The role of ErbB2 and BRCA1 in repair of drug-induced DNA damage

by

Julien Jacques Max Boone

A thesis submitted to the University of London for the degree of Doctor of Philosophy

October 2007

CRUK Drug-DNA Interaction Research Group
Department of Oncology
Royal Free and University College Medical School
University College London
91 Riding House Street, London, W1W 7BS, UK

ProQuest LLC
789 East Eisenhower Parkway
P.O. Box 1346
Ann Arbor, MI 48106-1346

A ma grand-mère maternelle

ABSTRACT

Breast cancer is the most common cause of cancer in women. Overexpression of ErbB2 (HER2) occurs in 25-30% of sporadic breast cancer and is associated with poor prognosis. New therapies targeting ErbB2 have been developed and shown to influence the activity of chemotherapeutic agents. The main aim of this investigation was to study the potential role of ErbB2 in the repair of drug-induced DNA damage. Synergistic effects of trastuzumab, a monoclonal anti-ErbB2 antibody, in combination with common chemotherapeutics were evaluated in cell lines expressing different level of ErbB2. In addition, effects of ErbB2 nuclear localisation on cisplatin sensitivity were also investigated. Using the comet assay, effects of ErbB2 expression and its nuclear translocation on the kinetic of damage and repair of DNA interstrand crosslinks and DNA strand breaks were examined. Effects of trastuzumab, alone and in combination with cisplatin, on the cell cycle and apoptosis were studied using FACS analysis. Trastuzumab was shown to enhance drug sensitivity in cell lines overexpressing ErbB2. ErbB2 overexpression caused increased resistance to cisplatin whereas deletion of its nuclear localisation signal sequence led to an increased sensitivity. Study of the repair of drug-induced DNA damage revealed that modulation of ErbB2 expression altered the kinetics of repair of cisplatin-induced DNA interstrand crosslinks but not DNA intrastrand crosslinks, and that ErbB2 nuclear translocation was important for the repair of cisplatin DNA damage. BRCA1 is another important protein, as germline mutations of this gene have been shown to substantially increase the risk of hereditary breast cancer. Sensitivity of BRCA1 down-regulated cells to radiotherapy, chemotherapeutic agents alone and in combination with gefitinib, an EGFR tyrosine kinase inhibitor, was also evaluated. Study of BRCA1 down-regulation produced conflicting results with published data but a synergistic effect was obtained between cisplatin and gefitinib in cells with down-regulated BRCA1 expression. These results establish a link between nuclear ErbB2 and repair of drug-induced DNA damage. In addition, they suggest an interaction between BRCA1 and the EGFR signalling pathway in cisplatin-induced DNA damage repair.

ACKNOWLEDGEMENTS

I carried out my PhD work in the Drug-DNA interaction research group of the Department of Oncology at UCL and was supervised by Professor John Hartley and Professor Daniel Hochhauser.

Firstly, I would like to thank John for his constant support and advice during these four years. Thank you as well to Daniel for his support, advice and insightful contributions.

I would like to thank Dr C. Lord, Dr. O. Segatto, Prof. Y. Yarden and Prof. M. Hung for supplying me with important reagents necessary for the accomplishment of the work carried out in this thesis. A special thank you to Dr. M. Tilby without whom I would not have been able to carry out the intrastrand crosslink assay.

I am grateful to all my colleagues in the laboratory and the office for all their help. A special thank you to Dr. Victoria Spanswick, Helen Lowe and Janet Hartley for their help and advice, especially during the first months of my PhD. A huge thank you as well to Dr. Minal Kotecha for her constant support, advice and friendship. "Un grand merci" to my colleague, friend and French ally in the lab, Dr. Jérome Kluza, for his advice and support during working hours, pub lunch and "fitness" sessions. Finally, I would like to thank Ali Hazrati for his friendship and without whom I would have been homeless more than once.

Life would not have been the same during these four years (and more) without my friends, Damien, Simon, Adrien, Benjamin, Cédric, Jérémie, Eléonore, Magalie, and Nadège, who surrounded me, kept me down to earth and helped me relax during those scarce but highly enjoyable week-ends and holidays away which I cannot always remember – and long may it continue. A special thank you as well to Géraldine for her constant support during the final part of this PhD.

Most of all, I am deeply grateful to my parents, my sister and Sylvain for all their support and wise words during my long years of study, and to Manon for all the lovely cuddles for her uncle. Thank you to "Famille Lemercher" for their support and regular visits. I would also like to thank Allan, Irina and Stoyko for giving me distraction at weekends and supporting me during these four years. Finally, I would like to thank Annie, for always encouraging me and putting up with me during stressful moments especially in the last few months.

COMMUNICATIONS

PRESENTATIONS

- **April 2006:** Oncology Department, UCL – Role of BRCA1 and ErbB2 in the repair of drug-induced DNA damage in breast cancer.

PUBLICATIONS

- **Boone J.J.M.**, Hochhauser D. and Hartley J.A. (2006). Modulation of the repair of cisplatin-induced DNA interstrand crosslinks by trastuzumab. Eur. J. Cancer, *Supl. 4(12)*, 151. (18th EORTC-NCI-AACR International Conference: "Synopsium on Molecular Targets and Cancer Therapeutics").

- Masterson L., Spanswick V.J., **Boone J.J.M.**, Howard P.W., Hartley J.A., Begent R.H. and Thurston D.E. (2005). Design, synthesis and evaluation of novel pyrrolobenzodiazepine (PBD) based prodrugs for use in antibody directed enzyme prodrug therapy (ADEPT). Proc. Am. Assoc. Cancer Res., *46*, 684. (96th Annual meeting American Association for Cancer Research, Anaheim).

TABLE OF CONTENTS

ABSTRACT 1

ACKNOWLEDGMENTS 2

COMMUNICATIONS 3

TABLE OF CONTENTS 4

INDEX OF FIGURES 14

INDEX OF TABLES 22

ABBREVIATIONS 24

CHAPTER 1 INTRODUCTION 28

1.1 Epidemiology of breast cancer 29

1.1.1 Definition of cancer 29

1.1.2 Importance of breast cancer 29

1.1.3 Molecular epidemiology of breast cancer 29

1.1.4 Treatment of breast cancer 30

1.2 Anti-cancer drugs and breast cancer 31

1.2.1 Cisplatin 32

1.2.2 Melphalan 33

1.2.3 Doxorubicin 33

1.2.4 Etoposide 34

1.2.5 Paclitaxel 36

1.2.6 Other chemotherapeutic treatments 37

1.3 DNA damage and repair mechanisms 38

1.4 Cellular response to DNA damage 40

1.4.1 DNA repair pathways 40

Nucleotide Excision Repair (NER) 41

Base Excision Repair (BER) 43

Homologous recombination (HR) and non homologous end joining (NHEJ) 45

1.4.2 Cell cycle alterations in cancer 47

G1/S cell cycle checkpoint 47

G2 cell cycle checkpoint 49

1.4.3 p53 and apoptosis 51

1.5 BReast-CAncer susceptibility gene 1 (BRCA1) 53

1.5.1 BRCA1 and DNA damage repair 55

1.5.2 BRCA1 as transcriptional regulator 58

1.5.3 BRCA1 and cell cycle regulation 59

1.5.4 BRCA1 and topoisomerase II 60

1.5.5 BRCA1 and cancer therapy 60

Response to chemotherapy 60

Response to radiotherapy 61

1.6 The epidermal growth factor receptors 62

1.6.1 The EGF receptor family 62

1.6.2 Epidermal growth factor receptors and cancer 64

Oncogenic tyrosine kinases (OTKs) 64

EGFR 65

ErbB2 67

1.6.3 EGFR and ErbB2 targeted therapies 72

Tyrosine kinase inhibitors 73

Antibodies blocking the extracellular binding region of the receptor 78

Ligand/antibody-toxin conjugates acting on the extracellular ligand binding region 82

Combination therapies 82

Resistance to targeted therapies 85

1.7 Aims and objectives 88

CHAPTER 2 MATERIALS AND METHODS 89

MATERIALS 90

2.1 Cell lines and culture conditions 90

2.2 Tissue culture 92

2.2.1 Cell lines maintenance 92

2.2.2 Storage and retrieval from liquid nitrogen 93

2.2.3 Cell count 93

2.2.4 Cell doubling time 93

2.3 Chemotherapeutic drugs and other reagents 94

METHODS 96

2.4 *In vitro* cytotoxicity assay 96

2.4.1 Single agent cytotoxicity 96

2.4.2 Dual agent treatments and synergistic effect 97

2.4.3 SRB assay and data analysis 97

2.5 Radiation survival curve 98

2.6 Isobologram analysis 98

2.7 Western blotting analysis 99

2.7.1 Total protein extraction 99

2.7.2 Nuclear and cytoplasmic protein extraction 100

2.7.3 Protein quantification 101

2.7.4 Immunoblotting 101

2.8 Reverse Transcriptase Polymerase Chain Reaction 103

2.8.1 RNA extraction and quantification 103

2.8.2 Synthesis of first strand cDNA 104

2.8.3 Reverse Transcriptase PCR amplification 104

2.9 Real Time Polymerase Chain Reaction 105

2.9.1 Real Time PCR 105

PCR products verification 106

Real Time PCR 107

2.9.2 Optimisation 110

2.9.3 Results analysis 111

2.10 Single cell gel electrophoresis Comet assay 112

2.10.1 The Comet assay 112

Study of drug concentration on DNA damage level 112

DNA damage repair study 113

Assay methodology 113

2.10.2 Data analysis 114

2.11 Cisplatin intrastrand crosslinks assay 116

2.11.1 Methodology 116

DNA extraction 116

Competitive ELISA 116

2.11.2 Data analysis 117
2.12 Cell cycle analysis 119
2.12.1 Methodology 119
2.12.2 Data analysis 120
2.13 Topoisomerase II activity assay 122
2.14 Immunofluorescence 123
2.15 Small interfering RNA transfection 124
2.16 Stable transfection 125
2.16.1 Stable transfection of ErbB2 plasmids 125
Plasmids transformation and amplification 125
Plasmids verification 127
Plasmids transfection 127
2.16.2 Plasmids encoding specific human BRCA1 siRNA 128
2.17 Drug treatments 129

CHAPTER 3 MODULATION OF THE REPAIR OF DRUG-INDUCED DNA DAMAGE BY ERBB2 INHIBITION 130
INTRODUCTION 131
3.1 Trastuzumab and ErbB2 protein expression 131
3.2 Trastuzumab and chemotherapeutic agents 132
3.3 Trastuzumab and DNA damage repair 132
3.4 Aims 133
RESULTS 134
3.5 EGF receptor protein expression 134
3.6 Effects of trastuzumab treatment 135
3.6.1 Down-regulation of ErbB2 by trastuzumab 135
3.6.2 Inhibition of cell proliferation by trastuzumab 139
3.7 Trastuzumab and chemotherapeutic treatments 140
3.7.1 Determination of IC_{50} of common chemotherapeutics 140
3.7.2 Combination of trastuzumab with chemotherapeutic agents 142
3.8 Modulation of DNA damage repair by ErbB2 inhibition 147
3.8.1 Measurement of DNA damage 147

Measurement of cisplatin and melphalan-induced DNA interstrand crosslink formation 147
Measurement of etoposide-induced DNA strand breaks 150
3.8.2 Effect of trastuzumab on the repair of drug-induced DNA damage 151
Effect of trastuzumab on the repair of cisplatin-induced interstrand crosslinks 151
Effect of trastuzumab on the repair of melphalan-induced interstrand crosslinks 153
Effect of trastuzumab on the repair of etoposide-induced strand breaks 155
3.8.3 Effect of trastuzumab dosage and drug treatment schedule 158
Inhibition of DNA repair in a dose dependent manner 158
Modulation of drug scheduling and inhibition of DNA repair 160
DISCUSSION 163
3.9 Trastuzumab affects ErbB2 overexpressing cells 163
3.10 Trastuzumab enhances chemotherapeutic cytotoxicity 164
3.11 Trastuzumab modulates DNA damage repair 165
3.12 Conclusion 167

CHAPTER 4 DNA REPAIR MODULATION AND CELL CYCLE REGULATION 169
INTRODUCTION 170
4.1 Effects of trastuzumab on the cell cycle 170
4.2 Effect of trastuzumab on apoptosis 171
4.3 ErbB2 signalling cascade and topoisomerase IIα 171
4.3.1 Role of Akt in ErbB2 signalling cascade 172
4.3.2 Topoisomerase IIα and cell cycle 173
4.4 Aims 174
RESULTS 175
4.5 Influence of DNA repair modulation on cell cycle regulation 175
4.6 Influence of DNA repair modulation on apoptosis 180

4.7 Identification of proteins involved in the modulation of DNA repair caused by ErbbB2 inhibition 182

4.7.1 Influence of DNA damage repair delay on the level of proteins involved in DNA damage repair and ErbB2 signalling pathways 182

Modulation of proteins level in MDA-MB-453 cells 182

Modulation of proteins level and their phosphorylated forms in MDA-MB-453 and SK-BR-3 cells 188

Effect of trastuzumab treatment of Akt protein level 193

4.7.2 Influence of ErbB2 inhibition on TOPO2α mRNA level 194

DISCUSSION 196

4.8 Cell cycle and apoptosis 196

4.9 Modulation of proteins level by trastuzumab 197

4.9.1 Akt and cytoplasmic localisation of $p21^{WAF1}$ 197

4.9.2 Akt and inhibition of $p27^{kip1}$ function 198

4.10 Trastuzumab and topoisomerase IIα 199

4.11 Conclusion 200

CHAPTER 5 MODULATION OF THE REPAIR OF DRUG-INDUCED DNA DAMAGE AND ERBB2 EXPRESSION 201

INTRODUCTION 202

5.1 ErbB2 overexpression 202

5.2 Cisplatin-induced DNA damage 202

5.3 Cell cycle modulation 203

5.3.1 Mitogen-Activated Protein Kinase (MAPK) 203

5.3.2 Phosphatase and Tensin homolog (PTEN) 204

5.3.3 Topoisomerase II activity 204

5.4 Aims 205

RESULTS 206

5.5 Downregulation of ErbB2 expression by siRNA 206

5.5.1 Determination of ErbB2 mRNA down-regulation by real time PCR 206

PCR product verification ant optimisation of the conditions 206
Modulation of ErbB2 mRNA level 207
5.5.2 Effect of ErbB2 siRNA on ErbB2 protein expression level 211
5.6 Transfection of ErbB2 in ErbB2 negative cell line 213
5.7 Effect of trastuzumab on MDA-MB-468 cells overexpressing ErbB2 215
5.7.1 Effect of trastuzumab on ErbB2 protein level 215
5.7.2 Effect of trastuzumab on cell proliferation 218
5.8 Trastuzumab and cisplatin treatment 219
5.8.1 Effect of combination treatment after continuous exposure 219
5.8.2 Effect of combination treatment after short exposure 222
5.9 Modulation of ErbB2 expression and DNA interstrand crosslink repair 224
5.9.1 Kinetics of cisplatin DNA damage and repair 224
Measurement of cisplatin-induced DNA interstrand crosslinks 224
Effect of ErbB2 modulation on the kinetics of formation and repair of cisplatin-induced DNA interstrand crosslinks 225
5.9.2 Kinetics of melphalan-induced DNA damage and repair 229
Measurement of melphalan-induced DNA interstrand crosslinks 229
Effect of ErbB2 modulation on the kinetics of formation and repair of melphalan-induced DNA interstrand crosslinks 230
5.10 Modulation of ErbB2 expression and DNA intrastrand crosslinks repair 233
5.10.1 Measurement of cisplatin-induced intrastrand crosslinks 234
5.10.2 Effect of ErbB2 modulation on the kinetics of formation and repair of cisplatin-induced DNA intrastrand crosslinks 235
5.11 Modulation of expression of DNA repair proteins and proteins of the ErbB2 signalling pathway 237
5.12 ErbB2 overexpression and topoisomerase II activity 243
DISCUSSION 244
5.13 ErbB2 expression and drug sensitivity 244

5.14 ErbB2 expression modulates the repair of drug-induced DNA damage 246
5.15 Modulation of cell cycle progression 247
5.15.1 Role of Akt in the modulation of cell cycle 247
5.15.2 Role of MAPK in the modulation of cell cycle 248
5.15.3 PTEN and PI3K/Akt signalling 248
5.16 ErbB2 overexpression increases topoisomerase II activity 249
5.17 Conclusion 250

CHAPTER 6 ROLE OF ERBB2 NUCLEAR LOCALISATION IN THE REPAIR OF CISPLATIN-INDUCED DNA ICL 251
INTRODUCTION 252
6.1 Nuclear localisation of EGFR family members 252
6.2 Wheat germ agglutinin and nuclear translocation 254
6.3 Aims 255
RESULTS 256
6.4 Expression of mutated ErbB2 with a deletion of the NLS sequence 256
6.4.1 ErbB2 protein expression by immunoblotting 256
6.4.2 ErB2 protein expression by immunofluorescence 258
6.5 Effect of trastuzumab and cisplatin on transfected cell lines 259
6.5.1 Effect of trastuzumab on MDA-MB-468 cell lines 259
Trastuzumab and ErbB2 protein expression 259
Effect of trastuzumab on cell proliferation 262
6.5.2 Sensitivity to cisplatin treatment 263
6.6 Modulation of DNA damage repair by inhibition of ErbB2 nuclear translocation 265
6.6.1 Modulation of the repair of cisplatin-induced DNA interstrand crosslinks 265
6.6.2 EGFR and ErbB2 nuclear localisation 269
DISCUSSION 273
6.7 Trastuzumab and ErbB2 nuclear translocation 273

6.8 Cisplatin sensitivity 274
6.9 Modulation of DNA damage repair 275
6.10 Conclusion 276

CHAPTER 7 EFFECT OF THE MODULATION OF BRCA1 EXPRESSION ON CELLULAR RESPONSE TO CHEMOTHERAPEUTIC AGENTS 277
INTRODUCTION 278
7.1 BRCA1 and chemotherapeutic response 278
7.2 Mutations and loss of BRCA function 279
7.2.1 BRCA1 expression and chemotherapy 279
7.2.2 BRCA1 expression and radiotherapy 280
7.3 BRCA1 and topoisomerase II activity 280
7.4 Aims 281
RESULTS 282
7.5 Modulation of BRCA1 mRNA level 282
7.5.1 Determination of BRCA1 mRNA level by RT-PCR 282
7.5.2 Quantification of BRCA1 mRNA level 284
Optimisation of the real time PCR conditions 284
Quantification of BRCA1 mRNA level 285
7.6 Modulation of BRCA1 protein expression level 287
7.7 Effects of gefitinib and chemotherapeutic treatments 288
7.7.1 IC_{50} for single agent treatments 288
7.7.2 Combination of cisplatin with gefitinib 290
7.8 Effects of X-ray irradiation 295
7.9 Topoisomerase II activity 296
CONCLUSION 297
7.10 Chemosensitivity of BRCA1 deficient cells 297
7.10.1 BRCA1 expression modulates chemosensitivity 297
7.10.2 BRCA1 expression and EGFR signalling pathway 298
7.11 Radiosensitivity of BRCA1 deficient cells 299
7.12 Role of BRCA1 in DNA decatenation 300
7.13 Conclusion 300

CHAPTER 8 CONCLUSIONS AND FUTURE WORK 301

8.1 ErbB2 protein expression and sensitivity to trastuzumab and chemotherapeutic agents 303

8.1.1 ErbB2 protein expression and trastuzumab sensitivity **303**

8.1.2 ErbB2 protein expression and chemotherapeutic response **304**

8.1.3 Nuclear ErbB2 and chemotherapeutic treatments **305**

8.2 ErbB2 expression and repair of drug-induced DNA damage 305

8.2.1 ErbB2 expression and repair of drug-induced DNA strand breaks **305**

8.2.2 ErbB2 expression and repair of drug-induced DNA interstrand crosslinks **306**

8.2.3 Nuclear ErbB2 and repair of cisplatin-induced DNA interstrand crosslinks **306**

8.3 ErbB2 and EGFR nuclear localisation 307

8.4 ErbB2 expression and DNA repair proteins 307

8.5 Role of BRCA1 in drug-induced DNA damage 308

8.6 Conclusion 308

REFERENCES 309

APPENDICES 368

Appendix 1: Student *t*-test 369

Appendix 2: Design of TaqMan probes and primers using Primer Express software 371

INDEX OF FIGURES

Figure 1.1 – Classification of anti-cancer drugs according to their mechanism of action. **31**

Figure 1.2 – Structure of cisplatin. **32**

Figure 1.3 – Structure of melphalan (L-phenylalanine). **33**

Figure 1.4 – Structure of doxorubicin. **34**

Figure 1.5 – Structure of etoposide (VP-16). **35**

Figure 1.6 – Inhibition of topoisomerase II by etoposide. **35**

Figure 1.7 – Structure of paclitaxel. **36**

Figure 1.8 – DNA damage and repair mechanisms. **39**

Figure 1.9 – Interaction of crosslinking drugs with DNA. **40**

Figure 1.10 – Nucleotide Excision Repair (NER) pathway. **42**

Figure 1.11 – Base Excision Repair (BER) pathway. **44**

Figure 1.12 – Homologous Recombination (HR) and Non Homologous End Joining (NHEJ or V(D)J recombination) molecular mechanism. **46**

Figure 1.13 – G1/S cell cycle checkpoint and signalling pathway. **48**

Figure 1.14 – G2/M cell cycle checkpoint and signalling pathway. **50**

Figure 1.15 – Apoptosis signalling pathway. **52**

Figure 1.16 – BRCA1 structure (1863 amino acids). **54**

Figure 1.17 – BRCA1 network. **54**

Figure 1.18 – BRCA1 and DNA double strand break repair. **57**

Figure 1.19 – Transcription and BRCA1. **59**

Figure 1.20 – ErbB family: their structure and binding ligands. **63**

Figure 1.21 – ErbB receptors signalling. **63**

Figure 1.22 – ErbB downstream signalling pathways. **69**

Figure 1.23 – ErbB targeted therapies: modulation of ErbB receptors activity. **73**

Figure 1.24 – Structure of gefitinib. **75**

Figure 1.25 – Internalisation of the ErbB2 receptor by trastuzumab. **80**

Figure 2.1 – Isobologram analysis. **99**

Figure 2.2 – Real Time PCR reaction: amplification of the fragment. **109**

Figure 2.3 – Typical real time PCR amplification plot. **112**

Figure 2.4 – Screen display of Komet analysis software. **114**
Figure 2.5 – Repair of DNA damage caused by etoposide treatment. **115**
Figure 2.6 – DNA damage repair profile of irradiated cells treated with cisplatin. **115**
Figure 2.7 – Typical curve fitting for two standards obtained with GraphPad Prism 4. **119**
Figure 2.8 – Histogram profile showing the number of events in each phase versus DNA quantity. **121**
Figure 2.9 – Histogram profile obtained with WinMDI software. **121**
Figure 2.10 – pcDNA3 plasmid map. **126**
Figure 2.11 – pEGFP-N1 plasmid map. **126**
Figure 3.1 – Western blotting of each EGF receptor in MCF-7, SK-BR-3 and MDA-MB-453 cell lines. **134**
Figure 3.2 – Immunoblots of ErbB2 and pErbB2 in MCF-7, SK-BR-3 and MDA-MB-453 cell lines treated with trastuzumab for 1 hour. **136**
Figure 3.3 – Immunoblots of ErbB2 and pErbB2 in MCF-7, SK-BR-3 and MDA-MB-453 cell lines treated with trastuzumab for 16 hours. **137**
Figure 3.4 – Immunoblots of ErbB2 and pErbB2 in MCF-7, SK-BR-3 and MDA-MB-453 cell lines treated with trastuzumab for 24 hours. **138**
Figure 3.5 – Inhibition of cell proliferation by trastuzumab in MCF-7, SK-BR-3 and MDA-MB-453 cells. **139**
Figure 3.6 – Inhibition of MCF-7, SK-BR-3 and MDA-MB-453 cell proliferation after single agent treatment. **141**
Figure 3.7 – Inhibition of MCF-7 cells proliferation after continuous treatment with trastuzumab combined with chemotherapeutic drugs. **144**
Figure 3.8 – Inhibition of SK-BR-3 cells proliferation after continuous treatment with trastuzumab combined with chemotherapeutic drugs. **145**

Figure 3.9 – Inhibition of MDA-MB-453 cells proliferation after continuous treatment with trastuzumab combined with chemotherapeutic drugs. **146**
Figure 3.10 – DNA interstrand crosslinks in MCF-7 after cisplatin and melphalan treatment. **148**
Figure 3.11 – DNA interstrand crosslinks in SK-BR-3 after cisplatin and melphalan treatment. **149**
Figure 3.12 – DNA interstrand crosslinks in MDA-MB-453 after cisplatin and melphalan treatment. **149**
Figure 3.13 – DNA strand breaks in MCF-7, SK-BR-3 and MDA-MB-453 cells after etoposide treatment. **150**
Figure 3.14 – Cisplatin-induced DNA interstrand crosslinks in MCF-7 cells. **152**
Figure 3.15 – Cisplatin-induced DNA interstrand crosslinks in SK-BR-3 cells. **152**
Figure 3.16 – Cisplatin-induced DNA interstrand crosslinks in MDA-MB-453 cells. **153**
Figure 3.17 – Melphalan-induced DNA interstrand crosslinks in MCF-7 cells. **154**
Figure 3.18 – Melphalan-induced DNA interstrand crosslinks in SK-BR-3 cells. **154**
Figure 3.19 – Melphalan-induced DNA interstrand crosslinks in MDA-MB-453 cells. **155**
Figure 3.20 – Etoposide-induced DNA strand breaks in MCF-7 cells. **156**
Figure 3.21 – Etoposide-induced DNA strand breaks in SK-BR-3 cells. **157**
Figure 3.22 – Etoposide-induced DNA strand breaks in MDA-MB-453 cells. **157**
Figure 3.23 – Trastuzumab dose dependent repair of cisplatin-induced DNA damage in MDA-MB-453 cells. **159**
Figure 3.24 – Effect of trastuzumab pre-treatment on cisplatin-induced DNA ICLs in MDA-MB-453 cells. **161**
Figure 3.25 – Effect of drug free media pre-incubation on cisplatin-induced DNA ICLs repair kinetics in MDA-MB-453 cells. **161**

Figure 3.26 – Inhibition of MDA-MB-453 cells proliferation after 48 hours of pre-incubation in drug free media. **162**
Figure 4.1 – Effect of Akt activation. **173**
Figure 4.2 – Histogram profile of MDA-MB-453 untreated cells. **176**
Figure 4.3 – Histogram profile of MDA-MB-453cells treated with trastuzumab. **177**
Figure 4.4 – Histogram profile of MDA-MB-453 cells treated with cisplatin. **178**
Figure 4.5 – Histogram profile of MDA-MB-453 cells treated with a combination of cisplatin. **179**
Figure 4.6 – Western blot analysis of PARP and cleaved PARP protein in MDA-MB-453 cells. **181**
Figure 4.7 – Immunoblots of MDA-MB-453 untreated cells. **184**
Figure 4.8 – Immunoblots of MDA-MB-453 cells treated with trastuzumab. **185**
Figure 4.9 – Immunoblots of MDA-MB-453 cells treated with cisplatin. **186**
Figure 4.10 – Immunoblots of MDA-MB-453 cells treated with cisplatin and trastuzumab. **187**
Figure 4.11 – Immunoblots of MD-MB-453 cells treated with cisplatin. **189**
Figure 4.12 – Immunoblots of MDA-MB-453 cells treated with cisplatin and trastuzumab. **190**
Figure 4.13 – Immunoblots of SK-BR-3 cells treated with cisplatin. **191**
Figure 4.14 – Immunoblots of SK-BR-3 cells treated with cisplatin and trastuzumab. **192**
Figure 4.15 – Akt and pAkt protein expression in MDA-MB-453 cells treated with trastuzumab. **193**
Figure 4.16 – TOPO2α mRNA level in MDA-MB-453 cells. **195**
Figure 5.1 – Effect of ErbB2 siRNA on ErbB2 mRNA level in MCF-7 cell line. **208**
Figure 5.2 – Effect of ErbB2 siRNA on ErbB2 mRNA level in SK-BR-3 cell line. **209**
Figure 5.3 – Effect of ErbB2 siRNA on ErbB2 mRNA level in MDA-MB-453 cell line. **210**

Figure 5.4 – ErbB2 protein level in MCF-7 cells transfected with ErbB2 siRNA. **212**

Figure 5.5 – ErbB2 protein level in SK-BR-3 cells transfected with ErbB2 siRNA. **212**

Figure 5.6 – ErbB2 protein level in MDA-MB-453 cells transfected with ErbB2 siRNA. **212**

Figure 5.7 – Protein expression of each ErbB receptor in MDA-MB-468, MDA-MB-468 pcDNA3 (vector control) and MDA-MB-468 pcDNA3-ErbB2 cells. **214**

Figure 5.8 – ErbB2 immunofluorescence of MDA-MB-453 and MDA-MB-468 cells. **214**

Figure 5.9 – ErbB2 and pErbB2 protein expression in MDA-MB-468 pcDNA3-ErbB2 cells treated with trastuzumab. **216**

Figure 5.10 – ErbB2 immunofluorescence in MDA-MB-468 pcDNA3-ErbB2 cells before and after trastuzumab treatment. **217**

Figure 5.11 – Inhibition of MDA-MB-468 cells proliferation by trastuzumab. **218**

Figure 5.12 – Inhibition of MDA-MB-468 cells proliferation by cisplatin alone and in combination with trastuzumab for 5 days. **221**

Figure 5.13 – Inhibition of MDA-MB-468 cells proliferation by cisplatin alone and in combination with trastuzumab for 1 hour. **223**

Figure 5.14 – DNA interstrand crosslinks in MDA-MB-468 wild type cells after cisplatin treatment. **225**

Figure 5.15 – Cisplatin-induced DNA interstrand crosslinks in MDA-MB-468 wild type cells. **226**

Figure 5.16 – Cisplatin-induced DNA interstrand crosslinks in MDA-MB-468 pcDNA3 vector control cells. **227**

Figure 5.17 – Cisplatin-induced DNA interstrand crosslinks in MDA-MB-468 pcDNA3-ErbB2 cells. **227**

Figure 5.18 – Cisplatin-induced DNA interstrand crosslinks in MDA-MB-468 cells. **228**

Figure 5.19 – DNA interstrand crosslinks in MDA-MB-468 wild type cells after melphalan treatment. **229**

Figure 5.20 – Melphalan-induced DNA interstrand crosslinks in MDA-MB-468 wild type cells. **231**

Figure 5.21 – Melphalan-induced DNA interstrand crosslinks in MDA-MB-468 pcDNA3 vector control cells. **231**

Figure 5.22 – Melphalan-induced DNA interstrand crosslinks in MDA-MB-468 pcDNA3-ErbB2 cells. **232**

Figure 5.23 – Melphalan-induced DNA interstrand crosslinks in MDA-MB-468 cells. **232**

Figure 5.24 – Cisplatin-induced DNA intrastrand crosslinks in MDA-MB-468 cells. **234**

Figure 5.25 – Cisplatin-induced DNA intrastrand crosslinks in MDA-MB-468 cells. **236**

Figure 5.26 – Repair of cisplatin-induced DNA intrastrand crosslinks in MDA-MB-468 cells. **236**

Figure 5.27 – Immunoblots of untreated MDA-MB-468 wild type cells. **239**

Figure 5.28 – Immunoblots of MDA-MB-468 wild type cells treated with trastuzumab. **239**

Figure 5.29 – Immunoblots of MDA-MB-468 wild type cells treated with cisplatin. **240**

Figure 5.30 – Immunoblots of MDA-MB-468 wild type cells treated with cisplatin and trastuzumab. **240**

Figure 5.31 – Immunoblots of untreated MDA-MB-468 pcDNA3-ErbB2 cells. **241**

Figure 5.32 – Immunoblots of MDA-MB-468 pcDNA3-ErbB2 cells treated with trastuzumab. **241**

Figure 5.33 – Immunoblots of MDA-MB-468 pcDNA3-ErbB2 cells treated with cisplatin. **242**

Figure 5.34 – Immunoblots of MDA-MB-468 pcDNA3-ErbB2 cells treated with cisplatin and trastuzumab. **242**

Figure 5.35 – Topoisomerase II α activity assay in MDA-MB-468 cells. **243**

Figure 6.1 – Protein expression of each ErbB receptor in MDA-MB-468 wild type, vector control, ErbB2 and ErbB2ΔNLS cells. **257**

Figure 6.2 – ErbB2 protein expression in MDA-MB-468 ErbB2 and MDA-MB-468 ErbB2ΔNLS cells. **257**

Figure 6.3 – Immunofluorescence ErbB2 protein expression in MDA-MB-468 cells. **258**

Figure 6.4 – Nuclear and cytoplasmic ErbB2 protein expression in MDA-MB-468 ErbB2 cells. **260**

Figure 6.5 – ErbB2 protein expression in MDA-MB-468 ErbB2ΔNLS cells. **261**

Figure 6.6 – Inhibition of MDA-MB-468 cells proliferation by trastuzumab. **262**

Figure 6.7 – Inhibition of MDA-MB-468 cells proliferation by cisplatin. **264**

Figure 6.8 – Cisplatin-induced DNA interstrand crosslinks in MDA-MB-468 wild type cells. **266**

Figure 6.9 – Cisplatin-induced DNA interstrand crosslinks in MDA-MB-468 pEGFP-N1 vector control cells. **267**

Figure 6.10 – Cisplatin-induced DNA interstrand crosslinks in MDA-MB-468 ErbB2 cells. **267**

Figure 6.11 – Cisplatin-induced DNA interstrand crosslinks in MDA-MB-468 cells treated with cisplatin. **268**

Figure 6.12 – Cisplatin-induced DNA interstrand crosslinks in MDA-MB-468 wild type, vector control, ErbB2 and ErbB2ΔNLS cells. **268**

Figure 6.13 – ErbB2 immunofluorescence of MDA-MB-468 ErbB2 cells. **270**

Figure 6.14 – EGFR immunofluorescence of MDA-MB-468 wild type cells. **271**

Figure 6.15 – EGFR immunofluorescence of MDA-MB-468 ErbB2ΔNLS cells. **272**

Figure 7.1 – Reverse Transcriptase PCR analysis of MCF-7 wild type, MCF-7 scrambled and MCF-7 3.23 cells. **283**

Figure 7.2 – BRCA1 mRNA level in MCF-7 cell lines. **286**

Figure 7.3 – EGFR and BRCA1 protein expression in MCF-7 cell lines. **287**

Figure 7.4 – Inhibition of MCF-7 cells proliferation by single agent treatment. **289**

Figure 7.5 – Inhibition of MCF-7 wild type cells proliferation by cisplatin/gefitinib combination treatment. **291**

Figure 7.6 – Inhibition of MCF-7 scrambled cells proliferation by cisplatin/gefitinib by combination treatment. **292**

Figure 7.7 – Inhibition of MCF-7 3.23 cells proliferation assay by cisplatin/gefitinib combination treatment. **292**

Figure 7.8 – Isobologram analysis at IC_{50} of cisplatin/gefitinib combination treatment using gefitinib 10%. **293**

Figure 7.9 – Isobologram analysis at IC_{50} of cisplatin/gefitinib combination treatment using gefitinib 20%. **294**

Figure 7.10 – Inhibition of MCF-7 cells proliferation after X-ray irradiation. **295**

Figure 7.11 – Topoisomerase IIα activity assay in MCF-7 cell lines. **296**

INDEX OF TABLES

Table 2.1 –	Transfected cell lines and corresponding plasmids.	**91**
Table 2.2 –	Summary of the cell lines used.	**92**
Table 2.3 –	Compounds used in the BRCA1 and ErbB2 studies.	**94-95**
Table 2.4 –	Antibodies used in the BRCA1 and ErbB2 studies.	**102-103**
Table 2.5 –	Sequences and annealing temperature for each primer set used in the BRCA1 study.	**105**
Table 2.6 –	Primers, probes and number of cycles used for Real Time PCR.	**108**
Table 2.7 –	Antibodies used for immunofluorescence experiments.	**123**
Table 2.8 –	ErbB2 siRNA sequences.	**124**
Table 2.9 –	List of enzymes used for plasmids restriction.	**127**
Table 2.10 –	Range of concentrations and lengths of exposure for drugs used in the different experiments.	**129**
Table 3.1 –	IC_{50}±SD results after single agent treatment in MCF-7, SK-BR-3 and MDA-MB-453 cells.	**140**
Table 3.2 –	IC_{50}±SD results for MCF-7 cells after single agent treatment and combination treatments.	**143**
Table 3.3 –	IC_{50}±SD results for SK-BR-3 cells after single agent treatment and combination treatments.	**143**
Table 3.4 –	IC_{50}±SD results for MDA-MB-453 cells after single agent treatment and combination treatments.	**143**
Table 3.5 –	IC_{50}±SD of cisplatin as a single agent and combined with trastuzumab, in MDA-MB-453 cells pre-incubated in drug-free media for 24 hours or 48 hours.	**162**
Table 4.1 –	Percentage of untreated MDA-MB-453 cells in each phase of the cell cycle.	**176**
Table 4.2 –	Percentage of MDA-MB-453 cells treated with trastuzumab in each phase of the cell.	**177**
Table 4.3 –	Percentage of MDA-MB-453 cells treated with cisplatin in each phase of the cell cycle.	**178**

Table 4.4 – Percentage of MDA-MB-453 cells treated with cisplatin and trastuzumab in each phase of the cell cycle. **179**

Table 4.5 – TOPO2α mRNA expression ratio in MDA-MB-453 cells. **195**

Table 5.1 – ErbB2 mRNA level in MCF-7 cells. **208**

Table 5.2 – ErbB2 mRNA level in SK-BR-3 cells. **209**

Table 5.3 – ErbB2 mRNA level in MDA-MB-453 cells. **210**

Table 5.4 – IC_{50}±SD results for MDA-MB-468 cells after cisplatin single agent and combination with trastuzumab for 5 days. **220**

Table 5.5 – IC_{50}±SD results for MDA-MB-468 cells after cisplatin treatment and combination with trastuzumab for 1 hour. **222**

Table 6.1 – IC_{50}±SD results for MDA-MB-468 cells treated with cisplatin alone. **264**

Table 7.1 – Quantification of BRCA1 mRNA level in MCF-7 cell lines. **285**

Table 7.2 – IC_{50} (±SD) results for single agent treatments in MCF-7 cell lines. **288**

Table 7.3 – IC_{50} (±SD) results for cisplatin/gefitinib combination treatments in MCF-7 cell lines. **291**

Table 7.4 – IC_{50} (±SD) results after X-ray irradiation of MCF-7 cell lines. **295**

Table I – Tabulated *t* values. **370**

ABBREVIATIONS

6-FAM	2',7'-bis(2-Carboxyethyl)-5(6)-carboxyfluorescein
Abl	Abelson
ADCC	Antibody-Dependent Cellular Cytotoxicity
ASK1	Apoptosis Signal-regulating Kinase 1
ATM	Ataxia Telangiectasia Mutated homolog protein
ATP	Adenosine TriPhosphate
ATR	Ataxia Telangiectasia and Rad3 related protein
AU	Arbitrary Unit
Bad	Bcl-2-associated death promoter
BARD1	BRCA1 Associated RING Domain
BASC	BRCA1 Associated genome Surveillance Complex
Bax	Bcl-2–associated X protein
Bcl-2	B-cell CLL/lymphoma 2
Bcr	Breakpoint cluster region
BER	Base Excision Repair
bp	base pair
BRCA1/2	BReast-CAncer susceptibility gene 1/2
BRCT	BRCA1 Carboxyl Terminus
Cdc	Cell division cycle
CDDP	*cis*-diamminedichloroplatinum(II), cisplatinum or cisplatin
Cdk	Cyclin-dependent kinases
cDNA	complementary DNA
CHK1/2	Choline Kinase
COMET	Single-cell gel electrophoresis
COX-2	CycloOXygenase 2
CPD	Cyclobutane Pyrimidine Dimer
CtIP	Carboxy-terminal BRCA1 Interacting Protein
DEPC	DiEthyl PyroCarbonate
DMEM	Dulbecco Modified Eagle's Minimal Essential Medium
DMSO	DiMethyl SulfOxide
DNA	Deoxyribose Nucleic Acid
DNA-PKcs	DNA-dependent Protein Kinase catalytic subunit (DNA-PK)

dNTP	deoxyNucleoside triphosphate
ECD	Extracellular Domain
EDTA	EthyleneDiamine Tetraacetic Acid
EGF	Epidermal Growth Factor
EGFR	HER1 or ErbB1, Epidermal Growth Factor Receptor
EGFRvIII	Epidermal Growth Factor Receptor variant III
ELISA	Enzyme-Linked ImmunoSorbent Assay
ER	Estrogen Receptor
ErbB2	HER2 or ErbB2/neu, Epidermal Growth Factor Receptor 2
ErbB3	HER3, Epidermal Growth Factor Receptor 3
ErbB4	HER4, Epidermal Growth Factor Receptor 4
ERCC	Excision Repair Cross-Complementing
ERK1/2	Extracellular signal-Regulated Kinase
FA	Fanconi Anemia
FACS	Fluorescence Activated Cell Sorting
FANCA	Fanconi Anemia Complementation group A
FANCC	Fanconi Anemia Complementation group C
FANCD	Fanconi Anemia Complementation group D
FCS	Foetal Calf Serum
Gadd45	Growth Arrest and DNA Damage gadd45 genes
GG-NER	Global Genome Nucleotide Excision Repair
GIST	GastroIntestinal Stromal Tumors
Grb2	Growth factor receptor-bound protein 2
GSK-3	Glycogen Synthase Kinase 3
H2AX	variant of the histone H2A
HAS	HER2-Associated Sequence
HR	Homologous Recombination
HRP	HorseRadish Peroxidase
IC_{50}	Inhibitory Concentration producing 50% growth inhibition
ICL	Interstrand CrossLinks
IF	ImmunoFluorescence
IGF-1R	Insulin-like Growth Factor 1 Receptor
IR	Ionizing Radiation
kDNA	kintoplast DNA

MAPK	Mitogen Activated Protein Kinase
MDM2	Murine Double Minute 2 protein
MEK1/2	MAPK/ERK kinase
MRE11	Meiotic Recombination 11
MRN	MRE11/NBS1/RAD51
mTOR	mammalian Target Of Rapamycin
n	degree of freedom
NBS1	Nijmegen Breakage Syndrome 1
NER	Nucleotide Excision Repair
NHEJ	Non Homologous End-Joining
NLS	Nuclear Localisation Signal
NLSs	Nuclear Localisation Signal sequence
NSCLC	Non Small Cell Lung Cancer
OD	Optical Density
OTK	Oncogenic Tyrosine Kinase
p	level of significance
PARP	Poly (ADP-Ribose) Polymerase
PBS	Phosphate Buffered Saline
PCNA	Proliferating Cell Nuclear Antigen
PCR	Polymerase Chain Reaction
PDGFR	Platelet-derived Growth Factor Receptor
PDK1/2	Phosphoinositide Dependent Kinase
PI	Propidium Iodide
PI3K	PhosphatidylInositol-3 Kinase
PIP_2	PhosphatidylInositol bisPhosphate
PIP_3	PhosphatidylInositol (3,4,5)-trisPhosphate
PKB	Protein Kinase B (Akt)
PKC	Protein Kinase C
PNK	PolyNucleotide Kinase
PTB	Phospho Tyrosine Binding domain
PTEN	Phosphatase and TENsin homolog
mRNA	messenger RiboNucleic Acid
RPA	Replication Protein A
RT-PCR	Reverse Transcriptase PCR

S473	Serine 473
scFv	single chain variable Fragment
SD	Standard Deviation
SE	Standard Error
siRNA	small interference RiboNucleic Acid
SRB	SulphoRhodamine B
Src	V-src sarcoma (Schmidt-Ruppin A-2) viral oncogene homolog
STAT	Signal Transducer and Activator of Transcription
T308	Threonine 308
TAMRA	N, N, N', N'-tetramethyl-6-carboxyrhodamine
TCR	Transcription Coupled Repair
TGF	Transforming Growth Factor
TK	Tyrosine Kinase
TOPO2α	Topoisomerase IIα
TP53	Tumour suppressor p53
UDS	Unscheduled DNA Synthesis
UV	UltraViolet
VEGF	Vascular Endothelial Growth Factor
WGA	Wheat Germ-Agglutinin
XPA	Xeroderma Pigmentosum A

Chapter 1

Introduction

1.1 Epidemiology of Breast cancer

1.1.1 Definition of cancer

Under normal conditions, the multiplication of cells is carefully regulated and responsive to specific needs of the body. Tumour development occurs through a multi-step process, in which a succession of genetic alterations, conferring growth advantages, leads to the progressive transformation of normal cells into cancer cells (Hanahan and Weinberg, 2000).

1.1.2 Importance of Breast cancer

Breast cancer is a disease affecting mainly women (especially women between 50 and 60 years old), with only 1% of all breast cancer cases affecting men (Weiss *et al.*, 2005). However, it is the second most common cause of female cancer death, after lung cancer. Nevertheless, the rate of breast cancer has been shown to vary around the world. Although the mortality rate for breast cancer has been decreasing since the late 1980s, statistics show that its incidence has increased by more than 50% in the same time period (www.cancerresearchuk.org).

1.1.3 Molecular epidemiology of breast cancer

Breast cancer is a multi-step disease of molecular and genetic changes affecting one or more regulatory genes. Several studies have established the existence of molecular markers for the prognosis of breast cancer. Dahiya and Deng (1998) reported many possible molecular prognostic markers in breast cancer: BRCA1 and BRCA2 (Breast Cancer genes), p53, ErbB oncogenes, loss of heterozygosity, chromosomal aberrations, microsatellite instability, transforming growth factor alpha and the multiple drug resistance gene. Nonetheless, two types of breast cancer have been identified, hereditary breast cancer and sporadic breast cancer (Kenemans *et al.*, 2004).

- Hereditary breast cancer is caused by an inherited susceptibility to breast cancer due to germline mutation of high risk susceptibility genes, such as BRCA1, BRCA2 or CHEK2. Indeed, several studies (Nkondjock and Ghadirian, 2004; Miki *et al.*, 1994; Wooster *et al.*, 1995) have shown the importance of BRCA1

and BRCA2, showing that germline mutations accounted for 5-10% of all breast cancers and 65% of hereditary cases. Cell-cycle-check-point kinase 2 (CHK2), responsible for the phosphorylation of p53 and BRCA1 in response to DNA damage, was also shown to be a good predictive marker in hereditary breast cancer, since CHK2 germline mutations were shown to be associated with increased risk of breast cancer (Weiss *et al.*, 2005; Vahteristo *et al.*, 2002).
In addition to germline mutations of high risk susceptibility genes, mutations of modest risk susceptibility genes have been identified, such as PTEN.

- Sporadic breast cancer results from an accumulation of unrepaired mutations in somatic genes, with no germline mutations. Oncogenes are then activated through mutations and their activation often associated with inactivation of tumour suppressor genes. Several oncogenes have been shown to play a major role in sporadic breast cancer, such as ErbB2. Slamon *et al.* (1987) reported that ErbB2 overexpression plays an important role in breast cancer development as it is overexpressed in 20-30% of breast cancer and causes oncogenesis. In addition, Harari and Yarden (2000) demonstrated that ErbB2 overexpression caused increased chemoresistance.

Nonetheless, many other factors have been described to have an impact on the increased risk of breast cancer (Okobia and Bunker, 2003; Kenemans *et al.*, 2004). Thus, gene expression profiling can be used as a tool to classify breast cancers.

1.1.4 Treatment of breast cancer

The development of a tumour being progressive, breast cancer growth has been divided in four stages. For the earliest stages (I – III) breast cancer can be treated using surgery, chemotherapy/radiotherapy and in some cases hormonal therapy.

- Surgery is divided into two types of operations for breast cancer, lumpectomy and mastectomy. Radiotherapy is usually used after a lumpectomy in order to destroy cancer cells that may still be present.

- Chemotherapy is usually used as a combination of chemotherapeutic drugs to increase efficacy and avoid drug resistance. It is usually given before or after breast surgery.

- Hormone therapy is used to modify the amount of estrogen in the blood, which is a major factor of growth in many breast cancers.

However, for advanced breast cancer, there are three type of treatments: hormonal therapies (tamoxifen is the most common but progestogens and aromatase inhibitors can also be used), chemotherapy using combinations of drugs in order to increase the efficacy, and monoclonal antibody therapy (trastuzumab or Herceptin®) targeting the epidermal growth factor receptor ErbB2. Trastuzumab being the only humanized monoclonal antibody which has been approved for the treatment of breast cancer.

1.2 Anti-cancer drugs and breast cancer

Anticancer drugs can be classified according to their mechanism of action, as described in Figure 1.1. The different classes of chemotherapeutic drugs have been briefly reviewed, with emphasis on the drugs used in the study of ErbB2 and BRCA1.

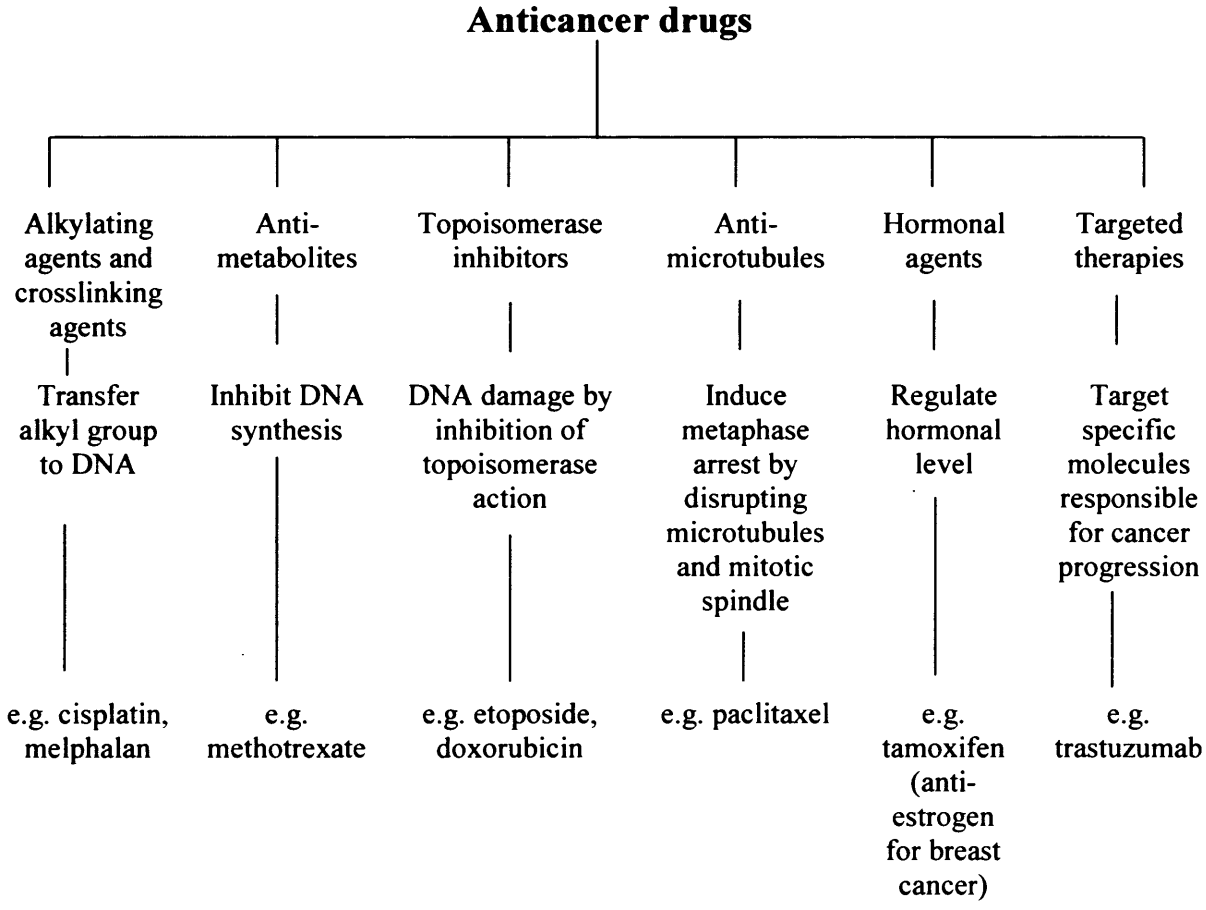

Figure 1.1 – Classification of anti-cancer drugs according to their mechanism of action.

1.2.1 Cisplatin

Cisplatin (CDDP – Figure 1.2), or *cis*-diamminedichloroplatinum(II), is a covalent DNA-binding agent (bifunctional alkylating agent). The pharmacological activity of cisplatin was identified in the late 1960s (Jakupec *et al.*, 2003). Alkylating agents form the largest class of anticancer drugs. These include nitrogen mustards, nitrosoureas, alkyl sulfonates and platinum compounds. Alkylating agents act non-specifically on the cell cycle by forming highly reactive electrophilic species which bind covalently with alkyl groups onto nucleophilic sites. These agents react with cellular macromolecules such as DNA bases (Adenine; Guanine; Cytosine and Thymine) and proteins. Cisplatin forms interstrand crosslinks and intrastrand adducts, chlorine atoms allow the group to bind to N^7 guanine atoms. By forming crosslinks, cisplatin inhibits DNA replication and transcription. Thus, causing inhibition of cell proliferation and apoptosis.

Cisplatin has become a widely used chemotherapeutic agent for a large number of cancers (e.g. bladder, ovarian, liver, gastric, brain, head, neck and lung). Cisplatin is also used in combination with radiation and other chemotherapeutic agents, to avoid resistance caused by the decrease of drug uptake and the increase of DNA repair. So far, cisplatin has not been widely used in the treatment of metastatic breast cancer due to its toxicity. Nonetheless, there has been an increasing interest in this compound in the past few years, as *in vitro* and *in vivo* studies demonstrated that combining cisplatin with the monoclonal antibody trastuzumab resulted in a higher response rate than either agent alone in metastatic breast cancer (Pegram *et al.*, 1998).

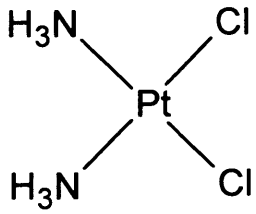

Figure 1.2 – Structure of cisplatin. Cisplatin (*cis*-diamminedichloroplatinum(II), CDDP) is an inorganic compound with a planar structure.

1.2.2 Melphalan

Melphalan or L-phenylalanine mustard (Figure 1.3) is also a bifunctional alkylating agent, belonging to the nitrogen mustard group. Similar to mechlorethamine but less reactive due to a slower rate of the chlorides ionisation, it forms bulky adducts by reacting with O^6 and N^7 guanine atoms. Melphalan is able to form two types of crosslinks: interstrand, intrastrand or between a DNA strand and a protein. Crosslinks result in the disruption of DNA replication and transcription, leading to cell cycle arrest and cell death. Melphalan is primarily used in the treatment of multiple myeloma and ovarian cancer.

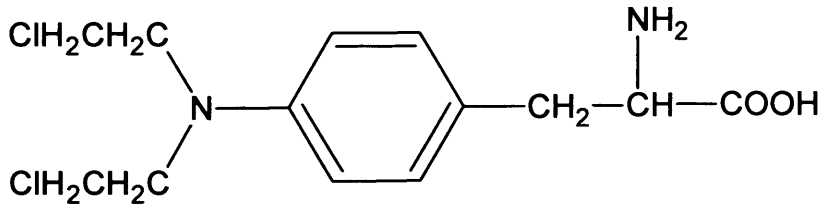

Figure 1.3 – Structure of melphalan (L-phenylalanine mustard).

1.2.3 Doxorubicin

Doxorubicin (or Adriamycin – Figure 1.4) is an anthracycline (produced by *Streptomyces peucetius*) and is classified as a non-covalent DNA binding drug that inhibits topoisomerase II activity. Doxorubicin is an intercalating agent with a planar region stacking between paired DNA bases, forming tight drug-DNA interactions. Doxorubicin also causes free radical damage of the DNA due to the metabolism of the quinone ring releasing active oxygen species. This results in partial unwinding of the DNA, impaired DNA and RNA synthesis and double strand breaks in DNA. Increase in resistance to treatment with doxorubicin was associated with an increase in glutathione peroxidase activity and a decrease in drug accumulation due to an increase in drug efflux, mediated by P-glycoprotein. Doxorubicin is used for the treatment of a wide range of cancers, including breast cancer.

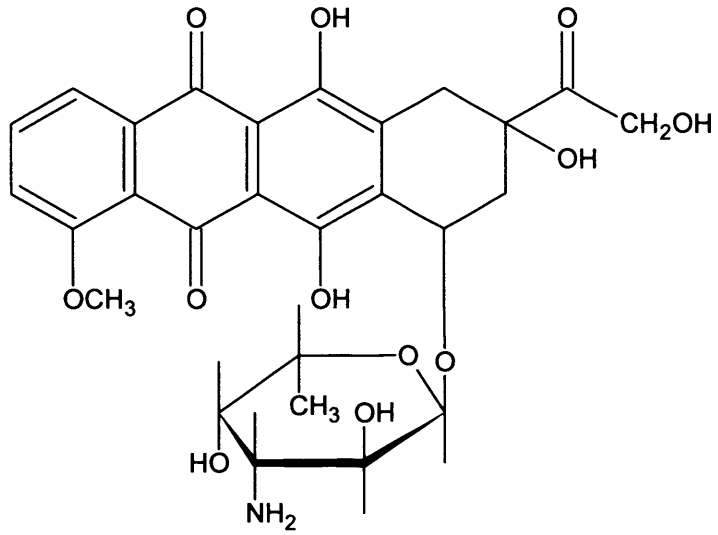

Figure 1.4 – Structure of doxorubicin.

1.2.4 Etoposide

Etoposide (VP-16 – Figure 1.5) is an inhibitor of chromatin function, and more precisely a topoisomerase II inhibitor. It is a semisynthetic derivative of podophyllotoxin from the mandrake plant. Topoisomerases are responsible for the unwinding of DNA to allow transcription and replication. They are also responsible for temporary DNA breakage and reseal, necessary for topological changes. The first type of topoisomerases (I) is responsible for transient single strand breaks whereas topoisomerase II produces double strand breaks to relieve tortional stress on the unwound DNA (topoisomerase I being responsible for the re-annealing).

Thus, etoposide stabilises the topoisomerase II-DNA complex (Figure 1.6), preventing topological changes, leading to double strand breaks, cell cycle arrest at S and G2 phases and apoptosis (Bromberg *et al.*, 2003). Etoposide is commonly used for the treatment of lung, testicular and ovarian cancers.

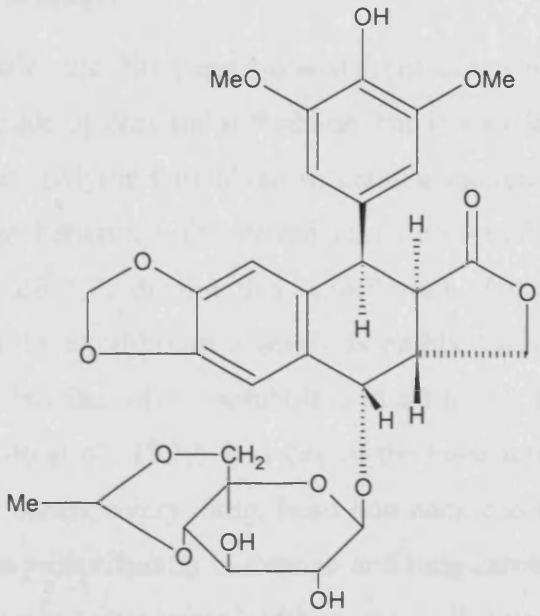

Figure 1.5 – Structure of etoposide (VP-16).

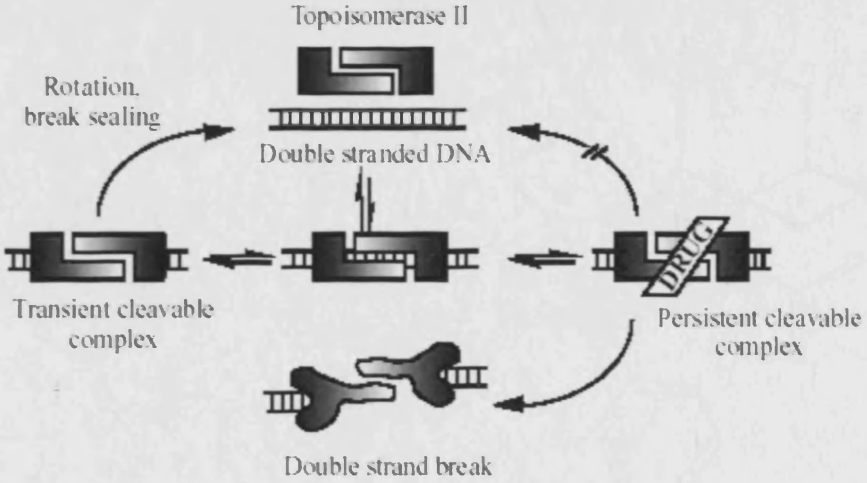

Figure 1.6 – Inhibition of topoisomerase II by etoposide (www.ovc.uoguelph.ca).

1.2.5 Paclitaxel

Paclitaxel (Taxol) is a tricyclic diterpene isolated from *Taxus brevifolia*, the Pacific yew. It is also an inhibitor of chromatin function but it also inhibits microtubules. Microtubules are proteins polymers involved in cellular movement and morphology occurring in equilibrium between polymerized and free tubulin dimers. Inhibitors, such as paclitaxel (Figure 1.7) disrupt this equilibrium. Paclitaxel binds to form microtubules and shifts the equilibrium towards assembly, causing stabilisation and formation of abnormal bundles of microtubules, resulting in the inhibition of cell proliferation (Mastropaolo *et al.*, 1995). It is one of the most active anti-cancer drugs and is effective against breast, ovary, lung, head and neck carcinomas. Paclitaxel is also used in combination with cisplatin in ovarian and lung carcinomas. Resistance to paclitaxel has been shown to be associated with increased P-glycoprotein and mutated tubulin. Paclitaxel is used in the treatment of breast, ovarian and lung cancer. In addition, recent studies have shown that combination of paclitaxel with trastuzumab increased the activity of either agent alone in ErbB2 overexpressing advanced breast cancer (Fountzilas *et al.*, 2001).

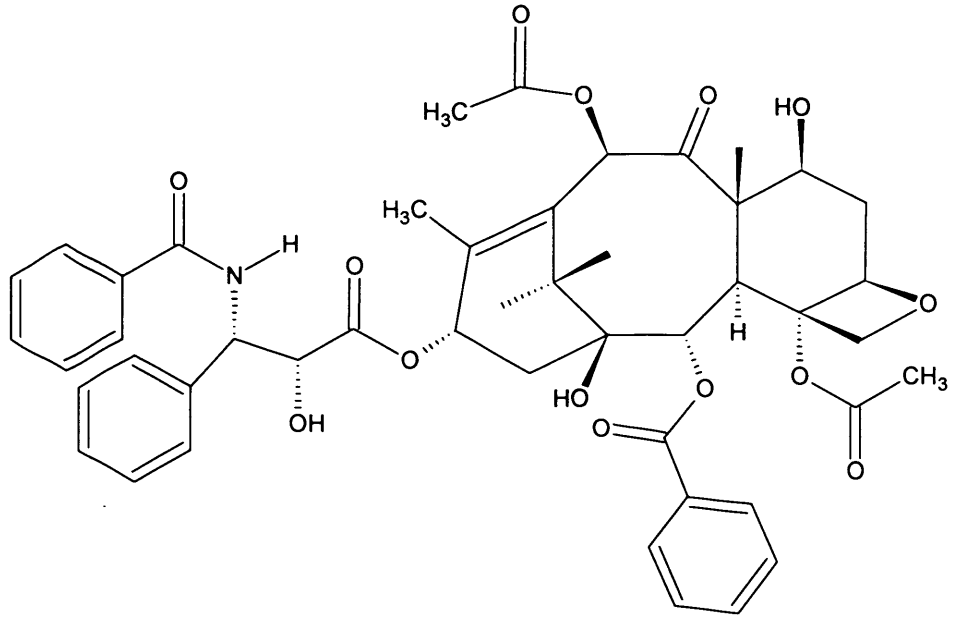

Figure 1.7 – Structure of paclitaxel.

1.2.6 Other chemotherapeutic treatments

There are two other categories of chemotherapeutic agents, antimetabolites and drugs affecting the endocrine function.

- Antimetabolites are usually cell cycle dependent and interfere with the production of nucleic acids resulting in the decrease of RNA and DNA synthesis, cell growth and proliferation. For example, methotrexate prevents the formation of tetrahydrofolate essential for purine and pyrimidine synthesis.

- Drugs affecting the endocrine function modify the growth of tumours by affecting steroid hormones or their antagonists. They can be separated into two groups, the antagonists (competitive antagonists) of estrogen receptors (used in treatment of breast cancer) inhibit the progression of the cell cycle between G1 and S phase and resulting in cell death. The second group is the glucocorticoids inhibiting protein synthesis, they attach to corticosteroid-binding proteins leading to apoptosis.

Finally, chemotherapeutic drugs can also be used as combination of two or more drugs in order to achieve a greater effect than either drug alone (e.g. synergistic or additive effect) and avoid drug resistance. However, each individual drug must have some anti-tumour activity. Moreover, each drug must also act by different mechanism to the other and have a different dose limiting toxicity when compared to its combination drug. In addition, for combination treatments, several cycles of treatment are usually given.

1.3 DNA damage and repair mechanisms

It has been previously established that tumours arise from genetic and molecular changes caused by DNA damage or mistakes of the DNA replication mechanism. The different type of damage can be classified in three main categories of DNA damage (Hoeijmakers, 2001a). The first is caused by environmental agents, such as ultraviolet (UV), ionizing radiation (IR) and genotoxic chemicals (e.g. cigarette smoke). Secondly, DNA damage can be caused by byproducts of normal cellular metabolism, such as reactive oxygen species and products of lipid peroxidation. Finally, DNA damage can be caused due to the intrinsic instability of chemical bonds in DNA, spontaneous hydrolysis will lead to disintegration of chemical bonds in DNA and chemical changes in DNA bases.

Therefore, these DNA lesions can result in different adverse effects summarised in Figure 1.8. Indeed, Although DNA lesions usually trigger cell cycle arrest, through specific cell cycle checkpoint, in order to allow DNA damage repair (the different repair pathways are detailed hereafter), improper repair of the lesions may occur, due to the large extent of the damage. This will cause permanent mutations and oncogenesis (Zhou and Elledge, 2000). In addition, if the extent of the damage is too large, cells usually trigger apoptosis. Furthermore, damage affecting both DNA strands such as double strand breaks may result in improper chromosome segregation and apoptosis. In addition, those double strand breaks can lead to chromosomes aberrations, such as deletions, leading to oncogenesis. Nevertheless, permanent changes of the DNA sequence and oncogenesis may also result from point mutations induced by lesions interfering with DNA replication.

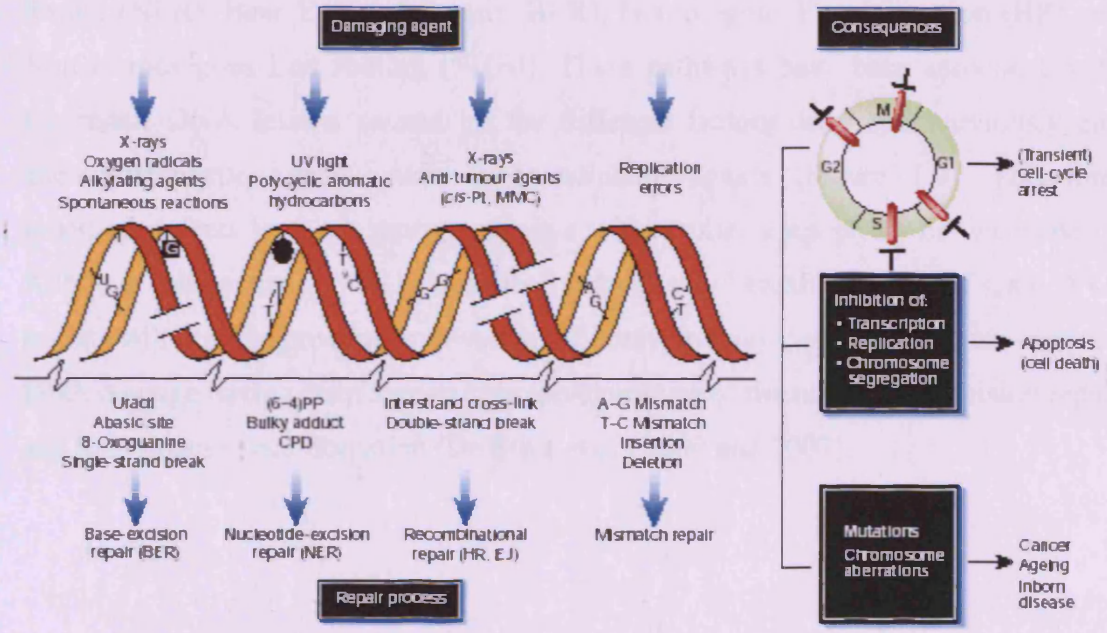

Figure 1.8 – DNA damage and repair mechanisms. Different DNA damage will trigger different mechanisms within the cell according to the type of damage and the extent: DNA damage repair, cell death or development of a tumour (oncogenesis). Figure obtained from Hoeijmakers J.H., Nature, 2001a, 411: 366-374.

1.4 Cellular response to DNA damage

Figure 1.8 describes the organisation of the DNA damage response: repair, cell arrest, apoptosis and angiogenesis. In the following sections, the DNA repair pathways, cell cycle arrest and cell death are discussed.

1.4.1 DNA repair pathways

Hoeijmakers (2001b) described four main DNA repair pathways: Nucleotide Excision Repair (NER), Base Excision Repair (BER), Homologous Recombination (HR) and Non Homologous End Joining (NHEJ). These pathways have been associated with the repair DNA lesions caused by the different factors described previously and chemotherapeutic agents, such as crosslinking agents (Figure 1.9). Therefore, inherited defects in these repair pathways will results in apoptosis or oncogenesis. Although each pathway will be described individually hereafter, repair of some DNA lesions will involve proteins involved in different pathways, such as cisplatin-induced DNA damage having been shown to involve proteins of the nucleotide excision repair and homologous recombination (De Silva *et al.*, 2000 and 2002).

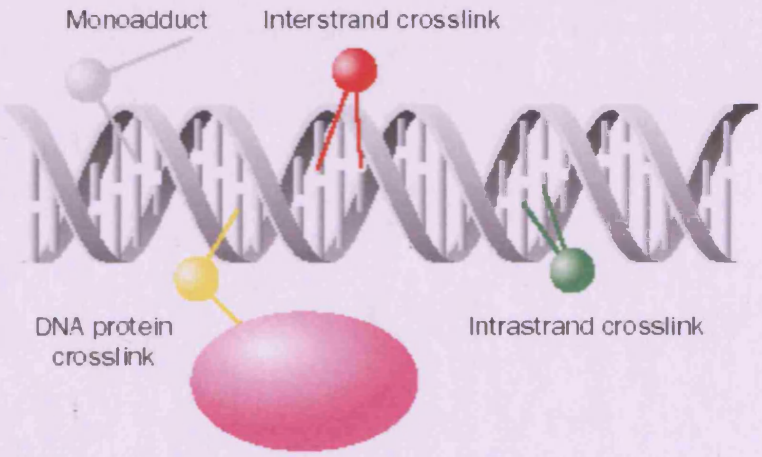

Figure 1.9 – Interaction of crosslinking drugs with DNA. McHugh P.J. *et al.*, The Lancet, 2001, 2: 483-490.

Nucleotide Excision Repair (NER)

NER pathway is mainly responsible for correcting lesions that arise spontaneously. It corrects inappropriate base pairing (mismatch and damaged bases), lesions causing transcription and replication inhibition, such as bulky adducts and helix-distorting DNA adducts (McHugh *et al.*, 2001). This repair pathway is divided into two sub-pathways (Figure 1.10): global genome NER (survey the entire genome of distorting injury) and transcription-coupled repair for damage that block elongating RNA polymerases (Hoeijmakers, 2001a; de Laat *et al.*, 1999). Although the recognition steps (I and II) of the damage is different for the two sub-pathways, subsequent steps are identical (III to V). Studies have shown that up to 25 proteins, including TFIIH, XPA and RPA, are necessary for the completion of the NER process involving lesion recognition, excision of 24-32 nucleotides strand containing the lesion and repair through normal replication mechanism (de Laat *et al.*, 1999; Lindahl and Wood, 1999). Finally, after repair the protein complex is disassembled. Defects in this repair pathway have shown to cause other symptoms beyond NER defect, revealing that proteins of the NER pathway have additional purposes, such as transcriptional functions (Hoeijmakers, 2001b; de Laat *et al.*, 1999).

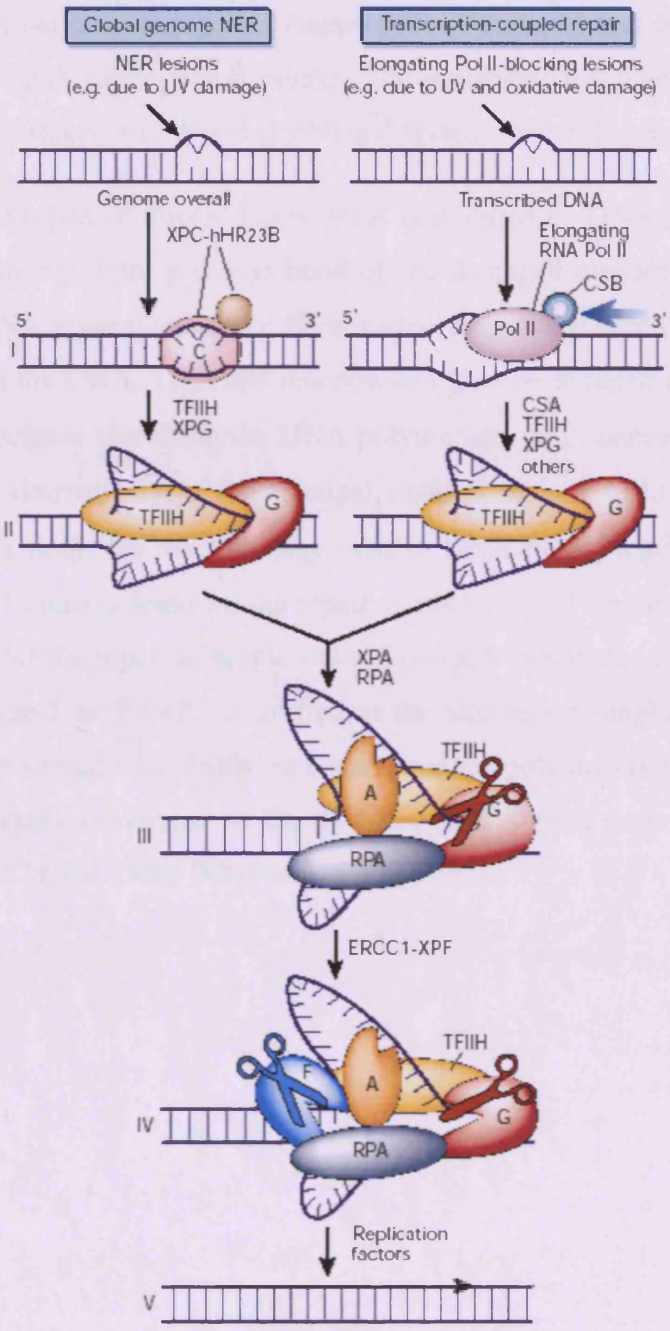

Figure 1.10 – Nucleotide Excision Repair (NER) pathway. This figure describes important proteins involved in the two sub-pathways of the NER pathway: global genome NER (GG-NER) and transcription-coupled repair (TCR). Hoeijmakers J.H., Nature, 2001a, 411: 366-374.

Base Excision Repair (BER)

BER pathway is mainly involved in the repair of damage caused by cellular metabolism. This pathway recognises inappropriate bases (mismatched or damaged), sites of base loss and single strand breaks. The molecular mechanism for BER has been reported by Lindahl and Wood (1999) and is described in Figure 1.11.

In the case of the repair of altered bases, BER is initiated by DNA glycosylases that cleave the base-deoxyribose glycosyl bond of the damaged nucleotide residue. It is noted that the DNA glycosylase are different according to the type of altered base to be removed from the DNA. The BER reaction will then be initiated at the abasic site, by APE1 endonuclease recruiting the DNA polymerase, polβ, necessary for the gap-filling reaction. Alternatively, if the terminal sugar-phosphate residue is resistant to cleavage of DNA polβ, the reaction may involve DNA polδ/ε together with PCNA protein and FEN1 endonuclease for the repair synthesis of 2-10 bases. When the BER pathway is used for the repair of single strand breaks, it is initiated by the poly(ADP-ribose) polymerase-1 or PARP1, recruited at the site of the single strand break to protect it from unwanted recombination events, and the polynucleotide kinase (PNK). The following events are similar to the one described for the removal of an altered base (Lindahl and Wood 1999; Whitehouse *et al.*, 2001).

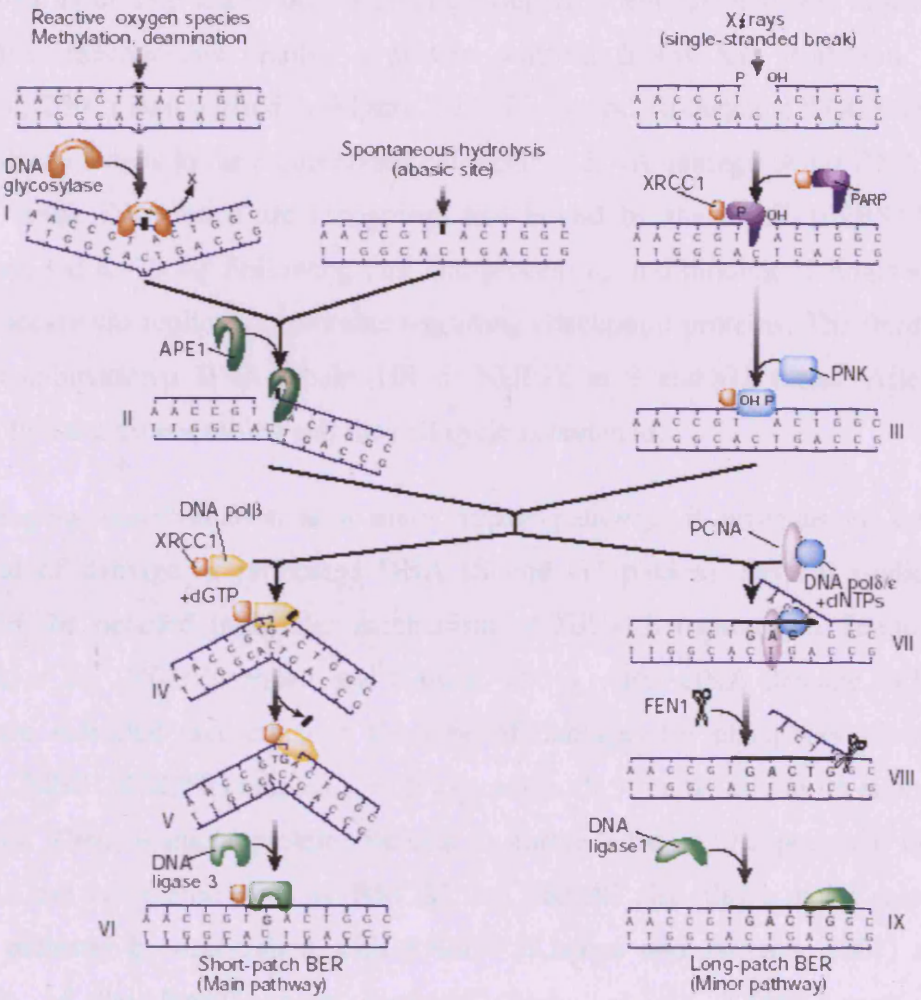

Figure 1.11 – Base Excision Repair (BER) pathway. Hoeijmakers J.H., Nature, 2001a, 411: 366-374.

Homologous recombination (HR) and non homologous end joining (NHEJ)

These two mechanisms are used during the replication of single strand break and in the repair of double strand breaks arising from IR, chemicals and free radicals. The molecular mechanisms involve a protein scaffold (Lisby and Rothstein, 2004b; Jackson, 2002) summarised in Figure 1.12. Lisby and Rothstein (2004a) described four different steps in the recombinational repair of DNA damage. After DNA double strand break DNA ends are recognised and bound by the MRE11/NBS1/RAD50 complex and Ku70/80. Following this, end-processing and binding of single stranded DNA occurs *via* replication proteins recruiting checkpoint proteins. The third step is the recombinational DNA repair (HR or NHEJ), at S and G2 phase. After DNA repair, foci are disassembled and the cell cycle is resumed.

Homologous recombination is a major repair pathway, it provides an error-free removal of damage of replicated DNA (S and G2 phases). Several studies have reported the detailed molecular mechanism of HR (Thompson and Schild, 2001; Pastink *et al.*, 2001; Dronkert and Kanaar, 2001). After DNA damage, ATM and ATR are recruited (according to the type of damage) for phosphorylation of the MRE11/NBS1/RAD50 complex which exposes both 3' ends (due to its exonuclease activity). Then, a nucleoprotein filament is formed due to the presence of RPA, RAD51 and the related proteins. BRCA1 and BRCA2 also play a major role in this repair pathway by associating with RAD51 (Khanna and Jackson, 2001) and the proteins of the BASC super complex (Wang *et al.*, 2000b), such as the MRE11/NBS1/RAD50 complex. This leads to the subsequent exchange of strands with the identical sister chromatid (homologous sequence). Finally, Holliday junctions are resolved by resolvases (Khanna and Jackson, 2001).

Figure 1.12 also describes the non homologous end-joining repair pathway (NHEJ repair or V(D)J recombination), mainly present in the G1 phase (only one copy of the gene present). This repair pathway is more error prone since a few nucleotides are lost (end joining without any template). End-joining is activated by ATM and DNA-PK_{cs} proteins. DNA-PK_{cs} consists of a heterodimeric DNA (signaling function) targeting Ku70/80 complex (ends protection and approximation). Furthermore, Khanna and Jackson (2001) reported that MRE11/NBS1/RAD50 complex was also

involved in the NHEJ repair, suggesting a role for BRCA1. Finally, both ends are ligated by XRCC4-ligaseIV (Hoeijmakers, 2001a; Pastwa and Blasiak, 2003). Therefore, DNA double strand breaks repair is an important repair pathway and is more difficult than the other type of DNA damage and erroneous rejoining may lead to oncogenesis.

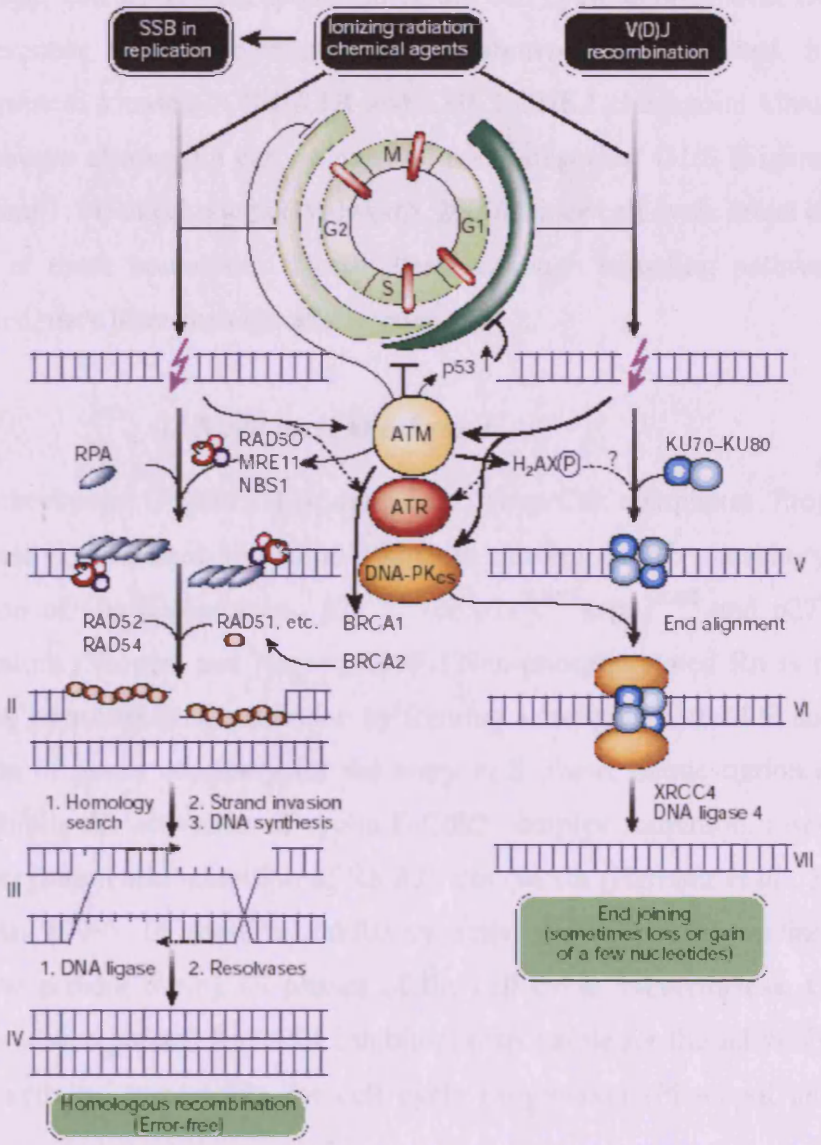

Figure 1.12 – Homologous Recombination (HR) and Non Homologous End Joining (NHEJ or V(D)J recombination) molecular mechanism. Hoeijmakers J.H., Nature, 2001a, 411: 366-374.

1.4.2 Cell cycle alterations in cancer

Cell cycle checkpoints are key transitions during the cell cycle progression. Checkpoints are present at different stages in the cell cycle, in order to arrest the cells, to repair DNA damage, dissipate an exogenous cellular stress signal or to wait for available growth factors, hormones or nutrients (Pietenpol and Stewart, 2002). Therefore, cell cycle checkpoints contribute to genomic stability. Thus, in response to DNA damage, cell cycle checkpoints integrate cell cycle control with DNA repair. Cellular response to DNA damage has been shown to be mediated through two groups of protein kinases, ATM/ATR and CHK1/CHK2 checkpoint kinases groups, and downstream checkpoint can be put into two categories: G1/S (Figure 1.13) and G2/M (Figure 1.14) checkpoints (Walworth, 2000), since cell cycle arrest occurs most frequently at these boundaries. Nonetheless, although signaling pathways can be distinguished, they have considerable overlap.

G1/S cell cycle checkpoint

The G1/S checkpoint (Figure 1.13) is ruled by cyclin/Cdk complexes. Progression of the cell cycle is facilitated by cyclin D kinases causing the Rb phosphorylation and sequestration of Cip/Kip proteins, $p21^{Cip1}$ (or $p21^{WAF1}$), $p57^{Kip2}$ and $p27^{Kip1}$, called Cdks inhibitors (Shapiro and Harper, 1999). Non-phosphorylated Rb is responsible for relieving transcriptional repression by forming a complex with E2F, and allowing transcription of genes necessary for the entry in S phase. Sequestration of Cip/Kip proteins inhibits the activation of cyclin E-Cdk2 complex formation, responsible for Rb phosphorylation and inhibition of Rb-E2F complexes (Harbour *et al.*, 1999; Sherr and Roberts, 1999). In addition, inhibitory activity of Cip/Kip proteins has been shown to be present during all phases of the cell cycle. Nevertheless, G1/S phase transition is also regulated by INK4 inhibitors responsible for the inhibition of Cdk4 and Cdk6 activity, responsible for cell cycle progression (Pietenpol and Stewart, 2002).

Therefore, exposure to DNA damaging agents will cause induction of INK4 inhibitors and Cip/Kip proteins are activated causing inhibition of cyclin D and Cdk4 and 6 and formation of cyclin E-Cdk2 complexes, leading to Rb phosphorylation and cell cycle

arrest. It is also noted that $p21^{WAF1}$ activation is p53-dependent, nonetheless, Liu *et al.* (1996) reported that it could be activated through the MAPK signaling pathway.

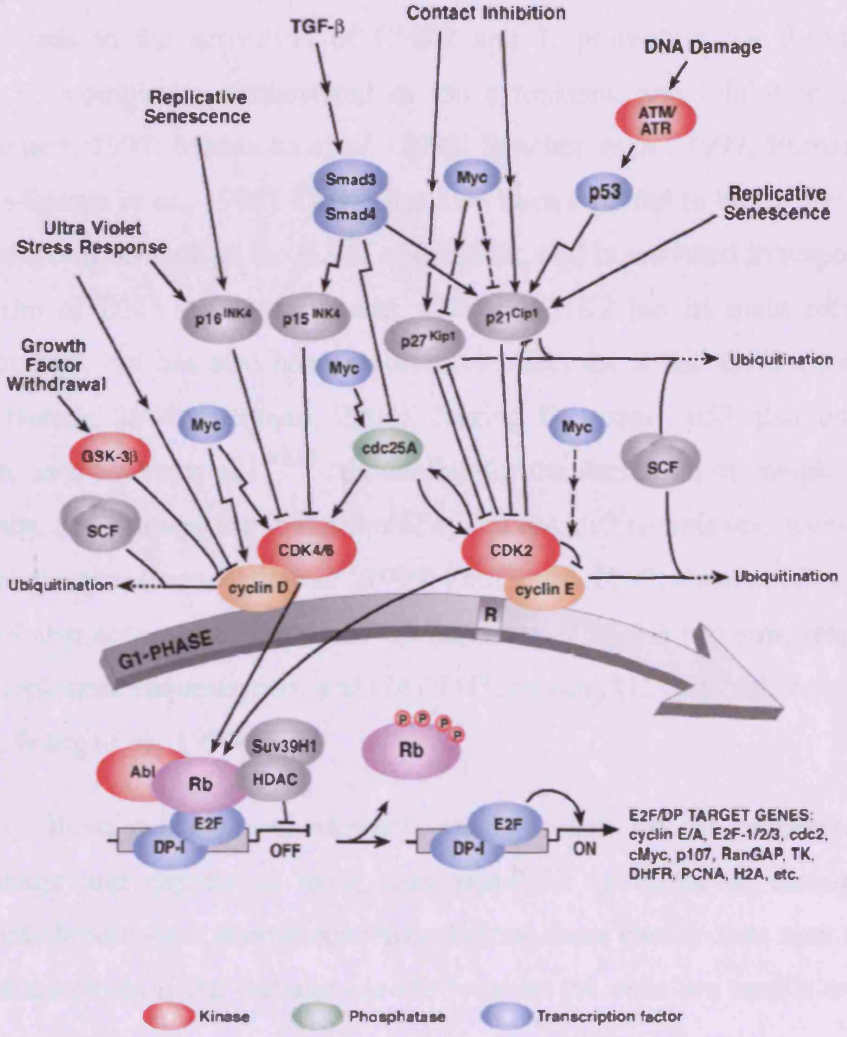

Figure 1.13 – G1/S cell cycle checkpoint and signalling pathway (www.cellsignal.com).

G2 cell cycle checkpoint

The G2 cell cycle arrest (Figure 1.14) is regulated through the inhibition of Cdc2 activation. Cdc2 is negatively regulated by its phosphorylation, preventing the formation of cyclin B-Cdc2 complexes and entry into mitosis (Pietenpol and Stewart, 2002; Walworth, 2000). DNA damage maintains the phosphorylated state of Cdc2, through the activation of the members of PI3K family, including DNA-PK, ATM and ATR. This leads to the activation of CHK2 and 1, promoting the formation of Cdc25C-14-3-3 complexes, sequestered in the cytoplasm, and inhibition of Cdc2 activity (Weinert, 1997; Matsuoka *et al.*, 1998; Sanchez *et al.*, 1997; Furnari *et al.*, 1997; Lopez-Girona *et al.*, 1999). CHK1 has also been reported to be involved in the S phase checkpoint, as well as the G2/M checkpoint, and is activated in response to a large spectrum of DNA damaging agents whereas CHK2 has its main role in IR-induced apoptosis, but has also been reported to affect the S and G1/S checkpoints (Zhou and Bartek, 2004; Eastman, 2004). During G2 arrest, p53 also undergoes modification, as it activates $p21^{WAF1}$ responsible for the formation of complexes with cyclin B. Thus, p53 reduces the formation of cyclin B-Cdc2 complexes, necessary for cell cycle progression (Innocente *et al.*, 1999; Flatt *et al.*, 2000; Chan *et al.*, 1999). In addition, p53 also acts as transcriptional up-regulator of 14-3-3 proteins, responsible for Cdc2 cytoplasmic sequestration, and GADD45, causing G2 cell cycle arrest (Chan *et al.*, 1999; Wang *et al.*, 1999a).

Consequently, those cell cycle checkpoints are important for the proper repair of cellular damage and defects in those may result in oncogenesis, through gene mutations and chromosome aberrations. Nonetheless, these checkpoints may result in activation of apoptosis if the damage are too large or the cells are unable to trigger DNA damage repair.

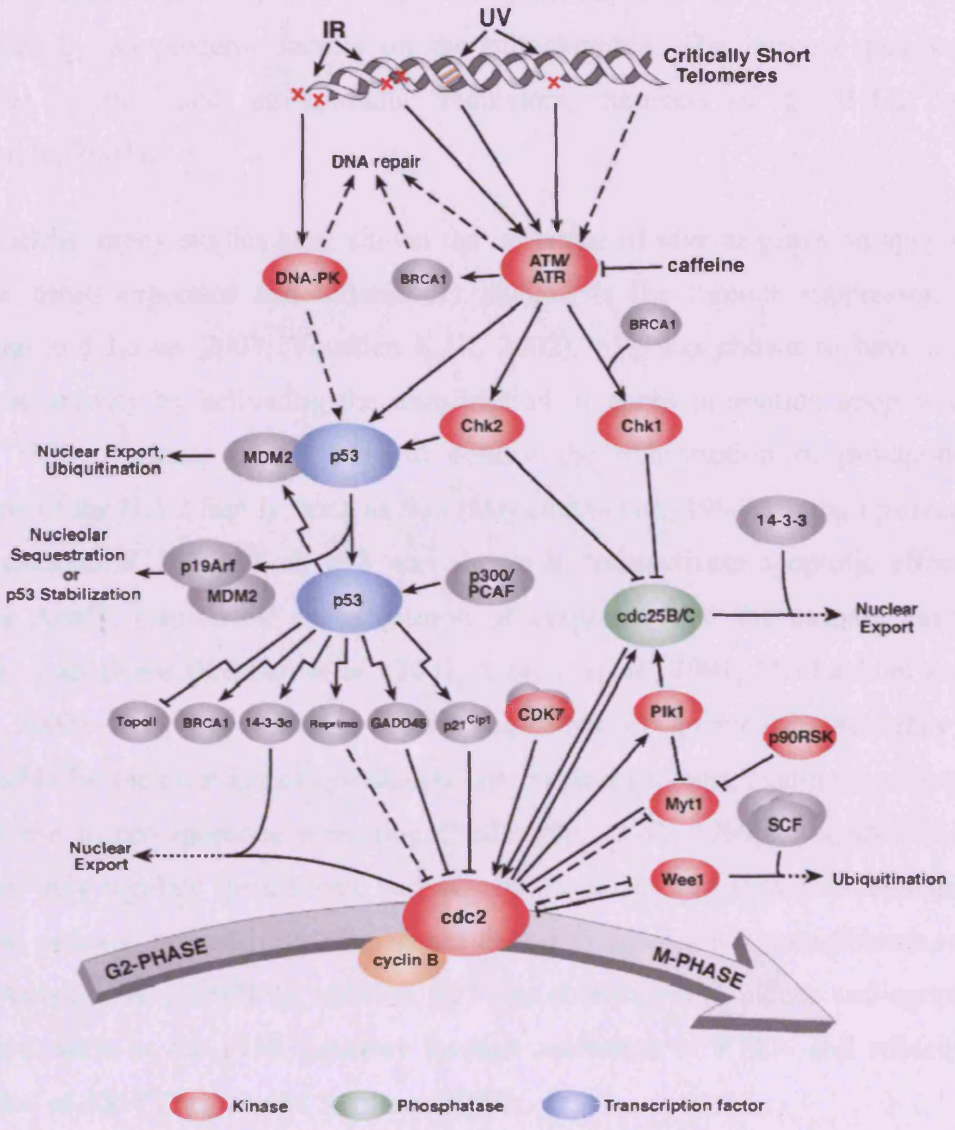

Figure 1.14 – G2/M cell cycle checkpoint and signalling pathway (www.cellsignal.com)

1.4.3 p53 and apoptosis

Apoptosis or cell death (Figure 1.15) is a gene-directed program (Lowe and Lin, 2000) leading to cell shrinkage, membrane blebbing and DNA fragmentation. Apoptosis can be divided into two pathways, the extrinsic, regulated by cell surface receptors, their inhibitors and associated proteins, and the intrinsic pathway, controlled by apoptogenic factors on the mitochondria. The intrinsic pathway is regulated by pro- and anti-apoptotic regulators, members of the Bcl-2 family (Tsujimoto, 2003).

Nevertheless, many studies have shown the influence of several genes on apoptosis, but the most important and extensively studied is the tumour suppressor, p53 (Fridman and Lowe, 2003; Vousden K.H., 2002). p53 was shown to have a pro-apoptotic activity by activating the transcription of genes promoting apoptosis (El Deiry, 1998). Indeed, p53 is able to control the transcription of pro-apoptotic members of the Bcl-2 family, such as Bax (Miyashita *et al.*, 1994), acting upstream of the mitochondria. In addition, p53 was shown to transactivate apoptotic effectors, such as Apaf1, responsible for activation of caspase 9 and the caspase cascade, leading to apoptosis (Kannan *et al.*, 2001; Moroni *et al.*, 2001; MacLachlan and El Deiry, 2002). Caspases are the central regulators of apoptosis since they are responsible for the cleavage of cytoskeletal and nuclear proteins, leading to apoptosis, in response to pro-apoptotic activation (Budihardjo *et al.*, 1999). Nonetheless, p53 does not only regulate the intrinsic pathway but has also been shown to regulate the extrinsic pathway and activate other genes linked to apoptosis (Owen-Schaub *et al.*, 1995; Attardi *et al.*, 2000). In addition, p53 was also shown to induce anti-apoptotic pathways, such as the PI3K pathway through activation of PTEN and subsequent activation of Akt (Vivanco and Sawyers, 2002).

Therefore, p53 is an important player of the apoptosis and mutations or loss-of-function mutations in p53 will be critical as they have been shown to modulate apoptosis and drug resistance (Fulda *et al.*, 1998; Petak *et al.*, 2000). Nonetheless, apoptosis is not the only form of programmed cell death, as senescence is a non-apoptotic cell death. It is described as being an irreversible program of cell cycle arrest (Lowe and Lin, 2000), with p53 being an important factor (Wynford-Thomas, 1999).

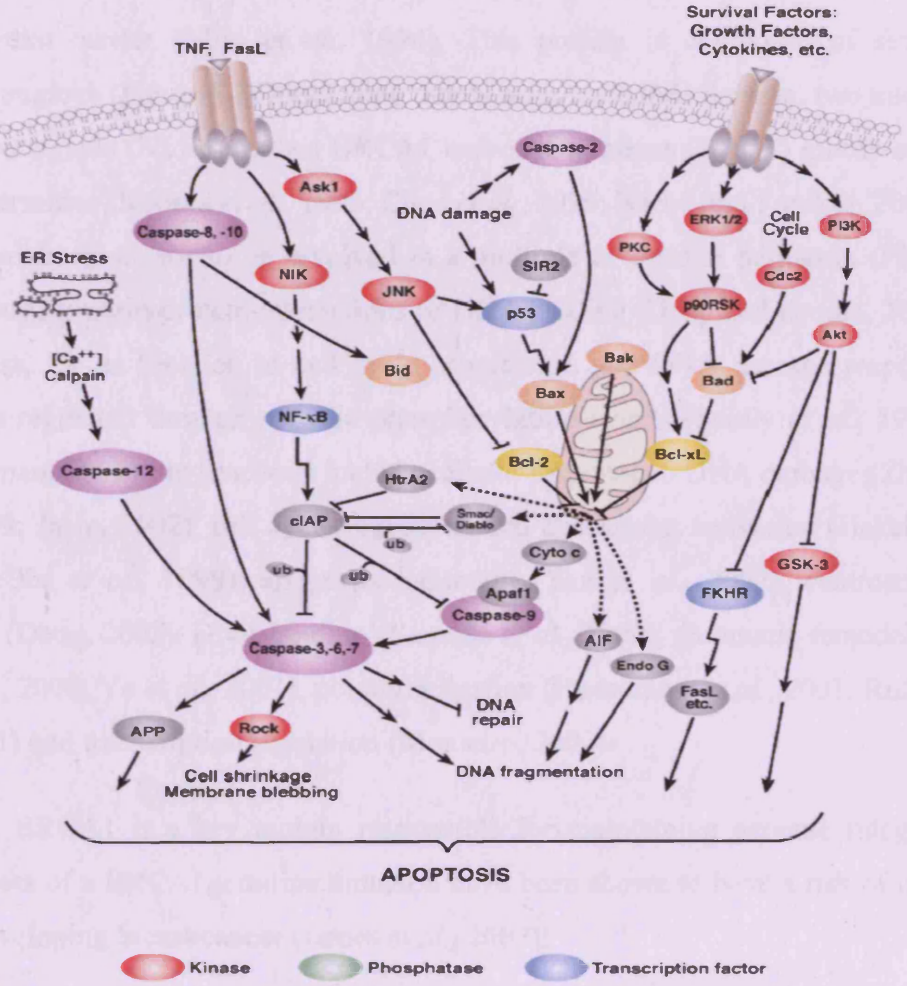

Figure 1.15 – Apoptosis signalling pathway (www.cellsignal.com).

1.5 BReast-CAncer susceptibility gene 1 (BRCA1)

BRCA1 is the BReast-CAncer susceptibility gene 1 encoding for a multifunctional phosphoprotein (Figure 1.16) and is mainly found in the nucleus and mitochondria (Coene *et al.*, 2005). BRCA1 is a tumour suppressor which plays an important role in nuclear DNA maintenance, and its mutations have been associated with the increased risk of breast cancer (Miki *et al.*, 1994). This protein is composed of several functional regions (Figure 1.16) including one N-terminal RING domain, two nuclear localization signals (NLS) and two BRCA1 carboxyl terminus (BRCT) motifs at the carboxyl terminus (Koonin *et al.*, 1996; Chen *et al.*, 1996; Narod and Foulkes, 2004). BRCA1 has been shown to be involved in a multiple of cellular pathways (Figure 1.17), through protein-protein interactions or DNA binding (Deng and Brodie, 2000). Nonetheless, for its function in cell cycle progression and DNA damage response, BRCA1 is regulated through specific phosphorylation events (Scully *et al.*, 1997a; Venkitaraman, 2002). Its functions include cellular response to DNA damage (Zhong *et al.*, 1999; Jasin, 2002), cell cycle regulation and checkpoint activation (Hakem *et al.*, 1997; Xu *et al.*, 1999), apoptosis induction (Yan *et al.*, 2002), centrosomes regulation (Deng, 2002), DNA binding (Yamane *et al.*, 2000), chromatin remodelling (Lou *et al.*, 2005; Ye *et al.*, 2001), ubiquitin ligation (Hashizume *et al.*, 2001; Ruffner *et al.*, 2001) and transcription regulation (Monteiro, 2000).

Therefore, BRCA1 is a key protein responsible for maintaining genome integrity, since carriers of a BRCA1germline mutation have been shown to have a risk of up to 85% of developing breast cancer (James *et al.*, 2007).

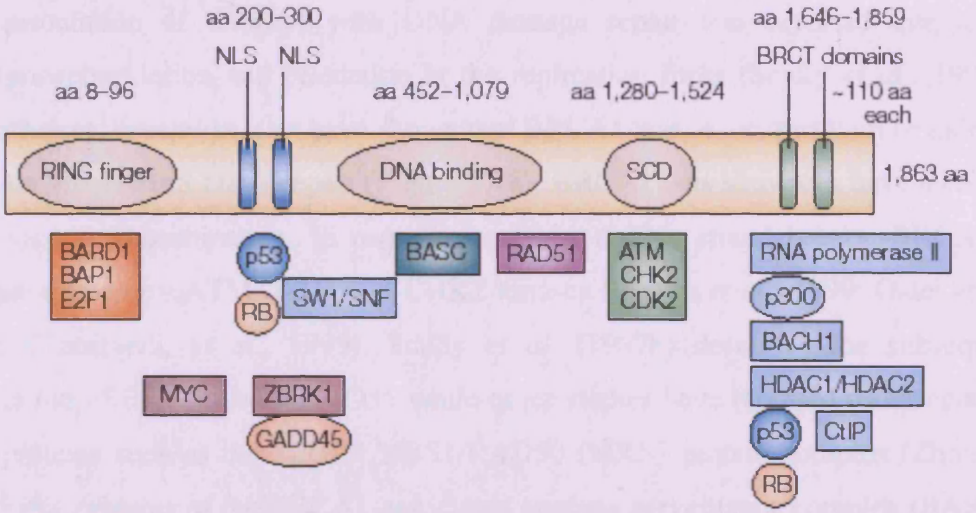

Figure 1.16 – BRCA1 structure (1863 amino acids). BRCA1 encodes a large number of proteins involved in DNA repair and cell cycle control. Narod S.A. and Foulkes W.D., Nature Reviews, 2004, 4: 665-676.

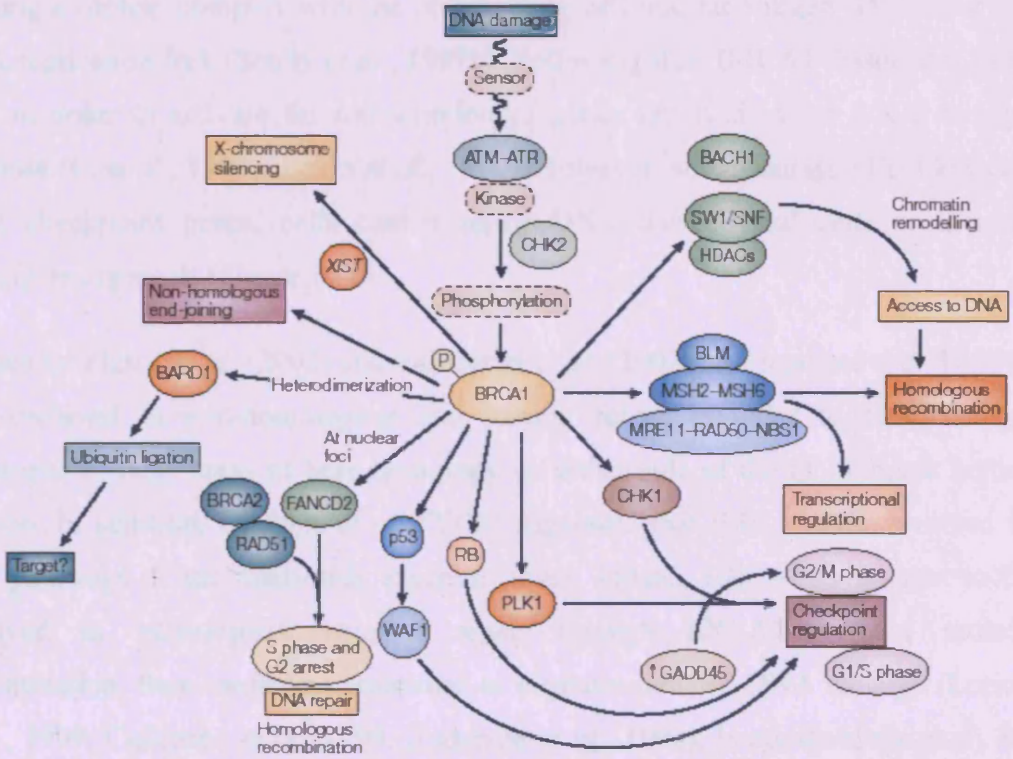

Figure 1.17 – BRCA1 network. BRCA1 interacts with molecules involved in different signalling pathways. Narod S.A. and Foulkes W.D., Nature Reviews, 2004, 4: 665-676.

1.5.1 BRCA1 and DNA damage repair

The association of BRCA1 with DNA damage repair was reported due to its hyperphosphorylation and relocation at the replication forks (Scully *et al.*, 1997a). Nevertheless, several studies have shown that BRCA1 was associated with or induced proteins involved in DNA repair (Figure 1.18). BRCA1 was shown to have a role in homologous recombination. In response to DNA double strand breaks, BRCA1 is phosphorylated by ATM, ATR and CHK2 kinases (Cortez *et al.*, 1999; Gatei *et al.*, 2001; Chaturvedi, *et al.*, 1999). Scully *et al.* (1997b) described the subsequent association of BRCA1 with RAD51 while other studies have reported its association with proteins such as the MRE11/NBS1/RAD50 (MRN) protein complex (Zhong *et al.*, 1999), proteins of the BRCA1-associated genome surveillance complex (BASC – Wang *et al.*, 2000b). By its association with the BASC super complex, BRCA1 will influence the type of repair used according to the type of DNA damage. Nonetheless, BRCA1 has a specific role in the homologous recombination by its association with the MRN protein complex, thus exposing the 3' ends on either side of the break (Hoeijmakers, 2001a). Subsequently, BRCA1 associates with BRCA2 and RAD51 forming a protein complex with the proliferating cell nuclear antigen (PCNA) at the DNA replication fork (Scully *et al.*, 1997b). Following this, BRCA1 dissociates from CtIP in order to activate the transcription of genes involved in the DNA damage response (Li *et al.*, 1999; Harkin *et al.*, 1999). However, when damage affect key cell cycle checkpoint genes, cells cannot repair DNA damage and cells proliferate, causing oncogenesis (Figure 1.18).

Studies by Zhong *et al.* (2002) and Baldeyron *et al.* (2002) also reported that BRCA1 was involved in non-homologous end joining repair in order to facilitate the alignment of short areas of base homology on either side of the DNA break before ligation. In addition, Le Page *et al.* (2000) suggested that BRCA1 was involved in both pathways of the nucleotide excision repair. Indeed, BRCA1 is thought to be involved in transcription coupled repair through BRCA1-mediated protein ubiquitination, thus conferring resistance to cisplatin-induced DNA damage (Lorick *et al.*, 1999; Cullinane *et al.*, 1999; Anderson *et al.*, 1998). In addition, the study by Hartman and Ford (2002) demonstrated that BRCA1 deficient cells were deficient in global genomic repair, suggesting its involvement in this repair pathway. Therefore, BRCA1 interacts with key proteins involved in DNA damage repair and its mutation

or loss of function will result reduction of DNA repair efficiency and increased toxicity or oncogenesis.

Moreover, BRCA1 has been reported to be associated with the Fanconi Anemia (FA – autosomal recessive disease) core complex through the formation of a complex with FANCA protein involved in the recognition of the DNA replication fork after chemotherapy and activation of the FANCAD2 protein (Folias *et al.*, 2002; Pichierri *et al.*, 2004). In addition, monoubiquitinated FANCD2 has been shown to co-localise with BRCA1 after DNA damage (Garcia-Higuera *et al.*, 2001). BRCA1 has also been shown to be associated with FANCAD1, which has been identified as BRCA2 and those two proteins have been shown to be involved in drug-induced DNA double strand breaks repair through homologous recombination (Howlett *et al.*, 2002; Tutt *et al.*, 2001). Taniguchi *et al.* (2003) also reported that reduction of Fanconi Anemia protein F led to an increase in cisplatin sensitivity and demonstrating that association of BRCA1 with FA proteins was important for the repair of drug-induced DNA damage. Furthermore, Yamamoto *et al.* (2005) and Nakanishi *et al.* (2005) reported that deficiency in some FA genes led to a defect in homologous recombination. Therefore, interaction of BRCA1 with Fanconi Anemia proteins needs to be considered when studying BRCA1 DNA repair machinery.

Hence, it is clear that BRCA1 plays a major role in DNA repair and that its mutation will have important implication on tumour development and response to drug-induced DNA damage.

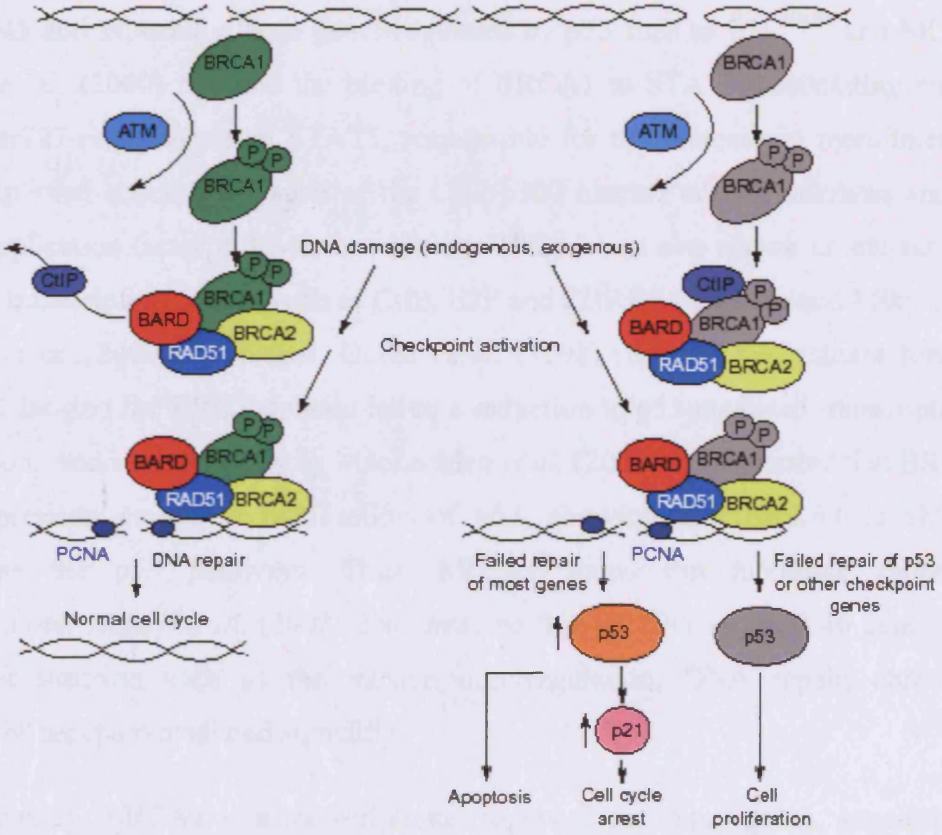

Figure 1.18 – BRCA1 and DNA double strand break repair. BRCA1 associates with proteins involved in repair of double strand break. Welcsh P.L. *et al.*, Trends in Genetics, 2000, 12(2): 69-74.

1.5.2 BRCA1 as transcriptional regulator

Several studies reported the transcriptional activity of BRCA1, such as its transcriptional function in response to ionizing radiation (Figure 1.19). Scully *et al.* (1997c) reported that C-terminus of BRCA1 interacts with RNA polymerase II through RNA helicase A, demonstrating the interaction BRCA1 with the basal transcriptional machinery. Studies by Somasundaram *et al.* (1997) and Ouchi *et al.* (1998) also reported that BRCA1 induced the transcription of the promoter of GADD45 and especially those genes regulated by p53 such as $p21^{WAF1}$ and MDM2. Ouchi *et al.* (2000) reported the binding of BRCA1 to STAT1, associating mainly with Ser727-phosphorylated STAT1, responsible for the increase in recruitment of transcriptional coactivators such as the CBP/p300 histone acetyltranferases and the DNA replication factor, MCM5. In addition, BRCA1 was also shown to interact with several transcription factors such as CtIP, E2F and ZBRK1 (Yoshida and Miki, 2004; Zheng *et al.*, 2000). Moreover, Ouchi *et al.* (1998) reported that mutant form of BRCA1 lacking the BRCT domain led to a reduction in p53-mediated transcriptional activation. And a recent study by MacLachlan *et al.* (2002) demonstrated that BRCA1 overexpression caused a stabilisation of p53, showing that BRCA1 is able to stimulate the p53 pathways. Thus, BRCA1 status can modulate apoptosis. Furthermore, Atalay *et al.* (2002) demonstrated that BRCA1 induced 46 genes with different function such as the transcription regulation, DNA repair, chromatin assembly, receptor-mediated signaling.

Consequently, BRCA1 is a transcriptional regulator for many genes, suggesting a bridging role for BRCA1 between DNA damage and stress response, leading to cell cycle arrest and apoptosis.

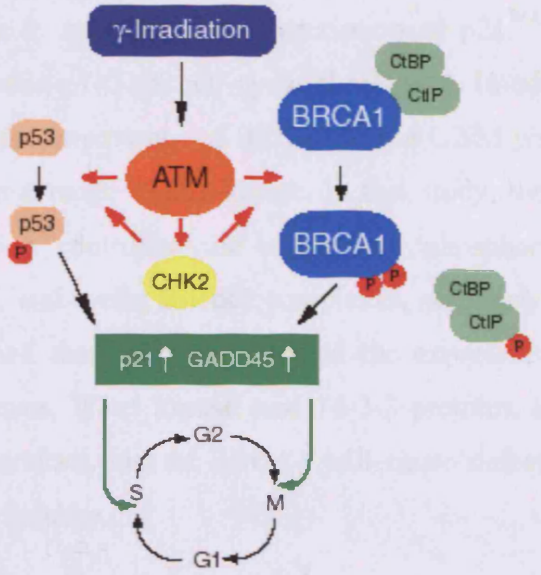

Figure 1.19 – Transcription and BRCA1. Example of BRCA1 transcriptional function in response to ionising radiation. Yoshida K. and Miki Y., Cancer science, 2004, 95(11): 866-871.

1.5.3 BRCA1 and cell cycle regulation

As described previously, after DNA damage, cells rely on the cell cycle checkpoints to stop their progression before DNA repair. Many studies have reported the implication of BRCA1 in the regulation of cell cycle checkpoints. Indeed, Quinn *et al.* (2003) demonstrated that BRCA1 was essential for G2/M cell cycle checkpoint, as they reported that cells deficient in BRCA1 were defective in this checkpoint, following exposure to spindle poisons and DNA damaging agents. Nonetheless, transfection of BRCA1 wild type gene restored the function of this checkpoint.

The role of BRCA1 as a regulator of cell cycle checkpoints has been shown to be due to its phosphorylation by ATM, ATR and the cell cycle checkpoint kinase 2 (CHK2). Indeed, Cortez *et al.* (1999) reported that ATM, activated by ionizing radiation-induced DNA double strand breaks, caused the phosphorylation of BRCA1 in response to DNA damage, necessary for efficient G2/M and intra-S phase checkpoints (Xu *et al.*, 2001 and 2002). In addition, ATR, activated by stalled DNA replication forks, and CHK2 were also shown to cause BRCA1 phosphorylation, upon DNA damage, necessary for cell cycle checkpoints activation (Lee *et al.*, 2000a; Tibbetts *et al.*, 2000).

Furthermore, Williamson *et al.* (2002) and Somasundaram *et al.* (1997) demonstrated that BRCA1 was able to stimulate the transcription of $p21^{WAF1}$ and $p27^{Kip1}$, both involved in the regulation of G1/S cell cycle checkpoint. In addition, Yarden *et al.* (2002) also described the importance of BRCA1 in the G2/M phase checkpoint since BRCA1 was shown to activate CHK1 kinase. In this study, they also demonstrated that BRCA1 expression controlled the expression, phosphorylation and cellular localisation of Cdc25C and cyclin B-Cdc2 complexes, necessary for G2/M transition. Finally, they established that BRCA1 regulated the expression of the inhibitor of cyclin B-Cdc2 complexes, Wee1 kinase, and 14-3-3 proteins, key regulators of the G2/M checkpoint. Therefore, loss of BRCA1 will cause defective checkpoints and accumulation of DNA damage.

1.5.4 BRCA1 and topoisomerase II

So far, BRCA1 has been shown to be a key player in the maintenance of genome integrity, through its participation in the response to DNA damage and the regulation of cell cycle checkpoints. Furthermore, BRCA1 has recently been shown to maintain genomic stability through its interaction and colocalisation with topoisomerase IIα in the S phase. Indeed, Lou *et al.* (2005) established that BRCA1 played a direct role in DNA decatenation and that deficiency in BRCA1 resulted in chromosome aberrations. In addition, it is suggested that BRCA1 participate in a decatenation checkpoint in order to maintain chromosome integrity (Deming *et al.*, 2001). Thus, this new function of BRCA1 provides a better understanding of the importance of BRCA1 for genomic stability.

1.5.5 BRCA1 and cancer therapy

Response to chemotherapy

Studies investigating the role of BRCA1 in response to chemotherapeutic treatment have established that BRCA1 is a modulator of DNA damage response. Indeed, Bhattacharyya *et al.* (2000) and Quinn *et al.* (2003) demonstrated BRCA1 caused an increased resistance to alkylating agents such as cisplatin and mitomycin C. Furthermore, they showed that BRCA1 deficient cells were more sensitive to crosslinking agents. Fedier *et al.* (2003) also established that BRCA1 conferred resistance to topoisomerase I and II poisons, such as topotecan and etoposide, but did

not alter the sensitivity to spindle poisons. Conversely, Tassone *et al.* (2003) reported that BRCA1 mutation caused an increase resistance to doxorubicin, acting similarly to etoposide. Thus more understanding on the effect of BRCA1 on doxorubicin-induced DNA damage is required. In addition, Tassone *et al.* (2003) and Quinn *et al.* (2003) also reported that wild type BRCA1 induced an increase in sensitivity to spindle poisons, such as paclitaxel and vinorelbine. Nevertheless, conflicting results still exist as a decrease in paclitaxel sensitivity was reported when BRCA1 function was restored in human ovarian cancer cells (Zhou *et al.*, 2003). Therefore, results suggest that BRCA1 blocks apoptosis after treatment with DNA damaging agents and induces it after spindle poisons treatment. Nonetheless, further understanding on the mechanisms involved is required as conflicting results have been published.

Response to radiotherapy

BRCA1 has been shown to play a role in DNA repair following radiation-induced DNA strand breaks. Many studies have reported the sensitivity of BRCA1 mutants to radiotherapy (Abbott *et al.*, 1999; Cortez *et al.*, 1999). They all showed that BRCA1 deficient cell lines failed to repair the damage caused by radiation resulting in radiation hypersensitivity. Furthermore, Bhattacharyya *et al.* (2000) demonstrated that BRCA1 contributed to increased resistance to radiation-induced DNA damage by promoting the assembly of RAD51. Thus, BRCA1 not only plays an important role in drug-induced DNA damage response is associated with radiation resistance. Nevertheless, Wang *et al.* (2001) did not show the role of BRCA1 in radiation-induced DNA damage and suggested that the increased radiosensitivity was independent of the BRCA1 status but was due to a defect in the repair pathway. Furthermore, studies on heterozygous BRCA1 mutations have shown that BRCA1 did not play a major role in radiosensitivity (Nieuwenhuis *et al.*, 2002; Baeyens *et al.*, 2004), as heterozygous BRCA1 mutation carriers did not have an increased radiosensitivity compared to non-carriers of the BRCA1 mutations. Therefore, further understanding is required to determine the role of BRCA1 in radiation-induced DNA damage.

1.6 The epidermal growth factor receptors

1.6.1 The EGF receptor family

The Epidermal Growth Factor Receptor (EGF receptor or ErbB) family is the subclass I of the receptor tyrosine kinase superfamily (Hynes and Lane, 2005). It consists of four members (Figure 1.20): EGFR (or ErbB1 or HER1), ErbB2 (or neu or HER2), ErbB3 (or HER3) and ErbB4 (or HER4). All four receptors are transmembrane glycoproteins (185KDa) formed of an extracellular domain (ligand binding region), a single membrane spanning region and a cytoplasmic tyrosine kinase domain (intracellular). Activation of the tyrosine kinase occurs *via* homo and heterodimerisation and ligand binding.

Different ligands (Figures 1.20 and 1.21) have been identified for each receptor (Hynes and Lane, 2005). EGF, transforming growth factor-α and amphiregulin bind to EGFR, whereas betacellulin, heparin-binding EGF and epiregulin to EGFR and ErbB4. Another group of ligands composed of neuregulins binds either to both ErbB3 and ErbB4 or only to ErbB4. Although, no ligand has been identified for ErbB2, Brennan *et al.* (2000) reported that it was activated through homo or heterodimerisation with other members of the ErbB family. Once activated, these receptors lead to the activation of a large number of intracellular signalling pathways (Figure 1.21). However, it is noted that ErbB3 is deficient in tyrosine kinase activity. Two main signalling pathways have been identified, the Mitogen-Activated Protein Kinase (MAPK) signalling pathway and the PhosphatidylInositol 3-kinase (PI3K)/Akt pathway (Riese and Stern, 1998; Yarden and Sliwkowski, 2001; Olayioye *et al.*, 2000). Thus, activation of EGFR tyrosine kinases affects a variety of signal transductions, leading to increase of proliferation and inhibition of apoptosis (Vlahovic and Crawford, 2003). Nevertheless, ErbB receptors have been implicated in the development of many cancers. EGFR and ErbB2 overexpression are the two main ErbB receptors which have been shown to play a major role cancer development (Ohgaki *et al.*, 2004; Sunpaweravong and Sunpaweravong, 2005; Slamon *et al.*, 1987). In addition, EGFR amplification is often accompanied by a mutated form of EGFR, EGFRvIII variant, having a deletion in the extracellular domain of the receptor (Ekstrand *et al.*, 1992). More recently, mutations of the receptor tyrosine kinase domain have also been identified in non-small-cell lung cancers (Pao *et al.*,

2004). Stephens *et al.* (2004) also identified mutations in the kinase domain of ErbB2, in non-small-cell lung cancers. Therefore, these two receptors are important to consider in the development of tumours.

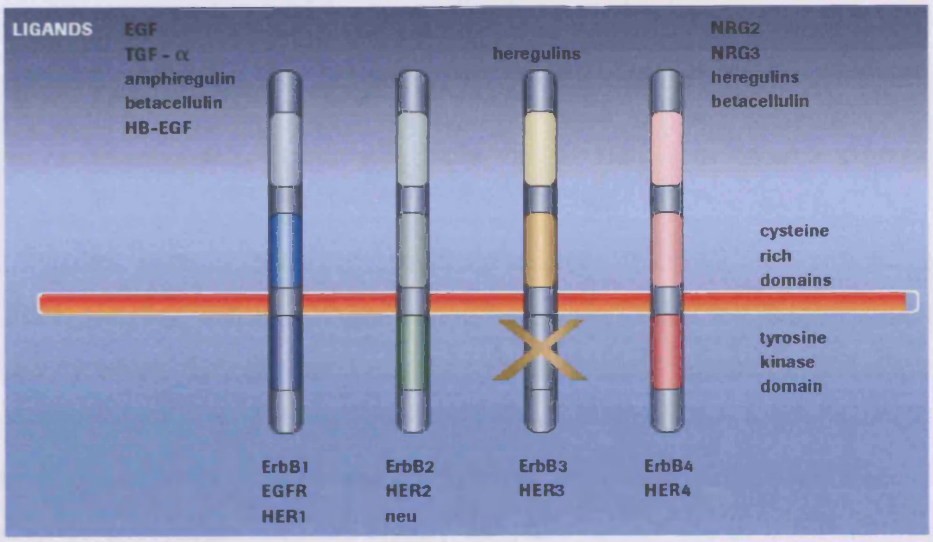

Figure 1.20 – ErbB family: their structure and binding ligands (www.roche.com). The cross indicates a deficiency in the tyrosine kinase activity of ErbB3.

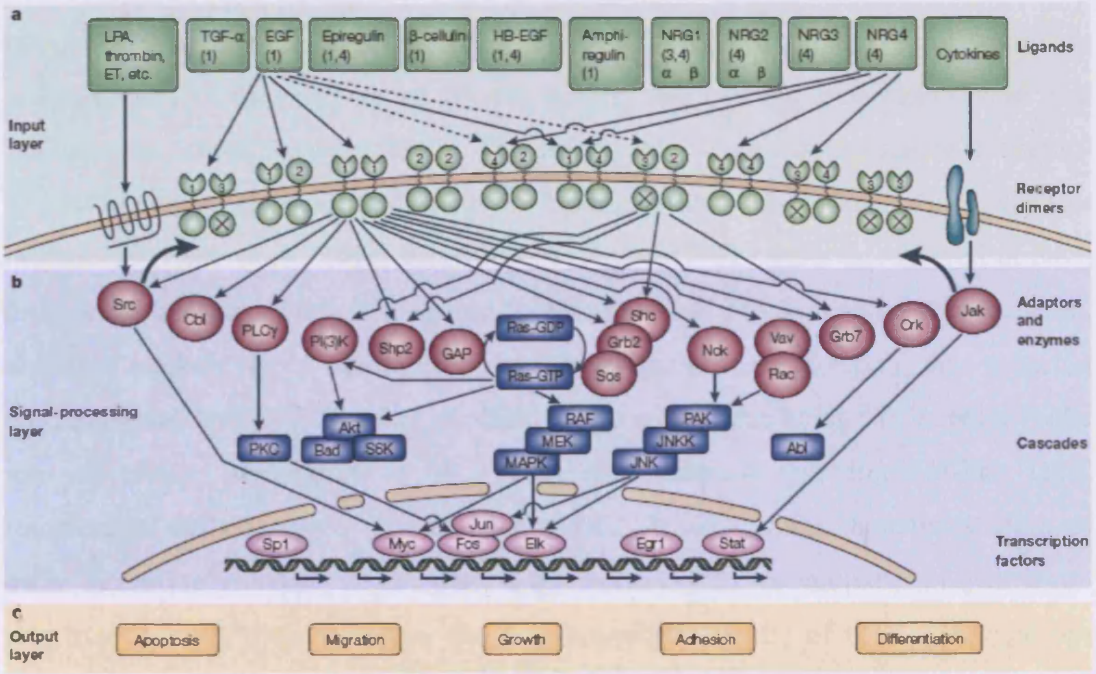

Figure 1.21 – ErbB receptors signalling. Activation (**a**), signalling network (**b**) and effects on cell proliferation (**c**) of ErbB receptors. Yarden Y. and Sliwkowski M.X., Molecular Cell Biology, 2001, 2: 127-137.

1.6.2 Epidermal growth factor receptors and cancer

Members of the EGFR family have been identified as being involved in development and progression of cancer. EGFR was the first to be linked with cancer (Gschwind *et al.*, 2004). However, ErbB2 was also described as being an important player in cell proliferation in cancer and particularly in breast cancer (Yarden, 2001a). These proteins have been shown to be largely overexpressed in tumours and cause uncontrolled cell proliferation due to their tyrosine kinase activity.

Oncogenic Tyrosine Kinases (OTKs)

Indeed, tyrosine kinases, acting to transfer phosphate from ATP to tyrosine residues on cellular proteins, are tightly controlled. However, three mechanisms have been described by which they become constitutively active and lead to the development of tumours, thus being oncogenic. The first one is the chromosomal translocation, generating fusion proteins allowing constitutive activation of the kinase activity, the second is by overexpression and finally by point mutations in the juxtamembrane region of a receptor causing constitutive dimerisation and activation of its kinase activity (Blume-Jensen and Hunter, 2001). These oncogenic tyrosine kinases have two complementary roles in cancer. One is to increase stimulation of signalling pathways enabling the cells to proliferate and protecting them from apoptosis independently of the presence of growth factors, thus causing metastasis (Porter and Vaillancourt, 1998; Sawyers, 1997). The second role is to cause resistance to chemo- and radiotherapy, thus accumulating DNA damage and genetic aberrations, such as mutations (Nishii *et al.*, 1996; Slupianek *et al.*, 2001). The latter is achieved through four possible mechanisms. One being the reduction of DNA damage accumulation, although unlikely, DNA damage may accelerate the process of repair, thus reducing the number of lesions (Michel *et al.*, 2001). The second one being the increase in the rate of repair, Masumoto *et al.* (1999) demonstrated that Bcr-Abl-like OTK transformed cells repaired cisplatin-induced DNA ICLs faster than untransformed cells. Indeed, to this date, it is suggested that homologous recombination repair is up-regulated in cells transformed by the Bcr-Abl-related family of OTKs, through up-regulation of RAD51 (Raderschall *et al.*, 2002), whereas Deutsch *et al.* (2001) showed that NHEJ repair is downregulated. However, it is not confirmed if this observation is general to all OTKs and if it can be applied to other repair pathways.

The third mechanism is the activation of cell cycle checkpoints. Although the mechanism, by which OTK-transformed cells increase the G2/M cell cycle arrest, is not known, Slupianek *et al.* (2002) reported that OTKs of the Bcr-Abl-related family induced G2/M checkpoint in response to different chemotherapeutic. Nevertheless, in response to radiation results have been more controversial (Nishii *et al.*, 1996; Salloukh *et al.*, 2000). Finally, OTKs can cause resistance to genotoxic damage through activation of anti-apoptotic proteins, such as Bcl-X_L and Bcl2 (Kumar *et al.*, 1996), and inhibit pro-apoptotic proteins, Bad and Bax (Salomoni *et al.*, 2000; Wang *et al.*, 1999b).

Therefore, oncogenic tyrosine kinases, such as EGFR or ErbB2 are important to consider in the progression and treatment of tumours, thus development of new targeted therapies is needed.

EGFR

EGFR activation and signalling – The Epidermal Growth Factor Receptor (EGFR) is a transmembrane glycoprotein, of the ErbB family, with a ligand-dependent intracellular tyrosine kinase activity (Velu, 1990). It is composed of an N-terminus extracellular region, a hydrophobic transmembrane region and a C-terminus intracellular region containing the tyrosine kinase domain. The N-terminus region is a ligand-binding site. Indeed, several studies have established that EGFR was the only receptor for EGF and TGFα ligands, nevertheless other ligands have also been shown to bind EGFR, such as amphiregulin, betacellulin (Kelloff *et al.*, 1996; Davies and Chamberlin, 1996). Both, EGF and TGFα, have a mitogenic activity amongst others (Velu, 1990), and have been implicated in the induction of angiogenesis, since EGFR has been shown to have a direct role in tumour development (Davies and Chamberlin, 1996). This activation of EGFR will result in the formation of homodimers and three functional heterodimers (Baselga and Arteaga, 2005). Nevertheless, the preferred partner of EGFR for heterodimerisation is ErbB2 which result in increased affinity for ligands and greater catalytic activity then EGFR homodimers. This causes receptor auto-phosphorylation or trans-phosphorylation, as tyrosine residues on one receptor are cross-phosphorylated by the other member of the receptor pair, will form a docking site for several Src homology 2 containing signal transducers. After ligand-induced activation, EGFR couple to different intracellular proteins involved in signal

transduction cascades, including the Mitogen-activated protein kinase (MAPK), phosphatidylinositol-3'-kinase (PI3K), the anti-apoptotic kinase Akt and several transcriptional regulators, such as STAT5 (Citri and Yarden, 2006, Hernandez-Sotomayor and Carpenter, 1992; Kelloff *et al.*, 1996). Nonetheless, EGFR signalling is negatively regulated through ubiquitylation by Cbl (Citri and Yarden, 2006).

EGFR nuclear localisation – Recent studies have demonstrated that EGFR was able to be internalised and induce endosomal signalling leading to cell proliferation and survival (Wang *et al.*, 2002). Furthermore, different studies have also established that EGFR was able to physically interact with proteins in the nucleus, such as STAT3 causing activation of transcription (Lo *et al.*, 2005 and 2006). In addition, Dittmann *et al.* (2005) established that nuclear EGFR is not only used as a transcriptional activator but also to trigger DNA damage repair in response to ionising radiation. Furthermore, they demonstrated that EGFR translocation occurs *via* a ligand-independent pathway in which stress induces the movement of the receptor from a perinuclear compartment into the nucleus. In addition, Hsu and Hung (2007) established that EGFR nuclear translocation was due to a tripartite nuclear localisation signal (NLS) sequence. Thus, EGFR endosomal and nuclear signalling need to be further characterised and will be important to consider when designing targeted therapies, as they need to act on the cell surface as well as in the nucleus.

EGFR and cancer – As described in Figure 1.21, activation of EGFR will cause increased cell proliferation as well as cell motility, adhesion, invasion and survival. Therefore, when overexpressed, EGFR contributes to angiogenesis (Woodburn, 1999). In addition, EGFR activation has an anti-apoptotic activity, since inhibitors of its tyrosine kinase activity have been shown to promote apoptosis (Kulik *et al.*, 1997; Bruns *et al.*, 2000). Consequently, deregulated expression of EGFR will result in increased EGFR signalling and angiogenesis.

Different mechanisms have been identified explaining the deregulated EGFR activity. The first one is the overexpression of EGFR, resulting from transcriptional or post-transcriptional mechanisms. EGFR overexpression has been observed in several cancers and was associated with invasiveness (Velu, 1990). The second mechanism is the activation of normal receptors, through autocrine overproduction of ligands. This will result in constant activation of EGFR and angiogenesis. Another mechanism is

also the loss of the negative feedback, responsible for the negative regulation of EGFR cell signalling (Amit *et al.*, 2007). Finally, is the mutation of EGFR, forming mutants which are constitutively actives without ligands. The best characterised is the EGFR variant III (EGFRvIII), lacking the dimerisation arm and an essential part of the ligand binding domain. Nonetheless, this mutation results in ligand-independent tyrosine kinase activation (Kelloff *et al.*, 1996). This mutation has been associated with increased resistance to chemotherapy and resistance to tyrosine kinase inhibitors (Learn *et al.*, 2004; Camp *et al.*, 2005). In addition, other kinase domain missense mutations, deletions and insertions have been observed, causing enhanced autophosphorylation and cell survival (Lynch *et al.*, 2004; Paez *et al.*, 2004). Therefore, further understanding of signal transduction pathways will help designing new targeted therapies and improve the therapeutic outcome.

ErbB2

ErbB2 activation and signalling – ErbB2 (human epidermal growth factor receptor 2) is the only receptor of the ErbB family to be ligand-less (Brennan *et al.*, 2000) whereas other members of the ErbB family are activated by large family of ligands. Upon activation, growth factor receptors dimerise and transduce their signals by auto-phosphorylation catalysed by the tyrosine kinase activity (Hunter, 2000). Nevertheless, ErbB2 having no known ligand, has been shown to be the preferred dimer partner of other ErbB receptors (Tzahar *et al.*, 1996; Graus-Porta *et al.*, 1997). In addition, Yarden and Sliwkowski (2001) reported that formation of ErbB2 heterodimers led to a stronger intracellular signal than the one originating from other complexes. Therefore, ErbB ligands activate ErbB2 together with the appropriate high affinity co-receptor (Harari *et al.*, 1999; Karunagaran *et al.*, 1996).

Similarly to EGFR, activated ErbB2 induces PI3K/Akt signalling pathway as well as the MAPK pathway, causing cell proliferation. ErbB receptor activation of the PI3K pathway (Figure 1.22) occurs through the Src-homology 2 (SH2)-mediated recruitment of the p85 regulatory subunit of PI3K. Once recruited, the p110 catalytic subunit of PI3K phosphorylates phosphatidylinositol-4,5-biphosphate (PIP_2) to form PIP_3. PIP_3 recruits phospholipid-binding domain containing proteins to the plasma membrane (Blume-Jensen and Hunter, 2001). Akt is one of the key effectors of the PI3K pathway and is recruited to the membrane through its PH domain, and

phosphorylated (at threonine 308) through activation of PDK1 (Meier and Hemmings, 1999). Akt phosphorylation at serine 473 occurs via PDK2 but the identity of PDK2 remains controversial. Nonetheless, it was suggested that phosphorylation at serine 473 could be caused by integrin-linked kinase (ILK), mammalian target of rapamycin (mTOR)-rictor complex, protein kinase C (PKC) and Akt itself (Delcommenne *et al.*, 1998; Toker and Newton, 2000; Kawakami *et al.*, 2004; Sarbassov *et al.*, 2005; Hay, 2005). Akt subsequently undergoes nuclear translocation and phosphorylates a number of downstream proteins. Indeed, Akt has been shown to phosphorylate Bad, blocking its pro-apoptotic activity (Danielsen and Maihle, 2002). In addition, Akt was shown to negatively regulate Raf and GSK-3 kinases and FKHR, a cell cycle regulatory transcription factor. Akt was also reported to promote protein translation through mTOR, initiation factor 4E and ribosomal p70-S6 (Li *et al.*, 2004). Finally, Akt was shown to promote cell cycle progression through downregulation of $p21^{WAF1}$ and $p27^{Kip1}$ (Zhou *et al.*, 2001b). Therefore, PI3K modulates cell proliferation and survival. Nonetheless, this pathway can be inhibited through the action of phosphatase and tensin homolog (PTEN) that the 3' phosphate from PIP_3, forming PIP_2. Thus, inhibiting Akt phosphorylation and downstream signaling, PTEN is then used as a balance for controlled cell growth (Cantley and Neel, 1999). Moreover, Hay (2005) also reported that Akt activation was negatively regulated by mTOR-raptor complex, thus playing an important role in cell progression regulation.

In addition to the PI3K pathway, ErbB2 also activates the Ras-MAPK pathway (or MAPK – Figure 1.22). This occurs either directly through the SH2 domain-mediated recruitment of Grb-2 or indirectly through the PTB domain-mediated binding of the Shc adaptor. By exchange of GDP for GTP, Gbr-2 activates Ras, which in turns binds and activates the Raf kinase (Schlessinger, 2000). This subsequently initiates the kinase cascade which involves phosphorylation of MEK1/2 and Erk1/2. Erk is responsible for the phosphorylation of cytoplasmic and cytoskeletal proteins such as MAPK-activated protein kinases and ribosomal p70-S6 kinase. In addition, Erk is translocated to the nucleus where it activates a number of transcription factors, such as E2F and AP1. Moreover, the MAPK pathway has also been implicated in chromatin remodeling through phosphorylation of histone H3 (Dunn *et al.*, 2005). Therefore, activation of the MAPK cascade results in gene expression and cell

proliferation. In addition, under stress, such as UV radiation, p38 MAPK stress pathway is activated causing cell proliferation, growth and survival. This pathway also modifies transcription factors, histones and chromatin remodeling factors (Dunn *et al.*, 2005).

Nonetheless, other signalling pathways are also activated in response to ErbB activation (Figure 1.22). Indeed, studies have shown that ErbB receptors induced activation of the phospholipase Cγ, causing increased intracellular calcium concentrations and phosphorylation of a number of substrates. In addition, STAT1, STAT3 and STAT5 have been shown to be phosphorylated and activate transcriptional gene involved in cell proliferation (Marmor *et al.*, 2004).

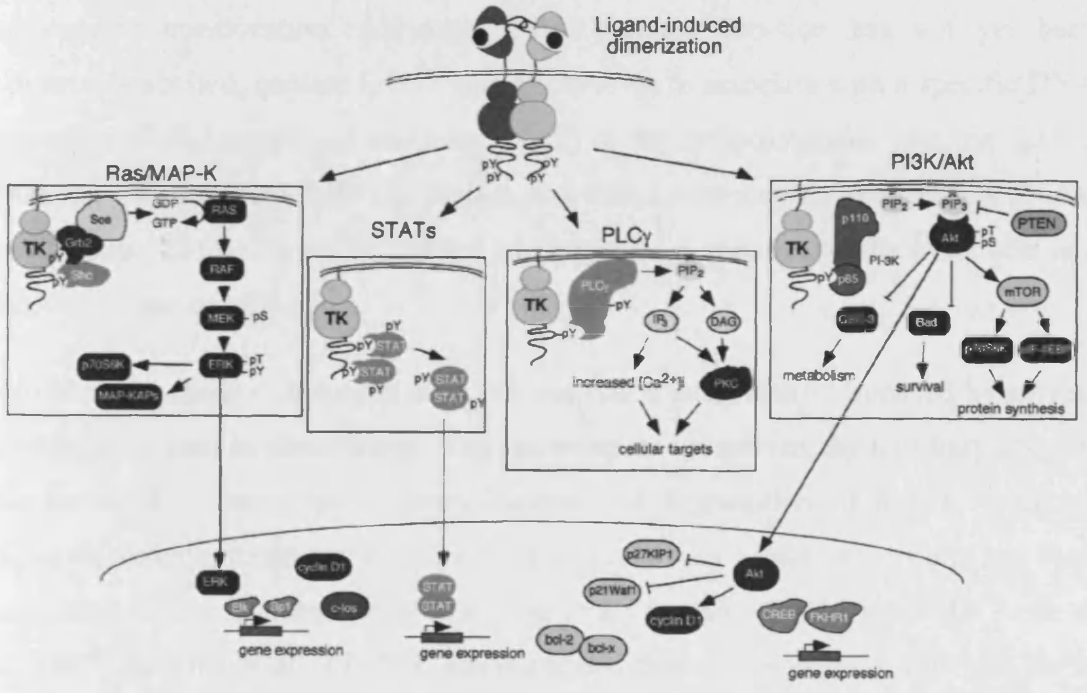

Figure 1.22 – ErbB downstream signalling pathways. Marmor M.D. *et al.*, International Journal of Radiation Oncology Biology Physics, 2004, 58(3): 903-913.

ErbB2 nuclear localisation – For growth factor receptors, nuclear translocation is more complex as they are integral membrane proteins, nuclear translocation requires a release from the lipid layer. So far, five mechanisms have been proposed, one is the internalisation of active receptors through dissociation from the endosomal compartment and direct entry into the nucleus (Myers *et al.*, 2003; Stachowiak *et al.*, 1996; Marti and Wells, 2000). Another mechanism is that the active receptor is

internalised into an endosomal compartment and then fuse with the nuclear envelope or transfer the receptor from an early-endosomal compartment into the nucleus (Giri *et al.*, 2005). Growth factor receptors may also be translocated to the nucleus by direct escape from the membrane at the cell surface and enter the nucleus using importin (Myers *et al.*, 2003). Proteolytic cleavage may also occur to release the cytoplasmic tail of the receptor which then associates with importin for nuclear entry (Ni *et al.*, 2001). Finally, receptors can use a ligand-independent pathway in which stress induces the movement of the receptor from a perinuclear compartment into the nucleus (Dittmann *et al.*, 2005; Offterdinger *et al.*, 2003). Nevertheless, Giri *et al.* (2005) established that ErbB2 was internalised through endocytosis, involving importinβ1 for nuclear entry. Furthermore, Hsu and Hung (2007) identified a nuclear localisation signal sequence, common to all ErbB family members, and responsible for nuclear translocation. Although ErbB2 nuclear function has not yet been extensively studied, nuclear ErbB2 was also shown to associate with a specific DNA sequence, HER-2 associated sequence (HAS) in the cyclooxygenase enzyme COX-2 promoter (Wang *et al.*, 2004), a protein associated with tumour progression (Turini and Dubois, 2002). Therefore, further investigation is required in the exact role and function of nuclear ErbB2.

ErbB2 and cancer – In normal cells this activation is carefully controlled by several mechanisms, such as dissociation of ligand-receptor complexes, dephosphorylation of the activated receptor, rapid internalisation and degradation of active receptors. However, overexpression of ErbB2 occurs in 20-30% of breast cancers and has been associated with enhancement of signalling pathways and angiogenesis (Di Fiore *et al.*, 1987; Hudziak *et al.*, 1987). It was suggested that overexpression of ErbB2 led to the formation of homodimers and auto-phosphorylation activity. Furthermore, overexpression of ErbB2 increases the formation of heterodimers, thus potentiating and prolonging the activation of downstream signalling pathways (Weiner *et al.*, 1989; Lonardo *et al.*, 1990). Nevertheless, different mechanisms of action of ErbB2 in the potentiation of cancer have been described. Several studies have reported that ErbB2 overexpression deccelerates the dissociation rates of ligands such as EGF (Wada *et al.*, 1990) and neuregulins (Peles *et al.*, 1993). Furthermore, Sorkin *et al.* (1993) demonstrated that ErbB2 could reduce the rate of internalization of EGFR, impairing the downregulation and degradation of the receptor, causing a longer

activation of intracellular signalling. Finally, ErbB2 overexpression was shown to enhance the rate of recycling of EGFR to the cell surface, such that the heterodimers will have a slow degradation rate (Lenferink *et al.*, 1998). Therefore, ErbB2 overexpression causes the potentiation of signalling by evading inactivation processes and prolonging the intracellular signalling.

ErbB2 overexpression has also been shown to affect the cell cycle regulation. Indeed, Lee *et al.* (2000b) demonstrated that ErbB2 overexpression was associated with an up-regulation of cyclin D1 protein expression, causing progression through the G1/S cell cycle checkpoint. It was also suggested that cyclin D was up regulated by ErbB2 signalling, through Akt activation (Lane *et al.*, 2000; Neve *et al.*, 2000). Thus, ErbB2 amplification can cause progression through G1/S cell cycle checkpoint and play a role in oncogenesis (Bartkova *et al.*, 1997). Concomitantly to the enhancement of the cyclin D activity, ErbB2 overexpression was associated with increased degradation and sequestration of $p27^{Kip1}$ (Lane *et al.*, 2000; Lenferink *et al.*, 2001). This effect is thought to be the result of up-regulation of MAPK and PI3K signalling pathways, causing its phosphorylation and subsequent degradation (Sheaff *et al.*, 1997; Busse *et al.*, 2000).

In addition to angiogenesis, ErbB2 overexpression causes resistance to chemotherapeutic agents and radiotherapy (Yu *et al.*, 1996 and 1998a; Tsai *et al.*, 1993. It is thought that ErbB2 causes increased resistance through the anti-apoptotic machinery involving the Cdk inhibitor $p21^{WAF1}$. Indeed, Yu *et al.* (1998b) demonstrated that ErbB2 transfected cells progressed less efficiently through the G2/M phase compared to untransfected cells. In addition, they reported that ErbB2 overexpressing cells wild type for $p21^{WAF1}$ conferred resistance to taxol-induced apoptosis and that this effect was abolished in ErbB2 overexpressing $p21^{WAF1}$ null cells. Thus, these data suggest that resistance to chemotherapy is driven by ErbB2-induced activation of $p21^{WAF1}$ through p53-dependent and independent mechanisms (Deng *et al.*, 1995; Pietras *et al.*, 1999).

Therefore, ErbB2 overexpression is an important factor in the development of tumours. Nevertheless, molecular mechanisms involved in ErbB2-induced chemoresistance are still unclear.

ErbB2 mutations – Mutations of ErbB2 have only recently been identified in non-small-cell-lung cancer (NSCLC) adenocarcinomas. These mutations involve somatic in-frame insertions within the exon 20 that correspond to the identical nine codon region in exon 20 of the EGFR gene where Stephens *et al.* (2004) reported insertions. The study by Wang *et al.* (2006) reported that cells carrying the ErbB2 in-frame YVMA insertion at residue 776 ($ErbB2^{YVMA}$), which is the most common mutations reported in a study by Shigematsu *et al.* (2005), activate cell proliferation and anti-apoptotic pathways more potently than ErbB2 wild type and remain sensitive ErbB2 targeted therapies, such as trastuzumab, but insensitive to EGFR tyrosine kinase inhibitors. Resistance to EGFR tyrosine kinase inhibitors was explained by the ability of $ErbB2^{YVMA}$ to increase association with and activate EGFR in the absence of ligands and kinase activity (Wang *et al.*, 2006). In addition, this mutation caused auto-phosphorylation of ErbB2. Another mutation, the VC insertion at G776 in exon 20 ($ErbB2^{VC}$) also found in NSCLC, causing increased anti-apoptotic signalling, as well as having highly phosphorylated wild-type EGFR, was shown to confer resistance to tyrosine kinase inhibitors, such as gefitinib and erlotinib (Wang *et al.*, 2006). Nevertheless, cells carrying this mutation were shown to be sensitive to HKI-272, an irreversible dual-specific kinase inhibitor targeting EGFR and ErbB2, trastuzumab and lapatinib.

Therefore, mutations of ErbB2 will need to be studied further in order to develop targeted therapies and improve patient prognosis, as mutations have been shown to alter the response to ErbB targeted therapies and no clinical data are available for ErbB2 targeted therapies in NSCLC.

1.6.3 EGFR and ErbB2 targeted therapies

Overexpression of ErbB receptors, causing increased cell proliferation and angiogenesis is a strong rationale for designing ErbB targeted therapies. Indeed, several agents have been designed to modulate ErbB receptors signalling (Figure 1.23). Nevertheless, they can be classified into two categories, small molecules inhibitors of the tyrosine kinase activity and monoclonal antibodies targeting the extracellular domain of the receptor (Baselga and Arteaga, 2005). Small inhibitors of the tyrosine kinase (TK) activity compete with ATP binding to the TK domain, thus inhibiting its activation and the ErbB signalling pathways. Different class of agents

are being developed against members of the ErbB family. Those agents differ by their potency but also by their capacity to inhibit a single receptor or more than one ErbB receptor. Monoclonal antibodies, so far developed, have been classified according to their mode of action, since they can prevent the ligand binding and ligand-dependent receptor activation (EGFR), interfere with ligand-independent receptor activation (ErbB2) or can also prevent receptor heterodimerisation. Nevertheless, a third class of agents has also been investigated: ligand/antibody-toxin conjugates, causing inhibition of receptor activation.

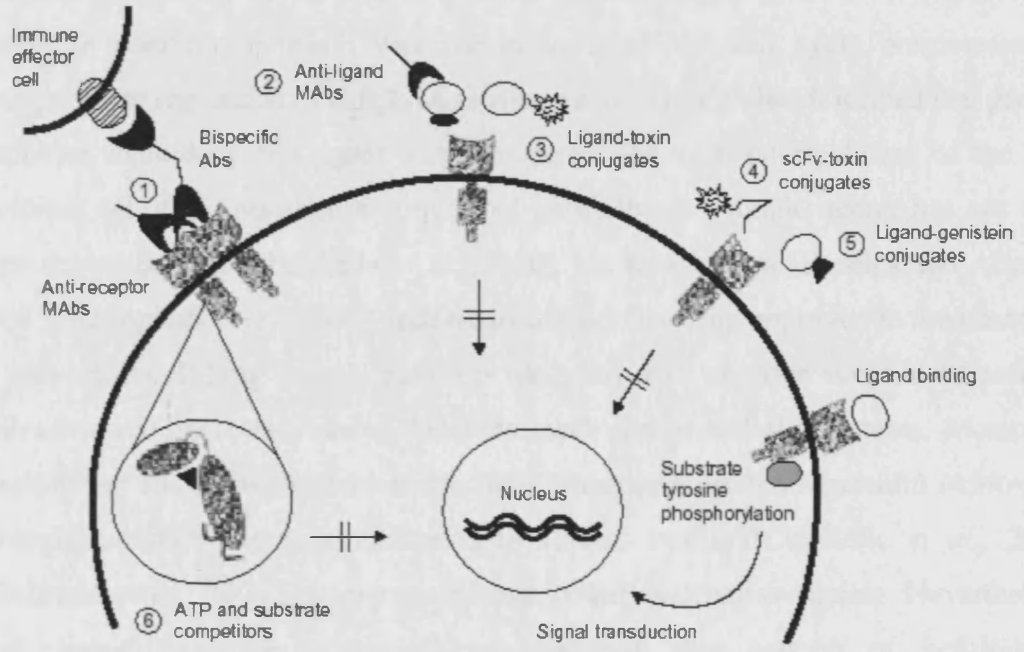

Figure 1.23 – ErbB targeted therapies: modulation of ErbB receptors activity. Raymond E. *et al.*, Drugs, 2000, 60(supll.1): 15-23.

Tyrosine kinase inhibitors

Tyrosine kinase inhibitors interfere with the ErbB receptors tyrosine kinases activity by inhibiting the phosphorylation of the tyrosine kinase, causing inhibition of ErbB signalling pathways. They are usually small molecules competing with the ATP binding site (number 6 in Figure 1.23). Those agents are mainly reversible inhibitors (Baselga and Averbuch, 2000) but irreversible inhibitors have recently been developed (Bridges, 1999; Fry, 1999). Nevertheless, other molecules inhibiting the tyrosine kinase have also been synthesised. Some act by mimicking the tyrosine moiety and substituting non-phosphorilable peptides at the binding region, and other

inhibit downstream signals by interrupting intracellular protein recognition (Raymond *et al.*, 2000). In addition, those agents differ by their potency against members of the ErbB family or by their capacity to inhibit a single receptor or on the contrary inhibit more than one receptor.

Gefitinib (Iressa^{TM}, ZD1839) – One of the most studied tyrosine kinase inhibitors is gefitinib. It is a low molecular weight anilinoquinazoline (Figure 1.24), acting as a potent, selective and reversible ATP-competitive inhibitor of EGFR tyrosine kinase. *In vitro* and *in vivo* studies have demonstrated its ability to inhibit the autophosphorylation of the EGFR tyrosine kinase activity (Baselga and Averbuch, 2000). In addition, gefitinib was shown to delay the cell cycle progression by disrupting the regulation of Cdk2. Di Gennaro *et al.* (2003) also described that growth inhibition caused by this agent was also associated with up-regulation of the Cdk inhibitor, $p27^{kip1}$. Anti-tumour activity of gefitinib, as a single agent, has not only been shown *in vitro* (Ciardiello *et al.*, 2000), but also *in vivo* (Baselga and Arteaga, 2005; Mellinghoff *et al.*, 2005). Indeed, in addition to being approved in the treatment of non-small-cell-lung cancer, gefitinib was shown to improve survival of patients with advanced pancreatic cancer, head-and-neck cancer and glioblastoma. Moreover, combination studies with chemotherapeutic drugs have proven successful *in vitro*, as synergistic effects were demonstrated in several studies (Ciardiello *et al.*, 2000; Friedmann *et al.*, 2004), but the mechanism of action remains unclear. Nevertheless, two clinical trials (in advanced non-small-cell lung cancer) of gefitinib in combination with gemcitabine and cisplatin (Giaccone *et al.*, 2004), and in combination with paclitaxel and carboplatin (Herbst *et al.*, 2004) have proved unsuccessful. Results did not show the additive effects observed *in vitro* and treatments did not improve patient survival.

Nevertheless, new studies have shown that patients with NSCLC for whom first and second line chemotherapy failed, had an improved response rate, when treated with gefitinib alone, but did not have an improvement of the survival (Thatcher *et al.*, 2005). In addition, discovery of somatic mutations of EGFR in a subset of NCLCs was shown to increase the response rate to gefitinib (Lynch *et al.*, 2004). Furthermore, Baselga (2006) reported that other markers of sensitivity and resistance have been identified, such as EGFR amplification, expression of ErbB3 and mutations in the Ras and ErbB2 genes. Additionally, although gefitinib is selective of

the EGFR tyrosine kinase activity, Cappuzzo *et al.* (2005) demonstrated that EGFR positive NSCLC patients with an increased ErbB2 gene amplification had a better response to gefitinib single agent therapy. This may be explained by the ability of ErbB2 to form heterodimers with EGFR and increase its kinase activity.

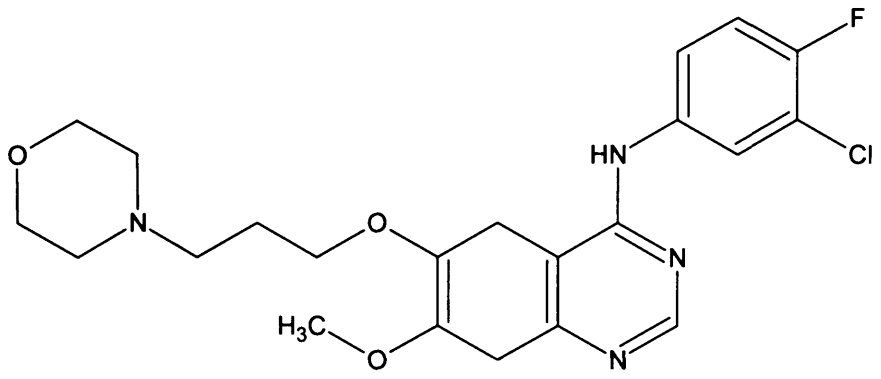

Figure 1.24 – Structure of gefitinib.

Erlotinib (Tarceva™, OSI-774) – Similarly to gefitinib, erlotinib is a selective, low molecular weight inhibitor that binds competitively to the ATP binding site of the EGFR kinase domain. Furthermore, Schaefer *et al.* (2007) demonstrated that erlotinib inhibits ErbB2 kinase activity in the absence of EGFR, at sub-micromolar levels, causing inhibition of the Akt and MAPK signalling pathways. In addition, they showed that erlotinib was able to inhibit ErbB2/ErbB3 heterodimers signalling and cell proliferation activity, in the absence of EGFR.

Single agent activity has been demonstrated *in vitro* and *in vivo* in NSCLC and metastatic pancreatic cancer (Akita and Sliwkowski, 2003; Grunwald and Hidalgo, 2003; Johnson *et al.*, 2005). Erlotinib was also studied in combination with conventional chemotherapeutics but clinical trials failed to shown an improved prognosis, compared to the single agent. Nevertheless, similarly to gefitinib, patients with NSCLC for whom first and second line chemotherapy failed, had an improved response rate and survival after treatment with erlotinib single agent. Moreover, mutations of EGFR have been shown to lead to an increase in sensitivity to erlotinib

(Hidalgo *et al.*, 2001). Several studies have shown that expression of other members of the ErbB family could modulate the response to erlotinib. Although *in vitro* assays have shown that erlotinib was not effective against ErbB2 kinase, studies showed that ErbB2 phosphorylation decreased after erlotinib treatment. In addition, ErbB2 overexpression was shown to render human tumour xenograft sensitive to erlotinib (Schaefer *et al.*, 2007).

Lapatinib (GW572016) – Lapatinib is a potent dual inhibitor of EGFR and ErbB2 tyrosine kinase activity. This compound has been shown to be active in normal cells and tumour cells, causing inhibition of EGFR and ErbB2 phosphorylation, phospho-Erk1/2, phospho-Akt and cyclin D (Rusnak *et al.*, 2001). In addition, its activity has been demonstrated *in vitro* and in breast xenografts (Xia *et al.*, 2003). Furthermore, clinical studies have shown its activity in advanced and metastatic cancers (Burris *et al.*, 2005). Phase II and III clinical trials have investigated the activity of lapatinib, in advanced breast cancer, as a single agent or in combination with capecitabine, a taxane or hormonal therapy in previously treated patients and untreated patients. Results indicated that lapatinib induced apoptosis and was associated with a higher clinical response (Burris, 2004). Xia *et al.* (2005) also demonstrated that combining lapatinib with trastuzumab, an anti-ErbB2 antibody, caused an enhancement of tumour apoptosis.

Other reversible tyrosine kinase inhibitors – In addition to lapatinib, other dual reversible inhibitors of EGFR and ErbB2 tyrosine kinase activity are being developed, such as BMS-599626 and AEE788 (also targets vascular endothelial growth factor receptor – VEGFR). Both of these compounds are being developed clinically, BMS-599626 has been shown to be a highly potent inhibitor of EGFR and ErbB2 kinases and inhibits cell proliferation through modulation of signalling pathways. Indeed, the preclinical study carried out by Wong *et al.* (2006) showed that BMS-599626 inhibits EGFR/ErbB2 heterodimerisation and provides an additional mechanism of inhibiting tumours in which receptor co-expression and heterodimerisation play a major role in inducing tumour growth.

Finally, other tyrosine kinase inhibitors have been developed, targeting tyrosine kinases other than the ErbB family members. Imatinib (Gleevec^{TM}, STI-571), is a competitive inhibitor of tyrosine kinase activity of additional tyrosine kinases,

including c-Kit receptor and the platelet derived growth factor receptor (PDGFR). Imatinib has been shown to be particularly efficient against gastrointestinal stromal tumours (GISTs) with mutations in the c-Kit gene, expressing its activated form permanently (Heinrich *et al.*, 2003). In addition, Imatinib has also been shown to be active against cancers associated with PDGFR alterations (Baselga and Arribas, 2004). Dasatinib (Sprycel™, BMS-354825) is a dual inhibitor of Src-Abl that binds Abl with less stringent conformational requirements than imatinib (Shah *et al.*, 2004). It has been shown to be active in patients with imatinib-resistant chronic myelogenous leukaemia (Talpaz *et al.*, 2005). In addition, mutations in GISTs causing resistance to imatinib have shown to be sensitive to sunitinib (Sutent™, SU-11248) a multitarget tyrosine kinase inhibitor blocking VEGFR, PDGFR and c-Kit activation (Demetri *et al.*, 2006).

Irreversible tyrosine kinase inhibitors – Compared to reversible inhibitors, irreversible kinase inhibitors have several advantages and potential. Indeed, irreversible inhibitors have been shown to have an enhanced potency. In addition, biological effect can be achieved at much lower doses since once the covalent bond has been formed, the biological effect persists (Denny, 2002; Bridges *et al.*, 2001). Moreover, some irreversible inhibitors have been shown to be active against the function of mutated kinases that are resistant to reversible inhibitors. Kwak *et al.* (2005) demonstrated the EKB-569 and HKI-272, 4-anilinoquinoline-3-carbonitrile-based irreversible inhibitors, covalently bind to a conserved cysteine residue present in some ErbB receptors and are active in erlotinib and gefitinib resistant cell lines. The clinical study by Yoshimura *et al.* (2006) confirmed that patients with NSCLC with acquired resistance to gefitinib were sensitive to EKB-569. Furthermore, several studies have also reported a similar effect with CI-1033 and EKI-785 other irreversible EGFR kinase inhibitor (Carter *et al.*, 2005; Kobayashi *et al.*, 2005; Greulich *et al.*, 2005). Therefore, designing new irreversible inhibitors may help overcoming acquired resistance.

Antibodies blocking the extracellular binding region of the receptor

These antibodies (numbers 1 and 2 in Figure 1.23) interfere with the activation of the receptor and modulate the intracellular cascade (Raymond *et al.*, 2000). There are four categories of antibodies: monoclonal antibodies that are directed against EGFR (cetuximab) or ErbB2 (trastuzumab and pertuzumab), bispecific anti-EGFR (MDX-447) or anti-ErbB2 (MDX-210) monoclonal antibodies linked to an anti-CD64 antibody.

Trastuzumab (Herceptin®) – This monoclonal antibody is the only humanized mouse monoclonal antibody that binds to the extracellular domain of ErbB2 and inhibit the growth of ErbB2 overexpressing cells (Leonard *et al.*, 2002). Currently, it is the only approved ErbB2 targeted therapy for the treatment of metastatic breast cancer. Trastuzumab has been shown to induce regression of ErbB2 overexpressing tumours. Nevertheless, mechanisms involved are not completely defined. Indeed, several molecular and cellular effects have been identified. The first one is the ability of trastuzumab to reduce cellular signalling from PI3K and MAPK cascades. Trastuzumab disrupts receptor dimerisation and mediates its internalisation and degradation, as shown in Figure 1.25 (Yarden, 2001b; Baselga *et al.*, 2001; Sliwkowski *et al.*, 1999). This process involves the recruitment of ubiquitin ligase (or Cbl) targeting the endosomes for lysosomal degradation by promoting receptor ubiquitination (Yarden, 2001b). Thus, trastuzumab down regulates ErbB2. Nonetheless, Lane *et al.* (2000) showed reduction of downstream signalling but no down regulation of ErbB2. Nagata *et al.* (2004) also suggested that trastuzumab disrupts the interaction between ErbB2 and Src tyrosine kinase, leading to the activation of PTEN, a PI3K inhibitor. It was also shown that reduction of downstream signalling pathways induced the Cdk inhibitor, $p27^{kip1}$, thus promoting cell cycle arrest during the G1 phase and apoptosis (Sliwkowski *et al.*, 1999; Lane *et al.*, 2000; Neve *et al.*, 2000; Baselga *et al.*, 2001). Trastuzumab was also shown to promote apoptosis through induction of an immune response or antibody-dependent cellular cytotoxicity (ADCC), but further investigation is required to fully understand the importance of ADCC in the response to trastuzumab (Cooley *et al.*, 1999; Clynes *et al.*, 2000; Gennari *et al.*, 2004). Furthermore, trastuzumab was shown to inhibit

angiogenesis through reduction of microvessel density, endothelial cell migration, reduction of VEGF expression and transforming growth factor-α (Izumi *et al.*, 2002; Klos *et al.*, 2003). In addition, angiogenesis inhibition was also improved when trastuzumab was combined with paclitaxel. Moreover, trastuzumab inhibits the proteolytic cleavage of ErbB2 extracellular domain, or ECD, mediated by metalloproteases. Indeed, a 95kDa N-terminal truncated membrane-associated ErbB2 fragment with increased kinase activity can be found on the cell surface, and an 110kDa ECD is released and can be detected in the culture media (Christianson *et al.*, 1998; Zabrecky *et al.*, 1991; Pupa *et al.*, 1993). Molina *et al.* (2001) reported that trastuzumab blocks this cleavage in vitro and high serum levels of ErbB2 ECD correlated with poor prognosis and a decreased response to chemotherapy in patients with advanced breast cancer (Molina *et al.*, 2002; Leitzel *et al.*, 1995; Yamauchi *et al.*, 1997; Hayes *et al.*, 2001). Finally, Pietras *et al.* (1994 and 1998) demonstrated that trastuzumab was able to inhibit DNA damage repair induced by cisplatin and unscheduled DNA synthesis after radiation. They reported that trastuzumab blocked DNA damage repair through inhibition of $p21^{WAF1}$. Thus, allowing cell cycle progression and accumulation of unrepaired DNA damage, causing increased apoptosis.

Trastuzumab was first studied as a single agent and was proved to be efficient in metastatic breast cancer, overexpressing ErbB2 (Cobleigh *et al.*, 1999). Nevertheless several studies have investigated the effect of trastuzumab in combination with common chemotherapeutic drugs, such as cisplatin, etoposide and paclitaxel, demonstrating the ability of trastuzumab to synergise with those drugs, *in vitro* and *in vivo* (Pegram *et al.*, 1999; Pegram *et al.*, 2004a; Naruse *et al.*, 2002). Pegram *et al.* (2004b) also demonstrated that a 3-way drug combination including trastuzumab, docetaxel and a platinum salt resulted in a higher response rate and a slower progression of the disease, in patients with advanced breast cancer overexpressing ErbB2. Robert *et al.* (2006) also reported, in a phase III randomised trial that patients treated with trastuzumab, paclitaxel and carboplatin had a slower disease progression than the patients treated with trastuzumab and paclitaxel. Similarly, Slamon *et al.* (2001) showed that combining trastuzumab with doxorubicin plus cyclophosphamide or single agent paclitaxel resulted in an improved survival rate compared to chemotherapy alone. Nevertheless, efficiency of trastuzumab treatment will depend

on the ErbB2 status, drug scheduling and side effects, since administration of trastuzumab with anthracyclines resulted in severe cardiac dysfunction (Seidman *et al.*, 2002).

Nonetheless, tumours have been shown to develop trastuzumab resistance. Indeed, resistance to trastuzumab has been shown to be associated with mutation of the ErbB2 gene, found in lung cancers (Stephens *et al.*, 2004 – ErbB2 mutations detailed previously). However, no data are available on the mutation status and the response to trastuzumab in breast cancer. Resistance may also be achieved through an increased cell signalling. Since trastuzumab only affects ErbB2-mediated signalling, other dimers are not affected and can function in presence of trastuzumab. Nevertheless, Nagata *et al.* (2004) reported that PTEN plays a major role in the development of trastuzumab resistance as its loss of function result in Akt activation. Down regulation of PTEN was shown to block trastuzumab-mediated inhibition of proliferation and induce a poor response to trastuzumab therapy. Finally, resistance to trastuzumab therapy was also shown to be induced by the modulation of $p27^{kip1}$ as growth inhibitory properties of trastuzumab depend on this Cdk inhibitor (Le *et al.*, 2003). In addition, increased insulin growth factor-I receptor signalling can also cause the inhibition of trastuzumab-mediated growth arrest (Lu *et al.*, 2001).
Therefore, future investigations will involve the study of novel drug combinations to overcome acquired resistance.

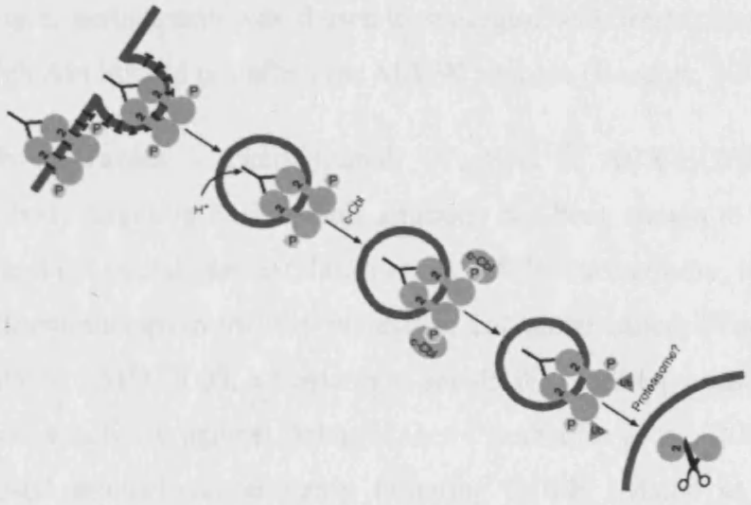

Figure 1.25 – Internalisation of the ErbB2 receptor by trastuzumab. Yarden Y., European Journal of Cancer, 2001b, 37: S3-S8.

Cetuximab (Erbitux®, IMC-C225) – It is a chimeric mouse anti-EGFR antibody, approved for the treatment of irinotecan-refractory colorectal cancer. Cetuximab blocks EGFR tyrosine kinase activation by interfering with ligand receptor binding. In addition, six mechanisms have been identified, by which cetuximab inhibits tumour progression: inhibition of cell cycle progression, induction of apoptosis, inhibition of angiogenesis, inhibition of metastasis, synergise with chemotherapeutic agents and induction of immune response similarly to trastuzumab (Mendelsohn, 2000). Single agent treatment has been shown to be efficient in variety of solid tumours including colon, head and neck, NSCLC and renal cell carcinoma. Similarly to other ErbB targeted therapies, cetuximab was also used in combination with chemotherapeutic agents and was shown to be able to reverse resistance to irinotecan in colorectal cancer (Prewett *et al.*, 2002). Furthermore, a randomised study (Cunningham *et al.*, 2004) confirmed the significant activity of cetuximab in combination of irinotecan in irinotecan-refractory disease.

Pertuzumab (Omnitarg™, 2C4) – This is the first monoclonal antibody that prevents receptor heterodimerisation. Pertuzumab binds to ErbB2 and sterically hinders ligand-associated heterodimerisation of ErbB2 with other ErbB receptors. Thus, inhibiting intracellular signalling, including PI3K and MAPK cascades (Franklin *et al.*, 2004). Pertuzumab has been shown to be active *in vitro* and *in vivo*, in breast and prostate cancer, independently of ErbB2 expression, through inhibition of the ErbB2-ErbB3 heterodimer formation (Agus *et al.*, 2002 and 2005; Baselga, 2002). Furthermore, pertuzumab was shown to synergise with trastuzumab, blocking signalling through Akt but did not affect the MAPK cascade (Baselga, 2002).

Other antibody therapies – Panitumumab (Vectibis™, ABX-EGF) is another monoclonal antibody targeting EGFR. This antibody has been shown to be active in prostate cancer and colorectal cancer (Harari *et al.*, 2007). Furthermore, it was shown to be active in chemotherapy-refractory metastatic colorectal cancer (Van Cutsem *et al.*, 2006). Similarly, EMD72000, a humanised anti-EGFR antibody, has been shown to have anti-tumour activity against colon cancer (Vanhoefer *et al.*, 2004). h-R3 is another humanised monoclonal antibody targeting EGFR (Mateo *et al.*, 1997). Preclinical studies have shown that h-R3 has anti-proliferative, pro-apoptotic and anti-angiogenic effects (Crombet-Ramos *et al.*, 2002). This antibody was also shown

to be active in combination with radiotherapy in head and neck cancer (Crombet *et al.*, 2004).

Bispecific anti-EGFR (MDX-447) or anti-ErbB2 (MDX-210) monoclonal antibodies linked to an anti-CD64 antibody have also been developed. These antibodies have potential anti-neoplastic activity since they enhance cellular immune response against EGFR or ErbB2 positive cells, resulting in increased tumour cell death. MDX-210 has been shown to be active in patients with advanced breast or ovarian cancer overexpressing ErbB2 (Valone *et al.*, 1995). MDX-447 was also shown to be active clinically in advanced solid tumours (Fury *et al.*, 2007). Many other monoclonal and bi-specific antibodies have been developed and shown to be active *in vitro* and *in vivo*, those have been reviewed by Booy *et al.* (2006). Although antibody therapy may have disadvantages due the specificity of antibodies, this review also demonstrates that antibody therapy is becoming an important therapeutic tool.

Ligand/antibody-toxin conjugates acting on the extracellular ligand binding region

Normal ligands such as TGFα and EGF can fuse with truncated forms of immunogenic cellular toxins (e.g. ETA) or genistein fusion protein in order to block the activation of EGFR (Raymond *et al.*, 2000 – Figure 1.23, numbers 3 and 5). In addition, scFv (side chain variable region-containing fragment) antibody-toxin conjugates have also been developed to target EGFR. Binding of such ligand/antibody-toxin conjugates (Figure 1.22, number 4), to EGFR, leads to the inhibition of downstream signalling pathways. Nevertheless, no agent has yet been shown to be active *in vivo*.

Combination therapies

ErbB targeted therapies have not only been used as single agents but also in combination with conventional chemotherapeutic agents, hormone therapy or other molecules-targeted therapies.

Combination with chemotherapeutic agents – Indeed, as described previously ErbB targeted therapies have been used in combination with common

chemotherapeutics, such as gefitinib with cisplatin (Friedmann *et al.*, 2004) or trastuzumab with cisplatin or etoposide (Pegram *et al.*, 1999; Pegram *et al.*, 2004a; Naruse *et al.*, 2002). Combination of trastuzumab with chemotherapeutic agents has also been used in a clinical study by Slamon *et al.* (2001). In addition, synergistic effects of trastuzumab with platinum salts and vinka alkaloids, described in the pre-clinical study by Pegram *et al.* (2004a), was also demonstrated clinically (Burstein *et al.*, 2003; Pegram *et al.*, 2004b). Similarly, efficacy of chemotherapeutic agents, such as cisplatin and paclitaxel, was shown to be enhanced when combined with gefitinib, in pre-clinical studies (Sirotnak *et al.*, 2000; Friedmann *et al.*, 2004). Nevertheless, phase III clinical trials, using gefitinib or erlotinib combined with gemcitabine and cisplatin or carboplatin and paclitaxel have proved unsuccessful (Giaccone *et al.*, 2004; Herbst *et al.*, 2004; Gatzemeier *et al.*, 2007). The failure of these trials can be explained by an antagonistic effect of the combination, as antagonism was demonstrated between cytostatic and cytotoxic agents such as tamoxifen and chemotherapeutic agents (Baselga, 2004; Albain *et al.*, 2002). In addition, failure of these trials could be explained by the mutations of the ErbB receptors causing the tumour to be insensitive to anti-EGFR therapy (as discussed later in the resistance to targeted therapies). Nonetheless, in order to obtain positive clinical results, it is important to consider if ErbB inhibitors can reverse the acquired and primary resistance to common chemotherapy. Indeed, Saltz *et al.* (2007) and Cunningham *et al.* (2004) demonstrated that combination of cetuximab with irinotecan was active in patients resistant to irinotecan treatment.

Therefore, the lack of concordance between pre-clinical and clinical outcome points the way to further studies to investigate combinations of anti-ErbB therapies and chemotherapeutic agents.

Combination with hormone therapy – Anti-ErbB therapies have also been combined with anti-estrogens in breast cancer and prostate cancer. Although EGFR tyrosine kinase inhibitors have shown limited activity in breast cancer patient, Baselga and Arteaga (2005) reported that, *in vitro*, combining gefitinib with tamoxifen caused an increased growth inhibition and anti-hormone resistance was overcome. Although the molecular basis of the cross-talk between ErbB receptors and estrogen receptors (ER) is unclear, it is suggested that EGFR and ErbB2 signalling phosphorylates and activates (ER) and its co-activator amplified in breast cancer-1

(AIB-1), thus causing tamoxifen to act as an ER agonist (Osborne *et al.*, 2003). Nevertheless, further clinical investigations are required to determine the potential benefit of such combinations

Combination with other targeted therapies – Such combination has recently become the focus of a number of studies. This is due to the fact that tumours are not dependent on just one receptor signalling pathway and that there is compensatory cross-talk among receptors signalling network (Gschwind *et al.*, 2004). Thus, three types of combinations have been identified.

The first one is the combination of ErbB targeted therapies with anti-receptor therapies. Indeed, ErbB2 was shown to potentiate EGFR signalling and its overexpression to counteract the activity of EGFR tyrosine kinase inhibitors (Karunagaran *et al.*, 1996; Christensen *et al.*, 2001). In addition, EGFR overexpression causing inhibition of trastuzumab activity was reversed in presence of TKIs (Motoyama *et al.*, 2002). Furthermore, Nahta *et al.* (2004) demonstrated, *in vitro*, that trastuzumab was able to synergise with pertuzumab in breast cancer cells. Therefore, these data are the rationale for the combination of anti-EGFR and anti-ErbB2. Nevertheless, clinical trial results combining gefitinib with trastuzumab have proved unsuccessful (Moulder and Arteaga, 2003). Thus, suggesting the need of alternative approaches. Nonetheless, another type of combination can be considered, anti-insulin like growth factor I (IGF-I) with anti-ErbB therapies. Indeed, Chakravarti *et al.* (2002) and Lu *et al.* (2001) demonstrated that inhibition of EGFR TKIs and trastuzumab by IGF-I overexpression could be reversed by IGF-I receptor inhibitors (Garcia-Echeverria *et al.*, 2004; Camirand *et al.*, 2005).

ErbB targeted therapies can also be combined with molecules targeting downstream signalling molecules. Indeed, abnormal activation of downstream molecules, due to mutations, can cause the tumours to be insensitive to ErbB targeted therapies (Bianco *et al.*, 2003). Mutations in PTEN, an inhibitor of Akt, have been shown to cause resistance to trastuzumab (Nahta *et al.*, 2006). Furthermore, *in vitro* combination of EGFR TKI, gefitinib, with mTOR inhibitor has produced promising results. Therefore, this points the way to further investigations and new combinations.

Finally, ErbB targeted therapies have been combined with agents interfering with essential components required for tumour growth. Hanahan and Weinberg (2000) identified six essential alterations for tumour growth: self-sufficiency in growth signals, insensitivity to growth inhibitory signals, evasion of apoptosis, limitless replicative potential, sustained angiogenesis and metastasis. Although anti-ErbB therapies interfere with the self-sufficiency in growth signals, they also have been shown to induce apoptosis, reduce VEGF, and inhibit angiogenesis and metastasis (Mendelsohn *et al.*, 2003; Petit *et al.*, 1997; Ciardiello *et al.*, 2001). Nevertheless, studies have shown that enhanced angiogenesis caused resistance to EGFR inhibition (Viloria-Petit *et al.*, 2001). Thus, Herbst *et al.* (2005) demonstrated that combining erlotinib with angiogenesis inhibitor, bevacizumab, increased the response rate. Nevertheless, tyrosine kinase inhibitors blocking EGFR and ErbB2 tyrosine kinase activity and the VEGF receptor tyrosine kinase have become available (Wedge *et al.*, 2002).

Therefore, future research is required to developed new drugs and drug targets, pointing the way to the development of new targeted therapies.

Resistance to targeted therapies

Over the past few years, several ErbB targeted therapies have been developed. Nevertheless, patients have been shown to become refractory to those therapies. Indeed, several mechanisms, responsible for the development of resistance, have been identified and lead to the improvement of targeted ErbB therapies.

Redundant tyrosine kinase receptors – Firstly, the presence of redundant tyrosine kinase receptors can also influence the activation of signalling pathways. Herynk *et al.* (2003) demonstrated that c-Met activation led to an increased cell proliferation and angiogenesis, thus countering the effect of ErbB inhibitors. In addition, Kulik *et al.* (1997) and Lu *et al.* (2001) also demonstrated that activation of the tyrosine kinase receptor IGF-1R was associated with resistance to tyrosine kinase inhibitors and trastuzumab. Therefore, activation of alternative tyrosine kinase receptor will override the effect of ErbB inhibitors.

Angiogenesis – Secondly, up-regulation of tumour angiogenesis promoting growth factors is another mechanism by which tumour cells overcome ErbB inhibition.

Indeed, Viloria-Petit *et al.* (2001) demonstrated that tumours resistant to ErbB therapy increased angiogenesis and they showed that this was associated with an increased VEGF expression. This finding was further confirmed by Ciardiello *et al.* (2003), showing that targeting EGFR could lead to increase angiogenesis and resistance to EGFR inhibitors but targeting EGFR together with VEGFR-2 did not result in resistant tumours. Therefore, targeting more than one survival pathway can cause greater tumour inhibition and the reduction of angiogenesis (Jung *et al.*, 2002).

Constitutive activation of downstream signalling pathways – This is the result of the alteration of signalling mediators, such as PTEN. Indeed, PTEN loss causes constitutive activation of PI3K, resulting in Akt activation and its anti-apoptotic functions. PTEN loss has been reported to cause resistance to gefitinib (Bianco *et al.*, 2003) and trastuzumab, as described previously. Nevertheless, other signalling mediators have been shown to cause resistance to targeted therapy, such as Src family kinases (Wiener *et al.*, 2003; Dehm and Bonham, 2002) and STAT family members (Ni *et al.*, 2000; Garcia *et al.*, 2001)

Ligand-independent activation – As demonstrated by Liu *et al.* (2002) and Moro *et al.* (2002), EGFR and several signalling mediators could be activated through interactions with integrins and their ligands in the cellular matrix, leading to the bypass of anti-EGFR antibody inhibitory effects and the activation of the tyrosine kinase activity.

Mutations – As previously described, specific mutations of EGFR or ErbB2 receptors have been shown confer resistance to targeted therapies. Mutations that cause resistance are usually mutations affecting amino acids within the kinase catalytic domain, preventing or weakening the interaction between this domain and the drug (Baselga, 2006). Furthermore, several studies reported untreated patients as well as patients responding to erlotinib or gefitinib can acquire secondary mutations, T790M mutation, localised within the ATP-binding site and rendering them resistant to those agents (Pao and Miller, 2005; Kobayashi *et al.*, 2005; Greulich *et al.*, 2005). Nevertheless, irreversible tyrosine kinase inhibitors have been shown to overcome this problem (Carter *et al.*, 2005).

Moreover, other mutations may play a role in the sensitivity or resistance to ErbB targeted therapies. Indeed, Pao *et al.* (2005) reported that K-ras mutations led to signalling in the absence of EGFR input, leading to a lower response rate to EGFR tyrosine kinase inhibitors. Thus, suggesting that K-ras can be used as a marker of resistance to EGFR inhibitors, such as gefitinib and erlotinib. In addition, several studies have identified mutations in PI3K gene in glioblastoma, colorectal, ovarian and breast cancers, demonstrating that these tumours were PI3K-signalling dependent and that these mutations were responsible for angiogenesis. Thus, these tumours are highly sensitive to PI3K-Akt-mTOR pathway (Campbell *et al.*, 2004; Bachman *et al.*, 2004).

1.7 Aims and objectives

ErbB2 and BRCA1 have been identified as playing a major role in the development of breast cancer. The aim of this investigation is to study the potential role of these proteins in the repair of drug-induced DNA damage. To this end, the following questions will be addressed:

- Does trastuzumab affect the chemosensitivity and the repair of drug-induced DNA damage of ErbB2 overexpressing breast cancer cells (Chapter 3)?
- Does ErbB2 inhibition by trastuzumab alter cell cycle regulation (Chapter 4)?
- How does ErbB2 expression affect the repair of cisplatin-induced DNA damage (Chapter 5)?
- Does nuclear ErbB2 play a role in the repair of cisplatin-induced DNA damage (Chapter 6)?
- How does BRCA1 expression affect chemotherapeutic response in breast cancer cells (Chapter 7)?

Chapter 2

Materials and Methods

MATERIALS

2.1 Cell lines and culture conditions

For the BRCA1 study, MCF-7 wild type, MCF-7 scrambled and MCF-7 3.23 (BRCA1 expression down-regulated by plasmids encoding specific human BRCA1 siRNA, based on the pSUPER plasmid) cell lines (plasmids detailed in Table 2.1) were kindly provided by Prof. A. Ashworth from the Institute of Cancer Research (Breakthrough Breast Cancer Research). MCF-7 wild type cells were grown in RPMI 1640 (Autogen Bioclear, UK) supplemented with 10% heat inactivated (at 56°C for 30 minutes) foetal calf serum, 1% of 200mM L-glutamine (Autogen Bioclear, UK), 1% of 10,000 units Penicillin – 10mg/ml Streptomycin (Sigma-Aldrich, UK) and 500µl insulin at 10mg/ml (Sigma-Aldrich, UK) incubated at 37°C in 5% CO_2. The MCF-7 scrambled and MCF-7 3.23 cell lines were grown in complete RPMI 1640 media, supplemented with 250µl of 10mg/ml of selection marker blasticidin (Invivogen, UK).

For the ErbB2 study, MCF-7 cells (obtained from CR-UK London Research Institute) were grown as described above. SK-BR-3 cells (obtained from CR-UK London Research Institute) were cultured in McCoy's 5A Modified Medium (Sigma-Aldrich, UK) supplemented with 10% foetal calf serum, 1% of 200mM L-glutamine (Autogen Bioclear, UK) and 1% of 10,000 units Penicillin – 10mg/ml Streptomycin (Sigma-Aldrich, UK) incubated at 37°C in 5% CO_2. MDA-MB-453 cells (obtained from CR-UK London Research Institute) were grown in Dulbecco's Minimal Essential Medium (DMEM) (Autogen Bioclear, UK) supplemented with 10% foetal calf serum, 1% of 200mM L-glutamine (Autogen Bioclear, UK) and 1% of 10,000 units Penicillin – 10mg/ml Streptomycin (Sigma-Aldrich, UK) incubated at 37°C in 5% CO_2. Human breast cancer cell line, MDA-MB-468, was grown in Dulbecco's Minimal Essential Medium (DMEM) (Autogen Bioclear, UK) supplemented with 10% foetal calf serum, 1% of 200mM L-glutamine (Autogen Bioclear, UK) and 1% of 10,000 units Penicillin – 10mg/ml Streptomycin (Sigma-Aldrich, UK) incubated at 37°C in 5% CO_2. Transfected MDA-MB-468 cells (list of plasmids detailed in Table 2.1) were grown in the same complete media containing G418 (Sigma-Aldrich, UK) selective agent at a concentration of 750µg/ml. All the cell lines used are summarised in Table 2.2.

Transfected cell line	Plasmid	Vector	Insert	Plasmid Supplier
MCF-7 scrambled	pSUPER vector control	pSUPER	None	Dr. C. Lord Institute of Cancer Research (provided us with the transfected cell line)
MCF-7 3.23	pSUPER BRCA1siRNA	pSUPER	BRCA1 siRNA sequence	Dr. Lord Institute of Cancer Research (provided us with the transfected cell line)
MDA-MB-468 pcDNA3	pcDNA3 vector control	pcDNA3	None	Dr. Segatto (Regina Elena Cancer Institute, Italy)
MDA-MB-468 pcDNA3-ErbB2	pcDNA3 ErbB2 wild type	pcDNA3	ErbB2	Dr. Segatto (Regina Elena Cancer Institute, Italy)
MDA-MB-468 pEGFP-N1	pEGFP-N1 vector control	pEGFP-N1	None	Prof. Hung (MD Anderson cancer center, USA)
MDA-MB-468 pEGFP-N1 ErbB2	pEGFP-N1 ErbB2 wild type	pEGFP-N1	ErbB2	Prof. Hung (MD Anderson cancer center, USA)
MDA-MB-468 pEGFP-N1 ErbB2ΔNLS	pEGFP-N1 ErbB2ΔNLS (ErbB2 with deletion of the Nuclear Localisation Signal)	pEGFP-N1	ErbB2ΔNLS	Prof. Hung (MD Anderson cancer center, USA)

Table 2.1 – Transfected cell lines and corresponding plasmids.

Cell line	Origin	Culture condition	Supplier
MCF-7	Human Caucasian breast adenocarcinoma	RPMI 1640	Cancer Research UK, London Research Institute
SK-BR-3	Human Caucasian breast adenocarcinoma	McCoy's 5A modified	Cancer Research UK, London Research Institute
MDA-MB-453	Human Caucasian breast metastatic carcinoma	Dulbecco's Minimal Essential Medium (DMEM)	Cancer Research UK, London Research Institute
MDA-MB-468	Human Black breast metastatic carcinoma	Dulbecco's Minimal Essential Medium (DMEM)	Cancer Research UK, London Research Institute

Table 2.2 – Summary of the cell lines used.

2.2 Tissue culture

2.2.1 Cell lines maintenance

All cell lines were grown in 75cm^2 flasks (T75), in humidity-saturated (95%) incubators (Forma Scientific, UK), at 37°C with 5% CO_2. All procedures were carried out in Class II MDH biological safety cabinet (Intermed MDH, UK) using aseptic techniques (cabinet was cleaned with 70% industrial methylated spirit – IMS – as well as the equipment used inside the cabinet). Cells were routinely passage twice a week, at 80-90% confluence. As all cell lines were adherent, media was removed and cells were washed with 3ml of sterile 0.01M phosphate-buffered saline solution (PBS, Sigma-Aldrich, UK) to remove the residual serum. Cells were subsequently detached using 5ml of 1xTrypsin/EDTA (Autogen Bioclear, UK) at 37°C. 5ml of complete medium was then added to inactivate the trypsin and cells were pelleted by centrifugation at 1500rpm for 5 minutes at room temperature. The supernatant was discarded and cells were resuspended in 10ml of complete medium. Cells were finally seeded into new flasks at a ratio of 1/2 to 1/5 according to the cell line. All cell lines were passaged to a maximum of 30 times, after which point fresh cells were retrieved from the liquid nitrogen stock.

2.2.2 Storage and retrieval from liquid nitrogen

In order to store cell lines, frozen cell stocks were prepared. Cells were grown in $175cm^2$ flasks (T175) to 80% confluence. Cells were trypsinised and resuspended to a concentration of $1x10^6$cells/ml in freezing medium (FCS containing 10% dimethylsulphoxide – DMSO – Sigma-Aldrich, UK). The cell suspension was aliquoted in 1ml cryotubes and frozen at -80°C for one day. Tubes were then transferred to a liquid nitrogen tank. Cells were recovered from liquid nitrogen by thawing the cryotubes rapidly in a 37°C water bath. The cell solution was added to a $25cm^2$ flask (T25) containing 9ml of complete growth medium. Flasks were incubated at 37°C with 5% CO_2. The medium was changed after 24 hours (once cells have re-attached to the bottom of the flask) to avoid toxicity due to the DMSO from the freezing mixture.

2.2.3 Cell count

Cells were counted, once resuspended in 10ml of complete growth medium (see cell line maintenance), using a haemocytometer. A haemocytometer has two chambers and each chamber has a microscopic grid etched on the glass surface (central counting area formed of 25 squares). The chambers are overlaid with a glass coverslip that rests on pillars exactly 0.1mm above the chamber floor. 60µl of cell suspension was mixed with 60µl of trypan blue (Sigma-Aldrich, UK) in order to exclude dead cells (1 in 2 dilution). Some of this solution was loaded into both chambers. The number of cells was determined for each central counting of the two chambers (each counting area has a surface of $1mm^2$ and a volume of $0.1mm^3$ or 0.1µl), since a 1 in 2 dilution was made. The total number of cells obtained was multiplied by $1x10^4$, giving the number of cells per ml of suspension.

2.2.4 Cell doubling time

Cells were seeded in 6 well plates at a concentration of $5x10^4$cells/ml with complete growth medium, each single well was used for one time point. Cells were counted (as in 2.2.3) and the concentration was determined. Cell concentration was determined every 24 hours until confluence. The doubling time was determined by plotting the cell concentration against the number of hours.

2.3 Chemotherapeutic drugs and other reagents

Clinical grade Gefitinib (Iressa, ZD 1839) was kindly provided by AstraZeneca (Macclesfield, UK). Etoposide, Melphalan, Doxorubicin, Paclitaxel were purchased from Sigma-Aldrich (Dorset, UK). Wheat germ agglutinin (Lectin from *Triticum vulgaris*) was purchased from Merck Biosciences (Nottingham, UK). Cisplatin (DBL, Warwick, UK) and trastuzumab (Herceptin® – Roche, Welwyn Garden City, UK) were obtained from The Middlesex Hospital (UCL Hospital, London, UK). Details of the compounds used for this study are described in Table 2.3. Stock solutions were either prepared in advance or fresh prior to experiments according to stability of each compound. Stock solution concentrations were adjusted according to the cytotoxicity of each drug. Trastuzumab and cisplatin were obtained pre-diluted at the indicated concentrations from the hospital.

Compounds	Type of drug	Structure	Dilution solvent	Stock solution
Gefitinib	Quinazoline derivative inhibiting EGFR (ErbB1) tyrosine kinase activity (small molecule)	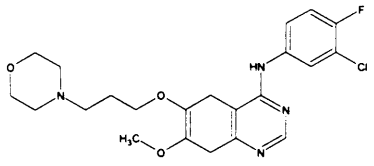	DMSO	10mM
Etoposide	Topoisomerase inhibitor (inhibitor of chromatin function)	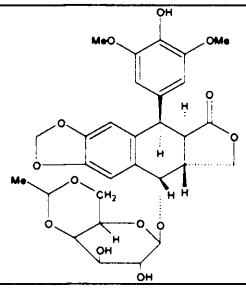	DMSO	10mM
Melphalan	Bifunctional alkylating agent - nitrogen mustard based (covalent DNA-binding drug)	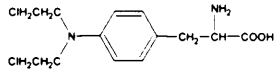	Ethanol with 1% HCl	10mM
Doxorubicin	DNA intercalating agent (non covalent DNA binding drug)	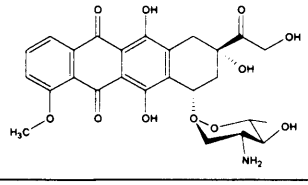	Sterile Water	1mM

Compounds	Type of drug	Structure	Dilution solvent	Stock solution
Paclitaxel	Microtubule inhibitor (inhibitor of chromatin function)	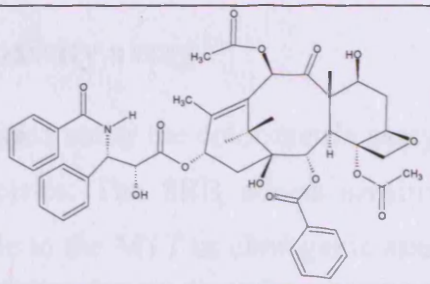	DMSO	1mM
Cisplatin	Alkylating agent – platinum compound (covalent DNA binding drug)	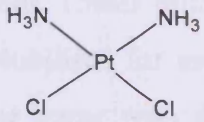	Sterile water	3.3mM
Trastuzumab	Monoclonal antibody inhibiting ErbB2 tyrosine kinase activity	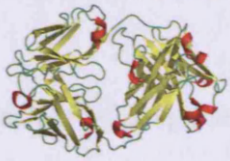 www.3dchem.com	Sterile Water	21mg/ml
Wheat germ agglutinin (WGA)	Lectin from *Triticum vulgaris* inhibiting nuclear import	 www.bmb.uga.edu	Sterile PBS	5mg/ml

Table 2.3 – Compounds used in the BRCA1 and ErbB2 studies.

METHODS

2.4 *In vitro* cytotoxicity assay

Cytotoxicity of drugs was assessed using the colorimetric assay Sulphorhodamine B (SRB) in 96-well microtiter plates. The SRB allows sensitive measure of drug-induced cytotoxicity comparable to the MTT or clonogenic assays. It is based on the ability of the protein dye sulforhodamine B to bind on protein basic amino acid residues of trichloroacetic acid-fixed cells. Under mild acidic conditions it binds to the cells and is easily extracted and solubilised for measurement (Voigt W., 2005). The SRB assay gives results which are linear with the number of cells and more sensitive than the Lowry and Bradford assays and twenty other visible dyes (Skehan *et al.*, 1990).

This assay was used to determine the effect of drugs and drug combinations on cell proliferation. Cells were seeded (200µl per well), according to their doubling time (MCF-7 wild type, MCF-7 3.23 and MCF-7 scrambled at $1x10^4$cells/ml, SK-BR-3 at $2x10^4$cells/ml, MDA-MB-453 at $5x10^4$cells/ml and MDA-MB-468 wild type and transfected MDA-MB-468 cell lines at $2x10^4$cells/ml) into 96-well microtitre plates (Nunclon, VWR, UK) and incubated for 24 hours at 37°C with 5% CO_2, prior to drug treatment.

2.4.1 Single agent cytotoxicity

For single agent assays, drugs were added at a range of concentrations (all drugs were used at clinically achievable peak plasma concentrations and adjusted to each cell line) to wells in triplicate and left in solution continuously for 5 days or one hour followed by 5 days in drug free media. Alternatively, cells were treated for 3 days continuously or one hour followed by 3 days in drug free media. Drugs were diluted in complete growth medium and 200µl of the appropriate concentration was added to the appropriate well. Each experiment included a solvent control lane and a drug-free media control lane (100% cell proliferation), treated in the same way with change of media at the appropriate time. Plates were incubated in a humid box at 37°C in 5% CO_2.

2.4.2 Dual agent treatments and synergistic effect

For dual agent treatments (combination assays), drugs were either added concomitantly (drug A and B together) for 5 days or added concomitantly for 24 hours (drug A+B) followed by 4 days of drug-free media (no drug) or media containing the drug B. Combination experiments included one control lane (drug-free media) and one solvent control lane. Plates were incubated in a humid box at 37°C in 5% CO_2. To determine synergy, drug B was used at a sub-toxic concentration (concentration producing 10-20% inhibition of proliferation) and combined with a range of concentration of drug A.

2.4.3 SRB assay and data analysis

At the end of the incubation period, cells were fixed by adding 100µl per well of ice-cold 10% w/v trichloroacetic acid for 20 minutes at 4°C, wells were then washed with distilled water and stained with 0.4% SRB in 1% v/v acetic acid for 20 minutes at room temperature (staining of living cells). Wells were finally washed using 1% acetic acid and left to dry at room temperature overnight. Purple crystals formed were dissolved in 100µl of 10mM Tris Base (Sigma-Aldrich, UK) / 1mM EDTA (Sigma-Aldrich, UK) for 20 minutes at room temperature. The absorbance (OD) of each well was read at 540nm using a Spectrafluor Plus plate reader (Tecan, UK). The mean absorbance of each drug concentration was expressed as a percentage of the untreated control wells absorbance:

$$\% \text{ proliferation} = \frac{\text{OD treated}}{\text{OD control}} \times 100$$

Data obtained were the average of three independent experiments, showing standard deviations. Dose-response curves obtained were used to determine the IC_{50}. The IC_{50} being the drug concentration required to produce 50% growth inhibition.

The Student *t*-test (Appendix 1) was used to statistically compare the IC_{50} obtained for two independent treatments. Data were said to be significantly different, at a 95% (p=0.05) or 99% (p=0.01) probability (p being the level of significance), if the calculated t value (Appendix 1) was superior to the tabulated t value. Each independent experiment was repeated in triplicate, so the degree of freedom (Appendix 1) used to read the tabulated t value was 4. When studying synergistic

effect of drugs producing IC_{50} individually, data were analysed using the isobologram analysis (detailed in section 2.6).

2.5 Radiation survival curve

Assessing the survival of cell after irradiation was achieved in a similar manner to the cell proliferation assay described in section 2.4. MCF-7 wild type, MCF-7 3.23 and MCF-7 scrambled were diluted at $1x10^4$cells/ml in 15ml falcon tubes (VWR, UK). Cells were exposed on ice to a range of radiation doses using the GEC Newton Victor X-ray machine at 25kV. As the machine delivers 2.5Gy per minute, time of exposure was varied to obtain the desired doses. Control cells were not exposed to any radiation. Cells were then plated in 96-well microtitre plates (200µl per well) and incubated for 6 days in a humid box at 37°C with 5% CO_2. After the incubation period, cells were treated as previously described in the SRB assay (fixing, staining and reading). Each experiment was repeated in triplicate, results were expressed as in section 2.3.

2.6 Isobologram analysis

Isobologram analysis (Tallarida, 2001) has been described in order to identify when two drugs that produce antagonistic, additive or synergistic effects. An isobologram was used to assess the effect of combination of any given chemotherapeutic agent with gefitinib. An example of an isobologram is shown in Figure 2.1. In order to analyse the results, a particular effect level is selected, in our case 50% of the maximum killing for gefitinib (IC_{50}) and doses of each drug alone that give this effect. These values are plotted as axial points in a Cartesian plot (i.e. IC_{50} for each drug - single agent treatment - is plotted on each axis). The straight line connecting the two IC_{50} values (A and B representing the IC_{50} of the two drugs) is the locus of points (isoboles) that produce the additive combination of compounds. Thus, all the combinations of IC_{50} of two drugs, on or close to the line (as defined by the red circle), have an additive effect (illustrated by the letter P). Combinations of IC_{50} above this line, such as R, have a sub-additive or an antagonistic effect. IC_{50} values such as point Q show a super-additive or a synergistic effect. However, the

isobologram does not allow a statistical distinction, due to the error inherent in the dose-effect data. Hence, points on or close to the line do not provide a conclusive distinction. For those points further statistical analysis such as regression analysis would be required (these analysis will not be required in our case).

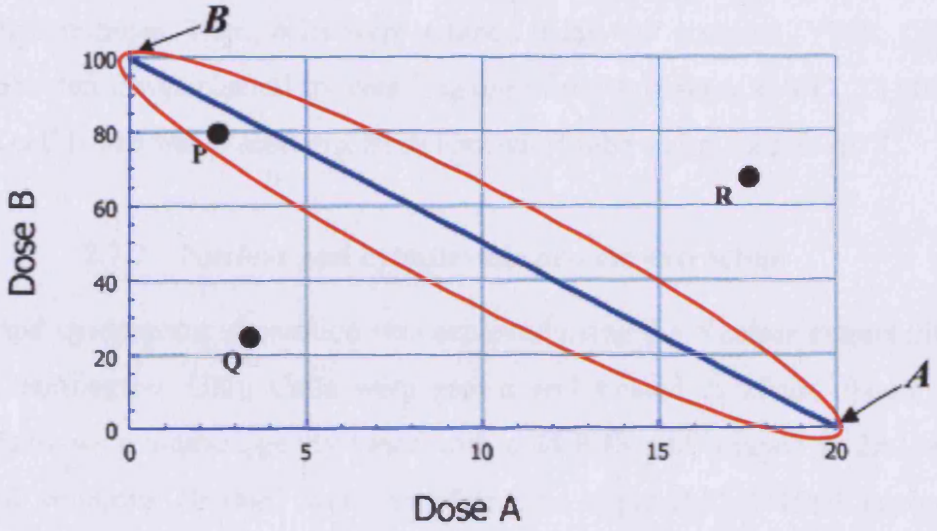

Figure 2.1 – Isobologram analysis. A and B are the IC_{50} of the two drugs studied in combination, R = sub-additive or antagonistic effect, P = additive effect, Q = super-additive or synergistic effect. The red circle defines the region giving additive effect. Tallarida R.J., Journal of Pharmacology and Experimental Therapeutics, 2001, 298(3):865-72.

2.7 Western blotting analysis

2.7.1 Total protein extraction

Two methods of protein extraction were used according to the protein extracted. The freeze-thaw method was used for the BRCA1 study. After treatment, cells were pelleted in an eppendorf tube using trypsin, and kept on dry ice. Lysis buffer (450mM NaCl, 25% glycerol, 5mM EDTA, 0.5mM DTT, 20mM Hepes pH 7.9 and protease inhibitor x1) containing fresh protease inhibitor (Roche, UK) was added to the cell pellet. The pellet with added lysis buffer was freeze-thawed five times (freeze for 1-2 minutes and thaw for 30 seconds at 30°C) and subsequently centrifuged for 10 minutes at 4°C (13,000rpm) in order to remove insoluble material. The total cell lysate (supernatant) was carefully transferred to a fresh eppendorf tube and stored at -80°C.

The RIPA method was used for the ErbB2 study, since ErbB2 is a cell surface receptor it can be damaged by trypsin. Treated cells were washed twice with PBS (phosphate buffered saline, pH 7.3). RIPA lysis buffer (1% deoxycholic acid, 1% Triton X-100, 0.1% SDS, 250mM NaCl, 50mM Tris HCl and protease inhibitor x1), containing fresh protease inhibitor (Roche, UK), was added to the cells (kept on wet ice) for five minutes. Then, cells were scraped using cell scrapers (VWR, UK) and insoluble material was cleared by centrifugation for 10 minutes at 4°C (13,000rpm). The total cell lysate was placed in a fresh eppendorf tube and placed at -80°C.

2.7.2 Nuclear and cytoplasmic protein extraction

Nuclear and cytoplasmic separation was achieved using the Nuclear extract kit from Perbio (Cramlington, UK). Cells were grown and treated in 25cm^2 flasks (T25). Briefly, cells were washed gently twice with cold PBS and scraped in 2ml of cold PBS. Cell solutions obtained were transferred to a pre-chilled 15ml falcon tube (VWR, UK) and centrifuged 5 minutes at 500g at 4°C (supernatant was discarded). Cell pellets were resuspended in 300µl of cold PBS and transferred to a cold eppendorf tube and centrifuged at 500g, 4°C for 5 minutes (supernatant was discarded – all the PBS must be removed). Pellets were finally resuspended in 100µl of ice cold CERI (Cytoplasmic Extraction Reagent I) buffer, containing protease inhibitor, and vortexed at high speed for 15 seconds. The cell suspensions were incubated 10 minutes on ice before adding 5.5µl of CERII (Cytoplasmic Extraction Reagent II) buffer. Cell solutions were vortexed for 5 seconds and incubated for 1 minute on ice. Solutions were vortexed once more for 5 seconds and centrifuged for 5 minutes at 16,000g at 4°C. The supernatant corresponds to the cytoplasmic fraction and was stored at -80°C (the last few microliters of supernatant were discarded to avoid contamination with the nuclear pellet).

The nuclear pellets were resuspended in 50µl of NER (Nuclear Extraction Reagent) buffer containing protease inhibitor and vortexed 15 seconds at high speed. Samples were vortexed for 15 seconds every 10 minutes for 40 minutes. Lysed nuclei were centrifuged for 10 minutes at 16,000g at 4°C and the nuclear fractions (supernatant) were stored at -80°C.

2.7.3 Protein quantification

Once extracted, proteins were quantified using the RC DC protein assay from Bio-Rad Laboratories. This assay is based on the Lowry protocol (Lowry *et al.*, 1951), using reagents A, S and B. Briefly, 2µl of each lysate was mixed with 18µl of distilled water, then 100µl of the mix of reagent A and S (20µl of reagent S with 1ml of reagent A) was added. Finally 800µl of reagent B is added and solutions are incubated for 15 minutes at room temperature. Absorbance (OD) was measured, against a blank containing only distilled water at 750nm on a Philips spectrophotometer (Beam PU8620 Series UV/Vis single) and total protein concentration was determined with the following formula:

$$\text{Concentration in } \mu g/\mu l = OD*25$$

Once the concentration was determined, loading dye (250mM Tris HCl, pH 6.8, 500mM DTT, 10% SDS, 0.5% Bromophenol Blue, 50% glycerol and distilled water were used to make a 5 times stock) was added to 50µg of protein (volume equivalent). Samples were boiled at 100°C for 4 minutes and then stored at -20°C until immunoblotting.

2.7.4 Immunoblotting

Samples prepared as in section 2.7.1 and 2.7.2 were centrifuged for 5 seconds and loaded onto 3-8% Tris acetate gels (Novex pre-cast gels, Invitrogen, UK), using the XCell SureLock™ Mini-Cell module (Invitrogen, UK) with NuPAGE tri-acetate SDS running buffer (60.5g Tris Base, 89.5 Tricine, 10.0g SDS and distilled water added to a volume of 1 litre were used to make a 20 times stock) in order to separate proteins at 150V, at room temperature. Proteins smaller than 40kDa were separated on 4-12% Bis-Tris gels (Novex pre-cast gels, Invitrogen, UK) using the same module as above but with MES running buffer (97.6g MES, 60.6g Tris Base, 10g SDS, 3g EDTA and distilled water added to a volume of 500ml was used to make a 20 times stock). Kaleidoscope marker (Bio-Rad, UK) was used as a size marker.

Proteins were transferred electrophoretically (40V at 4°C for 3 hours) onto activated immobilon P membranes (Sigma-Aldrich, UK) (membranes are activated by

immersion in 100% MeOH for 30 seconds, followed by 2 minute in distilled water and 5 minutes in transblot buffer), using the XCell II Blot module (Invitrogen, UK) with transblot buffer (100ml of running buffer stock x10 (30.3g Tris Base, 144.1 Glycine and distilled water to 1 litre – pH 8.3), 200ml MeOH and distilled water to 2 litre). Unbound sites on membranes were subsequently blocked using blocking buffer: 5% Marvel milk in Tris-Buffered Saline (TBS – 20mM Tris Base, 0.2M NaCl, pH 7.5 in distilled water) with 0.1% Tween 20 when probing for non-phosphorylated proteins and 5% BSA (Bovine Serum Albumin – Sigma-Aldrich, UK) in TBS with 0.1% Tween 20 for phosphorylated proteins. Proteins were probed using the appropriate antibody (see dilutions and preparation in Table 2.4). Finally, the primary antibody was probed with HRP-conjugated polyclonal antibodies (Mouse or Rabbit – 1/2000, Abcam – see Table 2.4) for chemiluminescence detection (ECL system, Amersham Biosciences, UK). To this end, blots were dried and incubated 1 minute with ECL reagents before covering them with cling film and exposing them to Kodak X-OMAT™LS film for various times (2 seconds to 10 minutes).

Membranes were subsequently re-hydrated and stripped of already bound antibodies, in order to re-probe for another antibody, using stripping buffer (100mM β-mercaptoethanol, 2% SDS and 62.5mM Tris HCl pH 6.8) in a hybridiser (Techne, UK) at 50°C for 30 minutes. Finally membranes were washed twice 10 minutes in TBS with 0.1% Tween 20, before blocking and re-probing as previously described.
For all experiments using total protein lysate, α-tubulin was used as a loading control. However, for the nuclear and cytoplasmic separation, lamin was used for the nuclear fraction and calnexin for the cytoplasmic fraction.

Antibodies	**Dilutions**	**Dilution buffer**	**Supplier**
Anti-BRCA1 (Ab-1)	1/50	3% milk	Oncogene, UK
Anti-EGFR	1/1000	5% BSA	Cell Signaling, UK
Anti-ErbB2	1/1000	5% BSA	Cell Signaling, UK
Anti-phosphoErbB2 (PY1248)	1/1000	5% BSA	Cell Signaling, UK
Anti-ErbB3	1/1000	5% BSA	Cell Signaling, UK
Anti-ErbB4	1/1000	5% BSA	Cell Signaling, UK
Anti-DNA-PK_{cs}	1/400	5% Milk	Abcam,UK
Anti-phosphoDNA-PK_{cs}	1/400	5% BSA	Abcam, UK
Anti-ATM	1/1000	5% Milk	Abcam, UK

Antibodies	Dilutions	Dilution buffer	Manufacturer
Anti-phosphoATM	1/500	5% BSA	Abcam, UK
Anti-ATR	1/500	5% Milk	Abcam, UK
Anti-phosphoATR	1/1000	5% BSA	Cell signaling, UK
Anti-TOPO2α	1/1000	5% Milk	Santa Cruz, UK
Anti-Artemis	1/500	5% Milk	Abcam, UK
Anti-Ku70	1/500	5% Milk	Abcam, UK
Anti-Akt	1/1000	5% BSA	Cell Signaling, UK
Anti-phosphoAkt (T308)	1/1000	5% BSA	Cell signaling, UK
Anti-phospho Akt (S473)	1/1000	5% BSA	Cell signaling, UK
Anti-RAD51	1/200	5% Milk	Abcam, UK
Anti-ERCC1 (clone 8F1)	1/200	5% Milk	Neomarker, UK
Anti-MAPK (p42/44)	1/1000	5% BSA	Cell signaling, UK
Anti-phosphoMAPK	1/1000	5% BSA	Cell signaling, UK
Anti-PARP (also detects cleaved PARP)	1/1000	5% Milk	Cell signaling, UK
Anti-PTEN	1/1000	5% BSA	Cell Signaling, UK
Anti-Calnexin	1/1000	5% BSA	Cell Signaling, UK
Anti-LaminA/C	1/1000	5% milk	Cell Signaling, UK
Anti-Mouse (ab6728)	1/2000	5% milk	Abcam, UK
Anti-Rabbit (ab6721)	1/2000	5% milk	Abcam, UK
Anti- α-tubulin (Clone B-5-1-2)	1/4000	5% milk	Sigma-Aldrich, UK

Table 2.4 – Antibodies used in the BRCA1 and ErbB2 studies

2.8 Reverse Transcriptase Polymerase Chain Reaction

2.8.1 RNA extraction and quantification

RNA was extracted from cell pellets using the RNeasy minikit (Qiagen, UK). Briefly, cells were disrupted using 600µl of buffer RLT containing β-mercaptoethanol and samples were homogenised by passing solutions trough a 20-gauge syringe. After adding 600µl of 70% ethanol, solutions were filtered using RNeasy mini-columns (15 seconds at 13,000rpm), 700µl of RWI buffer was then added to the column and centrifuged (15 seconds at 13,000rpm). Then, columns were washed twice with 500µl of buffer RPE. Finally, 40µl of RNase-free water was added onto the membrane of the column to elute the RNA (1 minute at 13,000rpm). RNA was kept at -80°C.

RNA was quantified by measuring the absorbance at 260nm (Philips spectrophotometer, Beam PU8620 Series UV/Vis single) of a 1 in 500 dilution of the RNA, in DEPC water (0.1% DEPC in distilled water, solution was left at room temperature overnight in foil and autoclaved): $Absorbance_{260}$ of 1 = 40µg/ml. Purity of the RNA was checked by calculating the ratio at 260nm and 280nm (A_{260}/A_{280}) – which should be between 1 and 2.

2.8.2 Synthesis of first strand cDNA

cDNA was synthesised from the RNA extracted, using Superscript II RNase H^- reverse transcriptase enzyme (Invitrogen, UK). Briefly, 2.5µl of oligo $(dT)_{15}$ (500µg/ml, Promega, UK) was mixed with 5µg RNA, 2.5µl of dNTP mix (10mM each – dTTP, dCTP, dATP and dGTP, Promega, UK) and DEPC water (distilled water containing 0.1% DEPC left in the dark overnight and autoclaved) to a volume of 30µl. Samples were heated at 65°C for 5 minutes then chilled quickly on ice before adding 10µl of 5 times first strand buffer (Invitrogen, UK) and 5µl of 0.1M DTT (Invitrogen, UK). Samples were heated for 2 minutes at 42°C and 2.5µl of superscript II RNase H^- reverse transcriptase (200 units per µl, Invitrogen, UK) as well as 2.5µl DEPC water was added. Finally, samples were incubated at 42°C for 50 minutes then 15 minutes at 70°C. cDNA was stored at -20°C.

2.8.3 Reverse Transcriptase PCR amplification

PCR amplification was performed using a PTC-225 thermal cycler (GRI, UK). Primers (MWG Biotech, Germany) and annealing temperatures used are shown in Table 2.5. BLASTN search (www.ncbi.nlm.nih.gov) was conducted in order to confirm the total gene specificity of the nucleotide sequences.

5µl of cDNA previously synthesised was mixed with 4µl of dNTP mix (2.5mM each, Promega, UK), 3µl of magnesium chloride at 25mM (Invitrogen, UK), 10µl of 5x GoTaq flexi PCR buffer (Promega, UK), 0.3µl of GoTaq polymerase (5 units per µl, Promega, UK), 5µl of each primer of interest at 10µM (BRCA1) and 2µl of each internal control primer at 10µM (β-actin). DEPC water was added to a volume of 50µl. β-actin was used as an internal control and sizes of the bands were determined using a 50bp DNA ladder (Invitrogen, UK). PCR was achieved on a PTC-225 (MJ

Research, UK) PCR machine and cycling parameters were as follows: 95°C (1 min – denaturation); 59°C (1 min – annealing); 72°C (1.5 min – elongation) for 35 cycles. A final step at 72°C for 10 minutes was used to allow annealing completion.

At the end of the PCR cycles, electrophoresis of the products on a 2% agarose ethidium bromide gel (using 1xTAE – 2.5mM EDTA, 40mM Tris Base and 0.1% acetic acid) was performed at 100V – gels were photographed using a dual intensity ultraviolet transilluminator coupled with camera (UVP, UK).

Genes	Primers	Sequences	Amplicons size (base pair)	Annealing temperature
BRCA1	BRCA1-forward	5'-TTGCGGGAGGAAAATG GGTAGTTA-3'	285bp	59°C
BRCA1	BRCA1-reverse	5'-TGTGCCAAGGGTGA ATGATGAAAG-3'		
β-actin	β-actin-forward	5'-GAGCACAGAGC CTCGCCTTTG-3'	636bp	59°C
β-actin	β-actin-reverse	5'-GGATCTTCATGAGG TAGTCAGTCAGG-3'		

Table 2.5 – Sequences and annealing temperature for each primer set used in the BRCA1 study (BRCA1 primer set originated from the paper published by Xian *et al.*, 2003, and the β-actin primer set from Kotecha *et al.*, 2003).

2.9 Real Time Polymerase Chain Reaction

2.9.1 Real Time PCR

This type of PCR is different from conventional PCR as it measures the formation of the PCR product as it is formed, using fluorescence emitted from the reporter dye on the probe (Figure 2.2). For that purpose, probes used are highly specific to the sequence amplified with the primer, and labelled with a quencher dye (TAMRA) and a reporter dye (6-FAM). Also, PCR products obtained must be of small size (50 to 150bp). Real Time PCR was performed using the ABI PRISM® 7000 Sequence Detection System (Perkin-Elmer Applied Biosystems, UK). Primers and probes (MWG Biotech, Germany) used are described in Table 2.6. Sequences were either obtained from the literature or designed (Appendix 2) using Primer Express® software (Applied Biosystem, UK). BLASTN search (www.ncbi.nlm.nih.gov) was conducted

in order to confirm the total gene specificity of the nucleotide sequences. Housekeeping gene β-glucuronidase (de Kok *et al.*, 2005) was purchased from Perkin-Elmer Applied Biosystems (UK) as a ready made mix of primers/probe.

PCR products verification

Primers were initially tested by reverse transcriptase PCR in order to ensure that a single product was amplified. This was performed as described previously in section 2.8 (no internal control, cycling parameters: 94°C 30 seconds, 60°C 30 seconds and 72°C 15 seconds for 45 cycles) with the primers described in Table 2.6 (annealing temperature during the real time PCR being 60°C). Part of the PCR product was analysed on a 2% agarose ethidium bromide gel (along with a 100bp DNA ladder) for a purity check and another part was used for TOPO TA cloning and sequencing.

As the small size of the PCR fragments did not allow for accurate sequencing, fragments had to be cloned into pCR®2.1-TOPO vector and amplified in competent cells. Cloning was carried out using TOPO TA cloning kit (Invitrogen, UK). Briefly, 2μl of PCR products were mixed with 1μl of salt solution, 2μl of water and 1μl of TOPO® vector (TA cloning is possible since Taq polymerase leave a 3' A overhang – no proofreading) to allow TA cloning for 5 minutes at room temperature. 2μl of this reaction was added to one vial of One shot® chemically competent (Invitrogen , UK) *Escherichia coli* (*E. coli*) for 15 minutes on ice. Cells were then heat shocked at 42°C for 30 seconds and 250μl of SOC medium was added. 40μl of the cells were plated on LB (Luria-Bertani) agar plates (Invitrogen, UK) containing 50μg/ml of ampicillin (Sigma-Aldrich, UK) and grown overnight at 37°C. As the sequence of interest was inserted in the lactose region of the plasmid, a blue/white selection was performed using blue/white select screening reagent (Sigma-Aldrich, UK). Colonies containing the plasmid with the insert appeared white. After selection, colonies were picked and grown overnight in 10ml of LB broth base (Lennox L Broth Base) medium (Invitrogen, UK) containing 50μg/ml of ampicillin (Sigma-Aldrich, UK), in 15ml falcon tubes at 37°C. Plasmids were finally extracted using the QIAprep Spin Miniprep kit (Qiagen, UK). Briefly, after harvesting the cells, 250μl of buffer P1 was added to resuspend the cells and 250μl of buffer P2 was added to lyse the cells. Then, 350μl of buffer N3 was added, creating precipitation, and the supernatant obtained by

centrifugation was applied onto QIAprep Spin columns and washed with 500µl of buffer PB. Finally, columns were washed with 750µl of buffer PE and plasmids were eluted in 50µl of DEPC water. Plasmids were sent to the Windeyer Institute of Medical Sciences for sequencing of the inserted PCR fragment, using M13 forward and reverse primers.

Real Time PCR

Once the PCR products were shown to match the desired gene sequence, primers were used in the real time PCR. To this end, 2.5µl of cDNA (synthesised as described in section 2.8.2) was mixed with 12.5µl of Taqman PCR master mix (Perkin-Elmer Applied Biosystem, UK), 1.25µl of β-glucuronidase primer/probe mix (Perkin-Elmer Applied Biosystem, UK), 0.5µl of probe specific to the gene amplified, 2.5µl of each primer (forward and reverse) of the gene of interest and DEPC water was added to a volume of 25µl. All reactions were performed in triplicate and included a water control reaction and a standard curve using a sample serially diluted (1/2, 1/5, 1/10, 1/20, 1/50, 1/100 – see section 2.9.2). Schematic representation of real time PCR is shown in figure 2.2. The amplification of the fragment was measured by the release of the reporter dye from the quencher (Figure 2.3 - Amplification plot). Cycling conditions used were as follows: 50°C 2 minutes (optimal AmpErase UNG enzyme activity), 95°C 10 minutes (activation of DNA polymerase), 40 cycles: 95°C for 15 seconds (strands separation) and 60°C 1 minute (annealing).

Genes / Accession number	Primers and probes	Sequences	Amplicons size (base pair)	Paper source
BRCA1 U14680	BRCA1 forward	5'-CAGAGGACAAT GGCTTCCATG-3'	81bp	Provided by Dr. Li (CRUK)
	BRCA1 reverse	5'-CTACACTGTCCA ACACCCACTCTC-3'		
	BRCA1 probe	5'(6-FAM)-CAGGTGCC TCACACATCTG CCCAATT-(TAMRA)3'		
ErbB2 M11730	ErbB2 forward	5'-GGATGTGCGG CTCGTACAC-3'	74bp	Designed
	ErbB2 reverse	5'-TAATTTTGACA TGGTTGGGACTCTT-3'		
	ErbB2 probe	5'(6-FAM)-CTTGGCC GCTCGGAACGT GC-(TAMRA)3'		
TOPO2α NM001067	TOPO2α forward	5'-ATTGAAGACGCT TCGTTATGGG-3'	96bp	Obtained from Dr. Kotecha (Oncology Dept - UCL)
	TOPO2α reverse	5'-GATGGATAAAAT TAATCAGCAAGCCT-3'		
	TOPO2α probe	5'(6-FAM)-CAGATCAGG ACCAAGATGGTTCCCAC ATC-(TAMRA)3'		

Table 2.6 – Primers, probes and number of cycles used for Real Time PCR. Primers and probe for ErbB2 gene have been designed using Primer Express (Perkin-Elmer Applied Biosystems). 6-FAM (6-carboxyfluorescein) being the reporter dye and TAMRA (N, N, N', N'-tetramethyl-6-carboxyrhodamine) the quencher dye. Details of the design of TaqMan probes and primers using Primer Express are in Appendix 2.

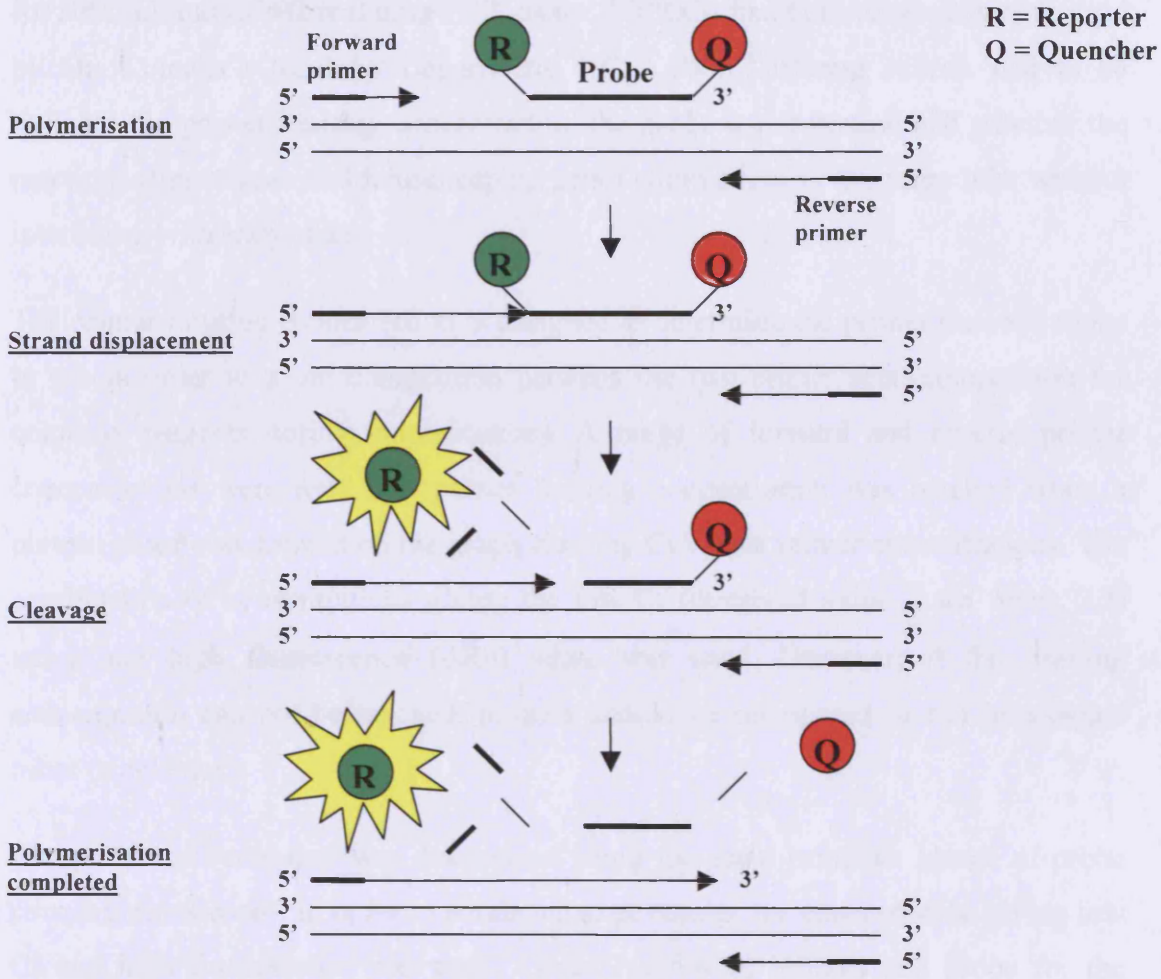

Figure 2.2 – Real Time PCR reaction: amplification of the fragment. When the target sequence is present, the probe anneals downstream from one of the primer sites and is cleaved by the 5' nuclease activity of Taq DNA polymerase as this primer is extended. Cleavage of the probe separates the reporter dye from quencher dye, increasing the reporter dye signal. Cleavage removes the probe, and primer extension continues to the end of the template strand. Thus, with fluorescent probes, non-specific amplification due to mis-priming or primer-dimer artifact does not generate signal. When two sets of primers / probes are used in the same reaction, probes must be labelled with different and distinguishable reporter dyes. Hence, amplification of two distinct sequences can be detected in a single PCR reaction (e.g. BRCA1 and β-glucuronidase).

2.9.2 Optimisation

Optimisation was mainly required to determine if reactions of the target gene and the internal control could be run in the same tube (multiplex). Optimisation was required for BRCA1 and ErbB2 real time PCR, as the TOPO2α had been previously optimised by Dr. Kotecha (Oncology Department, UCL, UK). Different criteria had to be defined: the primer limiting concentration, the probe concentration and whether the reactions (target gene and housekeeping gene) could occur in the same tube without interfering with each other.

The primer limiting concentration is designed to determine the primer concentrations to use in order to avoid competition between the two primer sets (competition for common reagents during amplification). A range of forward and reverse primer concentrations were used and primer limiting concentration was reached when a plateau phase was formed on the graph charting Ct versus primer concentrations. The combination of concentrations giving the low Ct (threshold value – see figure 2.3) value and high fluorescence (ΔRn) value was used. However, if the limiting concentration can not be reached, primers should be redesigned or run in separate tubes (singleplex).

The probe concentration was determined using the same principle (range of probe concentrations used). In order to obtain accurate results, the concentration giving low Ct and high fluorescence was used. Concentrations of primers and probe for the internal control β-glucuronidase (enzyme from the lysosome with hydrolase activity) did not need optimisation as these were purchased as a primer probe mix.

In order to compare multiplex and separate tube reactions, a relative standard curve (dilution of a sample set at a value of 1 – untreated control – is used to construct the standard curve: 1/2; 1/5; 1/10; 1/20; 1/50 and 1/100) was used. Reactions of the target gene and the housekeeping gene were carried out in the same tube if no interference occurred (distorsion of the fluorescence curve), and if the difference in efficiencies (see section 2.9.3) of the primer sets (for target and housekeeping genes) between the two methods (separate and same tube) was minimal (ABI, User Bulletin #2 and #5, 2001).

2.9.3 Results Analysis

Each run included a triplicate of the samples and a standard curve. Levels of BRCA1, ErbB2 and TOPO2α mRNA were expressed in relation to the reference housekeeping gene (gene regulating basic and ubiquitous cellular function and code) β-glucuronidase (exoglycosidase in lysosomes) as a ratio of target gene/housekeeping gene (all reactions were performed in triplicate). A new mathematical approach for quantification in real time PCR has been described by Pfaffl (2001). It is based on the relative expression ratio (R) of a target gene (BRCA1, ErbB2 or TOPO2α) versus an internal control (int. control) gene (β-glucuronidase):

$$R = \frac{E_{target}^{\Delta Ct_{target}}}{E_{int.control}^{\Delta Ct_{int.control}}} \quad \textbf{(1)}$$

Where $E = 10^{(-1/slope)}$ **(2)**

and $\Delta Ct_{target} = Ct_{target\ for\ reference} - Ct_{target\ for\ unknown}$ **(3)**

$\Delta Ct_{int.\ control} = Ct_{int.\ control\ for\ reference.} - Ct_{int.\ control\ for\ unknown}$ **(4)**

For all equations, Ct corresponds to the threshold cycle (see figure 2.3) which is defined as the fractional cycle number at which the fluorescence, generated by cleavage of the probe, passes a fixed threshold (defined by the user on the exponential phase of the fluorescence curve) above baseline (Bièche *et al.*, 1999). Hence, Ct is determined where the threshold crosses with the fluorescence curve and is read on the x axis (number of cycles). In equations **(3)** and **(4)**, reference is the sample of reference (i.e. wild type or untreated) and unknowns the samples which have an increased or decreased level of the target gene. Efficiencies (E) **(2)** for the target and the internal control are defined by the slope of the standard curve of the target and the internal control, respectively. For the relative standard curves, serial dilutions of the reference sample were used, in our studies: 1; 1/2; 1/5; 1/10; 1/20; 1/50; 1/100 (triplicate of each point). Hence, the quantification of the amount of target in an unknown sample is determined by measuring Ct and using the standard curve.

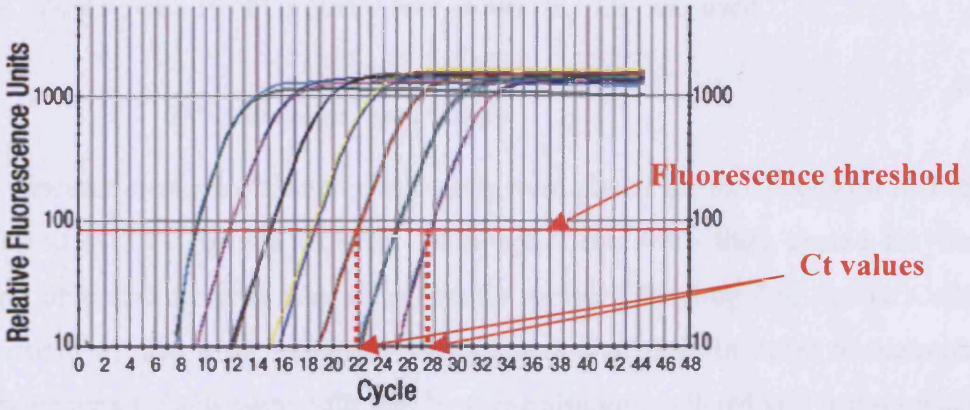

Figure 2.3 – Typical real time PCR amplification plot. Fluorescence signal versus cycle number, obtained with the standard curve serial dilutions – the figure shows the threshold cycle (determined by the user, anywhere on the exponential phase of the curves) and the Ct values read on the x axis (www.cambio.co.uk).

2.10 Single cell gel electrophoresis Comet assay

The comet assay was first developed as a method to measure DNA strand breaks at a single cell level (Ostling and Johanson, 1984). However, a modification of this assay has been shown to achieve sensitive detection of interstrand crosslinks (Hartley *et al.*, 1999; Spanswick *et al.*, 2002).

2.10.1 The Comet assay

Study of drug concentration on DNA damage level

Cells were plated at $10x10^4$cells/ml in $25cm^2$ flasks (Nunclon, VWR, UK) and incubated for 24 hours at 37°C in 5% CO_2. In order to analyse DNA damage and repair, cells were treated with the appropriate chemotherapeutic drug at a range of concentrations. Drugs were left in contact with the cells for a short period of time (1 to 2 hours according to the drug) and left to incubate in drug free media (if necessary), for DNA damage to reach its peak (e.g. 9 hours for cisplatin). From this, a fixed drug concentration was determined to treat the cell and observe the repair of drug-induced DNA damage. For strand breaks agents (such as etoposide), the drug concentration producing a tail moment (see section 2.10.2) of 10-12 was used. For

interstrand crosslink agents (such as melphalan or cisplatin), the drug concentration giving 50-70% decrease in tail moment (see section 2.10.2) was used.

DNA damage repair study

Once the concentration was selected, fresh cells were plated at $10x10^4$cells/ml in T25 and incubated at 37°C in 5% CO_2 for 24 hours. Cells were then treated for the appropriate time and the drug was subsequently replaced by drug free media. Cells were incubated in drug free media for various period of time in order to measure DNA damage repair. Cells were collected by trypsinisation, pelleted and resuspended in 1ml of foetal calf serum containing 10% DMSO, before to be stored at -80°C.

Assay methodology

When studying damage caused by a crosslinking agent, cells were thawed and resuspended in ice cold media to a concentration of $2.5x10^4$cells/ml. Those cell suspensions were divided into two samples, one of which being irradiated (12.5Gy) using an X-ray source (GEC Newton Victor X-ray machine 25kV) to deliver a fixed number of random DNA strand breaks (procedure carried out on ice), immediately before analysis. For strand breaking agents, cells were thawed and diluted to a concentration of $2.5x10^4$cells/ml without any irradiation.

In both cases, the following methodology was the same. All procedures were carried out on ice and in subdued light. Cells were embedded in 1% type VII agarose (Sigma-Aldrich, UK) (1ml of agarose + 0.5ml of cell suspension) on duplicate 1% type 1A agarose (Sigma-Aldrich, UK) pre-coated microscope slides. Cells were lysed, in the dark on ice, for one hour in ice cold lysis buffer (100mM disodium EDTA, 2.5M NaCl, 10mM Tris-HCl pH 10.5) containing 1% Triton X-100 (Sigma-Aldrich, UK) added fresh. Slides were subsequently washed every 15 minutes in ice cold distilled water for 1 hour. Slides were then incubated in ice cold alkali buffer (50mM NaOH, 1mM disodium EDTA, pH 12.5) for 45minutes followed by electrophoresis in the same buffer for 25 minutes at 18 V (0.6V/cm), 250mA. The slides were finally rinsed in neutralising buffer (0.5M Tris-HCl, pH 7.5) then saline (PBS). Slides left to dry overnight were re-hydrated for 20 minutes with distilled water and stained with

propidium iodide (2.5µg/mL) for 30 minutes (in the dark) then rinsed in distilled water. Finally, slides were left to dry in a drying oven and stored.

2.10.2 Data analysis

Images (illustrated in figure 2.4) were visualised using a NIKON inverted microscope with high-pressure mercury light source, 510-560nm excitation filter and 590nm barrier filter at x20 magnification. Images were captured using an on-line charge-couple device (CCD) camera and analysed using Komet Analysis software (Kinetic Imaging, Liverpool, U.K.). For each duplicate slide 25 individual cells were analysed. Tail moment for each cell was calculated using the Komet Analysis software as the product of the percentage DNA in the comet tail and the distance between the means of the head and tail distributions, based on the definition of Olive *et al.* (2002).

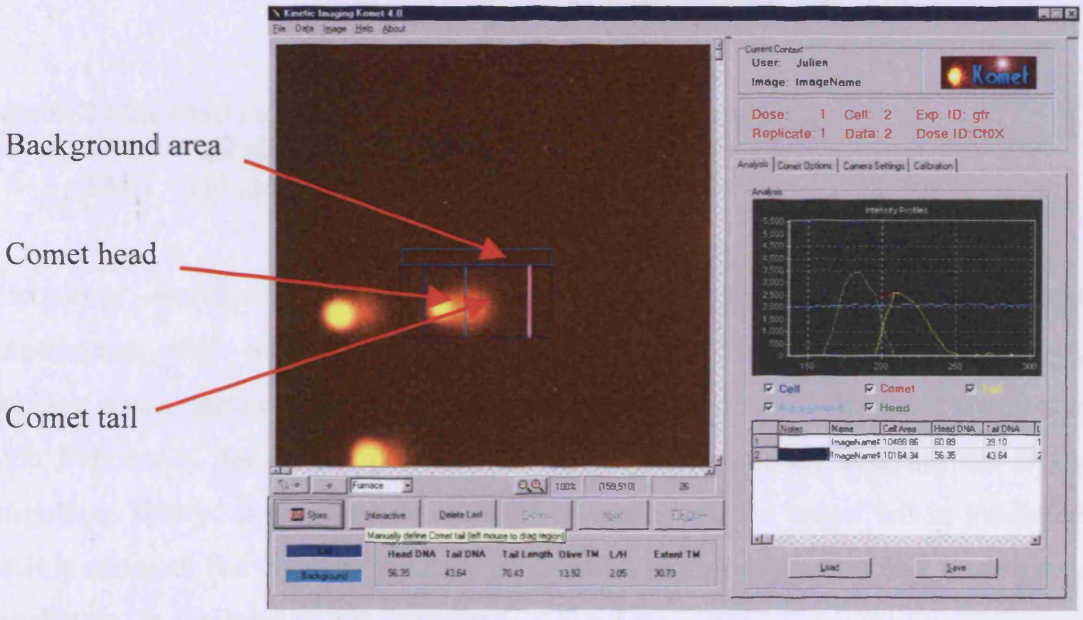

Figure 2.4 – Screen display of Komet analysis software. The figures shows untreated irradiated cells. Red arrows are showing the head and the tail of comet. The background is also taken into consideration by the software for calculation of the tail moment.

For strand breaks, tail moment data were analysed as a function of time post-incubation or drug concentration. Figure 2.5 illustrates the effect of etoposide after drug incubation. Data shown were the result of three independent experiments and included corresponding standard error bars.

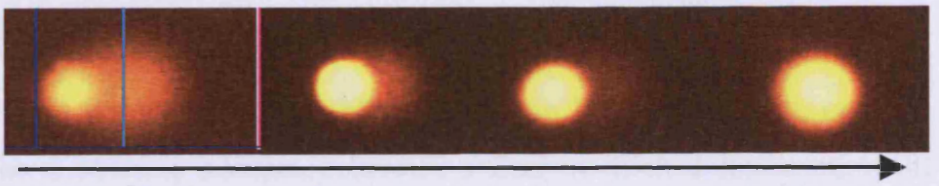

Time post-treatment (hours) 0 1 4 24

Figure 2.5 – Repair of DNA damage caused by etoposide treatment. Comet tail appears to be reduced as DNA strand breaks, caused by etoposide treatment, are repaired.

For crosslinking agents, results were expressed as percentage decrease in tail moment compared to untreated controls calculated by the following formula (tail moment was calculated from the same software as previously described):

$$\% \text{ decrease in tail moment} = \left[1 - \left(\frac{TMdi - TMcu}{TMci - TMcu} \right) \right] \times 100$$

where TMdi = tail moment of drug-treated irradiated sample
TMcu = tail moment of untreated, unirradiated control
TMci = tail moment of untreated, irradiated control

Percentage decrease in tail moment data were the result of three independent experiments, with corresponding standard error bars. Figure 2.6 represents DNA damage repair profile of irradiated cell treated with cisplatin. The short comet tail after 9 hours is due to the presence of interstrand crosslinks, delaying the DNA migration. Hence, as crosslinks are unhooked (repaired), the comet tail in irradiated cells is restored. For cisplatin the peak of crosslinking is observed after 9 hours post-incubation (for melphalan it is 16 hours).

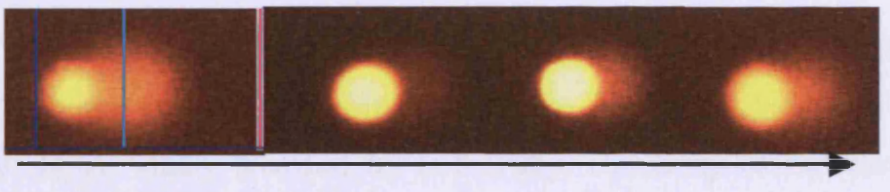

Time post-treatment (hours) 0 9 24 48

Figure 2.6 – DNA damage repair profile of irradiated cells treated with cisplatin. Cells were treated with cisplatin for 1 hour and subsequently incubated in drug-free media for various times. After 9 hours crosslinking reached its maximum (60-70% crosslinks) as the tail appears much shorter (crosslinks are causing the delay in DNA migration). At 24 and 48 hours, the unhooking (repair) of cisplatin crosslinks causes the comet tail to re-elongate.

2.11 Cisplatin intrastrand crosslink assay

Cisplatin intrastrand adducts represent 90% of cisplatin DNA damage. In order to determine the level of these adducts, competitive Enzyme-Linked ImmunoSorbant Assay (ELISA) method was used. This assay was developed by Tilby *et al.* (1987, 1991).

2.11.1 Methodology

DNA extraction

Prior to the assay 10ml of cells were plated in T25 at a concentration of $1x10^5$cells/ml. After drug treatment cells were pelleted and DNA was extracted using the DNeasy blood & tissue kit (Qiagen, UK). Briefly, cells were pelleted for 5 minutes at 300g at room temperature and cells were resuspended in 200µl of PBS and 20µl of proteinase K. 200µl of lysis buffer (AL) was added to the solution and vortexed for 10 seconds. The solution was incubated at 56°C for 10 minutes and 200µl of 100% ethanol was added before vortexing the solution for 10 seconds. The mixture was added onto a DNeasy mini spin column and centrifuge at 8,000rpm for 1 minute (supernatant was discarded). The column was then washed with 500µl of washing buffer (AW1) followed by a wash with 500µl of washing buffer (AW2) by centrifugation for 3 minutes at 14,000rpm. Finally, DNA was eluted with 200µl of AE buffer at 8,000rpm for 1 minute. DNA was quantified at 260nm using a NanoDrop® ND-1000 UV-Vis Spectrophotometer (NanoDrop, UK). DNA was stored at -20°C.

Competitive ELISA

High bind ELISA plates (Greiner, UK) were coated with 50µl of platinated DNA (denatured calf thymus DNA treated with cisplatin to give an adduct level of 25.5µmoles/g of DNA, kindly provided by M.J. Tilby, University of Newcastle) diluted 1 in 2,000 in high salt coating buffer (1M NaCl, 50mM sodium phosphate, pH 7.0). Plates were placed in a sealable box at 37°C, overnight.

On the following day ELISA wells were blocked with 150µl of blocking buffer (1% BSA in PBS w/v) for at least 30 minutes at room temperature. Samples were diluted in DB buffer (50mM NaCl, 50mM sodium phosphate, pH7.0), starting concentration

was determined by trial and error as it varies according to the level of cisplatin adducts. Samples and standards (one standard containing 801fmol of adduct/ml and another standard with 797fmol of adduct/ml, kindly provided by Dr. Tilby, University of Newcastle) were incubated for 5 minutes in boiling water to increase immunoreactivity, cooled on iced water and spun briefly. Samples and standard were serially diluted (one row = one sample) in a 96 well plate (Nunclon®, VWR, UK) in DB buffer. The monoclonal antibody CP9/19 (kindly provided by Dr. Tilby, University of Newcastle) was diluted 1 in 60,000 in PBS containing 0.2%BSA, 90mM sodium chloride, 0.2% Tween 20 and 0.2mg/ml phenol red. 55µl of this solution was mixed (30 minutes at 37°C) with 55µl of the serially diluted samples and standards to allow binding to intrastrand adducts. A low concentration of antibody is used in order to maximise the sensitivity of the assay. Each plate included four wells with no DNA (sample or standard) and no antibody for background measurement and wells with antibody but no DNA (100% fluorescence). ELISA plates were washed twice with PBS containing 0.1% tween 20 (PBS-Tween) and 50µl of the mix solutions were subsequently transferred into ELISA plates in duplicate wells and incubated for 1 hour at 37°C. Following five washes with PBS-Tween, 50µl of biotinylated anti-rat solution (biotinylated goat anti-rat – Sigma-Aldrich, UK – diluted at 1 in 2500 in 1% BSA, 0.2% Tween 20 and PBS) was added for 30 minutes at 37°C. Plates were washed three times with PBS-Tween and 50µl of β-galactosidase-streptavidin conjugate (Boehringer, UK) solution (β-galactosidase-streptavidin conjugate diluted at 1 in 10,000 in 1% BSA, 0.1% Tween 20, 10mM $MgCl_2$ and 2µl and PBS). Finally, after 30 minutes incubation at 37°C plates were washed seven times (PBS-Tween) and 50µl of substrate solution (PBS containing 80µg/ml 4-methyl-umbelliferyl-β-D-galactoside – Sigma-Aldrich, UK – and 10mM $MgCl_2$) was added to each well. Plates were placed in a sealable box, in the dark at room temperature, overnight.

2.11.2 Data analysis

Cleavage of 4-methyl-umbelliferyl-β-D-galactoside by β-galactosidase caused the release of fluorescent molecule 4-methylumbelliferone. Fluorescence was measured at 360nm excitation and 465nm emission, using a Spectrafluor Plus plate reader

(Tecan, UK). The mean background was substracted from all reading and the percentage of fluorescence (%FV) was calculated for each serial dilution (compared to the 100% fluorescence value). Data obtained were fitted to the logistic equation ($FV=MxC^s/(C^s+K^s)$)) as described by Tilby *et al.* (1987), and the 50% inhibition (K value) was determined using GraphPad Prism 4 software. A typical fitting curve, obtained with GraphPad Prism, is illustrated in Figure 2.7. The figure is showing the decrease of the fluorescence intensity as the concentration of adduct increases, a similar profile is obtained for the samples (reduction of fluorescence as DNA concentration increases). The choice of the initial DNA concentration in the samples is important as points on the curve must span the 50% inhibitory level so as to maximise the accuracy of the curve fitting to estimate the concentration of samples giving 50% inhibition.

Once the K values were calculated, the level of adduct was determined for each samples. In the case of the standards the K value corresponds to the level of adduct necessary to cause 50% reduction of assay signal this is then in femtomol (fmol) of cisplatin adduct per well (fmol Pt/well) as the concentration of cisplatin adducts is known. In the case of samples of DNA extracted from cells, these are the quantities of DNA per well (ng/well). Since reduction in assay signal is due only to cisplatin adducts (except at very high DNA concentrations, i.e. > 5 μg/well), the quantity of sample DNA that causes 50% reduction in signal must carry the same number of adducts that causes 50 % reduction of the signal in the standards. Results are expressed in moles of adducts per grams of DNA. E.g. If K value for samples = 50ng DNA per well and K value for standard = 2fmol Pt adduct per well, 50ng of DNA carries 2fmol of adduct. Thus 1 g DNA carries 40nmoles of adduct (40nmoles adduct/g DNA).

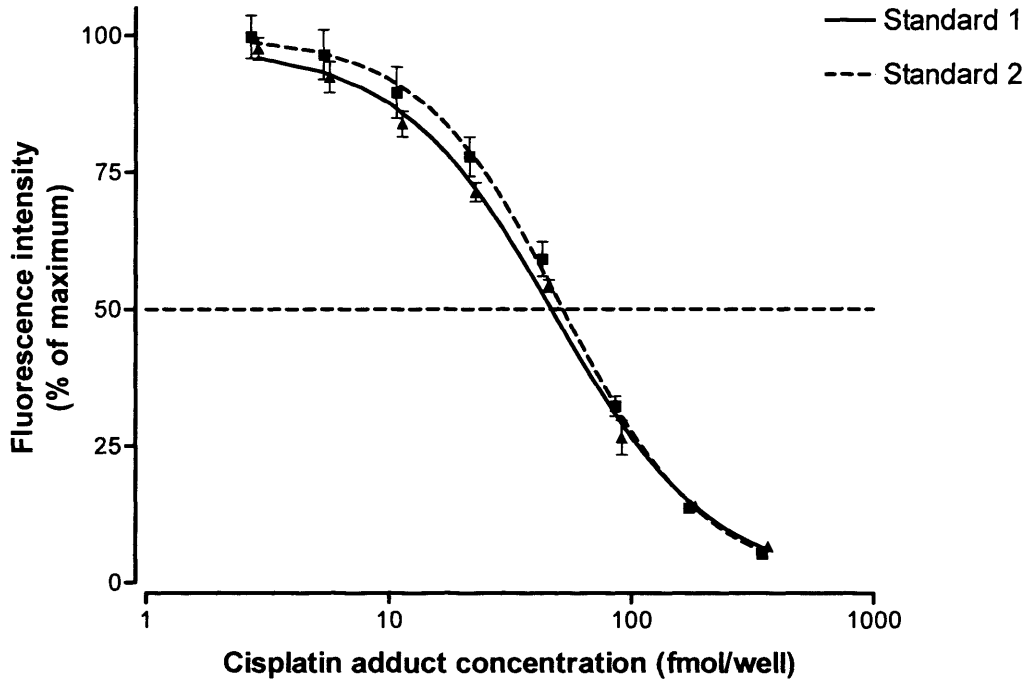

Figure 2.7 – Typical curve fitting for two standards obtained with GraphPad Prism 4. Points appear to span the 50% inhibitory level shown by the horizontal doted line. As the concentration in cisplatin adducts increases the fluorescence decreases (as adduct concentration increases the free antibody in solution is reduced).

2.12 Cell cycle analysis

Effect of drug treatment on cell cycle was studied using cytofluorimetry analysis.

2.12.1 Methodology

2ml of cells were plated at a concentration of $10x10^4$cells/ml in six well plates (Nunclon®, VWR, UK) and incubated at 37°C in 5%CO_2 for 24 or 48 hours prior to treatment. After treatment, media was collected in 5ml tubes and cells were washed with 0.5ml of cold PBS with 0.02% sodium azide (also collected). Cells were subsequently trypsinised (0.5ml of trypsin for 5 minutes at 37°C) and collected in the same tube. Each well was finally washed with 0.5ml of cold PBS azide (collected in the FACS tube). Cells were pelleted at 2,000rpm for 15 minutes at 4°C and supernatant was discarded. Cells were washed with PBS azide and spun at 2,000rpm for 5 minutes at 4°C. Supernatant was discarded and cells were fixed with 0.75ml of

cold 70% ethanol overnight. Samples were kept for up to a week at -20°C before staining.

Once collected and fixed, samples were spun at 2,000rpm for 5 minutes at 4°C. Supernatant was removed and cells were washed twice with 1ml of PBS with 0.01% azide. Cells were resuspended in 400µl of propidium iodide (PI) staining solution (0.05mg/ml of propidium iodide mixed with 0.5mg/ml of RNAse A and PBS azide to a volume of 35ml). Samples were incubated for 30 minutes at room temperature in the dark and placed on ice and analysed immediately.

2.12.2 Data analysis

Red fluorescence from PI staining was analysed with a Becton Dickinson FACscan (UK) cytofluorometer on the channel FL3. Gates were draw in order to only observe individual cells and eliminate clumped cells.

Data were analysed using WinMDI 2.8 and Cylchred software in order to quantify the number of cells in each phase of the cell cycle. Figure 2.8 represent a typical profile of normally cycling cells, with sub-G1, G1, S and G2 phases. Samples were taken at different time points to observe the evolution of the cell cycle with time (Figure 2.9).

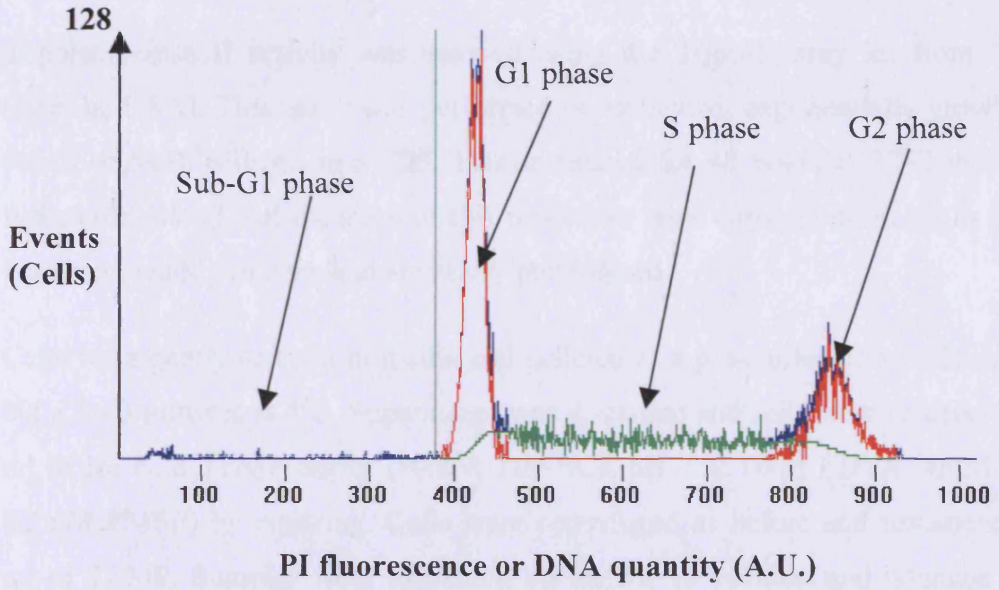

Figure 2.8 – Histogram profile showing the number of events in each phase versus DNA quantity. Arrows are pointing to the different phase of the cell cycle: Sub-G1 is in blue (on the left), G1 is the first peak in red, the S phase is represented in green and the last peak in red corresponds to the G2 phase. This figure was obtained from a screenshot of the Cylchred software.

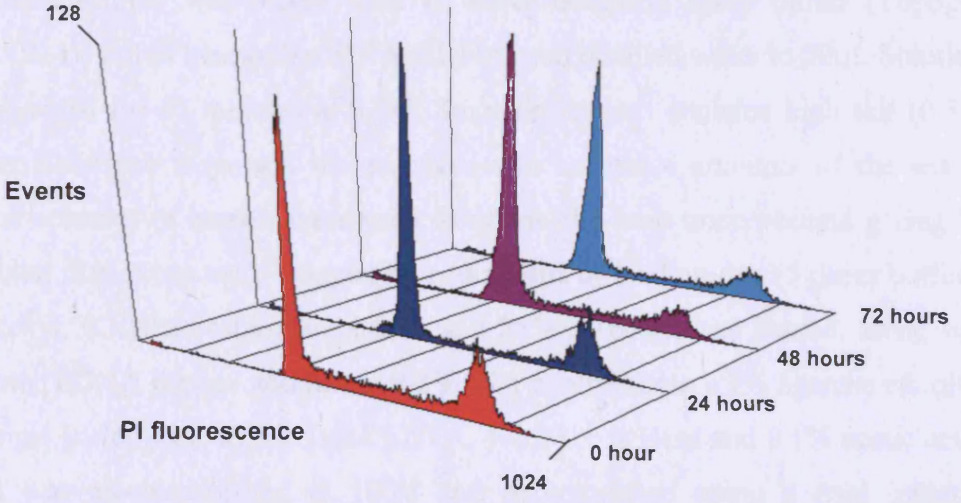

Figure 2.9 – Histogram profile obtained with WinMDI software. Untreated cells were collected every 24 hours. One event = one cell.

2.13 Topoisomerase II activity assay

Topoisomerase II activity was assayed using the TopoII assay kit from Topogen (Florida, USA). This assay was performed on untreated, exponentially growing cells (10ml of $5x10^4$cells/ml in a T25 flask incubated for 48 hours at 37°C in 5% CO_2, before the assay). All the steps of this procedure were carried out on ice as enzymes inactivate readily *in vitro* and are easily proteolysed.

Cells were gently scraped in media and pelleted in a pre-chilled 15ml falcon tube, at 800g for 3 minutes at 4°C. Supernatant was discarded and cells were resuspended in 4 ml of ice cold TEMP buffer (10mM Tris-HCl, pH 7.5, 1mM EDTA, 4mM MgCl2, 0.5mM PMSF) by pipetting. Cells were centrifuged as before and resuspended in 3 ml of TEMP. Samples were incubated on ice for 10 minutes and dounced in tight fitting homogeniser with eight strokes. Nuclei were pelleted at 1500g for 10 minutes at 4°C and subsequently resuspended in 1ml of ice cold TEMP buffer. Suspensions were transferred in an eppendorf tube and centrifuge at 4,000rpm for 2 minutes at 4°C. Supernatant was completely removed and pellets were resuspended in a small volume (no more than four pellet volumes) of TEP buffer (same as TEMP but lacking $MgCl_2$). An equal volume of 1M NaCl was added and solutions were vortexed for 5 seconds and incubated on ice for 45 minutes. Finally, suspensions were centrifuge at 15,000g for 15 minutes (at 4°C). The supernatant contains topo I and II activities. However, the kit used is specific of topisomerase II activity.

1µl of each sample was mixed with 10 times complete assay buffer (Topogen, Florida, USA), 2µl of kinetoplast DNA (kDNA) and distilled water to 20µl. Solutions were incubated for 45 minutes at 37°C. Since the extract contains high salt (0.5M) care was taken not to poison the reaction with excessive amounts of the extract (different volumes of extract were used to define the least toxic volume giving the best results). Reactions were stopped by adding 4µl of loading dye (5 times buffer is 5% sorkosyl, 0.125% bromophenol blue and 25% glycerol) and loaded, along with decatenated kDNA control and linearised kDNA control, onto a 1% agarose ethidium bromide gel (using 1xTAE – 2.5mM EDTA, 40mM Tris Base and 0.1% acetic acid). The gel was electrophoresed at 100V and photographed using a dual intensity ultraviolet transilluminator coupled with camera (UVP, UK).

2.14 Immunofluorescence

Exponentially growing cells were seeded in Labtek™ II chamber slides (Nunclon™, VWR, UK) at $2x10^4$cell/well (0.5ml per well). Cells were incubated in a humid box for 24 hours at 37°C in 5% CO_2, prior to treatment. At the end of the treatment, media was removed and wells were washed twice with cold PBS (0.5ml/well). Cells were fixed using cold 50% methanol/50% acetone solution (0.5ml/well) at 4°C for 8 minutes. Wells were then washed with cold PBS and 0.5ml of permeabilisation (0.5% Triton X-100 – Sigma-Aldrich, UK – in PBS) buffer was added for 5 minutes at room temperature. Wells were subsequently washed and 0.5ml of blocking buffer (0.2% skimmed dry milk, 0.1% Triton X-100 in PBS) was added overnight at 4°C. Three washes were performed with cold PBS. 200µl of the desired antibody (see Table 2.7) was added to each well, left overnight at 4°C, then washed three times with 0.1% Triton X-100 in PBS for 15 minutes. 200µl of FITC-labelled secondary antibody (Alexa fluor® 488 goat anti-rabbit IgG – see Table 2.7) was added for one hour in the dark. As before slides were washed three times for 15 minutes and counter-stained with 2µg/ml propidium iodide (PI) for 3 minutes. Slides were destained with distilled water for 20 minutes, mounted using VECTASHIELD® Mounting Medium H-1000 (Vector Labs, UK) and photographed using a LSM510 Axioplan 2 (Zeiss, UK) confocal microscope. Excitation wavelengths used were 488nm for the Alexa fluoro® and 543nm for PI.

Antibody	Colour under microscope and on pictures	Dilution	Supplier
Anti-ErbB1 (15F8)	Green	1/64	Cell Signaling, UK
Anti-ErbB2 (29D8)	Green	1/64	Cell Signaling, UK
Alexa fluor® 488 goat anti-rabbit IgG	Red	1/1000	Invitrogen, UK

Table 2.7 – Antibodies used for immunofluorescence experiments.

2.15 Small interfering RNA (siRNA) transfection

Small interfering RNA transfection was used in order to reduce the level of expression of the ErbB2 gene. siRNA sequences were obtained from the literature and synthesised by MWG Biotech. (Germany). The sequences are detailed in Table 2.8, and were transfected using RNAifect (Qiagen, UK) transfection reagent. Briefly, cells were plated out in 2ml (MCF-7 $1x10^5$ cells/well, SK-BR-3 $2x10^5$ cells/well and MD-MB-453 $5x10^5$ cells/well) in 6-well plates (Nunclon™, VWR, UK) 24 hours before transfection (time to reach 50% confluence). 5µg of siRNA was diluted in EC-R buffer (Qiagen, UK) to a volume of 100µl, then 15µl of RNAifect transfectant reagent was added to the diluted siRNA. The solutions were incubated for 15 minutes at room temperature. Media from the cells was removed and replaced by 1.9ml of complete media with no antibiotics, and the siRNA mix (115µl) was added dropwise. Cells were then incubated at 37°C in 5% CO_2. All siRNAs are 19-bp double stranded sequences with symmetric 3' overhangs of two deoxythymidines. Scrambled sequences have been determined using the siRNA design tool from Promega (www.promega.com). Total specificity of the siRNA sequences was confirmed by a BLASTN search (www.ncbi.nlm.nih.gov).

Transfected cells were collected every 24 hours over a period of 120 hours and cells were analysed by western blotting and real time PCR in order to observe the effect of siRNAs on protein and gene expression level.

Genes / Accession number	siRNA names	Coding Strands	Position on the gene	Paper source
ErbB2 M11730	ErbB2	5'-GGGGCUGGCUCCG AUGUAUTT-3'	3388 - 3406	Faltus T. *et al.*, 2004
	ErbB2 scrambled	5'-GCGCGUCGGGUGG UUACUATT-3'	Random sequence non specific of a gene	

Table 2.8 – ErbB2 siRNA sequences. Only the coding strand is shown (RNAi ordered as double stranded RNA sequences).

2.16 Stable transfection

2.16.1 Stable transfection of ErbB2 plasmids

Plasmids were obtained from Dr. Segatto (Regina Elena Cancer Institute, Italy) and Prof. Hung (MD Anderson Cancer Center, USA) as mentioned in section 2.1. In order to proceed to the transfection, plasmids were transformed and amplified in *Escherishia coli* (*E. coli*). The pcDNA3 plasmid (Invitrogen, UK) contains the ampicillin resistant gene and the pEGFP-N1 plasmid (Clontech, UK) the kanamycin resistant gene (illustrated in Figures 2.10 and 2.11), to assist selection after transformation.

Plasmids transformation and amplification

In order to transform the plasmids into *E. coli*, 100µl of TOP10F chemically competent *E. coli* (Invitrogen, UK) was mixed with 5µl of plasmid and incubated for 15 minutes on ice. Cells were heat shocked for 90 seconds at 42°C before incubation for 2 minutes on ice. 800µl of SOC medium was added and cells were pelleted for 6.5 minutes at 4,000rpm, at room temperature. Finally, 750µl of the supernatant was removed and the pellet was resuspended in the rest of the supernatant. Each transformed plasmid was plated on a pre-warmed LB (Luria-Bertani) agar plate (Invitrogen, UK), containing either 50µg/ml of ampicillin (Sigma-Aldrich, UK) or 30µg/ml of kanamycin (Sigma-Aldrich, UK) selective agent. Plates were incubated overnight at 37°C. After selection, colonies were picked and grown overnight in 10ml of LB broth base (Lennox L Broth Base) medium (Invitrogen, UK) containing 50µg/ml of ampicillin (Sigma-Aldrich, UK) or 30µg/ml of kanamycin (Sigma-Aldrich, UK), in an incubator shaker (37°C, 300rpm). Cells were harvested and plasmids were extracted (as previously described in section 2.9.1) using the QIAprep Spin Miniprep kit (Qiagen, UK) and quantified at 260nm using a NanoDrop® ND-1000 UV-Vis Spectrophotometer (NanoDrop, UK).

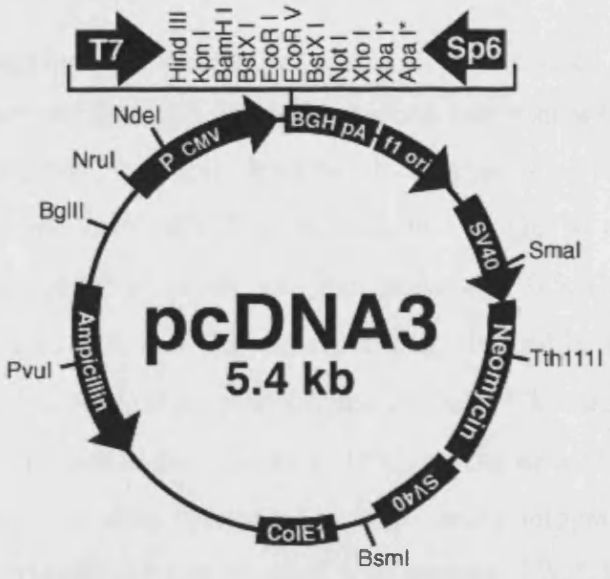

Figure 2.10 – pcDNA3 plasmid map. This plasmid carries the resistance gene ampicillin and neomycin. Unique restriction sites are indicated on the plasmid. (www.invitrogen.com).

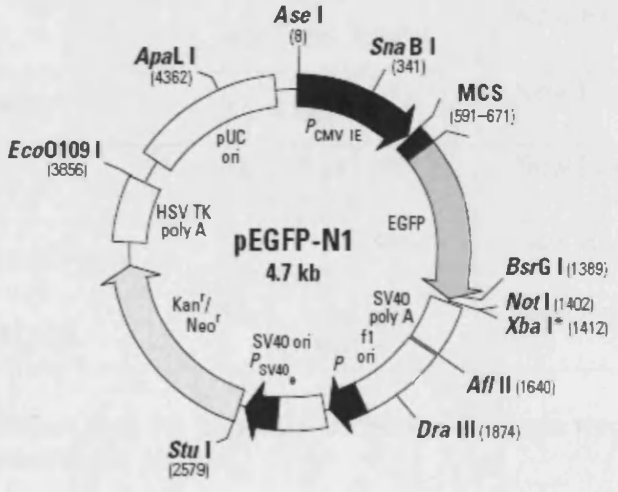

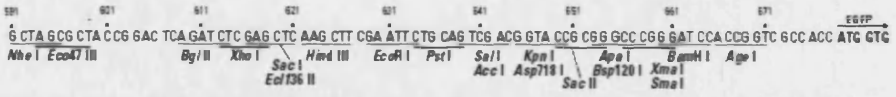

Figure 2.11 – pEGFP-N1 plasmid map. This plasmid carries the resistance gene kanamycin/neomycin. Unique restriction site are indicated on the plasmid and in the detailed MCS (Multiple Coning Site) sequence, shown below the plasmid map. (www.clontech.com).

Plasmids verification

After extraction, integrity and purity of the plasmids was checked. As plasmids have been previously described in the literature, restriction enzymes were used to confirm the inserts. pcDNA3-ErbB2 has been described by Tzahar *et al.* (1996) and pEGFP-N1-ErbB2 wild type and ErbB2ΔNLS were described by Giri *et al.* (2005). For the restriction reactions, 2µl of plasmids was incubated with 0.5µl of the appropriate enzyme (see Table 2.9), 1.5µl of the corresponding 10x buffer (supplied with the enzyme), 1µl of RNAse A at 30.3mg/ml (Sigma-Aldrich, UK) and distilled water to 15µl. Reactions were incubated for 2 hours at 37°C and run on a 1% agarose ethidium bromide gel. The gel was electrophoresed at 100V and photographed using a dual intensity ultraviolet transilluminator coupled with camera (UVP, UK). A 1Kb DNA ladder was used to determine the size of each fragment obtained. The expected sizes were as follow: ErbB2 ~ 4.4Kb; pcDNA3 ~ 5.4Kb; pEGFP-N1 ~ 4.7Kb; ErbB2ΔNLS ~ 3.7Kb; N-terminal part of ErbB2ΔNLS ~ 2.0Kb and C-terminal part of ErbB2ΔNLS ~ 1.7Kb.

Plasmid	Enzyme	Supplier
pcDNA3	XhoI and XbaI	New England Biolabs, UK
pcDNA3-ErbB2	XhoI and XbaI	New England Biolabs, UK
pEGFP-N1	NheI, AgeI and HindIII	New England Biolabs, UK
pEGFP-N1 ErbB2 wild type	NheI, AgeI and HindIII	New England Biolabs, UK
pEGFP-N1 ErbB2ΔNLS	NheI, AgeI and HindIII	New England Biolabs, UK

Table 2.9 – List of enzymes used for plasmids restriction. Enzymes were chosen according to the position of the insert on the plasmid.

Plasmids transfection

Transfection was achieved using GeneJuice® transfection reagent (Novagen® EMD Biosciences Darmstadt, Germany). Exponentially growing MDA-MB-468 cells were plated in 6 well plates (Nunclon™, VWR, UK) at a concentration of $2x10^5$cells/ml (2ml per well), without any antibiotics and incubated for 24 hours at 37°C (5% CO_2). 3µl was vortexed with 100µl of DMEM FCS free and incubated for 5 minutes in an

eppendorf. 1μg of plasmid was added to the solution and incubated at room temperature for 15 minutes. Media from the plates was removed and replaced by fresh complete media with no antibiotics. Each plasmid/GeneJuice mixture was added dropwise to one well. Cells were incubated at 37°C (5% CO_2) until confluence. Cells were subsequently trypsinised (0.5ml of trypsin) and pelleted before being plated in T25 flasks with media containing antibiotics and selective agent G418 (Sigma-Aldrich, UK). Transfected cells were incubated for 3 to 4 weeks to allow clones to grow (media was regularly changed to keep selective pressure). All the clones used were grown as stable transfected cell lines, maintaining selective pressure in the media.

2.16.2 Plasmids encoding specific human BRCA1 siRNA

DNA-directed RNA interference was used to reduce expression of BRCA1 gene. To this end, the MCF-7 cell line was stably transfected with a plasmid encoding specific human BRCA1 siRNA provided by Dr. C. Lord from the Institute of Cancer Research (UK). MCF-7 3.23 cells were transfected with a pSUPER-eCFP plasmid expressing siRNA directed against BRCA1 (BRCA1 siRNA sequence: 5'-GGAACCTGTCTCCACAAAG-3') and MCF-7 scrambled was transfected with the same plasmid but expressing a control sequence (Control siRNA sequence: 5'-CATGCCTGATCCGCTAGTC-3') which does not recognise any human gene. In order to maintain selective pressure, for stable transfection, cells were grown with media containing blasticidin (Invivogen, UK). Stably transfected cell lines were subsequently analysed to assess the effect of the siRNA on protein and gene expression.

2.17 Drug treatments

Prior to drug treatment, cells were seeded in flasks, 96 or 6 well plates and incubated at 37°C in 5% CO_2 for 24 to 48 hours. Cells were then treated at a range of concentrations and lengths of exposure (Table 2.10). Concentrations varied according to the sensitivity of the cell lines. Appropriate schedules were used for the different experiments, as outlined in the methods detailed previously.

Compounds	Lengths of exposure	Range of concentrations
Gefitinib	24 hours or continuously	0 – 50μM
Etoposide	2 hours for Comet assays and continuously for SRB assay	0 – 250μM
Melphalan	1 hour for Comet assay and continuously for SRB assay	0 – 250μM
Doxorubicin	Continuously for SRB assay	0 – 1μM
Paclitaxel	Continuously for SRB assay	0 – 100nM
Cisplatin	Continuously for SRB assay and 1 hour for all other assays	0 – 250μM
Trastuzumab	1 to 72 hours to determine the effect on ErbB2 level (western Blot) and continuously for all other assays	0 – 100μg/ml
Wheat germ agglutinin (WGA)	Continuously for SRB assay and 1.5hours for all other assays	0 – 100μg/ml

Table 2.10 – Range of concentrations and lengths of exposure for drugs used in the different experiments. The ranges of concentration indicated in the table reflect the minimum and maximum concentrations used.

Chapter 3

Modulation of the repair of drug-induced DNA damage by ErbB2 inhibition

INTRODUCTION

Overexpression of ErbB2 tyrosine kinase receptor occurs in approximately one third of breast cancer cases and has been shown to be important in the development of this disease (Harari and Yarden, 2000). There has been an increasing interest in studying its function in breast cancer development and its role and interactions within the EGF receptor family (EGFR; ErbB2; ErbB3; ErbB4). Furthermore, ErbB2 overexpression has been related to poor prognosis in cancer patients due to factors including increased proliferation rate (Harari and Yarden, 2000).

3.1 Trastuzumab and ErbB2 protein expression

Currently, trastuzumab (Herceptin®) is the only approved therapy specifically targeting ErbB2. Trastuzumab is a monoclonal antibody which has been reported to have successful therapeutic effects on malignant cell lines and xenografts with overexpressed ErbB2 levels. Its therapeutic effects involve receptor phosphorylation (Yarden, 1990), receptor internalisation (Yarden, 2001b), inhibition of ectodomain cleavage (Molina *et al.*, 2001), decrease in heterodimerisation (Emens and Davidson, 2004) and in some cases down-regulation of receptor expression (Guan *et al.*, 2005). Nevertheless, some conflicting studies have shown no cell surface ErbB2 down-regulation in tumour cells (Lane *et al.*, 2000; Nahta *et al.*, 2004). These events result in decreased cell proliferation.

Furthermore, by causing ErbB2 degradation, trastuzumab has been shown to lead to inhibition of the downstream PI3K and MAPK signalling cascades (Sliwkowski *et al.*, 1999; Lane *et al.*, 2000), G1 arrest through modulation of $p27^{kip1}$ (Sliwkowski *et al.*, 1999), induction of apoptosis and inhibition of angiogenesis (Izumi *et al.*, 2002). Trastuzumab monotherapy also proved successful clinically, as several studies (Baselga *et al.*, 1996 and 2005; Cobleigh *et al.*, 1999) have shown that it is well tolerated and clinically active in ErbB2 overexpressing metastatic breast cancer and causes tumour regression.

3.2 Trastuzumab and chemotherapeutic agents

Trastuzumab has also been studied, *in vitro* and *in vivo*, in combination with chemotherapeutic agents, in ErbB2 overexpressing cells. Hancock *et al.* (1991) and Pietras *et al.* (1994) demonstrated that anti-ErbB2 antibodies were able to potentiate the cytotoxicity of cisplatin by altering the DNA repair activity of the cells. In addition, Pietras *et al.* (1994) also established that the interaction between cisplatin and an anti-ErbB2 antibody (4D5), causing the inhibition of ErbB2 overexpressing cells, was synergistic. More recently, several studies (Pegram and Slamon, 1999; Pegram *et al.*, 2004a; Naruse *et al.*, 2002) have reported the synergistic effect between anti-ErbB2 antibodies, such as trastuzumab, and carboplatin, cisplatin, docetaxel or vinorelbine. Pegram *et al.* (2004a) also obtained synergistic or additive effects, in xenografts, between anti-ErbB2 antibody and chemotherapeutic agents, such as alkylating agents, platinum analogs and topoisomerase II inhibitors, demonstrating rational combinations for human clinical trials. Furthermore, in this study they also established that synergistic effect was obtained using a three-drug combination of trastuzumab, carboplatin and docetaxel together, at very low dose. This finding was further confirmed by a clinical trial (Pegram *et al.*, 2004b) showing that the three-drug combination leads to a higher response rate and a slower progression of the disease. Other clinical trials have also been carried out, investigating the combination of trastuzumab with paclitaxel (Seidman *et al.*, 2001; Slamon *et al.*, 2001) or docetaxel (Esteva *et al.*, 2002), demonstrating an increased response rate and a reduced progression of the disease compared to the monotherapy. However, many patients develop trastuzumab resistance after initial response. Therefore, in order to improve patient survival a better understanding of the molecular mechanisms of action and resistance of trastuzumab, as well as identifying more effective combinations, is necessary.

3.3 Trastuzumab and DNA damage repair

Although enhancement of the cytotoxicity of chemotherapeutic agents was suggested to be due to an inhibition of DNA damage repair, only a few studies have investigated the effect of trastuzumab on the kinetics of DNA damage formation and repair. Studies by Pietras *et al.* (1994 and 1999) have established that trastuzumab caused a

reduction of the DNA repair ability of tumour cells, by measuring unscheduled DNA synthesis. Those studies have shown that combining the anti-ErbB2 antibody with radiation or cisplatin, led to a decrease in unscheduled DNA synthesis compared to the treatments with cisplatin or radiation alone.

However, unscheduled DNA synthesis analysis, based on the replication of DNA during the excision repair of certain types of DNA lesions, as demonstrated by the incorporation of tritiated thymidine into the DNA repair sites, requires the use of radioactivity, has a limited sensitivity and is a non-specific assay. In contrast, single cell gel electrophoresis, used in this study, is a very sensitive method to detect low levels of DNA damage, requires a small number of cells, can be used *in vitro* and *in vivo* and requires a short time period to complete the experiment (Tice *et al.*, 2000). Therefore, a more extensive investigation of the modulation of the repair of drug-induced DNA damage by ErbB2 inhibition was required, using the comet assay.

3.4 Aims

This chapter investigated the effect of ErbB2 inhibition on drug sensitivity and repair of DNA damage. Three breast cancer cell lines having been described in the literature as having different level of ErbB2 protein (Moasser *et al.*, 2001), were used: MCF-7, MDA-MB-453 and SK-BR-3 cells. In order to study the effect of ErbB2 expression on drug-induced DNA damage response, the following questions have been addressed:

- How does trastuzumab affect ErbB2 protein expression and cell proliferation?
- Does trastuzumab enhance the cytotoxic effect of chemotherapeutic drugs?
- Does trastuzumab modulate the kinetics of formation and repair of drug-induced DNA damage?

However, as a starting point for this investigation, the normal protein expression level of each EGF receptor was identified for each cell line studied.

RESULTS

3.5 EGF receptor protein expression

The level of expression of EGFR (ErbB1), ErbB2, ErbB3 and ErbB4 was determined by western blotting from total protein lysate of exponentially growing cells. Figure 3.1 shows that ErbB2 is overexpressed in SK-BR-3 and MDA-MB-453 cell lines, whereas ErbB2 is detectable but not overexpressed in MCF-7 cells.

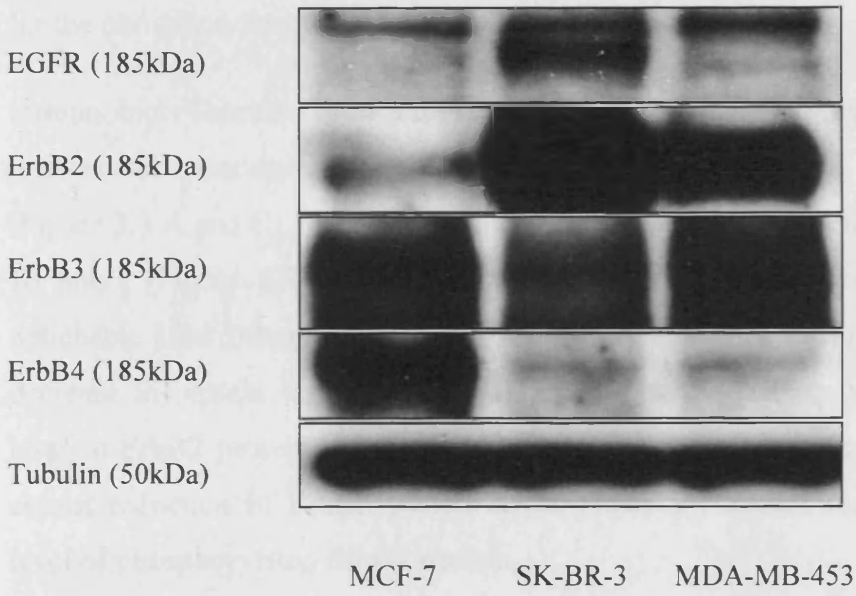

Figure 3.1 – Western blotting of each EGF receptor in MCF-7, SK-BR-3 and MDA-MB-453 cell lines. α-tubulin was used as a loading control.

3.6 Effects of trastuzumab treatment

In order to investigate the effect of ErbB2 inhibition on DNA damage repair, effects of trastuzumab on the ErbB2 protein level and on cell proliferation were assessed.

3.6.1 Down-regulation of ErbB2 by trastuzumab

ErbB2 expression was assessed by immunoblotting after treating the cells continuously with a range of trastuzumab concentrations (0-30μg/ml). Figures 3.2, 3.3 and 3.4 represent the immunoblots obtained after 1 hour, 16 hours and 24 hours, respectively, of trastuzumab treatment for all three cell lines. Blots were also probed for the phosphorylated form of ErbB2 (pErbB2).

Immunoblots obtained show a reduction of ErbB2 protein expression after 16 hours at trastuzumab concentrations above 0.3μg/ml, for MCF-7 and MDA-MB-453 cells (Figure 3.3 A and C). For SK-BR-3, a reduction of ErbB2 protein level was seen after 16 hours (Figure 3.3 B) with 3μg/ml of trastuzumab. However, the fall is more noticeable after 24hours (Figure 3.4 B), with 0.3μg/ml of trastuzumab. To detect the decrease in protein level, in SK-BR-3 cells, short exposures were required, as the level in ErbB2 protein in extremely high. Hence, in all three cell lines, trastuzumab causes reduction of ErbB2 protein level. However, trastuzumab did not affect the level of phosphorylated ErbB2 protein.

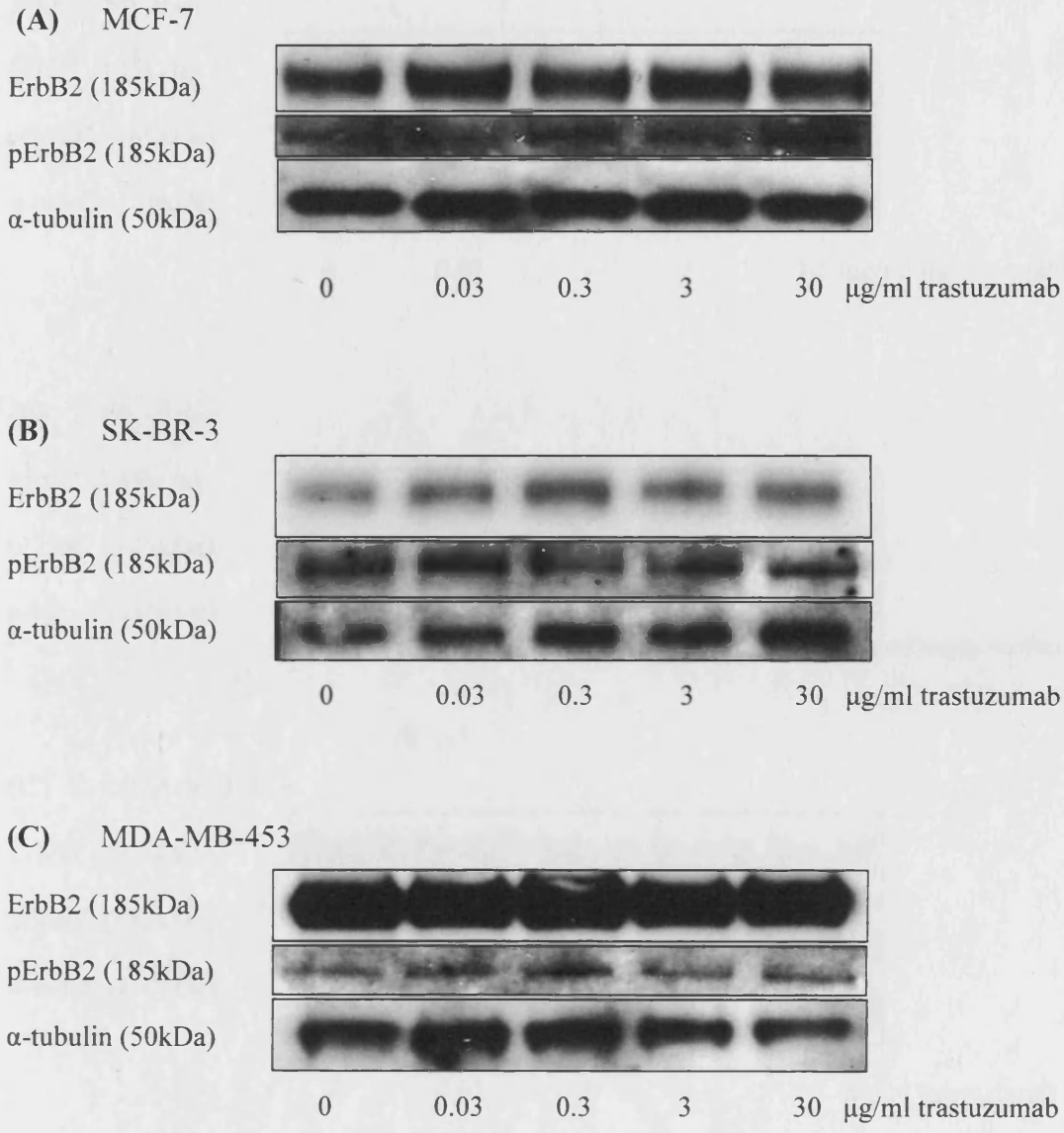

Figure 3.2 – Immunoblots of ErbB2 and pErbB2 in MCF-7, SK-BR-3 and MDA-MB-453 cell lines treated with trastuzumab for 1 hour. MCF-7 (**A**), SK-BR-3 (**B**) and MDA-MB-453 (**C**) cells were exposed to a range of trastuzumab concentrations (0-30μg/ml) for 1 hour. α-tubulin was used as a loading control.

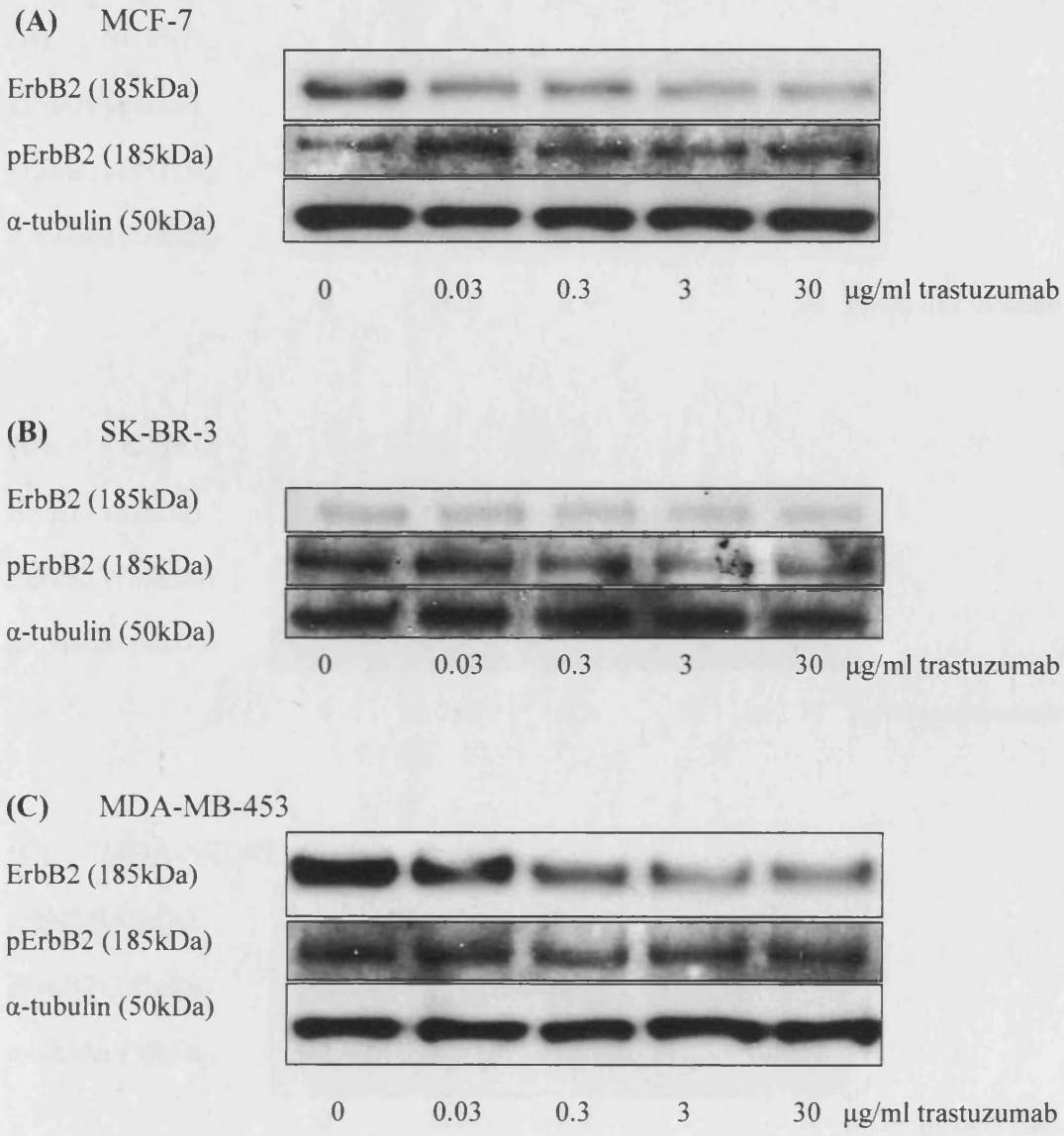

Figure 3.3 – Immunoblots of ErbB2 and pErbB2 in MCF-7, SK-BR-3 and MDA-MB-453 cell lines treated with trastuzumab for 16 hours. MCF-7 (**A**), SK-BR-3 (**B**) and MDA-MB-453 (**C**) cells were exposed to a range of trastuzumab concentrations (0-30μg/ml) for 16 hours. α-tubulin was used as a loading control.

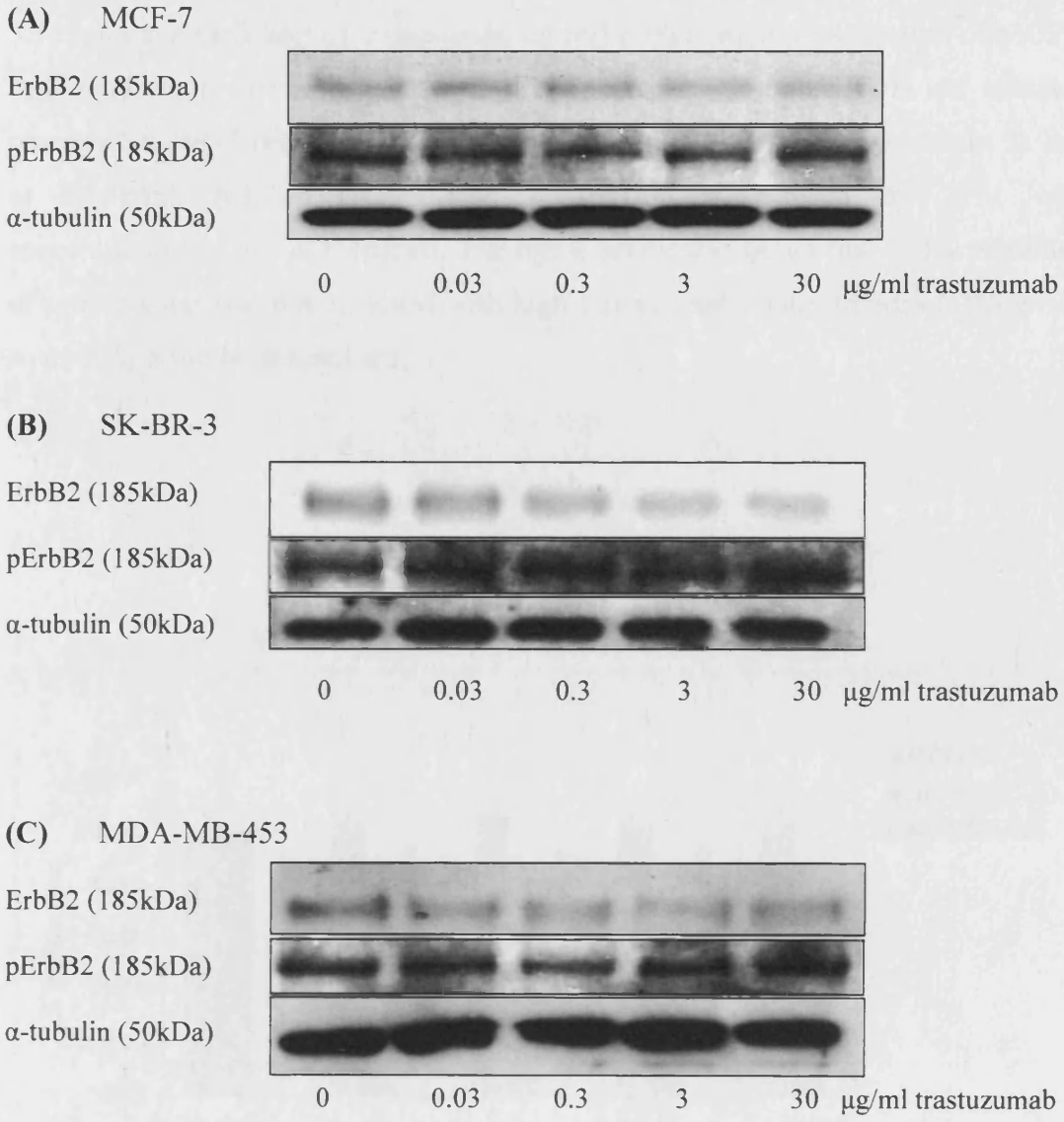

Figure 3.4 – Immunoblots of ErbB2 and pErbB2 in MCF-7, SK-BR-3 and MDA-MB-453 cell lines treated with trastuzumab for 24 hours. MCF-7 (**A**), SK-BR-3 (**B**) and MDA-MB-453 (**C**) cells were exposed to a range of trastuzumab concentrations (0-30μg/ml) for 24 hours. α-tubulin was used as a loading control.

3.6.2 Inhibition of cell proliferation by trastuzumab

Having shown the reduction of total ErbB2 protein level after continuous exposure to trastuzumab, its effects on cell proliferation was studied using the SRB assay. Figure 3.5 represents the effect of trastuzumab on cell proliferation. Proliferation of MCF-7 cells (expressing the lowest level of ErbB2 protein – Figure 3.1) is not affected, whereas SK-BR-3 cells proliferation is reduced by 40%, with concentrations as low as 0.1µg/ml. MDA-MB-453 cells proliferation is reduced by 20%, with concentrations as low as 0.1µg/ml. The figure below also shows that >50% inhibition of proliferation was not achieved with high trastuzumab concentrations (100µg/ml), so no IC_{50} could be determined.

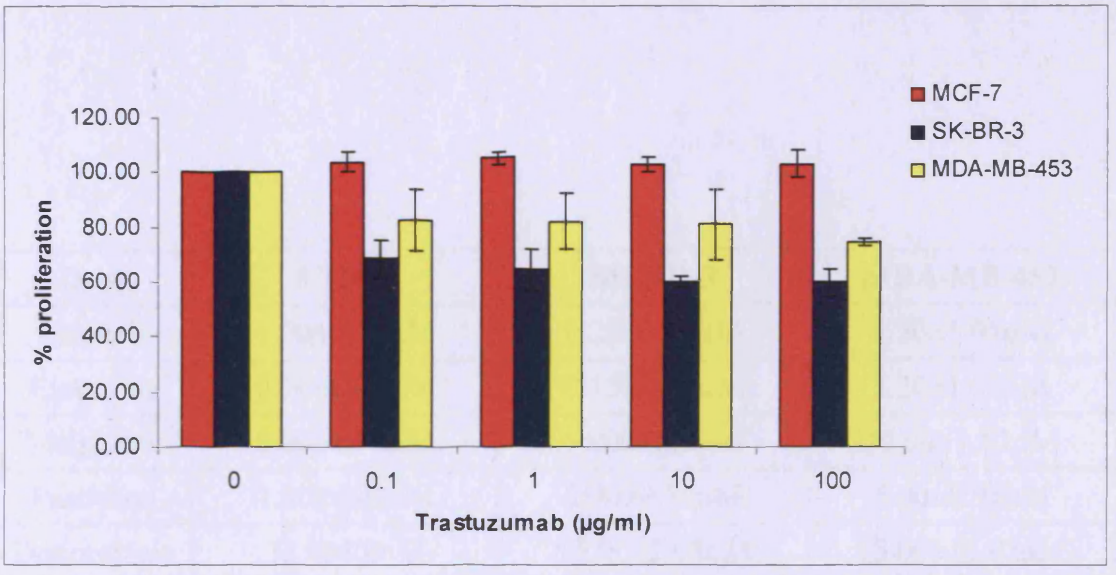

Figure 3.5 – Inhibition of cell proliferation by trastuzumab in MCF7, SK-BR-3 and MDA-MB-453 cells. MCF-7 (red), SK-BR-3 (blue) and MDA-MB-453 (yellow) cells were treated continuously for 5 days with a range of trastuzumab concentrations. This result is the average of triplicate experiments (standard deviation indicated on the figure).

3.7 Trastuzumab and chemotherapeutic treatments

3.7.1 Determination of IC_{50} of common chemotherapeutics

Several studies have reported an enhanced activity, *in vitro* and in xenograft models, of chemotherapeutic drugs when used in combination with trastuzumab (Pegram *et al.*, 2004a; Baselga *et al.*, 1998). Using the SRB assay, the effects of cisplatin, etoposide, melphalan, doxorubicin and paclitaxel were investigated as single agents. All cells were incubated for 5 days with the drugs, at a range of concentrations, in triplicate wells. To assure accuracy and reproducibility, all assays were repeated in triplicate. Inhibition of proliferation caused by each drug is represented in Figure 3.6 and results for the 50% growth inhibition (IC_{50}) are presented in Table 3.1. IC_{50} values in Table 3.1 show that SK-BR-3 cells are the most sensitive to all chemotherapeutic drugs used (except for paclitaxel) compared to the other cell lines. Therefore, the ErbB2 protein expression level could not be associated with an increased chemoresistance.

Drug	MCF-7	SK-BR-3	MDA-MB-453
Cisplatin	1.00±0.16μM	0.25±0.05μM	2.50±1.01μM
Etoposide	0.70±0.02μM	0.15±0.05μM	5.20±1.07μM
Melphalan	8.00±1.76μM	5.00±1.42μM	15.00±1.53μM
Paclitaxel	1.80±0.42nM	2.90±0.30nM	5.00±0.91nM
Doxorubicin	32.0±8.0nM	15.00±2.08nM	75.00±11.02nM

Table 3.1 – IC_{50}±SD results after single agent treatment in MCF-7, SK-BR-3 and MDA-MB-453 cells. Cells were treated continuously for 5 consecutive days.

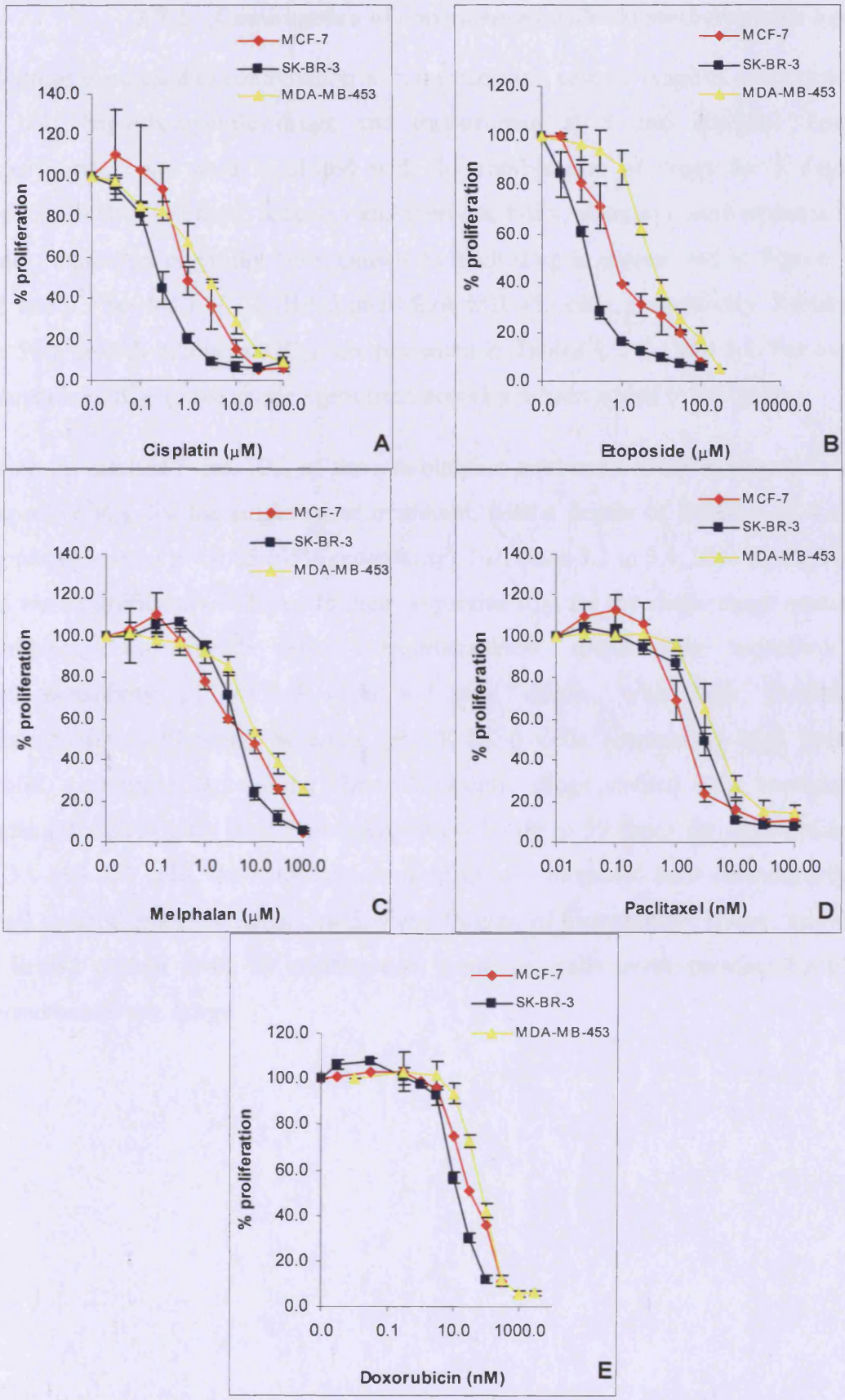

Figure 3.6 – Inhibition of MCF-7, SK-BR-3 and MDA-MB-453 cell proliferation after single agent treatment. MCF-7 (♦), SK-BR-3 (■) and MDA-MB-453 (▲) cells were treated for 5 consecutive days with cisplatin (**A**), etoposide (**B**) melphalan (**C**), paclitaxel (**D**) or doxorubicin (**E**). Experiments have been repeated in triplicate.

3.7.2 Combination of trastuzumab with chemotherapeutic agents

All drugs were used in combination with trastuzumab, using a range of concentrations of the chemotherapeutic drugs and trastuzumab at 3 and 20μg/ml. For all experiments, cells were incubated with the combination of drugs for 5 days, in triplicate wells. To ensure accuracy and reproducibility, all assays were repeated three times. Inhibition of proliferation caused by each drug is represented in Figures 3.7, 3.8 and 3.9 for MCF-7, SK-BR-3 and MDA-MB-453 cells, respectively. Results for the 50% growth inhibition (IC_{50}) are presented in Tables 3.2, 3.3 and 3.4. For ease of comparison, IC_{50} of the single agent treatments have been added to the tables.

Using the student *t*-test, IC_{50} of the combination treatments were compared to their respective IC_{50} for the single agent treatment, with a degree of freedom of 4 and a significance level $p = 0.05$ (95% probability). In Tables 3.2 to 3.4, IC_{50} highlighted in red were significantly different to their respective IC_{50} for the single agent treatment. Combining trastuzumab with chemotherapeutic drugs only increased the chemosensitivity of MCF-7 cells to some agents, with high trastuzumab concentrations (20μg/ml), whereas for SK-BR-3 cells (expressing high level of ErbB2) combining any of the chemotherapeutic drugs studied with trastuzumab, increased significantly their chemosensitivity, by up to 50 times for doxorubicin. In MDA-MB-453 cells, the combination of drugs also increased their chemosensitivity to all chemotherapeutic agents used, with 20μg/ml of trastuzumab. Hence, inhibition of ErbB2 protein level, by trastuzumab, sensitised cells overexpressing ErbB2 to chemotherapeutic drugs.

Drug	IC_{50} (single agent)	IC_{50} (combination with trastuzumab 3µg/ml)	IC_{50} (combination with trastuzumab 20 µg/ml)
Cisplatin	1.00±0.16µM	1.10±0.67µM	1.40±0.35µM
Etoposide	0.70±0.02µM	0.70±0.15µM	0.41±0.19µM
Melphalan	8.00±1.76µM	7.00±2.08µM	4.00±1.32µM
Paclitaxel	1.80±0.42nM	1.10±0.38nM	0.90±0.15nM
Doxorubicin	32.00±8.00nM	24.00±6.66nM	21.00±7.00nM

Table 3.2 – IC_{50}±SD results for MCF-7 cells after single agent treatment and combination treatments. Cells were treated with the combination of drugs for 5 consecutive days. IC_{50} highlighted in red were significantly different to their respective IC_{50} for the single agent treatment (Student *t*-test, degree of freedom = 4 and significance level $p = 0.05$).

Drug	IC_{50} (single agent)	IC_{50} (combination with trastuzumab 3µg/ml)	IC_{50} (combination with trastuzumab 20 µg/ml)
Cisplatin	0.25±0.05µM	0.02±0.01µM	0.02±0.01µM
Etoposide	0.15±0.05µM	0.02±0.01µM	0.02±0.01µM
Melphalan	5.00±1.42µM	1.10±0.70µM	0.07±0.04µM
Paclitaxel	2.90±0.30nM	0.90±0.46nM	0.46±0.09nM
Doxorubicin	15.00±2.08nM	0.30±0.06nM	0.85±0.20nM

Table 3.3 – IC_{50}±SD results for SK-BR-3 cells after single agent treatment and combination treatments. Cells were treated with the combination of drugs for 5 consecutive days. IC_{50} highlighted in red were significantly different to their respective IC_{50} for the single agent treatment (Student *t*-test, degree of freedom = 4 and significance level $p = 0.05$).

Drug	IC_{50} (single agent)	IC_{50} (combination with trastuzumab 3µg/ml)	IC_{50} (combination with trastuzumab 20 µg/ml)
Cisplatin	2.50±1.01µM	1.80±1.23µM	0.40±0.15µM
Etoposide	5.20±1.07µM	1.90±1.11µM	0.08±0.01µM
Melphalan	15.00±1.53µM	13.00±3.51µM	2.50±0.47µM
Paclitaxel	5.00±0.91nM	1.00±0.90nM	1.00±0.21nM
Doxorubicin	75.00±11.02nM	12.00±2.00nM	11.0±1.00nM

Table 3.4 – IC_{50}±SD results for MDA-MB-453 cells after single agent treatment and combination treatments. Cells were treated with the combination of drugs for 5 consecutive days. IC_{50} highlighted in red were significantly different to their respective IC_{50} for the single agent treatment (Student *t*-test, degree of freedom = 4 and significance level $p = 0.05$).

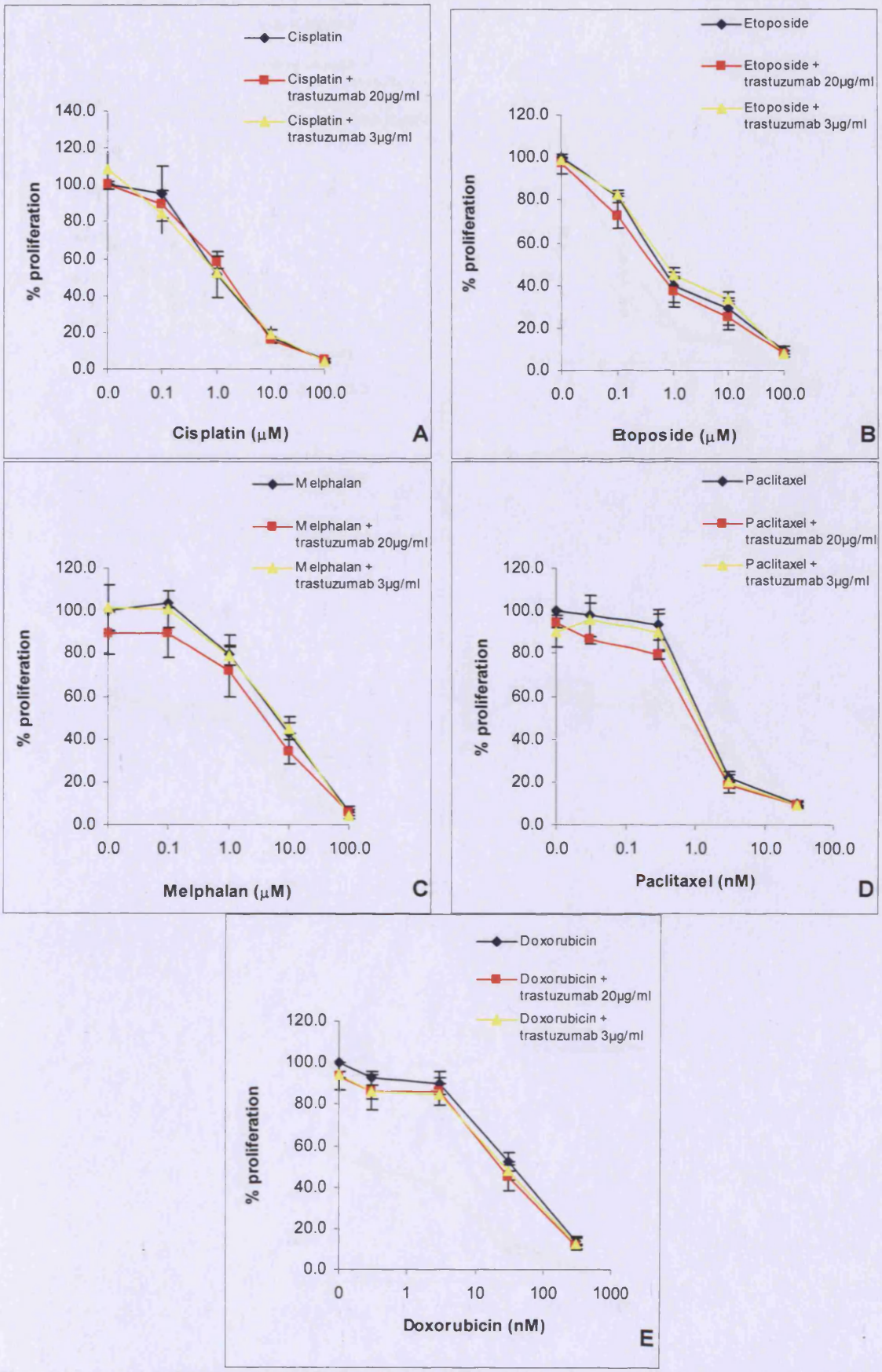

Figure 3.7 – Inhibition of MCF-7 cells proliferation after continuous treatment with trastuzumab combined with chemotherapeutic drugs. Cells were treated for 5 days with cisplatin (**A**), etoposide (**B**), melphalan (**C**), paclitaxel (**D**) or doxorubicin (**E**), alone (♦) and in combination with trastuzumab 3µg/ml (▲) and 20µg/ml (■). Error bars correspond to the standard deviation obtained from three independent experiments.

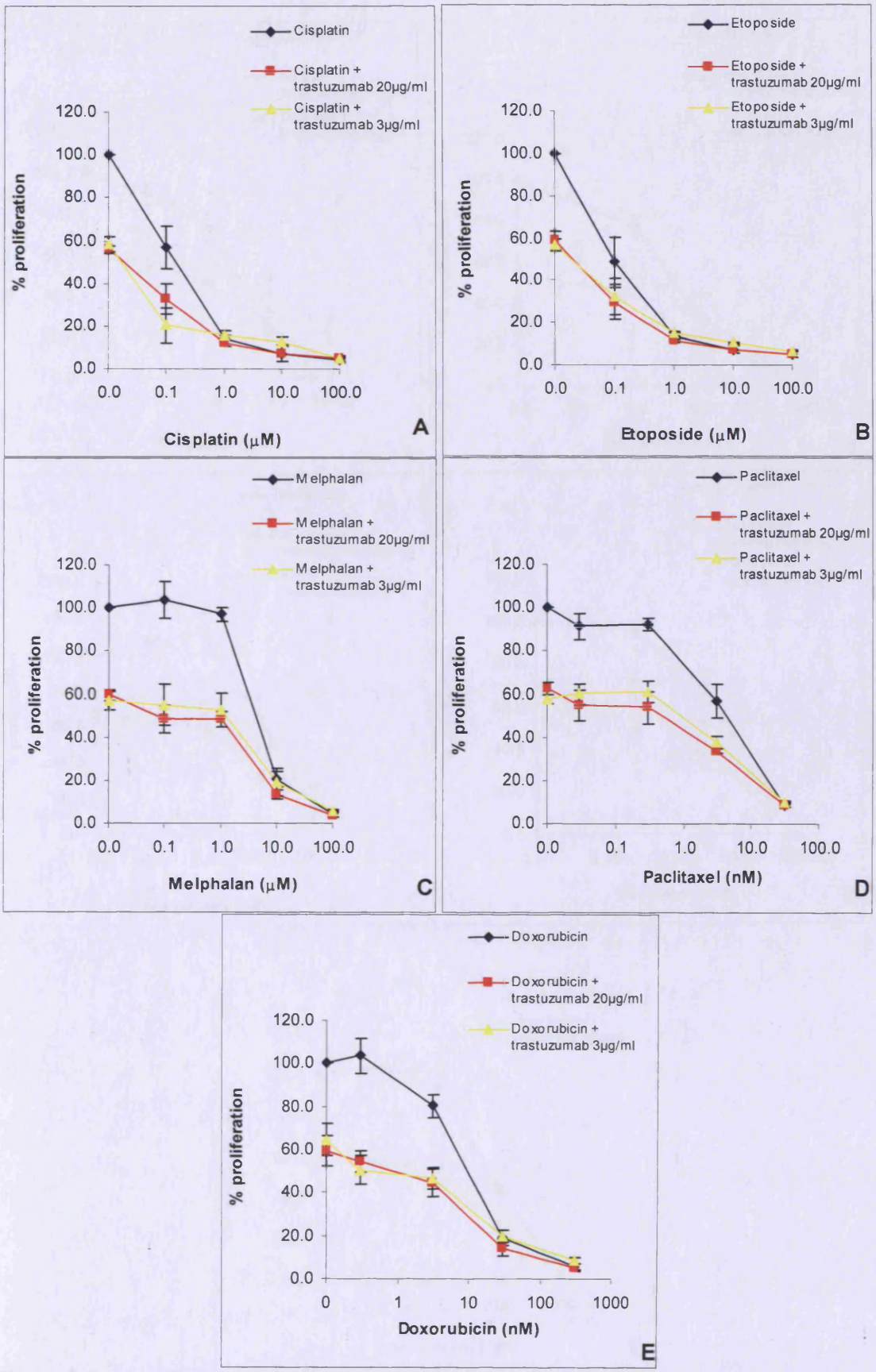

Figure 3.8 – Inhibition of SK-BR-3 cells proliferation after continuous treatment with trastuzumab combined with chemotherapeutic drugs. Cells were treated for 5 days with cisplatin (**A**), etoposide (**B**), melphalan (**C**), paclitaxel (**D**) or doxorubicin (**E**), alone (♦) and in combination with trastuzumab 3µg/ml (▲) and 20µg/ml (■). Error bars correspond to the standard deviation obtained from three independent experiments.

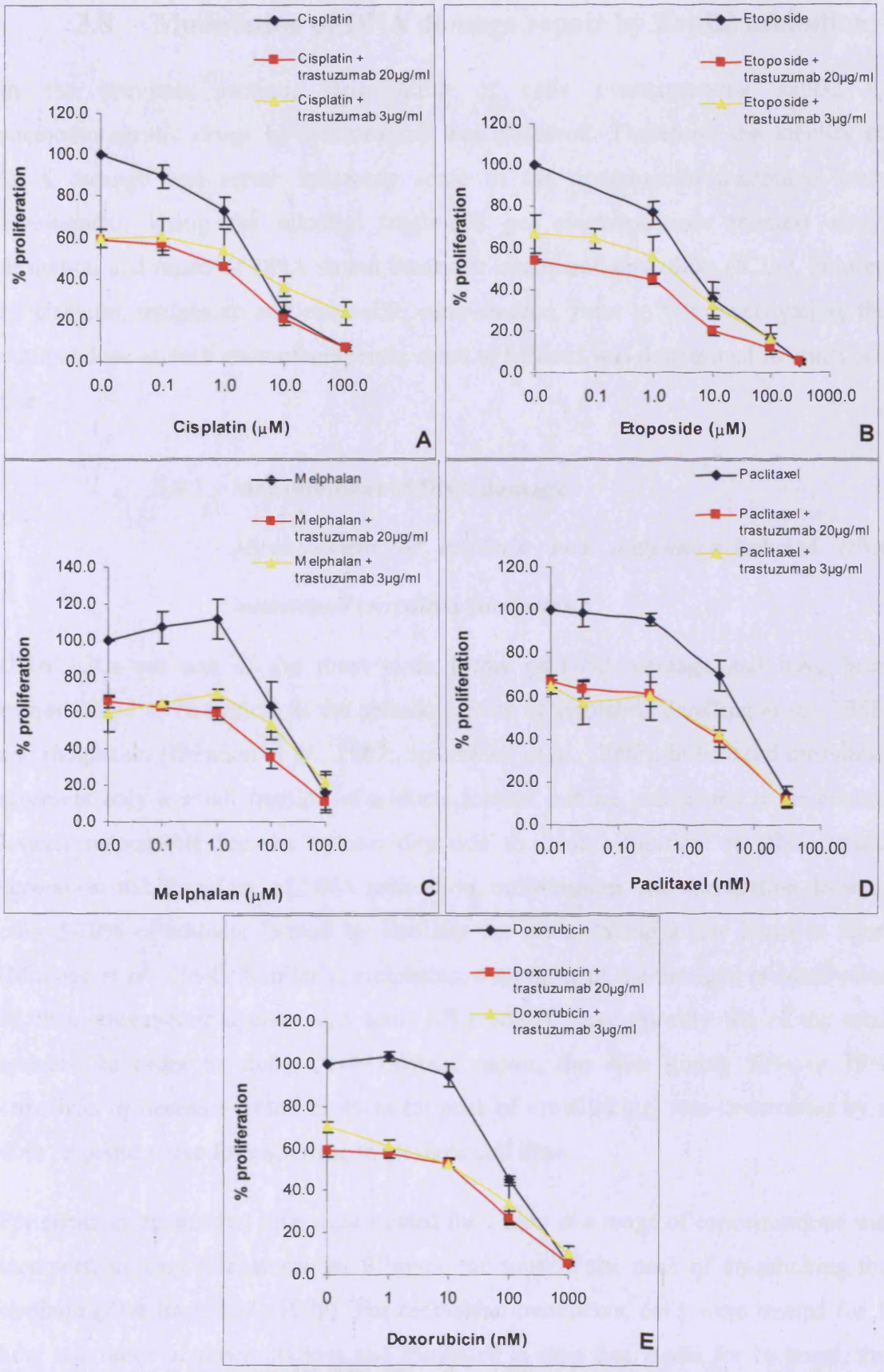

Figure 3.9 – Inhibition of MDA-MB-453 cells proliferation after continuous treatment with trastuzumab combined with chemotherapeutic drugs. Cells were treated for 5 days with cisplatin (**A**), etoposide (**B**), melphalan (**C**), paclitaxel (**D**) or doxorubicin (**E**), alone (♦) and in combination with trastuzumab 3µg/ml (▲) and 20µg/ml (■). Error bars correspond to the standard deviation obtained from three independent experiments.

3.8 Modulation of DNA damage repair by ErbB2 inhibition

In the previous section, sensitisation of cells overexpressing ErbB2 to chemotherapeutic drugs by trastuzumab was observed. Therefore, the kinetics of DNA damage and repair following some of the combination treatments were investigated. Using the alkaline single-cell gel electrophoresis (comet) assay, formation and repair of DNA strand breaks or interstrand crosslinks (ICLs), induced by cisplatin, melphalan and etoposide, were studied. Prior to this investigation, the optimal dose of each chemotherapeutic agent to be used was determined for each cell line.

3.8.1 Measurement of DNA damage

Measurement of cisplatin and melphalan-induced DNA interstrand crosslinks formation

DNA ICLs are one of the most toxic forms of DNA damage and have been demonstrated to be critical in the cellular effects of cisplatin (Zwelling *et al.*, 1981) and melphalan (Hansson *et al.*, 1987; Spanswick *et al.*, 2002). Interstrand crosslinks represent only a small fraction of adducts formed but are considered to be critical lesions responsible for the cytotoxicity due to their inhibition of DNA strand separation and, therefore, of DNA replication, transcription, and segregation. Indeed, only 5-10% of adducts formed by cisplatin are ICLs, taking a few hours to form (Malinge *et al.*, 1994). Similarly, melphalan, a member of the nitrogen mustard class of chemotherapeutic agents, also form ICLs which make up only 5% of the total adducts. In order to study DNA damage repair, the dose giving 50% to 70% crosslinks or decrease in tail moment (at peak of crosslinking) was determined by a dose response curve for each drug in all three cell lines.

For cisplatin treatments, cells were treated for 1 hour at a range of concentrations and incubated in drug free media for 9 hours, the time of the peak of crosslinking for cisplatin (Zwelling *et al.*, 1979). For melphalan treatments, cells were treated for 1 hour at a range of concentrations and incubated in drug free media for 16 hours, the time of the peak of crosslinking for melphalan (Spanswick *et al.*, 2002). Results obtained for cisplatin and melphalan treatments are represented in Figures 3.10, 3.11 and 3.12, for MCF-7, SK-BR-3 and MDA-MB-453, respectively. All three figures

show that 150μM of cisplatin and 200μM of melphalan are required to produce ~50% interstrand crosslinks in each cell line, except for SK-BR-3 where 150μM of cisplatin caused ~45% interstrand crosslinks.

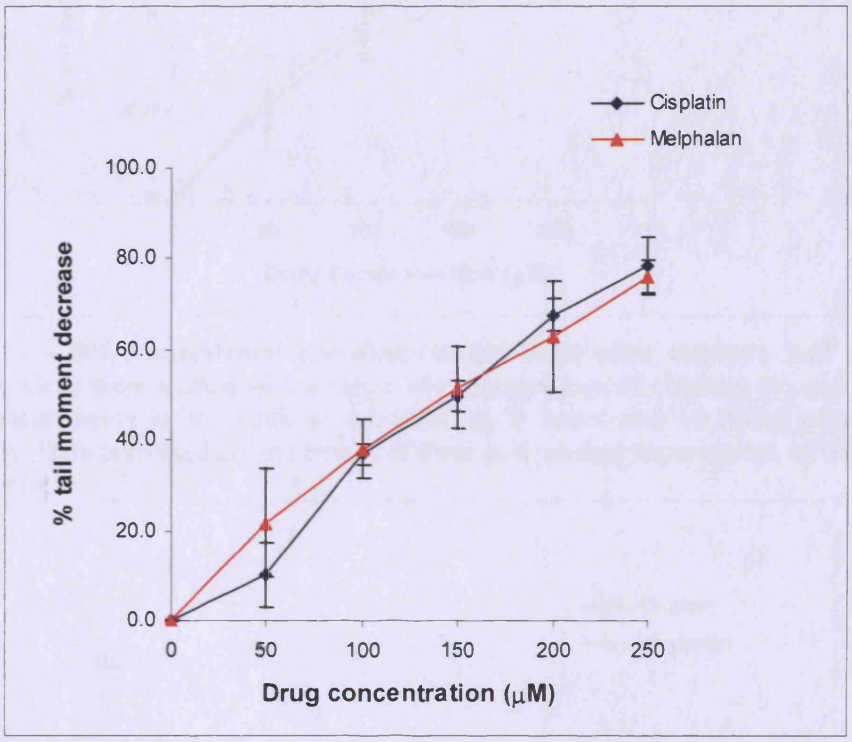

Figure 3.10 – DNA interstrand crosslinks in MCF-7 after cisplatin and melphalan treatment. Cells were treated with a range of concentrations of cisplatin (♦) and melphalan (▲) – measurements at the peak of crosslinking, 9 hours and 16 hours post-treatment, respectively. Data presented are the results of three independent experiments, as shown by the standard error.

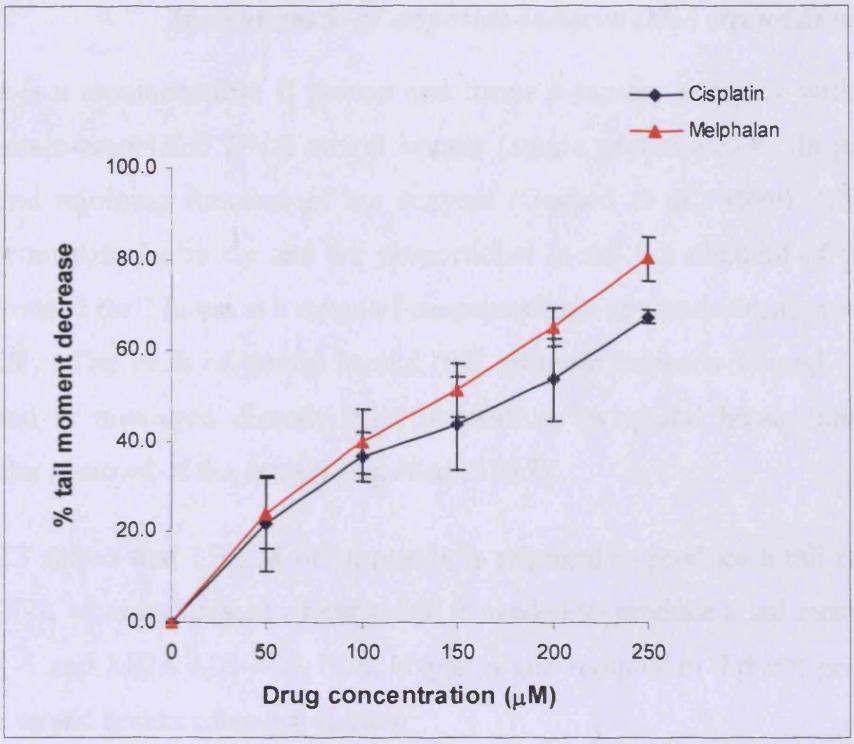

Figure 3.11 – DNA interstrand crosslinks in SK-BR-3 after cisplatin and melphalan treatment. Cells were treated with a range of concentrations of cisplatin (♦) and melphalan (▲) – measurements at the peak of crosslinking, 9 hours and 16 hours post-treatment, respectively. Data presented are the results of three independent experiments, as shown by the standard error.

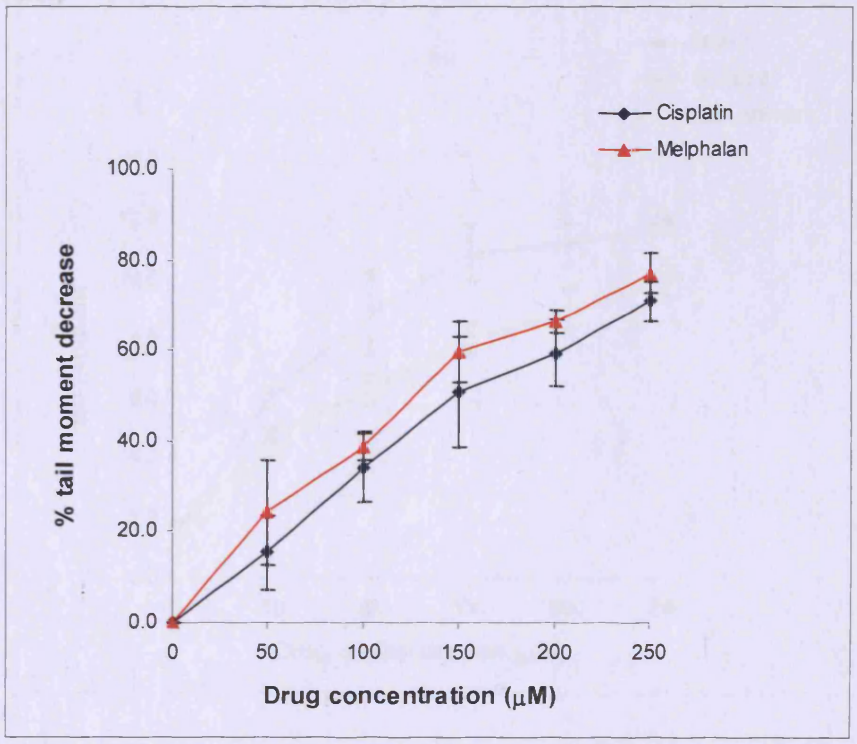

Figure 3.12 – DNA interstrand crosslinks in MDA-MB-453 after cisplatin and melphalan treatment. Cells were treated with a range of concentrations of cisplatin (♦) and melphalan (▲) – measurements at the peak of crosslinking, 9 hours and 16 hours post-treatment, respectively. Data presented are the results of three independent experiments, as shown by the standard error.

Measurement of etoposide-induced DNA strand breaks

Etoposide is a topoisomerase II poison and forms a ternary complex with DNA. It causes protein-associated DNA strand breaks (single or double) by impairing the DNA strand rejoining function of the enzyme (Godard *et al.*, 1999). DNA strand breaks are measured directly and are proportional to the tail moment of the comet. Cells are treated for 2 hours at a range of concentrations of etoposide, as strand breaks form rapidly. The peak of strand breaks (tail moment between 10 and 12) occurs quickly and is measured directly after incubation, as strand breaks are repaired quickly after removal of the drug (Long *et al.*, 1985).

Figure 3.13 shows that 150μM of etoposide is required to produce a tail moment of 11 in MCF-7, whereas 250μM of etoposide is needed to produce a tail moment of 10 in SK-BR-3 and MDA-MB-453. Both cisplatin and melphalan did not produce any detectable strand breaks (data not shown).

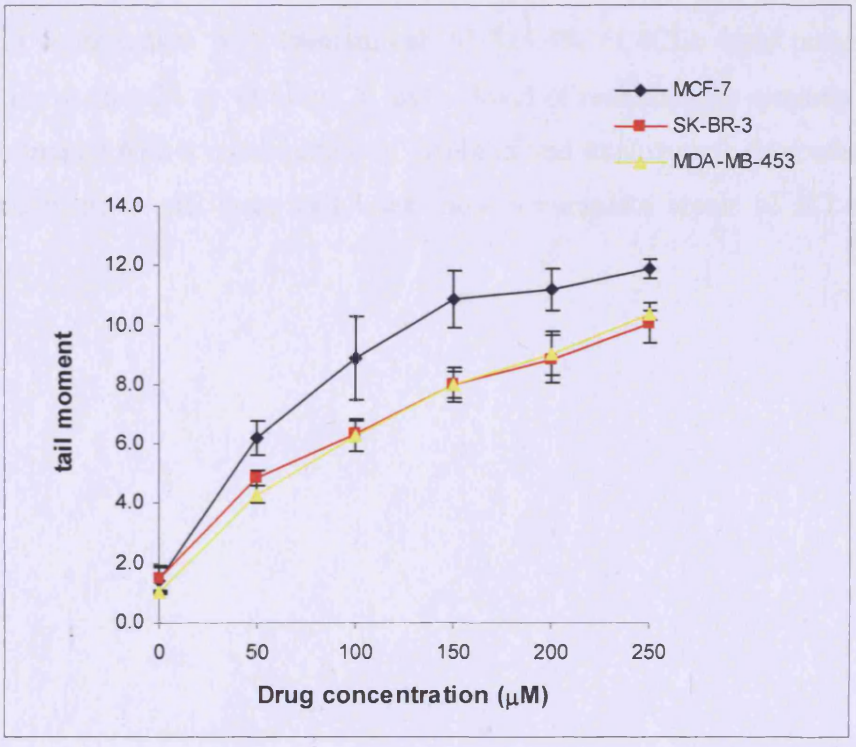

Figure 3.13 – DNA strand breaks in MCF-7, SK-BR-3 and MDA-MB-453 cells after etoposide treatment. MCF-7 (♦), SK-BR-3 (■) and MDA-MB-453 (▲) cells were treated with a range of concentrations of etoposide – measurements of strand breaks directly after the 2 hours treatment. Data presented are the results of three independent experiments, as shown by the standard error.

3.8.2 Effect of trastuzumab on the repair of drug-induced DNA damage

Effect of trastuzumab on cisplatin-induced interstrand crosslinks repair

Using 20μg/ml of trastuzumab, a clinically achievable dose (Baselga *et al.*, 2005), and 150μM of cisplatin (determined as previously described), cells were either treated with cisplatin alone or a combination of both drugs for 1 hour. Cells were subsequently incubated in drug free media or media containing trastuzumab and repair of DNA damage was measured over 72 hours post-incubation. Results are presented in Figures 3.14, 3.15 and 3.16 for MCF-7, SK-BR-3 and MDA-MB-453 cell lines, respectively. In all three cell lines, trastuzumab did not affect the level of cisplatin-induced ICLs. However, compared to cells treated with cisplatin alone, trastuzumab caused a clear delay in DNA ICLs repair when combined with cisplatin. The most significant inhibition in DNA repair was in SK-BR-3 cells (Figure 3.15). After 24 hours, 36.6±1.2% of ICLs were present in cells treated with cisplatin alone whereas in combination with trastuzumab 61.7±4.4% of ICLs were present. In all three cell lines, after 24 or 48 hours, a higher level of residual ICL remains when the cells were treated with a combination of cisplatin and trastuzumab than when treated with cisplatin alone. All three cell lines show a complete repair of ICLs after 72 hours.

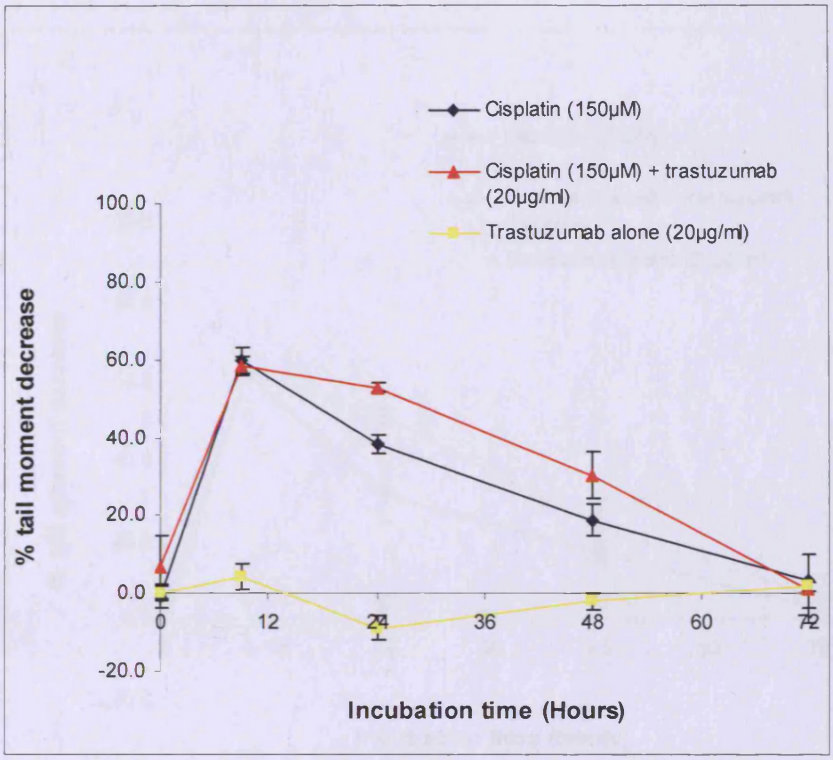

Figure 3.14 – Cisplatin-induced DNA interstrand crosslinks in MCF-7 cells. Cells treated with trastuzumab alone (■), cisplatin alone (♦) or a combination of cisplatin with trastuzumab (▲).Data presented are the results of three independent experiments, as shown by the standard error.

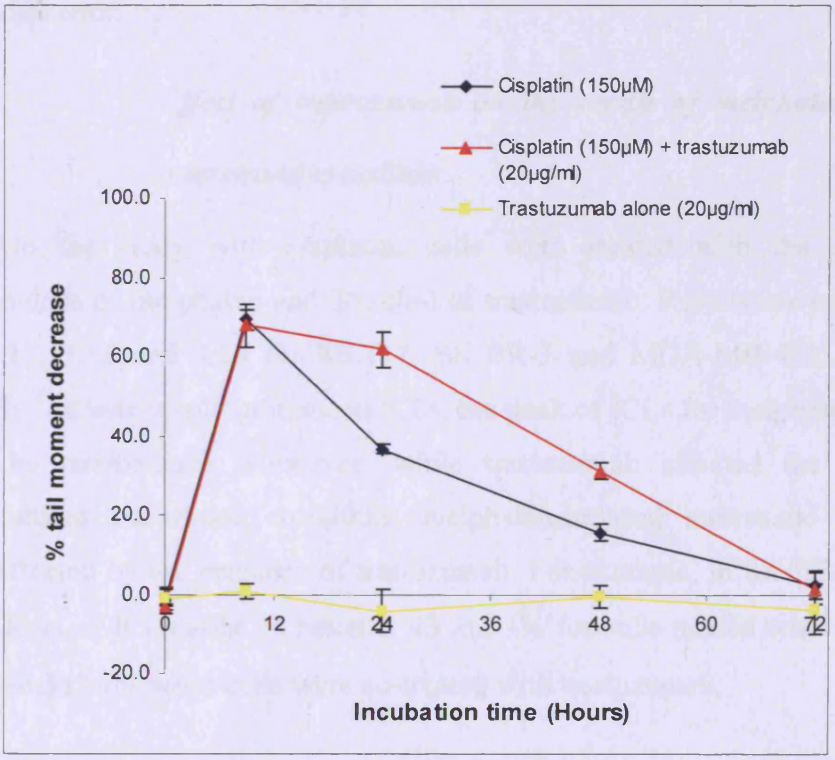

Figure 3.15 – Cisplatin-induced DNA interstrand crosslinks in SK-BR-3 cells. Cells treated with trastuzumab alone (■), cisplatin alone (♦) or a combination of cisplatin with trastuzumab (▲).Data presented are the results of three independent experiments, as shown by the standard error.

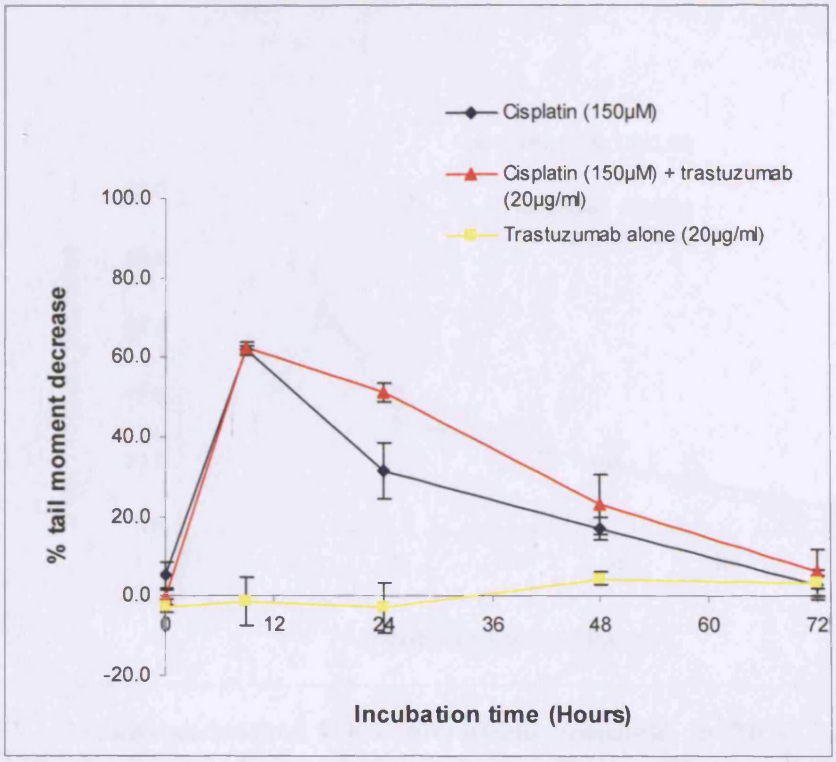

Figure 3.16 – Cisplatin-induced DNA interstrand crosslinks in MDA-MB-453 cells. Cells treated with trastuzumab alone (■), cisplatin alone (♦) or a combination of cisplatin with trastuzumab (▲).Data presented are the results of three independent experiments, as shown by the standard error.

Effect of trastuzumab on the repair of melphalan-induced interstrand crosslinks

Similarly to the study with cisplatin, cells were treated with the previously determined dose of melphalan and 20μg/ml of trastuzumab. Results are presented in Figures 3.17, 3.18 and 3.19 for MCF-7, SK-BR-3 and MDA-MB-453 cell lines, respectively. As with cisplatin-induced ICLs, the peak of ICLs for melphalan was not modified by trastuzumab. However, while trastuzumab affected the repair of cisplatin-induced interstrand crosslinks, melphalan-induced interstrand crosslinks were not affected by the presence of trastuzumab. For example, in SK-BR-3 (Figure 3.19), the level of ICLs after 24 hours is 43.5±5.1% for cells treated with melphalan alone and 46.3±2.7% when cells were co-treated with trastuzumab.

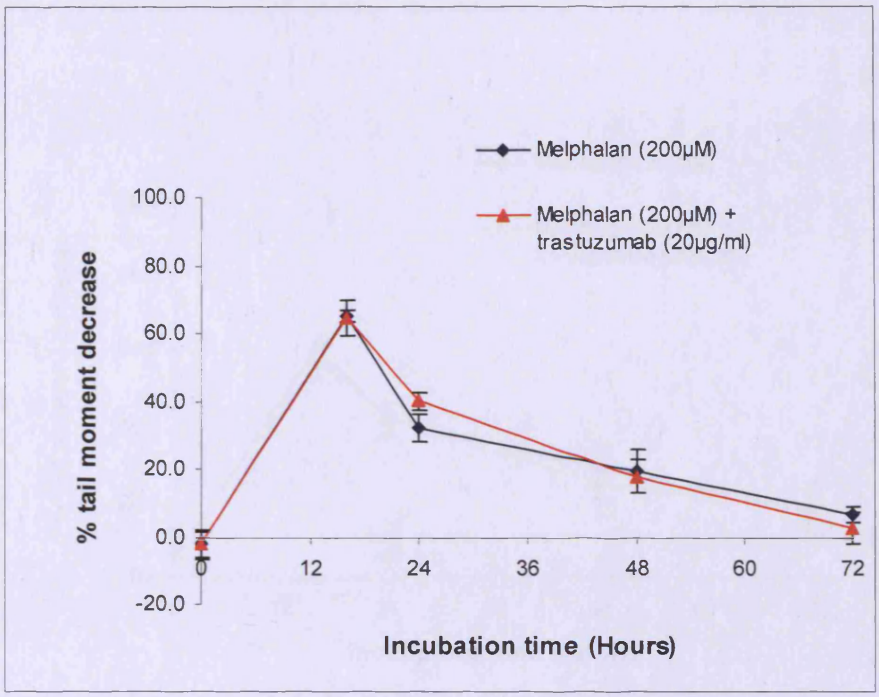

Figure 3.17 – Melphalan-induced DNA interstrand crosslinks in MCF-7 cells. Cells treated with melphalan alone (♦) or a combination of melphalan with trastuzumab (▲). Data presented are the results of three independent experiments, as shown by the standard error.

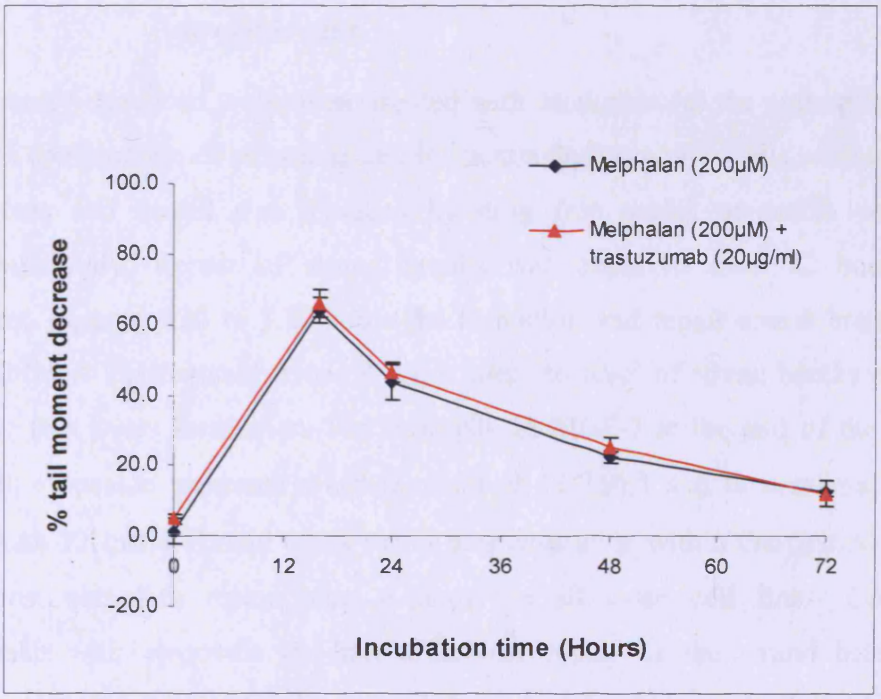

Figure 3.18 – Melphalan-induced DNA interstrand crosslinks in SK-BR-3 cells. Cells treated with melphalan alone (♦) or a combination of melphalan with trastuzumab (▲). Data presented are the results of three independent experiments, as shown by the standard error.

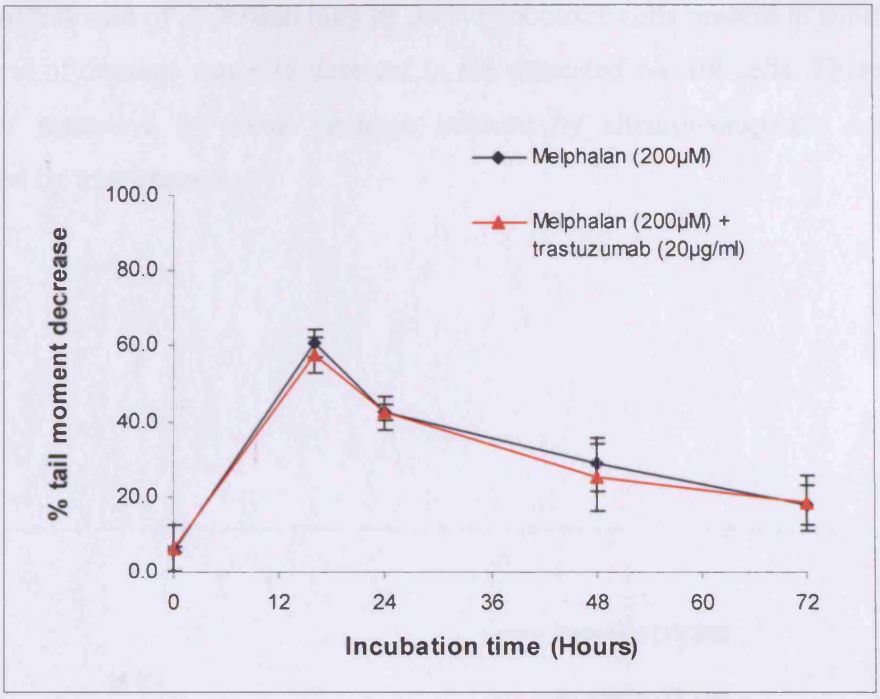

Figure 3.19 – Melphalan-induced DNA interstrand crosslinks in MDA-MB-453 cells. Cells treated with melphalan alone (♦) or a combination of melphalan with trastuzumab (▲). Data presented are the results of three independent experiments, as shown by the standard error.

Effect of trastuzumab on the repair of etoposide-induced strand breaks

As previously described, cells were treated with etoposide (at the appropriate dose) alone or a combination of etoposide and trastuzumab (20μg/ml). Cells were incubated for 2 hours and media was replaced by drug free media or media containing trastuzumab only. Repair of strand breaks was observed over 72 hours post-incubation. Figures 3.20 to 3.22 show the formation and repair strand breaks in all three cell lines. Trastuzumab alone did not alter the level of strand breaks produced following two hours incubation. For example, in MCF-7 at the end of the 2 hours treatment, etoposide produces a tail moment of 11.7±0.5 and in combination with trastuzumab 12.1±0.4. Strand break repair was detectable within the first 30 minutes and almost complete repair after 6 hours in all three cell lines. Combining trastuzumab with etoposide did not affect the repair of the strand breaks. For example, in MDA-MB-453 cells, after 1 hour post-incubation, the tail moment of cells treated with etoposide alone was 4.7±0.1 and the combination treatment gave a tail moment of 4.4±0.1. In all cell lines a small level of damage persisted after 72

hours (tail moment of 2), which may be due to apoptotic cells present in solution, as a small level of damage was also detected in the untreated control cells. Therefore not all repair pathways for DNA damage induced by chemotherapeutic agents are modulated by trastuzumab.

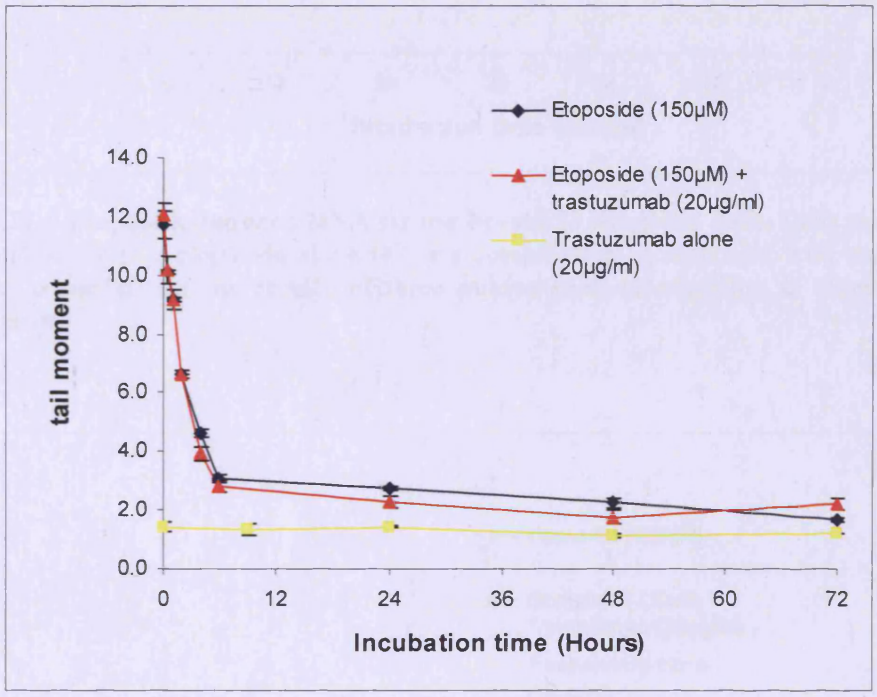

Figure 3.20 – Etoposide-induced DNA strand breaks in MCF-7 cells. Cells treated with trastuzumab alone (■), etoposide alone (♦) or a combination of etoposide with trastuzumab (▲). Data presented are the results of three independent experiments, as shown by the standard error.

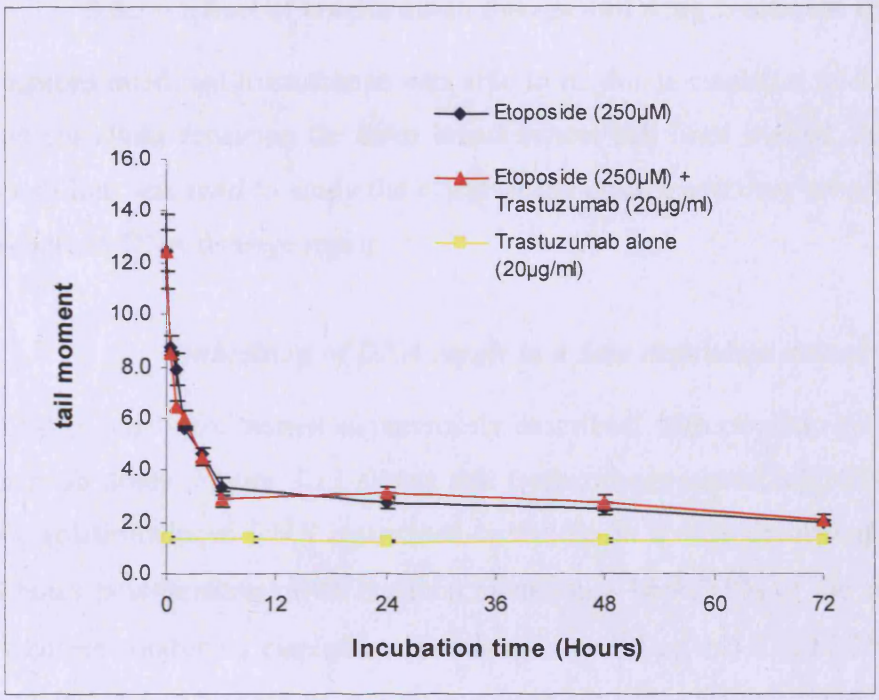

Figure 3.21 – Etoposide-induced DNA strand breaks in SK-BR-3 cells. Cells treated with trastuzumab alone (■), etoposide alone (♦) or a combination of etoposide with trastuzumab (▲). Data presented are the results of three independent experiments, as shown by the standard error.

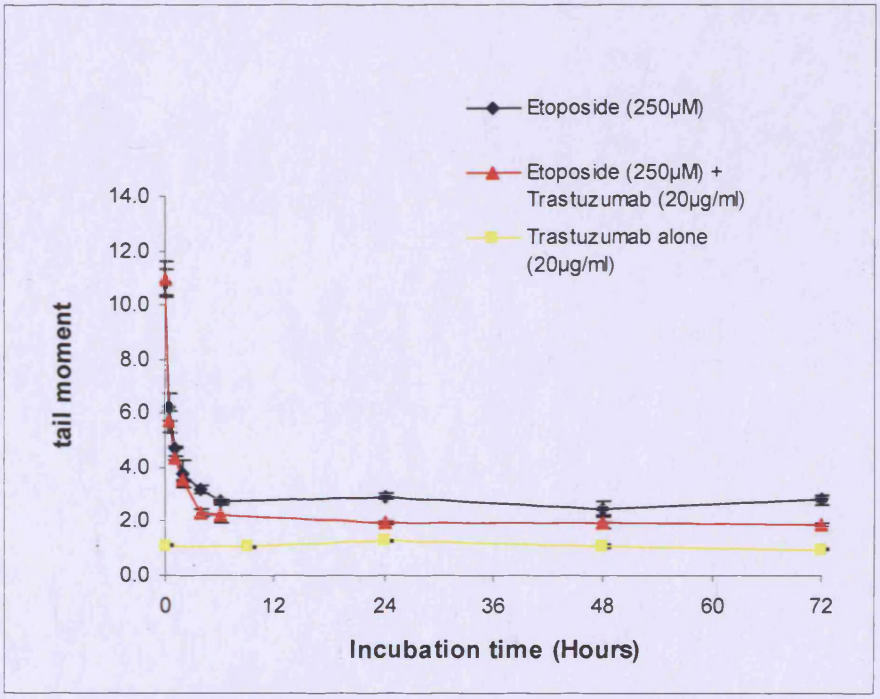

Figure 3.22 – Etoposide-induced DNA strand breaks in MDA-MB-453 cells. Cells treated with trastuzumab alone (■), etoposide alone (♦) or a combination of etoposide with trastuzumab (▲). Data presented are the results of three independent experiments, as shown by the standard error.

3.8.3 Effect of trastuzumab dosage and drug treatment schedule

Having demonstrated that trastuzumab was able to modulate cisplatin-induced DNA interstrand crosslinks repair on the three breast cancer cell lines studied, the MDA-MB-453 cell line was used to study the effect of the dosage and drug scheduling on cisplatin-induced DNA damage repair.

Inhibition of DNA repair in a dose dependent manner

MDA-MB-453 cells were treated as previously described, with cisplatin and a range of trastuzumab doses. Figure 3.23 shows that trastuzumab caused inhibition of the repair of cisplatin-induced DNA interstrand crosslinks in a dose dependent manner. After 48 hours post-treatment with cisplatin alone, only 16.9±2.8% of the crosslinks remain, whereas combining cisplatin with trastuzumab (20μg/ml) 23.1±7.7% remain and 48.1±3.1% of crosslinks persist if trastuzumab is used at 40μg/ml. Using a high trastuzumab concentration (100μg/ml), 55.5±0.5% of crosslinks remain unhooked after 48 hours. 300μg/ml of trastuzumab is a much higher dose than can be achieved clinically. However, at this dose of trastuzumab DNA repair can be almost completely inhibited, with only 26.3±3.0% of the damage being repaired after 72 hours.

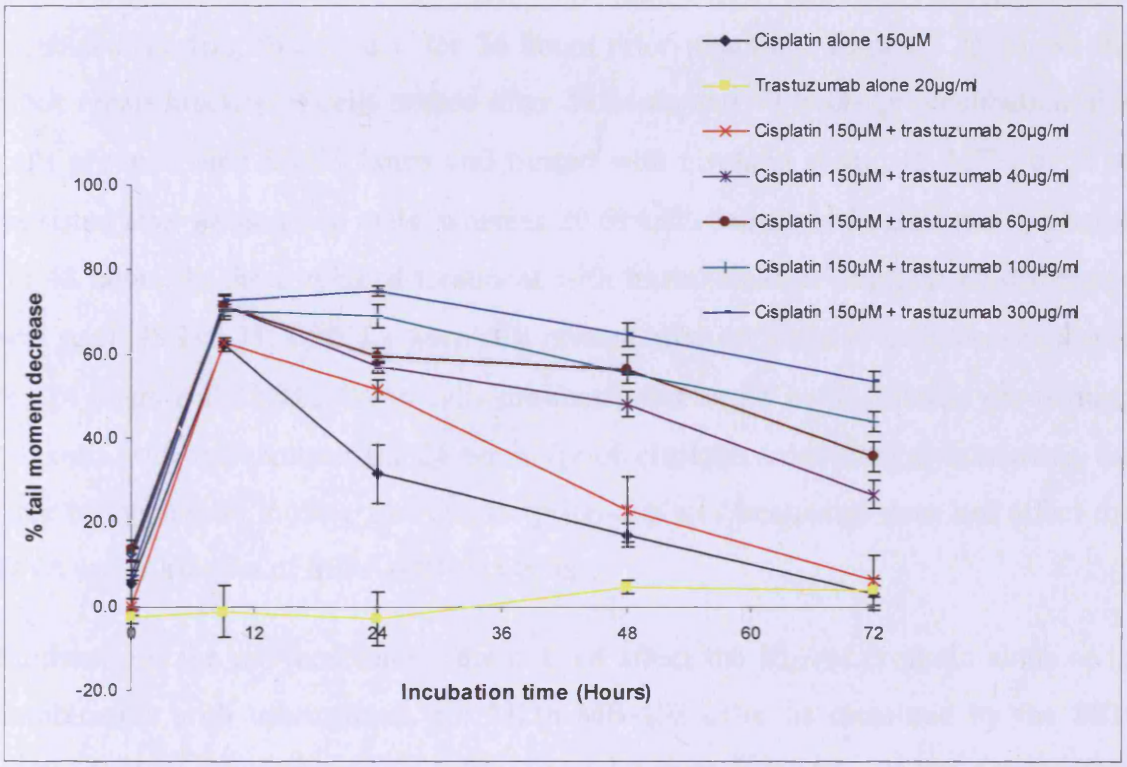

Figure 3.23 – Trastuzumab dose dependent repair of cisplatin-induced DNA damage in MDA-MB-453 cells. Cisplatin-induced DNA interstrand crosslinks were measured following treatment using a range of trastuzumab doses, on MDA-MB-453 cells. Data presented are the results of three independent experiments, as shown by the standard error.

Modulation of drug scheduling and inhibition of DNA repair

Trastuzumab has been shown to inhibit DNA repair in a dose dependent manner, but drug scheduling may also affect this as in the case of EGFR with gefitinib (Friedmann *et al.*, 2004). Firstly, prior to cisplatin treatment, MDA-MB-453 cells were pre-treated with 20μg/ml of trastuzumab for 24 hours. However, as shown in Figure 3.24, inhibition of DNA damage repair was not increased. After 24 hours, 50.1±1.2% of the ICLs persisted in cells pre-treated with trastuzumab and 51.4±2.5% were not repaired in non pre-treated cells. The second modification was the time of pre-incubation before treatment of the cells. Previously, all cells were plated and incubated, in drug free media, for 24 hours prior treatment. Figure 3.25 shows the DNA repair kinetics of cells treated after 24 hours and 48 hours pre-incubation. For cells pre-incubated for 24 hours and treated with cisplatin alone, 16.2±7% of ICLs persisted after 48 hours in cells, whereas 20.6±4.6% remained in cells pre-incubated for 48 hours. In the combined treatment with trastuzumab at 40μg/ml no difference was seen, 48.1±3.1% of ICLs were still present after 48 hours in cells pre-incubated for 24 hours and 47.9±2.4% in cells pre-incubated for 48 hours. Hence, pre-treating the cells with trastuzumab for 24 hours (prior cisplatin treatment) or increasing the time of incubation in drug free media (prior cisplatin treatment) does not affect the DNA repair kinetics of MDA-MB-453 cells.

Furthermore, the pre-incubation time did not affect the IC_{50} of cisplatin alone or in combination with trastuzumab, for MDA-MB-453 cells, as measured by the SRB assay. Results are presented in Table 3.5 and Figure 3.26, IC_{50} of the combination treatments have been statistically compared to the IC_{50} of cisplatin single agent treatment, using the student *t*-test (degree of freedom = 4 and $p = 0.05$). Data for the 24 hours pre-incubation are the same as the one presented in section 3.4.2. Similarly to section 3.4.2, IC_{50} of cisplatin combined with trastuzumab (20μg/ml) were significantly different to the IC_{50} of the cisplatin alone with a 95% probability (data highlighted in red). In addition, comparing the data obtained with 24 hours and 48 hours pre-incubation did not show any significant difference. Thus, pre-incubation time, in drug free media, does not alter the cytotoxic effect cisplatin and trastuzumab. Although the effect of drug scheduling has not been studied extensively, these data demonstrated that drug scheduling does not alter the DNA repair kinetics, *in vitro*.

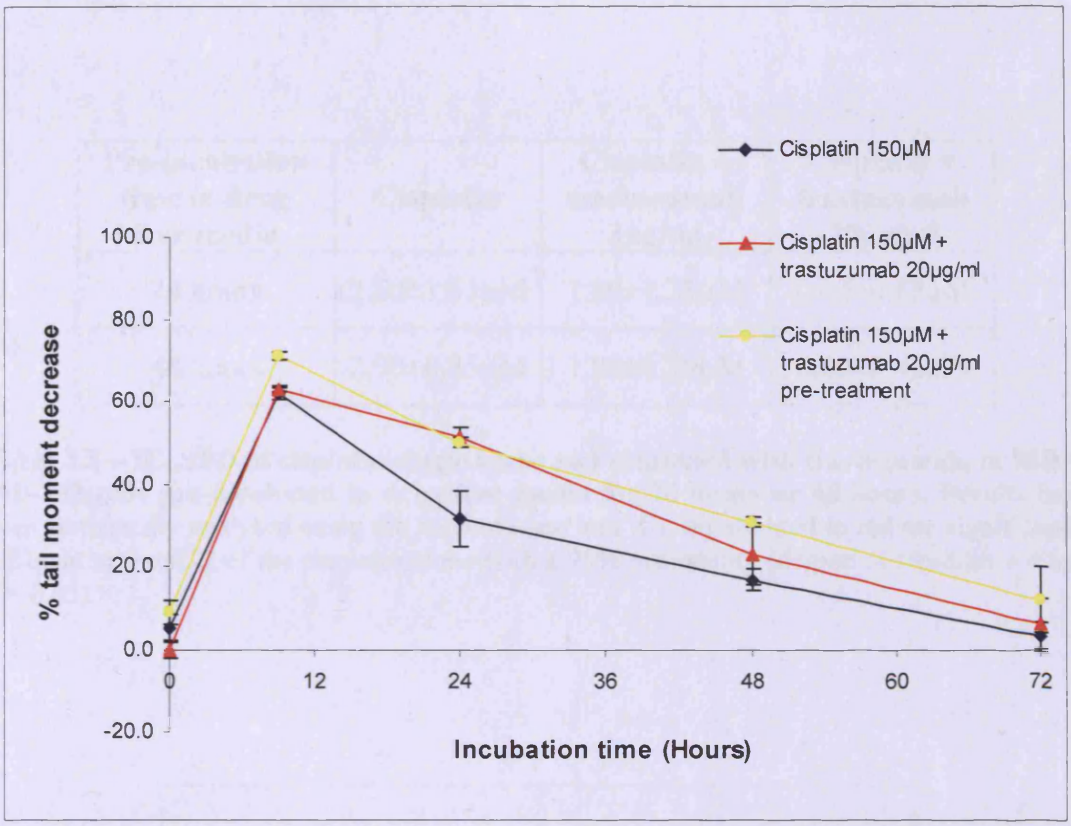

Figure 3.24 – Effect of trastuzumab pre-treatment on cisplatin-induced DNA ICLs in MDA-MB-453 cells. Cells were treated with cisplatin (♦) or cisplatin and trastuzumab, with (■) or without (▲) trastuzumab pre-treatment. Data presented are the results of three independent experiments, as shown by the standard error.

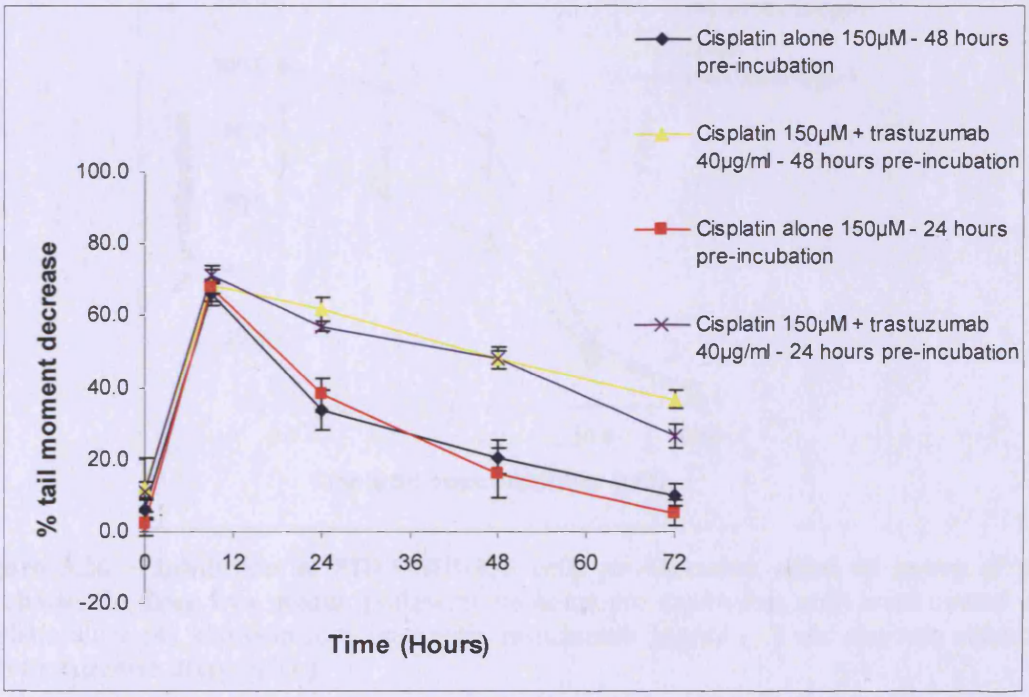

Figure 3.25 – Effect of drug free media pre-incubation on cisplatin-induced DNA ICLs repair kinetics in MDA-MB-453 cells. Cells were pre-incubated in drug free media for 24 hours or 48 hours. Data presented are the results of three independent experiments, as shown by the standard error.

Pre-incubation time in drug free media	Cisplatin	Cisplatin + trastuzumab 3µg/ml	Cisplatin + trastuzumab 20µg/ml
24 hours	2.50±1.01µM	1.80±1.23µM	0.40±0.15µM
48 hours	2.90±0.85µM	1.80±0.50µM	0.80±0.41µM

Table 3.5 – IC_{50}±SD of cisplatin single agent and combined with trastuzumab, in MDA-MB-453 cells pre-incubated in drug-free media for 24 hours or 48 hours. Results have been statistically analysed using the student *t*-test and IC_{50} highlighted in red are significantly different to the IC_{50} of the cisplatin alone with a 95% probability (degree of freedom = 4 and $p = 0.05$).

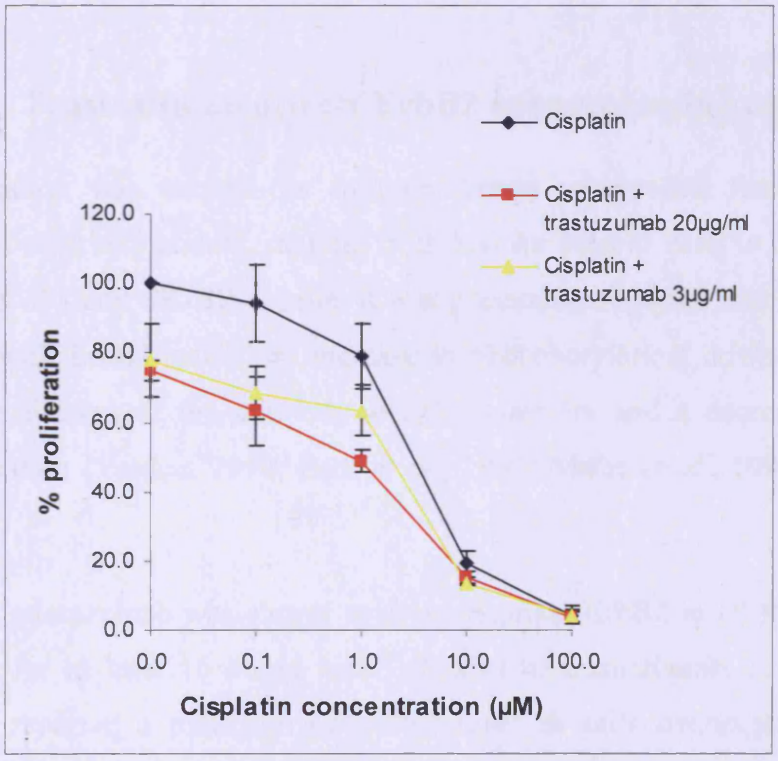

Figure 3.26 – Inhibition of MDA-MB-453 cells proliferation after 48 hours of pre-incubation in drug free media. Following 48 hours pre-incubation, cells were treated with cisplatin alone (♦), cisplatin combined with trastuzumab 3µg/ml (▲) and cisplatin combined with trastuzumab 20µg/ml (■).

DISCUSSION

Results presented in this chapter described the effect of trastuzumab on ErbB2, its effect on sensitivity to chemotherapeutic agents and the modulation of DNA damage repair in breast cancer cells MCF-7, SK-BR-3 and MDA-MB-453. The DNA damaging agents used for this study are widely used clinically and their mechanism of action is well understood. Although conflicting studies exist on the exact mechanism of action of trastuzumab, several investigations have shown the therapeutic benefits in breast cancer of trastuzumab alone (Vogel *et al.*, 2002; Mass *et al.*, 2005) and in combination of chemotherapeutic agents (Slamon *et al.*, 2001; Burstein *et al.*, 2003). Results demonstrated that trastuzumab inhibited ErbB2 expression and enhanced the anti-proliferative effects of cisplatin, melphalan, etoposide, paclitaxel and doxorubicin, in ErbB2 overexpressing cells. Furthermore, trastuzumab was shown to cause a delay in cisplatin-induced DNA damage repair.

3.9 Trastuzumab affects ErbB2 overexpressing cells

This investigation was carried out in three breast cancer cell lines, expressing different level of ErbB2 protein, ranging from low for MCF-7 cells to overexpressed for MDA-MB-453 and SK-BR-3 cells. It was previously reported that interaction of trastuzumab with ErbB2 caused an increase in phosphorylation, down-regulation of ErbB2, internalisation of the antibody-receptor complex and a decrease in ErbB2 heterodimerisation (Yarden, 1990; Park *et al.*, 1992; Maier *et al.*, 1991; Klapper *et al.*, 1997).

In this study, trastuzumab was shown to down-regulate ErbB2 in all three cell lines when treated for at least 16 hours with 0.3μg/ml of trastuzumab. Although many studies have reported a reduction of ErbB2 level in cells overexpressing ErbB2 (Cuello *et al.*, 2001; Guan *et al.*, 2005; Lee *et al.*, 2002b), there are conflicting results (Lane *et al.*, 2000; Nahta *et al.*, 2004). This may be explained by the time of exposure to trastuzumab, since ErbB2 protein level in SK-BR-3 cells was not affected before 24 hours of treatment. Another effect of trastuzumab is the inhibition of cell proliferation, as reported by Longva *et al.* (2005), where SK-BR-3 cells proliferation was inhibited after treatment with trastuzumab at 15μg/ml. In addition, Pegram *et al.*

(1999) demonstrated that anti-ErbB2 antibody led to an inhibition of tumour progression in xenografts. The results obtained there established that trastuzumab caused inhibition of cell proliferation of ErbB2 overexpressing cells, SK-BR-3 and MDA-MB-453, with concentration as low as 0.1μg/ml.

Trastuzumab causing ErbB2 down-regulation in all cell lines but inhibition of cell proliferation only in ErbB2 overexpressing cells, its anti-proliferative effect was therefore not directly associated with ErbB2 down-regulation.

3.10 Trastuzumab enhances chemotherapeutic cytotoxicity

Different studies (Pegram and Slamon, 1999; Pegram *et al.*, 2004a; Naruse *et al.*, 2002) have reported increased cytotoxic effect or synergistic effect of the monoclonal antibody (at relevant concentration – Arteaga, 2003) when used in combination with cisplatin, *in vitro* and in xenografts. Additive effects have also been reported with doxorubicin and paclitaxel (Pegram *et al.*, 2004a). A study by Hancock *et al.* (1991), using a monoclonal antibody specific to ErbB2 (TAb250), also demonstrated the inhibition of cell proliferation in a dose dependent manner and an enhance cytotoxicity of cisplatin when combined with this antibody. *In vivo*, Slamon *et al.* (2001) also established that trastuzumab increased the clinical benefit of first-line chemotherapy, such as paclitaxel and doxorubicin, in metastatic breast cancer overexpressing ErbB2. In the data presented, using chemotherapeutic drugs as single agents or in combination with trastuzumab (at clinically achievable concentrations), cells overexpressing ErbB2 (SK-BR-3 and MDA-MB-453 cells) were sensitised in the presence of the monoclonal antibody. In addition, this result was most significant in SK-BR-3, as with 3μg/ml trastuzumab sensitivity of the cells increased with all chemotherapeutic drugs used. The increased sensitivity observed in combination treatments was also related to the inhibition of proliferation caused by trastuzumab. Doses of 3μg/ml and 20μg/ml of trastuzumab produced growth inhibition of 20% to 40% in those two cell lines but did not affect MCF-7 cells which have a low level of ErbB2 proteins.

Comparing dose response curves of ErbB2 transfected cells with their parent cell lines, Pegram *et al.* (1997) established that the association between ErbB2 expression

and chemoresistance, to agents such as cisplatin, doxorubicin, paclitaxel or etoposide, was cell line specific. In addition, *in vivo* results for parent/daughter xenografts, differing only by their ErbB2 expression level, demonstrated that ErbB2 overexpression did not cause increased chemoresistance. Nevertheless, they showed that ErbB2 overexpressing xenografts had a more rapid re-growth in response to chemotherapeutic agents. Similarly, *in vitro* results obtained for single agent treatments showed that a higher level of ErbB2 did not correlate with an increased chemoresistance, as the SK-BR-3 cell line, with a high level of ErbB2, was the most sensitive to the chemotherapeutic agents studied. However, MDA-MB-453 cells, with a high ErbB2 protein level, were more chemoresistant than MCF-7 cells. Nonetheless, as cell lines used are derived from different sources, they may inherently differ in characteristics other than the ErbB2 expression level, which could have an impact on drug sensitivity.

Thus, it is difficult to compare the chemoresistance of different cell lines based solely on their ErbB2 protein level since chemoresistance is controlled by several genes which can be more or less amplified in different cell lines. Furthermore enhancement of cytotoxicity effect of chemotherapeutic agents by trastuzumab was less significant than the one described in published data. This may be explained by the use of the SRB assay as clonogenic assay or xenograft studies have been proved to be more sensitive. Nevertheless, as synergistic effects between trastuzumab and chemotherapeutic agents have been extensively described in published studies, the SRB assay will be sufficient to confirm enhancement of chemotherapeutic cytotoxicity.

3.11 Trastuzumab modulates DNA damage repair

Although synergistic mechanisms of trastuzumab with chemotherapeutic agents are not fully understood, it has been suggested that these mechanisms are due to the inhibition of repair by trastuzumab. Hancock *et al.* (1991) suggested that the enhancement of cisplatin cytotoxicity, by an ErbB2 inhibitor, could be explained by an inhibition of DNA repair. In addition, studies by Pietras *et al.* (1994 and 1998), demonstrated that trastuzumab was able to inhibit partially the repair of DNA damage induced by cisplatin and radiation, by blocking unscheduled DNA synthesis (UDS).

Nonetheless, the use of UDS analysis is limited as it does not measure specifically one type of repair but overall genome repair. Furthermore, in their study trastuzumab was used at 200μg/ml which is much higher than the clinically achievable doses described in the study by Baselga *et al.* (2005).

Cisplatin and melphalan-induced DNA ICLs – Using clinically achievable doses of trastuzumab and the more sensitive comet assay, results obtained here established that trastuzumab did not affect the peak of crosslinking of cisplatin or melphalan. Nonetheless, whilst the repair of melphalan-induced DNA ICLs was not affected by trastuzumab, a clear delay in cisplatin-induced DNA ICLs repair was observed. This delay persisted for more than 48 hours after drug treatment, in all three cell lines. In addition, trastuzumab was shown to induce DNA repair inhibition in a dose dependent manner, when using a range of trastuzumab doses, in MDA-MB-453 cells. Thus, trastuzumab affects the downstream pathway responsible for the repair of interstrand crosslinks induced by cisplatin. These results are similar to those obtained by Friedmann *et al.* (2004) in this laboratory, when they demonstrated that inhibition of EGFR tyrosine kinase inhibited cisplatin-induced DNA damage but not melphalan-induced DNA damage.

Although both melphalan and cisplatin caused the formation of ICLs, the repair mechanisms of those damages are affected differently by the inhibition of ErbB2. This could be explained by the type and frequency of ICLs that differ between cisplatin and melphalan. Indeed, De Silva *et al.* (2002) demonstrated that repair of cisplatin ICLs does not involve the formation of double strand breaks, in contrast to other conventional crosslinking agents, such as melphalan. Several studies have identified the importance of the XPF-ERCC1 heterodimer component of nucleotide excision repair (De Silva *et al.*, 2000; Mu *et al.*, 2000; Kuraoka *et al.*, 2000) for the unhooking of cisplatin ICLs. Nevertheless, De Silva *et al.* (2002) suggested that homologous recombination was initiated prior to excision of cisplatin ICLs since they found that XRCC2 and XRCC3 HR mutants were defective in the unhooking step of cisplatin ICLs. For melphalan, Clingen *et al.* (2005) demonstrated that the repair of DNA ICLs was dependent on the XPF-ERCC1 heterodimer component of the nucleotide excision repair pathway. Therefore, inhibition of the mechanisms of repair of melphalan and cisplatin-induced ICLs requires further investigation.

Furthermore, the molecular mechanisms by which trastuzumab blocks DNA repair is thought to involve the inhibition of $p21^{WAF1}$. Indeed, Pietras *et al.* (1999) reported that combining radiation therapy with trastuzumab caused inhibition of $p21^{WAF1}$ induction, leading to cell cycle progression and accumulation of unrepaired DNA damage. Thus, further investigation of the modulation of the cell cycle induced by trastuzumab after cisplatin-induced DNA damage will be required.

Etoposide-induced DNA strand breaks – Investigating the effect of trastuzumab on etoposide-induced DNA strand breaks did not show any increase of strand breaks by trastuzumab, in any of the cell line studied, as had been reported previously by Mayfield *et al.* (2001). In their study, they demonstrated that treating ErbB2 overexpressing cells, such as SK-BR-3 cells, with trastuzumab at 10µg/ml caused an increase in DNA strand breaks. Furthermore, results obtained established that trastuzumab did not alter the repair of etoposide-induced DNA strand breaks. Although no study has investigated the repair of etoposide-induced strand breaks following trastuzumab treatment, a study by Pietras *et al.* (1999) investigated the effect of ErbB2 on ionising radiation-induced DNA damage repair, using unscheduled DNA synthesis analysis. Their results demonstrated that trastuzumab caused a decrease in radiation-induced DNA strand break repair and highlighted that signal transduction pathways provided by ErbB2 were essential to the repair of this type of DNA damage. Therefore, further investigation of the effect of ErbB2 inhibition, by trastuzumab, on DNA strand break repair is needed using the more sensitive comet assay.

3.12 Conclusion

These results demonstrated that the inhibition of ErbB2 protein expression has an effect on cells sensitivity to chemotherapeutic drugs, suggesting a biological role for ErbB2 in the resistance to chemotherapy. These experiments have also proved that a clear inhibition of cisplatin-induced DNA ICLs repair was obtained by ErbB2 inhibition. Moreover, this delay in DNA repair was not seen after strand break damage and was specific to ICLs caused by cisplatin, as the repair of melphalan-induced DNA ICL was not affected.

Therefore, it is reasonable to conclude that enhancement of cisplatin cytotoxicity, by inhibition of ErbB2, is caused, at least in part, by an alteration of DNA repair mechanisms.

Further understanding of the mechanisms, involved in the interaction between ErbB2 and DNA damage repair, will be essential in order to improve the clinical management of breast cancer. To this end, the next chapter will discuss the effects of ErbB2 inhibition on cell cycle and downstream proteins.

Chapter 4

DNA repair modulation and cell cycle regulation

INTRODUCTION

In the previous chapter, enhancement of the cytotoxicity of chemotherapeutic agents in combination with trastuzumab, an inhibitor of ErbB2 protein, was seen in cells overexpressing ErbB2. It was also demonstrated that the inhibition of ErbB2 led to the inhibition of the repair of cisplatin-induced DNA interstrand crosslink. Thus, the effects of ErbB2 inhibition might be due primarily to cell cycle arrest. Therefore, the influence of the DNA repair modulation, by trastuzumab, on cell cycle regulation, apoptosis and the expression level of key DNA repair and downstream proteins involved in ErbB2 signalling pathways was investigated.

4.1 Effects of trastuzumab on the cell cycle

During cell division, genetic integrity is maintained through the proper execution of the cell cycle mechanism. Upon trastuzumab treatment, some studies have shown cells undergo cell cycle arrest in the G1 phase (Sliwkowski *et al.*, 1999). In addition, several studies (Marches and Uhr, 2004; Lane *et al.*, 2000; Le *et al.*, 2003) suggested that this cell cycle arrest in G1 was due to a reduction of proteins responsible for the cyclin-dependent kinase (cdk) inhibitor $p27^{kip1}$ sequestration, causing its accumulation. Sliwkowski *et al.* (1999) reported that an anti-ErbB2 antibody led to an increase in $p27^{kip1}$ in reducing the number of cells entering the S phase of the cell cycle. This cdk was shown to bind to cyclinE/cdk2 complexes, causing their inhibition (Lane *et al.*, 2001) and subsequent cell cycle arrest. However, increased Akt was shown to cause down-regulation of $p27^{kip1}$ (Di Cristofano *et al.*, 2001) or phosphorylation of $p27^{kip1}$ causing its cytoplasmic retention (Yakes *et al.*, 2002).

In other studies, anti-ErbB2 antibodies also caused a reduction in $p21^{WAF1}$ level in cells overexpressing ErbB2. $p21^{WAF1}$ is another cyclin-dependent kinase which was shown to lead to cell cycle arrest upon nuclear localisation and activation (El-Deiry *et al.*, 1993; Xiong *et al.*, 1993; Waga *et al.*, 1994). However, studies have demonstrated that the inhibition of cell cycle progression, by $p21^{WAF1}$, was not due to the reduction in cyclin D1 (Pietras *et al.*, 1998 and 1999) but a dramatic diminution in cyclins D2 and D3 (Lane *et al.*, 2000; Neve *et al.*, 2000). In addition, in response to DNA damage, $p21^{WAF1}$ was shown to be activated and caused cell cycle arrest upon

cyclin/cdk binding (El-Deiry *et al.*, 1993; Chen *et al.*, 1994). Using trastuzumab in combination with radiation, Pietras *et al.* (1999) established that the monoclonal antibody was able to inhibit $p21^{WAF1}$. Hence, this reduction in $p21^{WAF1}$ caused cell cycle progression and accumulation of unrepaired DNA damage, leading to an enhanced cell killing. Therefore, the study of trastuzumab effects on the cell cycle may potentially explain the modulation in DNA damage repair.

4.2 Effect of trastuzumab on apoptosis

In Chapter 3, single agent trastuzumab was shown to reduce cell proliferation of ErbB2 overexpressing cells. However, conflicting results have been obtained on the effect of trastuzumab on the induction of apoptosis. As demonstrated by the clinical data from Mohsin *et al.* (2005), trastuzumab induced a significant increase in apoptotic cell death in ErbB2 overexpressing breast cancer patients receiving trastuzumab as a single agent followed by trastuzumab in combination with docetaxel. On the contrary, in a similar study, Gennari *et al.* (2004) did not find any decrease in proliferation in patients with ErbB2 overexpressing operable breast cancer treated with single agent trastuzumab. Nevertheless, the latter was carried out in a small number of patients and over a short period of time. Therefore, apoptosis and a decrease in breast cancer proliferation need to be observed over a longer period.

Thus, more research is required to characterise the cytotoxic effect of trastuzumab, since induction of apoptosis by trastuzumab could explain the increase in chemosensitivity reported in Chapter 3.

4.3 ErbB2 signalling cascade and topoisomerase IIα

In order to investigate the observed delay in DNA damage repair, modulation of the level of proteins involved in DNA damage repair will be studied. Additionally, other important proteins need to be considered, such as Akt involved in the ErbB2 signalling cascade and topoisomerase IIα expression, which is dependent on the cell cycle phase.

4.3.1 Role of Akt in ErbB2 signalling cascade

As described previously, alteration of the cell cycle by trastuzumab has been shown to be mediated through the PI3K/Akt signalling pathway (Le *et al.*, 2005). In addition, several studies (Normanno *et al.*, 2002; Yakes *et al.*, 2002) have demonstrated that inhibition of PI3K and its target Akt was required to obtain trastuzumab anti-tumour activity. Akt is a downstream component of the PI3K signalling pathway, which is activated upon phosphorylation of receptor tyrosine kinases such as EGFR and ErbB2. This protein has been shown to be important in regulation of metabolism, cell survival motility, transcription and cell cycle regulation (Figure 4.1).

Upon activation of the PI3K signalling pathway, Akt is phosphorylated at threonine 308 for Akt activation and serine 473 for maximal activity (Fayard *et al.*, 2005). Activated Akt has been shown to have anti-apoptotic effects by inactivating pro-apoptotic factors BAD and pro-caspase 9. Moreover, Akt was shown to prevent the release of cytochrome c from mitochondria, inactivating forkhead transcription factors and expression of pro-apoptotic factors (Datta *et al.*, 1999). Activation of Akt was also previously described to cause degradation of $p27^{kip1}$ leading to stability of cyclin D and cell cycle progression (Collado *et al.*, 2000). In addition, Akt also inhibits the function of cell cycle suppressor $p21^{WAF1}$ and $p27^{kip1}$ through their phosphorylation and subsequent cytoplasmic retention (Zhou *et al.*, 2001b; Motti *et al.*, 2005). Cytoplasmic $p21^{WAF1}$ will then bind ASK1, inhibiting apoptosis (Zhou *et al.*, 2001b). Finally, activated Akt also phosphorylates MDM2, causing an increase in nuclear localisation and inhibition of its interaction with $p19^{ARF}$. In the absence of interaction with $p19^{ARF}$, MDM2 associates with the tumour suppressor, p53, causing its cytoplasmic translocation and degradation (Zhou *et al.*, 2001a).

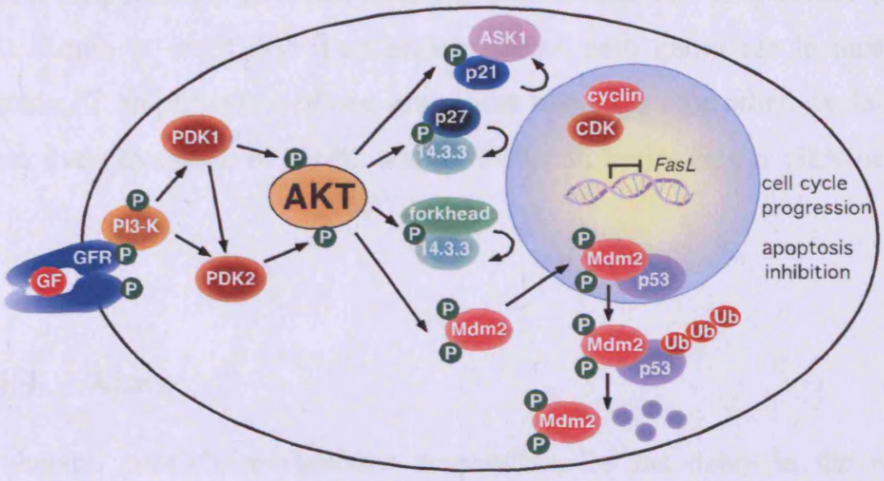

Figure 4.1 – Effect of Akt activation. Testa J.R. *et al.*, Proceedings of the National Academy of Sciences, 2001, 98(20): 10983-10985.

4.3.2 Topoisomerase IIα and cell cycle

Topoisomerase II is an enzyme responsible for relaxation of DNA supercoils, DNA decatenation of circular double stranded DNA and is involved in chromatin remodelling during mitosis (Nitiss, 1998). There are two homologous forms, α and β. The gene coding for topoisomerase IIα is adjacent to the ErbB2 oncogene at the chromosome location 17q12-q21 (Järvinen and Liu, 2006). In addition, the α form is regulated with the cell cycle and becomes detectable in late G1 phase with an increasing level up to G2/M phase (Woessner *et al.*, 1991). Topoisomerase IIα activity is increased by phosphorylation through casein kinase II. A recent study suggested the involvement of MAPK-regulated kinase pathway (Shapiro *et al.*, 1999). Furthermore, topoisomerase II has been shown to be influenced by p53 and retinoblastoma susceptibility gene product (Rb). p53 down-regulates topoisomerase IIα expression by transcriptional regulation (Wang *et al.*, 1997). Conversely, several studies (Carrier *et al.*, 1999; Hochhauser *et al.*, 1999) have shown that p53 was able to stimulate topoisomerase IIα. Similarly to p53, Rb has been shown to inhibit the activity of this enzyme (Bhat *et al.*, 1999). Moreover, a protein of the 14-3-3 family, responsible for cell cycle control, apoptosis and stress response, has recently been shown to inhibit the DNA binding capacity of topoisomerase IIα (Van Hemert *et al.*, 2001; Kurz *et al.*, 2000).

Therefore, topoisomerase IIα activity plays an important role in tumour progression. Several studies also demonstrated that TOPO2α amplification was associated with ErbB2 gene amplification in breast cancer and non-small cell lung cancer (Keith *et al.*, 1992; Smith *et al.*, 1993). Furthermore, since both genes are located on the chromosome 17, amplification of one gene locus may affect the other, explaining the concurrent overexpression of ErbB2 and TOPO2α in breast cancer (Järvinen *et al.*, 1996).

4.4 Aims

In this chapter, possible mechanisms responsible for the delay in the repair of cisplatin-induced DNA ICLs, described in Chapter 3, will be investigated. Using the MDA-MB-453 cell line overexpressing ErbB2, the following questions will be addressed:

- How do the combinations in the doses used in this study affect the cell cycle?
- Does trastuzumab induce apoptosis?
- How are proteins involved in DNA damage repair and ErbB2 signalling cascade affected by trastuzumab?
- Is topoisomerase IIα expression altered by trastuzumab in these cell lines?

RESULTS

4.5 Influence of DNA repair modulation on cell cycle regulation

Inhibition of ErbB2 has been shown to modulate the repair of cisplatin-induced DNA damage and it is possible that this effect might be due to cell cycle modulation. Therefore, to investigate this, the cell cycle of MDA-MB-453 cells was studied using flow cytometry (FACS analysis). Cells were treated with cisplatin alone (150μM) for one hour or cisplatin in combination with trastuzumab (40μg/ml) for one hour. Cells were subsequently incubated in drug-free media or media containing trastuzumab (40μg/ml). Two controls were included, cells treated continuously with trastuzumab alone and untreated cells. Cells were then collected at different time points over 72 hours (post-treatment). The percentages of cells in each phase of the cell cycle are presented in Tables 4.1 to 4.4 and with each table the appropriate histogram profile of the cells, from representative experiments, was associated (Figures 4.2 to 4.5).

Trastuzumab alone (Figure 4.3 and Table 4.2) caused the cells to accumulate in the G1 phase by 14 hours, resulting in a reduction in the cells entering the S phase, compared to untreated cells (Figure 4.2). 32.9±4.3% of the cells were in S phase after 4 hours of trastuzumab treatment whereas 16.5±1.7% were in S phase after 48 hours of treatment. In contrast, 24.1±1.0% of untreated cells were in S-phase after 48 hours. It is also noted that, compared to untreated cells, trastuzumab treatment did not cause a significant increase in sub-G1, characteristic of apoptotic cells.

Cells treated for 1 hour with cisplatin (Figure 4.4 and Table 4.3) accumulated in G2 phase by 48 hours. After cisplatin treatment (0 hour), 16.8±2.7% of cells were in G2 phase, whereas 34.4±0.3% of cells were in G2 after 72 hours. This accumulation in G2 stopped the cells from entering the G1 phase, as 48.7±2.0% of cells were in G1 after treatment and only 13.8±1.4% after 72 hours. Furthermore, cisplatin caused an increase of cells in sub-G1, as 2.4±0.4% of cells were in sub-G1 after treatment and 14.8±1.2% after 72 hours. Nevertheless, it is noted that at the peak of ICLs (9 hours), no change in the cell cycle was observed.

Combining trastuzumab with cisplatin (Figure 4.5 and Table 4.4) caused a smaller reduction in cells undergoing G2 arrest. After 72 hours, 22.9±3.5% of cells were in arrested in G2 whereas 34.4±0.3% of cells treated with cisplatin alone were arrested in G2. There was also an increase in cells entering sub-G1, as 14.8±1.2% of cells were in sub-G1 72 hours after cisplatin treatment whereas 22.7±2.4% were in sub-G1 72 hours after the combination treatment. It was also noted that cisplatin alone or in combination with trastuzumab caused an increase in sub-G1 after 14 to 19 hours, which may be due to cells arrested in G2 entering apoptosis.

Therefore, the delay in the repair of cisplatin-induced DNA ICLs caused by trastuzumab may be due to the progression of the cells through the G2 arrest, induced by cisplatin. It is also noted that the increase in cell sensitivity observed in the previous chapter (section 3.4.2) with the combination treatment is reflected in an increase in apoptotic cells (sub-G1).

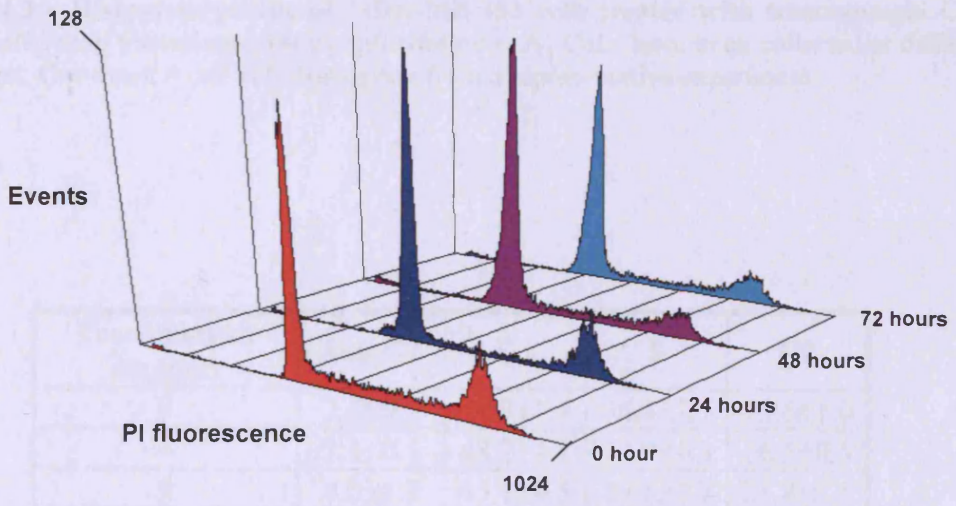

Figure 4.2 – Histogram profile of MDA-MB-453 untreated cells. Cells have been collected every 24 hours. One event = one cell. Histogram from a representative experiment.

Control	Sub G1	G1	S	G2
0	1.4±0.4	47.1±3.8	31.5±3.1	20.0±0.6
24	4.1±1.0	57.8±2.0	21.3±2.5	16.8±1.0
48	5.2±1.0	61.4±2.1	24.1±1.0	9.3±1.7
72	4.3±0.4	59.9±1.3	26.1±0.8	9.8±1.4

Table 4.1 – Percentage of untreated MDA-MB-453 cells in each phase of the cell cycle. These values are an average of three independent experiments. Data presented are the average of three independent experiments as shown by the standard error.

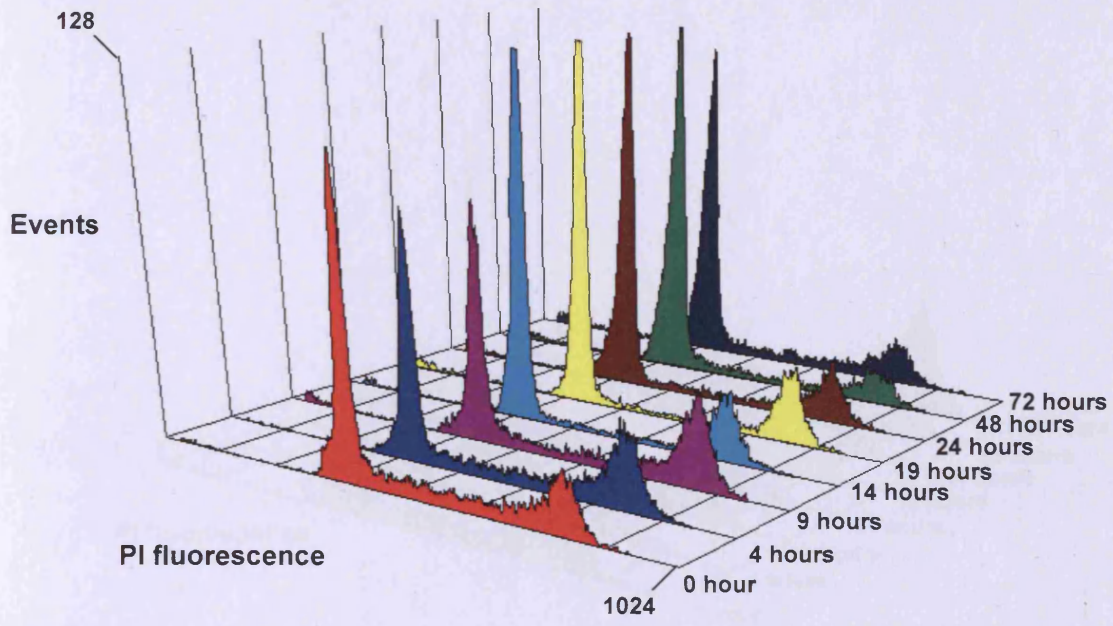

Figure 4.3 – Histogram profile of MDA-MB-453 cells treated with trastuzumab. Cells were treated with trastuzumab (40μg/ml) continuously. Cells have been collected at different time point. One event = one cell. Histogram from a representative experiment.

Trastuzumab 40μg/ml	Sub G1	G1	S	G2
0	2.1±0.3	49.9±1.4	34.4±2.1	13.6±1.0
4	2.4±0.5	48.2±4.7	32.9±4.3	16.5±0.5
9	4.0±1.3	45.1±4.5	29.1±4.7	21.8±1.5
14	4.9±1.0	64.6±0.7	14.8±1.2	15.7±0.3
19	5.8±1.8	62.4±1.1	13.0±1.4	18.8±0.4
24	6.9±1.3	60.3±2.6	20.7±1.8	12.4±2.0
48	7.1±0.3	66.1±1.3	16.5±1.7	10.3±0.3
72	6.2±0.9	59.1±0.5	22.1±0.5	12.7±0.1

Table 4.2 – Percentage of MDA-MB-453 cells treated with trastuzumab in each phase of the cell cycle. Cells were treated with trastuzumab (40μg/ml) continuously. These values are an average of three independent experiments. Data presented are the average of three independent experiments as shown by the standard error.

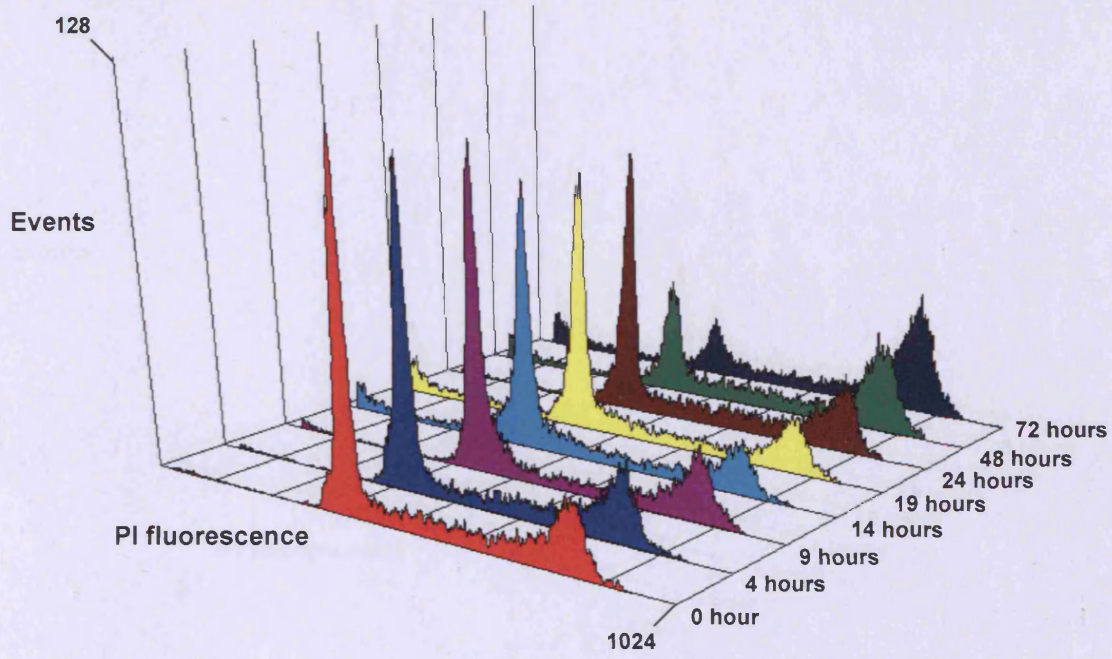

Figure 4.4 – Histogram profile of MDA-MB-453 cells treated with cisplatin. Cells were treated with cisplatin (150μM) for one hour. Cells have been collected at different time point after the 1 hour treatment. One event = one cell. Histogram from a representative experiment.

Cisplatin 150μM	Sub G1	G1	S	G2
0	2.4±0.4	48.7±2.0	32.1±3.0	16.8±2.7
4	2.5±0.9	50.3±3.4	32.5±3.8	14.7±1.3
9	2.8±0.2	45.4±3.9	39.0±4.0	12.7±0.3
14	16.3±2.1	41.8±2.1	32.3±1.0	9.6±1.0
19	16.7±1.5	40.2±0.7	31.5±1.1	11.5±1.3
24	4.9±0.7	40.8±1.4	41.9±1.3	12.4±0.2
48	11.3±0.4	23.2±0.9	41.2±1.3	24.3±0.6
72	14.8±1.2	13.8±1.4	37.0±0.7	34.4±0.3

Table 4.3 – Percentage of MDA-MB-453 cells treated with cisplatin in each phase of the cell cycle. Cells were treated with cisplatin (150μM) for one hour (±standard error). These values are an average of three independent experiments. Data presented are the average of three independent experiments as shown by the standard error.

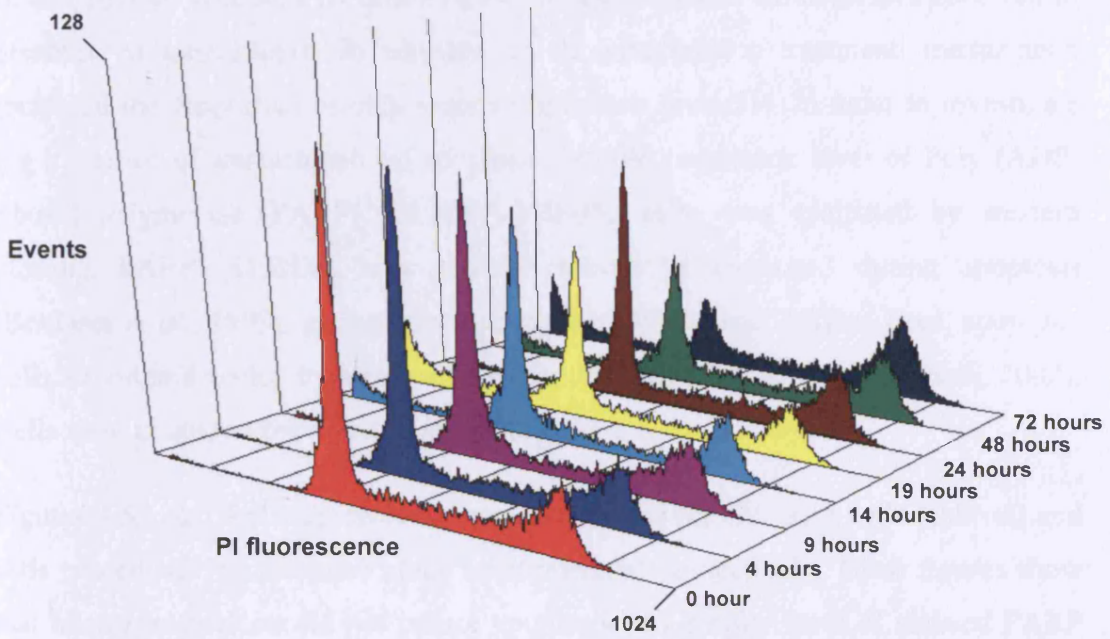

Figure 4.5 – Histogram profile of MDA-MB-453 cells treated with a combination of cisplatin and trastuzumab. Cells were treated with cisplatin (150μM) for one hour and trastuzumab (40μg/ml) continuously. Cells have been collected at different time point after the 1 hour treatment with both drugs. One event = one cell. Histogram from a representative experiment.

Trastuzumab 40μg/ml + Cisplatin 150μM	Sub G1	G1	S	G2
0	2.0±0.4	51.2±2.9	33.9±4.3	13.0±1.9
4	2.6±0.3	51.7±4.0	33.9±3.8	11.8±0.9
9	4.1±0.4	44.5±2.0	36.9±5.2	14.4±3.3
14	21.0±1.9	38.5±2.2	29.6±1.6	10.9±1.9
19	26.0±3.9	35.3±1.4	28.3±1.7	10.3±1.4
24	9.0±0.6	38.5±0.7	38.8±2.9	13.7±1.9
48	18.1±1.8	28.8±1.2	35.7±0.4	17.3±1.9
72	22.7±2.4	15.9±1.5	38.5±3.0	22.9±3.5

Table 4.4 – Percentage of MDA-MB-453 cells treated with cisplatin and trastuzumab in each phase of the cell cycle. Cells were treated with a combination of cisplatin (150μM) for one hour and trastuzumab (40μg/ml) continuously. Data presented are the average of three independent experiments as shown by the standard error.

4.6 Influence of DNA repair modulation on apoptosis

In the previous section, a reduction of the cisplatin-induced G2 arrest was observed in presence of trastuzumab. In addition, in the combination treatment, trastuzumab increased the proportion of cells entering apoptosis (sub-G1). In order to investigate the influence of trastuzumab on apoptosis, protein expression level of Poly (ADP-ribose) polymerase (PARP), in MDA-MB-453 cells, was evaluated by western blotting. PARP (113kDa) is a protein cleaved by caspase-3 during apoptosis (Boulares *et al.*, 1999), giving two fragments of 89kDa and 24kDa. Thus, apoptotic cells are often detected by monitoring PARP cleavage (Soldani and Scovassi, 2002). Cells were treated as previously described in the cell cycle analysis.

Figures 4.6A and 4.6B represent the results obtained for untreated cells (control) and cells treated with trastuzumab alone (continuously), respectively. These figures show that trastuzumab alone did not induce apoptosis as a similar level of cleaved PARP was observed in untreated cells and trastuzumab cells, after 48 hours. Figure 4.6C represents the level of PARP and cleaved PARP obtained in cells treated with cisplatin alone for 1 hour. A marked increase of cleaved PARP is seen at the peak of crosslinking (9 hours), increasing steadily up to 48 hours, demonstrating that cisplatin induces apoptosis. Nonetheless, the level of cleaved PARP is inferior to the level of total PARP, as no variation of PARP expression level can be noticed. When combining cisplatin with trastuzumab (Figure 4.6D), a similar level of cleaved PARP was observed after 9 hours, increasing steadily up to 48 hours, similarly to cells treated with cisplatin alone.

Consequently, measurement of PARP cleavage did not demonstrate that trastuzumab induced apoptosis. Nonetheless, trastuzumab may induce apoptosis after a longer period of time. Therefore, the results of the experiment on cisplatin/trastuzumab combinations were not due to induction of apoptosis.

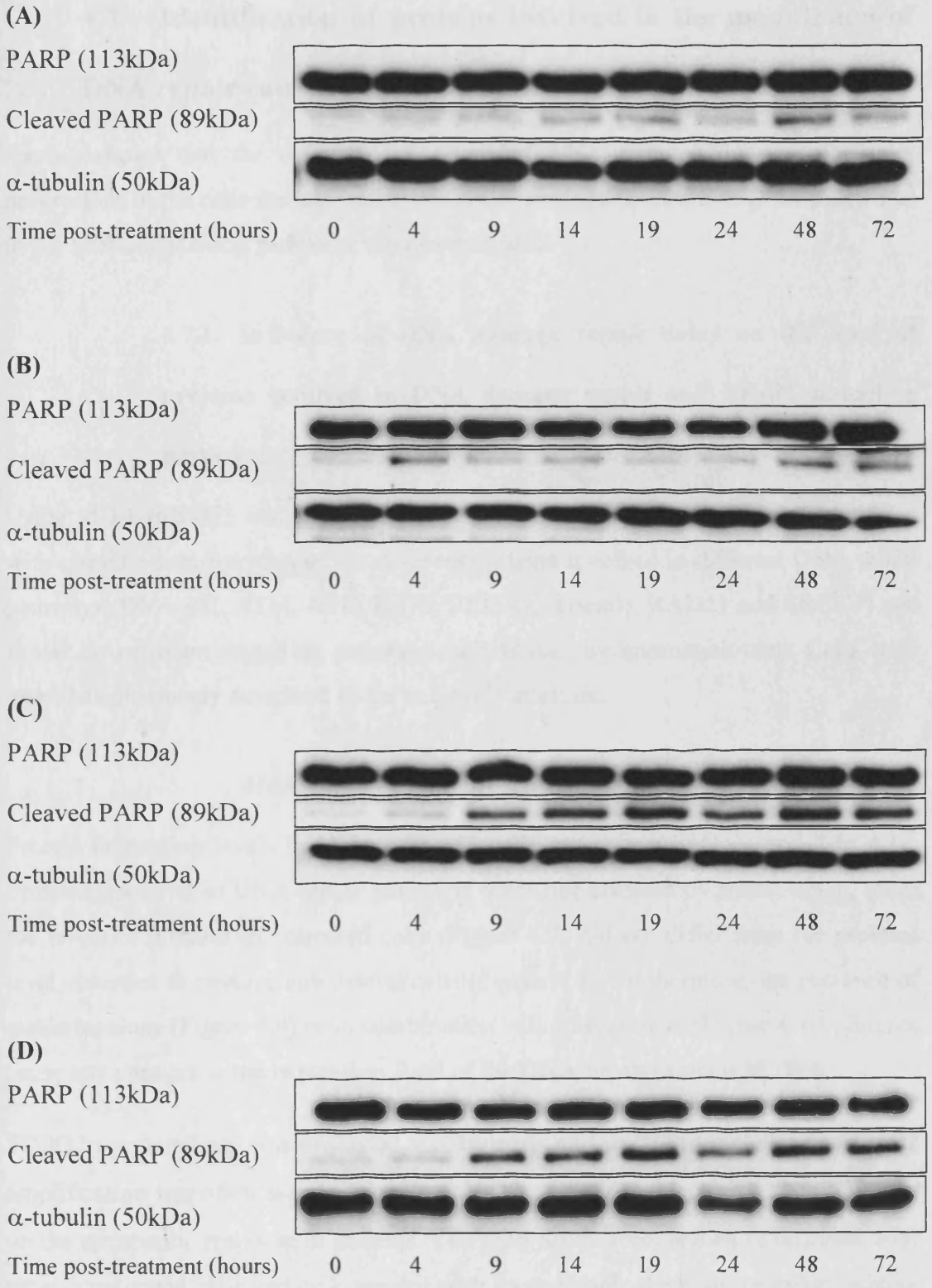

Figure 4.6 – Western blot analysis of PARP and cleaved PARP protein in MDA-MB-453 cells. MDA-MB-453 cells untreated (**A**), cells treated continuously with trastuzumab (40μg/ml) – **B**, cells treated for one hour with cisplatin (150μM) – **C**, and cells treated for one hour with cisplatin (150μM) and continuously with trastuzumab (40μg/ml) – **D**. Cleaved PARP is an indicator of apoptosis. α-tubulin was used as a loading control.

4.7 Identification of proteins involved in the modulation of DNA repair caused by ErbB2 inhibition

Having shown that the delay in the repair of DNA damage may be due to a progression of the cells through cell cycle arrest, proteins involved in DNA repair and in the ErbB2 signalling pathways were investigated.

4.7.1 Influence of DNA damage repair delay on the level of proteins involved in DNA damage repair and ErbB2 signalling pathways

Using MDA-MB-453 and SK-BR-3 cells, the effect of trastuzumab in combination with cisplatin was investigated on different proteins involved in different DNA repair pathways (DNA-PK, ATM, ATR, Ku70, BRCA1, Artemis, RAD51 and ERCC1) and ErbB2 downstream signalling pathway, such as Akt, by immunoblotting. Cells were treated as previously described in the cell cycle analysis.

Modulation of proteins level in MDA-MB-453 cells

Protein expression levels in MDA-MB-453 cells are shown in Figures 4.7 to 4.10. Proteins involved in DNA repair pathways were not affected by trastuzumab, since the levels of proteins in untreated cells (Figure 4.7) did not differ from the proteins level observed in trastuzumab treated cells (Figure 4.8). Furthermore, the presence of cisplatin, alone (Figure 4.9) or in combination with trastuzumab (Figure 4.10), did not cause any changes in the expression level of the DNA repair proteins studied.

TOPO2α protein level was evaluated, as Järvinen and Liu (2006) reported that ErbB2 amplification was often associated with TOPO2α amplification which had an impact on the therapeutic response in patients. TOPO2α levels were shown to decrease with time in untreated cells and cells treated with trastuzumab alone, in a similar fashion. Therefore ErbB2 inhibition by trastuzumab did not cause any alteration of TOPO2α expression. This reduction after 49 hours can be explained by the cells reaching confluence and not being able to grow exponentially. In cells treated with cisplatin alone (Figure 4.9), TOPO2α protein level was reduced after treatment (1 hour) but

quickly increased after 10 hours to reach a level higher than untreated cells. This reduction was explained by the accumulation of cells in G2 due to the formation of cisplatin-induced interstrand crosslinks, reaching a peak 9 hours post-treatment. These ICLs were then repaired allowing the cells to cycle normally. In combination with trastuzumab the reduction of TOPO2α was not present (Figure 4.10) but the protein level of TOPO2α increased steadily up to 73 hours.

As expected, ErbB2 was down-regulated in the presence of trastuzumab alone or in combination with cisplatin (Figures 4.8 and 4.10). This downregulation is noticeable after 10 hours of treatment. EGFR (which forms heterodimers with ErbB2 causing its activation) protein level is not affected by any of the treatments.

Akt protein level was not affected by any of the treatments but a major change in its phosphorylated form (pAkt Serine 473 – S473) was noticed in presence of trastuzumab (Figures 4.8 and 4.10). pAkt was not detectable in untreated MDA-MB-453 cells or in cells treated with cisplatin alone, however, in presence of trastuzumab for 1 hour, Akt became phosphorylated (pAkt S473). Activated Akt was then down-regulated when cells were treated with trastuzumab alone. Whereas, pAkt was not reduced in cells treated with cisplatin and trastuzumab. Therefore, cisplatin treatment maintained the phosphorylation state of Akt (pAkt S473), after activation by trastuzumab.

In conclusion, proteins levels investigated were not affected dramatically by trastuzumab, except for the phosphorylated form of Akt (S473) which was activated by trastuzumab. As a result, the phosphorylated forms of other proteins were investigated.

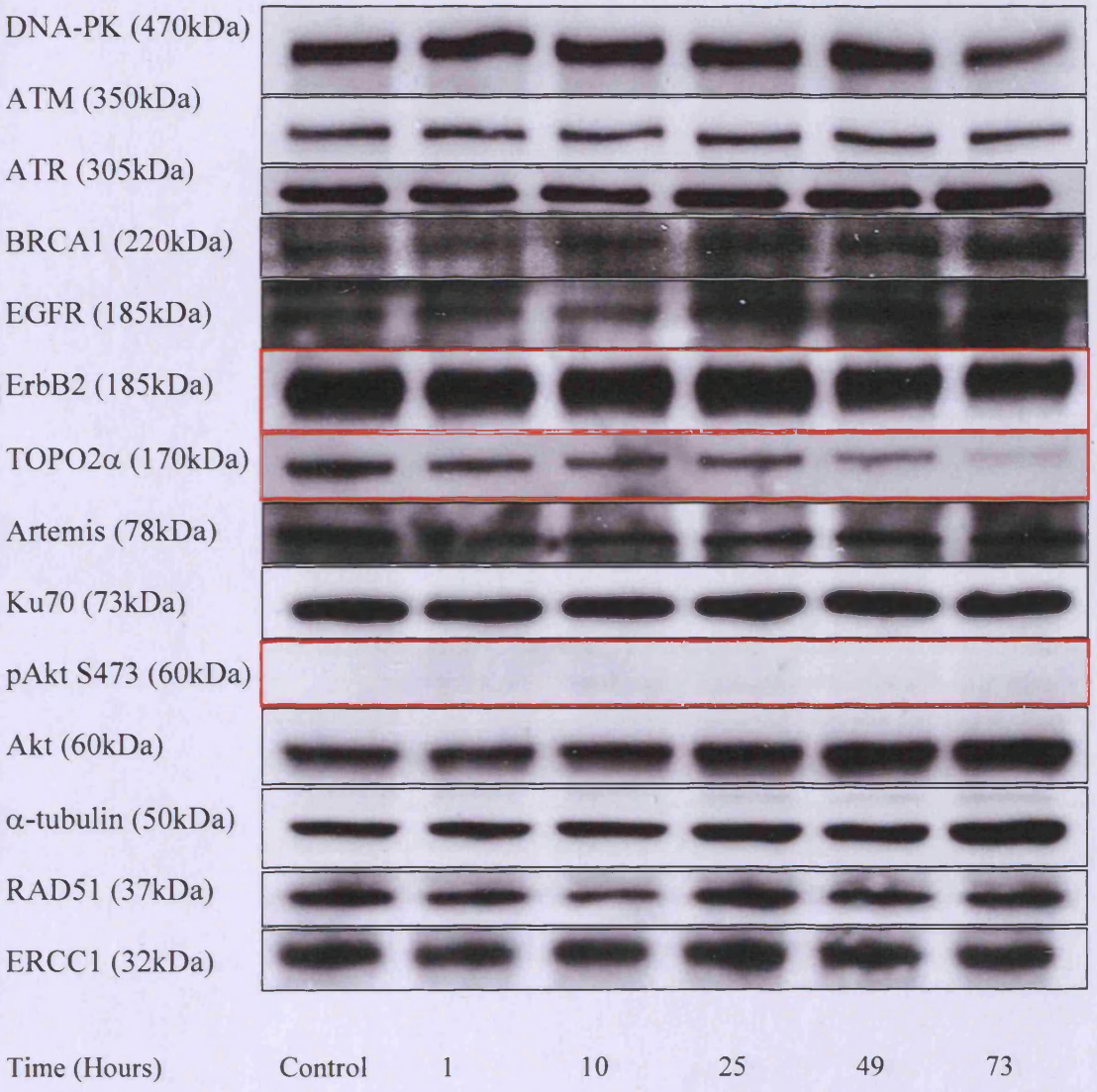

Figure 4.7 – Immunoblots of MDA-MB-453 untreated cells. Immunoblots were probed for DNA repair proteins and proteins involved in ErbB2 signalling pathways. α-tubulin was used as a loading control.

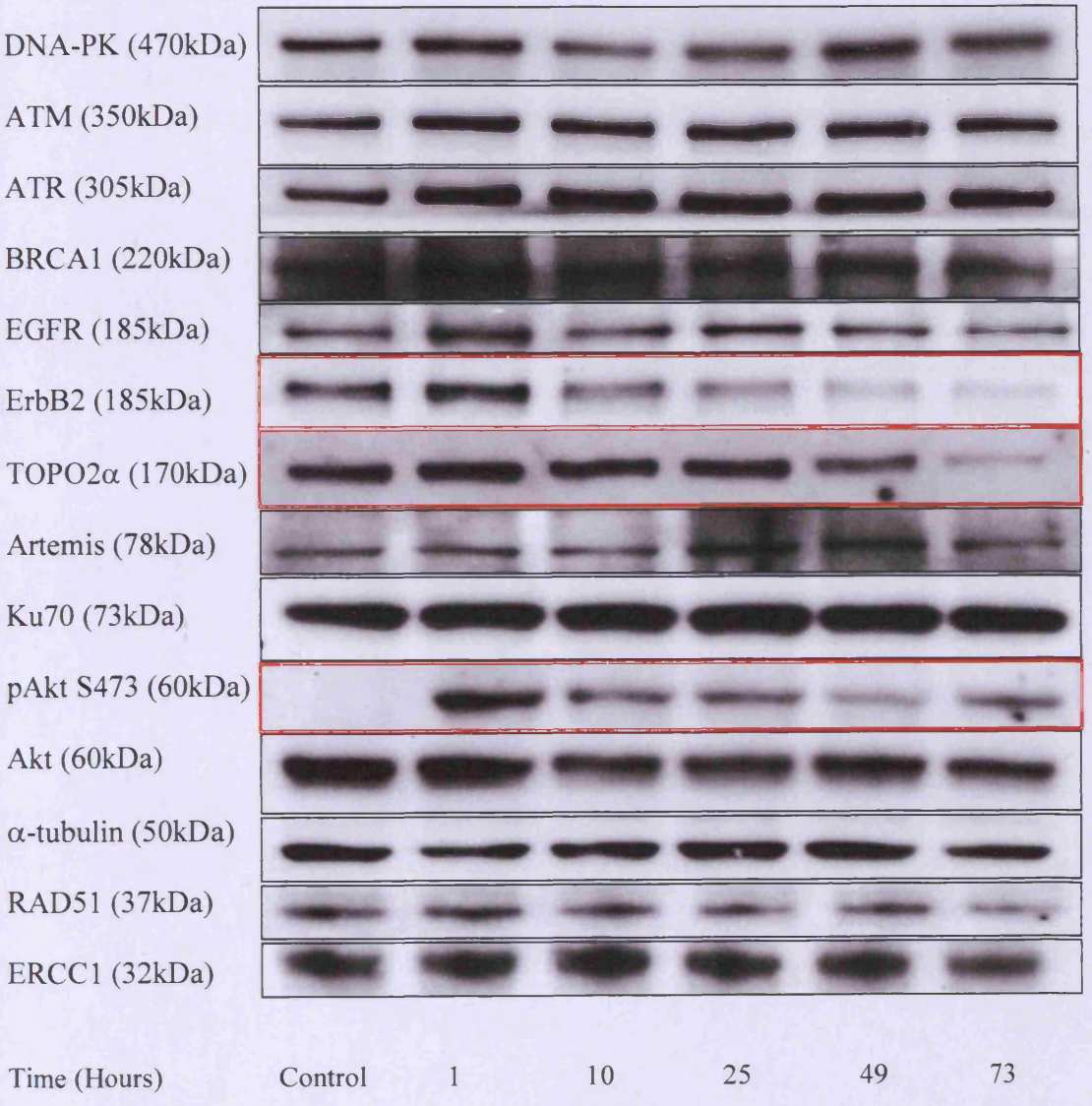

Figure 4.8 – Immunoblots of MDA-MB-453 cells treated with trastuzumab. Cells were treated with trastuzumab alone (40μg/ml) continuously and immunoblots were probed for DNA repair proteins and proteins involved in ErbB2 signalling pathways. α-tubulin was used as a loading control.

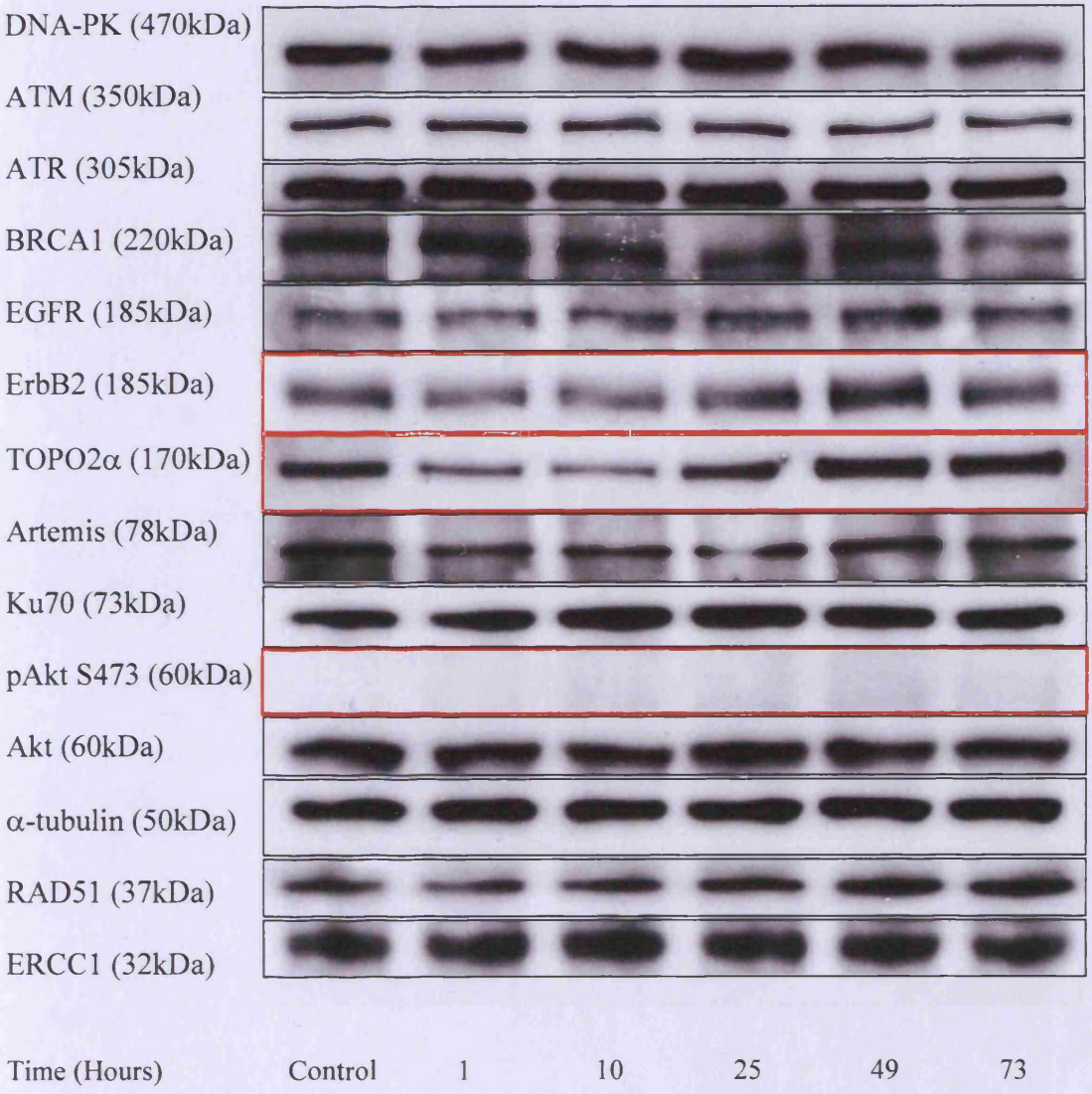

Figure 4.9 – Immunoblots of MDA-MB-453 cells treated with cisplatin. Cells were treated with cisplatin alone (150μM) for one hour then incubated in drug-free media. Immunoblots were probed for DNA repair proteins and proteins involved in ErbB2 signalling pathways. α-tubulin was used as a loading control.

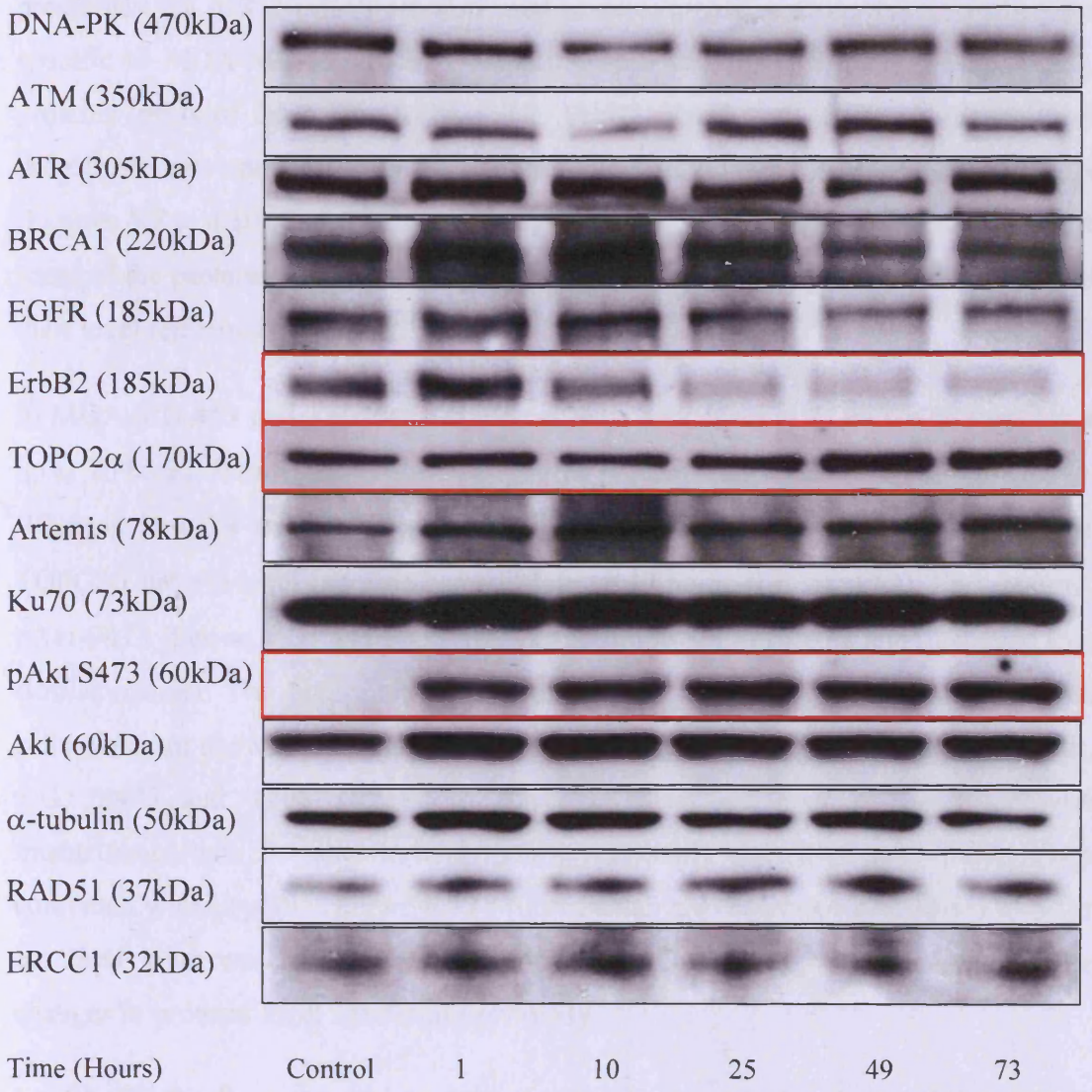

Figure 4.10 – Immunoblots of MDA-MB-453 cells treated with cisplatin and trastuzumab. Cells were treated with cisplatin (150μM) + trastuzumab (40μg/ml) for one hour then incubated in media containing trastuzumab alone (40μg/ml). Immunoblots were probed for DNA repair proteins and proteins involved in ErbB2 signalling pathways. α-tubulin was used as a loading control.

Modulation of proteins level and their phosphorylated forms in MDA-MB-453 and SK-BR-3 cells

MDA-MB-453 and SK-BR-3 cell lines were used to examine the effect of trastuzumab on the phosphorylated forms of some of the proteins investigated previously. SK-BR-3 cells were also used to determine if any observed effects were specific to MDA-MB-453 cells. Comparing both cell lines (Figures 4.11 to 4.14), proteins levels of DNA-PK, ATM, ATR, ErbB2, Ku70 and Akt were unaltered by drug treatments and similar to the one presented previously for MDA-MB-453 cells (Figures 4.7 to 4.10). In addition, pDNA-PK, pATM, pATR (phosphorylated forms of some of the proteins mentioned before) were not altered by any of the treatments and their level remained constant.

In MDA-MB-453 cells, cisplatin alone caused a reduction in TOPO2α protein level up to 10 hours, followed by an increase in the protein level by 25 hours (Figure 4.11). Whereas in cells treated with the combination of cisplatin and trastuzumab the TOPO2α protein level increased steadily up to 49 hours (Figure 4.12). Furthermore, pAkt S473 (Serine 473) and pAkt T308 (Threonine 308) proteins level behaved in a similar manner. The phosphorylated forms of Akt were not detectable in untreated cells (data not shown) or in cells treated with cisplatin alone (Figure 4.11). However, pAkt S473 and T308 were both activated after one hour of treatment with trastuzumab (data not shown) and their level slowly decreased with time. When combined with cisplatin (Figure 4.12), trastuzumab also activated both forms of pAkt but their level was maintained with time. Therefore, these results confirmed the changes in proteins level described previously.

For SK-BR-3 cells, immunoblots showed that cells treated with trastuzumab, alone or in combination with cisplatin, had their ErbB2 protein level reduced. Similarly to MDA-MB-453 cells, phosphorylated forms of Akt (pAkt S473 and T308) were not detectable in SK-BR-3 cells untreated (data not shown) or treated with cisplatin (Figure 4.13), but trastuzumab alone (data not shown) or in combination with cisplatin (Figure 4.14) caused phosphorylation of Akt (pAkt S473 and T308) after 1 hour. In addition, activated Akt was only reduced in cells treated with trastuzumab alone, similarly to MDA-MB-453 cells. Finally, in SK-BR-3 cells, cisplatin (Figure 4.13) also caused a reduction in TOPO2α protein expression level up to 10 hours (not

as detectable as in MDA-MB-453 cells) followed by an increase in protein level by 25 hours. Cells treated with a combination of trastuzumab and cisplatin (Figure 4.14) had no reduction in TOPO2α protein but a steady increase.

Therefore, results from SK-BR-3 cells confirmed those obtained with MDA-MB-453 cells; trastuzumab in combination with cisplatin modulates protein expression level of TOPO2α and alone, or in combination with cisplatin, modulates activation of Akt.

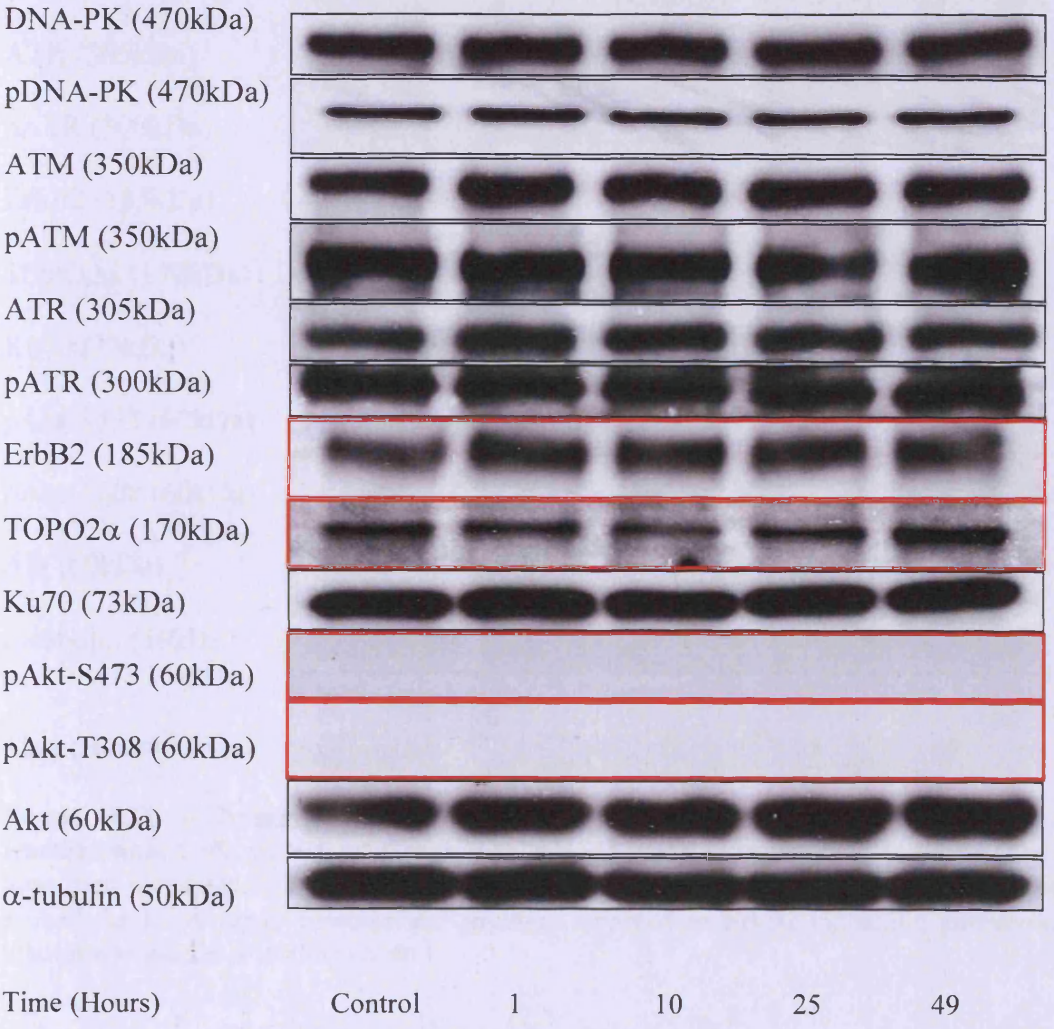

Figure 4.11 – Immunoblots of MD-MB-453 cells treated with cisplatin. Cells were treated with cisplatin alone (150μM) for one hour then incubated in drug-free media. Immunoblots were probed for DNA repair proteins and proteins involved in ErbB2 signalling pathways. α-tubulin was used as a loading control.

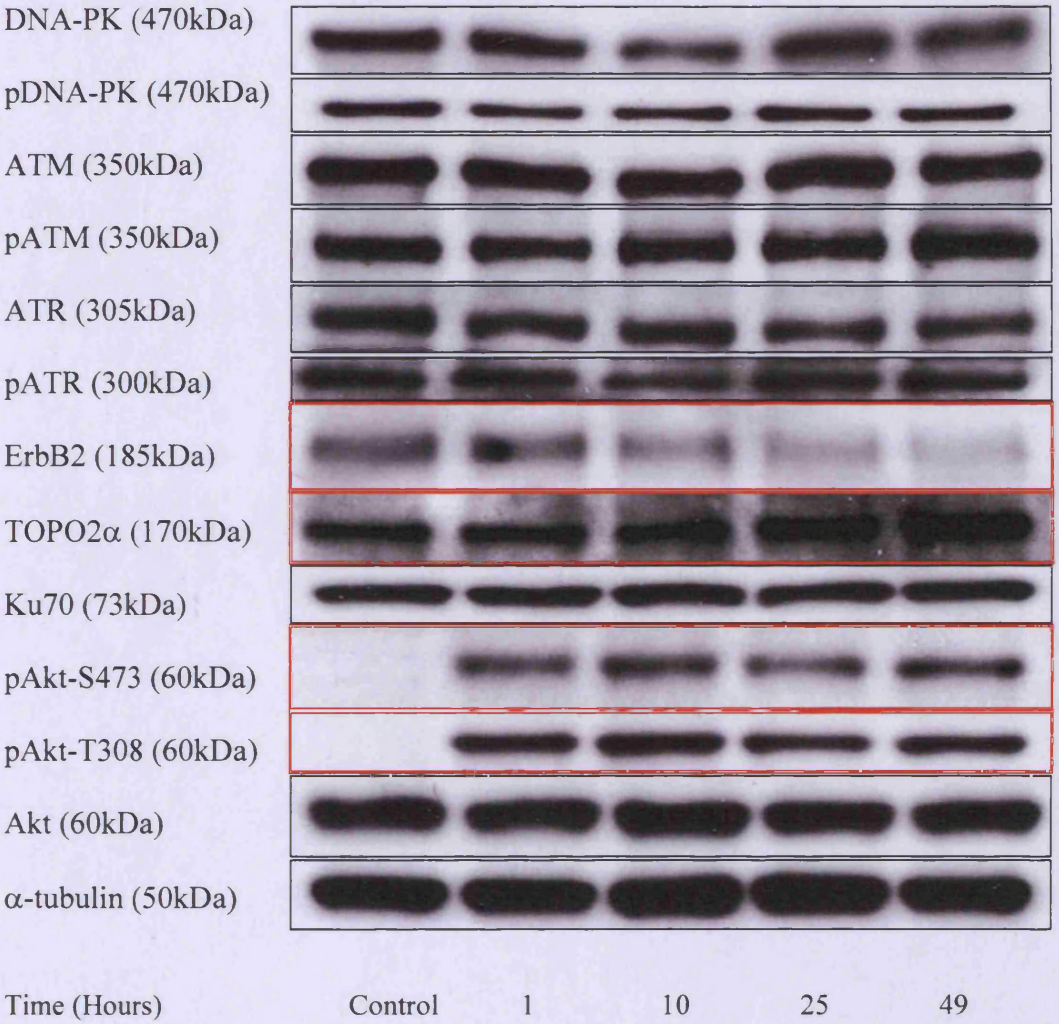

Figure 4.12 – Immunoblots of MDA-MB-453 cells treated with cisplatin and trastuzumab. Cells were treated with cisplatin (150μM) + trastuzumab (40μg/ml) for one hour then incubated in media containing trastuzumab alone (40μg/ml). Immunoblots were probed for DNA repair proteins and proteins involved in ErbB2 signalling pathways. α-tubulin was used as a loading control.

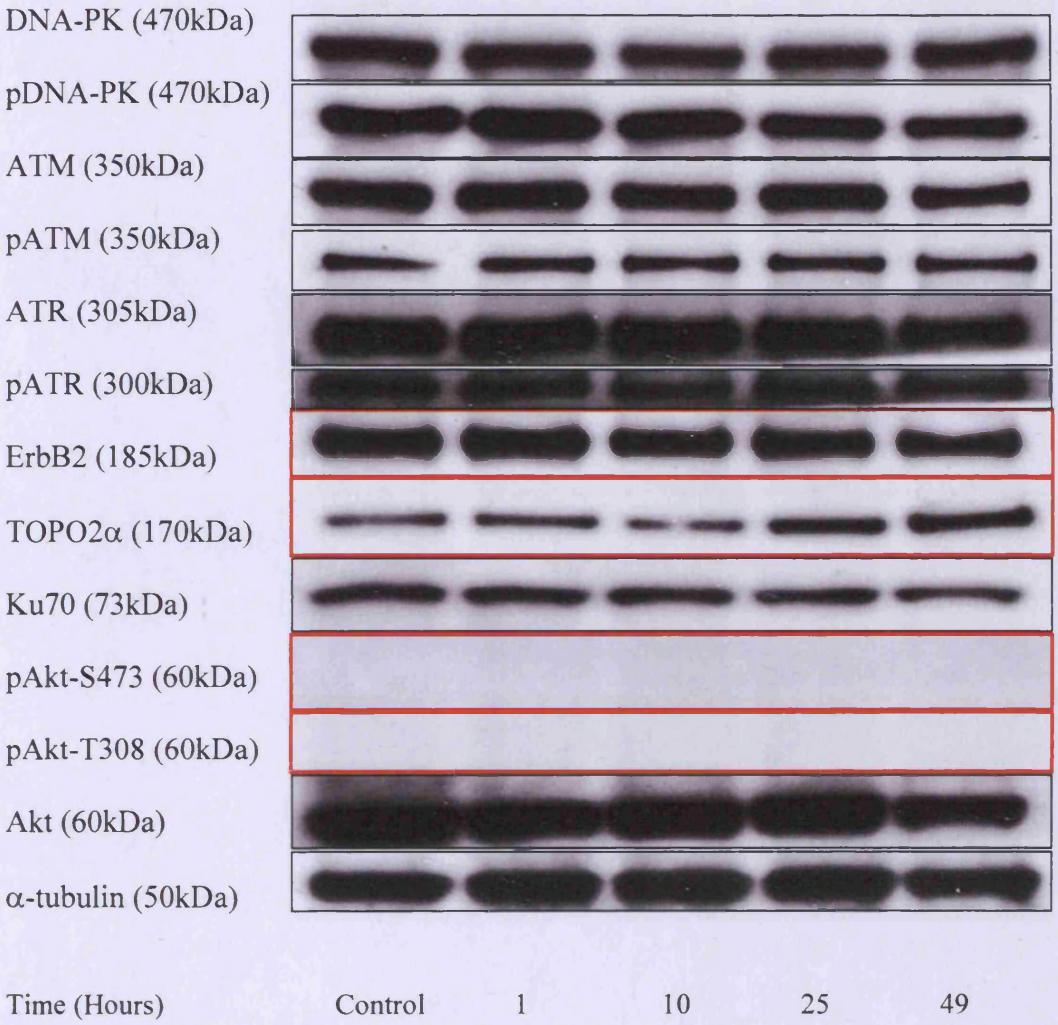

Figure 4.13 – Immunoblots of SK-BR-3 cells treated with cisplatin. Cells were treated with cisplatin alone (150μM) for one hour then incubated in drug-free media. Immunoblots were probed for DNA repair proteins and proteins involved in ErbB2 signalling pathways. α-tubulin was used as a loading control.

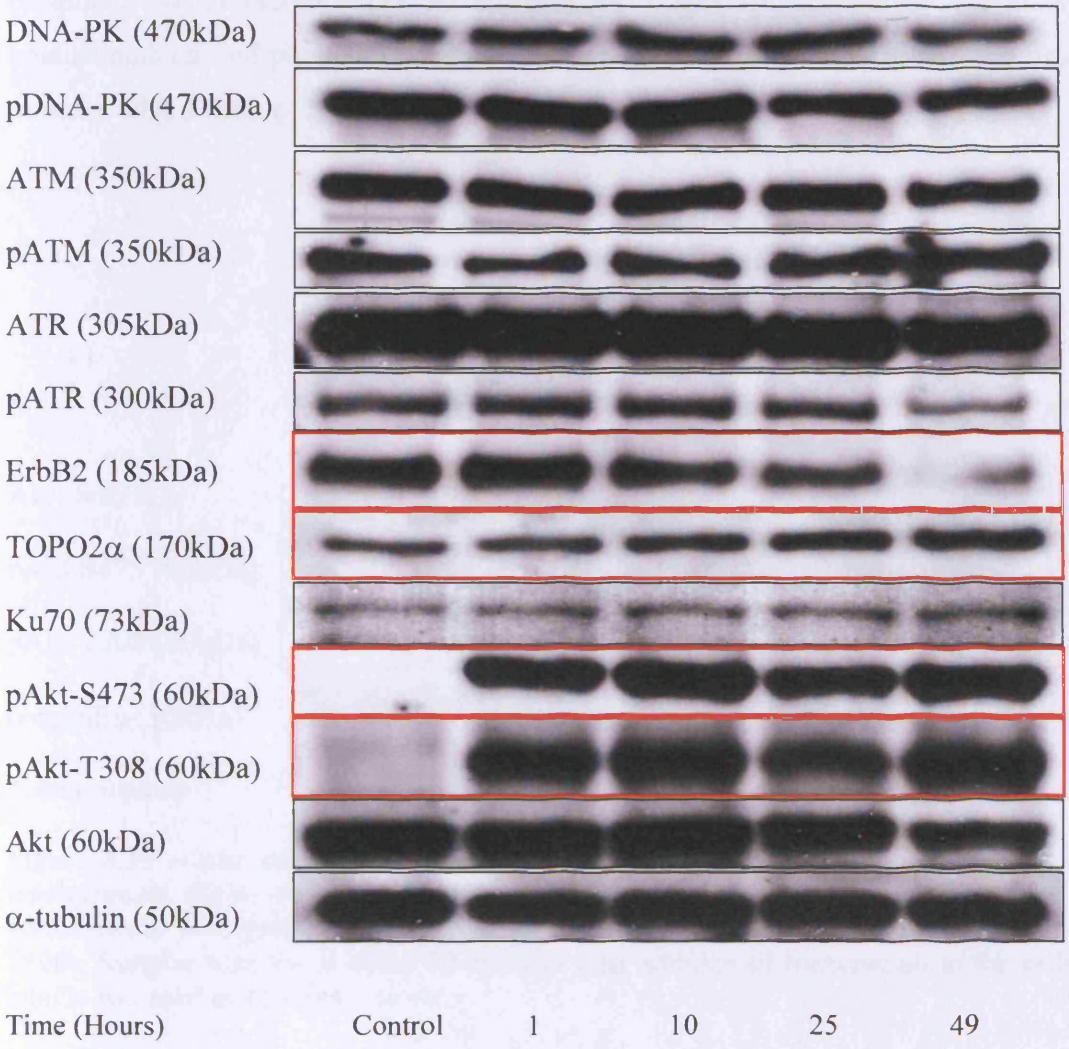

Figure 4.14 – Immunoblots of SK-BR-3 cells treated with cisplatin and trastuzumab. Cells were treated with cisplatin (150μM) + trastuzumab (40μg/ml) for one hour then incubated in media containing trastuzumab alone (40μg/ml). Immunoblots were probed for DNA repair proteins and proteins involved in ErbB2 signalling pathways. α-tubulin was used as a loading control.

Effect of trastuzumab treatment of Akt protein level

Having demonstrated that trastuzumab has a striking effect on the phosphorylation of Akt after 1 hour, the effect was further investigated within the first hour of trastuzumab treatment. MDA-MB-453 cells were treated with trastuzumab and proteins were extracted every 10 minutes for 1 hour. As shown by Figure 4.15, trastuzumab caused phosphorylation of Akt (pAkt S473 and T308) within the first 10 minutes with a peak of phosphorylation at 30 minutes.

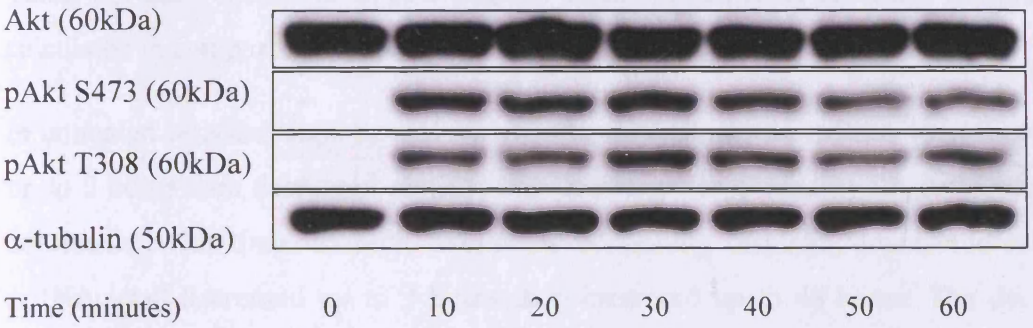

Figure 4.15 – Akt and pAkt protein expression in MDA-MB-453 cells treated with trastuzumab. Cells were treated with trastuzumab alone (40μg/ml) continuously and immunoblots were probed for Akt and the two phosphorylated forms of Akt (S473 and T308). Samples were taken every 10 minutes after addition of trastuzumab to the cells. α-tubulin was used as a loading control.

4.7.2 Influence of ErbB2 inhibition on TOPO2α mRNA level

It was shown that almost 90% of primary breast tumours with ErbB2 amplification have the simultaneous up-regulation of TOPO2α (Järvinen and Liu, 2006; Järvinen *et al.*, 2000). Furthermore, TOPO2α has been shown to be involved in important processes of cell cycle regulation. In section 4.7.1, trastuzumab was shown to block the decrease in TOPO2α protein level observed in cells treated with cisplatin alone. Therefore, it is important to consider the effect of ErbB2 inhibition, by trastuzumab, on TOPO2α mRNA expression level. In order to examine the effect of trastuzumab on TOPO2α amplification, MDA-MB-453 cells were treated with cisplatin and trastuzumab, and TOPO2α mRNA level was measured by real time PCR. As PCR conditions and primers had already been optimised, no optimisation was carried out. Figure 4.16 represent the level of TOPO2α mRNA post-treatment, with the values in Table 4.5. Each control is set at a value of 1 and mRNA level of treated samples are calculated in comparison to their control.

In untreated cells and cells treated with trastuzumab alone, the mRNA level increased up to 9 hours then decreased rapidly, this decrease was caused by the cells reaching confluence with time. In both treatments containing cisplatin, topoisomerase IIα mRNA level decreased up to 9 hours then increased up to 48 hours. The decrease observed can be attributed to the accumulation of cells in the G2 phase caused by cisplatin, thus arresting cell cycle progression to allow the repair of DNA damage. mRNA level increased up to 3 fold in cells treated with the combination of cisplatin and trastuzumab.

Therefore, these data are in accordance with the results obtained at the protein level (Figures 4.11 and 4.12), and demonstrate that inhibiting ErbB2 in cisplatin-induced DNA damaged cells increases topoisomerase IIα mRNA level, suggesting a progression of the cells through cell cycle arrest.

Time post-treatment (Hours)	Control	Trastuzumab (40µg/ml)	Cisplatin (150µM)	Cisplatin (150µM) + trastuzumab (40µg/ml)
Control	1.00±0.00	1.00±0.00	1.00±0.00	1.00±0.00
9	2.10±0.05	1.90±0.19	0.60±0.10	0.50±0.02
24	0.90±0.05	1.20±0.22	0.70±0.22	1.50±0.04
48	0.50±0.04	0.60±0.01	1.20±0.17	3.10±0.40

Table 4.5 – TOPO2α mRNA expression in MDA-MB-453 cells. TOPO2α mRNA expression ratio in treated MDA-MB-453 cells compared to untreated cells. For each treatment one untreated control was used, set at a value of 1. Data presented are the average of three independent experiments as shown by the standard error.

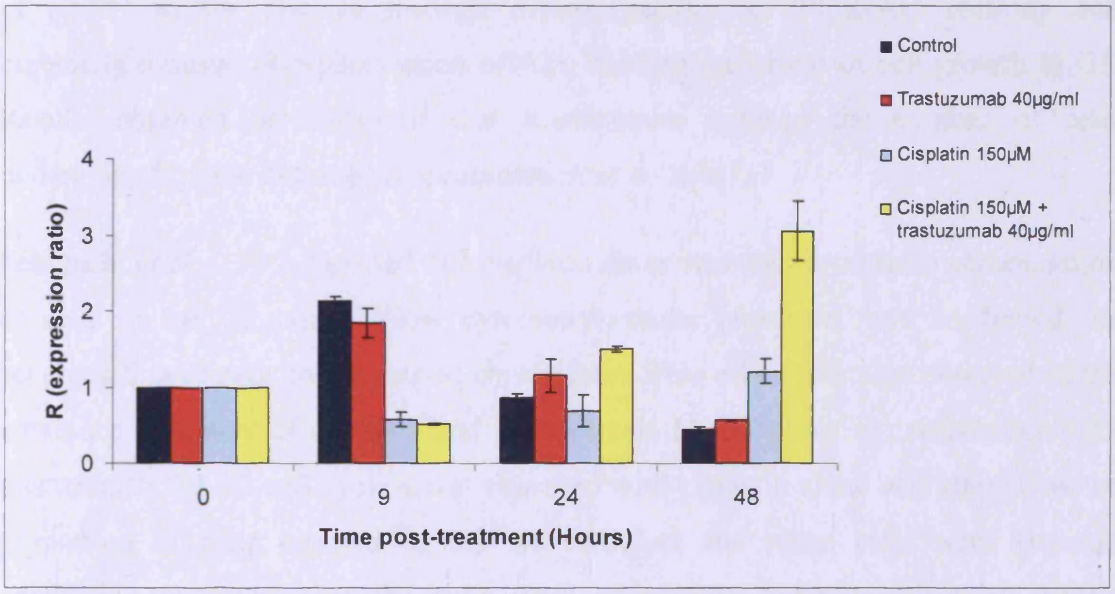

Figure 4.16 – TOPO2α mRNA level in MDA-MB-453 cells. Expression ratio in untreated MDA-MB-453 cells (dark blue), trastuzumab treated cells (red), cisplatin treated cells (light blue) and trastuzumab + cisplatin treated cells (yellow). Data presented are the average of three independent experiments as shown by the standard error.

DISCUSSION

In this chapter the effect of DNA repair modulation by trastuzumab, on the cell cycle, the induction of apoptosis and the expression level of proteins involved in DNA repair and ErbB2 signalling were investigated. Results established that the delay in the repair of cisplatin-induced DNA damage, caused by trastuzumab, may be explained by a progression of the cells through cell cycle arrest. Inhibition of ErbB2 was also shown to modulate Akt activation and topoisomerase IIα mRNA and protein expression.

4.8 Cell cycle and apoptosis

The study of the effects of DNA repair modulation, on the cell cycle, was carried out on MDA-MB-453 cells and showing a delay in the repair of cisplatin-induced DNA ICLs following treatment with trastuzumab. Sliwkowski *et al.* (1999) and Gong *et al.* (2004) demonstrated that trastuzumab alone caused a reduction of cells undergoing S phase and an accumulation of cells in the G1 phase. Furthermore, studies by Le *et al.* (2005) and Yakes *et al.* (2002) also demonstrated that trastuzumab led to an increase of $p27^{kip1}$ in the nucleus through down-regulation of PI3K/Akt pathway and especially reduced phosphorylation of Akt, causing inhibition of cell growth in G1. Results obtained here showed that trastuzumab reduced the number of cells undergoing S phase causing an accumulation of cells in G1.

Sekiguchi *et al.* (1996) reported that cisplatin alone was shown to cause accumulation of cells in the G2 phase. Flow cytometry results presented here confirmed the accumulation of cells in G2 caused by cisplatin. This effect was also observed in the combined treatment of cisplatin and trastuzumab. Nonetheless, in combination with trastuzumab the G2 cell cycle arrest observed with cisplatin alone was altered, as the proportion of cells arrested in G2 was reduced and more cells were entering apoptosis, suggesting that the cells were progressing through cell cycle arrest. Sliwkowski *et al.* (1999) reported that combining trastuzumab with chemotherapeutic agents results in increased anti-tumour activity than either agent given alone. However, study of the effect of trastuzumab on apoptosis has so far produced conflicting results (Mohsin *et al.*, 2005; Gennari *et al.*, 2004). The increase in sub-G1

observed is a marker of apoptosis and the increase in chemosensitivity (Chapter 3) is related to the increase in sub-G1. Nevertheless, the increase in apoptotic cells was not confirmed by measurement of PARP cleavage.

Therefore, the delay in the repair of cisplatin-induced DNA damage reported in Chapter 3 can be explained by the progression of the cells through cell cycle arrest caused by cisplatin. Further experiments need to be carried out to determine the effect of cisplatin/trastuzumab combination on apoptosis as results from flow cytometry and PARP cleavage were conflicting.

4.9 Modulation of proteins level by trastuzumab

4.9.1 Akt and cytoplasmic localisation of $p21^{WAF1}$

$p21^{WAF1}$ is a cyclin-dependent kinase which was shown to be activated by the tumour suppressor p53 following DNA damage, leading to cell cycle arrest (El-Deiry *et al.*, 1993; Xiong *et al.*, 1993; Waga *et al.*, 1994). In addition, $p21^{WAF1}$ was also shown to be induced by MAPK (Bottazzi *et al.*, 1999; Liu *et al.*, 1996) and PI3K (Zhou *et al.*, 2001b) signalling pathways. Zhou *et al.* (2001b) suggested that ErbB2 overexpressing cell lines promoted cell growth through activation of Akt and subsequent phosphorylation of $p21^{WAF1}$ at threonine 145, resulting in its cytoplasmic localisation and cell cycle progression. Furthermore, Yakes *et al.* (2002) demonstrated that trastuzumab caused a down-regulation of phosphorylated Akt, but no up regulation was noted within the first hour. A study by Pietras *et al.* (1999) also established that combining radiation with trastuzumab (100μg/ml) caused a delay in DNA repair and inhibition of $p21^{WAF1}$. They demonstrated that in presence of trastuzumab cells were able to escape cell cycle arrest, by inhibition of $p21^{WAF1}$, which did not allow enough time for DNA damage repair and caused an accumulation of unrepaired DNA damage. In addition, the study by McDonald *et al.* (1996) established that following DNA damage, caused by UV irradiation or cisplatin, $p21^{WAF1}$ deficient cells had a prominent defect in DNA repair compared to $p21^{WAF1}$ +/+ cells. Finally, Yu *et al.* (1998b) demonstrated that $p21^{WAF1}$ up-regulation, causing cell cycle arrest allowing DNA damage repair, was associated with chemoresistance in ErbB2 overexpressing cells.

Results obtained for MDA-MB-453 and SK-BR-3 cells demonstrated that after activation of Akt by trastuzumab (within the first 10 minutes – Figure 4.17), pAkt was down-regulated in the presence of trastuzumab alone but not in combination with cisplatin. These results, taken together with published data, demonstrate that trastuzumab leads to a G1 arrest and a reduction of cells undergoing S phase, due to decreased Akt activation and subsequent $p21^{WAF1}$ nuclear localisation. In contrast, in combination with cisplatin, pAkt level was maintained causing an increase in $p21^{WAF1}$ cytoplasmic localisation and inhibition of cell cycle arrest. In addition, Kandel *et al.* (2002) suggested that activation of Akt can overcome the p53-dependent G2/M cell cycle arrest and apoptosis induced by DNA damage. Thus, combining trastuzumab and cisplatin reduces the number of cells arresting in G2 and causes accumulation of unrepaired DNA damage, leading to apoptosis.

Although expression level of $p21^{WAF1}$ was not studied, results suggest that the delay in the repair of cisplatin-induced DNA damage by trastuzumab was due to a modulation of $p21^{WAF1}$. Nevertheless, other signal transduction pathways may be involved in the escape of cells from cell cycle arrest.

4.9.2 Akt and inhibition of $p27^{kip1}$ function

Another important protein involved in cell cycle regulation is the cdk inhibitor $p27^{kip1}$. Previous studies (Sliwkowski *et al.*, 1999; Marches and Uhr, 2004; Lane *et al.*, 2000; Le *et al.*, 2003) have shown that the anti-proliferative effect of trastuzumab was associated with cell cycle arrest in G1, by inhibition of proteins responsible for $p27^{kip1}$ sequestration. $p27^{kip1}$ has also been shown to be degraded following up-regulation of MAPK and PI3K pathways (Busse *et al.*, 2000; Lenferink et *al.*, 2001). Lenferink *et al.* (2001) suggested that blocking ErbB2 caused inhibition of MAPK and its mediated phosphorylation of $p27^{kip1}$, causing its stability. This study also demonstrated that the PI3K/Akt signalling pathway was inhibited, through inhibition of phosphorylated Akt, causing downregulation of cyclin D1. In addition, $p27^{kip1}$ was also shown to be transcriptionally activated through PI3K/Akt signalling pathway inhibition (Medema *et al.*, 2000). Therefore, these data taken together with the results obtained here for Akt activation, suggest that trastuzumab alone causes a G1 arrest by down-regulation of activated Akt and $p27^{kip1}$ activation. In combination with cisplatin, however, activated Akt is not reduced and leads to an escape from cell cycle

arrest, through continued activation of the PI3K/Akt pathway and progression of the cell cycle by $p27^{kip1}$ degradation or cytoplasmic retention (Medema *et al.*, 2000; Motti *et al.*, 2005).

Consequently, the decrease in the number of cells arrested in G2 when trastuzumab was combined with cisplatin, compared to cells treated with cisplatin alone, is explained by the cells escaping cell cycle arrest due to a degradation of $p27^{kip1}$ as well as a cytoplasmic localisation of $p27^{kip1}$ and $p21^{WAF1}$. Furthermore, progression of the cells through cell cycle arrest results in accumulation of unrepaired DNA damage as shown by the delay in DNA repair (Chapter3), and sensitisation of ErbB2 overexpressing cells to chemotherapeutic agents, by trastuzumab (Chapter 3). Nevertheless, further analysis of proteins involved in the escape of cells from cell cycle arrest is required, as Crowder *et al.* (2004) have reported that PTEN was also involved in PI3K/Akt signalling and may confer resistance to trastuzumab.

4.10 Trastuzumab and topoisomerase IIα

Topoisomerase IIα is a protein regulated by the cell cycle and involved in many cell cycle regulation processes. Järvinen and Liu (2003) reported that TOPO2α amplification was often associated with ErbB2 gene co-amplification in breast cancer. Although trastuzumab alone was not shown to affect the expression levels of TOPO2α, cisplatin caused a decrease in TOPO2α mRNA and protein levels. This decrease was associated with the DNA damage caused by cisplatin at 9 hours post-treatment, which corresponds to the peak of cisplatin crosslinks. As reported by Wang *et al.* (1997), p53 can down-regulate topoisomerase IIα expression by transcriptional regulation to stop the replication after DNA damage. The level of TOPO2α slowly increased again as DNA ICLs were repaired, as shown by the comet assay in Chapter 3. However, combining trastuzumab with cisplatin caused a decrease in TOPO2α mRNA level but not in the protein level, and the increase was much more dramatic than with cells treated with cisplatin alone. This would suggest that fewer cells undergo cell cycle arrest, as TOPO2α protein level is not reduced, and that there is cell cycle progression as topoisomerase IIα increased. Furthermore, Akt activation

was shown to cause p53 degradation, through MDM2 degradation (Zhou *et al.*, 2001a), blocking p53-induced topoisomerase IIα down-regulation.

Therefore, this observation supports the idea that cells treated with the combination of cisplatin and trastuzumab escaped cell cycle arrest due to activation of Akt and subsequent p53 degradation.

4.11 Conclusion

These results established that the delay in the repair of cisplatin-induced DNA ICLs observed in Chapter 3 could be attributed to a progression of the cells through cell cycle arrest. Furthermore, trastuzumab alone was shown to cause a reduction in cells undergoing S phase associated with an increase in G1, similarly to previous published studies. In addition, in combination with cisplatin, trastuzumab was shown to induce apoptosis. Although results were not confirmed by the PARP cleavage, further investigation need to be carried out. Results obtained also established that in combination with cisplatin, trastuzumab caused continuous activation of Akt and subsequent escape of cells from cell cycle arrest, through $p21^{WAF1}$ and $p27^{kip1}$ degradation or cytoplasmic retention. Furthermore, p53 degradation is also thought to be involved in the inhibition of induction of apoptosis.

Therefore, considering those results with other published studies on the effect of trastuzumab, it is reasonable to suggest that the delay in DNA damage repair is caused by an escape of the cells from cell cycle arrest. However, further analysis of the effect of trastuzumab on proteins involved in MAPK and PI3K/Akt signalling pathways is required to confirm this finding.

As the molecular mechanism of trastuzumab within the cells remains unclear, further understanding of the role of ErbB2 in DNA damage repair is required. To this end, the next chapter will discuss the specific role of ErbB2 on DNA damage repair using ErbB2 negative MDA-MB-468 cells, stably transfected with a plasmid containing ErbB2.

Chapter 5

Modulation of the repair of drug-induced DNA damage and ErbB2 expression

INTRODUCTION

In Chapter 4 it was suggested that the observed delay caused by ErbB2 inhibition of the repair of cisplatin-induced DNA ICLs was caused by an escape of cells from cell cycle arrest. Therefore, it is important to investigate further the specific role of ErbB2 overexpression in the repair of drug-induced DNA damage. In order to study the specific role of ErbB2, two approaches were considered: the use of ErbB2 siRNA in ErbB2 positive cell lines and the transfection of ErbB2 in ErbB2 negative cells. Using the most suitable approach, the effect on the repair of cisplatin-induced DNA damage will be studied further.

5.1 ErbB2 overexpression

In breast cancer, ErbB2 overexpression has been previously associated with increased cell proliferation and poor patient prognosis. Nevertheless, the role of ErbB2 overexpression in chemotherapeutic response remains unclear. Indeed, conflicting results have been published, clinical studies by Allred *et al.* (1992) and Wright *et al.* (1992) demonstrated that ErbB2 overexpression in patients was associated with increased resistance to chemotherapeutic treatments such as cyclophosphamide and carboplatin. Whereas Muss *et al.* (1994) reported that ErbB2 overexpression increased the response to doxorubicin. Furthermore, *in vitro* studies have also produced conflicting results showing that ErbB2 could be associated with increased resistance to cisplatin and paclitaxel whereas no difference was seen with doxorubicin and fluorouracil (Benz *et al.*, 1992). Nonetheless, Pegram *et al.* (1997) reported that chemosensitivity associated with ErbB2, *in vitro*, was cell line specific, and that *in vivo* ErbB2 overexpression did not alter the chemosensitivity but caused a more rapid re-growth.

5.2 Cisplatin-induced DNA damage

Cisplatin or *cis*-Diamminedichloroplatinum (II) is a widely used chemotherapeutic agent, its cytotoxic effects are due to the formation of two main types of adducts, the 1,2-intrastrand crosslinks forming up to 90% of the platinum-DNA adducts and the

interstrand crosslinks adducts (Jakupec, 2003). Although DNA interstrand crosslinks represent only 10% of the lesions caused by cisplatin, they have been described as being critical cytotoxic lesions in diving cells (Dronkert and Kanaar, 2001; Lawley and Phillips, 1996). Intrastrand crosslinks have been shown to be repaired by nucleotide excision repair (Zamble *et al.*, 1996). The mechanism of repair of cisplatin-induced interstrand crosslinks adducts remains unclear. Nevertheless, many studies have suggested that repair of cisplatin ICLs relies upon XPF-ERCC1 for the unhooking of the crosslink (De Silva *et al.*, 2000; Mu *et al.*, 2000; Kuraoka *et al.*, 2000). De Silva *et al.* (2002) also described that homologous recombination played an important role in the repair of cisplatin induced DNA ICLs repair, as they demonstrated the importance of XRCC2 and XRCC3 proteins in this repair pathway. Having shown that inhibition of ErbB2, by trastuzumab, led to a delay in the repair of cisplatin-induced DNA interstrand crosslinks, it is important to consider its effect on the repair of each of those two types of adducts.

Therefore, when studying the repair of cisplatin-induced DNA damage it is important to consider both types of adducts, as different protein are involved. As previously described in Chapter 3, DNA interstrand crosslinks formation and repair was studied using the comet assay. However, formation and repair of cisplatin-induced DNA intrastrand crosslinks can be measured using the competitive ELISA assay (described in Chapter 2), as developed by Tilby *et al.* (1987; 1991). This method is based on the use of an antibody that recognise cisplatin1,2-intrastrand adducts.

5.3 Cell cycle modulation

Chapter 4 suggested that Akt and topoisomerase IIα were involved in the escape of cells from cell cycle arrest, following combination treatment with cisplatin and trastuzumab. Nevertheless, other proteins have been shown to be involved.

5.3.1 Mitogen-Activated Protein Kinase (MAPK)

In addition to the PI3K pathway, ErbB2 overexpression was shown to prolong and enhance signalling from the MAPK pathway (Karunagaran *et al.*, 1996; Waterman *et al.*, 1999). Activation of the Ras/MAPK pathway causes degradation of $p27^{kip1}$ and

inhibits its ability to bind cdk2, increasing cyclin D1 expression and cell cycle progression (Kawada *et al.*, 1997; Rivard *et al.*, 1999). Furthermore, Lenferink *et al.* (2001) established that ErbB2 was able to modulate $p27^{kip1}$ and cyclin D1 protein levels through modulation of Ras/MAPK and PI3K/Akt signalling pathways. In addition, they demonstrated that inhibition of MAPK led to $p27^{kip1}$ stability and G1 cell cycle arrest. Moreover, MAPK was shown to induce $p21^{WAF1}$ (Bottazzi *et al.*, 1999; Liu *et al.*, 1996), leading to cell cycle arrest in G1 phase.

5.3.2 Phosphatase and Tensin homolog (PTEN)

PTEN is as a tumour suppressor gene causing inhibition of the PI3K pathway through inhibition of Akt activity. Indeed, upon ErbB2 phosphorylation, tyrosine kinase residues of the receptor recruit intracellular signalling molecules to the intracellular domain, including the non-receptor tyrosine kinase Src. Phosphorylated Src becomes activated and phosphorylates PTEN preventing its translocation to the plasma membrane and the dephosphorylation of PIP3, generated by PI3K (Crowder *et al.*, 2004). In addition, Nagata *et al.* (2004) reported that ErbB2 overexpression caused inhibition of PTEN through its phosphorylation, potentiating the activation of PI3K. Nevertheless, they showed that in presence of trastuzumab, PTEN becomes activated through dephosphorylation and inhibits the PI3K/Akt signalling pathway, leading to inhibition of tumour progression. However, loss of PTEN function from PTEN mutations has been shown to increase trastuzumab resistance *in vitro* and *in vivo*, as PTEN cannot be activated and inhibit PI3K/Akt pathway. Thereby, causing tumourigenesis and trastuzumab resistance. Fujita *et al.* (2006) further confirmed that PTEN could be used a predictive marker for trastuzumab resistance. Therefore, it is important to consider the expression of PTEN in cell cycle regulation and the response to combination treatments with trastuzumab.

5.3.3 Topoisomerase II activity

The study by Pu and Bezwoda (1999) reported that elevated topoisomerase IIα level as well as increase of topoisomerase II activity was associated with an increase resistance to alkylating agents. Furthermore, Harris *et al.* (2001) demonstrated that ErbB2 signalling activation caused an increase of topoisomerase II protein and enzymatic activity, leading to chemoresistance to the alkylating agent

cyclophosphamide. In addition, the study by Pietras *et al.* (1994) reported that modulation of ErbB2 expression by trastuzumab led to a reduction of the repair of cisplatin-induced DNA damage. Therefore, it is possible that topoisomerase II is involved in the modulation of repair activity causing modulation of chemosensitivity.

5.4 Aims

ErbB2 expression was modulated using siRNA and ErbB2 plasmid transfection. Nevertheless, only one of these two models was used to evaluate the effect of ErbB2 expression on the repair of cisplatin-induced DNA damage. To this end, the following questions were addressed:

- How does ErbB2 protein expression affect sensitivity to cisplatin and trastuzumab?
- Does ErbB2 overexpression affect the repair of cisplatin and melphalan-induced DNA interstrand crosslinks?
- Is the repair of cisplatin-induced DNA intrastrand crosslinks also affected?
- How is expression of proteins involved in DNA damage repair and ErbB2 signalling pathway modified by ErbB2 expression and drug treatment?
- Is topoisomerase II activity affected by ErbB2 overexpression?

5.5 Down-regulation of ErbB2 expression by siRNA

In order to study the specific role of ErbB2, its expression level needed to be altered. To this end, specific ErbB2 siRNA, from Faltus *et al.* (2004), was used to cause down-regulation of ErbB2. RNA interference (RNAi or siRNA) regulates endogenous gene expression, the siRNA technique using the introduction of small double stranded RNA with a sequence specific to the gene being silenced. As siRNA does not always have the same efficiency in each cell line, all three breast cancer cell lines previously studied (MCF-7, SK-BR-3 and MDA-MB-453 cells) were used.

5.5.1 Determination of ErbB2 mRNA down-regulation by real time PCR

In order to determine the efficiency of the siRNA, down-regulation caused by specific human ErbB2 siRNA was measured by real time PCR. However, initially PCR conditions needed to be optimised.

PCR product verification and optimisation of the conditions

Prior to analysis, the purity of the product formed, using the designed primers, was checked by reverse transcriptase PCR (result not shown) and PCR samples were sequenced. The sequence below represents the sequence amplified during PCR (forward primer in red and reverse primer in blue):

5'-GGATGTGCGGCTCGTACACAGGGACTTGGCCGCTCGGAACGTGC TGGTCAAGAGTCCCAACCATGTCAAAATTA-3'

Conditions for the PCR were optimised by determining the primer limiting concentration, the probe concentration and the conditions of the PCR (internal control and ErbB2 reactions in the same tube or separate tube). All optimisation experiments were carried out with cDNA from untreated cells.

The primer limiting concentration was defined by using a range of concentrations, which were: forward primer (μM): 0.1; 0.4; 0.7; 1.0 and 1.4, and reverse primer (μM): 0.1; 0.4; 0.7; 1.0 and 1.4. No plateau phase could be observed, the absence of plateau phase indicated that the primer limiting concentration could not be reached.

Therefore, each set of primer needed to be run in separate wells. Primers concentrations were then determined using separate tubes for each experiment (results not shown). The concentrations of forward and reverse primers that yield the lowest Ct and the highest ΔRn values were 1.3μM of forward primer and 0.7μM of reverse primer. The probe concentration was determined using the same criteria (low Ct and high ΔRn) and 350nM of the probe was found to be enough to achieve a low Ct value and a high ΔRn.

Having determined the optimum concentrations, standard curves for β-glucuronidase (internal control) and ErbB2 were obtained using serial dilutions of the wild type cDNA. Reactions of the internal control and the ErbB2 gene were run in separate tubes and in the same tubes, in order to compare efficiencies. Results (not shown) indicated that interference occurred between the primer sets since efficiencies were affected if both reactions were run in the same tube. Furthermore, low correlation coefficients were obtained for the standard curves. Hence, reactions needed to be carried out in separate tubes.

Modulation of ErbB2 mRNA level

MCF-7, SK-BR-3 and MDA-MB-453 cells were transfected (as detailed in Chapter 2, section 2.15) with the siRNA and samples were analysed every 24 hours. Results obtained using the previously defined conditions are presented in Tables 5.1 to 5.3 and Figures 5.1 to 5.3. For each time point, untransfected cells were used as the control set at a value of 100% expression (or 1). A scrambled siRNA, which did not recognise any specific gene, was also used as a negative control.

Results showed that ErbB2 siRNA down-regulated the ErbB2 mRNA level in all cell lines. However, efficiency of the siRNA varied between cell lines. MCF-7 cells (Figure 5.1 and Table 5.1) had the ErbB2 mRNA level reduced to greater extent than the SK-BR-3 (Figure 5.2 and Table 5.2) and MDA-MB-453 cells (Figure 5.3 and Table 5.3) cells. In MCF-7 cells, transfected with ErbB2 siRNA, the mRNA level was reduced by 76% at the maximum effect, after 72 hours, and then increased from 96 hours. Similarly, in MDA-MB-453 cells the maximum mRNA reduction (55%) was seen after 72 hours and increased from 96 hours. In SK-BR-3 cells ErbB2 mRNA level was not affected before 96 hours, reaching a maximum effect after 120 hours,

with 62% reduction. It was also noted that ErbB2 mRNA level of MCF-7 and SK-BR3 cells transfected with scrambled siRNA was up regulated. This could possibly be explained by the effect of the transfection itself. However, in MDA-MB-453 cells transfected with scrambled siRNA the level of ErbB2 mRNA remained constant up to 96 hours.

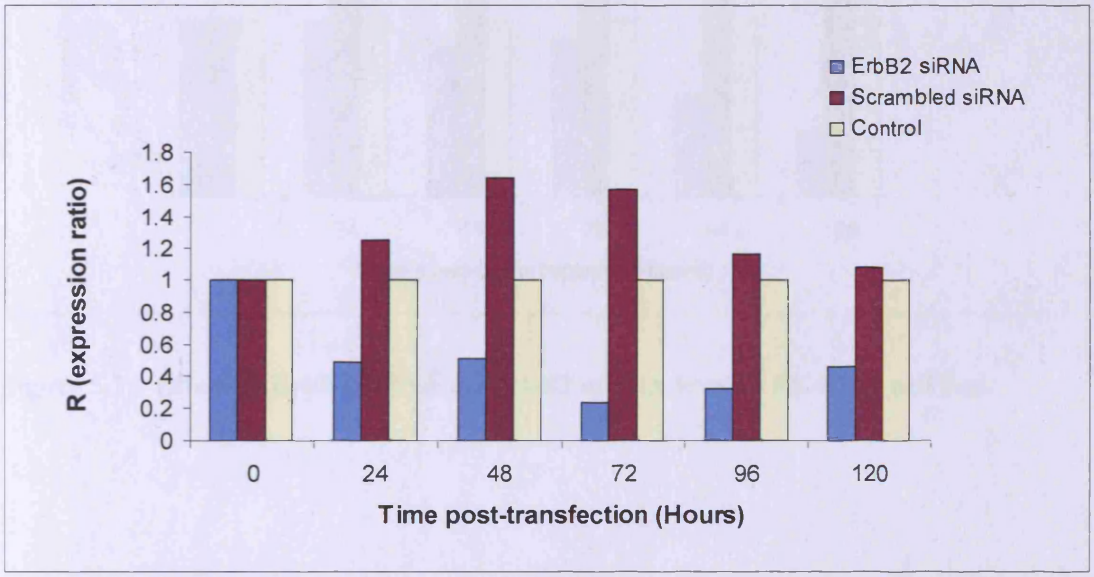

Figure 5.1 – Effect of ErbB2 siRNA on ErbB2 mRNA level in MCF-7 cell line.

Time (Hours)	Control untransfected	Scrambled siRNA	ErbB2 siRNA
0	1.00	1.00	1.00
24	1.00	1.25	0.49
48	1.00	1.64	0.51
72	1.00	1.57	0.24
96	1.00	1.17	0.32
120	1.00	1.08	0.46

Table 5.1 – ErbB2 mRNA level in MCF-7 cells. Cells were transfected with scrambled siRNA and ErbB2 specific siRNA. Time indicated was post-transfection.

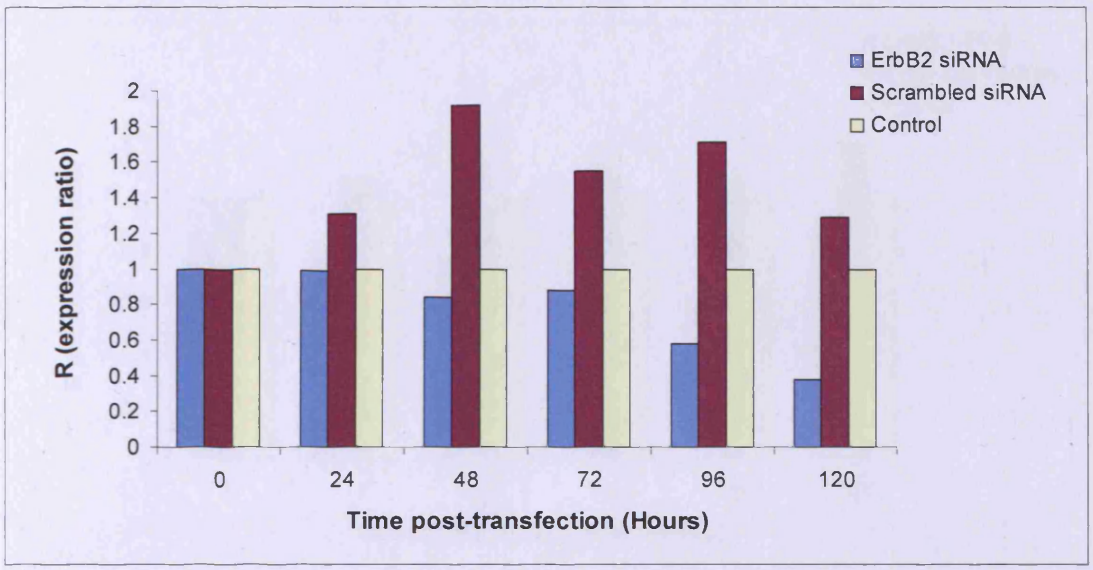

Figure 5.2 – Effect of ErbB2 siRNA on ErbB2 mRNA level in SK-BR-3 cell line.

Time (Hours)	Control untransfected	Scrambled siRNA	ErbB2 siRNA
0	1.00	1.00	1.00
24	1.00	1.31	0.99
48	1.00	1.92	0.84
72	1.00	1.55	0.88
96	1.00	1.71	0.58
120	1.00	1.29	0.38

Table 5.2 – ErbB2 mRNA level in SK-BR-3 cells. Cells were transfected with scrambled siRNA and ErbB2 specific siRNA. Time indicated was post-transfection.

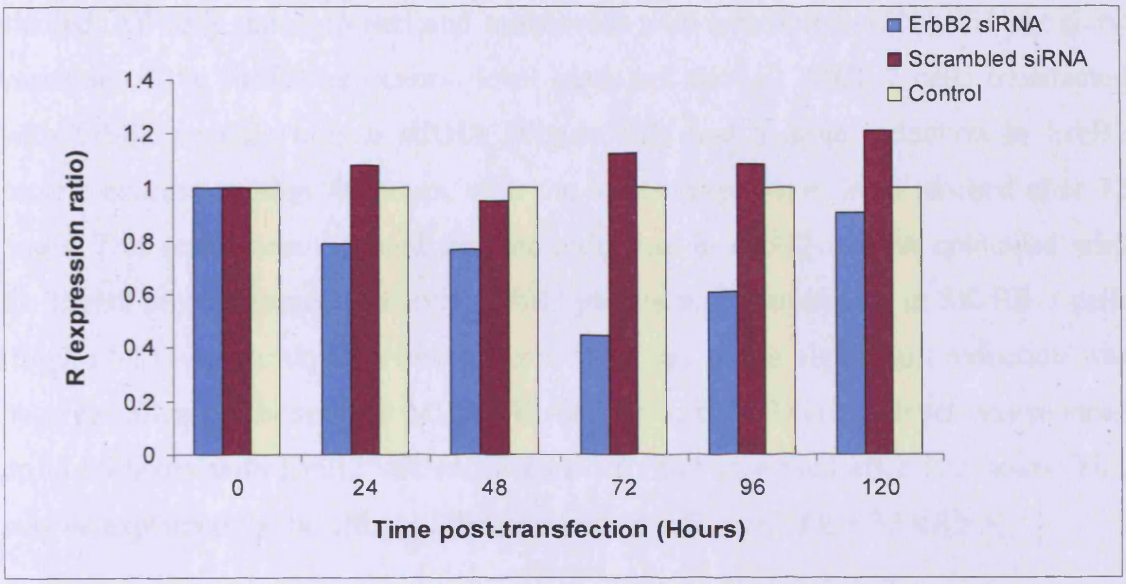

Figure 5.3 – Effect of ErbB2 siRNA on ErbB2 mRNA level in MDA-MB-453 cell line.

Time (Hours)	Control	Scrambled siRNA	ErbB2 siRNA
0	1.00	1.00	1.00
24	1.00	1.08	0.79
48	1.00	0.95	0.77
72	1.00	1.13	0.45
96	1.00	1.08	0.61
120	1.00	1.21	0.91

Table 5.3 – ErbB2 mRNA level in MDA-MB-453 cells. Cells were transfected with scrambled siRNA and ErbB2 specific siRNA. Time indicated was post-transfection.

5.5.2 Effect of ErbB2 siRNA on ErbB2 protein expression level

As the level of ErbB2 mRNA was shown to be reduced in all three cell lines, levels of ErbB2 proteins were evaluated by western blotting. Figures 5.4 to 5.6 represent the immunoblots obtained for cells transfected with ErbB2 siRNA, in all three cell lines studied. All cells untransfected and transfected with scrambled siRNA did not show variation of the ErbB2 expression level (data not shown). MCF-7 cells transfected with ErbB2 specific human siRNA (Figure 5.4) had a large reduction in ErbB2 protein expression after 48 hours, with the lowest expression level reached after 72 hours. This result demonstrated that the reduction in ErbB2 mRNA coincided with the ErbB2 protein expression level. ErbB2 protein expression level in SK-BR-3 cells (Figure 5.5) was slowly decreasing up to 96 hours, but a significant reduction was observed after 120 hours. For MDA-MB-453 cells, ErbB2 protein level was reduced up to 96 hours with ErbB2 siRNA (Figure 5.6) and increased after 120 hours. This may be explained by the effect of the transient transfection of ErbB2 siRNA.

All those observations concur with the effect of the siRNA on the mRNA level detailed previously. It also demonstrates that ErbB2 siRNA reduces ErbB2 protein in all the cell lines studied. Furthermore, the main reduction in protein level was seen in MCF-7 cells, expressing the lowest level of ErbB2 protein. Therefore, more optimisation work, on the amount of siRNA to be used and the conditions of transfection, would be required before using this siRNA in ErbB2 overexpressing cells for the study of ErbB2 modulation.

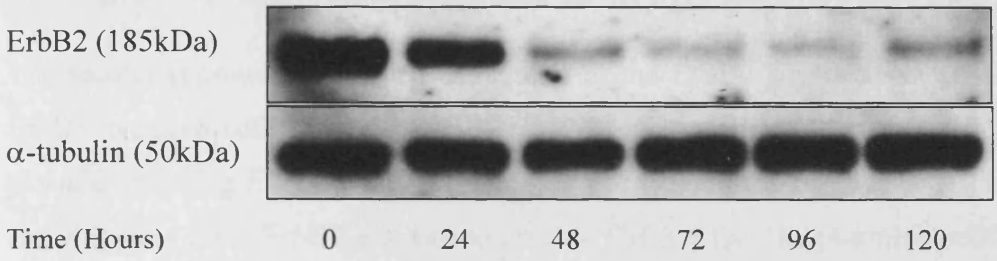

Figure 5.4 – ErbB2 protein level in MCF-7 cells transfected with ErbB2 siRNA. Cells were transfected for 120 hours (sample taken every 24 hours). α-tubulin was used as a loading control.

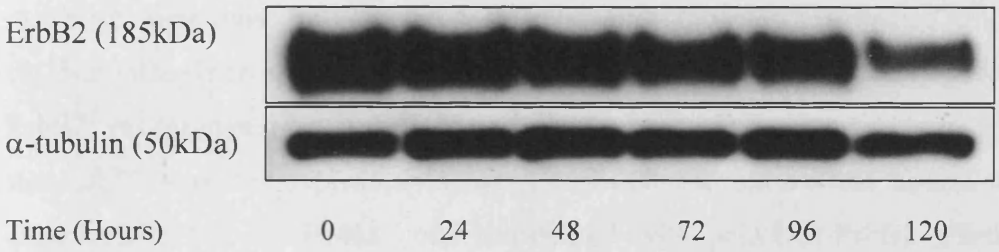

Figure 5.5 – ErbB2 protein level in SK-BR-3 cells transfected with ErbB2 siRNA. Cells were transfected for 120 hours (sample taken every 24 hours). α-tubulin was used as a loading control.

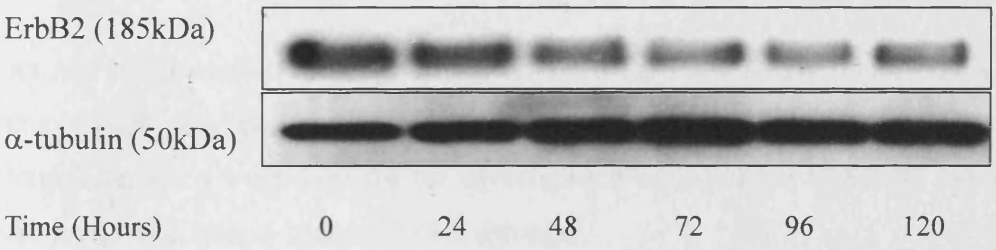

Figure 5.6 – ErbB2 protein level in MDA-MB-453 cells transfected with ErbB2 siRNA. Cells were transfected for 120 hours (sample taken every 24 hours). α-tubulin was used as a loading control.

5.6 Transfection of ErbB2 in ErbB2 negative cell line

The second approach developed in parallel of the ErbB2 siRNA, was the use of an ErbB2 negative cell line, MDA-MB-468 (Moasser *et al.*, 2001), transfected with a plasmid encoding ErbB2. This plasmid has been described by Tzahar *et al.* (1996), showing very good ErbB2 expression level in CHO cells. The plasmids pcDNA3 and pcDNA3-ErbB2 were a kind gift from Dr O. Segatto (Regina Elena Cancer Institute, Italy).

ErbB2 negative cell line, MDA-MB-468, was stably transfected with pcDNA3 and pcDNA3-ErbB2 in order to create a MDA-MB-468 cell line expressing ErbB2 and a MDA-MB-468 cell line used as a vector control. Stable transfection was carried out as described in Chapter 2 (section 2.16). Pooled transfection was carried out to minimise interclonal variation and selective pressure was maintained using G418 (0.75µg/ml). Once the two cell lines were growing exponentially, expression of ErbB2 was measured by western blotting and immunofluorescence. Figure 5.7 shows that ErbB2 was not expressed in MDA-MB-468 and shows that ErbB2 was only expressed in MDA-MB-468 cells transfected with pcDNA3-ErbB2. Furthermore, transfection did not affect the expression level of the other receptors of the ErbB family. Immunofluorescence confirmed that ErbB2 (green) was only expressed in MDA-MB-468 cells transfected with pcDNA3-ErbB2 (Figure 5.8 C), in the cytoplasm and the nucleus (stained red). In addition, MDA-MB-468 wild type cells (Figure 5.8 A) and MDA-MB-468 pcDNA3 (vector control – Figure 5.8 B) did not express ErbB2. It is also noted that the level of ErbB2 expression was comparable to the one observed in MDA-MB-453 cells as shown in Figure 5.8 D. Another characteristic of those cell lines is that EGFR was largely overexpressed.

As no further optimisation work was required for these stably transfected cell lines, this model was easier to use than the siRNA transfected cells. Thus, ErbB2 transfected cells were used for the investigation of the effect of ErbB2 expression in the repair of cisplatin-induced DNA damage.

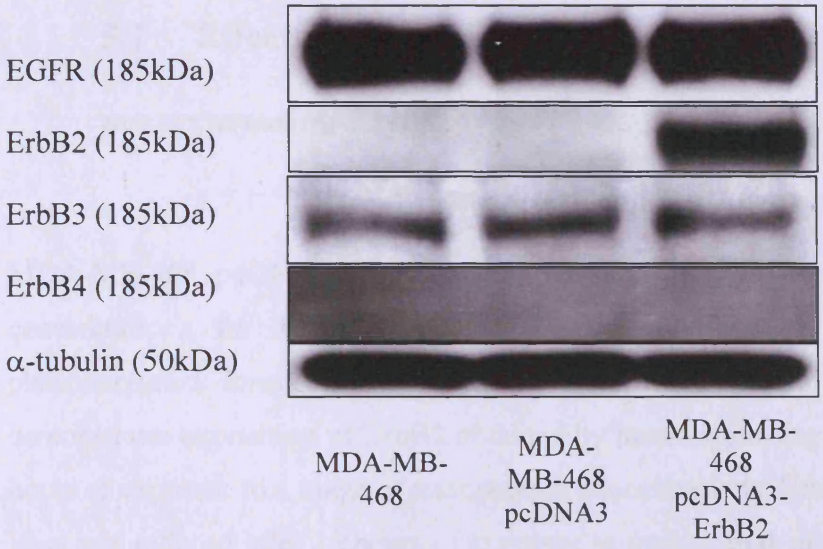

Figure 5.7 – Protein expression of each ErbB receptor in MDA-MB-468, MDA-MB-468 pcDNA3 (vector control) and MDA-MB-468 pcDNA3-ErbB2 cells. α-tubulin was used as a loading control.

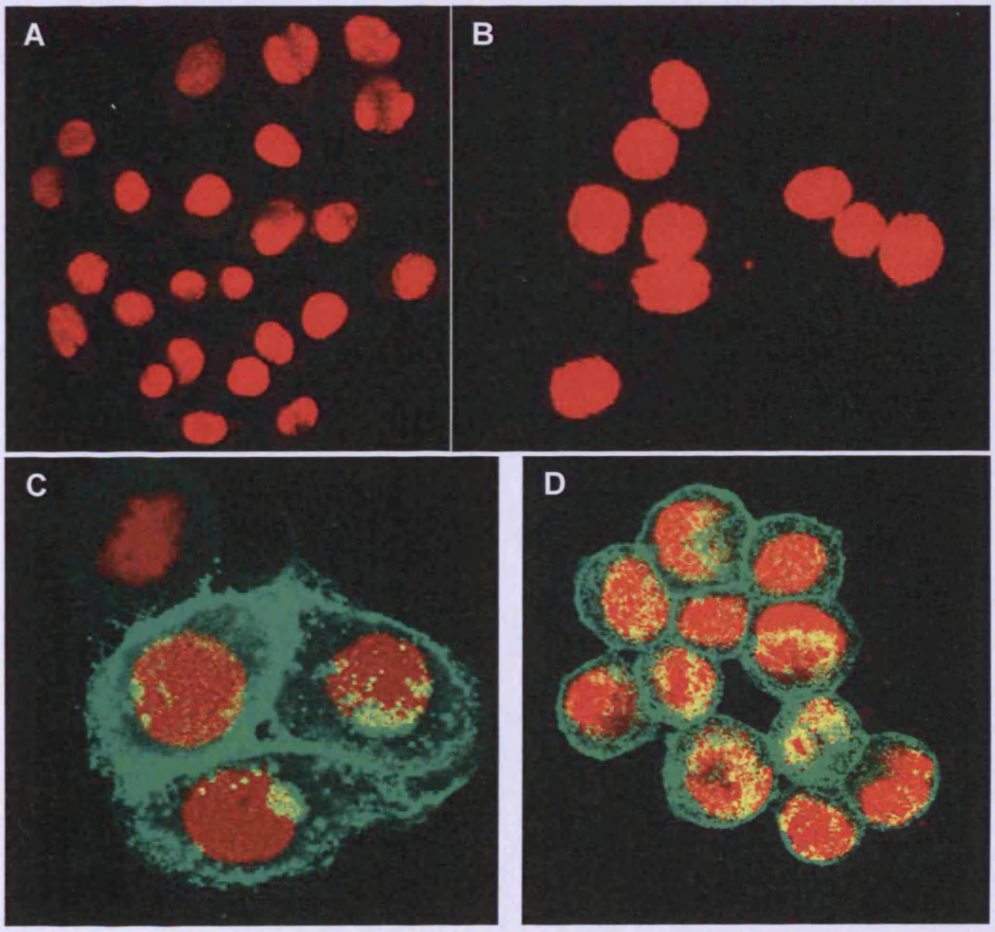

Figure 5.8 – ErbB2 immunofluorescence of MDA-MB-453 and MDA-MB-468 cells. MDA-MB-468 wild type cells (**A**), MDA-MB-468 cells transfected with pcDNA3 (**B**), MDA-MB-468 cells transfected with pcDNA3-ErbB2 (**C**) and MDA-MB-453 cells (**D**) were stained with anti-ErbB2 (green) and counter-stained with propidium iodide (red).

5.7 Effect of trastuzumab on MDA-MB-468 cells overexpressing ErbB2

5.7.1 Effect of trastuzumab on ErbB2 protein level

MDA-MB-468 pcDNA3-ErbB2 cells were treated with a range of trastuzumab concentrations, for different periods of exposure. Expression of ErbB2 and the phosphorylated form of Erb2 were measured by western blotting. Figure 5.9 demonstrates expression of ErbB2 obtained by immunoblotting after 1, 16, 24 and 72 hours of exposure to a range of trastuzumab concentrations. ErbB2 protein expression level was reduced after 16 hours of exposure to trastuzumab at 0.04μg/ml (Figure 5.9 B). After 1 hour of exposure, no reduction was observed. Similarly to the experiment in Chapter 3 (section 3.3), trastuzumab did not affect the level of phosphorylated ErbB2.

Down-regulation of ErbB2 by trastuzumab was also confirmed by immunofluorescence (Figure 5.10 A and B). After 24 hours with 40μg/ml of trastuzumab (Figure 5.10 B) ErbB2 protein level was reduced. This concentration of trastuzumab was used for the study of DNA interstrand crosslinks in the next section.

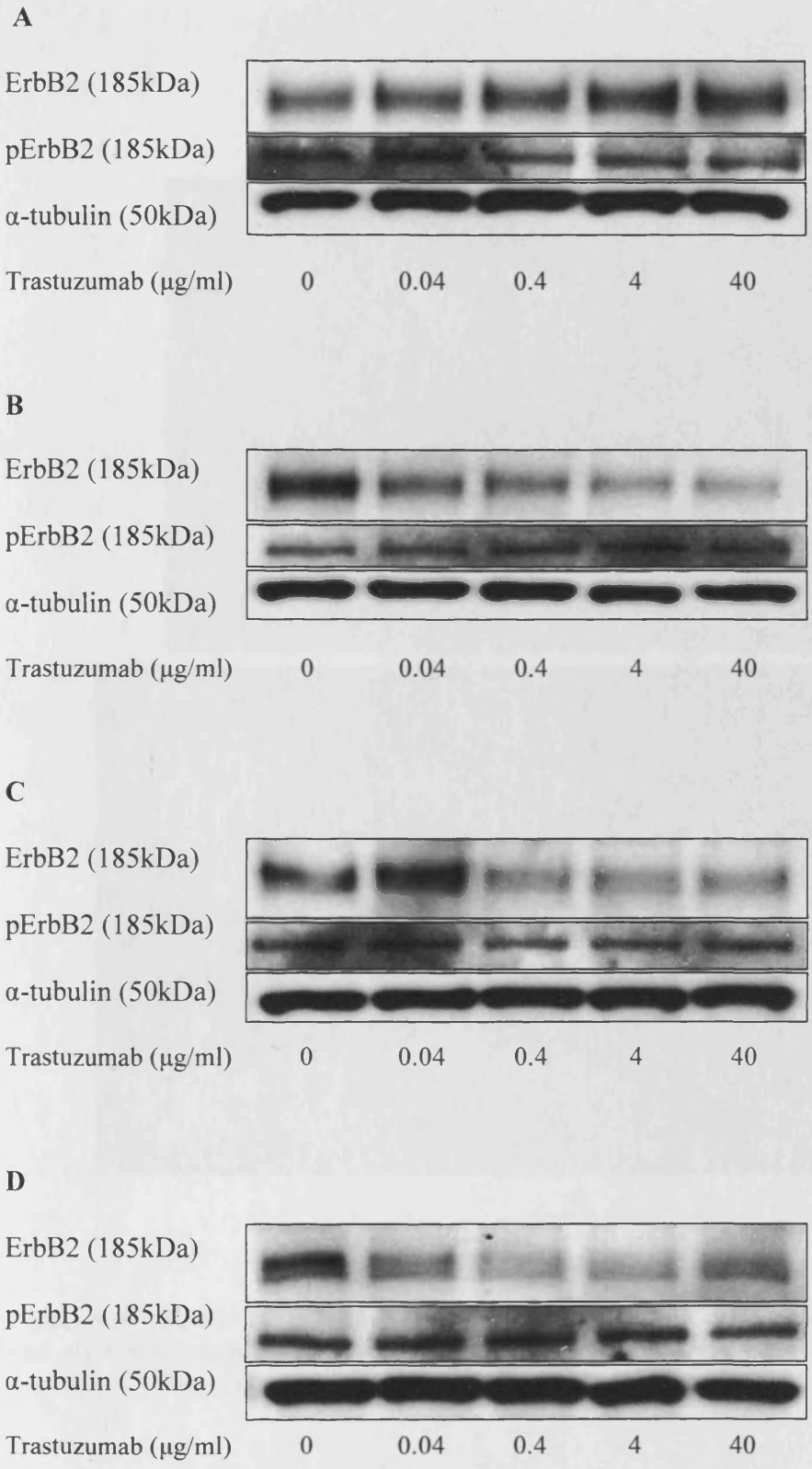

Figure 5.9 – ErbB2 and pErbB2 protein expression in MDA-MB-468 pcDNA3-ErbB2 cells treated with trastuzumab. Cells were treated with a range of trastuzumab concentrations for 1 hour (**A**), 16 hours (**B**), 24 hours (**C**) and 72 hours (**D**). α-tubulin was used as a loading control.

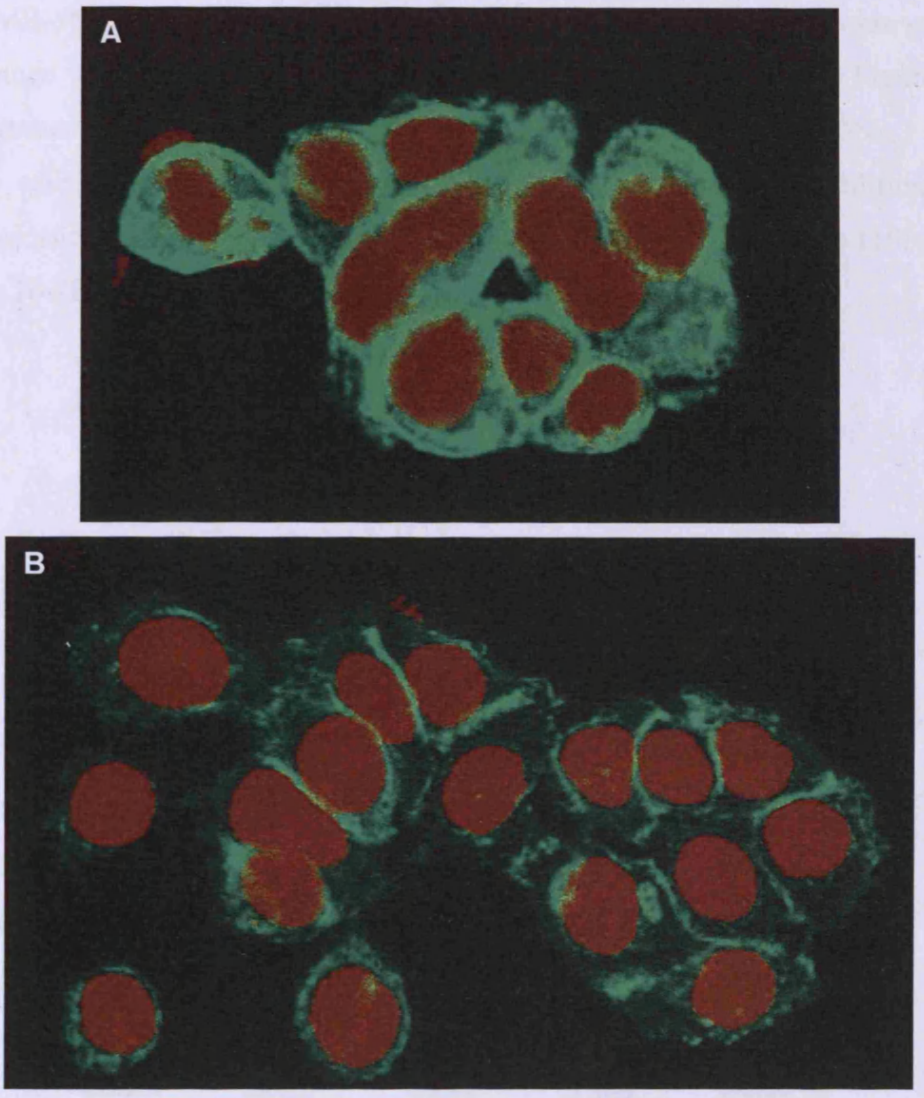

Figure 5.10 – ErbB2 immunofluorescence in MDA-MB-468 pcDNA3-ErbB2 cells before and after trastuzumab treatment. ErbB2 was measured in untreated cells (**A**) and cells treated for 24 hours with 40µg/ml of trastuzumab (**B**).

5.7.2 Effect of trastuzumab on cell proliferation

Having shown the reduction of total ErbB2 protein level after continuous exposure to trastuzumab, effects on cell proliferation were investigated using the SRB assay. MDA-MB-468 wild type cells and the two stably transfected cell lines were exposed to a range of trastuzumab concentrations for 5 consecutive days. Figure 5.11 demonstrates that MDA-MB-468 wild type and MDA-MB-468 pcDNA3 vector control cells proliferation were not affected by trastuzumab. In addition, cells overexpressing ErbB2 were only affected by high doses of trastuzumab (100µg/ml), causing 10-20% inhibition of proliferation.

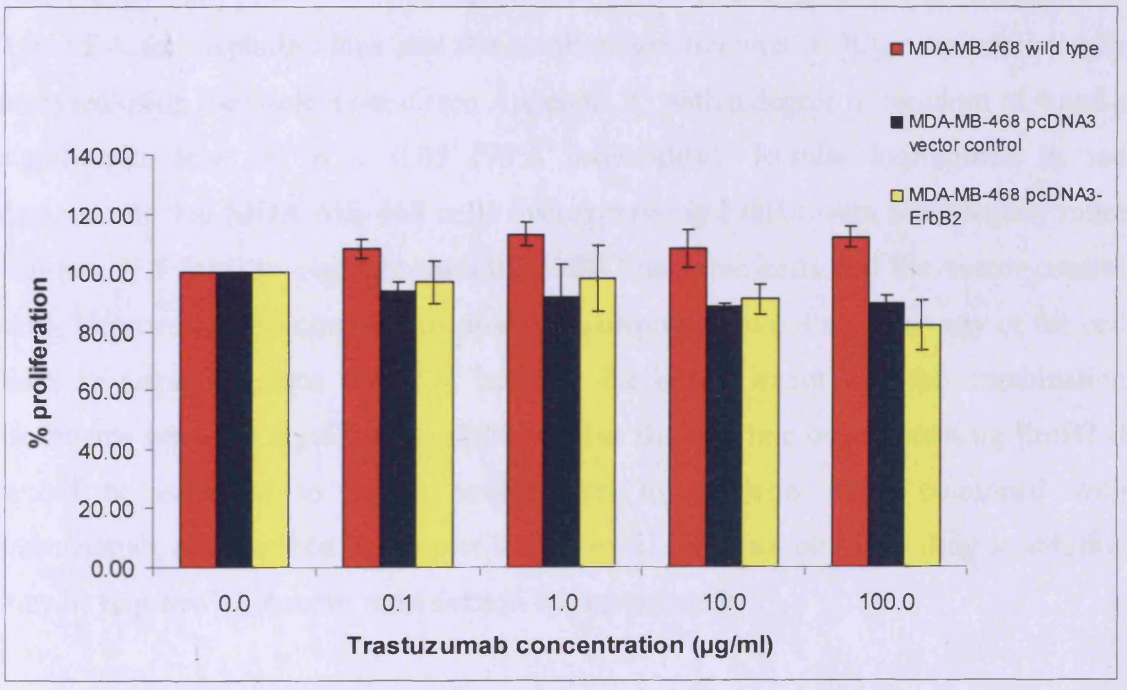

Figure 5.11 – Inhibition of MDA-MB-468 cells proliferation by trastuzumab. MDA-MB-468 wild type cells (red), MDA-MB-468 pcDNA3 vector control cells (blue) and MDA-MB-468 pcDNA3-ErbB2 cells (yellow) were treated with a range of trastuzumab concentrations. Data presented are the result of three independent experiments, as shown by the standard deviation.

5.8 Trastuzumab and cisplatin treatment

As demonstrated in Chapter 3 (section 3.4), trastuzumab was capable of enhancing the anti-tumour activity of chemotherapeutic drugs (Pegram *et al.*, 2004a). In Chapter 3, trastuzumab was shown to enhance cisplatin anti-tumour activity but also to delay the repair of cisplatin-induced DNA ICL. Therefore, the effect of cisplatin in combination with trastuzumab was studied on MDA-MB-468 wild type cells and the transfected cell lines.

5.8.1 Effect of combination treatment after continuous exposure

Cells were treated with trastuzumab at 4μg/ml or 40μg/ml and a range of cisplatin concentrations, for 5 consecutive days. To ensure accuracy and reproducibility, all assays were performed in triplicate. Proliferation curves are presented in Figure 5.12 A, B and C for MDA-MB-468 pcDNA3-ErbB2, MDA-MB-468 pcDNA3 (vector control) and MDA-MB-468 wild type cells, respectively. IC_{50} results are presented in Table 5.4, for cisplatin alone and the combination treatments. IC_{50} were statistically analysed using the student *t*-test (see Appendix 1) with a degree of freedom of 4 and a significance level of $p = 0.05$ (95% probability). Results highlighted in red demonstrate that MDA-MB-468 cells overexpressing ErbB2 were significantly more resistant (1.5 fold) to cisplatin than the ErbB2 negative cells and the vector control cells. However, combining trastuzumab with cisplatin did not sensitise any of the cell lines to cisplatin, since the IC_{50} between the single agent and the combination treatments were not significantly different. For the cell line overexpressing ErbB2 it would be expected to see a sensitisation to cisplatin when combined with trastuzumab, as described in Chapter 3. However, optimisation of the drug scheduling may be required to observe sensitisation by trastuzumab.

Cell line	IC_{50} (cisplatin alone)	IC_{50} (cisplatin with trastuzumab 4µg/ml)	IC_{50} (cisplatin with trastuzumab 40µg/ml)
MDA-MB-468 pcDNA3-ErbB2	0.28±0.05µM	0.28±0.04µM	0.31±0.03µM
MDA-MB-468 pcDNA3 vector control	0.21±0.04µM	0.15±0.0.04µM	0.22±0.07µM
MDA-MB-468 wild type	0.20±0.02µM	0.15±0.06µM	0.20±0.06µM

Table 5.4 – IC_{50}±SD results for MDA-MB-468 cells after cisplatin single agent treatment and combination with trastuzumab. MDA-MB-468 wild type, MDA-MB-468 pcDNA3-ErbB2 and MDA-MB-468 pcDNA3 vector control cells were treated for five consecutive days. IC_{50} were statistically compared to the IC_{50} of the wild type cells, using the student *t*-test, n = 4 and p = 0.05. Results highlighted in red are significantly different to the corresponding IC_{50} in the wild type cells.

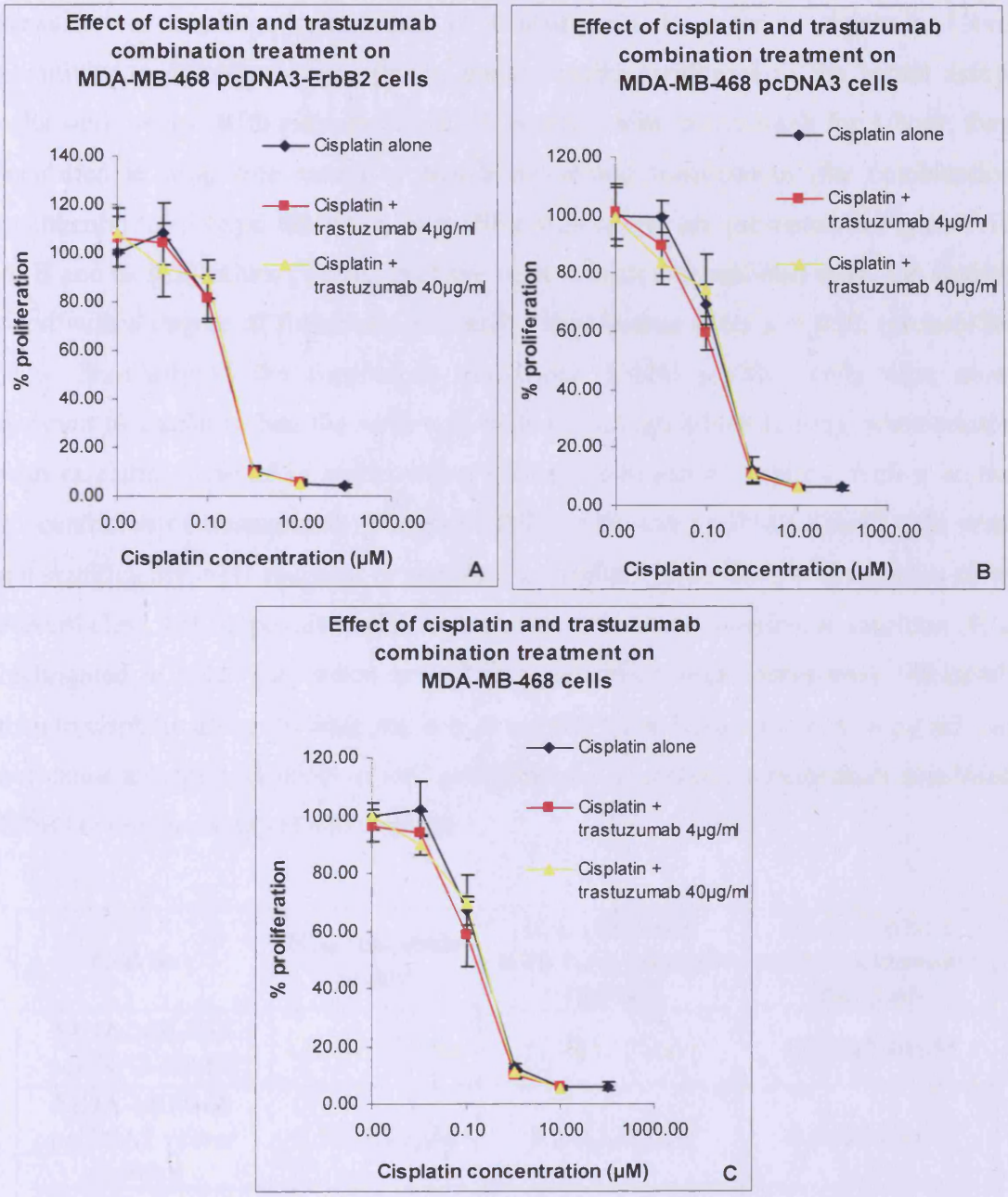

Figure 5.12 – Inhibition of MDA-MB-468 cells proliferation by cisplatin alone and in combination with trastuzumab for 5 days. MDA-MB-468 pcDNA3-ErbB2 (**A**), MDA-MB-468 pcDNA3 (**B**) and MDA-MB-468 wild type cells (**C**) were treated by cisplatin alone (♦) and cisplatin in combination with trastuzumab 4µg/ml (■) and 40µg/ml (▲) for 5 consecutive days. Data presented are the result of three independent experiments, as shown by the standard deviation.

5.8.2 Effect of combination treatment after short exposure

MDA-MB-468 cells overexpressing ErbB2 were shown to be more resistant to cisplatin than the wild type cells, after continuous exposure. However, cells were not sensitised to cisplatin in presence of trastuzumab. In order to determined cell sensitivity to combination treatment, under similar conditions to the comet assay, cells were treated with cisplatin alone or cisplatin with trastuzumab for 1 hour, then incubated in drug free media or media containing trastuzumab (for combination treatments) for 5 days. Inhibition of proliferation curves are presented in Figure 5.13 A, B and C. IC_{50} values (Table 5.5) have been statistically analysed using the student *t*-test with a degree of freedom n = 4 and a significance level $p = 0.05$ (probability 95%). Similarly to the continuous treatments, ErbB2 positive cells were more resistant to cisplatin than the wild type cells (IC_{50} highlighted in red), when treated with cisplatin alone or in combination with trastuzumab at 4µg/ml. With a higher concentration of trastuzumab (40µg/ml), MDA-MB-468 pcDNA3-ErbB2 cells were not significantly more resistant or sensitive to cisplatin, than the ErbB2 negative cells. Nevertheless, ErbB2 positive cells were shown to be more sensitive to cisplatin (IC_{50} highlighted in bold blue) when treated in combination with trastuzumab (40µg/ml) than to cisplatin alone. In addition, it is noted that trastuzumab alone, at 40µg/ml, did not cause a large inhibition of cell proliferation. Therefore, trastuzumab sensitised ErbB2 overexpressing cells to cisplatin.

Cell line	IC_{50} (cisplatin alone)	IC_{50} (cisplatin with trastuzumab 4µg/ml)	IC_{50} (cisplatin with trastuzumab 40µg/ml)
MDA-MB-468 pcDNA3-ErbB2	18.00±3.21µM	17.00±2.75µM	**12.00±3.40µM**
MDA-MB-468 pcDNA3 vector control	9.50±3.11µM	9.50±3.62µM	8.50±3.04µM
MDA-MB-468 wild type	10.00±3.00µM	8.50±3.79µM	8.50±3.88µM

Table 5.5 – IC_{50}±SD results for MDA-MB-468 after cisplatin single agent treatment and combination with trastuzumab, for 1 hour. Cells were treated for 1 hour followed by 5 days in drug free media or media containing trastuzumab alone. Results were statistically analysed with the student *t*-test, n = 4 and $p = 0.05$. MDA-MB-468 pcDNA3-ErbB2 cells were more resistant to cisplatin than ErbB2 negative cells (IC_{50} highlighted in red). IC_{50} in blue shows that trastuzumab (40µg/ml) sensitised ErbB2 overexpressing cells to cisplatin.

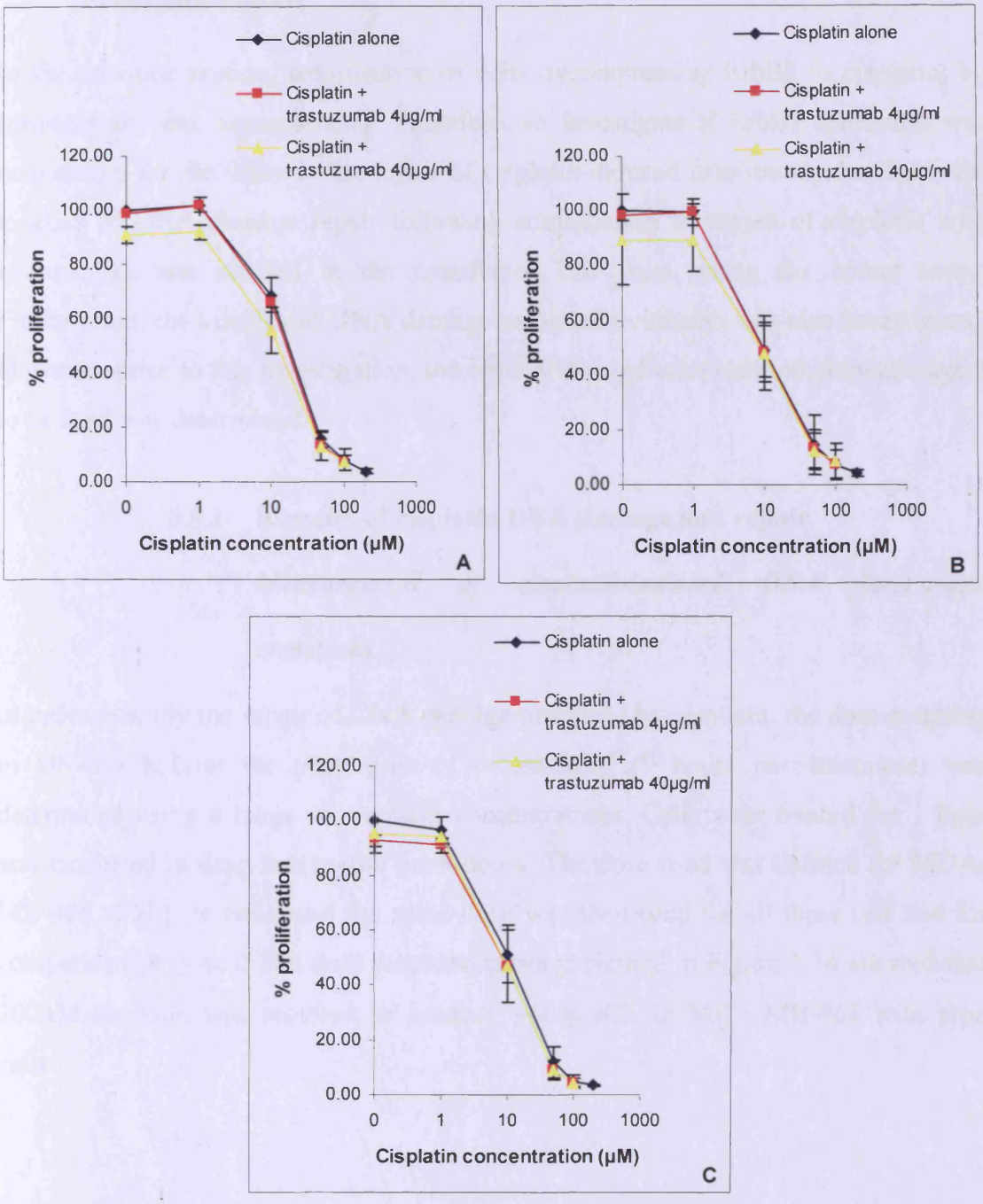

Figure 5.13 – Inhibition of MDA-MB-468 cells proliferation by cisplatin alone and in combination with trastuzumab for 1 hour. MDA-MB-468 pcDNA3-ErbB2 (**A**), MDA-MB-468 pcDNA3 (**B**) and MDA-MB-468 wild type (**C**) cells were treated with cisplatin alone (♦) or cisplatin with trastuzumab 4µg/ml (■) and 40µg/ml (▲) for 1 hour, then incubated in drug free media or media containing trastuzumab (for combination treatments) for 5 days. Data presented are the result of three independent experiments, as shown by the standard deviation.

5.9 Modulation of ErbB2 expression and DNA interstrand crosslink repair

In the previous section, sensitisation of cells overexpressing ErbB2 to cisplatin, by trastuzumab, was demonstrated. Therefore, to investigate if ErbB2 inhibition was responsible for the delay in the repair of cisplatin-induced interstrand crosslinks, the kinetics of DNA damage repair following combination treatment of cisplatin with trastuzumab was studied in the transfected cell lines, using the comet assay. Furthermore, the kinetics of DNA damage repair of melphalan was also investigated. However, prior to this investigation, the optimal dose of each chemotherapeutic agent to be used was determined.

5.9.1 Kinetics of cisplatin DNA damage and repair

Measurement of cisplatin-induced DNA interstrand crosslinks

In order to study the repair of DNA damage produced by cisplatin, the dose resulting in 50-70% ICL at the peak time of crosslinking (9 hours post-treatment) was determined using a range of cisplatin concentrations. Cells were treated for 1 hour and incubated in drug free media for 9 hours. The dose used was defined for MDA-MB-468 wild type cells, and the same dose was then used for all three cell line for comparison purposes. The dose response curve presented in Figure 5.14 showed that 100μM cisplatin was required to produce ~60% ICL in MDA-MB-468 wild type cells.

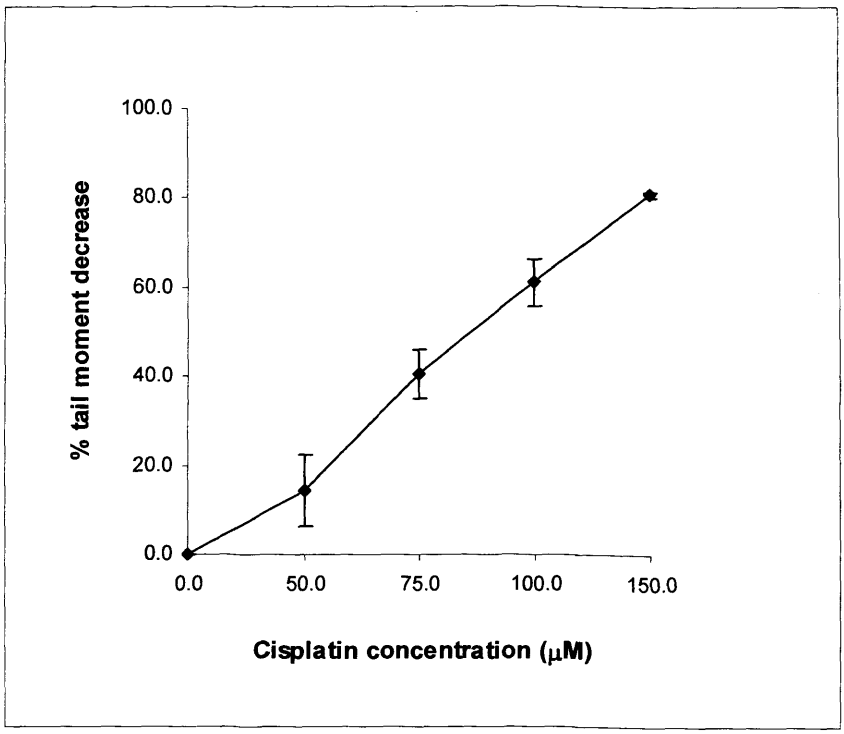

Figure 5.14 – DNA interstrand crosslinks in MDA-MB-468 wild type cells after cisplatin treatment. Cells were treated with a range of cisplatin concentrations, for 1 hour. Measurements at the peak of crosslinking, 9 hours post-incubation. Data presented are the result of three independent experiments, as shown by the standard error.

Effect of ErbB2 modulation on the kinetics of formation and repair of cisplatin-induced DNA interstrand crosslinks

Using trastuzumab at 40μg/ml and cisplatin at 100μM, as defined previously, MDA-MB-468 wild type, MDA-MB-468 pcDNA3 and MDA-MB-468 pcDNA3-ErbB2 cells were treated with either cisplatin alone or cisplatin in combination with trastuzumab for 1 hour, followed by incubation in drug free media or media containing trastuzumab (for combination treatment). ICLs were measured at different time points, post-treatment.

Trastuzumab did not alter the kinetics of repair of cisplatin-induced DNA damage in MDA-MB-468 wild type (Figure 5.15) and MDA-MB-468 pcDNA3 (Figure 5.16) cells, non expressing ErbB2. For example, in the wild type cell line, after 48 hours, 36.1±3.0% of ICLs remained in cells treated with cisplatin alone, and 32.0±3.9% were unrepaired in cells treated with the combined drugs. Inhibition of ErbB2 by trastuzumab, in MDA-MB-468 pcDNA3-ErbB2 (Figure 5.17) caused a delay in the

repair of cisplatin-induced DNA ICL. After 48 hours 24.2±3.8% of ICLs remained in cells treated with cisplatin alone, whereas 55.7±3.6% was unrepaired in cells treated with cisplatin in combination with trastuzumab. Therefore, these results concur with the data obtained in Chapter 3 on the effect of trastuzumab in the repair of cisplatin-induced DNA damage.

Furthermore, Figure 5.18 demonstrates that ErbB2 plays a direct role in the repair of cisplatin-induced DNA damage, since ErbB2 overexpressing cells treated with cisplatin alone repaired cisplatin ICLs faster (24.2±3.8% after 48 hours) than ErbB2 negative cells (36.1±3.0% after 48 hours). It is also noted that the transfection of ErbB2 did not affect the level of formation of crosslinks, as 61.7±3.6% of crosslinks were formed after 9 hours post-treatment in MDA-MB-468 wild type cells and 66.8±2.1% in ErbB2 overexpressing cells. The cells transfected with the vector control having 70.4±1.8% of crosslinks formed, after 9 hours.

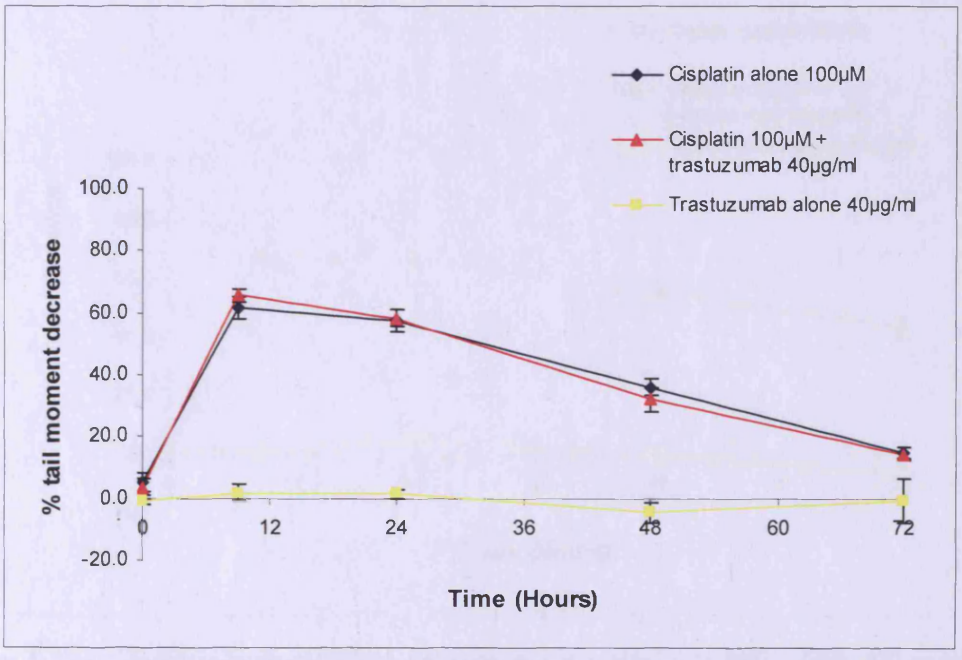

Figure 5.15 – Cisplatin-induced DNA interstrand crosslinks in MDA-MB-468 wild type cells. Cells were treated with trastuzumab alone (■), trastuzumab in combination with cisplatin (▲) or cisplatin alone (♦). Data presented are the result of three independent experiments, as shown by the standard error.

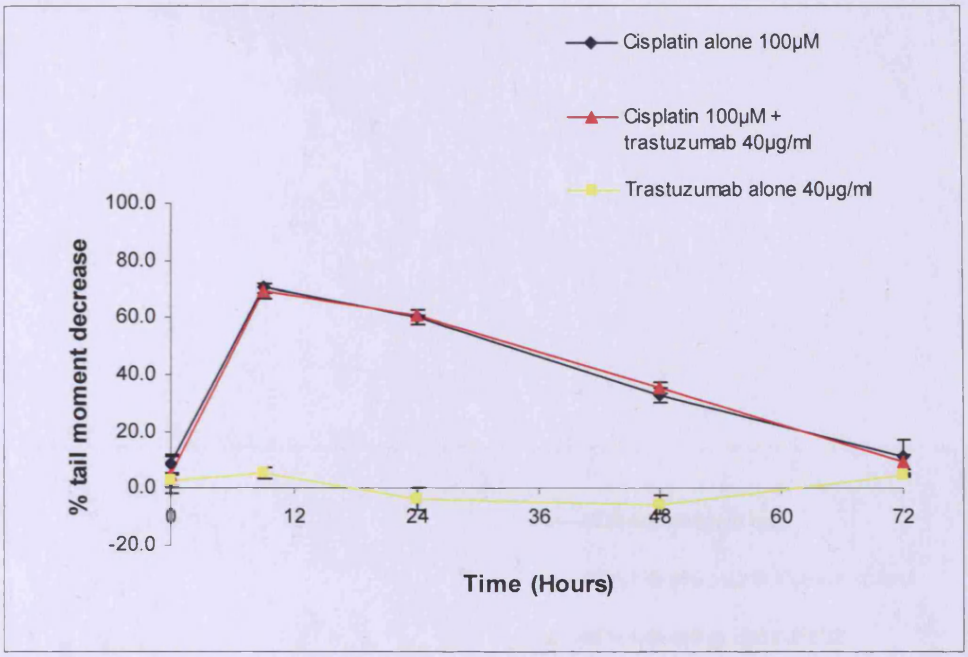

Figure 5.16 – Cisplatin-induced DNA interstrand crosslinks in MDA-MB-468 pcDNA3 vector control cells. Cells were treated with trastuzumab alone (■), trastuzumab in combination with cisplatin (▲) or cisplatin alone (♦). Data presented are the result of three independent experiments, as shown by the standard error.

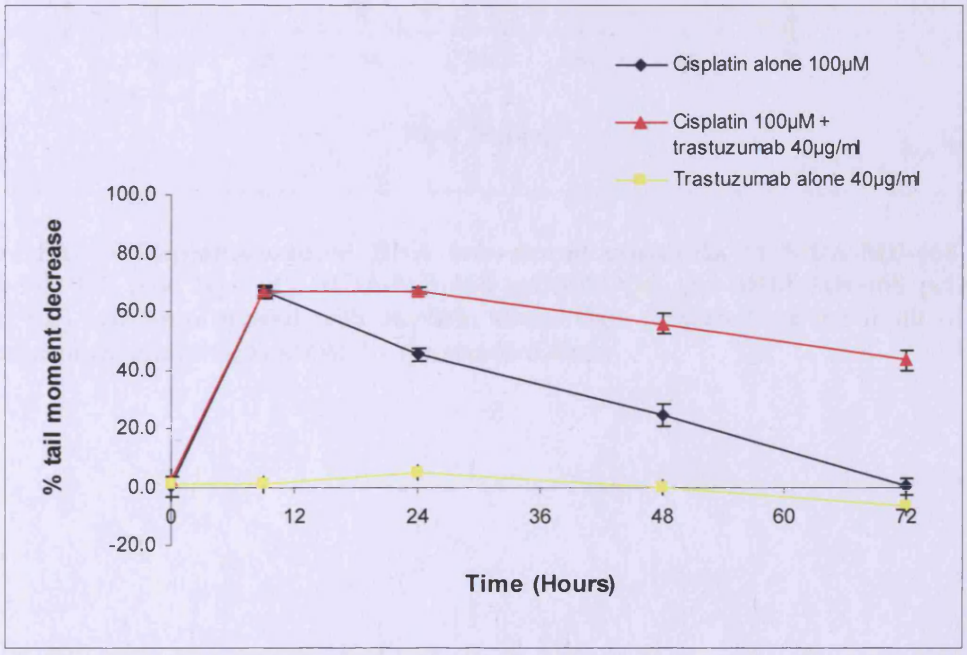

Figure 5.17 – Cisplatin-induced DNA interstrand crosslinks in MDA-MB-468 pcDNA3-ErbB2 cells. Cells were treated with trastuzumab alone (■), trastuzumab in combination with cisplatin (▲) or cisplatin alone (♦). Data presented are the result of three independent experiments, as shown by the standard error.

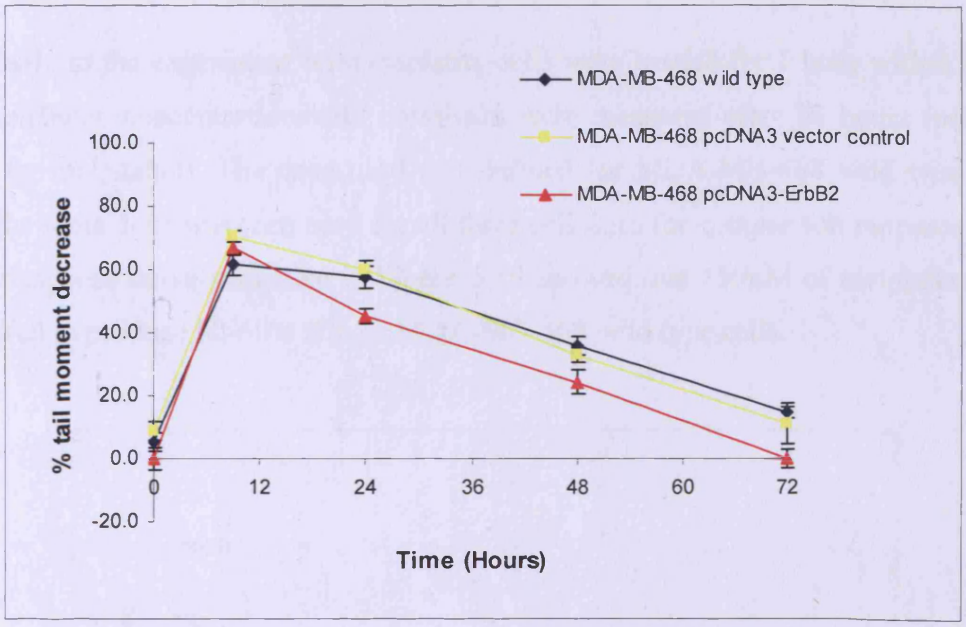

Figure 5.18 – Cisplatin-induced DNA interstrand crosslinks in MDA-MB-468 cells. MDA-MB-468 wild type (♦), MDA-MB-468 pcDNA3 (■) and MDA-MB-468 pcDNA3-ErbB2 (▲) cells were treated with cisplatin alone. Data presented are the result of three independent experiments, as shown by the standard error.

5.9.2 Kinetics of melphalan-induced DNA damage and repair

Although melphalan-induced DNA interstrand crosslinks were shown to be unaffected by the inhibition of ErbB2 (see Chapter 3), it was interesting to consider the effect of ErbB2 overexpression on the kinetics of melphalan-induced DNA damage and repair.

Measurement of melphalan-induced DNA interstrand crosslinks

Similarly to the experiment with cisplatin, cells were treated for 1 hour with a range of melphalan concentrations and crosslinks were measured after 16 hours (peak of ICL for melphalan). The dose used was defined for MDA-MB-468 wild type cells and the same dose was then used for all three cell lines for comparison purposes. The dose response curve presented in Figure 5.19 showed that 150μM of melphalan was required to produce 50-60% ICL in MDA-MB-468 wild type cells.

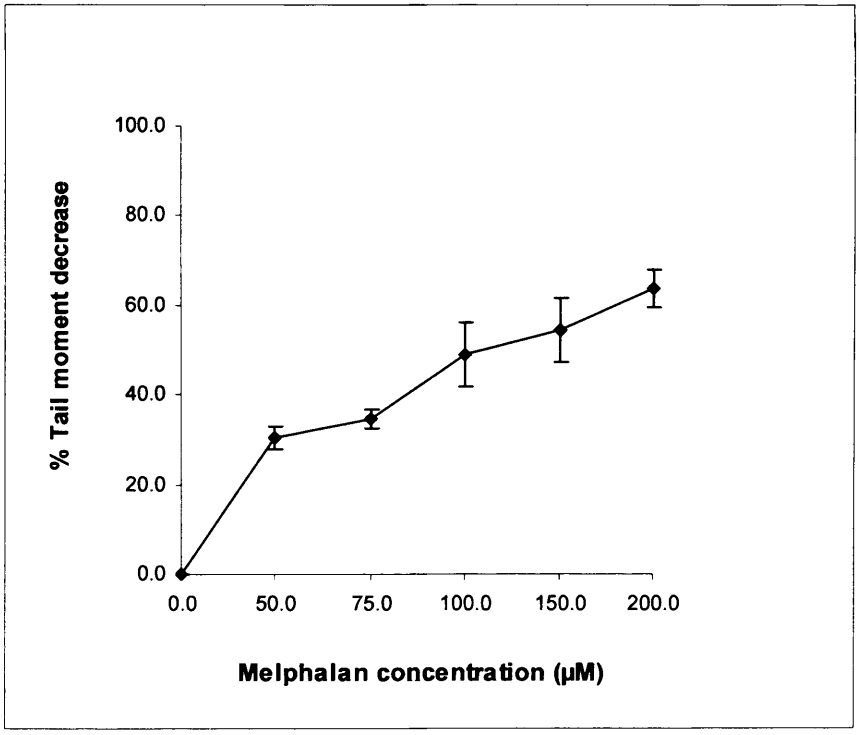

Figure 5.19 – DNA interstrand crosslinks in MDA-MB-468 wild type cells after melphalan treatment. Cells were treated with a range of melphalan concentrations, for 1 hour. Measurements at the peak of crosslinking, 16 hours post-incubation. Data presented are the result of three independent experiments, as shown by the standard error.

Effect of ErbB2 modulation on the kinetics of formation and repair of melphalan-induced DNA interstrand crosslinks

Using trastuzumab at 40μg/ml and melphalan at the previously defined dose of 150μM, MDA-MB-468 wild type, MDA-MB-468 pcDNA3 and MDA-MB-468 pcDNA3-ErbB2 cells were treated with either melphalan alone or melphalan in combination with trastuzumab for 1 hour, followed by incubation in drug free media or media containing trastuzumab alone (for combination treatment). ICLs were measured at different time points, post-treatment.

The repair kinetics of melphalan-induced DNA ICL remained unaffected by the presence of trastuzumab, in MDA-MB-468 cells (Figure 5.20) and MDA-MB-468 pcDNA3 vector control cells (Figure 5.21). Those results were comparable to the one obtained for MDA-MB-453 cells in Chapter 3. As shown in Figure 5.22, inhibition of ErbB2 (MDA-MB-468 pcDNA3-ErbB2), by trastuzumab, did not cause any delay in the repair of melphalan interstrand crosslinks. After 24 hours, 45.7% of crosslinks remained unrepaired in cells treated with cisplatin alone and 47.3% in cells treated with the combination of both drugs.

Furthermore, Figure 5.23 shows that overexpression of ErB2 alone did not alter the kinetics of melphalan-induced DNA ICL damage and repair. After 24 hours 40.5±3.7% of ICLs remained in MDA-MB-468 wild type cells and 45.7±1.1% were still unrepaired in MDA-MB-468 cells overexpressing ErbB2. Similarly to the result obtained with cisplatin, transfection of ErbB2 did not affect the peak of crosslinking, since 58.1±1.3% of ICLs were formed after 16 hours post-treatment in the wild type cells and 59.7±1.4% in the ErbB2 transfected cell line. In the same way, melphalan treatment of cells transfected with the empty vector produced 58.3±4.8% of ICLs after 16 hours.

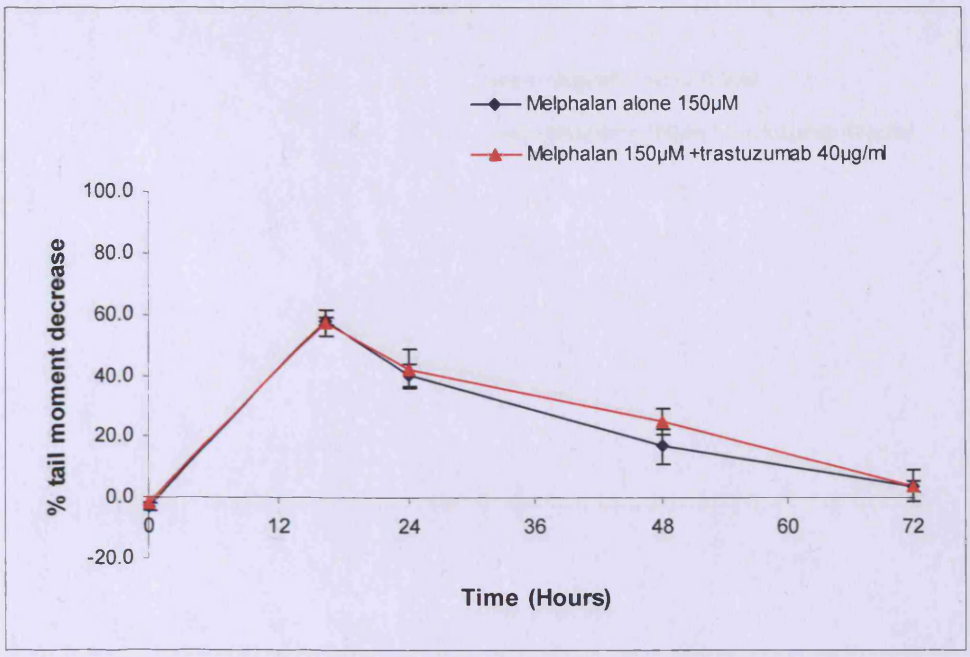

Figure 5.20 – Melphalan-induced DNA interstrand crosslinks in MDA-MB-468 wild type cells. Cells were treated with trastuzumab in combination with cisplatin (▲) or cisplatin alone (♦). Data presented are the result of three independent experiments, as shown by the standard error.

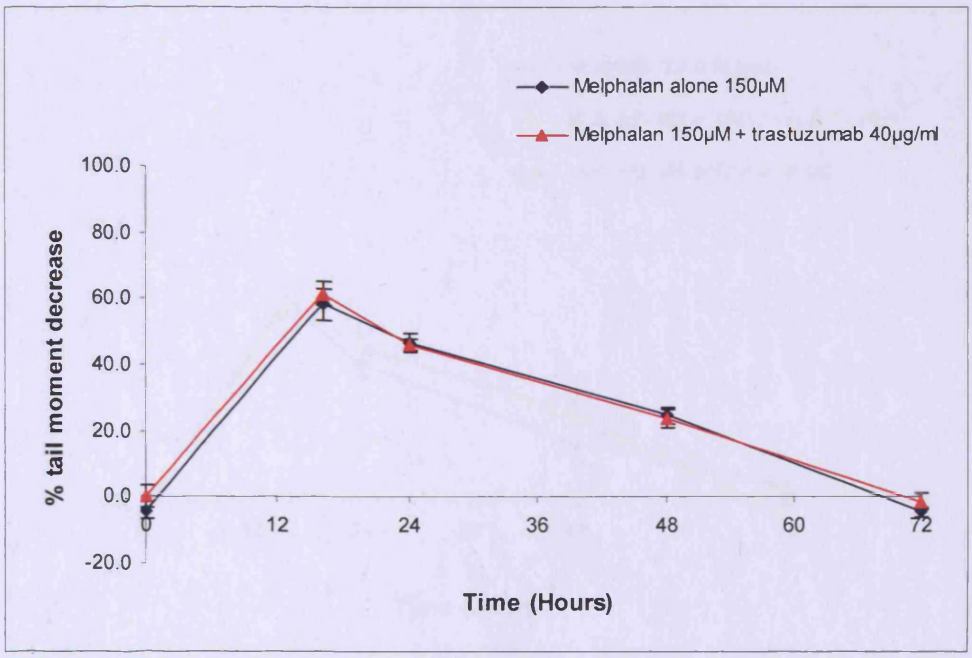

Figure 5.21 – Melphalan-induced DNA interstrand crosslinks in MDA-MB-468 pcDNA3 vector control cells. Cells were treated with trastuzumab in combination with cisplatin (▲) or cisplatin alone (♦). Data presented are the result of three independent experiments, as shown by the standard error.

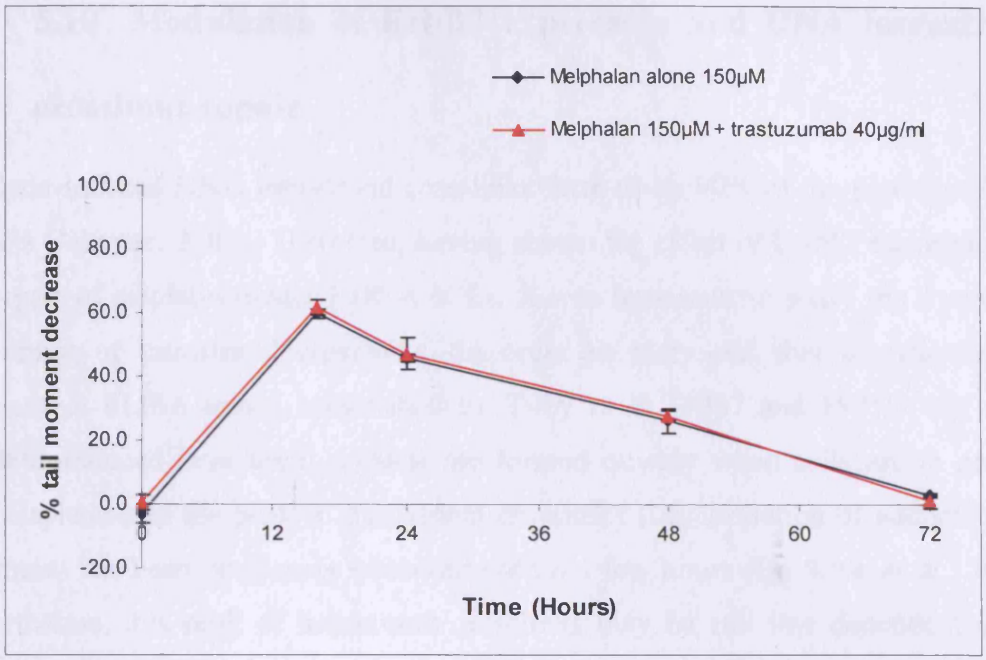

Figure 5.22 – Melphalan-induced DNA interstrand crosslinks in MDA-MB-468 pcDNA3-ErbB2 cells. Cells were treated with trastuzumab in combination with cisplatin (▲) or cisplatin alone (♦).Data presented are the result of three independent experiments, as shown by the standard error.

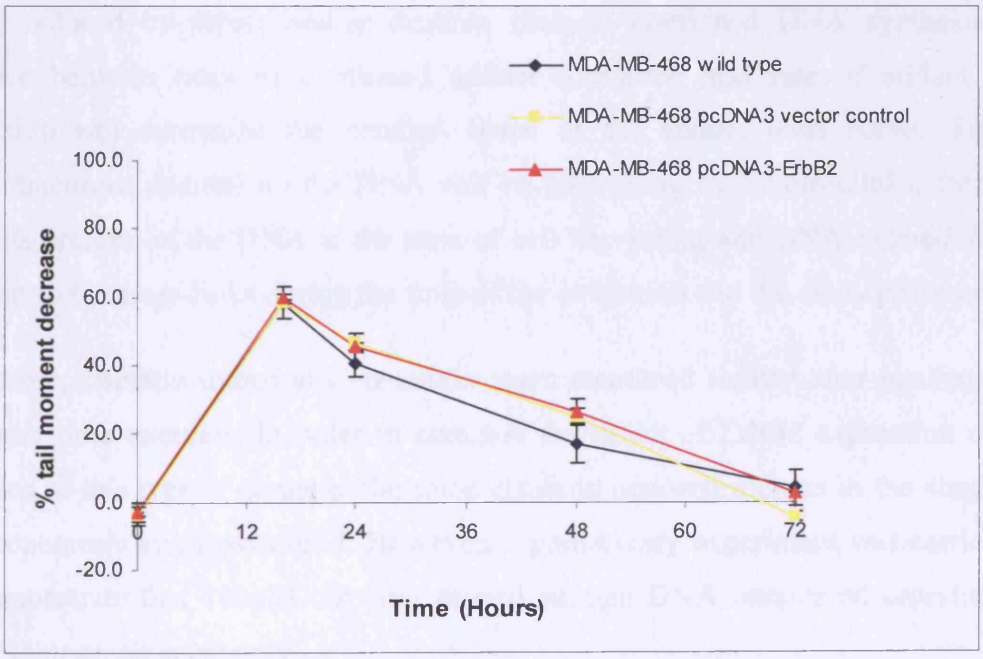

Figure 5.23 – Melphalan-induced DNA interstrand crosslinks in MDA-MB-468 cells. MDA-MB-468 wild type (♦), MDA-MB-468 pcDNA3 (■) and MDA-MB-468 pcDNA3-ErbB2 (▲) cells were treated with melphalan alone. Data presented are the result of three independent experiments, as shown by the standard error.

5.10 Modulation of ErbB2 expression and DNA intrastrand crosslinks repair

Cisplatin-induced DNA intrastrand crosslinks form up to 90% of the platinum-DNA adducts (Jakupec, 2003). Therefore, having shown the effect of ErbB2 expression on the repair of cisplatin-induced DNA ICLs, it was important to study the formation and repair of intrastrand crosslinks. In order to carry out this investigation, a competitive ELISA assay, established by Tilby *et al.* (1987 and 1991), was used. Cisplatin-induced intrastrand adducts are formed quickly when cells are in contact with cisplatin and the peak of intrastrand crosslinks (i.e. formation of adducts post-treatment) has been previously observed within a few hours (De Silva *et al.*, 2002). Nevertheless, this peak of intrastrand crosslinks may be cell line dependent and a number of factors need to taken into consideration. Firstly, the intracellular drug concentration will vary between cells and residual cisplatin in the cells after removal of extra-cellular drug will continue to react with DNA, react with other molecules and/or be exported. The balance between these factors will determine how many more adducts are formed post-drug removal. Secondly, levels of adducts on DNA being reduced by repair and/or dilution through continued DNA synthesis, the balance between rates of continued adduct formation and rate of adduct level reduction will determine the detailed shape of the adduct level curve. Finally, monofunctional adducts on the DNA will be converting to 1,2-crosslinks, therefore adducts present on the DNA at the time of cell harvesting and DNA extraction may convert to the cross-links during the time of the extraction and the assay procedures.

Therefore, cisplatin intrastrand crosslinks were measured shortly after incubation at different time intervals. In order to compare the effect of ErbB2 expression on the kinetics of this type of damage, the same cisplatin concentration as in the single gel electrophoresis assay, was used. However, a preliminary experiment was carried out to demonstrate that 100μM cisplatin caused enough DNA intrastrand crosslinks to study their repair accurately.

5.10.1 Measurement of cisplatin-induced intrastrand crosslinks

As the vector control cell line did not show any differences with MDA-MB-468 cells, only the wild type and ErbB2 transfected cells have been studied in this experiment. Cells were treated for 1 hour with a range of cisplatin concentrations and samples were analysed at the end of the drug treatment. As shown in Figure 5.24, 100μM of cisplatin caused the formation of 430nmol of adduct/ g of DNA. Therefore, the transfection of ErbB2 did not affect the formation of 1,2-intrastrand crosslinks.

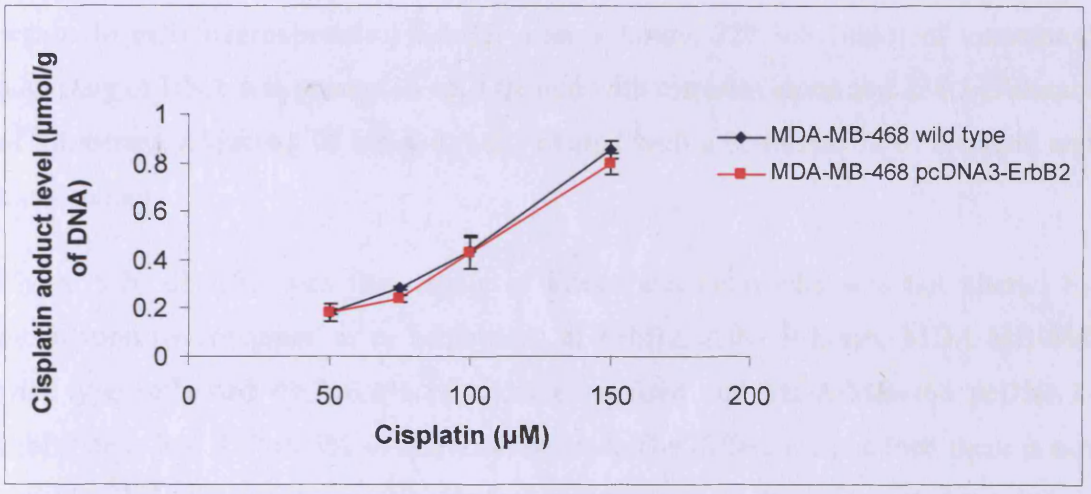

Figure 5.24 – Cisplatin-induced intrastrand crosslinks in MDA-MB-468 cells. MDA-MB-468 wild type (♦) and MDA-MB-468 pcDNA3-ErbB2 (■) cells were treated with a range of cisplatin concentrations, for 1 hour. Measurements were made at the end of the 1 hour treatment. Data presented are the result of three independent experiments, as shown by the standard error.

5.10.2 Effect of ErbB2 modulation on the kinetics of formation and repair of cisplatin-induced intrastrand crosslinks

Cells were treated with cisplatin alone or with a combination of cisplatin and trastuzumab, as detailed in the study of interstrand crosslinks. As shown in Figure 5.25, formation of cisplatin-induced intrastrand crosslinks was not affected by ErbB2 overexpression. In these two cell lines the peak of intrastrand adduct formation was observed immediately after the 1 hour treatment, and was not modified by ErbB2 overexpression. Furthermore, adducts were rapidly repaired within the first 5 hours post-treatment. After 24 hours, 162.0±8.4nmol of intrastrand adducts/g of DNA remained in wild type cells and 160.5±9.7nmol of intrastrand adducts/g of DNA was present in cells overexpressing ErbB2. Furthermore, inhibition of ErbB2 by trastuzumab did not affect the kinetics of DNA intrastrand crosslink formation or repair. In cells overexpressing ErbB2, after 9 hours, 222.3±9.1nmol of intrastrand adducts/g of DNA was present in cells treated with cisplatin alone and 238.5±9.0nmol of intrastrand adducts/g of DNA in cells treated with a combination of cisplatin and trastuzumab.

Figure 5.26 demonstrates that repair of intrastrand crosslinks was not altered by modulation (overexpression or inhibition) of ErbB2. After 9 hours, MDA-MB-468 wild type cells had 49.7±6.4% of adducts repaired and MDA-MB-468 pcDNA3-ErbB2 cells had 37.7±4.3% of adducts repaired. The difference obtained there is not considered significant due to the standard errors obtained. It is also noted that repair of intrastrand adducts was not complete, since the repair of adducts reached a plateau at ~60% after 48 hours post-treatment. This was explained by the high level of adducts obtained with 100μM of cisplatin, resulting in incomplete repair. Using the same technique, incomplete repair of cisplatin intrastrand adducts was also observed in the study by De Silva *et al.* (2002).

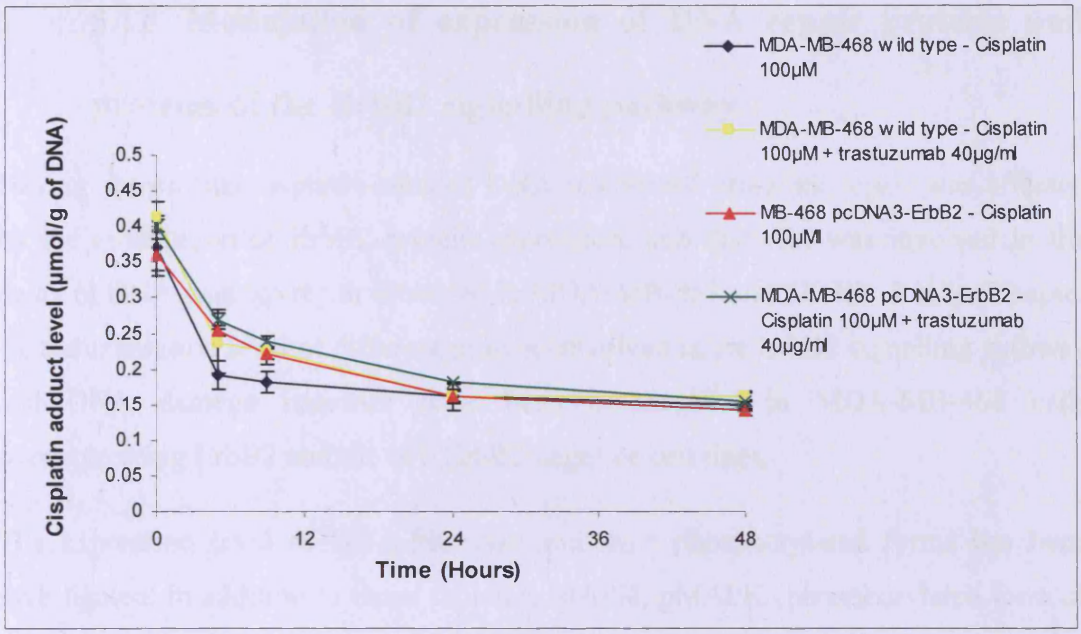

Figure 5.25 – Cisplatin-induced DNA intrastrand crosslinks in MDA-MB-468 cells. MDA-MB-468 wild type (♦ and ■) and MDA-MB-468 pcDNA3-ErbB2 (▲ and ×) cells (with standard error), after treatment with cisplatin alone or cisplatin and trastuzumab. Data presented are the result of three independent experiments, as shown by the standard error.

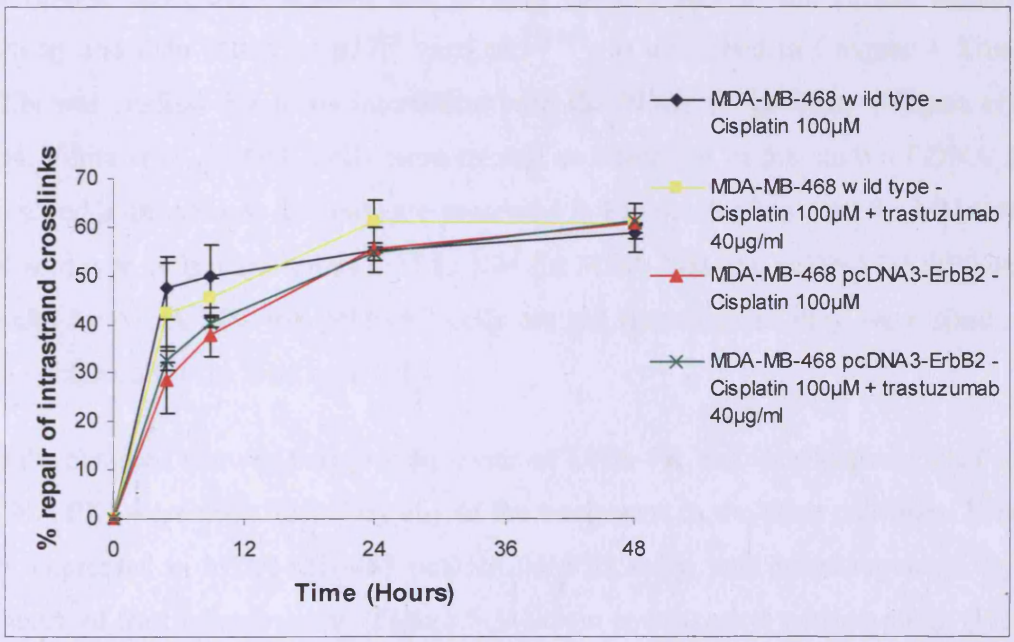

Figure 5.26 – Repair of cisplatin-induced DNA intrastrand crosslinks in MDA-MB-468 cells. MDA-MB-468 wild type (♦ and ■) and MDA-MB-468 pcDNA3-ErbB2 (▲ and ×) cells (with standard error), after treatment with cisplatin alone or cisplatin and trastuzumab. Data presented are the result of three independent experiments, as shown by the standard error.

5.11 Modulation of expression of DNA repair proteins and proteins of the ErbB2 signalling pathway

Having shown that cisplatin-induced DNA interstrand crosslink repair was affected by the modulation of ErbB2 protein expression, and that Akt was involved in the delay of DNA damage repair observed in MDA-MB-453 and SK-BR-3 cells (Chapter 4), the expression level of different proteins involved in the ErbB2 signalling pathway and DNA damage response have been investigated in MDA-MB-468 cells overexpressing ErbB2 and the two ErbB2 negative cell lines.

The expression level of DNA-PK, Akt and their phosphorylated forms has been investigated. In addition to those proteins, MAPK, pMAPK (phosphorylated form of MAPK) and PTEN protein expression levels were examined. Although DNA-PK expression was not shown to be altered by the inhibition of ErbB2 (Chapter 4, section 4.4), it remains an important protein as it was shown to physically interact with EGFR, another member of the epidermal growth factor family, following the inhibition of the tyrosine kinase activity of EGFR (Friedmann B. *et al.*, 2004). Akt and MAPK have been studied due to their involvement in the ErbB2 signalling pathway and their effect on $p27^{kip1}$ and $p21^{WAF1}$, as described in Chapter 4. Finally, PTEN was studied due to its interaction with the PI3K/Akt pathway (Nagata *et al.*, 2004; Fujita *et al.*, 2006). Cells were treated as described in the study of DNA ICL repair and immunoblots obtained are presented in Figures 5.27 to 5.30 for MDA-MB-468 wild type cells and Figures 5.31 to 5.34 for MDA-MB-468 pcDNA3-ErbB2 cells. Results for MDA-MB-468 pcDNA3 cells are not presented as they were similar to those obtained for the wild type cells.

Results obtained showed that protein levels of DNA-PK and its phosphorylated form (pDNA-PK) were not affected by any of the treatments in the three cell lines. ErbB2, only expressed in MDA-MB-468 pcDNA3-ErbB2 cells, was down-regulated in the presence of trastuzumab alone (Figure 5.34) or in combination with cisplatin (Figure 5.34). In untreated MDA-MB-468 pcDNA3-ErbB2 cells (Figure 5.31) or cells treated with cisplatin alone (Figure 5.33), ErbB2 protein level remained unaltered.

As shown in Chapter 4, the protein level of Akt was not affected by trastuzumab or cisplatin, and Akt phosphorylated at serine 473 (pAkt S473) was not detectable in

untreated cells (Figures 5.27 and 5.31) or cells treated with cisplatin alone (Figures 5.29 and 5.33). However, a low level of Akt phosphorylated at threonine 308 (pAkt T308) was present in all three untreated cell lines (the strength of the pAkt band may differ between the immunoblots presented due to the length of exposure of the films). In addition, level of pAkt T308 was higher in cells overexpressing ErbB2 (Figure 5.31) than in ErbB2 negative cells (Figures 5.27). Moreover, pAkt T308 and pAkt S473 increased in presence of trastuzumab alone for 1 hour (Figures 5.28, 5.32). This level reduced slowly with time in ErbB2 negative cells whereas the reduction in ErbB2 positive cells was much more rapid. It was also noted that pAkt S473 reduced dramatically in ErbB2 positive cells after 10 hours (Figure 5.32). In combination with cisplatin (Figure 5.30 and 5.34), trastuzumab also caused phosphorylation of Akt after 1 hour but there was no reduction of pAkt (S473 and T308) with time in ErbB2 negative cells, while in MDA-MB-468 pcDNA3-ErbB2 cells, only pAkt T308 level was maintained.

Therefore, trastuzumab caused similar effects in ErbB2 positive and negative cells, identical to the one described in Chapter 4. However, overexpression of ErbB2 caused an increase in phosphorylation of Akt (pAkt T308) compared to ErbB2 negative cells. Moreover, ErbB2 overexpression caused a rapid reduction of pAkt S473, after activation by trastuzumab.

MAPK was present in all cell lines but its expression was not affected by any of the treatments. However, MAPK became phosphorylated (pMAPK) after treatment with cisplatin alone or in combination, and its phosphorylated state was maintained with time. In addition, trastuzumab or ErbB2 overexpression did not alter its phosphorylation level.

PTEN was not detectable in any of the three untreated cell lines. However, after 1 hour of treatment with trastuzumab alone it was present in all three cell lines with a level reducing quickly with time. In combination with cisplatin, trastuzumab caused activation of PTEN with its level reducing slowly with time. Therefore similarly to pAkt cisplatin maintained the activated level of PTEN caused by trastuzumab.

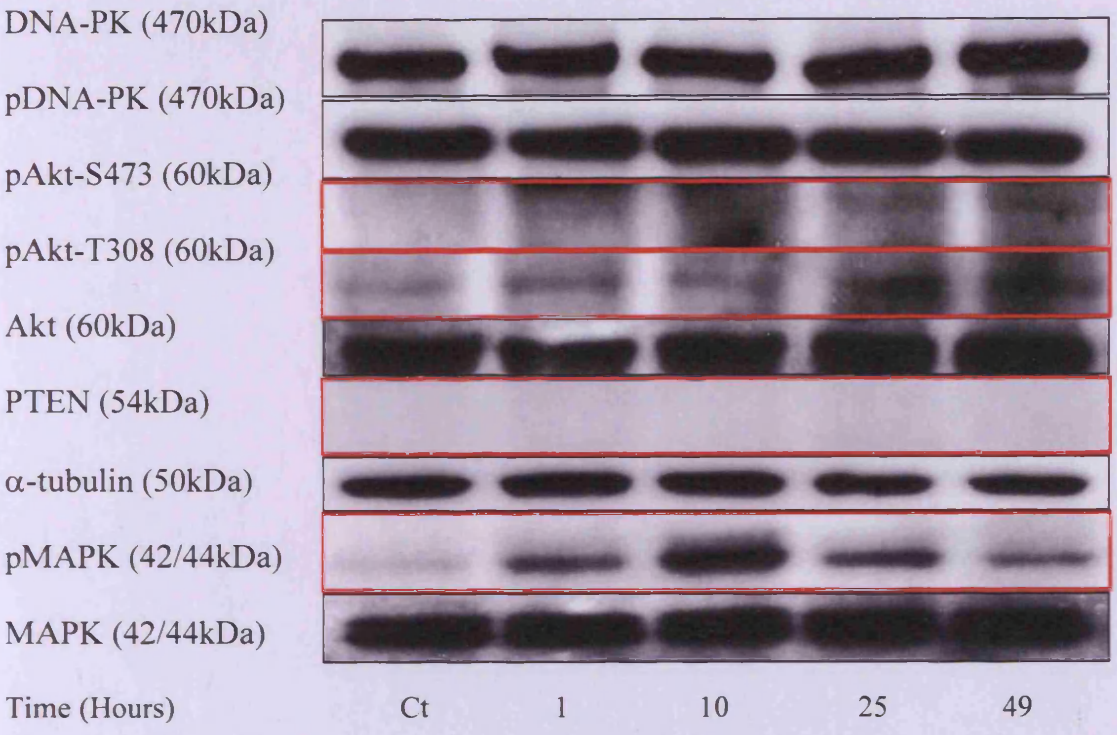

Figure 5.27 – Immunoblots of untreated MDA-MB-468 wild type cells. Immunoblots were probed for DNA repair proteins and proteins involved in ErbB2 signalling pathways. α-tubulin was used as a loading control.

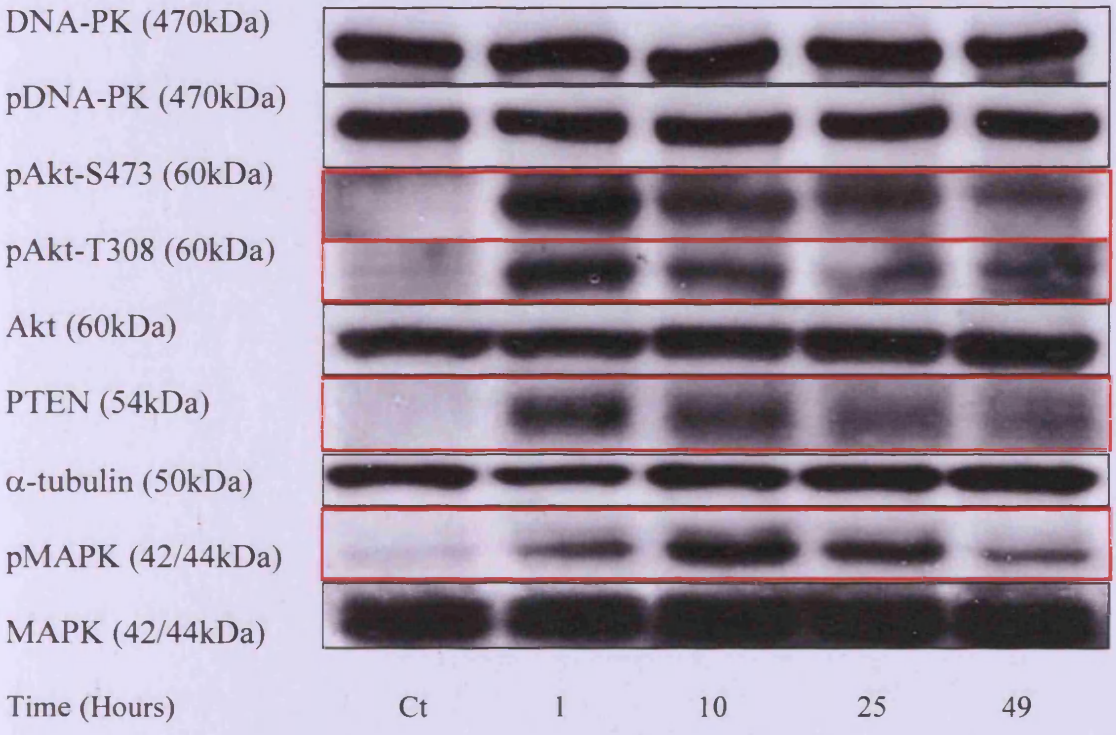

Figure 5.28 – Immunoblots of MDA-MB-468 wild type cells treated with trastuzumab. Cells were treated with trastuzumab (40μg/ml) and immunoblots were probed for DNA repair proteins and proteins involved in ErbB2 signalling pathways. α-tubulin was used as a loading control.

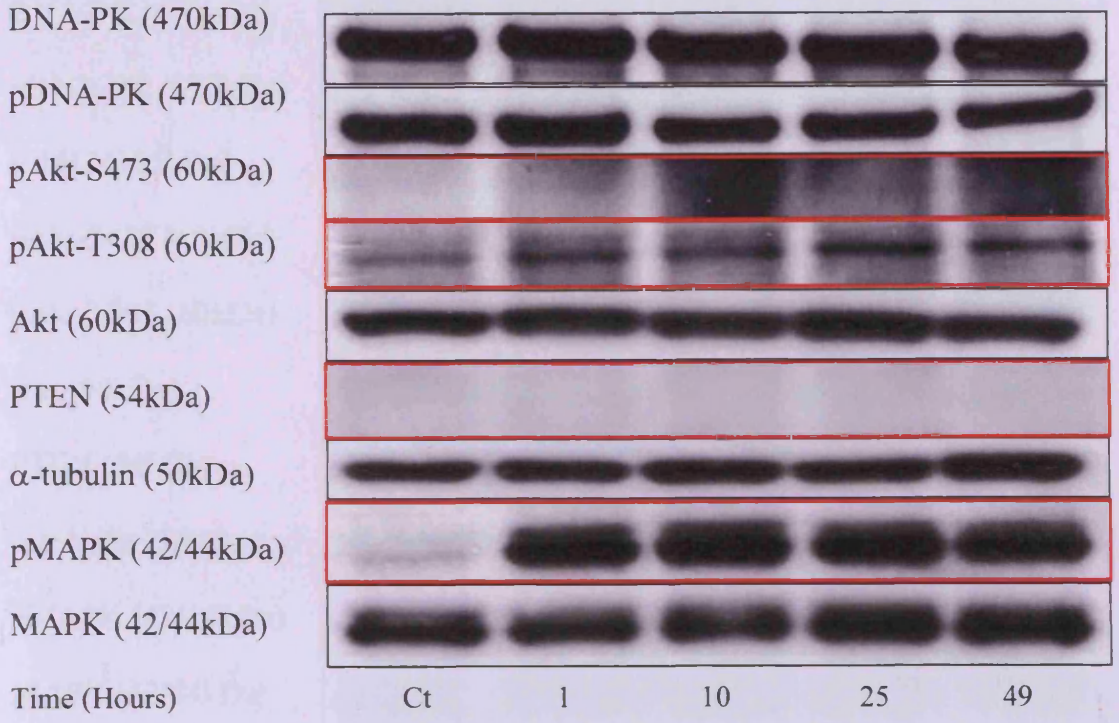

Figure 5.29 – Immunoblots of MDA-MB-468 wild type cells treated with cisplatin. Cells were treated with cisplatin (100μM) for 1 hour and immunoblots were probed for DNA repair proteins and proteins involved in ErbB2 signalling pathways. α-tubulin was used as a loading control.

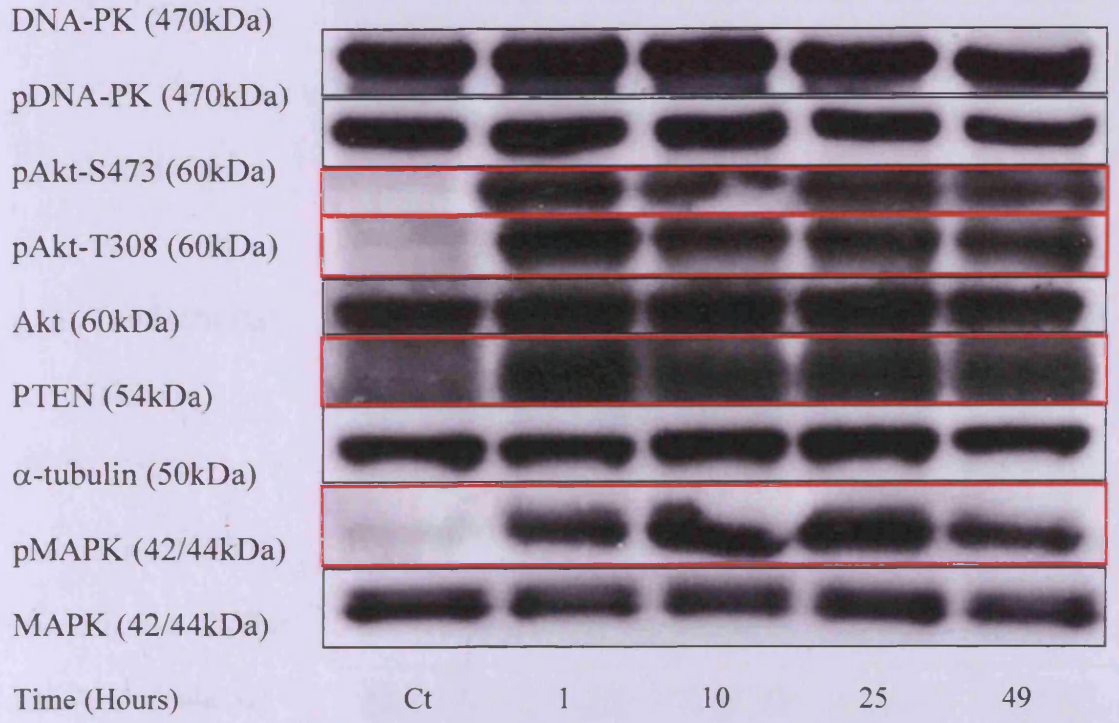

Figure 5.30 – Immunoblots of MDA-MB-468 wild type cells treated with cisplatin and trastuzumab. Cells were treated with cisplatin (100μM) and trastuzumab (40μg/ml) for 1 hour then incubated in media containing trastuzumab alone (40μg/ml), immunoblots were probed for DNA repair proteins and proteins involved in ErbB2 signalling pathways. α-tubulin was used as a loading control.

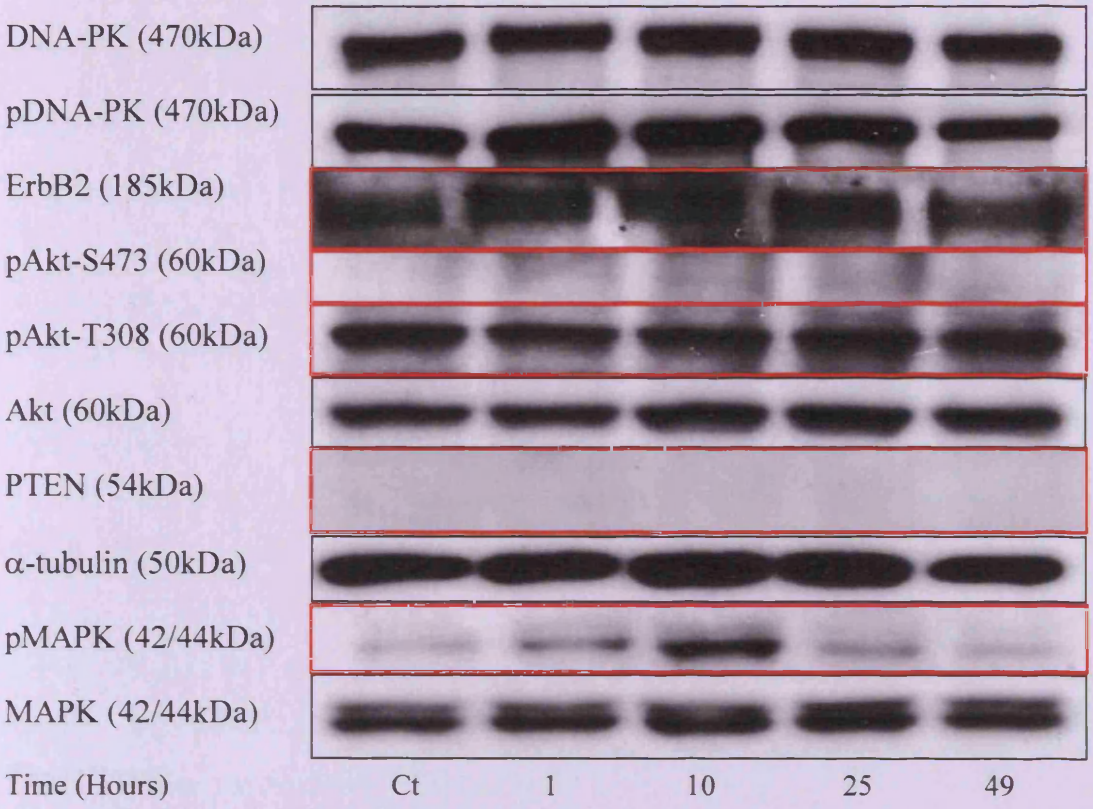

Figure 5.31 – Immunoblots of untreated MDA-MB-468 pcDNA3-ErbB2 cells. Immunoblots were probed for DNA repair proteins and proteins involved in ErbB2 signalling pathways. α-tubulin was used as a loading control.

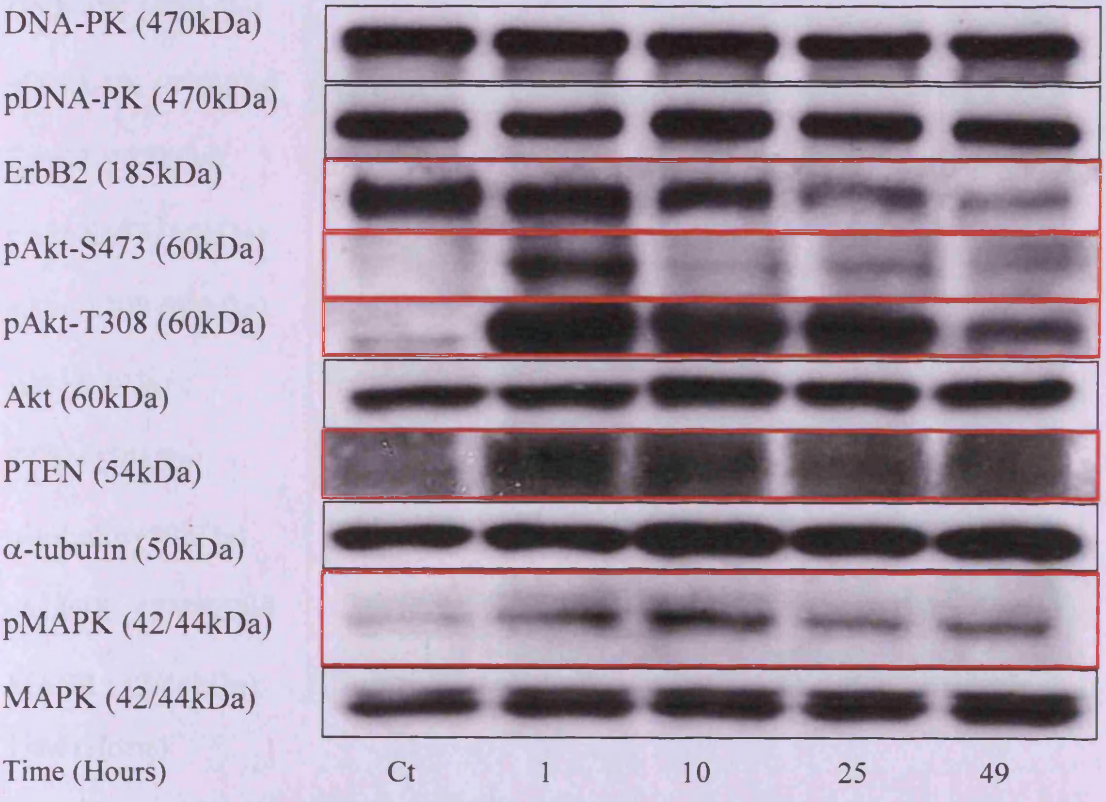

Figure 5.32 – Immunoblots of MDA-MB-468 pcDNA3-ErbB2 cells treated with trastuzumab (40μg/ml). Immunoblots were probed for DNA repair proteins and proteins involved in ErbB2 signalling pathways. α-tubulin was used as a loading control.

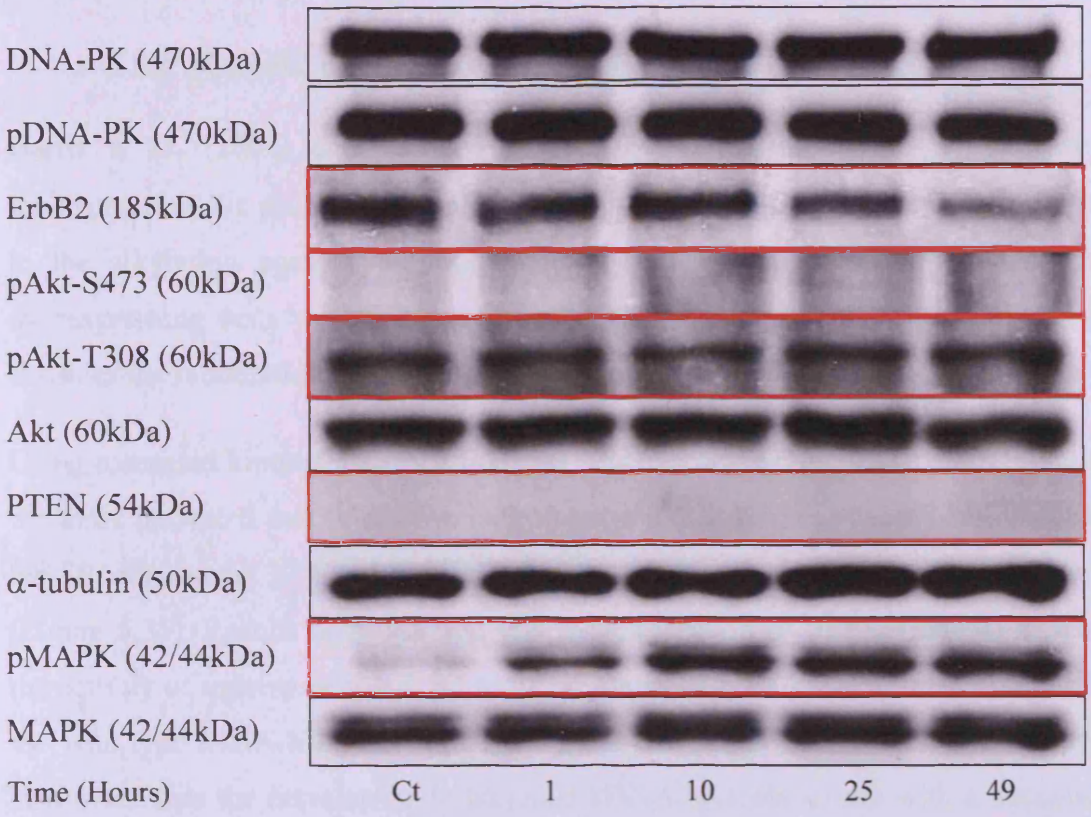

Figure 5.33 – Immunoblots of MDA-MB-468 pcDNA3-ErbB2 cells treated with cisplatin (100μM). Cells were treated for 1 hour and immunoblots probed for DNA repair proteins and proteins involved in ErbB2 signalling pathways. α-tubulin was used as a loading control.

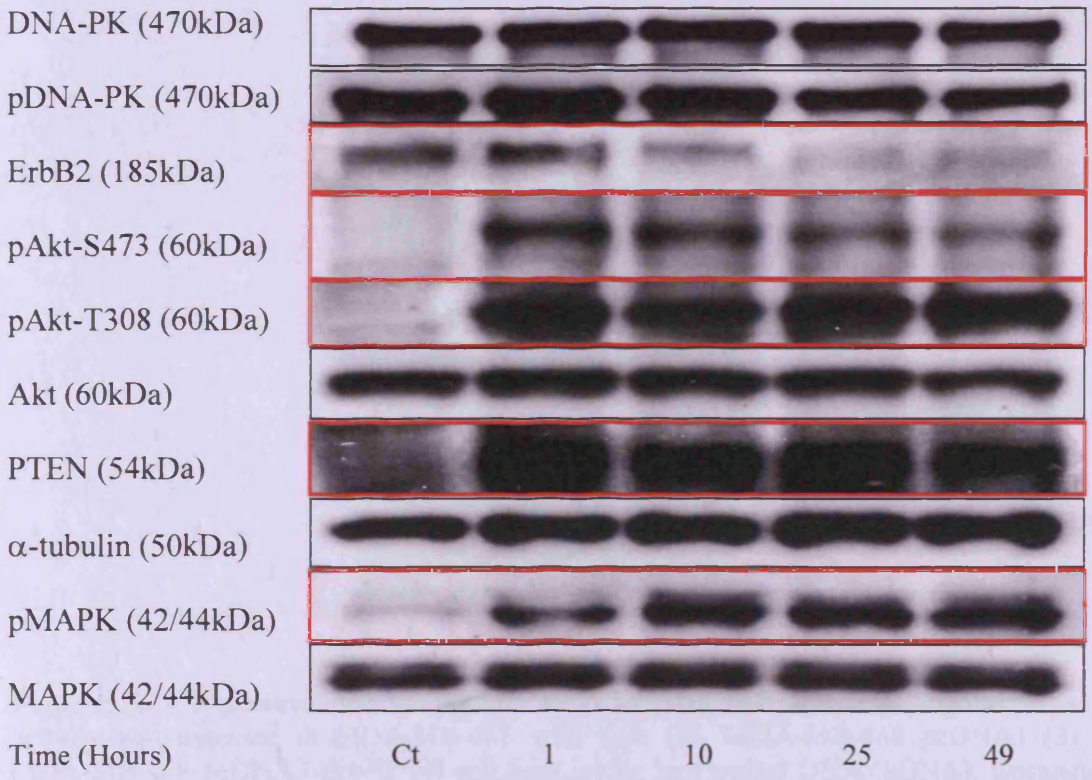

Figure 5.34 – Immunoblots of MDA-MB-468 pcDNA3-ErbB2 cells treated with cisplatin (100μM) **and trastuzumab** (40μg/ml). Cells were treated for 1 hour then incubated in media containing trastuzumab alone (40μg/ml) and immunoblots probed for DNA repair proteins and proteins involved in ErbB2 signalling pathways. α-tubulin was used as a loading control.

5.12 ErbB2 overexpression and topoisomerase II activity

Harris *et al.* (2001) demonstrated that ErbB2 signalling led to an increase in topoisomerase IIα protein and topoisomerase II activity, causing increased resistance to the alkylating agent cyclophosphamide. Therefore, having shown that ErbB2 overexpressing cells were more resistant to cisplatin treatment, it was important to consider the modulation of topoisomerase II activity due to ErbB2 overexpression.

Using catenated kinetoplast DNA (kDNA), DNA decatenation activity was studied in the three untreated cell lines described in section 5.6. Nuclear extract was incubated for 30 minutes at 37°C with kDNA before being separated on a 1% agarose gel (Figure 5.35). Results demonstrated that overexpression of ErbB2 (lane 4) increased the activity of topoisomerase II, as more decatenated kDNA was formed compared to the wild type MDA-MB-468 cells (lane 2) or the vector control cells (lane 3). It is also noted that the increase in decatenated kDNA was associated with a decrease in catenated kDNA.

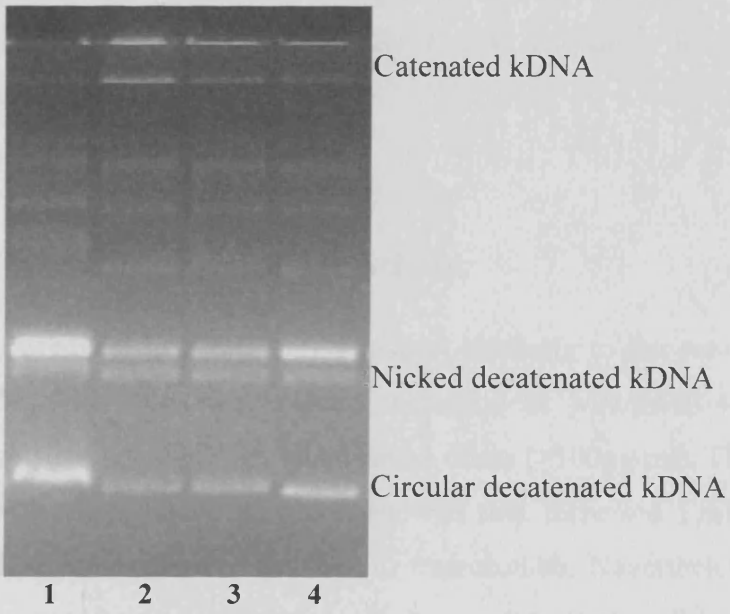

Figure 5.35 – Topoisomerase IIα activity assay in MDA-MB-468 cells. Topoisomerase IIα activity was assessed in MDA-MB-468 wild type (**2**), MDA-MB-468 pcDNA3 (**3**) and MDA-MB-468 pcDNA3-ErbB2 (**4**) cell lines, using kinetoplast DNA (kDNA). Decatenated kDNA (**1**) was used as a positive control. Reactions were stopped after 30 minutes. Increase in decatenated kDNA was observed in cells overexpressing ErbB2 (**4**).

DISCUSSION

In this chapter, the specific role of ErbB2 in the repair of cisplatin-induced DNA damage was investigated. To this end two approaches were considered. The first one was the use of siRNA to down-regulate ErbB2 expression in a breast cancer cell line overexpressing ErbB2. Although successful results were obtained with the siRNA, only partial down-regulation was achieved in cell lines overexpressing ErbB2 such as MDA-MB-453 cells. Therefore, the second approach using MDA-MB-468 cells, ErbB2 negative, stably transfected with a plasmid coding ErbB2 expression, was chosen. Results demonstrated that overexpression of ErbB2 was obtained and that ErbB2 was present in the cytoplasm and in the nucleus (immunofluorescence data). Using the same plasmid, Tzahar *et al.* (1996) obtained similar results as they showed overexpression of ErbB2 in CHO cells, negative for ErbB2. In addition, ErbB2 overexpression was shown to increase resistance to cisplatin and subsequent inhibition by trastuzumab caused an increase in sensitivity. Furthermore, modulation of ErbB2 expression caused a modulation of the kinetics of repair of cisplatin-induced DNA ICL but not repair of DNA intrastrand crosslinks. Finally, results demonstrated that modulation of Akt and PTEN activation was independent of the ErbB2 status. In addition, DNA decatenation activity by topoisomerase II was shown to be up-regulated by ErbB2 overexpression.

5.13 ErbB2 expression and drug sensitivity

Trastuzumab was shown to reduce the ErbB2 protein level similarly to the results obtained in MDA-MB-453 cells. However, growth inhibition of MDA-MB-468 ErbB2 positive cells was only observed at high trastuzumab doses (>100μg/ml). This result differs from the results in Chapter 3, which showed that increased ErbB2 expression was associated with increased sensitivity to trastuzumab. Nevertheless, Gong *et al.* (2004) demonstrated that trastuzumab single agent treatment did not always reduce cell proliferation of ErbB2 overexpressing cells.

In Chapter 3, breast cancer cells overexpressing ErbB2 (e.g. SK-BR-3) were not shown to be more resistant to chemotherapeutic agents than cells with a lower level of ErbB2 protein (e.g. MCF-7 and SK-BR-3 cells). As reported by Pegram *et al.* (1997)

resistance to chemotherapeutic agents is not only associated with the ErbB2 expression and is often cell line specific. Nevertheless, results from Benz *et al.* (1992) demonstrated that ErbB2 overexpression in transfected MCF-7 cells caused a 2-4 fold increase in resistance to cisplatin. Similarly, clinical trial studies (Allred *et al.*, 1992; Wright *et al.*, 1992) have also suggested the association of ErbB2 overexpression with increased resistance to chemotherapeutic agents. Results obtained here demonstrated that ErbB2 transfection in MDA-MB-468 wild type cells caused an increase in resistance to cisplatin, by 1.5 fold after continuous exposure and by almost 2 fold after short exposure (1 hour).

Studies by Pegram *et al.* (1997) and Orr *et al.* (2000) demonstrated that ErbB2 overexpression is not always sufficient to account for increased resistance to chemotherapeutic agents. Conversely, Hancock *et al.* (1991) also reported that ErbB2 negative cells sensitivity to cisplatin was not affected by trastuzumab. Furthermore, the study by Pegram and Slamon (1999) established that combining trastuzumab with cisplatin enhances chemosensitivity of ErbB2 overexpressing cells. Naruse *et al.* (2002) also confirmed that trastuzumab was able to enhance the cytotoxic effect of cisplatin. The results obtained in the present study demonstrated that combining trastuzumab with cisplatin did not increase the chemosensitivity of ErbB2 negative cells. They also showed that trastuzumab was able to sensitise ErbB2 overexpressing cells to cisplatin, as an increase of 1.5 folds in sensitivity to cisplatin was observed when cells were treated with trastuzumab and cisplatin. Therefore, a direct association can be made between ErbB2 overexpression and cisplatin chemoresistance.

It was also demonstrated that drug scheduling played an important role, as sensitisation of ErbB2 positive cells to cisplatin, by trastuzumab, was only seen after short exposure to cisplatin. Thus, there is an important need to define the optimal schedule of administration of anticancer drugs with trastuzumab. A study of trastuzumab in combination with paclitaxel and carboplatin in metastatic breast cancer reported that drug scheduling played an important role in determining toxicity and efficacy of the treatment *in vivo* (Perez, 2004). Similarly, studies have shown that drug scheduling was important to consider in order to obtain synergistic effect between gefitinib, an EGFR tyrosine kinase inhibitor, and chemotherapeutic agents, such as cisplatin (Friedmann *et al.*, 2004; Xu *et al.*, 2003).

5.14 ErbB2 expression modulates repair of drug-induced DNA damage

Studying the repair of cisplatin-induced interstrand crosslink established that ErbB2 overexpression caused an increase in DNA ICL repair efficiency, compared to the ErbB2 negative cells. Moreover, subsequent inhibition of ErbB2, by trastuzumab, caused a significant delay in DNA ICL repair, similarly to the results obtained for MDA-MB-453 cells in Chapter 3. Pietras *et al.* (1994) reported that inhibition of ErbB2 led to a decrease in the rate of unscheduled DNA synthesis, used as a measure of DNA damage repair, after cisplatin treatment. Therefore, overexpression of ErbB2 in MDA-MB-468 cells caused an increased resistance to cisplatin due to a more efficient repair of DNA ICLs, and combination of trastuzumab with cisplatin increased significantly the sensitivity to cisplatin, due to ErbB2 inhibition, and caused a delay in the repair of cisplatin-induced DNA interstrand crosslinks. It was also demonstrated that melphalan-induced DNA interstrand crosslinks were not affected by the modulation of ErbB2 expression. This difference from cisplatin can be explained by the type and frequency of ICLs formed, as De Silva *et al.* (2002) demonstrated that repair of cisplatin ICLs did not involve the formation of double strand breaks, in contrast to other conventional crosslinking agents, such as melphalan.

In contrast to interstrand crosslinks, the kinetics of formation and repair of intrastrand crosslinks formed by cisplatin was not altered by ErbB2 overexpression or subsequent down-regulation by trastuzumab. However, Arteaga *et al.* (1994) demonstrated that cisplatin-induced DNA intrastrand crosslinks were affected by ErbB2 inhibition. Using a competitive cisplatin-DNA ELISA, they showed that inhibition of ErbB2, using the anti-ErbB2 antibody Tab250, caused an increase in the formation of DNA intrastrand adducts and a delay in the repair of this type of adducts.

Therefore, according to the results obtained modulation of ErbB2 protein expression affects specifically the repair of cisplatin-induced DNA interstrand crosslinks. This specificity relies on the difference in the repair pathway involved for each type cisplatin adduct formed (De Silva *et al.*, 2002). As described previously, Zamble *et*

al. (1996) established that cisplatin-induced intrastrand crosslinks were repaired by nucleotide excision repair. Whereas the repair of interstrand crosslinks adducts, which represent only 10% of the lesions caused by cisplatin, has been shown to involve the XPF-ERCC1 heterodimer component of nucleotide excision repair (De Silva *et al.*, 2000; Mu *et al.*, 2000; Kuraoka *et al.*, 2000) and XRCC2 and XRCC3 proteins of the homologous recombination repair pathway (De Silva *et al.*, 2002). Although DNA interstrand crosslinks represent only 10% of cisplatin-DNA adducts, they have been described as being critical cytotoxic lesions in diving cells (Dronkert and Kanaar, 2001; Lawley and Phillips, 1996).

Consequently, it is logical that ErbB2 transfected cells, repairing cisplatin ICLs more efficiently than ErbB2 negative cells, are more resistant to cisplatin than the ErbB2 negative wild type cells. Hence, ErbB2 plays a role in the repair of cisplatin-induced ICLs and cisplatin chemoresistance.

5.15 Modulation of cell cycle progression

Proteins investigated in order to establish a possible explanation for the delay in DNA damage repair demonstrated that Akt, PTEN and pMAPK were affected by trastuzumab and the combination with cisplatin.

5.15.1 Role of Akt in the modulation of cell cycle

Results obtained were similar to those described in Chapter 4, with an activation of Akt (pAkt S473 and T308) by trastuzumab. Interestingly, trastuzumab had similar effects on pAkt in ErbB2 positive and negative cells, suggesting that escape of cells from the cell cycle, through inhibition of $p21^{WAF1}$ and $p27^{kip1}$ activity (Zhou *et al.*, 2001b; Medema *et al.*, 2000), also occurred in MDA-MB-468 wild type cells. This may be explained by the presence of undetectable level of ErbB2 protein in MDA-MB468 wild type cells. However, overexpression of ErbB2 caused an increase of pAkt T308 level in untreated cells compared to ErbB2 negative cells. In addition, in ErbB2 positive cells, trastuzumab alone caused a more rapid decrease in pAkt following its activation. Yakes *et al.* (2002) also reported that inhibition of pAkt was only observed in cell lines with the highest ErbB2 protein expression. This finding

could explain why inhibition of pAkt is faster in MDA-MB-468 cells positive for ErbB2 than in ErbB2 negative cells, leading to an increase in G1 arrest (discussed in Chapter 4). Furthermore, in ErbB2 positive cells, reduction of pAkt S473 was more rapid than reduction of pAkt T308 after activation by trastuzumab. A similar effect was observed with trastuzumab in combination with cisplatin, since only pAkt T308 level was maintained with time. Thus, ErbB2 expression modulates differently phosphorylation of Akt at S473 and T308. This can be explained by the difference in phosphorylation mechanism, since threonine 308 has been shown to be phosphorylated by the kinase PDK1 (Alessi *et al.*, 1997) whereas phosphorylation at serine 473 remains controversial (Toker and Newton, 2000).

Consequently, trastuzumab alone caused cell cycle arrest through inhibition of Akt activation, but in combination with cisplatin cells escaped cell cycle arrest due to the continuous activation of Akt. Furthermore, increased pAkt in ErbB2 cells may account for the increased resistance to cisplatin as Akt activation causes cell cycle progression and inhibition of apoptosis.

5.15.2 Role of MAPK in the modulation of cell cycle

Although ErbB2 overexpression was previously described to enhance MAPK signalling, results presented here did not show increased MAPK or pMAPK protein levels. However, in the presence of cisplatin, MAPK was shown to be activated. This concurs with the study by Wang *et al.* (2000a) which demonstrated that cisplatin caused activation of MAPK signalling and that it played a major role in mediating cisplatin-induced apoptosis. Contrary to the study by Yakes *et al.* (2002), in combination with cisplatin, trastuzumab did not cause inhibition of pMAPK in ErbB2 overexpressing cells.

Therefore, cisplatin activates the MAPK signalling pathway and contributes to cell cycle arrest through modulation of $p27^{kip1}$ and cyclin D1 (Lenferink *et al.*, 2001).

5.15.3 PTEN and PI3K/Akt signalling

Studies by Nagata *et al.* (2004) and Fujita *et al.* (2006) have previously established that trastuzumab caused activation of PTEN through its dephosphorylation. Furthermore, they reported that activation of PTEN led to an inhibition of the

PI3K/Akt pathway. Results obtained here demonstrated that PTEN was rapidly activated by trastuzumab. Therefore, in the presence of trastuzumab alone, reduction of activated Akt and G1 arrest was mediated through PTEN activation. However, in combination with cisplatin, trastuzumab activated PTEN continuously but no down-regulation of pAkt was observed, suggesting that PTEN activation is not sufficient to cause inhibition of the PI3K pathway and cell growth inhibition.

Therefore, further investigation is required to determine the role of PTEN when combining trastuzumab with chemotherapeutic drugs and proteins regulating the PI3K/Akt signalling pathway.

5.16 ErbB2 overexpression increases topoisomerase II activity

A study by Harris *et al.* (2001) demonstrated that activation of ErbB2 led to an increase in topoisomerase II protein and activity, conferring increased resistance to cyclophosphamide, an alkylating agent. In addition, they also showed that inhibition of ErbB2, by trastuzumab, led to the reversal of this effect. Although no decrease in topoisomerase IIα protein level was observed in Chapter 4, after combination of trastuzumab with cisplatin, an increase in sensitivity to cisplatin was reported. As demonstrated by several studies (Larsen *et al.*, 1998; Pu and Bezwoda, 1999; Eder *et al.*, 1995), the increase of topoisomerase II activity and protein level contribute, in some cell lines, to resistance to DNA crosslinking agent, cisplatin. Furthermore, topoisomerase II was also suggested to play a role in DNA repair through modulation of the chromatin structure. Investigating the DNA decatenation ability of stably transfected ErbB2 positive and negative cells, demonstrated that ErbB2 overexpression caused an increase in topoisomerase II activity.

Therefore, together with published data, results suggest that ErbB2 overexpression increased topoisomerase II activity leading to a modulation of DNA repair activity and resistance to cisplatin. It is also suggested that combining cisplatin with trastuzumab causes a reduction in topoisomerase II activity. Nevertheless, further understanding of the molecular mechanism involved here is required.

5.17 Conclusion

The results presented in this chapter demonstrated that ErbB2 overexpression increased the repair of cisplatin-induced DNA interstrand crosslinks and subsequent down-regulation of ErbB2 by trastuzumab led to a delay in the repair of this type of cisplatin-DNA adduct. In addition, results also established that cisplatin-induced intrastrand crosslinks were not affected by ErbB2 expression modulation. Furthermore, ErbB2 overexpression was shown to increase resistance to cisplatin which was associated with the increased DNA ICLs repair efficiency, pAkt protein level and topoisomerase II activity. Trastuzumab was also shown to enhance the sensitivity of ErbB2 overexpressing cells to cisplatin and cause a delay in the repair of cisplatin-induced DNA ICLs. Finally, studying the expression of proteins involved in DNA damage repair and ErbB2 signalling pathway confirmed the results obtained in Chapter 4, however, PTEN activation did not cause inhibition of pAkt in the combination treatment, contrary to some published studies. Cisplatin was also suggested to induce cell cycle arrest and apoptosis through activation of the MAPK signalling pathway.

Therefore, considering those results it is reasonable to conclude that ErbB2 expression can alter the repair of cisplatin-induced DNA ICLs. In addition, the delay in the repair of DNA damage was also suggested to be caused by an escape of the cells from cell cycle arrest.

ErbB2 having been shown to localise in the cytoplasm and the nucleus and since DNA repair occurs in the nucleus, its nuclear localisation may play an important role in the repair of cisplatin-induced DNA damage. In order to determine the effect of ErbB2 nuclear localisation, MDA-MB-468 cells, ErbB2 negative, will be used and stably transfected with a plasmid encoding a mutated form of ErbB2, with a deletion of the nuclear localisation signal (NLS).

Chapter 6

Role of ErbB2 nuclear localisation in the repair of cisplatin-induced DNA ICL

INTRODUCTION

The previous chapter demonstrated that ErbB2 overexpression caused an increase in efficiency in the repair of cisplatin-induced DNA interstrand crosslink. In addition, ErbB2 protein inhibition, by trastuzumab, led to a delay in the repair of DNA ICLs induced by cisplatin. Finally, it was demonstrated that ErbB2 overexpression induced an increased in DNA decatenation activity. Since ErbB2 was shown, in certain cancer cell lines, to be expressed in the cytoplasm and the nucleus, it is important to consider the potential role of ErbB2 nuclear localisation in the repair of cisplatin-induced DNA interstrand crosslink.

6.1 Nuclear localisation of EGFR family members

The epidermal growth factor receptor family of receptor tyrosine kinases, including EGFR, ErbB2, ErbB3 and ErbB4, are expressed at the cell surface. Binding of these receptors to their respective ligands causes heterodimerisation and homodimerisation leading to activation of the tyrosine kinase activities (Schlessinger, 2002). This will subsequently relay information from the cell surface to the nucleus through a network of downstream signalling pathways, such as the MAPK and PI3K pathways, regulating cellular proliferation, differentiation and programmed cell death (Olayioye *et al.*, 2000). However, recent studies have shown that EGFR family members are able to translocate to the nucleus (Massie and Mills, 2006). Nuclear localisation has been shown to be mediated by a nuclear localisation signal sequence (NLS – Pemberton L.F. and Paschal B.M., 2005), and transported to the nucleus through the formation of a complex with importin α/β (Hu and Jans, 1999) or importin β alone (Truant and Cullen, 1999).

Similarly, Chen *et al.* (2005) recently identified a NLS (KRRQQKIRKYTMRR) that is responsible for ErbB2 nuclear localisation. This sequence may provide an explanation for the mechanism underlying ErbB2 nuclear function. Although the mechanism responsible for nuclear translocation of ErbB2 remains unclear, Giri *et al.* (2005) established a mechanism, involving importin $\beta 1$ as a driver, for ErbB2 nuclear translocation from the cell surface. It is also suggested that this translocation route may serve as a general mechanism for other receptor tyrosine kinases. Hsu and Hung

(2007) recently characterised a tripartite nuclear localisation sequence formed of 13 amino acids, which is conserved among the EGFR family members and responsible for their nuclear translocation. Conflicting results have also shown that this tripartite NLS is required for receptor dimerisation (Aifa *et al.*, 2005). Conversely, Giri *et al.* (2005) demonstrated that deletion of the ErbB2 tripartite NLS did not affect its membrane localisation and its ability to activate MAPK signalling pathway. Therefore, association between dimerisation of EGFR and nuclear localisation needs to be investigated further. Although nuclear translocation of the four members of the EGFR family has been shown, it was reported that they were translocated into the nucleus under different forms.

For EGFR (Lin *et al.*, 2001), the complete full ligand length receptor complex is translocated into the nucleus, for ErbB2 and ErbB3 the full length protein is translocated (Wang *et al.*, 2004; Offterdinger *et al.*, 2002), whereas for ErbB4 only the intracellular domain is translocated into the nucleus (Lee *et al.*, 2002a). Detection of nuclear EGFR was first reported by Kamio *et al.* (1990). Although nuclear EGFR lacks DNA binding domain/function, Lin *et al.* (2001) established that nuclear EGFR acts as a transcriptional activator through binding to adenine/thymidine-rich DNA sequences. In their study they showed that EGFR was able to activate cyclin D1 through binding to the promoter region. In a different study (Lo *et al.*, 2005), nuclear EGFR was shown to associate with the signal transducers and activators of transcription 3 (STAT3) leading to activation of inducible nitric oxide synthase (iNOS) and subsequent tumour growth and angiogenesis (Cianchi *et al.*, 2003; Vakkala *et al.*, 2000). A recent study by Hanada *et al.* (2006) suggested that nuclear function of EGFR can be phosphorylation dependent, since nuclear EGFR was able to phosphorylate E2F1 which is responsible for the activation of B-Myb, a transcription factor. Upon cell irradiation, EGFR has also been shown to translocate, together with Ku70/80, into the nucleus for regulation of DNA-PK (Dittmann *et al.*, 2005). Therefore, nuclear EGFR is not only used as a transcriptional activator but can serve to trigger DNA repair. Although nuclear EGFR has been more widely studied, unidentified transcriptional targets may exist. Clark *et al.* (2005) also demonstrated that nuclear ErbB4 was able to act as a transcriptional activator through phosphorylation of the serine of STAT5a transcription factor and subsequent activation of the β-casein gene (Williams *et al.*, 2004). Nuclear ErbB2 was also

shown to associate with a specific DNA sequence, HER-2 associated sequence (HAS) in the cyclooxygenase enzyme COX-2 promoter (Wang *et al.*, 2004), a protein associated with tumour progression (Turini and Dubois, 2002). Indeed, Wang *et al.* (2004) demonstrated that nuclear ErbB2 was used as a transcriptional regulator by forming a complex with the COX-2 promoter. In addition, they also identified a HAS in the Fanconi Anemia Complementation group C (FANCC) promoter, suggesting that nuclear ErbB2 acts as a transcriptional regulator of the FANCC protein, involved in the repair of DNA damage generated from oxidative stress.

Together, these observations suggest that nuclear localisation of ErbB2 may also affect other nuclear events since it contains intrinsic ability to enhance gene transcription, through transcription co-factors with DNA binding ability. In addition, ErbB2 nuclear localisation may have other functions such as DNA damage repair.

6.2 Wheat germ agglutinin and nuclear translocation

Nuclear translocation of large molecules depends on the nuclear localisation signal, as previously described. This nuclear import is divided into two steps, binding in or near the nuclear pore and translocation through it (Newmeyer and Forbes, 1988). The translocation step is energy dependent and can be inhibited by the lectin wheat germ agglutinin (WGA – Yoneda *et al.*, 1987; Newmeyer and Forbes, 1988; Wolff *et al.*, 1988) which binds specifically to the glycoconjugates of the nuclear pore complex (Davis and Blobel, 1987; Finlay *et al.*, 1987). Therefore, WGA does not physically block the pore and does not affect the signal sequence-dependent binding step. This inhibition has been shown to be reversed by addition of competing sugars (Finlay *et al.*, 1987).

Therefore, WGA can be used as a pharmacological method to block nuclear translocation. As Dittmann *et al.* (2005) reported, radiation-induced nuclear translocation of EGFR was blocked after treating the cells with 100μg/ml of WGA for 30 minutes, prior to irradiation. Although WGA can be used to block nuclear translocation of EGFR, it is not specific for this protein and effects observed may be due to the inhibition of nuclear translocation of other proteins. Furthermore, after removal of WGA, nuclear translocation inhibition will gradually decrease. WGA may

therefore be used for the inhibition of ErbB2 nuclear translocation, in order to study the effect on the repair of cisplatin-induced DNA interstrand crosslinks.

6.3 Aims

To investigate the role of ErbB2 nuclear localisation in the repair of drug-induced DNA damage, using MDA-MB-468 wild type cells stably transfected with a plasmid encoding ErbB2 with a deletion of the nuclear localisation signal (as described by Giri *et al.*, 2005), the following questions will be addressed:

- Is ErbB2 nuclear localisation blocked by the deletion of the NLSs?
- Does ErbB2 nuclear localisation affect the sensitivity to trastuzumab and cisplatin?
- Does inhibition of ErbB2 nuclear translocation affect the repair of cisplatin-induced DNA interstrand crosslinks?
- How does the modulation of the repair of cisplatin-induced DNA ICL correlate with EGFR and ErbB2 nuclear localisation?

RESULTS

6.4 Expression of mutated ErbB2 with a deletion of the NLS sequence

The plasmid encoding the mutated form of ErbB2 containing a deletion of the NLSs (amino acids 676-KRRQQKIRKYTMRR-689) was described by Giri *et al.* (2005) and was a kind gift from Prof. M.C. Hung (MD Anderson Cancer Center, USA). Similarly to Chapter 5, MDA-MB-468 cells were used for stable transfection, in order to express the mutated form of ErbB2.

6.4.1 ErbB2 protein expression by immunoblotting

The ErbB2 negative cell line, MDA-MB-468, was stably transfected with the three plasmids as previously described. Cells were pooled transfected and selective pressure was maintained using G418. After four to five weeks, the three new cell lines (MDA-MB-468 vector control, MDA-MB-468 ErbB2 and MDA-MB-468 ErbB2ΔNLS) were exponentially growing. It is noted that MDA-MB-468 vector control and ErbB2 are different from the one described in Chapter 5 as the vector used is pEGFP-N1. Figure 6.1 shows that ErbB2 is overexpressed in MDA-MB-468 ErbB2 cells and in MDA-MB-468 ErbB2ΔNLS cells. Other ErbB receptors protein expression levels are not affected by the transfection. Furthermore, results presented in Figure 6.2 revealed that ErbB2 is not present in the nucleus of MDA-MB-468 ErbB2ΔNLS cells (Figure 6.2 B) but is present in both the nucleus and the cytoplasm of MDA-MB-468 ErbB2 cells (Figure 6.2 A).

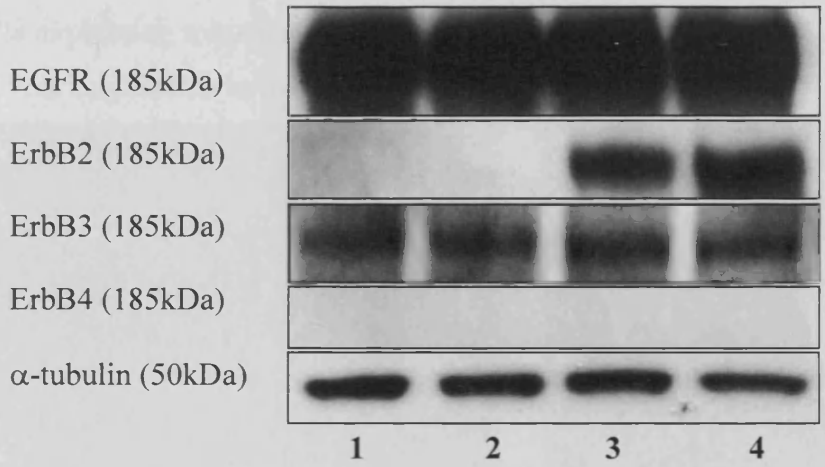

Figure 6.1 – Protein expression of each ErbB receptor in MDA-MB-468 wild type (1), vector control (2), ErbB2 (3) and ErbB2ΔNLS (4) cells. α-tubulin was used as a loading control.

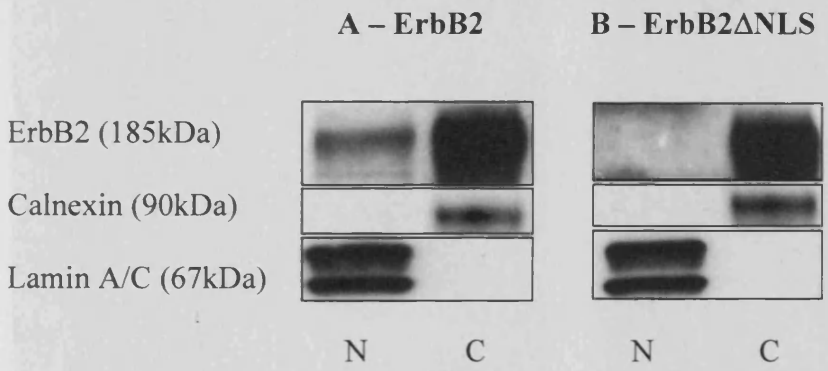

Figure 6.2 – ErbB2 protein expression in MDA-MB-468 ErbB2 (A) and MDA-MB-468 ErbB2ΔNLS (B) cells. Calnexin is used as a loading control for the cytoplasmic fraction (C) and Lamin A/C as a loading control for the nuclear fraction (N).

6.4.2 ErbB2 protein expression by immunofluorescence

Immunofluorescence confirmed that ErbB2 was present in the nucleus of MDA-MB-468 ErbB2 cells (red arrow Figure 6.3 C), but not in the nucleus of MDA-MB-468 ErbB2ΔNLS cells (Figure 6.3 D). Therefore, the stably transfected MDA-MB-468 cells expressing a mutated form of ErbB2 was used to investigate the role of ErbB2 nuclear localisation in the repair of cisplatin-induced DNA damage.

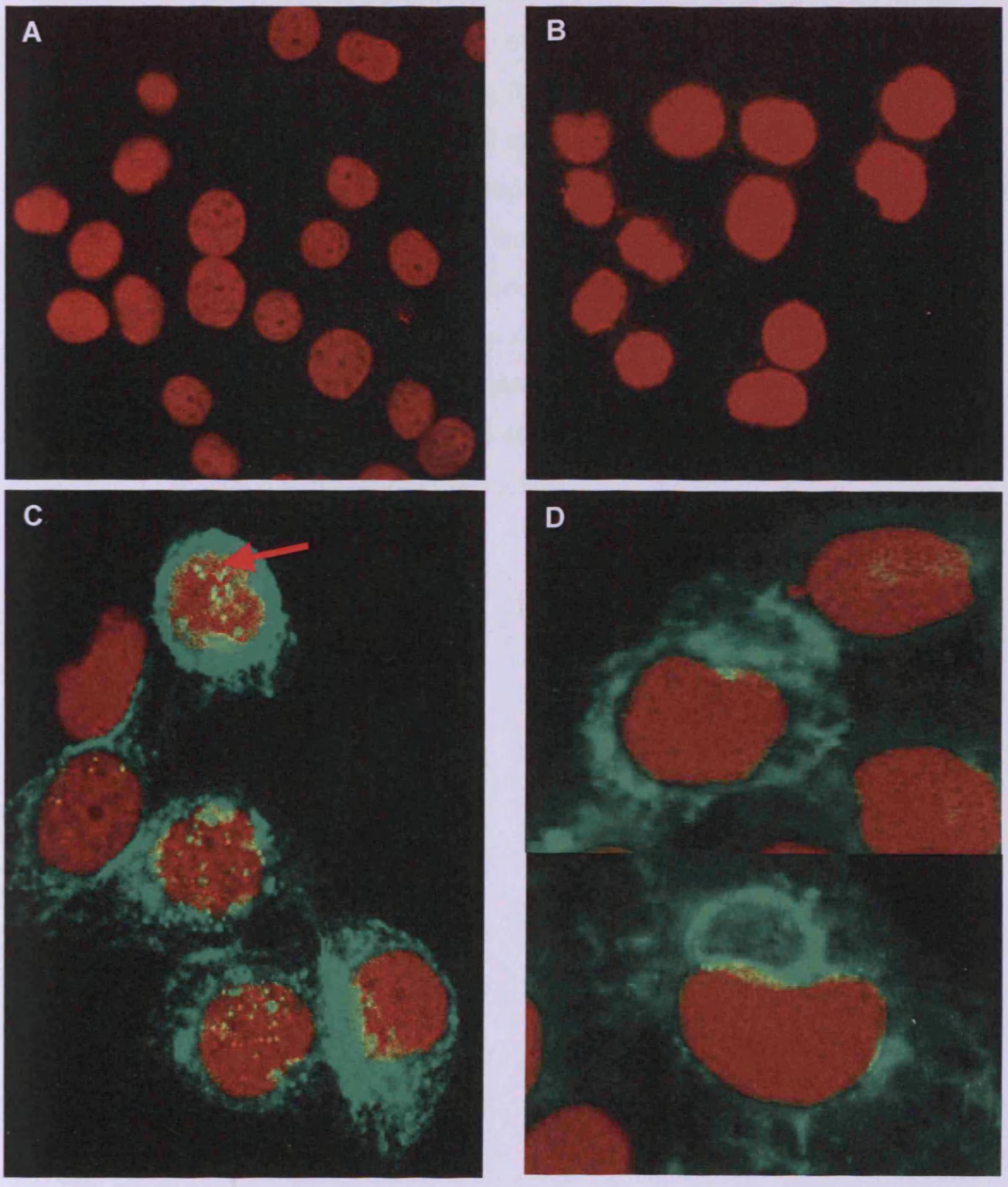

Figure 6.3 – Immunofluorescence ErbB2 protein expression in MDA-MB-468 cells. MDA-MB-468 wild type (**A**), MDA-MB-468 pEGFP-N1 vector control (**B**), MDA-MB-468 ErbB2 (**C**) and MDA-MB-468 ErbB2ΔNLS (**D**) cells were stained with anti-ErbB2 (green) and counter stained with propidium iodide (red). The red arrow indicates that ErbB2 is expressed in the nucleus.

6.5 Effect of trastuzumab and cisplatin on transfected cell lines

6.5.1 Effect of trastuzumab on MDA-MB-468 cell lines

Trastuzumab and ErbB2 protein expression

MDA-MB-468 ErbB2 and ErbB2ΔNLS cell lines were treated with trastuzumab at 40μg/ml for 24 hours. ErbB2 protein expression was measured by immunofluorescence and western blotting (total protein level). Trastuzumab caused a reduction of the total ErbB2 protein level after treatment for 24 hours in MDA-MB-468 ErbB2 cells (Figure 6.4 B and C) compared to the untreated cells (Figure 6.4 A). It is also noted that nuclear ErbB2 is reduced by trastuzumab in MDA-MB-468 ErbB2 cells (Figure 6.4 D). Indeed, although trastuzumab does not affect nuclear ErbB2 directly, it is suggested that less membrane bound ErbB2 (cytoplasmic fraction) was available for nuclear translocation, thus reducing nuclear ErbB2. A similar result was obtained for MDA-MB-468 ErbB2ΔNLS cells (Figure 6.5 B and C) but no ErbB2 protein was present in the nucleus.

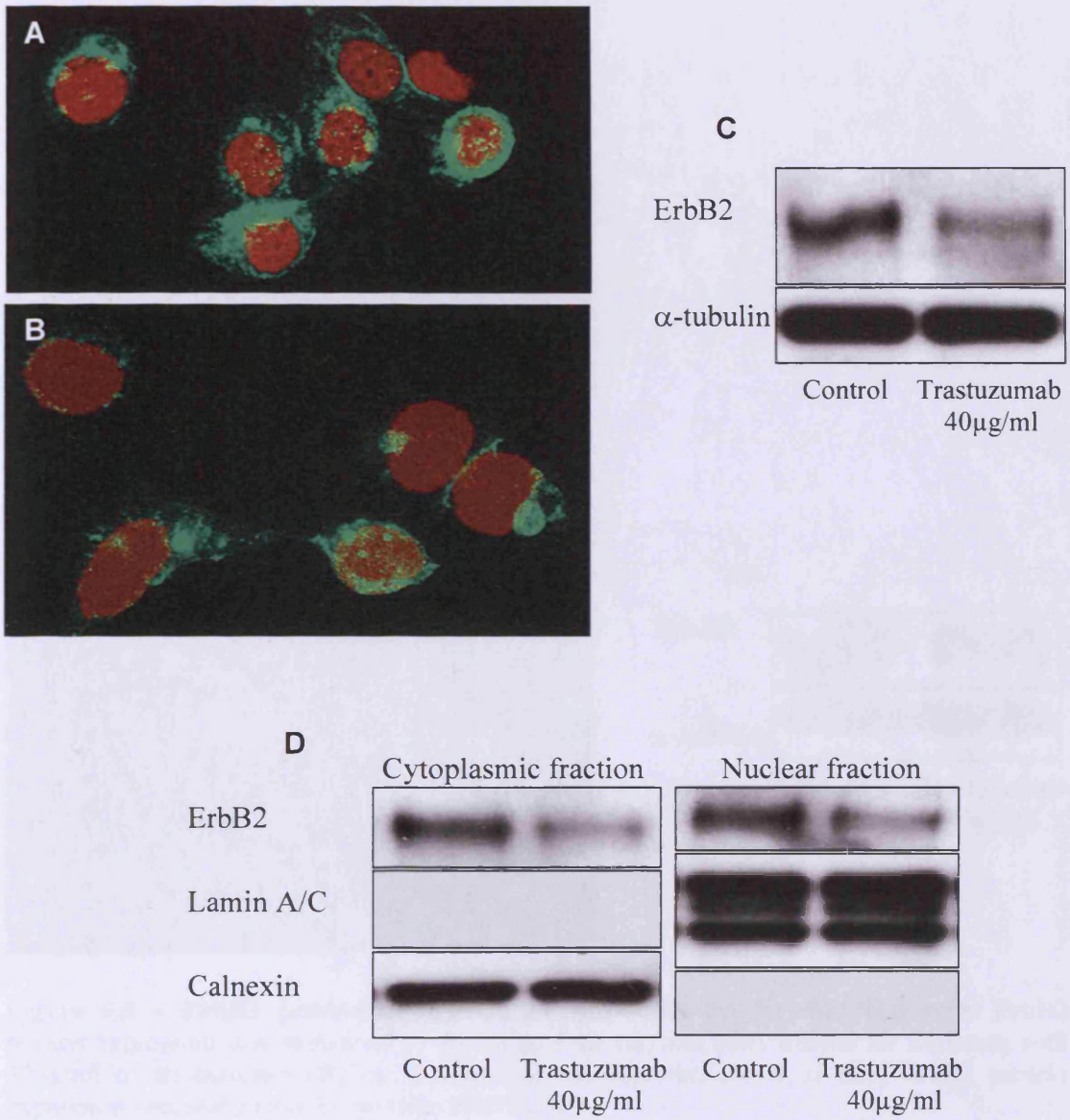

Figure 6.4 – Nuclear and cytoplasmic ErbB2 protein expression in MDA-MB-468 ErbB2 cells. ErbB2 protein expression was measured in untreated cells (**A**) and cells treated for 24 hours with 40µg/ml of trastuzumab (**B**) by immunofluorescence. Total ErbB2 protein expression was measured by western blotting (**C**). ErbB2 protein level was also measured separately in the nuclear fraction and cytoplasmic fraction (**D**).

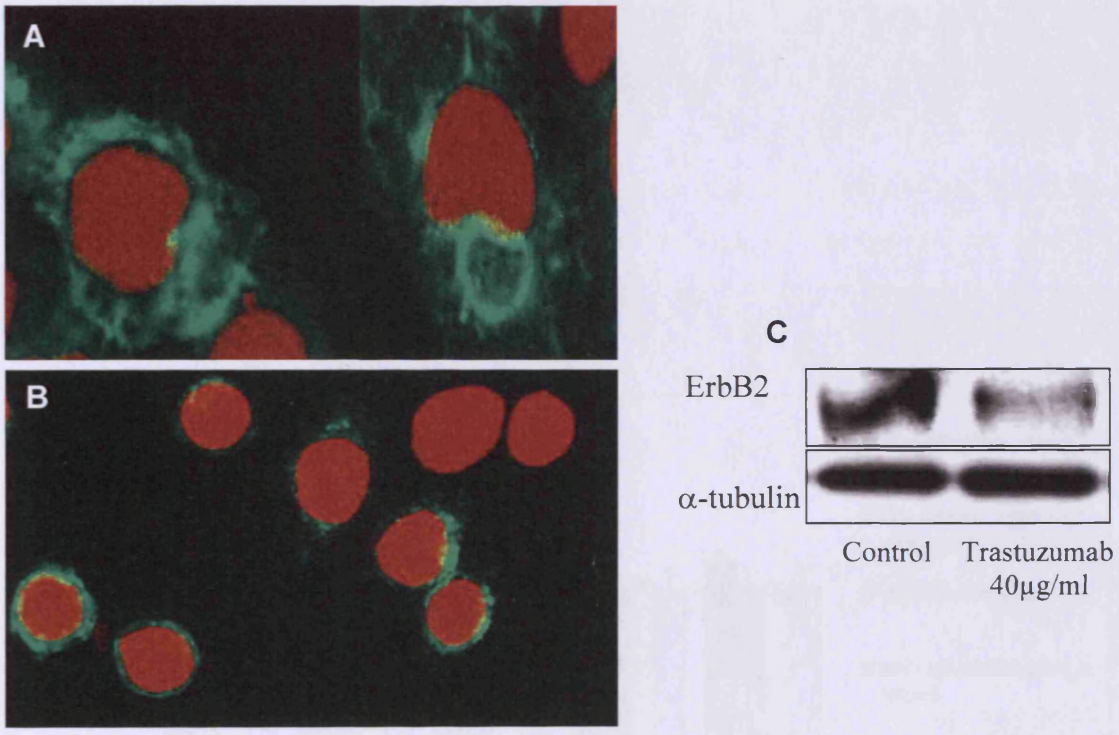

Figure 6.5 – ErbB2 protein expression in MDA-MB-468 ErbB2ΔNLS cells. ErbB2 protein expression was measured in untreated cells (**A**) and cells treated for 24 hours with 40μg/ml of trastuzumab (**B**) by immunofluorescence. Reduction of total ErbB2 protein expression was also shown by western blotting (**C**).

Effect of trastuzumab on cell proliferation

Having shown that trastuzumab caused the down-regulation of ErbB2 protein level in both cell lines expressing ErbB2 (mutated and non-mutated), its effect was observed on the proliferation of cells. All four cell lines were exposed to a range of trastuzumab concentrations for 5 consecutive days, experiment were repeated in triplicate. The inhibition of proliferation assay revealed that cell proliferation was not affected by trastuzumab with concentrations up to 100µg/ml (Figure 6.6). Therefore, ErbB2 overexpression and inhibition of its nuclear localisation did not alter inhibition of proliferation by trastuzumab.

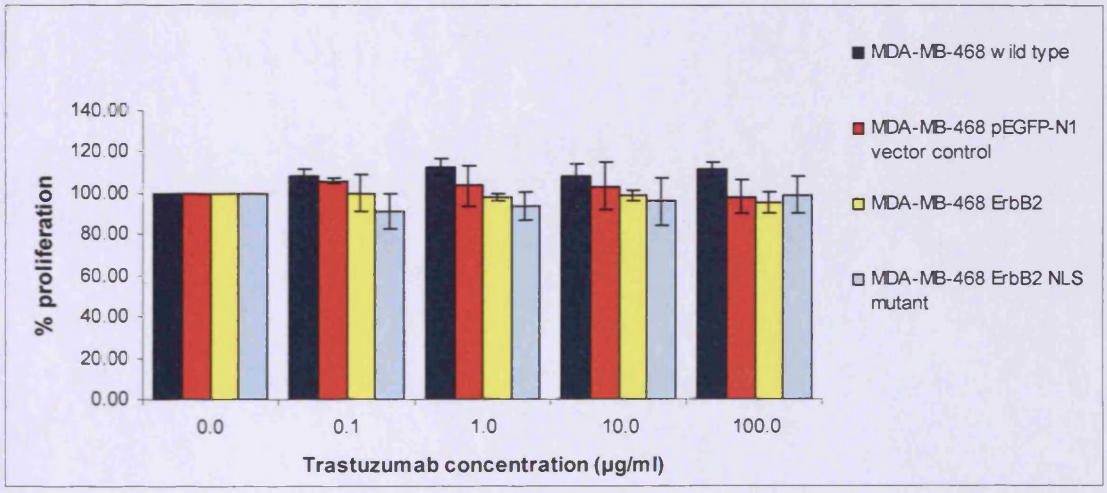

Figure 6.6 – Inhibition of MDA-MB-468 cells proliferation by trastuzumab. MDA-MB-468 wild type (dark blue), MDA-MB-468 vector control (red), MDA-MB-468 ErbB2 (yellow) and MDA-MB-468 ErbB2ΔNLS (light blue) cells were treated with a range of trastuzumab concentrations. Data presented are the result of three independent experiments, as shown by the standard deviation.

6.5.2 Sensitivity to cisplatin treatment

Cells were exposed to a range of cisplatin concentrations for 1 hour and incubated in drug free media for 3 days. For accuracy and repeatability all experiments have been repeated in triplicate. Results of the inhibition of proliferation assay are presented in Figure 6.7 and IC_{50} obtained in Table 6.1. IC_{50} were statistically analysed using the student *t*-test with a degree of freedom n = 4 and a significance level $p = 0.01$ (99% probability). Result obtained for the cell line overexpressing the normal form of ErbB2 was comparable to the result obtained in Chapter 5. As shown in Table 6.1, overexpression of the non-mutated ErbB2 protein caused an increase in resistance (1.5 fold) to cisplatin (result in red) whereas deletion of the nuclear localisation signal sequence caused an increase in sensitivity (3 fold – result in bold blue). Sensitivity of the NLS mutant increased by 3 fold compared to ErbB2 negative cells and by 5 fold compared to the cells that could translocate ErbB2 into the nucleus. Consequently, these results suggest that ErbB2 nuclear translocation plays an important role in the response to cisplatin-induced DNA damage.

	MDA-MB-468 wild type	MDA-MB-468 pEGFP-N1 vector control	MDA-MB-468 ErbB2	MDA-MB-468 ErbB2ΔNLS
Cisplatin IC_{50}	9.00±0.75μM	9.10±1.01μM	15.00±1.53μM	**3.10±0.25μM**

Table 6.1 – IC_{50}±SD results for MDA-MB-468 cells treated with cisplatin alone. MDA-MB-468 wild type, MDA-MB-468 vector control, MDA-MB-468 ErbB2 and MDA-MB-468 ErbB2ΔNLS cells were treated with cisplatin for one hour, followed by 3 days in drug free media. Results were statistically compared to the wild type cells, using the student *t*-test with n = 4 and $p = 0.01$ (99% probability). Cells overexpressing the normal form of ErbB2 were more resistant (result in red) to cisplatin but with the deletion of the NLS sequence cells became more sensitive (result in bold blue).

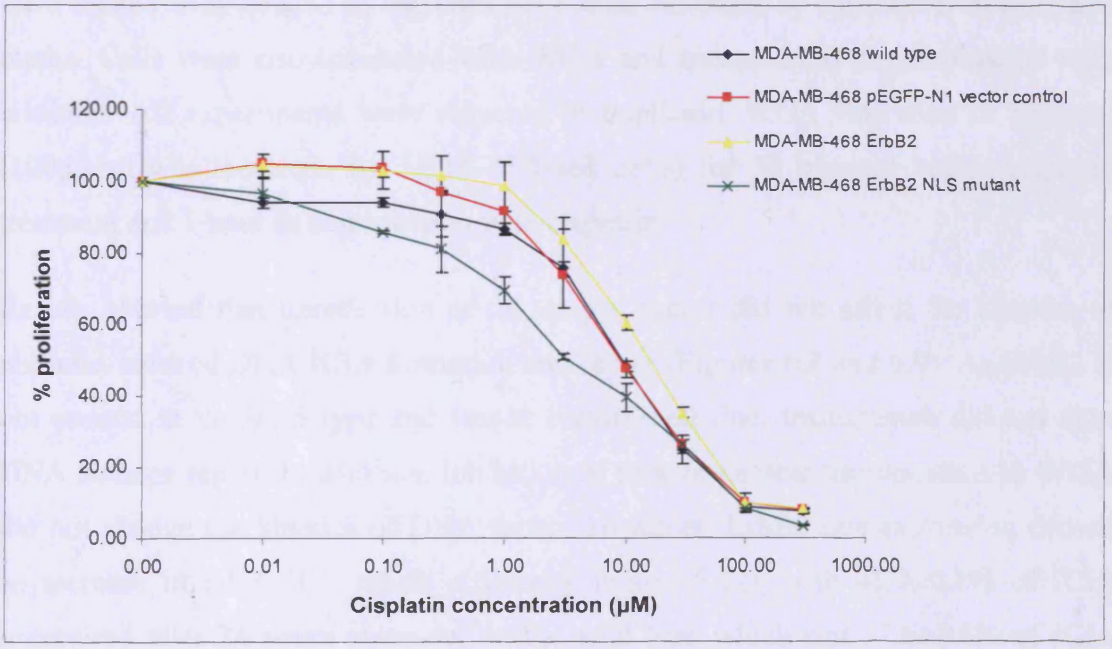

Figure 6.7 – Inhibition of MDA-MB-468 cells proliferation by cisplatin. MDA-MB-468 wild type (♦), MDA-MB-468 vector control (■), MDA-MB-468 ErbB2 (▲) and MDA-MB-468 ErbB2ΔNLS (×) cells were incubated 1 hour with a range of cisplatin concentration followed by 3 days in drug free media. Data presented are the result of three independent experiments, as shown by the standard deviation.

6.6 Modulation of DNA damage repair by inhibition of ErbB2 nuclear translocation

The importance of ErbB2 nuclear translocation in the response to cisplatin-induced DNA damage was shown in the previous section. However, to determine whether nuclear translocation plays a role in the repair of cisplatin-induced DNA interstrand crosslink, kinetics of formation and repair of cisplatin-induced DNA ICLs was studied using the same cisplatin dose defined in Chapter 5.

6.6.1 Modulation of the repair of cisplatin-induced DNA interstrand crosslinks

In order to study the role of nuclear translocation, the cell line expressing the mutated form of ErbB2 as well as WGA were used. MDA-MB-468 wild type, MDA-MB-468 pEGFP-N1 vector control, MDA-MB-468 ErbB2 and MDA-MB-468 ErbB2ΔNLS were treated with 100μM of cisplatin for 1 hour followed by incubation in drug free media. Cells were also incubated with WGA and trastuzumab in combination with cisplatin. All experiments were repeated in duplicate. WGA was used at 50μg/ml (100μg/ml was too toxic for MDA-MB-468 cells) for 30 minutes before cisplatin treatment and 1 hour in combination with cisplatin.

Results showed that transfection of the empty vector did not affect the kinetics of cisplatin-induced DNA ICLs formation and repair (Figures 6.8 and 6.9). As ErbB2 is not present in the wild type and vector control cell line, trastuzumab did not alter DNA damage repair. In addition, inhibition of protein nuclear translocation by WGA did not change the kinetics of DNA repair. However, ErbB2 overexpression caused an increase in DNA ICL repair efficiency Figure 6.12), with 41.7±0.1% of ICLs unrepaired after 24 hours compared to the wild type which had 57.6±3.6% of ICLs unrepaired after 24 hours. Subsequent inhibition of ErbB2, by trastuzumab, led to a delay in the kinetics of repair of cisplatin-induced DNA ICLs (Figure 6.10) causing 66.5±0.3% unrepaired ICLs after 24 hours. The effect of trastuzumab is comparable to the effect of WGA, which caused 67.2±3.6% of interstrand crosslinks to be unrepaired after 24 hours. Down-regulating ErbB2 by trastuzumab and blocking its nuclear translocation increased the delay in DNA damage repair only after 72 hours.

This result, together with the data from the ErbB2 negative cells lines, demonstrates that ErbB2 nuclear translocation plays a major role in the repair of cisplatin-induced DNA ICLs.

Deletion of the ErbB2 NLS sequence caused a delay in DNA ICLs repair (Figure 6.12), since after 24 hours 66.8±2.0% of ICLs are unrepaired compared to 57.6±3.6% in the wild type cells and 41.7±0.1% in cells overexpressing the normal form of ErbB2. Trastuzumab and WGA did not change the kinetics of DNA ICLs formation and repair of MDA-MB-468 ErbB2ΔNLS cells (Figure 6.11). After 24 hours 66.8±2.0% of ICLs remained unrepaired in cells treated with cisplatin alone and 68.9±0.1% were unrepaired in cells treated with a combination of cisplatin and trastuzumab. Nevertheless,

Therefore, ErbB2 overexpression was confirmed to cause an increase in DNA ICLs repair efficiency whereas blocking its nuclear translocation led to a decrease of the effectiveness of this repair. Furthermore, using WGA demonstrated that nuclear ErbB2 has a role in repair of ICLs induced by cisplatin.

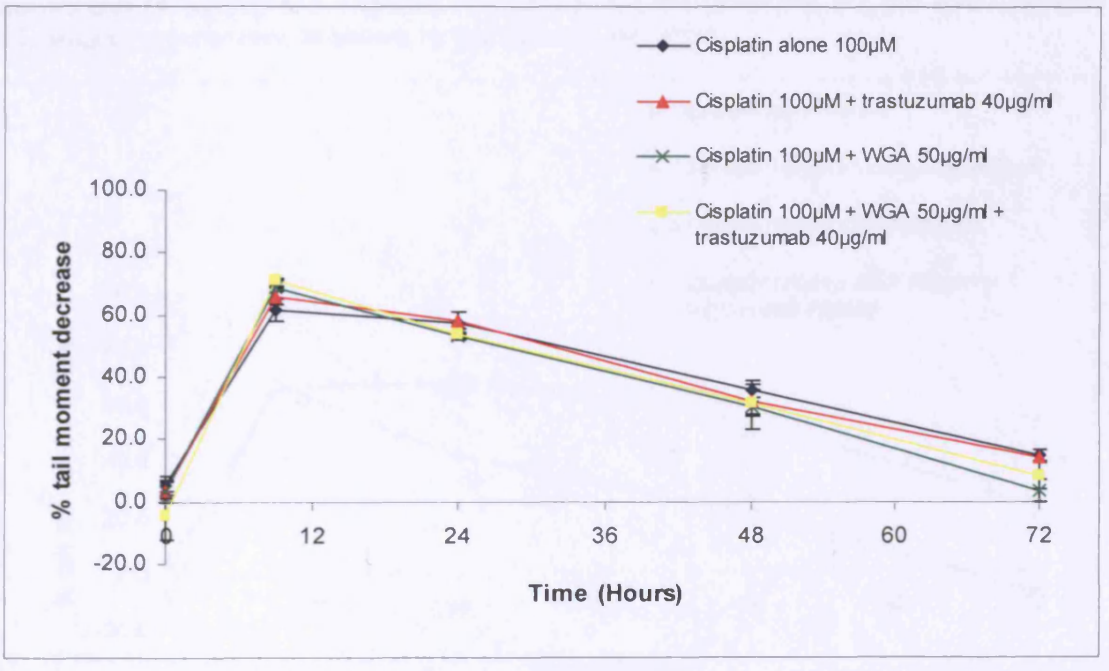

Figure 6.8 – Cisplatin-induced DNA interstrand crosslinks in MDA-MB-468 wild type cells. Cells were treated with cisplatin alone (100μM) for one hour followed by incubation in drug free media (♦), cisplatin (100μM) with trastuzumab (40μg/ml) for one hour followed by incubation in media containing trastuzumab alone (▲), WGA (50μg/ml) for 30 minutes followed by cisplatin (100μM) with WGA for 1 hour then incubated in drug free media (×), or WGA (50μg/ml) and trastuzumab (40μg/ml) for 30 minutes then cisplatin (100μM) was added for 1 hour and cells were incubated in media containing trastuzumab alone (■). Data presented are the result of three independent experiments, as shown by the standard deviation.

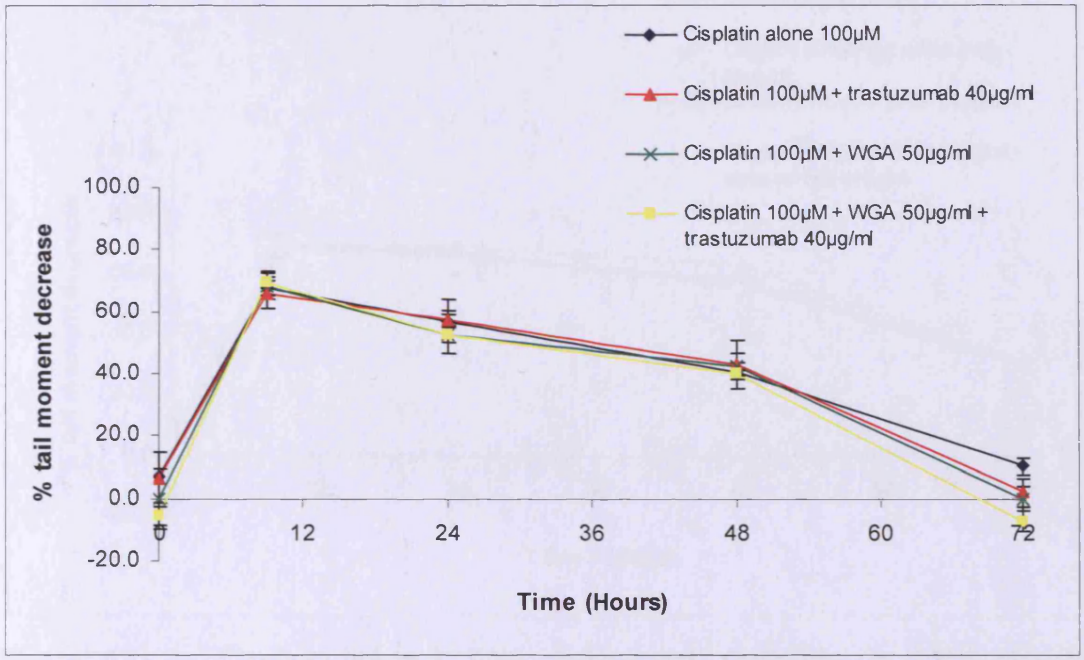

Figure 6.9 – Cisplatin-induced DNA interstrand crosslinks in MDA-MB-468 pEGFP-N1 vector control cells. Cells were treated as MDA-MB-468 wild type cells. Cells were treated as MDA-MB-468 wild type cells: with cisplatin alone (100µM) (♦), cisplatin (100µM) with trastuzumab (40µg/ml) (▲), WGA (50µg/ml) and cisplatin (100µM) (×) or WGA (50µg/ml), trastuzumab (40µg/ml) and cisplatin (100µM) (■). Data presented are the result of three independent experiments, as shown by the standard deviation.

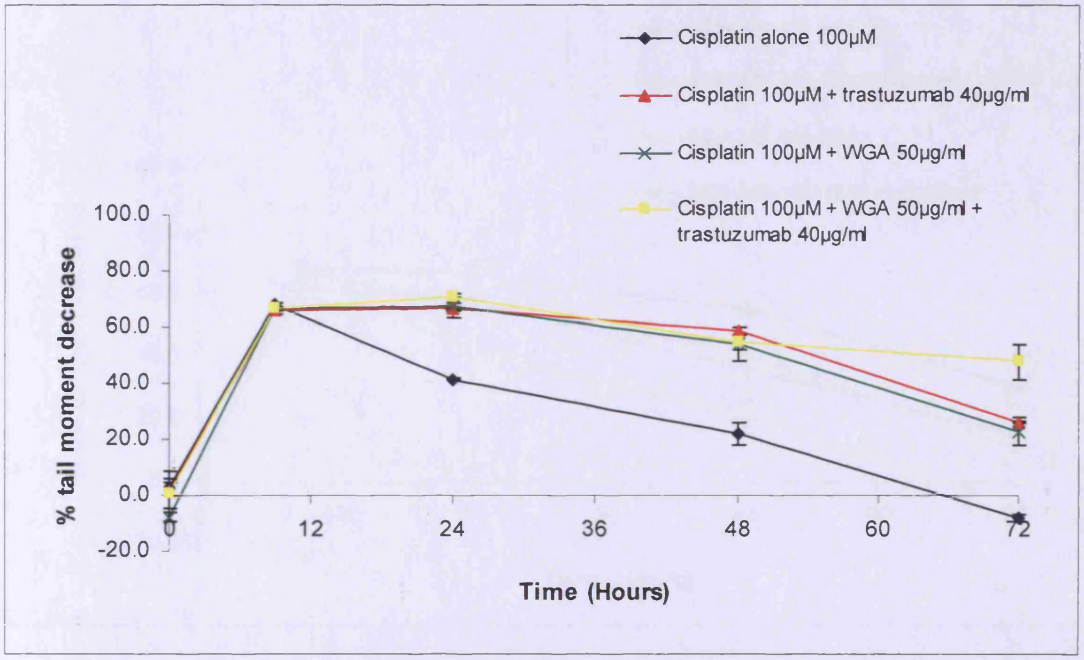

Figure 6.10 – Cisplatin-induced DNA interstrand crosslinks in MDA-MB-468 ErbB2 cells. Cells were treated as MDA-MB-468 wild type cells. Cells were treated as MDA-MB-468 wild type cells: with cisplatin alone (100µM) (♦), cisplatin (100µM) with trastuzumab (40µg/ml) (▲), WGA (50µg/ml) and cisplatin (100µM) (×) or WGA (50µg/ml), trastuzumab (40µg/ml) and cisplatin (100µM) (■). Data presented are the result of three independent experiments, as shown by the standard deviation.

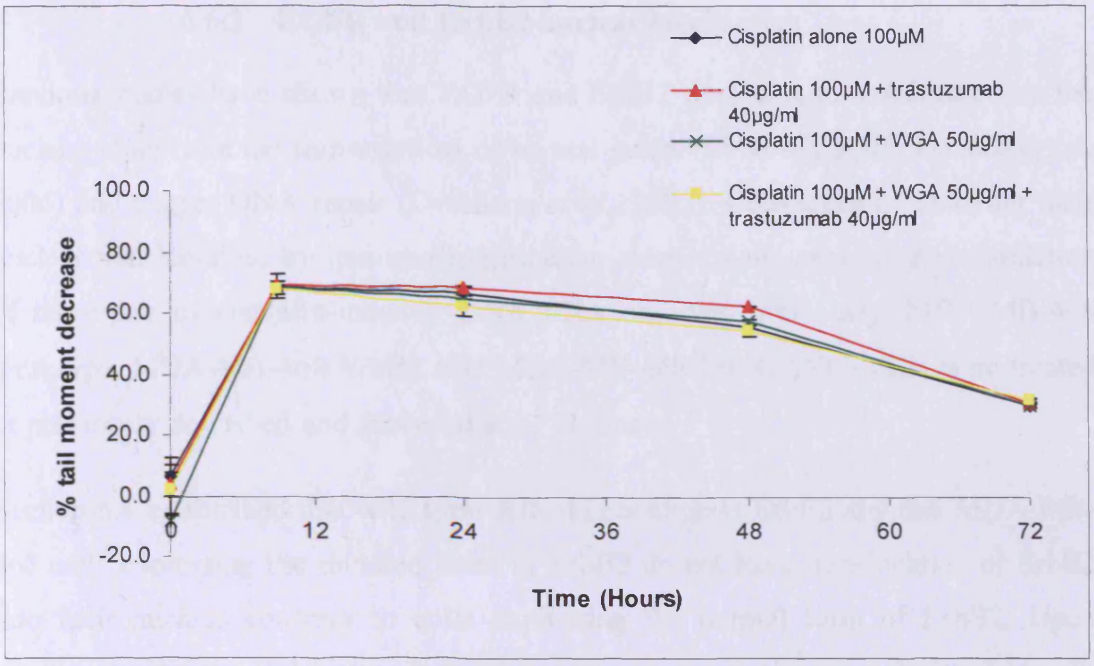

Figure 6.11 – Cisplatin-induced DNA interstrand crosslinks in MDA-MB-468 ErbB2ΔNLS cells. Cells were treated as MDA-MB-468 wild type cells. Cells were treated as MDA-MB-468 wild type cells: with cisplatin alone (100µM) (♦), cisplatin (100µM) with trastuzumab (40µg/ml) (▲), WGA (50µg/ml) and cisplatin (100µM) (×) or WGA (50µg/ml), trastuzumab (40µg/ml) and cisplatin (100µM) (■). Data presented are the result of three independent experiments, as shown by the standard deviation.

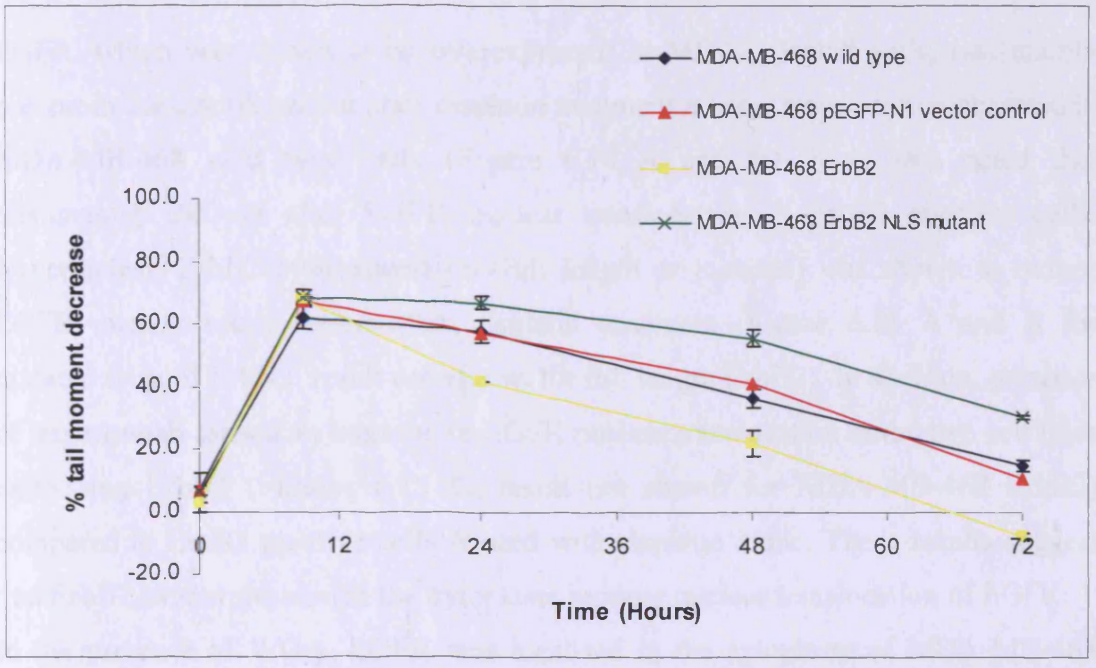

Figure 6.12 – Cisplatin-induced DNA interstrand crosslinks in MDA-MB-468 cells treated with cisplatin. MDA-MB-468 wild type (♦), vector control (▲), ErbB2 (■) and ErbB2ΔNLS (×) cells were treated cisplatin alone (100µM) for one hour then incubated in drug-free media. Data presented are the result of three independent experiments, as shown by the standard deviation.

6.6.2 EGFR and ErbB2 nuclear localisation

Previous studies have shown that EGFR and ErbB2 were able to translocate into the nucleus to activate the transcription of several genes (Lo *et al.*, 2005; Hanada *et al.*, 2006) and trigger DNA repair (Dittmann *et al.*, 2005). Consequently, studying their nuclear translocation, by immunofluorescence, may explain some of the modulation of the repair of cisplatin-induced DNA ICLs observed previously. MDA-MB-468 wild type, MDA-MB-468 ErbB2 and MDA-MB-468 ErbB2ΔNLS cells were treated as previously described and analysed after 24 hours.

Section 6.4 established that wild type cells do not express ErbB2 and that MDA-MB-468 cells expressing the mutated form of ErbB2 do not have translocation of ErbB2 into their nucleus contrary to cells expressing the normal form of ErbB2. Upon cisplatin treatment, an increase in ErbB2 nuclear translocation was observed in cells transfected with full length ErbB2 (Figure 6.13 B). However, in the presence of trastuzumab ErbB2 present in the cytoplasm and the nucleus was reduced (Figure 6.13 C). WGA in combination with cisplatin caused a complete inhibition of ErbB2 nuclear translocation (Figure 6.13 D and E).

EGFR, which was shown to be overexpressed in MDA-MB-468 cells, was mainly present in the cytoplasm but after cisplatin treatment nuclear translocation occurred in MDA-MB-468 wild type cells (Figure 6.14 A and B). It is also noted that trastuzumab did not alter EGFR nuclear translocation in ErbB2 negative cells. Nevertheless, ErbB2 overexpression (full length or mutated) was shown to reduce EGFR nuclear translocation after cisplatin treatment (Figure 6.15 A and B for mutated form of ErbB2, result not shown for full length ErbB2). In addition, presence of trastuzumab caused an increase in EGFR nuclear translocation in the two cell lines expressing ErbB2 (Figures 6.15 C, result not shown for MDA-MB-468 ErbB2) compared to ErbB2 positive cells treated with cisplatin alone. These results suggest that ErbB2 overexpression in the cytoplasm reduces nuclear translocation of EGFR.
In the presence of WGA, EGFR was localised in the cytoplasm of MDA-MB-468 ErbB2 cells (result not shown) and MDA-MB-468 ErbB2ΔNLS cells (Figure 6.15 D and E). Nevertheless, in MDA-MB-468 wild type cells (Figure 6.14 D and E), after 24 hours, some EGFR was seen re-entering into the nucleus.

Therefore, these results demonstrate that, by overexpressing ErbB2 (full length or with a deletion of the NLSs) in MDA-MB-468 cells, EGFR nuclear translocation is limited, possibly caused by the formation of ErbB2-EGFR heterodimers.

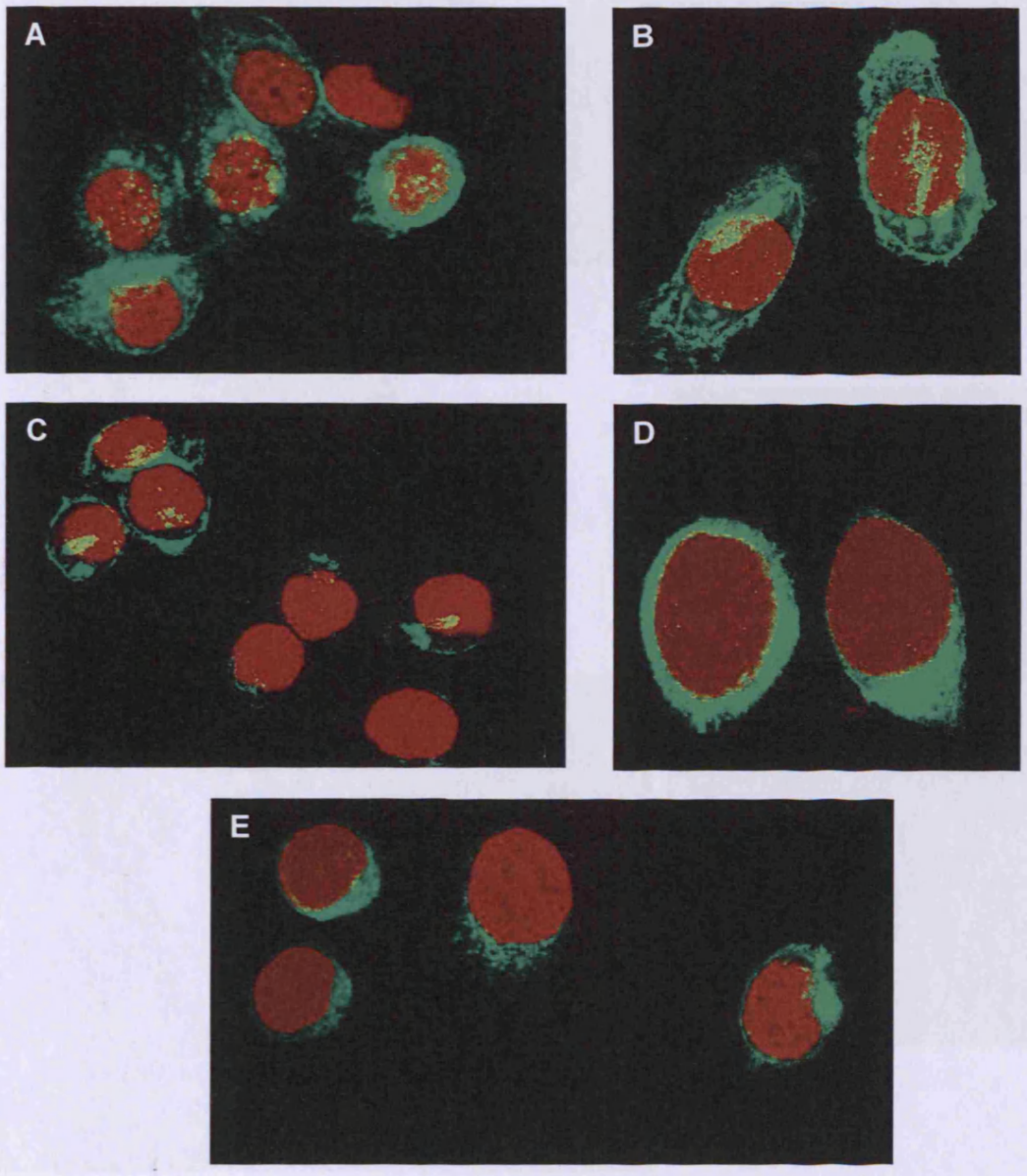

Figure 6.13 – ErbB2 immunofluorescence of MDA-MB-468 ErbB2. ErbB2 was measured in untreated cells (**A**), cells treated with cisplatin alone 100μM (**B**), cisplatin 100μM and trastuzumab 40μg/ml (**C**), cisplatin 100μM and WGA 50μg/ml (**D**), cisplatin 100μM, WGA 50μg/ml and trastuzumab 40μg/ml (**E**). Cells were analysed 24 hours post-treatment.

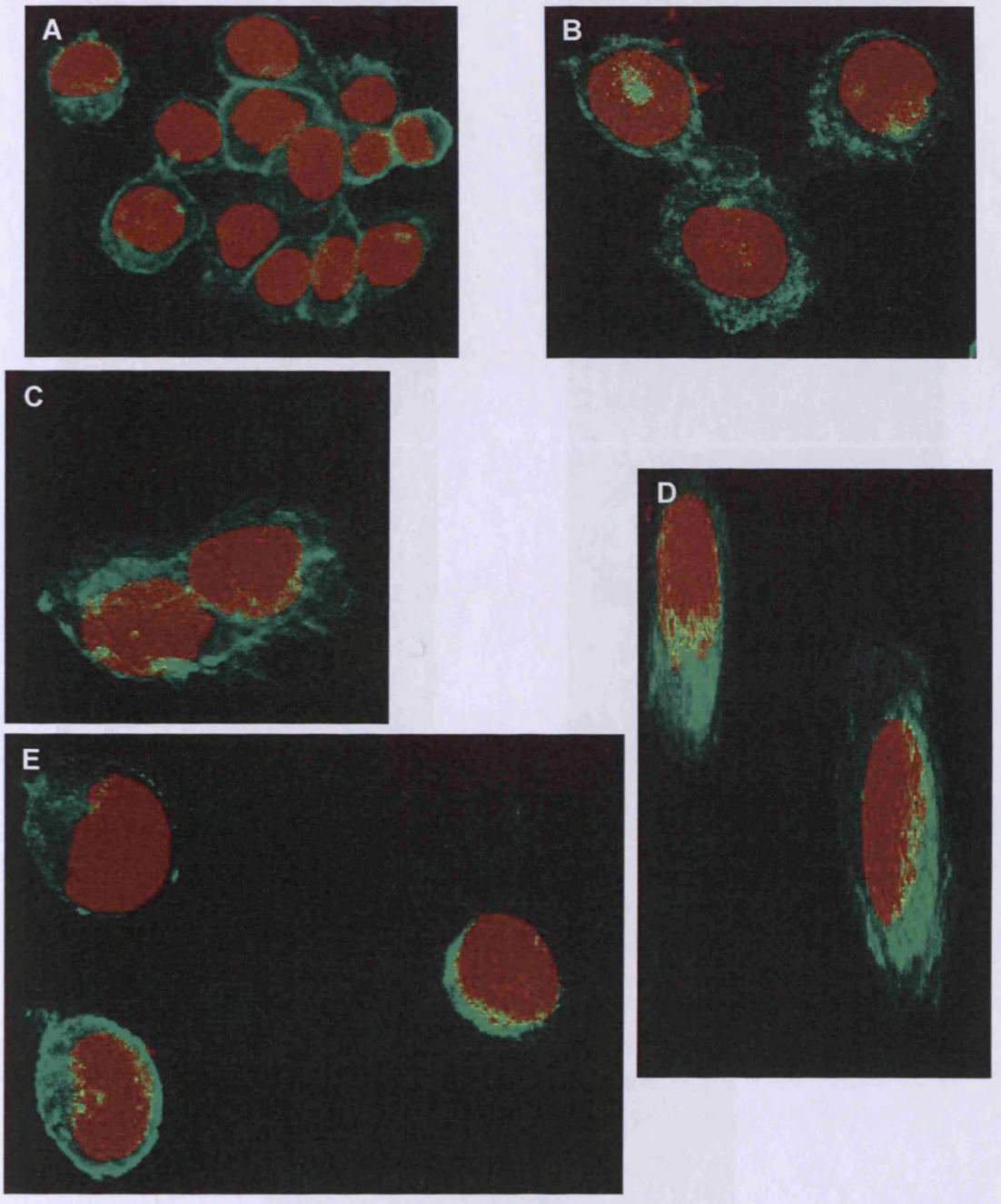

Figure 6.14 – EGFR immunofluorescence of MDA-MB-468 wild type cells. EGFR was measured in untreated cells (**A**), cells treated with cisplatin alone 100μM (**B**), cisplatin 100μM and trastuzumab 40μg/ml (**C**), cisplatin 100μM and WGA 50μg/ml (**D**), cisplatin 100μM, WGA 50μg/ml and trastuzumab 40μg/ml (**E**). Cells were analysed 24 hours post-treatment.

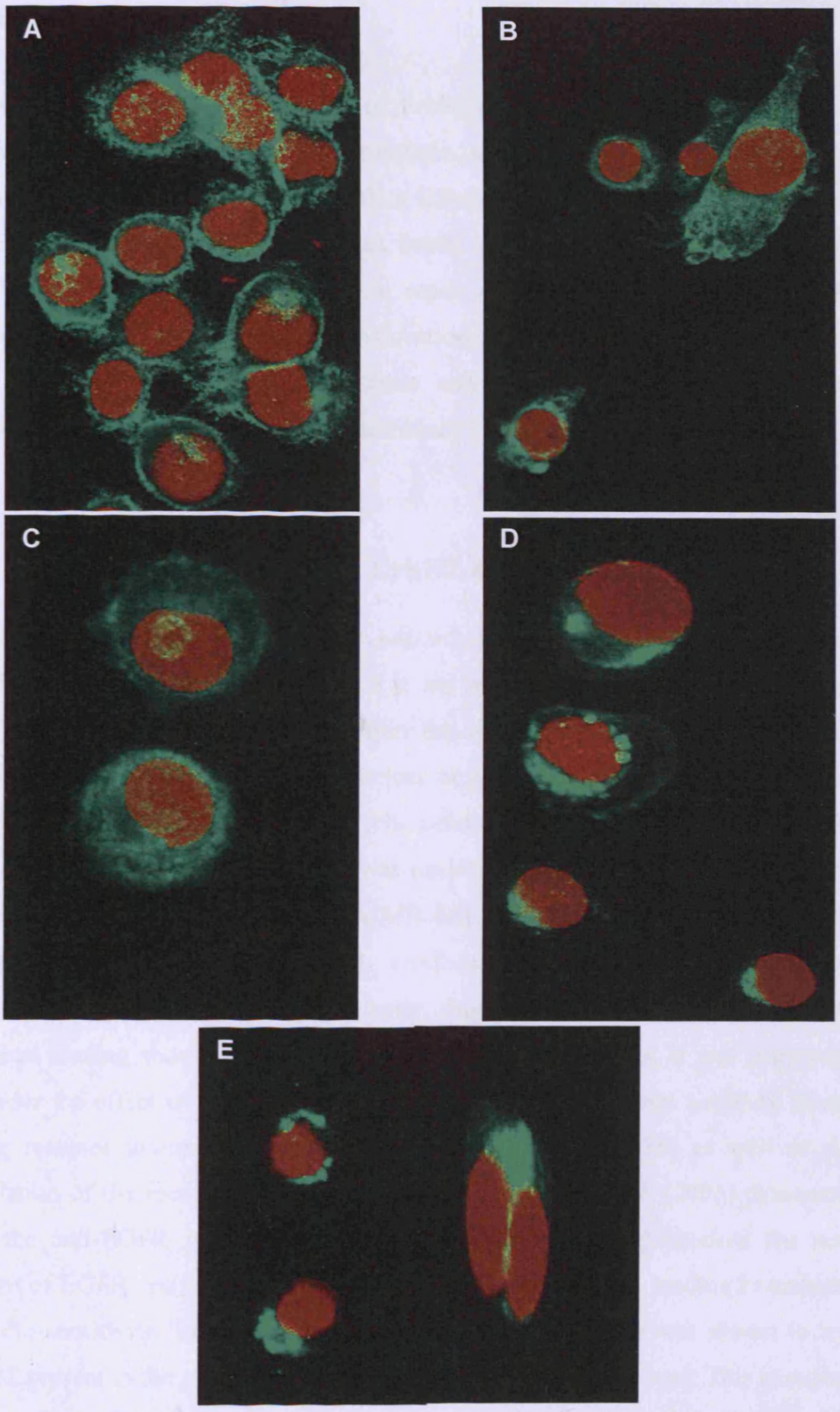

Figure 6.15 – EGFR immunofluorescence of MDA-MB-468 ErbB2ΔNLS cells. EGFR was measured in untreated cells (**A**), cells treated with cisplatin alone 100μM (**B**), cisplatin 100μM and trastuzumab 40μg/ml (**C**), cisplatin 100μM and WGA 50μg/ml (**D**), cisplatin 100μM, WGA 50μg/ml and trastuzumab 40μg/ml (**E**). Cells were analysed 24 hours post-treatment.

DISCUSSION

These results demonstrate the role of ErbB2 nuclear localisation in the repair of cisplatin-induced DNA interstrand crosslinks, using MDA-MB-468 cells transfected with a plasmid encoding ErbB2 with a deletion of the nuclear localisation signal sequence. Results have confirmed that ErbB2 overexpression caused an increase in cisplatin resistance and an increase in repair efficiency of cisplatin-induced DNA ICLs. However, blocking ErbB2 translocation to the nucleus increased significantly the sensitivity of the cells to cisplatin and delays DNA ICLs repair. Finally, overexpression of ErbB2 was shown to reduce EGFR nuclear translocation.

6.7 Trastuzumab and ErbB2 nuclear translocation

Although ErbB2 nuclear translocation has only recently been investigated (Giri *et al.*, 2005), nuclear ErbB2 has been shown to act as a transcriptional activator (Wang *et al.*, 2004). Nevertheless, its role within the nucleus has not yet been extensively studied and potential unidentified nuclear targets may exist. Based on the nuclear function of EGFR during DNA repair, the potential role of nuclear ErbB2 in cisplatin-induced DNA interstrand crosslinks was investigated. Similarly to Giri *et al.* (2005), expression of nuclear ErbB2 in MDA-MB-468 ErbB2ΔNLS cells was not visible, as shown by western blotting and confocal microscopy. Furthermore, cells overexpressing full length ErbB2 clearly showed that ErbB2 was present in the nucleus. Having shown that ErbB2 was present in the nucleus, it was interesting to consider the effect of trastuzumab as an anti-ErbB2 monoclonal antibody shown to cause receptor internalisation and degradation (Yarden, 2001b) as well as down-regulation of the receptor (Guan *et al.*, 2005). Dittmann *et al.* (2005) demonstrated that the anti-EGFR monoclonal antibody C225 (Cetuximab) blocked the nuclear import of EGFR and radiation-induced activation of DNA-PK, leading to an increase in radio-sensitivity. In the results presented here, trastuzumab was shown to reduce ErbB2 present in the cytoplasmic membrane but also in the nucleus. This is explained by the effect of trastuzumab causing degradation of the receptor, thus limiting ErbB2 nuclear translocation and reducing nuclear ErbB2. Furthermore, although trastuzumab was previously shown to reduce cell proliferation of ErbB2 overexpressing cells, such

as MDA-MB-453 or SK-BR-3 cells, no effect was observed on cells overexpressing ErbB2 and ErbB2ΔNLS. A study by Gong *et al.* (2004) also reported the absence of growth inhibition by trastuzumab alone in ErbB2 overexpressing gastric cancer cells. In this study, they demonstrated that this phenomenon did not affect the ability of trastuzumab to increase the cytotoxicity of chemotherapeutic drugs when used in combination.

6.8 Cisplatin sensitivity

Unpublished data obtained in our laboratory demonstrated that radiation treatment caused EGFR nuclear translocation which was blocked upon gefitinib and cetuximab treatment. In addition, Dittmann *et al.* (2005) established that inhibition of EGFR nuclear translocation caused inhibition of DNA repair and increased radiosensitivity of cells. In this study, full length ErbB2 overexpression was confirmed to cause increased cellular resistance to cisplatin. However, cells overexpressing ErbB2ΔNLS showed increased sensitivity to cisplatin compared to cells overexpressing ErbB2. Therefore, trastuzumab causing a reduction in membrane bound ErbB2 protein level and ErbB2 nuclear translocation explains the increase in sensitivity to cisplatin, caused by trastuzumab, previously described. These data taken together reinforce the idea that nuclear ErbB2 plays a role in DNA repair processes. Furthermore, overexpressing ErbB2ΔNLS also caused in increase in sensitivity to cisplatin compared to ErbB2 negative cells. This suggests that deletion of the ErbB2 nuclear localisation signal sequence inhibited the effect of ErbB2 and also altered the normal response to cisplatin-induced DNA damage present in ErbB2 negative cell line. In the same way, Aifa *et al.* (2005) demonstrated that the tripartite NLS sequence was required for EGFR receptor dimerisation and phosphorylation. However, Giri *et al.* (2005) demonstrated that deletion of the ErbB2 tripartite NLS did not affect its membrane localisation and its ability to activate MAPK signalling pathway. Consequently, these results taken together demonstrate that ErbB2 nuclear translocation plays an important role in the response to cisplatin-induced DNA damage and that deletion of the nuclear localisation signal sequence causes a sensitisation of the cells to chemotherapeutic drugs, such as cisplatin.

6.9 Modulation of DNA damage repair

So far, there has been little study of the implication of a nuclear ErbB family member during DNA repair processes. Studies by Dittmann *et al.* (2005) and Friedmann *et al.* (2006) have demonstrated the implication of EGFR nuclear translocation and its association with the DNA repair protein, DNA-PK. Therefore, having shown that overexpression of full length ErbB2 increased dramatically the repair efficiency of cisplatin-induced DNA ICLs, in the previous chapter, the importance of nuclear ErbB2 remained to be determined. Deletion of the ErbB2 NLSs resulted in a significant inhibition of the repair of cisplatin-induced DNA ICLs compared to cells overexpressing full length ErbB2. This result was confirmed using WGA in cells overexpressing full length ErbB2. Indeed, wheat germ agglutinin which caused inhibition of ErbB2 nuclear translocation, also resulted in a delay in the repair of cisplatin-induced DNA interstrand crosslinks, compared to cells treated with cisplatin alone. In addition, a similar delay in DNA repair was obtained with trastuzumab, suggesting that trastuzumab causes a delay in DNA damage repair through reduction of nuclear ErbB2. These results indicate that nuclear ErbB2 has role in DNA repair processes. Furthermore, the novel link between ErbB2 and DNA repair may partly explains the association between ErbB2 overexpression and chemoresistance (Benz *et al.*, 1992; Allred *et al.*, 1992; Wright *et al.*, 1992). Moreover, inhibition of ErbB2 nuclear translocation, by WGA or deletion of ErbB2 NLSs, did not restore the kinetics of repair of cisplatin-induced DNA ICLs observed in ErbB2 negative cells. In fact, inhibition of ErbB2 nuclear translocation led to a large decrease in DNA repair efficiency compared to the wild type cells.

Having shown, by immunofluorescence, that overexpression of ErbB2 caused a reduction in EGFR nuclear translocation, it is possible that overexpression of ErbB2 leads to a dimerisation of the two receptors causing an increase in DNA repair efficiency. Whereas overexpression of ErbB2ΔNLS inhibits the DNA repair function of nuclear ErbB2, it is suggested to form non-functional EGFR-ErbB2 heterodimers that sequester EGFR in the cytoplasmic membrane and are unable to trigger the DNA repair signalling cascade. Furthermore, deletion of the NLS may also lead to a disruption of the normal ErbB2 signalling cascade thereby further reducing the capacity of the cells to repair cisplatin-induced DNA ICLs. Similar results were

obtained using WGA in cells overexpressing full length ErbB2, since WGA also inhibits EGFR translocation and translocation of proteins involved in the DNA repair signalling cascades.

In this study, only EGFR was considered as it is overexpressed in MDA-MB-468 cells and its ability to translocate to the nucleus and activate DNA repair processes has already been shown (Dittmann *et al.*, 2005). Nevertheless, dimerisation with other ErbB family members needs to be considered.

A novel link between ErbB2 nuclear localisation and DNA repair has been established and it is suggested that ErbB2 overexpression affects EGFR nuclear localisation and deletion of ErbB2 NLSs alters the DNA repair signalling cascade.

6.10 Conclusion

This chapter confirmed that ErbB2 overexpression increased resistance to cisplatin and increased the repair efficiency of cisplatin-induced DNA ICLs. In addition, deletion of ErbB2 NLS inhibits ErbB2 nuclear translocation and was shown to increase cell sensitivity to cisplatin. Furthermore, ErbB2 nuclear translocation was shown to play an important role in the repair of cisplatin-induced DNA interstrand crosslinks. Finally, ErbB2 overexpression reduced EGFR nuclear translocation and it was suggested that deletion of the ErbB2 tripartite NLSs impairs DNA repair signalling cascade and EGFR functional activity.

Considering those results, it is reasonable to conclude that a novel function for nuclear ErbB2 has been established in the repair of cisplatin-induced DNA ICLs. It is also suggested that increase in sensitivity to chemotherapeutic drugs, caused by trastuzumab, was partially due to the reduction in nuclear ErbB2. However, potential targets for nuclear ErbB2 need to be identified in order to establish a molecular mechanism for the modulation of DNA repair. In addition, further investigation is required to determine the effects of NLSs deletion on ErbB2 and EGFR dimerisation and the proteins involved in the DNA repair signalling cascade.

Chapter 7

Effect of the modulation of BRCA1 expression on cellular response to chemotherapeutic agents

INTRODUCTION

In the previous chapters, the importance of ErbB2 in the repair of drug-induced DNA damage has been demonstrated in breast cancer cells. BRCA1 is another important protein in breast cancer, since loss-of-function mutations have been reported to cause an 82% risk of developing breast cancer and a 54% risk to develop ovarian cancer. However, germline mutations in BRCA1 account for only 5% of breast and ovarian cancers (King *et al.*, 2003).

Furthermore, several studies have shown that BRCA1 is involved in fundamental processes such as DNA repair (homologous recombination), cell cycle checkpoint and transcription (Venkitaraman, 2002; Yoshida and Miki, 2004; Turner *et al.*, 2005). Thus, it is an important protein for the maintenance of genomic integrity (Powell and Kachnic, 2003). A study by Wang *et al.* (2000b) also reported that BRCA1 was associated with a large number of proteins, named the BRCA1-associated genome super-complex (or BASC super-complex), which plays an important role in DNA damage recognition and repair, conferring BRCA1 with an important biological role within the cell.

7.1 BRCA1 and chemotherapeutic response

Chemotherapeutic drugs commonly used in breast and ovarian cancer cause DNA double strand breaks either directly or indirectly (Kennedy *et al.*, 2004). BRCA1 is a protein involved in DNA damage repair through association with proteins involved in DNA double strand break repair by homologous recombination and non homologous end-joining (Scully *et al.*, 1997c; Zhong *et al.*, 1999). In addition, Wang *et al.* (2000b) reported that BRCA1 was associated with the BASC super-complex formed of proteins involved in nucleotide excision repair (NER), which can be sub-divided into transcription-coupled repair and genomic repair pathways.

Therefore, BRCA1 has a critical role in promoting cell survival and preventing apoptosis after DNA damage (Bernstein *et al.*, 2002; MacLachlan *et al.*, 2002). As shown by Tassone *et al.* (2003) BRCA1 expression is critical in the response to chemotherapeutic treatment and can modulate the chemosensitivity of cells.

Consequently, BRCA1 can be used as a useful predictive marker for the response to chemotherapeutic treatment. Nevertheless, in addition to its role in DNA repair pathways and cell cycle regulation, the importance of BRCA1 in the response to DNA damaging agents has also been shown to be due to its association with Fanconi anemia proteins. Indeed, Folias *et al.* (2002) reported that BRCA1 associated with different Fanconi anemia proteins in order to detect the arrest of the replication fork after DNA damage and was implicated in the repair of DNA crosslinks through homologous recombination (Pichierri and Rosselli, 2004; Howlett *et al.*, 2002; Tutt *et al.*, 2001). Furthermore, Taniguchi *et al.* (2003) demonstrated that disruption of the Fanconi anemia-BRCA pathway, through reduced expression of the Fanconi anemia F protein, led to an increase in sensitivity to cisplatin in ovarian cancer. Therefore, BRCA1 is an important protein participating in genome integrity *via* regulation of cell cycle checkpoint and DNA damage repair.

7.2 Mutations and loss of BRCA1 function

7.2.1 BRCA1 expression and chemotherapy

The loss of BRCA1 function has been associated with increased sensitivity to DNA-damaging agents (Kennedy *et al.*, 2004), such as cisplatin (Bhattacharyya *et al.*, 2000), and mitomycin C (Moynahan *et al.*, 2001). Tassone *et al.* (2003) demonstrated that inhibition of BRCA1 expression led to an increase in chemosensitivity following cisplatin-induced DNA damage, similarly to the studies by Lafarge *et al.* (2001) and Husain *et al.* (1998). However, they also showed that BRCA1 expression caused an increased sensitivity to doxorubicin and paclitaxel. Nevertheless, conflicting results exist as Brodie *et al.* (2001) demonstrated that BRCA1 inactivation led to an increased sensitivity to doxorubicin.

Furthermore, Quinn *et al.* (2003) established that BRCA1 is a modulator of apoptosis according to the nature of the damaging agent. They showed that absence of BRCA1 increased the resistance to some spindle poisons, paclitaxel and vinorelbine, and increased sensitivity to agents causing double strand breaks such as etoposide, indicating that BRCA1 functions as a differential regulator of chemotherapy-induced

apoptosis. Therefore, the nature of the agent used in the treatment of breast cancer will need to be considered according to the BRCA1 expression status.

7.3.2 BRCA1 expression and radiotherapy

Several studies have also investigated the effect of BRCA1 mutations on DNA double strand breaks caused by ionizing radiation. Conflicting results have been obtained on the importance of BRCA1 in ionising radiation-induced DNA strand break repair. Indeed, Scully *et al.* (1999) demonstrated that wild type BRCA1 reduced sensitivity to ionizing radiation and increased the efficiency of double strand break repair, compared to BRCA1-/- cells. Conversely, Wang *et al.* (2001) reported that BRCA1 did not play a role in the rejoining of DNA double strand breaks induced by ionising radiation. They demonstrated that cells with a mutant BRCA1 status were able to repair radiation-induced DNA double strand breaks, through the DNA-PK-dependent non homologous end joining pathway, as efficiently as the cells expressing wild type BRCA1. Therefore, the role of BRCA1 in radiation-induced DNA double strand breaks repair remains unclear.

7.3 BRCA1 and topoisomerase II activity

In addition to its role in DNA damage repair described previously, BRCA1 has also been shown to maintain chromosome integrity through its involvement in DNA decatenation. Deming *et al.* (2001) established that BRCA1 was involved in the decatenation G2 checkpoint. Furthermore, Lou *et al.* (2005) have recently demonstrated that BRCA1 deficient cells had a defect in DNA decatenation and chromosome segregation. In addition, they showed that BRCA1 co-localised with topoisomerase IIα in the S phase and that BRCA1 deficient cells had a lower decatenation activity. Therefore, these findings establish a further role for BRCA1 and reinforce its role in the maintenance of chromosome integrity.

7.4 Aims

This chapter will discuss the effect of modulation of BRCA1 expression on DNA damage repair, using MCF-7, a breast cancer cell line, transfected with a plasmid encoding specific human BRCA1 siRNA. Moreover, similarly to the study by Friedmann *et al.* (2004) which demonstrated that inhibition of EGFR tyrosine kinase activity sensitised MCF-7 cells to cisplatin, the effect of BRCA1 down-regulation will be investigated. To this end, the following question will be addressed:

- Does BRCA1 expression modulate sensitivity to gefitinib and chemotherapeutic agents?
- Does BRCA1 down-regulation enhance the effect of gefitinib and cisplatin in combination?
- Does BRCA1 expression modulate radiosensitivity?
- Is topoisomerase II activity affected by BRCA1 down-regulation?

RESULTS

7.5 Modulation of BRCA1 mRNA level

Using the MCF-7 cell line, stably transfected with a plasmid encoding specific human BRCA1 siRNA, modulation of BRCA1 was studied. Three breast cancer cell lines were kindly provided by Prof. A. Ashworth and Dr. C Lord (Institute of Cancer Research): MCF-7 wild type, MCF-7 scrambled (MCF-7 transfected with a vector encoding a scrambled siRNA sequence) and MCF-7 3.23 (MCF-7 transfected with a plasmid encoding human specific BRCA1 siRNA) cells. The level of BRCA1 mRNA was measured by RT-PCR and real time PCR for quantification.

7.5.1 Determination of BRCA1 mRNA level by RT-PCR

BRCA1 mRNA level was evaluated in MCF-7 wild type, MCF-7 scrambled and MCF-7 3.23 cells using reverse transcriptase PCR, in order to demonstrate the efficacy of the siRNA. Figure 7.1 shows a large reduction of BRCA1 mRNA level in the BRCA1 siRNA transfected cell line compared to the wild type and the scrambled cell line. The level of BRCA1 mRNA in the scrambled cell line was also slightly reduced. However, standard reverse transcription PCR only detected the amount of final amplified product at the end of the reaction and was not appropriate for accurate quantification. Real time PCR is a more specific and sensitive technique as it quantifies the initial amount of the template and monitors the progress of the PCR as it occurs. Therefore, this technique was required to quantify the level of BRCA1 mRNA.

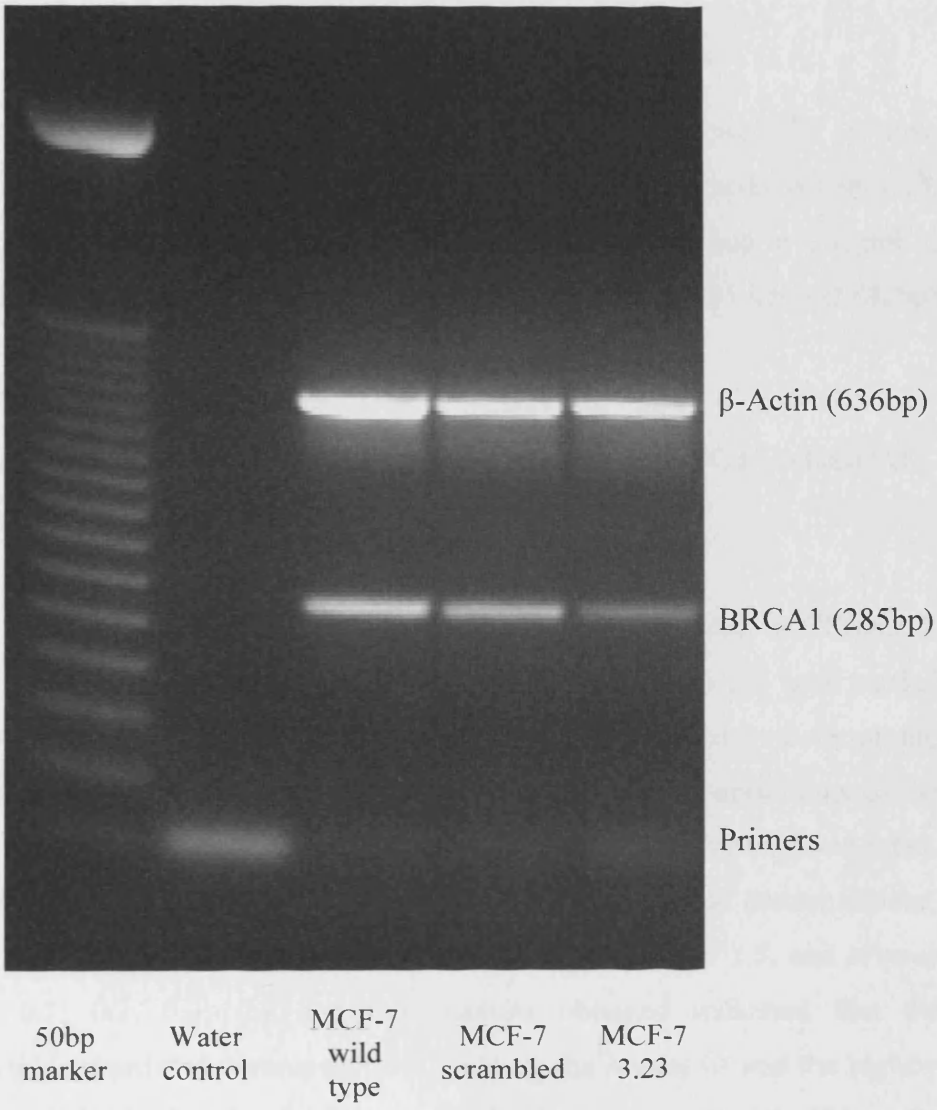

Figure 7.1 – Reverse Transcriptase PCR analysis of MCF-7 wild type, MCF-7 scrambled and MCF-7 3.23 cells. β-actin was used as an internal control.

7.5.2 Quantification of BRCA1 mRNA level

Having determined that BRCA1 mRNA was reduced in MCF-7 3.23 cell line, the reduction of mRNA was quantified by real time PCR. However, prior to analysis PCR conditions were optimised.

Optimisation of the real time PCR conditions

Primers sequences provided by Fiona Li (CRUK) were analysed by reverse transcriptase PCR to confirm that the correct product was formed (result not shown). PCR products were also checked by sequencing analysis, as explained in Chapter 2, section 2.9.1. Each PCR product sequenced matched the sequence of interest (81bp) detailed below (forward primer in red and reverse primer in blue):

5'-**CAGAGGACAATGGCTTCCATGCAATTGGGCAGATGTGTGAGGCAC CTGTGGTGACCCGAGAGTGGGTGTTGGACAGTGTAG**-3'

Subsequently, real time PCR conditions were optimised (as indicated in Chapter 2, section 2.9) to obtain accurate and reliable results. All optimisation steps were carried out using cDNA from MCF-7 wild type. Optimisation was achieved by determining the primer limiting concentration, the probe concentration and the conditions of the PCR (internal control and BRCA1 reactions run in the same tube or separate tube). The primer limiting concentration was defined by using a range of concentrations, which were as follow: forward primer (μM): 0.5; 0.7; 0.9; 1.1 and 1.5, and reverse primer (μM): 0.1; 0.2; 0.3; 0.4 and 0.5. Results obtained indicated that the concentrations of forward and reverse primers yielding the lowest Ct and the highest ΔRn values were 0.9μM of forward primer and 0.3μM of reverse primer. The probe concentration used was 200nM and was determined using the same criteria (low Ct and high ΔRn). Finally, β-glucuronidase (internal control) and BRCA1 primer sets were shown to be detected in a multiplex reaction without causing interference as the difference in efficiency between the standard curves was small and correlation coefficients were high (above 0.95).

Quantification of BRCA1 mRNA level

Using the PCR conditions defined previously, results obtained for BRCA1 mRNA levels are presented in Table 7.1 and Figure 7.2 (each cell line was compared to the wild type set at a value of 100%). Efficiencies obtained for the standard curve were 2.29 for BRCA1 and 2.16 for β-glucuronidase. Compared to the MCF-7 wild type cells, the level of BRCA1 in MCF-7 3.23 cells was reduced by 77%, nevertheless the scrambled cell line BRCA1 mRNA level was also reduced by 28%. Therefore, the real reduction in BRCA1 mRNA level compared to MCF-7 scrambled cells was 68%.

Samples	Ct_{BRCA1}	$Ct_{\beta\text{-glucuronidase}}$	ΔCt_{BRCA1}	$\Delta Ct_{\beta\text{-glucuronidase}}$	R
MCF-7 wild type	24.69	23.17	0.00	0.00	1.00
MCF-7 wild type	24.94	22.85			
MCF-7 wild type	24.97	23.05			
Average	**24.87**	**23.02**			
MCF-7 scrambled	25.56	23.34	-0.72	-0.36	0.72
MCF-7 scrambled	25.83	23.54			
MCF-7 scrambled	25.38	23.26			
Average	**25.59**	**23.38**			
MCF-7 3.23	26.42	22.61	-1.56	0.22	0.23
MCF-7 3.23	26.54	23.22			
MCF-7 3.23	26.33	22.59			
Average	**26.43**	**22.81**			

Table 7.1 – Quantification of BRCA1 mRNA level in MCF-7 cell lines. R is the expression ratio for BRCA1 in each cell line compared to MCF-7 wild type cell line (set at a value of 100% or 1).

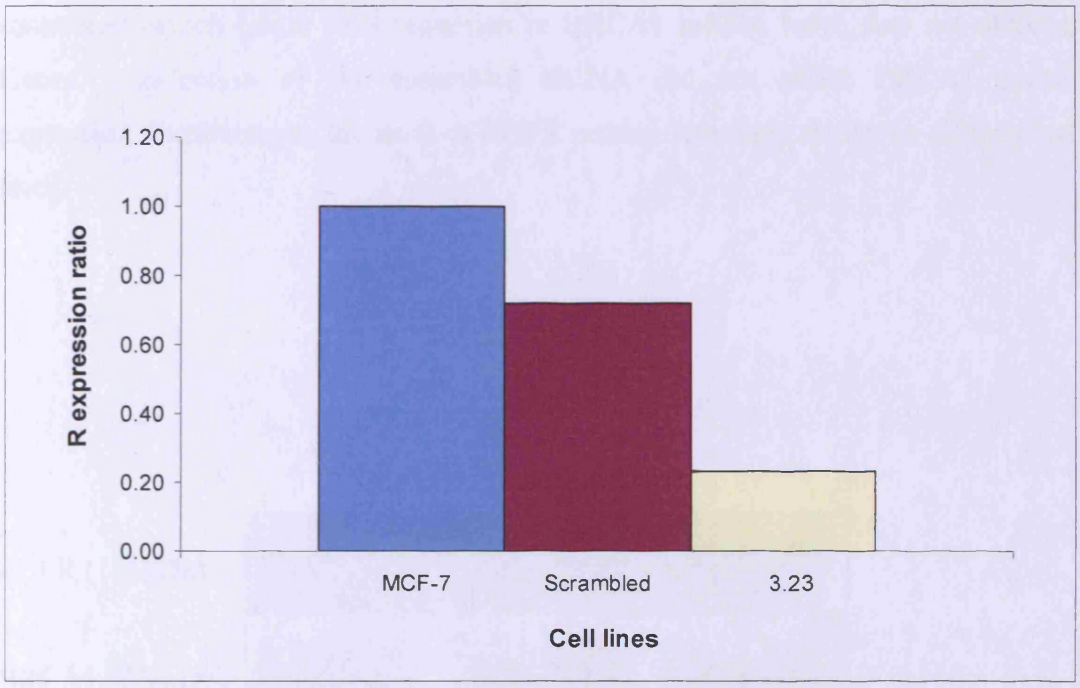

Figure 7.2 – BRCA1 mRNA level in MCF-7 cell lines. MCF-7 wild type was used as reference to determine the BRCA1 mRNA level in MCF-7 scrambled and MCF-7 3.23 cell lines.

7.6 Modulation of BRCA1 protein expression level

As the level of BRCA1 mRNA in MCF-7 3.23 was shown to be reduced by 68% compared to MCF-7 scrambled, BRCA1 protein expression level was detected by western blotting. Figure 7.3 indicates that the level of BRCA1 protein was reduced in the MCF-7 3.23 cell line. This result correlated with the results obtained by reverse transcriptase PCR and real time PCR. However, the BRCA1 protein level of MCF-7 scrambled, which had a 28% reduction in BRCA1 mRNA level, was not affected. Hence, transfection of the scrambled siRNA did not affect BRCA1 protein expression. Furthermore, the level of EGFR protein remained similar in all three cell lines.

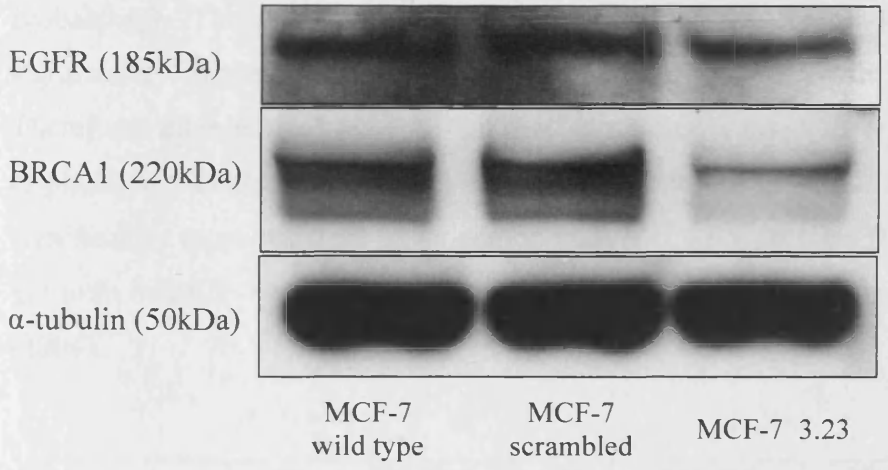

Figure 7.3 – EGFR and BRCA1 protein expression in MCF-7 cell lines. Protein levels were measured by immunoblotting in MCF-7 wild type, MCF-7 scrambled and MCF-7 3.23 cell lines. α-tubulin was used as internal control.

7.7 Effects of gefitinib and chemotherapeutic treatments

Having confirmed that the transfected MCF-7 (3.23) cell line had a reduced expression of BRCA1 protein, effects of gefitinib and common chemotherapeutic agents were investigated. Several studies having reported synergistic interactions between chemotherapeutic drugs and gefitinib (Ciardiello *et al.*, 2001; Sirotnak *et al.*, 2000), the effects of gefitinib, cisplatin, etoposide and melphalan were investigated as single agents, using the SRB assay.

7.7.1 IC_{50} for single agent treatments

For the single agent treatments, all drugs were incubated for 5 days with the cells, at a range of concentrations, in sextuplet wells. To assure accuracy and reproducibility, all sets of assays were repeated in triplicate. Results for the 50% growth inhibition (IC_{50}) are presented in Table 7.2 and Figure 7.4. IC_{50} obtained for MCF-7 scrambled and 3.23 were statistically compared to the IC_{50} for MCF-7 wild type, using the student *t*-test, with a degree of freedom of 4 and a significance level $p = 0.01$ (99% probability). The IC_{50} for cisplatin in MCF-7 3.23 (highlighted in red) was significantly higher than the IC_{50} obtained in MCF-7 with 99% confidence. Therefore, inhibition of BRCA1 protein expression caused increased resistance to cisplatin. It was also noted that with a 95% probability ($p = 0.05$) MCF-7 3.23 was significantly more resistant to etoposide than MCF-7 wild type. The IC_{50} found for gefitinib in MCF-7 wild type was similar to the one described by Friedmann *et al.* (2004).

Drug	IC_{50} in MCF-7 wild type	IC_{50} in MCF-7 scrambled	IC_{50} in MCF-7 3.23
Gefitinib	16.0 ± 2.4μM	10.0 ± 0.5μM	18.0 ± 1.0μM
Cisplatin	0.9 ± 0.1μM	1.2 ± 0.3μM	2.5 ± 0.6μM
Etoposide	1.1 ± 0.2μM	0.8 ± 0.1μM	2.1 ± 0.7μM
Melphalan	2.9 ± 1.5μM	2.5 ± 1.3μM	2.5 ± 1.5μM

Table 7.2 – IC_{50} (±SD) results for single agent treatments of MCF-7 cell lines. MCF-7 wild type, MCF-7 scrambled and MCF-7 BRCA1 cell lines were treated for 5 consecutive days with gefitinib, cisplatin, etoposide or melphalan. Data have been statistically analysed with the student *t*-test with n = 4 and $p = 0.01$, comparing IC_{50} of the wild type cell line with IC_{50} of the transfected cell lines.

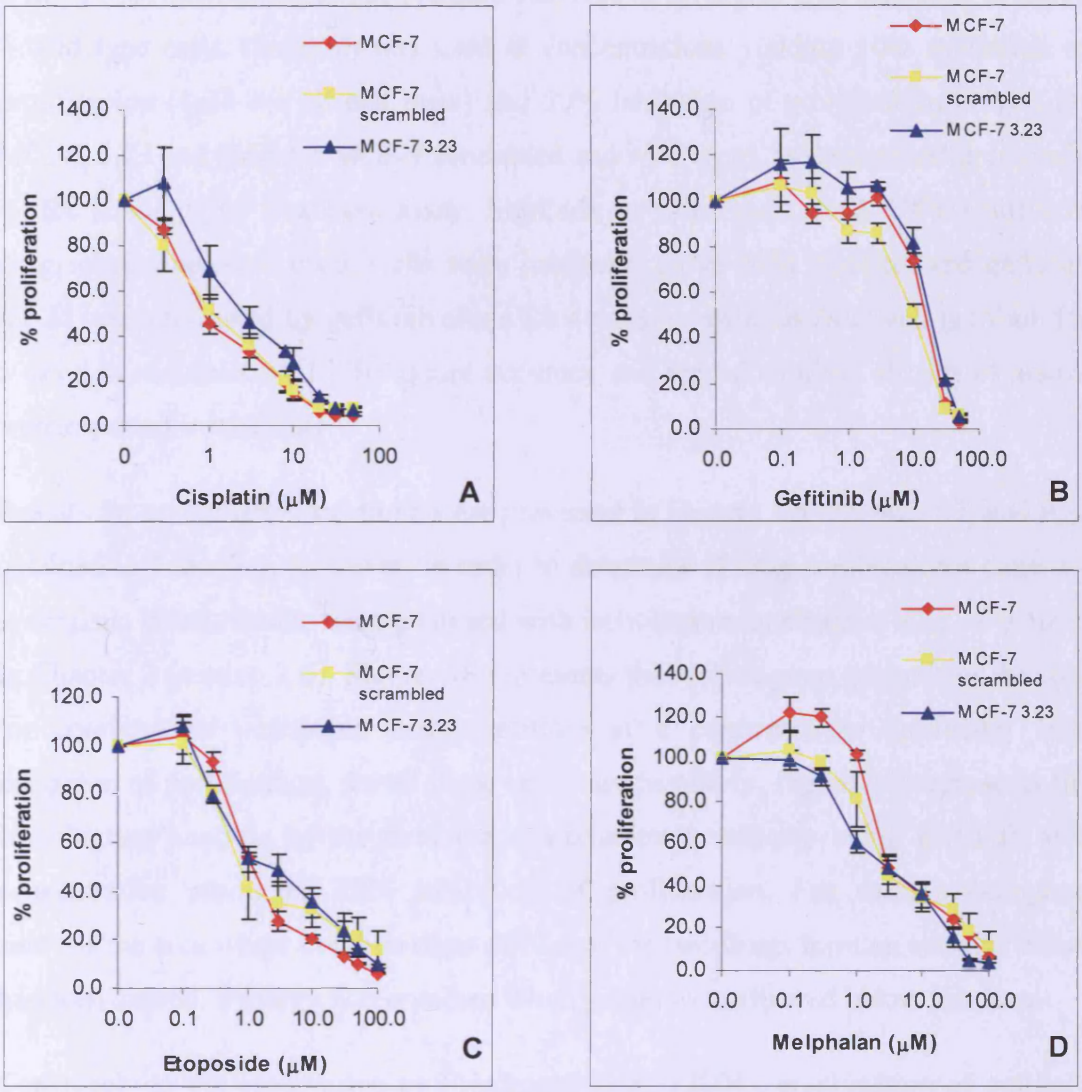

Figure 7.4 – Inhibition of MCF-7 cells proliferation by single agent treatment. MCF-7 wild type, MCF-7 scrambled and MCF-7 3.23 cell lines were treated with cisplatin (**A**), gefitinib (**B**), etoposide (**C**) or melphalan (**D**) for 5 consecutive days. Data presented are the result of three independent experiments, as shown by the standard deviation.

7.7.2 Combination of cisplatin with gefitinib

Cisplatin being the only drug to show a significant difference between MCF-7 wild type and 3.23, it was studied in combination with gefitinib. Furthermore, Friedmann *et al.* (2004) demonstrated that gefitinib was able to synergise with cisplatin, in MCF-7 wild type cells. Gefitinib was used at concentrations yielding 10% inhibition of proliferation (4μM for all cell lines) and 20% inhibition of proliferation (10μM for MCF-7 3.23 and 6μM for MCF-7 scrambled and wild type), as determined previously by the single agent treatment assay. Similarly to Friedmann *et al.* (2004) different drug scheduling were used. Cells were incubated either with cisplatin and gefitinib for 24 hours followed by gefitinib alone for 4 days, or with cisplatin and gefitinib for 5 days, in sextuplet wells. To assure accuracy and reproducibility, all sets of assays were repeated in triplicate.

Results for combination treatments are presented in Figures 7.5, 7.6 and 7.7, and IC_{50} obtained in Table 7.3. However, in order to determine if drug combinations caused a synergistic effect, results were analysed with isobologram analysis at IC_{50}, as defined in Chapter 2 (section 2.6). Figure 7.8 represents the isobologram analysis of the data for combination treatments using gefitinib at a concentration producing 10% inhibition of proliferation, for all three cell lines. Similarly, Figure 7.9 represents the isobologram analysis of the data for combination treatments using gefitinib at a concentration producing 20% inhibition of proliferation. For each isobologram analysis the area where combinations of IC_{50} of the two drugs have an additive effect has been circled. Synergy was obtained when points were situated below this area.

Conversely to the observation by Friedmann *et al.* (2004), combination of gefitinib with cisplatin, in MCF-7 wild type cells, did not produce a synergistic effect. Surprisingly, with MCF-7 scrambled a synergistic effect was obtained when cells were treated with a combination of cisplatin and gefitinib (10%) for 24 hours (Figure 7.8 B). Therefore, no conclusion can be drawn from this result since the wild type and the scrambled cell line gave different results. Nevertheless, when cells were treated for 5 consecutive days with cisplatin and gefitinib (20%) a synergistic effect was only observed in MCF-7 3.23 cell line (Figure 7.9 C). This effect was not seen in the two other cell lines with the same conditions.

Therefore, BRCA1 down-regulation sensitised the cells to the combination treatment, suggesting a role of BRCA1 in EGFR signalling pathway in response to cisplatin-induced DNA damage.

Cell line	IC_{50} cisplatin continuous exposure	IC_{50} (combination 5 days)		IC_{50} (combination 24hrs then gefitinib alone)	
		With gefitinib causing 10% inhibition of proliferation	With gefitinib causing 20% inhibition of proliferation	With gefitinib causing 10% inhibition of proliferation	With gefitinib causing 20% inhibition of proliferation
MCF-7 wild type	0.9 ± 0.1μM	0.9 ± 0.3μM	0.8 ± 0.5μM	0.6 ± 0.1μM	0.7 ± 0.2μM
MCF-7 scrambled	1.2 ± 0.3μM	1.0 ± 0.4μM	0.9 ± 0.3μM	0.3 ± 0.2μM	0.3 ± 0.1μM
MCF-7 3.23	2.5 ± 0.6μM	1.4 ± 0.4μM	0.4 ± 0.3μM	1.3 ± 0.4μM	0.8 ± 0.3μM

Table 7.3 – IC_{50} (±SD) results for cisplatin/gefitinib combination treatments in MCF-7 cell lines. MCF-7 wild type, MCF-7 scrambled and MCF-7 3.23 cells were treated with a combination of cisplatin and gefitinib.

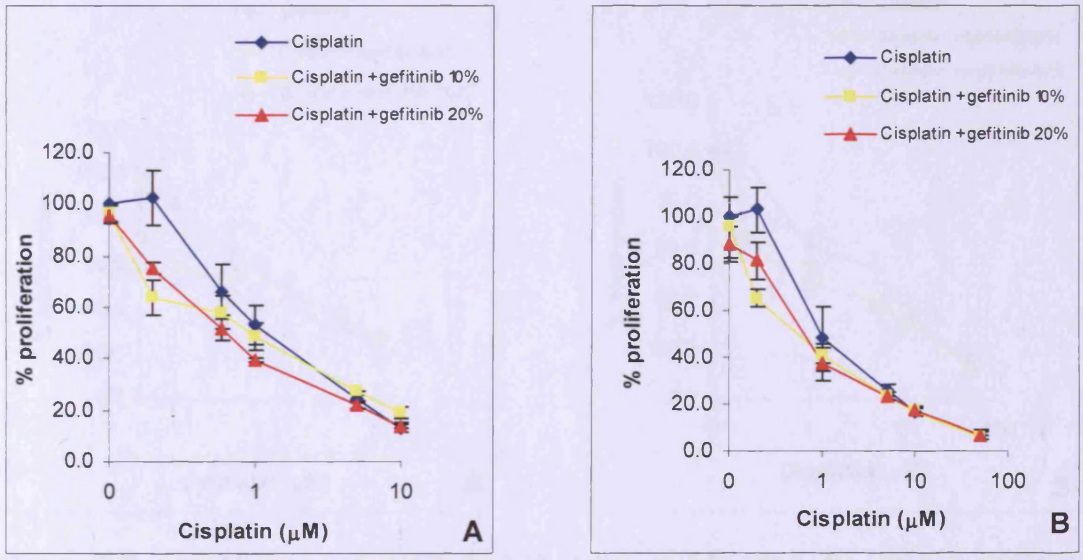

Figure 7.5 – Inhibition of MCF-7 wild type cells proliferation by cisplatin/gefitinib combination treatment. Cells were treated with cisplatin and gefitinib for 5 consecutive days (**A**) or with cisplatin and gefitinib for 24 hours followed by 4 days in drug media or media containing gefitinib alone (**B**). Gefitinib was used at doses giving 10% or 20% inhibition of proliferation. Data presented are the result of three independent experiments, as shown by the standard deviation.

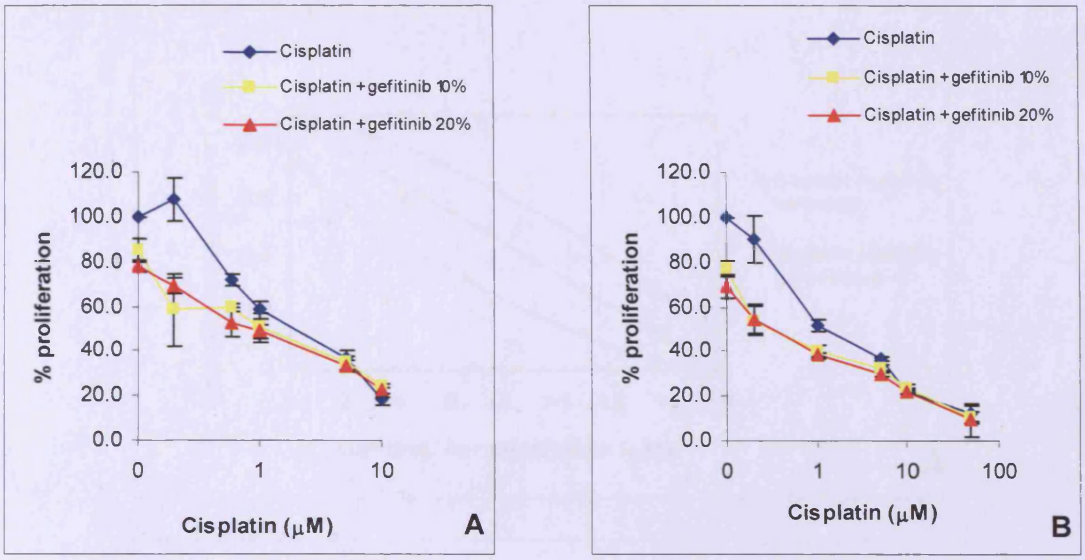

Figure 7.6 – Inhibition of MCF-7 scrambled cells proliferation by cisplatin/gefitinib combination treatment. Cells were treated with cisplatin and gefitinib for 5 consecutive days (**A**) or with cisplatin and gefitinib for 24 hours followed by 4 days in drug media or media containing gefitinib alone (**B**). Gefitinib was used at doses giving 10% or 20% inhibition of proliferation. Data presented are the result of three independent experiments, as shown by the standard deviation.

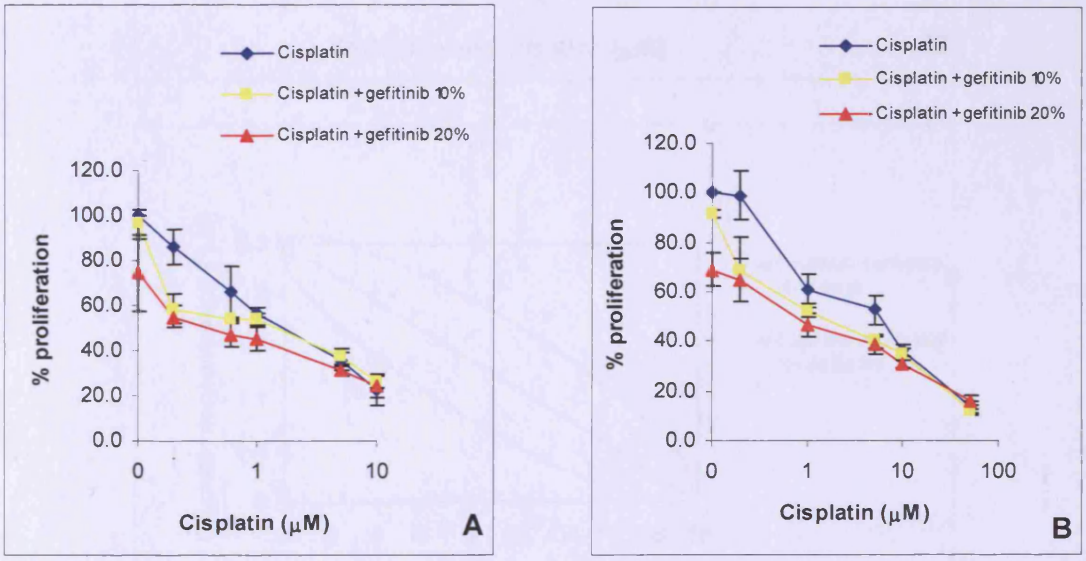

Figure 7.7 – Inhibition of MCF-7 3.23 cells proliferation by cisplatin/gefitinib combination treatment. Cells were treated with cisplatin and gefitinib for 5 consecutive days (A) or with cisplatin and gefitinib for 24 hours followed by 4 days in drug media or media containing gefitinib alone (**B**). Gefitinib was used at doses giving 10% or 20% inhibition of proliferation. Data presented are the result of three independent experiments, as shown by the standard deviation.

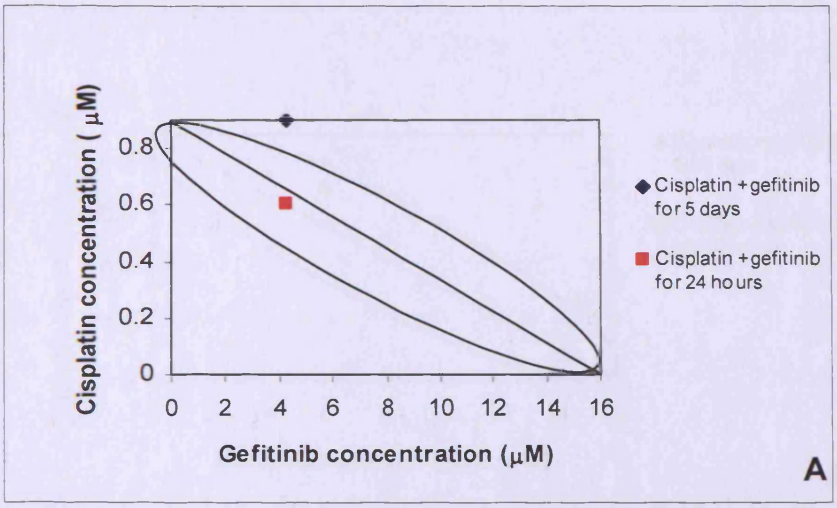

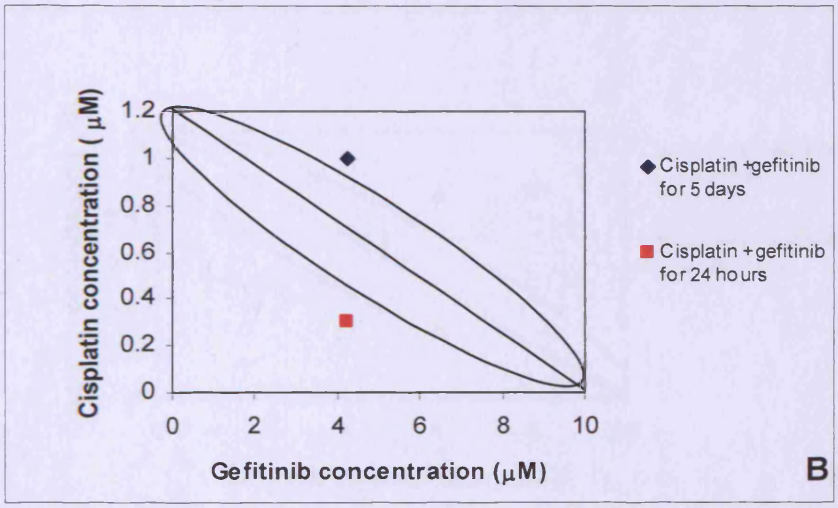

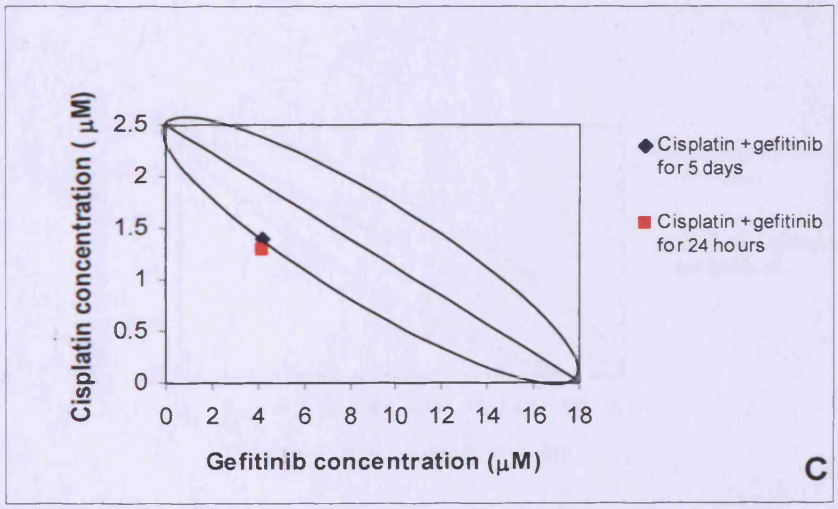

Figure 7.8 – Isobologram analysis at IC_{50} of cisplatin/gefitinib combination treatment using gefitinib 10%. Gefitinib was used at a concentration giving 10% inhibition of proliferation combined with a range of cisplatin concentrations, on MCF-7 wild type (**A**), MCF-7 scrambled (**B**) and MCF-7 3.23 (**C**) cell lines. The circled area defines the combinations of IC_{50} of cisplatin and gefitinib that have an additive effect.

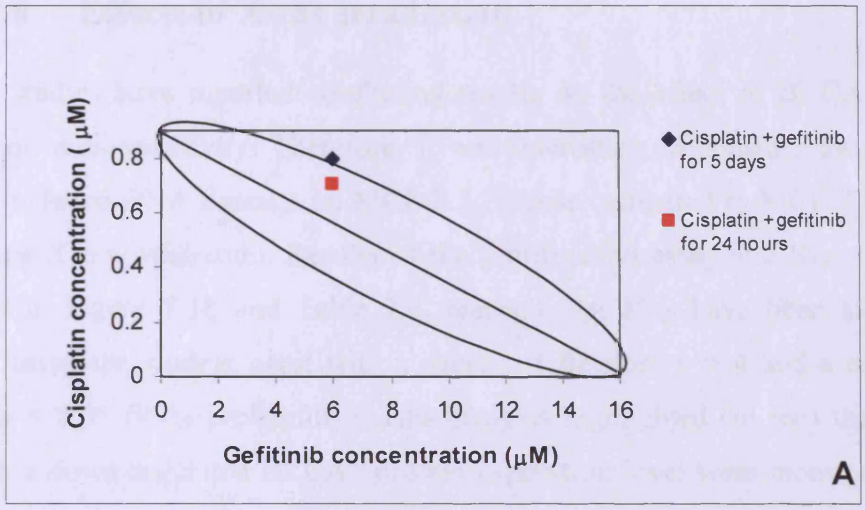

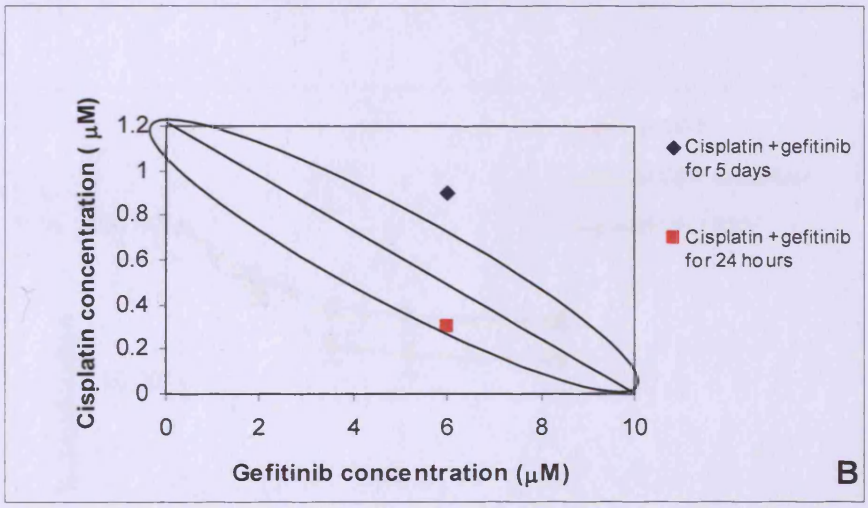

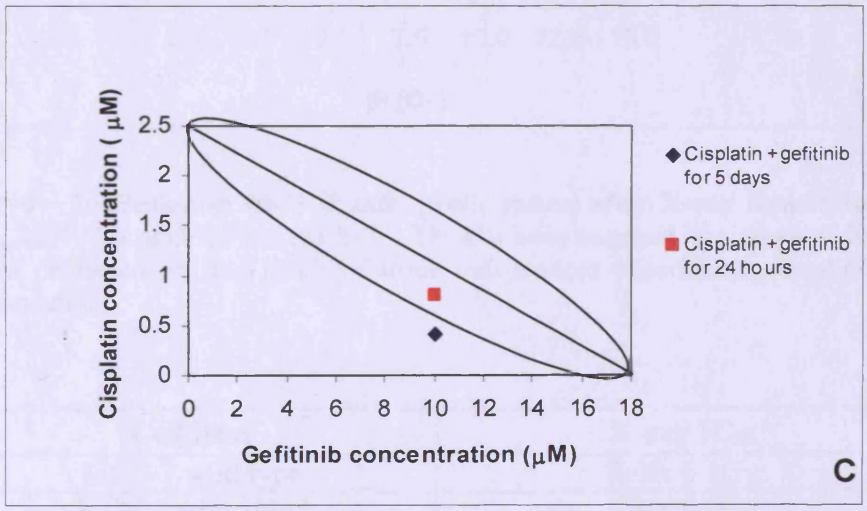

Figure 7.9 – Isobologram analysis at IC_{50} of cisplatin/gefitinib combination treatment using gefitinib 20%. Gefitinib was used at a concentration giving 20% inhibition of proliferation combined with a range of cisplatin concentrations, on MCF-7 wild type (**A**), MCF-7 scrambled (**B**) and MCF-7 3.23 (**C**) cell lines. The circled area defines the combinations of IC_{50} of cisplatin and gefitinib that have an additive effect.

7.8 Effects of X-ray irradiation

Previous studies have reported conflicting results on the effect of BRCA1 loss of function on radiosensitivity. Therefore, it was interesting to consider the effect of radiation-induced DNA damage on MCF-7 3.23 cells compared to MCF-7 wild type cells, using X-ray irradiation. Results of the proliferation assay and IC_{50} values are presented in Figure 7.10 and Table 7.4, respectively. IC_{50} have been statistically analysed using the student *t*-test with a degree of freedom n = 4 and a confidence interval $p = 0.05$ (95% probability). This analysis highlighted (in red) that MCF-7 cells with a down-regulated BRCA1 protein expression level were more resistant to irradiation than MCF-7 wild type cells.

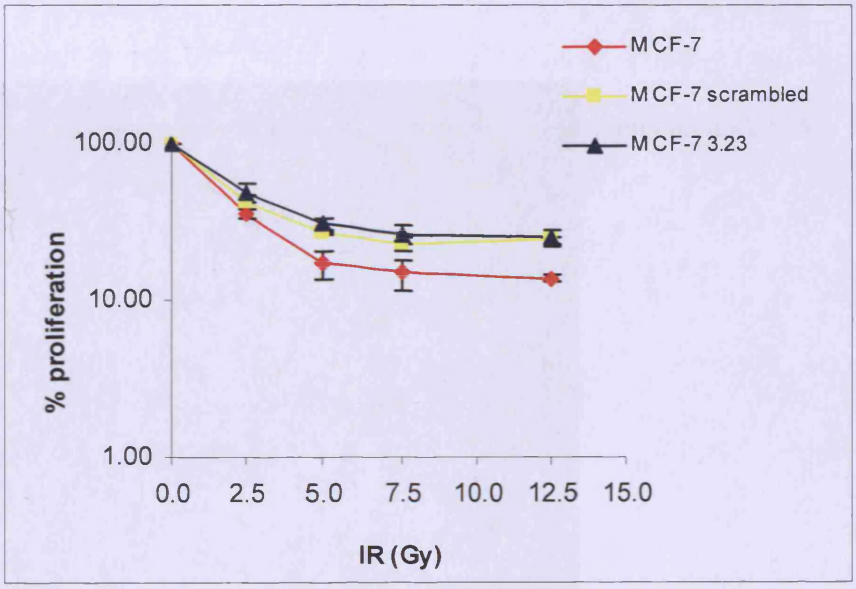

Figure 7.10 – Inhibition of MCF-7 cells proliferation after X-ray irradiation. MCF-7 wild type, MCF-7 scrambled and MCF-7 3.23 cells were exposed to a range of X-ray doses (Gy). Data presented are the result of three independent experiments, as shown by the standard deviation.

Cell lines	X-ray IC_{50}
MCF-7 wild type	2.0 ± 0.1Gy
MCF-7 scrambled	2.1 ± 0.2Gy
MCF-7 3.23	2.5 ± 0.3Gy

Table 7.4 – IC_{50} (±SD) results after X-ray irradiation of MCF-7 cell lines. MCF-7 wild type, MCF-7 scrambled and MCF-7 3.23 were exposed to a range of X-ray doses. Data obtained from the proliferation assay and analysed with the student *t*-test with n = 4 and $p = 0.05$, comparing IC_{50} of the wild type cell line with IC_{50} of the transfected cell lines.

7.9 Topoisomerase II activity

The study by Lou *et al.* (2005) suggested that BRCA1 interacted with topoisomerase IIα and was able to modulate DNA decatenation. Therefore, topoisomerase II activity was measured in all three cell lines. Topoisomerase II activity was measured by assessing the efficiency of DNA decatenation using catenated kintoplast DNA (kDNA). Upon efficient decatenation, topoisomerase IIα formed nicked decatenated kDNA and circular decatenated kDNA. Results presented in Figure 7.11 show that there was no difference in decatenation efficiency between the three cell lines, since there was no alteration of the level of decatenated kDNA. Therefore, BRCA1 down-regulation in MCF-7 3.23 cells (lane 6) did not modify the DNA decatenation efficiency of the cells.

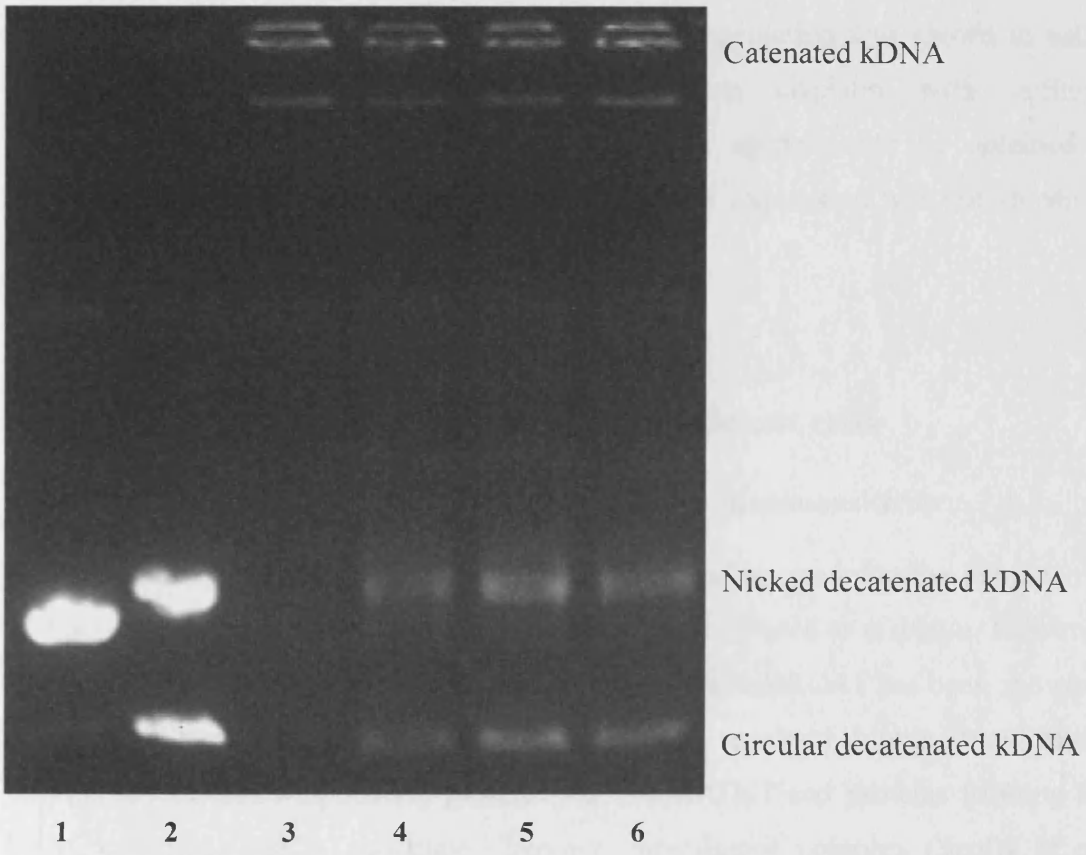

Figure 7.11 – Topoisomerase IIα activity assay in MCF-7 cell lines. Topoisomerase IIα activity was assessed in MCF-7 wild type (**4**), MCF-7 scrambled (**5**) and MCF-7 3.23 (**6**) cell lines using kintoplast DNA (kDNA). Decatenated kDNA (**2**) and linearised kDNA (**1**) were used as positive control and kDNA as negative control (**3**). Reactions were stopped after 30 minutes.

DISCUSSION

Using MCF-7 cells stably transfected, with a plasmid containing BRCA1 siRNA, this chapter investigated the effect of BRCA1 down-regulation on cell sensitivity to gefitinib, an inhibitor of EGFR tyrosine kinase activity, and common chemotherapeutic agents, cisplatin, melphalan and etoposide. BRCA1 is a protein involved in several DNA repair pathways which has been shown to be mutated in some hereditary forms of breast and ovarian cancers. Loss-of-function mutations in BRCA1 have been reported to confer up to an 82% risk of developing breast cancer (King *et al.*, 2003). Using the plasmid encoding human specific BRCA1 siRNA transfected in MCF-7 cells, a 68% down-regulation in BRCA1 mRNA was achieved and a similar reduction of the protein level was also observed. Reduction in BRCA1 expression caused increased resistance to the anti-proliferative effect of cisplatin and etoposide single agents. In addition, BRCA1 down-regulation was shown to cause increased radioresistance. Furthermore, combining cisplatin with gefitinib demonstrated that a synergistic effect between the agents could be obtained in BRCA1 deficient cells. Finally, reduction of BRCA1 expression was not shown to affect DNA decatenation activity.

7.10 Chemosensitivity of BRCA1 deficient cells

7.10.1 BRCA1 expression modulates chemosensitivity

Sensitivities of the transfected cells were evaluated and showed that the reduction in BRCA1 expression caused a significant increase in resistance to cisplatin. However, this result was in contradiction with published data, since BRCA1 has been shown in several studies as being involved in recombinational repair of double strand break, through association with several proteins such as RAD51 and proteins forming the BASC complex, BRCA1-associated genome surveillance complex (Scully *et al.*, 1997c; Moynahan *et al.*, 1999; Snouwaert *et al.*, 1999; Wang *et al.*, 2000b). Furthermore, BRCA1 has also been shown to promote cell survival after DNA damage by preventing apoptosis and activating DNA damage repair (Bernstein *et al.*, 2002). Bhattacharyya *et al.* (2000) demonstrated that the loss of BRCA1 function was

associated with an increased sensitivity to cisplatin, in BRCA1-/- isogenic mouse embryonic stem cell lines. In a separate study, the increased sensitivity to cisplatin by inhibition of BRCA1 using antisense RNAs was also shown to be associated with a decrease in DNA repair efficiency (Husain *et al.*, 1998). Nonetheless, conflicting results have been obtained on the effect of BRCA1 expression on the sensitivity to topoisomerase II inhibitors. The studies by Lafarge *et al.* (2001) and Quinn *et al.* (2003) established that a reduction in BRCA1 expression caused an increase in sensitivity to etoposide, whereas Tassone *et al.* (2003) reported that BRCA1 deficiency increased resistance to doxorubicin that like etoposide is a topoisomerase II inhibitor like etoposide. The results obtained in the present study demonstrated that, similarly to cisplatin, reduction of BRCA1 expression also conferred resistance to etoposide (results compared to the wild type are significantly different with a lower probability).

Therefore, results obtained demonstrate that BRCA1 down-regulation caused an increase in resistance to chemotherapeutic agents, cisplatin and etoposide. The difference with published data suggests that the down-regulation of BRCA1 expression is not sufficient to inhibit BRCA1 activity. However, the reason for the increased chemoresistance remains unclear.

7.10.2 BRCA1 expression and EGFR signalling pathway

Friedmann *et al.* (2004) demonstrated that gefitinib, an inhibitor of EGFR tyrosine kinase, in combination with cisplatin, enhanced the anti-proliferative effect of cisplatin, resulting in a synergistic effect, in MCF-7 cells. In this study, they reported that synergistic effects were drug scheduling dependent. In order to investigate further the result obtained here with cisplatin, cells were treated with a combination of gefitinib (using concentrations producing 10% and 20% inhibition of proliferation), an EGFR inhibitor of tyrosine kinase, and cisplatin. Although synergistic effects between gefitinib and a variety of anticancer agents, including chemotherapeutic agents and radiation, have been reported in cell lines and xenografts (Friedmann *et al.*, 2004; Huang *et al.*, 2002), no such effect was observed in MCF-7 wild type cells. However, using gefitinib at a concentration causing 20% inhibition of proliferation, a synergistic effect was observed in BRCA1 deficient MCF-7 cells when treated with the drug combination for 24 hours.

Therefore, synergistic effect between cisplatin and gefitinib was dependent on the drug scheduling. Moreover, since synergy was only obtained in the cell line with a down-regulated BRCA1 level, it suggests that both EGFR signalling pathway and BRCA1 are involved in the repair of cisplatin-induced DNA damage.

7.11 Radiosensitivity of BRCA1 deficient cells

Regarding the role of BRCA1 in radiation-induced DNA damage response, published results have been more conflicting than with chemotherapeutic agents. The result obtained here suggests that the partial loss of BRCA1 function increased the resistance to ionizing radiation. However, results obtained by Scully *et al.* (1999) suggested that BRCA1 confer radioresistance to cells and is required to efficient repair of radiation-induced DNA double strand breaks. Hypersensitivity, to ionizing radiation, of BRCA1 deficient cell line was also demonstrated by Scully *et al.* (1999). This finding was contradicted by Wang *et al.* (2001) showing that BRCA1 did not play a major role in the modulation of radiosensitivity. Furthermore, several studies demonstrated that heterozigosity of BRCA1 did not account for radiation hypersensitivity (Nieuwenhuis *et al.*, 2002). The study by Trenz *et al.* (2005) reported the absence of radiosensitivity of lymphoblastoid cell lines with a heterozygous BRCA1 mutation. However, conflicting results have been obtained as DNA end joining was shown to be reduced in other lymphoblastoid cell lines with a heterozygous BRCA1 mutation (Baldeyron *et al.*, 2002).

Although published results suggest that BRCA1 mutant cell lines have an increased radiosensitivity, the direct role of BRCA1 in the repair of radiation-induced DNA double strand breaks remains unclear. Taken together with previous studies, the results obtained with MCF-7 cells, deficient in BRCA1, show that reduction of BRCA1 protein expression does not induce radiosensitivity but that modulation of radiosensitivity may rely on the deficiency in the non-homologous repair pathway, used to repair radiation-induced double strand breaks (Jeggo, 1998; Wang *et al.*, 2001). Nevertheless, similarly to the effect on chemosensitivity, the reason for the increased radioresistance remains unclear.

7.12 Role of BRCA1 in DNA decatenation

Lou *et al.* (2005) have established that BRCA1 plays an important role in DNA decatenation, by causing topoisomerase IIα ubiquitination affecting topoisomerase IIα distribution and DNA decatenation activity. Indeed, they demonstrated that BRCA1 and topoisomerase IIα co-localised during the S-phase and that BRCA1 deficiency resulted in lower DNA decatenation activity and defect in chromosome segregation. Conversely, the results obtained in the present study failed to show the effect of BRCA1 down-regulation on topoisomerase II activity and DNA decatenation activity. However, Lou *et al.* (2005) used BRCA1 siRNA causing complete inhibition of BRCA1 protein expression.

Therefore, the reduction in BRCA1 protein expression level achieved may not be sufficient to inhibit completely BRCA1 activity and observe an effect on DNA decatenation activity.

7.13 Conclusion

These results obtained demonstrate that partial inhibition of BRCA1 protein expression could be obtained using siRNA. However, BRCA1 down-regulation caused an increase in resistance to chemotherapeutic agents and ionising radiation, contrary to the results reported in published studies. Furthermore, reduction of decatenation activity was not demonstrated in cells deficient in BRCA1. Nevertheless, a synergistic effect obtained between gefitinib and cisplatin in BRCA1 deficient cells.

Therefore, it is reasonable to conclude that down-regulation of BRCA1 protein level achieved was not sufficient to inhibit BRCA1 activity. Nonetheless, results suggest a role of BRCA1 and EGFR signalling pathway in the repair of cisplatin-induced DNA damage. Thus, it would be interesting to investigate further the interaction between BRCA1 and EGFR signalling pathway. In order to study further the role of BRCA1 in drug-induced DNA damage, a more efficient plasmid encoding BRCA1 siRNA need to be designed, to achieve a significant reduction in BRCA1 activity.

Chapter 8

Conclusions and future work

This study investigated the role of ErbB2 and BRCA1 in repair of drug-induced DNA damage. ErbB2 is overexpressed in 20-30% of breast cancer and has been shown to correlate with increased tumour chemoresistance and poor patient prognosis. Although many published studies have investigated the function of ErbB2 and the effect of the anti-ErbB2 monoclonal antibody, trastuzumab, its role in the repair of drug-induced DNA damage remains unclear. Firstly, effects of ErbB2 down-regulation, on chemotherapeutic response, were studied using trastuzumab. An increase in sensitivity caused by trastuzumab was identified in cells overexpressing ErbB2, for cisplatin and other chemotherapeutic drugs (Chapter 3). Furthermore, overexpression of ErbB2 demonstrated that ErbB2 caused an increase in topoisomerase activity and an increased chemoresistance to cisplatin. Combination of the chemotherapeutic agent with trastuzumab led to a sensitisation of the cells to cisplatin (Chapter 5). In addition, results obtained revealed that inhibition of ErbB2 nuclear translocation led to an increase in cisplatin sensitivity (Chapter 6). Secondly, effects of ErbB2 overexpression and down-regulation by trastuzumab in the repair of drug-induced DNA damage was investigated using the comet assay. Modulation of ErbB2 expression was shown to affect the repair of cisplatin-induced DNA damage, but not the kinetics of damage and repair of melphalan and etoposide-induced DNA damage (Chapter 3). More specifically, ErbB2 was shown to only alter the repair of cisplatin-induced DNA interstrand crosslink and not cisplatin-DNA intrastrand adducts (Chapter 5). Furthermore, in Chapter 6, results obtained demonstrated that ErbB2 nuclear localisation was essential to the repair of cisplatin-induced DNA interstrand crosslinks. It was also demonstrated that abolishing ErbB2 nuclear translocation reduced the normal DNA repair activity of the cells, similarly to the effect observed with trastuzumab on ErbB2 overexpressing cells. Therefore, this suggests that trastuzumab modulates the repair of cisplatin-induced DNA ICLs by reducing ErbB2 nuclear translocation. In addition, ErbB2 overexpression was shown to reduce EGFR nuclear localisation, possibly through the formation of EGFR/ErbB2 heterodimers, suggesting that ErbB2 and its NLSs have an impact on EGFR nuclear translocation. Chapter 4 revealed that the delay of the repair of cisplatin-induced DNA interstrand crosslinks, by down-regulation of ErbB2 expression, was due to a progression of the cell through cell cycle arrest. Investigating the effects of trastuzumab on the expression of proteins involved in DNA damage repair and ErbB2 downstream signalling pathways revealed that trastuzumab caused activation of Akt

followed by its downregulation. Moreover, in combination with cisplatin, trastuzumab caused an escape of cells from cell cycle arrest, associated with activation of Akt and increase in topoisomerase IIα expression. Therefore the delay in the repair of cisplatin-induced DNA damage, of ErbB2 overexpressing cells, could not be attributed to this effect. In addition, further investigation is required to elucidate the molecular mechanism behind the delay in the repair of cisplatin-induced DNA damage.

BRCA1 is a protein involved in different cellular pathways and germline mutations have been associated with an increased risk of breast and ovarian cancer and account for 50% of hereditary breast cancer. Therefore, it is important to fully understand its role in the repair of drug-induced DNA damage. Chapter 7 demonstrated that BRCA1 down-regulation caused an increase in resistance to cisplatin, etoposide and ionizing radiation. In addition, BRCA1 down-regulation did not alter DNA decatenation activity as previously suggested. Nevertheless, BRCA1 and EGFR signalling pathways were shown to play a role in the repair of cisplatin-induced DNA damage, as shown by the synergistic effect obtained between cisplatin and gefitinib in cells with BRCA1 down-regulated.

These experiments have opened new questions which will be the work of future investigations.

8.1 ErbB2 protein expression and sensitivity to trastuzumab and chemotherapeutic agents

8.1.1 ErbB2 protein expression and trastuzumab sensitivity

Studying the effect of trastuzumab on cells overexpressing ErbB2, identified its ability to inhibit cell proliferation in some cell lines, since trastuzumab did not alter the MDA-MB-468 ErbB2 cell proliferation. As reported by Gong *et al.* (2004) and Kasprzyk *et al.* (1992), trastuzumab does not always alter cell proliferation regardless of the ErbB2 expression level. Furthermore, Esteva *et al.* (2002; 2005) reported that response to trastuzumab was predictable in part by the presence of elevated serum ErbB2 extracellular domain (ECD - causing increased kinase activity and increased

metastasis) levels prior treatment. Therefore, the effect of trastuzumab may be cell line dependent but future work will need to consider levels of ECD in culture media as a way to predict the response to trastuzumab.

8.1.2 ErbB2 protein expression and chemotherapeutic response

Studying the chemosensitivity of different breast cancer cell lines, expressing different ErbB2 protein level, did not show any correlation between ErbB2 overexpression and chemosensitivity to common chemotherapeutics. In addition, ErbB2 overexpression was shown to increase the activity of topoisomerase II. Published data have shown that increase in topoisomerase II activity causes an increased resistance to alkylators but an increased sensitivity to topoisomerase II inhibitors (Larsen *et al.*, 1998; Pu and Bezwoda, 1999). Therefore, it would be interesting to investigate the effect of ErbB2 expression on the response to different classes of damaging agents, as a better understanding of the relationship between a given molecular lesion and the chemotherapeutic response will help designing new drug combinations for therapeutic use.

Using clinically achievable doses of trastuzumab, ErbB2 overexpressing cells were sensitised to chemotherapeutic agents. This effect was shown to be more significant in cells overexpressing ErbB2 and with increasing doses of trastuzumab. Therefore, it would be interesting to study further enhancement of cytotoxicity caused by trastuzumab as altering drug scheduling may change effect on cell proliferation. In addition, similarly to the study by Nahta *et al.* (2004) combining trastuzumab with other ErbB inhibitors/anti-ErbB antibodies may highlight new drug combination beneficial for therapeutic use. Indeed, using pertuzumab (Nahta *et al.*, 2004), sterically blocking ErbB2 dimerisation with other ErbB receptors and blocking ligand-activated signalling from ErbB2/EGFR and ErbB2/ErbB3 heterodimers, or lapatinib (Xia *et al.*, 2005), an inhibitor of the tyrosine kinase of EGFR and ErbB2, in combination with trastuzumab have been shown to be more effective than monotherapy. Finally, three drug combinations will need to be considered using a combination of ErbB inhibitors/anti-ErbB antibodies with a chemotherapeutic agent. Thus, future development in drug combination will help overcome drug resistance and cell signalling redundancy.

8.1.3 Nuclear ErbB2 and chemotherapeutic treatments

Inhibiting ErbB2 nuclear translocation caused an increase in cisplatin sensitivity compared to cells overexpressing full length ErbB2 and ErbB2 negative cells. These results suggested that nuclear ErbB2 plays a significant role in the response to cisplatin-induced DNA damage and that deletion of ErbB2 nuclear localisation signal sequence caused a sensitisation of the cells to cisplatin. Furthermore, as trastuzumab was shown to reduce membrane bound ErbB2 protein level and ErbB2 nuclear translocation, it is suggested that the increase in sensitivity to chemotherapeutic agents, caused by trastuzumab, was due to a reduction in nuclear ErbB2. However, further analysis is required to determine the molecular mechanism by which trastuzumab sensitises cells to chemotherapeutic drugs. In addition, further investigation will be required to identify new molecular targets of nuclear ErbB2 as the potential nuclear activity of ErbB family members has only been recently considered.

8.2 ErbB2 expression and repair of drug-induced DNA damage

8.2.1 ErbB2 expression and repair of drug-induced DNA strand break

ErbB2 overexpression or subsequent inhibition by trastuzumab did not affect the kinetics of formation and repair of etoposide-induced DNA strand breaks. However, its cytotoxicity was shown to be enhanced by the presence of trastuzumab. Studies by Mayfield *et al.* (2001) and Pietras *et al.* (1999) suggesting that trastuzumab was able to alter the formation and repair of DNA strand breaks. Moreover, by inhibiting EGFR tyrosine kinase activity, Friedmann *et al.* (2004) showed that the repair of etoposide-induced DNA strand break activity was reduced. Therefore, ErbB2-EGFR heterodimerisation will need to be considered for further investigation of the role of ErbB2 in the repair of etoposide-induced DNA strand breaks.

8.2.2 ErbB2 expression and repair of drug-induced DNA interstrand crosslink

Effects of ErbB2 down-regulation by trastuzumab on the repair of drug-induced DNA ICL were also investigated after melphalan and cisplatin-induced DNA damage. Similarly to etoposide, the kinetic of formation and repair of melphalan-induced DNA ICL was not affected, although trastuzumab was shown to increase its cytotoxic effect. In contrast, trastuzumab and ErbB2 overexpression modulated the kinetic of repair of cisplatin-induced DNA ICLs. De Silva *et al.* (2002) and Clingen *et al.* (2005) demonstrated that increased cytotoxicity of cisplatin and melphalan-induced ICLs was associated with defects in ERCC1-XPF heterodimers of the NER pathway and in XRCC2 and XRCC3 of the homologous recombination pathway. In addition, contrary to cisplatin, melphalan was shown to induce the formation of double strand breaks. Thus, for further investigation, the effects of trastuzumab should be studied on mutant cell lines defective in these pathways.

8.2.3 Nuclear ErbB2 and repair of cisplatin-induced DNA interstrand crosslinks

Studying the role of nuclear ErbB2 revealed a novel link between ErbB2 nuclear localisation and the repair of cisplatin-induced DNA ICLs. Results obtained established that ErbB2 nuclear translocation has a key role in the repair of cisplatin-induced DNA ICLs. In addition, results obtained showed that deletion of ErbB2 nuclear localisation signal sequence caused an increased delay in the repair of cisplatin-induced DNA ICL, suggesting a role of the NLSs in ErbB2 dimerisation or DNA repair signalling cascade. Since the role of nuclear ErbB2 has not yet been extensively studied, further experiments will need to be carried out to identify molecular targets, for nuclear ErbB2, involved in DNA damage repair. Furthermore, it will be interesting to investigate the role of ErbB2 tripartite NLS in ErbB2 dimerisation and signalling cascade.

8.3 ErbB2 and EGFR nuclear localisation

Immunofluorescence revealed that overexpression of ErbB2 or ErbB2ΔNLS led to a reduction of EGFR nuclear translocation. Therefore, it is suggested that ErbB2 dimerises with EGFR, blocking EGFR nuclear translocation. In addition, overexpressing full length ErbB2 causes an amplification of DNA repair efficiency whereas overexpressing ErbB2ΔNLS may lead to the formation of non-functional EGFR-ErbB2 heterodimers that sequestrate EGFR in the cytoplasmic membrane and are unable to trigger the DNA repair signalling cascade, causing a delay in DNA repair. For future investigation it will be interesting to determine the effects of ErbB2 overexpression and its NLS on the EGFR-ErbB2 heterodimers formation and its signalling cascade. In addition, dimerisation with other ErbB family members will need to be considered.

8.4 ErbB2 expression and DNA repair proteins

Results of the effect of the trastuzumab/cisplatin combination on the cell cycle and proteins involved in the ErbB2 downstream signaling cascade suggested that cells progressed through cell cycle arrest, leading to accumulation of unrepaired DNA damage and a delay of the repair kinetics of cisplatin-induced DNA damage. Therefore, a robust molecular mechanism needs to be established to explain the effects of trastuzumab within the cell. Future investigations will study the transcriptional changes associated with ErbB2 expression in cells overexpressing full length ErbB2 and ErbB2ΔNLS, treated with cisplatin and cisplatin/trastuzumab combination. To this end, cDNA microarray analysis will be used, similarly to Mackay *et al.* (2003), to highlight modulation of gene amplification. The data will be statistically analysed and significant results will be confirmed by investigating changes in protein levels. In addition, since topoisomerase II activity was shown to be increased by ErbB2 overexpression and topoisomerase IIα was suggested to be involved in DNA damage repair, it will be interesting to examine further the role of topoisomerase IIα in the repair of DNA damage in ErbB2 overexpressing cells.

8.5 Role of BRCA1 in drug-induced DNA damage

Using a plasmid encoding specific siRNA, BRCA1 protein expression level was reduced, however, results obtained for the chemosensitivity and radiosensitivity conflicted with published data, as the study showed that BRCA1 downregulation caused an increase in resistance. Synergistic effect obtained with cisplatin and gefitinib suggested an interaction between BRCA1 and EGFR signalling pathway in the repair of cisplatin-induced DNA damage. Therefore, for future investigation, a new siRNA sequence will be designed to increase BRCA1 down-regulation efficiency. Moreover, it will be interesting to study the effect of BRCA1 down-regulation on EGFR signalling pathway, using gefitinib and cisplatin and other platinum based compounds, such as carboplatin. In addition, having shown that synergistic effect between cisplatin and gefitinib was dependent on the drug scheduling, it will be important to consider other classes of DNA damaging agents as well as non-DNA damaging agents, as Friedmann *et al.* (2004) also demonstrated the synergistic effect between gefitinib and etoposide, in MCF-7 wild type cells.

8.6 Conclusion

In conclusion, these results have established a novel link between nuclear ErbB2 and DNA damage repair, showing the importance of ErbB2 expression. Therefore, future work will investigate the nuclear role of ErbB2 and will be extended to other ErbB family members. Furthermore, BRCA1 having been shown to induce gene expression of ErbB2 interacting protein (Atalay *et al.*, 2002), it will be interesting to examine the influence of BRCA1 on ErbB2 expression and activity. Results of this study together with further understanding of the molecular mechanisms involved will help in designing new targeted therapies and drug combinations.

References

Abbott,D.W., Thompson,M.E., Robinson-Benion,C., Tomlinson,G., Jensen,R.A., and Holt,J.T. (1999). BRCA1 expression restores radiation resistance in BRCA1-defective cancer cells through enhancement of transcription-coupled DNA repair. J. Biol. Chem. *274*, 18808-18812.

Agus,D.B., Akita,R.W., Fox,W.D., Lewis,G.D., Higgins,B., Pisacane,P.I., Lofgren,J.A., Tindell,C., Evans,D.P., Maiese,K., Scher,H.I., and Sliwkowski,M.X. (2002). Targeting ligand-activated ErbB2 signaling inhibits breast and prostate tumor growth. Cancer Cell *2*, 127-137.

Agus,D.B., Gordon,M.S., Taylor,C., Natale,R.B., Karlan,B., Mendelson,D.S., Press,M.F., Allison,D.E., Sliwkowski,M.X., Lieberman,G., Kelsey,S.M., and Fyfe,G. (2005). Phase I clinical study of pertuzumab, a novel HER dimerization inhibitor, in patients with advanced cancer. J. Clin. Oncol. *23*, 2534-2543.

Aifa,S., Miled,N., Frikha,F., Aniba,M.R., Svensson,S.P., and Rebai,A. (2006). Electrostatic interactions of peptides flanking the tyrosine kinase domain in the epidermal growth factor receptor provides a model for intracellular dimerization and autophosphorylation. Proteins *62*, 1036-1043.

Akita,R.W. and Sliwkowski,M.X. (2003). Preclinical studies with Erlotinib (Tarceva). Semin. Oncol. *30*, 15-24.

Albain,K.S., Crowley,J.J., Turrisi,A.T., III, Gandara,D.R., Farrar,W.B., Clark,J.I., Beasley,K.R., and Livingston,R.B. (2002). Concurrent cisplatin, etoposide, and chest radiotherapy in pathologic stage IIIB non-small-cell lung cancer: a Southwest Oncology Group phase II study, SWOG 9019. J. Clin. Oncol. *20*, 3454-3460.

Alessi,D.R., James,S.R., Downes,C.P., Holmes,A.B., Gaffney,P.R., Reese,C.B., and Cohen,P. (1997). Characterization of a 3-phosphoinositide-dependent protein kinase which phosphorylates and activates protein kinase Balpha. Curr. Biol. *7*, 261-269.

Allred,D.C., Clark,G.M., Tandon,A.K., Molina,R., Tormey,D.C., Osborne,C.K., Gilchrist,K.W., Mansour,E.G., Abeloff,M., Eudey,L., and . (1992). HER-2/neu in node-negative breast cancer: prognostic significance of overexpression influenced by the presence of in situ carcinoma. J. Clin. Oncol. *10*, 599-605.

Amit,I., Citri,A., Shay,T., Lu,Y., Katz,M., Zhang,F., Tarcic,G., Siwak,D., Lahad,J., Jacob-Hirsch,J., Amariglio,N., Vaisman,N., Segal,E., Rechavi,G., Alon,U., Mills,G.B., Domany,E., and Yarden,Y. (2007). A module of negative feedback regulators defines growth factor signaling. Nat. Genet. *39*, 503-512.

Anderson,S.F., Schlegel,B.P., Nakajima,T., Wolpin,E.S., and Parvin,J.D. (1998). BRCA1 protein is linked to the RNA polymerase II holoenzyme complex via RNA helicase A. Nat. Genet. *19*, 254-256.

Arteaga,C.L., Winnier,A.R., Poirier,M.C., Lopez-Larraza,D.M., Shawver,L.K., Hurd,S.D., and Stewart,S.J. (1994). p185c-erbB-2 signal enhances cisplatin-induced cytotoxicity in human breast carcinoma cells: association between an oncogenic receptor tyrosine kinase and drug-induced DNA repair. Cancer Res. *54*, 3758-3765.

Arteaga,C.L. (2003). Trastuzumab, an appropriate first-line single-agent therapy for HER2-overexpressing metastatic breast cancer. Breast Cancer Res. *5*, 96-100.

Atalay,A., Crook,T., Ozturk,M., and Yulug,I.G. (2002). Identification of genes induced by BRCA1 in breast cancer cells. Biochem. Biophys. Res. Commun. *299*, 839-846.

Attardi,L.D., Reczek,E.E., Cosmas,C., Demicco,E.G., McCurrach,M.E., Lowe,S.W., and Jacks,T. (2000). PERP, an apoptosis-associated target of p53, is a novel member of the PMP-22/gas3 family. Genes Dev. *14*, 704-718.

Bachman,K.E., Argani,P., Samuels,Y., Silliman,N., Ptak,J., Szabo,S., Konishi,H., Karakas,B., Blair,B.G., Lin,C., Peters,B.A., Velculescu,V.E., and Park,B.H. (2004). The PIK3CA gene is mutated with high frequency in human breast cancers. Cancer Biol. Ther. *3*, 772-775.

Baeyens,A., Thierens,H., Claes,K., Poppe,B., de,R.L., and Vral,A. (2004). Chromosomal radiosensitivity in BRCA1 and BRCA2 mutation carriers. Int. J. Radiat. Biol. *80*, 745-756.

Baldeyron,C., Jacquemin,E., Smith,J., Jacquemont,C., De,O., I, Gad,S., Feunteun,J., Stoppa-Lyonnet,D., and Papadopoulo,D. (2002). A single mutated BRCA1 allele leads to impaired fidelity of double strand break end-joining. Oncogene *21*, 1401-1410.

Bartkova,J., Lukas,J., and Bartek,J. (1997). Aberrations of the G1- and G1/S-regulating genes in human cancer. Prog. Cell Cycle Res. *3*, 211-220.

Baselga,J., Tripathy,D., Mendelsohn,J., Baughman,S., Benz,C.C., Dantis,L., Sklarin,N.T., Seidman,A.D., Hudis,C.A., Moore,J., Rosen,P.P., Twaddell,T., Henderson,I.C., and Norton,L. (1996). Phase II study of weekly intravenous recombinant humanized anti-p185HER2 monoclonal antibody in patients with HER2/neu-overexpressing metastatic breast cancer. J. Clin. Oncol. *14*, 737-744.

Baselga,J., Norton,L., Albanell,J., Kim,Y.M., and Mendelsohn,J. (1998). Recombinant humanized anti-HER2 antibody (Herceptin) enhances the antitumor activity of paclitaxel and doxorubicin against HER2/neu overexpressing human breast cancer xenografts. Cancer Res. *58*, 2825-2831.

Baselga,J. and Averbuch,S.D. (2000). ZD1839 ('Iressa') as an anticancer agent. Drugs *60 Suppl 1*, 33-40.

Baselga,J., Albanell,J., Molina,M.A., and Arribas,J. (2001). Mechanism of action of trastuzumab and scientific update. Semin. Oncol. *28*, 4-11.

Baselga,J. (2002). Combined anti-EGF receptor and anti-HER2 receptor therapy in breast cancer: a promising strategy ready for clinical testing. Ann. Oncol. *13*, 8-9.

Baselga,J. (2004). Combining the anti-EGFR agent gefitinib with chemotherapy in non-small-cell lung cancer: how do we go from INTACT to impact? J. Clin. Oncol. *22*, 759-761.

Baselga,J. and Arribas,J. (2004). Treating cancer's kinase 'addiction'. Nat. Med. *10*, 786-787.

Baselga,J. and Arteaga,C.L. (2005). Critical update and emerging trends in epidermal growth factor receptor targeting in cancer. J. Clin. Oncol. *23*, 2445-2459.

Baselga,J., Carbonell,X., Castaneda-Soto,N.J., Clemens,M., Green,M., Harvey,V., Morales,S., Barton,C., and Ghahramani,P. (2005). Phase II study of efficacy, safety, and pharmacokinetics of trastuzumab monotherapy administered on a 3-weekly schedule. J. Clin. Oncol. *23*, 2162-2171.

Baselga,J. (2006). Targeting tyrosine kinases in cancer: the second wave. Science *312*, 1175-1178.

Benz,C.C., Scott,G.K., Sarup,J.C., Johnson,R.M., Tripathy,D., Coronado,E., Shepard,H.M., and Osborne,C.K. (1992). Estrogen-dependent, tamoxifen-resistant tumorigenic growth of MCF-7 cells transfected with HER2/neu. Breast Cancer Res. Treat. *24*, 85-95.

Bernstein,C., Bernstein,H., Payne,C.M., and Garewal,H. (2002). DNA repair/pro-apoptotic dual-role proteins in five major DNA repair pathways: fail-safe protection against carcinogenesis. Mutat. Res. *511*, 145-178.

Bhat,U.G., Raychaudhuri,P., and Beck,W.T. (1999). Functional interaction between human topoisomerase IIalpha and retinoblastoma protein. Proc. Natl. Acad. Sci. U. S. A *96*, 7859-7864.

Bhattacharyya,A., Ear,U.S., Koller,B.H., Weichselbaum,R.R., and Bishop,D.K. (2000). The breast cancer susceptibility gene BRCA1 is required for subnuclear assembly of Rad51 and survival following treatment with the DNA cross-linking agent cisplatin. J. Biol. Chem. *275*, 23899-23903.

Bianco,R., Shin,I., Ritter,C.A., Yakes,F.M., Basso,A., Rosen,N., Tsurutani,J., Dennis,P.A., Mills,G.B., and Arteaga,C.L. (2003). Loss of PTEN/MMAC1/TEP in EGF receptor-expressing tumor cells counteracts the antitumor action of EGFR tyrosine kinase inhibitors. Oncogene *22*, 2812-2822.

Bieche,I., Onody,P., Laurendeau,I., Olivi,M., Vidaud,D., Lidereau,R., and Vidaud,M. (1999). Real-time reverse transcription-PCR assay for future management of ERBB2-based clinical applications. Clin. Chem. *45*, 1148-1156.

Blume-Jensen,P. and Hunter,T. (2001). Oncogenic kinase signalling. Nature *411*, 355-365.

Booy,E.P., Johar,D., Maddika,S., Pirzada,H., Sahib,M.M., Gehrke,I., Loewen,S., Louis,S.F., Kadkhoda,K., Mowat,M., and Los,M. (2006). Monoclonal and bispecific antibodies as novel therapeutics. Arch. Immunol. Ther. Exp. (Warsz.).

Bottazzi,M.E., Zhu,X., Bohmer,R.M., and Assoian,R.K. (1999). Regulation of p21(cip1) expression by growth factors and the extracellular matrix reveals a role for transient ERK activity in G1 phase. J. Cell Biol. *146*, 1255-1264.

Boulares,A.H., Yakovlev,A.G., Ivanova,V., Stoica,B.A., Wang,G., Iyer,S., and Smulson,M. (1999). Role of poly(ADP-ribose) polymerase (PARP) cleavage in apoptosis. Caspase 3-resistant PARP mutant increases rates of apoptosis in transfected cells. J. Biol. Chem. *274*, 22932-22940.

Brennan,P.J., Kumagai,T., Berezov,A., Murali,R., and Greene,M.I. (2000). HER2/neu: mechanisms of dimerization/oligomerization. Oncogene *19*, 6093-6101.

Bridges,A.J. (1999). The rationale and strategy used to develop a series of highly potent, irreversible, inhibitors of the epidermal growth factor receptor family of tyrosine kinases. Curr. Med. Chem. *6*, 825-843.

Bridges,A.J. (2001). Chemical inhibitors of protein kinases. Chem. Rev. *101*, 2541-2572.

Brodie,S.G., Xu,X., Qiao,W., Li,W.M., Cao,L., and Deng,C.X. (2001). Multiple genetic changes are associated with mammary tumorigenesis in Brca1 conditional knockout mice. Oncogene *20*, 7514-7523.

Bromberg,K.D., Burgin,A.B., and Osheroff,N. (2003). Quinolone action against human topoisomerase IIalpha: stimulation of enzyme-mediated double-stranded DNA cleavage. Biochemistry *42*, 3393-3398.

Bruns,C.J., Solorzano,C.C., Harbison,M.T., Ozawa,S., Tsan,R., Fan,D., Abbruzzese,J., Traxler,P., Buchdunger,E., Radinsky,R., and Fidler,I.J. (2000). Blockade of the epidermal growth factor receptor signaling by a novel tyrosine kinase inhibitor leads to apoptosis of endothelial cells and therapy of human pancreatic carcinoma. Cancer Res. *60*, 2926-2935.

Budihardjo,I., Oliver,H., Lutter,M., Luo,X., and Wang,X. (1999). Biochemical pathways of caspase activation during apoptosis. Annu. Rev. Cell Dev. Biol. *15*, 269-290.

Burris,H.A., III (2004). Dual kinase inhibition in the treatment of breast cancer: initial experience with the EGFR/ErbB-2 inhibitor lapatinib. Oncologist. *9 Suppl 3*, 10-15.

Burris,H.A., III, Hurwitz,H.I., Dees,E.C., Dowlati,A., Blackwell,K.L., O'Neil,B., Marcom,P.K., Ellis,M.J., Overmoyer,B., Jones,S.F., Harris,J.L., Smith,D.A., Koch,K.M., Stead,A., Mangum,S., and Spector,N.L. (2005). Phase I safety, pharmacokinetics, and clinical activity study of lapatinib (GW572016), a reversible dual inhibitor of epidermal growth factor receptor tyrosine kinases, in heavily pretreated patients with metastatic carcinomas. J. Clin. Oncol. *23*, 5305-5313.

Burstein,H.J., Harris,L.N., Marcom,P.K., Lambert-Falls,R., Havlin,K., Overmoyer,B., Friedlander,R.J., Jr., Gargiulo,J., Strenger,R., Vogel,C.L., Ryan,P.D., Ellis,M.J., Nunes,R.A., Bunnell,C.A., Campos,S.M., Hallor,M., Gelman,R., and Winer,E.P. (2003). Trastuzumab and vinorelbine as first-line therapy for HER2-overexpressing metastatic breast cancer: multicenter phase II trial with clinical outcomes, analysis of serum tumor markers as predictive factors, and cardiac surveillance algorithm. J. Clin. Oncol. *21*, 2889-2895.

Busse,D., Doughty,R.S., Ramsey,T.T., Russell,W.E., Price,J.O., Flanagan,W.M., Shawver,L.K., and Arteaga,C.L. (2000). Reversible G(1) arrest induced by inhibition of the epidermal growth factor receptor tyrosine kinase requires up-regulation of p27(KIP1) independent of MAPK activity. J. Biol. Chem. *275*, 6987-6995.

Camirand,A., Zakikhani,M., Young,F., and Pollak,M. (2005). Inhibition of insulin-like growth factor-1 receptor signaling enhances growth-inhibitory and proapoptotic effects of gefitinib (Iressa) in human breast cancer cells. Breast Cancer Res. *7*, R570-R579.

Camp,E.R., Summy,J., Bauer,T.W., Liu,W., Gallick,G.E., and Ellis,L.M. (2005). Molecular mechanisms of resistance to therapies targeting the epidermal growth factor receptor. Clin. Cancer Res. *11*, 397-405.

Campbell,I.G., Russell,S.E., Choong,D.Y., Montgomery,K.G., Ciavarella,M.L., Hooi,C.S., Cristiano,B.E., Pearson,R.B., and Phillips,W.A. (2004). Mutation of the PIK3CA gene in ovarian and breast cancer. Cancer Res. *64*, 7678-7681.

Cantley,L.C. and Neel,B.G. (1999). New insights into tumor suppression: PTEN suppresses tumor formation by restraining the phosphoinositide 3-kinase/AKT pathway. Proc. Natl. Acad. Sci. U. S. A *96*, 4240-4245.

Cappuzzo,F., Varella-Garcia,M., Shigematsu,H., Domenichini,I., Bartolini,S., Ceresoli,G.L., Rossi,E., Ludovini,V., Gregorc,V., Toschi,L., Franklin,W.A., Crino,L., Gazdar,A.F., Bunn,P.A., Jr., and Hirsch,F.R. (2005). Increased HER2 gene copy number is associated with response to gefitinib therapy in epidermal growth factor receptor-positive non-small-cell lung cancer patients. J. Clin. Oncol. *23*, 5007-5018.

Carrier,F., Georgel,P.T., Pourquier,P., Blake,M., Kontny,H.U., Antinore,M.J., Gariboldi,M., Myers,T.G., Weinstein,J.N., Pommier,Y., and Fornace,A.J., Jr. (1999). Gadd45, a p53-responsive stress protein, modifies DNA accessibility on damaged chromatin. Mol. Cell Biol. *19*, 1673-1685.

Carter,T.A., Wodicka,L.M., Shah,N.P., Velasco,A.M., Fabian,M.A., Treiber,D.K., Milanov,Z.V., Atteridge,C.E., Biggs,W.H., III, Edeen,P.T., Floyd,M., Ford,J.M., Grotzfeld,R.M., Herrgard,S., Insko,D.E., Mehta,S.A., Patel,H.K., Pao,W., Sawyers,C.L., Varmus,H., Zarrinkar,P.P., and Lockhart,D.J. (2005). Inhibition of drug-resistant mutants of ABL, KIT, and EGF receptor kinases. Proc. Natl. Acad. Sci. U. S. A *102*, 11011-11016.

Chakravarti,A., Loeffler,J.S., and Dyson,N.J. (2002). Insulin-like growth factor receptor I mediates resistance to anti-epidermal growth factor receptor therapy in primary human glioblastoma cells through continued activation of phosphoinositide 3-kinase signaling. Cancer Res. *62*, 200-207.

Chan,T.A., Hermeking,H., Lengauer,C., Kinzler,K.W., and Vogelstein,B. (1999). 14-3-3Sigma is required to prevent mitotic catastrophe after DNA damage. Nature *401*, 616-620.

Chaturvedi,P., Eng,W.K., Zhu,Y., Mattern,M.R., Mishra,R., Hurle,M.R., Zhang,X., Annan,R.S., Lu,Q., Faucette,L.F., Scott,G.F., Li,X., Carr,S.A., Johnson,R.K., Winkler,J.D., and Zhou,B.B. (1999). Mammalian Chk2 is a downstream effector of the ATM-dependent DNA damage checkpoint pathway. Oncogene *18*, 4047-4054.

Chen,C.F., Li,S., Chen,Y., Chen,P.L., Sharp,Z.D., and Lee,W.H. (1996). The nuclear localization sequences of the BRCA1 protein interact with the importin-alpha subunit of the nuclear transport signal receptor. J. Biol. Chem. *271*, 32863-32868.

Chen,C.Y., Oliner,J.D., Zhan,Q., Fornace,A.J., Jr., Vogelstein,B., and Kastan,M.B. (1994). Interactions between p53 and MDM2 in a mammalian cell cycle checkpoint pathway. Proc. Natl. Acad. Sci. U. S. A *91*, 2684-2688.

Chen,Q.Q., Chen,X.Y., Jiang,Y.Y., and Liu,J. (2005). Identification of novel nuclear localization signal within the ErbB-2 protein. Cell Res. *15*, 504-510.

Christensen,J.G., Schreck,R.E., Chan,E., Wang,X., Yang,C., Liu,L., Cui,J., Sun,L., Wei,J., Cherrington,J.M., and Mendel,D.B. (2001). High levels of HER-2 expression alter the ability of epidermal growth factor receptor (EGFR) family tyrosine kinase inhibitors to inhibit EGFR phosphorylation in vivo. Clin. Cancer Res. *7*, 4230-4238.

Christianson,T.A., Doherty,J.K., Lin,Y.J., Ramsey,E.E., Holmes,R., Keenan,E.J., and Clinton,G.M. (1998). NH2-terminally truncated HER-2/neu protein: relationship with shedding of the extracellular domain and with prognostic factors in breast cancer. Cancer Res. *58*, 5123-5129.

Cianchi,F., Cortesini,C., Fantappie,O., Messerini,L., Schiavone,N., Vannacci,A., Nistri,S., Sardi,I., Baroni,G., Marzocca,C., Perna,F., Mazzanti,R., Bechi,P., and Masini,E. (2003). Inducible nitric oxide synthase expression in human colorectal cancer: correlation with tumor angiogenesis. Am. J. Pathol. *162*, 793-801.

Ciardiello,F., Caputo,R., Bianco,R., Damiano,V., Pomatico,G., De,P.S., Bianco,A.R., and Tortora,G. (2000). Antitumor effect and potentiation of cytotoxic drugs activity in human cancer cells by ZD-1839 (Iressa), an epidermal growth factor receptor-selective tyrosine kinase inhibitor. Clin. Cancer Res. *6*, 2053-2063.

Ciardiello,F., Caputo,R., Bianco,R., Damiano,V., Fontanini,G., Cuccato,S., De,P.S., Bianco,A.R., and Tortora,G. (2001). Inhibition of growth factor production and angiogenesis in human cancer cells by ZD1839 (Iressa), a selective epidermal growth factor receptor tyrosine kinase inhibitor. Clin. Cancer Res. *7*, 1459-1465.

Ciardiello,F., Caputo,R., Damiano,V., Caputo,R., Troiani,T., Vitagliano,D., Carlomagno,F., Veneziani,B.M., Fontanini,G., Bianco,A.R., and Tortora,G. (2003). Antitumor effects of ZD6474, a small molecule vascular endothelial growth factor receptor tyrosine kinase inhibitor, with additional activity against epidermal growth factor receptor tyrosine kinase. Clin. Cancer Res. *9* , 1546-1556.

Citri,A. and Yarden,Y. (2006). EGF-ERBB signalling: towards the systems level. Nat. Rev. Mol. Cell Biol. *7*, 505-516.

Clark,D.E., Williams,C.C., Duplessis,T.T., Moring,K.L., Notwick,A.R., Long,W., Lane,W.S., Beuvink,I., Hynes,N.E., and Jones,F.E. (2005). ERBB4/HER4 potentiates STAT5A transcriptional activity by regulating novel STAT5A serine phosphorylation events. J. Biol. Chem. *280*, 24175-24180.

Clingen,P.H., De,S., I, McHugh,P.J., Ghadessy,F.J., Tilby,M.J., Thurston,D.E., and Hartley,J.A. (2005). The XPF-ERCC1 endonuclease and homologous recombination contribute to the repair of minor groove DNA interstrand crosslinks in mammalian cells produced by the pyrrolo[2,1-c][1,4]benzodiazepine dimer SJG-136. Nucleic Acids Res. *33*, 3283-3291.

Clynes,R.A., Towers,T.L., Presta,L.G., and Ravetch,J.V. (2000). Inhibitory Fc receptors modulate in vivo cytoxicity against tumor targets. Nat. Med. *6*, 443-446.

Cobleigh,M.A., Vogel,C.L., Tripathy,D., Robert,N.J., Scholl,S., Fehrenbacher,L., Wolter,J.M., Paton,V., Shak,S., Lieberman,G., and Slamon,D.J. (1999). Multinational study of the efficacy and safety of humanized anti-HER2 monoclonal antibody in women who have HER2-overexpressing metastatic breast cancer that has progressed after chemotherapy for metastatic disease. J. Clin. Oncol. *17*, 2639-2648.

Coene,E.D., Hollinshead,M.S., Waeytens,A.A., Schelfhout,V.R., Eechaute,W.P., Shaw,M.K., Van Oostveldt,P.M., and Vaux,D.J. (2005). Phosphorylated BRCA1 is predominantly located in the nucleus and mitochondria. Mol. Biol. Cell *16*, 997-1010.

Collado,M., Medema,R.H., Garcia-Cao,I., Dubuisson,M.L., Barradas,M., Glassford,J., Rivas,C., Burgering,B.M., Serrano,M., and Lam,E.W. (2000). Inhibition of the phosphoinositide 3-kinase pathway induces a senescence-like arrest mediated by p27Kip1. J. Biol. Chem. *275*, 21960-21968.

Cooley,S., Burns,L.J., Repka,T., and Miller,J.S. (1999). Natural killer cell cytotoxicity of breast cancer targets is enhanced by two distinct mechanisms of antibody-dependent cellular cytotoxicity against LFA-3 and HER2/neu. Exp. Hematol. *27*, 1533-1541.

Cortez,D., Wang,Y., Qin,J., and Elledge,S.J. (1999). Requirement of ATM-dependent phosphorylation of brca1 in the DNA damage response to double-strand breaks. Science *286*, 1162-1166.

Crombet-Ramos,T., Rak,J., Perez,R., and Viloria-Petit,A. (2002). Antiproliferative, antiangiogenic and proapoptotic activity of h-R3: A humanized anti-EGFR antibody. Int. J. Cancer *101*, 567-575.

Crombet,T., Osorio,M., Cruz,T., Roca,C., del,C.R., Mon,R., Iznaga-Escobar,N., Figueredo,R., Koropatnick,J., Renginfo,E., Fernandez,E., Alvarez,D., Torres,O., Ramos,M., Leonard,I., Perez,R., and Lage,A. (2004). Use of the humanized anti-epidermal growth factor receptor monoclonal antibody h-R3 in combination with radiotherapy in the treatment of locally advanced head and neck cancer patients. J. Clin. Oncol. *22*, 1646-1654.

Crowder,R.J., Lombardi,D.P., and Ellis,M.J. (2004). Successful targeting of ErbB2 receptors-is PTEN the key? Cancer Cell *6*, 103-104.

Cuello,M., Ettenberg,S.A., Clark,A.S., Keane,M.M., Posner,R.H., Nau,M.M., Dennis,P.A., and Lipkowitz,S. (2001). Down-regulation of the erbB-2 receptor by trastuzumab (herceptin) enhances tumor necrosis factor-related apoptosis-inducing ligand-mediated apoptosis in breast and ovarian cancer cell lines that overexpress erbB-2. Cancer Res. *61*, 4892-4900.

Cullinane,C., Mazur,S.J., Essigmann,J.M., Phillips,D.R., and Bohr,V.A. (1999). Inhibition of RNA polymerase II transcription in human cell extracts by cisplatin DNA damage. Biochemistry *38*, 6204-6212.

Cunningham,D., Humblet,Y., Siena,S., Khayat,D., Bleiberg,H., Santoro,A., Bets,D., Mueser,M., Harstrick,A., Verslype,C., Chau,I., and Van,C.E. (2004). Cetuximab monotherapy and cetuximab plus irinotecan in irinotecan-refractory metastatic colorectal cancer. N. Engl. J. Med. *351*, 337-345.

Danielsen,A.J. and Maihle,N.J. (2002). The EGF/ErbB receptor family and apoptosis. Growth Factors *20*, 1-15.

Datta,S.R., Brunet,A., and Greenberg,M.E. (1999). Cellular survival: a play in three Akts. Genes Dev. *13*, 2905-2927.

Davies,D.E. and Chamberlin,S.G. (1996). Targeting the epidermal growth factor receptor for therapy of carcinomas. Biochem. Pharmacol. *51* , 1101-1110.

Davis,L.I. and Blobel,G. (1987). Nuclear pore complex contains a family of glycoproteins that includes p62: glycosylation through a previously unidentified cellular pathway. Proc. Natl. Acad. Sci. U. S. A *84*, 7552-7556.

De Kok,J.B., Roelofs,R.W., Giesendorf,B.A., Pennings,J.L., Waas,E.T., Feuth,T., Swinkels,D.W., and Span,P.N. (2005). Normalization of gene expression measurements in tumor tissues: comparison of 13 endogenous control genes. Lab Invest *85*, 154-159.

de Laat,W.L., Jaspers,N.G., and Hoeijmakers,J.H. (1999). Molecular mechanism of nucleotide excision repair. Genes Dev. *13*, 768-785.

De,S., I, McHugh,P.J., Clingen,P.H., and Hartley,J.A. (2000). Defining the roles of nucleotide excision repair and recombination in the repair of DNA interstrand cross-links in mammalian cells. Mol. Cell Biol. *20*, 7980-7990.

De,S., I, McHugh,P.J., Clingen,P.H., and Hartley,J.A. (2002). Defects in interstrand cross-link uncoupling do not account for the extreme sensitivity of ERCC1 and XPF cells to cisplatin. Nucleic Acids Res. *30*, 3848-3856.

Dehm,S.M. and Bonham,K. (2004). SRC gene expression in human cancer: the role of transcriptional activation. Biochem. Cell Biol. *82*, 263-274.

Delcommenne,M., Tan,C., Gray,V., Rue,L., Woodgett,J., and Dedhar,S. (1998). Phosphoinositide-3-OH kinase-dependent regulation of glycogen synthase kinase 3 and protein kinase B/AKT by the integrin-linked kinase. Proc. Natl. Acad. Sci. U. S. A *95*, 11211-11216.

Demetri,G.D., van Oosterom,A.T., Garrett,C.R., Blackstein,M.E., Shah,M.H., Verweij,J., McArthur,G., Judson,I.R., Heinrich,M.C., Morgan,J.A., Desai,J., Fletcher,C.D., George,S., Bello,C.L., Huang,X., Baum,C.M., and Casali,P.G. (2006). Efficacy and safety of sunitinib in patients with advanced gastrointestinal stromal tumour after failure of imatinib: a randomised controlled trial. Lancet *368*, 1329-1338.

Deming,P.B., Cistulli,C.A., Zhao,H., Graves,P.R., Piwnica-Worms,H., Paules,R.S., Downes,C.S., and Kaufmann,W.K. (2001). The human decatenation checkpoint. Proc. Natl. Acad. Sci. U. S. A *98*, 12044-12049.

Deng,C., Zhang,P., Harper,J.W., Elledge,S.J., and Leder,P. (1995). Mice lacking p21CIP1/WAF1 undergo normal development, but are defective in G1 checkpoint control. Cell *82*, 675-684.

Deng,C.X. and Brodie,S.G. (2000). Roles of BRCA1 and its interacting proteins. Bioessays *22*, 728-737.

Deng,C.X. (2002). Roles of BRCA1 in centrosome duplication. Oncogene *21*, 6222-6227.

Denny,W.A. (2002). Irreversible inhibitors of the ErbB family of protein tyrosine kinases. Pharmacol. Ther. *93*, 253-261.

Deutsch,E., Dugray,A., Abdulkarim,B., Marangoni,E., Maggiorella,L., Vaganay,S., M'Kacher,R., Rasy,S.D., Eschwege,F., Vainchenker,W., Turhan,A.G., and Bourhis,J. (2001). BCR-ABL down-regulates the DNA repair protein DNA-PKcs. Blood *97*, 2084-2090.

Di Fiore,P.P., Pierce,J.H., Kraus,M.H., Segatto,O., King,C.R., and Aaronson,S.A. (1987). erbB-2 is a potent oncogene when overexpressed in NIH/3T3 cells. Science *237*, 178-182.

Di,C.A., De,A.M., Koff,A., Cordon-Cardo,C., and Pandolfi,P.P. (2001). Pten and p27KIP1 cooperate in prostate cancer tumor suppression in the mouse. Nat. Genet. *27*, 222-224.

Di,G.E., Barbarino,M., Bruzzese,F., De,L.S., Caraglia,M., Abbruzzese,A., Avallone,A., Comella,P., Caponigro,F., Pepe,S., and Budillon,A. (2003). Critical role of both p27KIP1 and p21CIP1/WAF1 in the antiproliferative effect of ZD1839 ('Iressa'), an epidermal growth factor receptor tyrosine kinase inhibitor, in head and neck squamous carcinoma cells. J. Cell Physiol *195*, 139-150.

Dittmann,K., Mayer,C., Fehrenbacher,B., Schaller,M., Raju,U., Milas,L., Chen,D.J., Kehlbach,R., and Rodemann,H.P. (2005). Radiation-induced epidermal growth factor receptor nuclear import is linked to activation of DNA-dependent protein kinase. J. Biol. Chem. *280*, 31182-31189.

Dronkert,M.L. and Kanaar,R. (2001). Repair of DNA interstrand cross-links. Mutat. Res. *486*, 217-247.

Dunn,K.L., Espino,P.S., Drobic,B., He,S., and Davie,J.R. (2005). The Ras-MAPK signal transduction pathway, cancer and chromatin remodeling. Biochem. Cell Biol. *83*, 1-14.

Duxbury,M.S. and Whang,E.E. (2004). RNA interference: a practical approach. J. Surg. Res. *117*, 339-344.

Eastman,A. (2004). Cell cycle checkpoints and their impact on anticancer therapeutic strategies. J. Cell Biochem. *91*, 223-231.

Eder,J.P., Jr., Chan,V.T., Ng,S.W., Rizvi,N.A., Zacharoulis,S., Teicher,B.A., and Schnipper,L.E. (1995). DNA topoisomerase II alpha expression is associated with alkylating agent resistance. Cancer Res. *55*, 6109-6116.

Ekstrand,A.J., Sugawa,N., James,C.D., and Collins,V.P. (1992). Amplified and rearranged epidermal growth factor receptor genes in human glioblastomas reveal deletions of sequences encoding portions of the N- and/or C-terminal tails. Proc. Natl. Acad. Sci. U. S. A *89*, 4309-4313.

El-Deiry,W.S., Tokino,T., Velculescu,V.E., Levy,D.B., Parsons,R., Trent,J.M., Lin,D., Mercer,W.E., Kinzler,K.W., and Vogelstein,B. (1993). WAF1, a potential mediator of p53 tumor suppression. Cell *75*, 817-825.

El-Deiry,W.S. (1998). p21/p53, cellular growth control and genomic integrity. Curr. Top. Microbiol. Immunol. *227*, 121-137.

Elbashir,S.M., Harborth,J., Lendeckel,W., Yalcin,A., Weber,K., and Tuschl,T. (2001). Duplexes of 21-nucleotide RNAs mediate RNA interference in cultured mammalian cells. Nature *411*, 494-498.

Emens,L.A. and Davidson,N.E. (2004). Trastuzumab in breast cancer. Oncology (Williston. Park) *18*, 1117-1128.

Esteva,F.J., Sahin,A.A., Cristofanilli,M., Arun,B., and Hortobagyi,G.N. (2002). Molecular prognostic factors for breast cancer metastasis and survival. Semin. Radiat. Oncol. *12*, 319-328.

Esteva,F.J., Cheli,C.D., Fritsche,H., Fornier,M., Slamon,D., Thiel,R.P., Luftner,D., and Ghani,F. (2005). Clinical utility of serum HER2/neu in monitoring and prediction of progression-free survival in metastatic breast cancer patients treated with trastuzumab-based therapies. Breast Cancer Res. *7*, R436-R443.

Faltus,T., Yuan,J., Zimmer,B., Kramer,A., Loibl,S., Kaufmann,M., and Strebhardt,K. (2004). Silencing of the HER2/neu gene by siRNA inhibits proliferation and induces apoptosis in HER2/neu-overexpressing breast cancer cells. Neoplasia. *6*, 786-795.

Fayard,E., Tintignac,L.A., Baudry,A., and Hemmings,B.A. (2005). Protein kinase B/Akt at a glance. J. Cell Sci. *118*, 5675-5678.

Fedier,A., Steiner,R.A., Schwarz,V.A., Lenherr,L., Haller,U., and Fink,D. (2003). The effect of loss of Brca1 on the sensitivity to anticancer agents in p53-deficient cells. Int. J. Oncol. *22*, 1169-1173.

Finlay,D.R., Newmeyer,D.D., Price,T.M., and Forbes,D.J. (1987). Inhibition of in vitro nuclear transport by a lectin that binds to nuclear pores. J. Cell Biol. *104*, 189-200.

Flatt,P.M., Tang,L.J., Scatena,C.D., Szak,S.T., and Pietenpol,J.A. (2000). p53 regulation of G(2) checkpoint is retinoblastoma protein dependent. Mol. Cell Biol. *20*, 4210-4223.

Folias,A., Matkovic,M., Bruun,D., Reid,S., Hejna,J., Grompe,M., D'Andrea,A., and Moses,R. (2002). BRCA1 interacts directly with the Fanconi anemia protein FANCA. Hum. Mol. Genet. *11*, 2591-2597.

Franklin,M.C., Carey,K.D., Vajdos,F.F., Leahy,D.J., de Vos,A.M., and Sliwkowski,M.X. (2004). Insights into ErbB signaling from the structure of the ErbB2-pertuzumab complex. Cancer Cell *5*, 317-328.

Fridman,J.S. and Lowe,S.W. (2003). Control of apoptosis by p53. Oncogene *22*, 9030-9040.

Friedmann,B., Caplin,M., Hartley,J.A., and Hochhauser,D. (2004). Modulation of DNA repair in vitro after treatment with chemotherapeutic agents by the epidermal growth factor receptor inhibitor gefitinib (ZD1839). Clin. Cancer Res. *10*, 6476-6486.

Friedmann,B.J., Caplin,M., Savic,B., Shah,T., Lord,C.J., Ashworth,A., Hartley,J.A., and Hochhauser,D. (2006). Interaction of the epidermal growth factor receptor and the DNA-dependent protein kinase pathway following gefitinib treatment. Mol. Cancer Ther. *5*, 209-218.

Fry,D.W. (1999). Inhibition of the epidermal growth factor receptor family of tyrosine kinases as an approach to cancer chemotherapy: progression from reversible to irreversible inhibitors. Pharmacol. Ther. *82*, 207-218.

Fujita,T., Doihara,H., Kawasaki,K., Takabatake,D., Takahashi,H., Washio,K., Tsukuda,K., Ogasawara,Y., and Shimizu,N. (2006). PTEN activity could be a predictive marker of trastuzumab efficacy in the treatment of ErbB2-overexpressing breast cancer. Br. J. Cancer *94*, 247-252.

Fulda,S., Friesen,C., and Debatin,K.M. (1998). Molecular determinants of apoptosis induced by cytotoxic drugs. Klin. Padiatr. *210*, 148-152.

Furnari,B., Rhind,N., and Russell,P. (1997). Cdc25 mitotic inducer targeted by chk1 DNA damage checkpoint kinase. Science *277*, 1495-1497.

Fury,M.G., Lipton,A., Smith,K.M., Winston,C.B., and Pfister,D.G. (2007). A phase-I trial of the epidermal growth factor receptor directed bispecific antibody MDX-447 without and with recombinant human granulocyte-colony stimulating factor in patients with advanced solid tumors. Cancer Immunol. Immunother.

Garcia-Echeverria,C., Pearson,M.A., Marti,A., Meyer,T., Mestan,J., Zimmermann,J., Gao,J., Brueggen,J., Capraro,H.G., Cozens,R., Evans,D.B., Fabbro,D., Furet,P., Porta,D.G., Liebetanz,J., Martiny-Baron,G., Ruetz,S., and Hofmann,F. (2004). In vivo antitumor activity of NVP-AEW541-A novel, potent, and selective inhibitor of the IGF-IR kinase. Cancer Cell *5*, 231-239.

Garcia-Higuera,I., Taniguchi,T., Ganesan,S., Meyn,M.S., Timmers,C., Hejna,J., Grompe,M., and D'Andrea,A.D. (2001). Interaction of the Fanconi anemia proteins and BRCA1 in a common pathway. Mol. Cell *7*, 249-262.

Garcia,R., Bowman,T.L., Niu,G., Yu,H., Minton,S., Muro-Cacho,C.A., Cox,C.E., Falcone,R., Fairclough,R., Parsons,S., Laudano,A., Gazit,A., Levitzki,A., Kraker,A., and Jove,R. (2001). Constitutive activation of Stat3 by the Src and JAK tyrosine kinases participates in growth regulation of human breast carcinoma cells. Oncogene *20*, 2499-2513.

Fountzilas,G., Tsavdaridis,D., Kalogera-Fountzila,A., Christodoulou,C.H., Timotheadou,E., Kalofonos,C.H., Kosmidis,P., Adamou,A., Papakostas,P., Gogas,H., Stathopoulos,G., Razis,E., Bafaloukos,D., and Skarlos,D. (2001). Weekly paclitaxel as first-line chemotherapy and trastuzumab in patients with advanced breast cancer. A Hellenic Cooperative Oncology Group phase II study. Ann. Oncol. *12*, 1545-1551.

Gatei,M., Zhou,B.B., Hobson,K., Scott,S., Young,D., and Khanna,K.K. (2001). Ataxia telangiectasia mutated (ATM) kinase and ATM and Rad3 related kinase mediate phosphorylation of Brca1 at distinct and overlapping sites. In vivo assessment using phospho-specific antibodies. J. Biol. Chem. *276*, 17276-17280.

Gatzemeier,U., Pluzanska,A., Szczesna,A., Kaukel,E., Roubec,J., De,R.F., Milanowski,J., Karnicka-Mlodkowski,H., Pesek,M., Serwatowski,P., Ramlau,R., Janaskova,T., Vansteenkiste,J., Strausz,J., Manikhas,G.M., and Von,P.J. (2007). Phase III study of erlotinib in combination with cisplatin and gemcitabine in advanced non-small-cell lung cancer: the Tarceva Lung Cancer Investigation Trial. J. Clin. Oncol. *25*, 1545-1552.

Gennari,R., Menard,S., Fagnoni,F., Ponchio,L., Scelsi,M., Tagliabue,E., Castiglioni,F., Villani,L., Magalotti,C., Gibelli,N., Oliviero,B., Ballardini,B., Da,P.G., Zambelli,A., and Costa,A. (2004). Pilot study of the mechanism of action of preoperative trastuzumab in patients with primary operable breast tumors overexpressing HER2. Clin. Cancer Res. *10*, 5650-5655.

Giaccone,G., Herbst,R.S., Manegold,C., Scagliotti,G., Rosell,R., Miller,V., Natale,R.B., Schiller,J.H., Von,P.J., Pluzanska,A., Gatzemeier,U., Grous,J., Ochs,J.S., Averbuch,S.D., Wolf,M.K., Rennie,P., Fandi,A., and Johnson,D.H. (2004). Gefitinib in combination with gemcitabine and cisplatin in advanced non-small-cell lung cancer: a phase III trial--INTACT 1. J. Clin. Oncol. *22*, 777-784.

Ginestier,C., Adelaide,J., Goncalves,A., Repellini,L., Sircoulomb,F., Letessier,A., Finetti,P., Geneix,J., Charafe-Jauffret,E., Bertucci,F., Jacquemier,J., Viens,P., and Birnbaum,D. (2007). ERBB2 phosphorylation and trastuzumab sensitivity of breast cancer cell lines. Oncogene.

Giri,D.K., li-Seyed,M., Li,L.Y., Lee,D.F., Ling,P., Bartholomeusz,G., Wang,S.C., and Hung,M.C. (2005). Endosomal transport of ErbB-2: mechanism for nuclear entry of the cell surface receptor. Mol. Cell Biol. *25*, 11005-11018.

Godard,T., Fessard,V., Huet,S., Mourot,A., Deslandes,E., Pottier,D., Hyrien,O., Sichel,F., Gauduchon,P., and Poul,J. (1999). Comparative in vitro and in vivo assessment of genotoxic effects of etoposide and chlorothalonil by the comet assay. Mutat. Res. *444*, 103-116.

Gong,S.J., Jin,C.J., Rha,S.Y., and Chung,H.C. (2004). Growth inhibitory effects of trastuzumab and chemotherapeutic drugs in gastric cancer cell lines. Cancer Lett. *214*, 215-224.

Graus-Porta,D., Beerli,R.R., Daly,J.M., and Hynes,N.E. (1997). ErbB-2, the preferred heterodimerization partner of all ErbB receptors, is a mediator of lateral signaling. EMBO J. *16*, 1647-1655.

Greulich,H., Chen,T.H., Feng,W., Janne,P.A., Alvarez,J.V., Zappaterra,M., Bulmer,S.E., Frank,D.A., Hahn,W.C., Sellers,W.R., and Meyerson,M. (2005). Oncogenic transformation by inhibitor-sensitive and -resistant EGFR mutants. PLoS. Med. *2*, e313.

Grunwald,V. and Hidalgo,M. (2003). Development of the epidermal growth factor receptor inhibitor Tarceva (OSI-774). Adv. Exp. Med. Biol. *532*, 235-246.

Gschwind,A., Fischer,O.M., and Ullrich,A. (2004). The discovery of receptor tyrosine kinases: targets for cancer therapy. Nat. Rev. Cancer *4*, 361-370.

Guan,H., Jia,S.F., Zhou,Z., Stewart,J., and Kleinerman,E.S. (2005). Herceptin down-regulates HER-2/neu and vascular endothelial growth factor expression and enhances taxol-induced cytotoxicity of human Ewing's sarcoma cells in vitro and in vivo. Clin. Cancer Res. *11*, 2008-2017.

Hakem,R., de la Pompa,J.L., Elia,A., Potter,J., and Mak,T.W. (1997). Partial rescue of Brca1 (5-6) early embryonic lethality by p53 or p21 null mutation. Nat. Genet. *16*, 298-302.

Hanada,N., Lo,H.W., Day,C.P., Pan,Y., Nakajima,Y., and Hung,M.C. (2006). Co-regulation of B-Myb expression by E2F1 and EGF receptor. Mol. Carcinog. *45*, 10-17.

Hanahan,D. and Weinberg,R.A. (2000). The hallmarks of cancer. Cell *100*, 57-70.

Hancock,M.C., Langton,B.C., Chan,T., Toy,P., Monahan,J.J., Mischak,R.P., and Shawver,L.K. (1991). A monoclonal antibody against the c-erbB-2 protein enhances the cytotoxicity of cis-diamminedichloroplatinum against human breast and ovarian tumor cell lines. Cancer Res. *51*, 4575-4580.

Hansson,J., Lewensohn,R., Ringborg,U., and Nilsson,B. (1987). Formation and removal of DNA cross-links induced by melphalan and nitrogen mustard in relation to drug-induced cytotoxicity in human melanoma cells. Cancer Res. *47*, 2631-2637.

Harari,D., Tzahar,E., Romano,J., Shelly,M., Pierce,J.H., Andrews,G.C., and Yarden,Y. (1999). Neuregulin-4: a novel growth factor that acts through the ErbB-4 receptor tyrosine kinase. Oncogene *18*, 2681-2689.

Harari,D. and Yarden,Y. (2000). Molecular mechanisms underlying ErbB2/HER2 action in breast cancer. Oncogene *19*, 6102-6114.

Harari,P.M., Allen,G.W., and Bonner,J.A. (2007). Biology of interactions: antiepidermal growth factor receptor agents. J. Clin. Oncol. *25*, 4057-4065.

Harbour,J.W. (1999). Tumor suppressor genes in ophthalmology. Surv. Ophthalmol. *44*, 235-246.

Harkin,D.P., Bean,J.M., Miklos,D., Song,Y.H., Truong,V.B., Englert,C., Christians,F.C., Ellisen,L.W., Maheswaran,S., Oliner,J.D., and Haber,D.A. (1999). Induction of GADD45 and JNK/SAPK-dependent apoptosis following inducible expression of BRCA1. Cell *97*, 575-586.

Harris,L.N., Yang,L., Liotcheva,V., Pauli,S., Iglehart,J.D., Colvin,O.M., and Hsieh,T.S. (2001). Induction of topoisomerase II activity after ErbB2 activation is associated with a differential response to breast cancer chemotherapy. Clin. Cancer Res. *7*, 1497-1504.

Hartley,J.M., Spanswick,V.J., Gander,M., Giacomini,G., Whelan,J., Souhami,R.L., and Hartley,J.A. (1999). Measurement of DNA cross-linking in patients on ifosfamide therapy using the single cell gel electrophoresis (comet) assay. Clin. Cancer Res. *5*, 507-512.

Hartman,A.R. and Ford,J.M. (2002). BRCA1 induces DNA damage recognition factors and enhances nucleotide excision repair. Nat. Genet. *32*, 180-184.

Hashizume,R., Fukuda,M., Maeda,I., Nishikawa,H., Oyake,D., Yabuki,Y., Ogata,H., and Ohta,T. (2001). The RING heterodimer BRCA1-BARD1 is a ubiquitin ligase inactivated by a breast cancer-derived mutation. J. Biol. Chem. *276*, 14537-14540.

Hay,N. (2005). The Akt-mTOR tango and its relevance to cancer. Cancer Cell *8*, 179-183.

Hayes,D.F., Yamauchi,H., Broadwater,G., Cirrincione,C.T., Rodrigue,S.P., Berry,D.A., Younger,J., Panasci,L.L., Millard,F., Duggan,D.B., Norton,L., and Henderson,I.C. (2001). Circulating HER-2/erbB-2/c-neu (HER-2) extracellular domain as a prognostic factor in patients with metastatic breast cancer: Cancer and Leukemia Group B Study 8662. Clin. Cancer Res. *7*, 2703-2711.

Heinrich,M.C., Corless,C.L., Demetri,G.D., Blanke,C.D., von,M.M., Joensuu,H., McGreevey,L.S., Chen,C.J., Van den Abbeele,A.D., Druker,B.J., Kiese,B., Eisenberg,B., Roberts,P.J., Singer,S., Fletcher,C.D., Silberman,S., Dimitrijevic,S., and Fletcher,J.A. (2003). Kinase mutations and imatinib response in patients with metastatic gastrointestinal stromal tumor. J. Clin. Oncol. *21*, 4342-4349.

Herbst,R.S., Giaccone,G., Schiller,J.H., Natale,R.B., Miller,V., Manegold,C., Scagliotti,G., Rosell,R., Oliff,I., Reeves,J.A., Wolf,M.K., Krebs,A.D., Averbuch,S.D., Ochs,J.S., Grous,J., Fandi,A., and Johnson,D.H. (2004). Gefitinib in combination with paclitaxel and carboplatin in advanced non-small-cell lung cancer: a phase III trial--INTACT 2. J. Clin. Oncol. *22*, 785-794.

Herbst,R.S., Johnson,D.H., Mininberg,E., Carbone,D.P., Henderson,T., Kim,E.S., Blumenschein,G., Jr., Lee,J.J., Liu,D.D., Truong,M.T., Hong,W.K., Tran,H., Tsao,A., Xie,D., Ramies,D.A., Mass,R., Seshagiri,S., Eberhard,D.A., Kelley,S.K., and Sandler,A. (2005). Phase I/II trial evaluating the anti-vascular endothelial growth factor monoclonal antibody bevacizumab in combination with the HER-1/epidermal growth factor receptor tyrosine kinase inhibitor erlotinib for patients with recurrent non-small-cell lung cancer. J. Clin. Oncol. *23*, 2544-2555.

Hernandez-Sotomayor,S.M. and Carpenter,G. (1992). Epidermal growth factor receptor: elements of intracellular communication. J. Membr. Biol. *128*, 81-89.

Herynk,M.H., Stoeltzing,O., Reinmuth,N., Parikh,N.U., Abounader,R., Laterra,J., Radinsky,R., Ellis,L.M., and Gallick,G.E. (2003). Down-regulation of c-Met inhibits growth in the liver of human colorectal carcinoma cells. Cancer Res. *63*, 2990-2996.

Hidalgo,M., Siu,L.L., Nemunaitis,J., Rizzo,J., Hammond,L.A., Takimoto,C., Eckhardt,S.G., Tolcher,A., Britten,C.D., Denis,L., Ferrante,K., Von Hoff,D.D., Silberman,S., and Rowinsky,E.K. (2001). Phase I and pharmacologic study of OSI-774, an epidermal growth factor receptor tyrosine kinase inhibitor, in patients with advanced solid malignancies. J. Clin. Oncol. *19*, 3267-3279.

Hochhauser,D., Valkov,N.I., Gump,J.L., Wei,I., O'Hare,C., Hartley,J., Fan,J., Bertino,J.R., Banerjee,D., and Sullivan,D.M. (1999). Effects of wild-type p53 expression on the quantity and activity of topoisomerase IIalpha and beta in various human cancer cell lines. J. Cell Biochem. *75*, 245-257.

Hoeijmakers,J.H. (2001a). Genome maintenance mechanisms for preventing cancer. Nature *411*, 366-374.

Hoeijmakers,J.H. (2001b). DNA repair mechanisms. Maturitas *38*, 17-22.

Howlett,N.G., Taniguchi,T., Olson,S., Cox,B., Waisfisz,Q., De Die-Smulders,C., Persky,N., Grompe,M., Joenje,H., Pals,G., Ikeda,H., Fox,E.A., and D'Andrea,A.D. (2002). Biallelic inactivation of BRCA2 in Fanconi anemia. Science *297*, 606-609.

Hsu,S.C. and Hung,M.C. (2007). Characterization of a novel tripartite nuclear localization sequence in the EGFR family. J. Biol. Chem. *282*, 10432-10440.

Hu,W. and Jans,D.A. (1999). Efficiency of importin alpha/beta-mediated nuclear localization sequence recognition and nuclear import. Differential role of NTF2. J. Biol. Chem. *274*, 15820-15827.

Huang,S.M., Li,J., Armstrong,E.A., and Harari,P.M. (2002). Modulation of radiation response and tumor-induced angiogenesis after epidermal growth factor receptor inhibition by ZD1839 (Iressa). Cancer Res. *62*, 4300-4306.

Hudziak,R.M., Schlessinger,J., and Ullrich,A. (1987). Increased expression of the putative growth factor receptor p185HER2 causes transformation and tumorigenesis of NIH 3T3 cells. Proc. Natl. Acad. Sci. U. S. A *84*, 7159-7163.

Hunter,T. (1998). The role of tyrosine phosphorylation in cell growth and disease. Harvey Lect. *94*, 81-119.

Husain,A., He,G., Venkatraman,E.S., and Spriggs,D.R. (1998). BRCA1 up-regulation is associated with repair-mediated resistance to cis-diamminedichloroplatinum(II). Cancer Res. *58*, 1120-1123.

Hynes,N.E. and Lane,H.A. (2005). ERBB receptors and cancer: the complexity of targeted inhibitors. Nat. Rev. Cancer *5*, 341-354.

Innocente,S.A., Abrahamson,J.L., Cogswell,J.P., and Lee,J.M. (1999). p53 regulates a G2 checkpoint through cyclin B1. Proc. Natl. Acad. Sci. U. S. A *96*, 2147-2152.

Izumi,Y., Xu,L., di,T.E., Fukumura,D., and Jain,R.K. (2002). Tumour biology: herceptin acts as an anti-angiogenic cocktail. Nature *416*, 279-280.

Jackson,S.P. (2002). Sensing and repairing DNA double-strand breaks. Carcinogenesis *23*, 687-696.

Jakupec,M.A., Galanski,M., and Keppler,B.K. (2003). Tumour-inhibiting platinum complexes--state of the art and future perspectives. Rev. Physiol Biochem. Pharmacol. *146*, 1-54.

James,C.R., Quinn,J.E., Mullan,P.B., Johnston,P.G., and Harkin,D.P. (2007). BRCA1, a potential predictive biomarker in the treatment of breast cancer. Oncologist. *12*, 142-150.

Järvinen,T.A., Kononen,J., Pelto-Huikko,M., and Isola,J. (1996). Expression of topoisomerase IIalpha is associated with rapid cell proliferation, aneuploidy, and c-erbB2 overexpression in breast cancer. Am. J. Pathol. *148*, 2073-2082.

Järvinen,T.A., Tanner,M., Rantanen,V., Barlund,M., Borg,A., Grenman,S., and Isola,J. (2000). Amplification and deletion of topoisomerase IIalpha associate with ErbB-2 amplification and affect sensitivity to topoisomerase II inhibitor doxorubicin in breast cancer. Am. J. Pathol. *156*, 839-847.

Järvinen,T.A. and Liu,E.T. (2003). HER-2/neu and topoisomerase IIalpha in breast cancer. Breast Cancer Res. Treat. *78*, 299-311.

Järvinen,T.A. and Liu,E.T. (2006). Simultaneous amplification of HER-2 (ERBB2) and topoisomerase IIalpha (TOP2A) genes--molecular basis for combination chemotherapy in cancer. Curr. Cancer Drug Targets. *6*, 579-602.

Jasin,M. (2002). Homologous repair of DNA damage and tumorigenesis: the BRCA connection. Oncogene *21*, 8981-8993.

Jeggo,P.A. (1998). Identification of genes involved in repair of DNA double-strand breaks in mammalian cells. Radiat. Res. *150*, S80-S91.

Johnson,J.R., Cohen,M., Sridhara,R., Chen,Y.F., Williams,G.M., Duan,J., Gobburu,J., Booth,B., Benson,K., Leighton,J., Hsieh,L.S., Chidambaram,N., Zimmerman,P., and Pazdur,R. (2005). Approval summary for erlotinib for treatment of patients with locally advanced or metastatic non-small cell lung cancer after failure of at least one prior chemotherapy regimen. Clin. Cancer Res. *11*, 6414-6421.

Jung,Y.D., Mansfield,P.F., Akagi,M., Takeda,A., Liu,W., Bucana,C.D., Hicklin,D.J., and Ellis,L.M. (2002). Effects of combination anti-vascular endothelial growth factor receptor and anti-epidermal growth factor receptor therapies on the growth of gastric cancer in a nude mouse model. Eur. J. Cancer *38*, 1133-1140.

Kamio,T., Shigematsu,K., Sou,H., Kawai,K., and Tsuchiyama,H. (1990). Immunohistochemical expression of epidermal growth factor receptors in human adrenocortical carcinoma. Hum. Pathol. *21*, 277-282.

Kandel,E.S., Skeen,J., Majewski,N., Di,C.A., Pandolfi,P.P., Feliciano,C.S., Gartel,A., and Hay,N. (2002). Activation of Akt/protein kinase B overcomes a G(2)/m cell cycle checkpoint induced by DNA damage. Mol. Cell Biol. *22*, 7831-7841.

Kannan,K., Kaminski,N., Rechavi,G., Jakob-Hirsch,J., Amariglio,N., and Givol,D. (2001). DNA microarray analysis of genes involved in p53 mediated apoptosis: activation of Apaf-1. Oncogene *20*, 3449-3455.

Karunagaran,D., Tzahar,E., Beerli,R.R., Chen,X., Graus-Porta,D., Ratzkin,B.J., Seger,R., Hynes,N.E., and Yarden,Y. (1996). ErbB-2 is a common auxiliary subunit of NDF and EGF receptors: implications for breast cancer. EMBO J. *15*, 254-264.

Kasprzyk,P.G., Song,S.U., Di Fiore,P.P., and King,C.R. (1992). Therapy of an animal model of human gastric cancer using a combination of anti-erbB-2 monoclonal antibodies. Cancer Res. *52*, 2771-2776.

Kawada,M., Yamagoe,S., Murakami,Y., Suzuki,K., Mizuno,S., and Uehara,Y. (1997). Induction of p27Kip1 degradation and anchorage independence by Ras through the MAP kinase signaling pathway. Oncogene *15*, 629-637.

Kawakami,Y., Nishimoto,H., Kitaura,J., Maeda-Yamamoto,M., Kato,R.M., Littman,D.R., Leitges,M., Rawlings,D.J., and Kawakami,T. (2004). Protein kinase C betaII regulates Akt phosphorylation on Ser-473 in a cell type- and stimulus-specific fashion. J. Biol. Chem. *279*, 47720-47725.

Keith,W.N., Tan,K.B., and Brown,R. (1992). Amplification of the topoisomerase II alpha gene in a non-small cell lung cancer cell line and characterisation of polymorphisms at the human topoisomerase II alpha and beta loci in normal tissue. Genes Chromosomes. Cancer *4*, 169-175.

Kellner,U., Sehested,M., Jensen,P.B., Gieseler,F., and Rudolph,P. (2002). Culprit and victim -- DNA topoisomerase II. Lancet Oncol. *3*, 235-243.

Kelloff,G.J., Fay,J.R., Steele,V.E., Lubet,R.A., Boone,C.W., Crowell,J.A., and Sigman,C.C. (1996). Epidermal growth factor receptor tyrosine kinase inhibitors as potential cancer chemopreventives. Cancer Epidemiol. Biomarkers Prev. *5*, 657-666.

Kenemans,P., Verstraeten,R.A., and Verheijen,R.H. (2004). Oncogenic pathways in hereditary and sporadic breast cancer. Maturitas *49*, 34-43.

Kennedy,R.D., Quinn,J.E., Mullan,P.B., Johnston,P.G., and Harkin,D.P. (2004). The role of BRCA1 in the cellular response to chemotherapy. J. Natl. Cancer Inst. *96*, 1659-1668.

Khanna,K.K. and Jackson,S.P. (2001). DNA double-strand breaks: signaling, repair and the cancer connection. Nat. Genet. *27*, 247-254.

King,M.C., Marks,J.H., and Mandell,J.B. (2003). Breast and ovarian cancer risks due to inherited mutations in BRCA1 and BRCA2. Science *302*, 643-646.

Klapper,L.N., Vaisman,N., Hurwitz,E., Pinkas-Kramarski,R., Yarden,Y., and Sela,M. (1997). A subclass of tumor-inhibitory monoclonal antibodies to ErbB-2/HER2 blocks crosstalk with growth factor receptors. Oncogene *14* , 2099-2109.

Klos,K.S., Zhou,X., Lee,S., Zhang,L., Yang,W., Nagata,Y., and Yu,D. (2003). Combined trastuzumab and paclitaxel treatment better inhibits ErbB-2-mediated angiogenesis in breast carcinoma through a more effective inhibition of Akt than either treatment alone. Cancer *98*, 1377-1385.

Kobayashi,S., Ji,H., Yuza,Y., Meyerson,M., Wong,K.K., Tenen,D.G., and Halmos,B. (2005). An alternative inhibitor overcomes resistance caused by a mutation of the epidermal growth factor receptor. Cancer Res. *65*, 7096-7101.

Koonin,E.V., Altschul,S.F., and Bork,P. (1996). BRCA1 protein products ... Functional motifs.. Nat. Genet. *13*, 266-268.

Kotecha,M.T., Afghan,R.K., Vasilikopoulou,E., Wilson,E., Marsh,P., Kast,W.M., Davies,D.H., and Caparros-Wanderley,W. (2003). Enhanced tumour growth after DNA vaccination against human papilloma virus E7 oncoprotein: evidence for tumour-induced immune deviation. Vaccine *21*, 2506-2515.

Kulik,G., Klippel,A., and Weber,M.J. (1997). Antiapoptotic signalling by the insulin-like growth factor I receptor, phosphatidylinositol 3-kinase, and Akt. Mol. Cell Biol. *17*, 1595-1606.

Kumar,R., Mandal,M., Lipton,A., Harvey,H., and Thompson,C.B. (1996). Overexpression of HER2 modulates bcl-2, bcl-XL, and tamoxifen-induced apoptosis in human MCF-7 breast cancer cells. Clin. Cancer Res. *2*, 1215-1219.

Kuraoka,I., Kobertz,W.R., Ariza,R.R., Biggerstaff,M., Essigmann,J.M., and Wood,R.D. (2000). Repair of an interstrand DNA cross-link initiated by ERCC1-XPF repair/recombination nuclease. J. Biol. Chem. *275*, 26632-26636.

Kurz,E.U., Leader,K.B., Kroll,D.J., Clark,M., and Gieseler,F. (2000). Modulation of human DNA topoisomerase IIalpha function by interaction with 14-3-3epsilon. J. Biol. Chem. *275*, 13948-13954.

Lafarge,S., Sylvain,V., Ferrara,M., and Bignon,Y.J. (2001). Inhibition of BRCA1 leads to increased chemoresistance to microtubule-interfering agents, an effect that involves the JNK pathway. Oncogene *20*, 6597-6606.

Lane,H.A., Beuvink,I., Motoyama,A.B., Daly,J.M., Neve,R.M., and Hynes,N.E. (2000). ErbB2 potentiates breast tumor proliferation through modulation of p27(Kip1)-Cdk2 complex formation: receptor overexpression does not determine growth dependency. Mol. Cell Biol. *20*, 3210-3223.

Lane,H.A., Motoyama,A.B., Beuvink,I., and Hynes,N.E. (2001). Modulation of p27/Cdk2 complex formation through 4D5-mediated inhibition of HER2 receptor signaling. Ann. Oncol. *12 Suppl 1*, S21-S22.

Larsen,A.K., Gobert,C., Gilbert,C., Markovits,J., Bojanowski,K., and Skladanowski,A. (1998). DNA topoisomerases as repair enzymes: mechanism(s) of action and regulation by p53. Acta Biochim. Pol. *45*, 535-544.

Larsen,A.K. and Skladanowski,A. (1998). Cellular resistance to topoisomerase-targeted drugs: from drug uptake to cell death. Biochim. Biophys. Acta *1400*, 257-274.

Lawley,P.D. and Phillips,D.H. (1996). DNA adducts from chemotherapeutic agents. Mutat. Res. *355*, 13-40.

Le,P.F., Randrianarison,V., Marot,D., Cabannes,J., Perricaudet,M., Feunteun,J., and Sarasin,A. (2000). BRCA1 and BRCA2 are necessary for the transcription-coupled repair of the oxidative 8-oxoguanine lesion in human cells. Cancer Res. *60*, 5548-5552.

Le,X.F., Claret,F.X., Lammayot,A., Tian,L., Deshpande,D., LaPushin,R., Tari,A.M., and Bast,R.C., Jr. (2003). The role of cyclin-dependent kinase inhibitor p27Kip1 in anti-HER2 antibody-induced G1 cell cycle arrest and tumor growth inhibition. J. Biol. Chem. *278*, 23441-23450.

Le,X.F., Lammayot,A., Gold,D., Lu,Y., Mao,W., Chang,T., Patel,A., Mills,G.B., and Bast,R.C., Jr. (2005). Genes affecting the cell cycle, growth, maintenance, and drug sensitivity are preferentially regulated by anti-HER2 antibody through phosphatidylinositol 3-kinase-AKT signaling. J. Biol. Chem. *280*, 2092-2104.

Learn,C.A., Hartzell,T.L., Wikstrand,C.J., Archer,G.E., Rich,J.N., Friedman,A.H., Friedman,H.S., Bigner,D.D., and Sampson,J.H. (2004). Resistance to tyrosine kinase inhibition by mutant epidermal growth factor receptor variant III contributes to the neoplastic phenotype of glioblastoma multiforme. Clin. Cancer Res. *10*, 3216-3224.

Lee,H.J., Jung,K.M., Huang,Y.Z., Bennett,L.B., Lee,J.S., Mei,L., and Kim,T.W. (2002a). Presenilin-dependent gamma-secretase-like intramembrane cleavage of ErbB4. J. Biol. Chem. *277*, 6318-6323.

Lee,J.S., Collins,K.M., Brown,A.L., Lee,C.H., and Chung,J.H. (2000a). hCds1-mediated phosphorylation of BRCA1 regulates the DNA damage response. Nature *404*, 201-204.

Lee,R.J., Albanese,C., Fu,M., D'Amico,M., Lin,B., Watanabe,G., Haines,G.K., III, Siegel,P.M., Hung,M.C., Yarden,Y., Horowitz,J.M., Muller,W.J., and Pestell,R.G. (2000b). Cyclin D1 is required for transformation by activated Neu and is induced through an E2F-dependent signaling pathway. Mol. Cell Biol. *20*, 672-683.

Lee,S., Yang,W., Lan,K.H., Sellappan,S., Klos,K., Hortobagyi,G., Hung,M.C., and Yu,D. (2002b). Enhanced sensitization to taxol-induced apoptosis by herceptin pretreatment in ErbB2-overexpressing breast cancer cells. Cancer Res. *62*, 5703-5710.

Leitzel,K., Teramoto,Y., Konrad,K., Chinchilli,V.M., Volas,G., Grossberg,H., Harvey,H., Demers,L., and Lipton,A. (1995). Elevated serum c-erbB-2 antigen levels and decreased response to hormone therapy of breast cancer. J. Clin. Oncol. *13*, 1129-1135.

Lenferink,A.E., Pinkas-Kramarski,R., Van de Poll,M.L., Van Vugt,M.J., Klapper,L.N., Tzahar,E., Waterman,H., Sela,M., Van Zoelen,E.J., and Yarden,Y. (1998). Differential endocytic routing of homo- and hetero-dimeric ErbB tyrosine kinases confers signaling superiority to receptor heterodimers. EMBO J. *17*, 3385-3397.

Lenferink,A.E., Busse,D., Flanagan,W.M., Yakes,F.M., and Arteaga,C.L. (2001). ErbB2/neu kinase modulates cellular p27(Kip1) and cyclin D1 through multiple signaling pathways. Cancer Res. *61*, 6583-6591.

Leonard,D.S., Hill,A.D., Kelly,L., Dijkstra,B., McDermott,E., and O'Higgins,N.J. (2002). Anti-human epidermal growth factor receptor 2 monoclonal antibody therapy for breast cancer. Br. J. Surg. *89*, 262-271.

Li,S., Chen,P.L., Subramanian,T., Chinnadurai,G., Tomlinson,G., Osborne,C.K., Sharp,Z.D., and Lee,W.H. (1999). Binding of CtIP to the BRCT repeats of BRCA1 involved in the transcription regulation of p21 is disrupted upon DNA damage. J. Biol. Chem. *274*, 11334-11338.

Li,Y., Corradetti,M.N., Inoki,K., and Guan,K.L. (2004). TSC2: filling the GAP in the mTOR signaling pathway. Trends Biochem. Sci. *29*, 32-38.

Lin,S.Y., Makino,K., Xia,W., Matin,A., Wen,Y., Kwong,K.Y., Bourguignon,L., and Hung,M.C. (2001). Nuclear localization of EGF receptor and its potential new role as a transcription factor. Nat. Cell Biol. *3*, 802-808.

Lindahl,T. and Wood,R.D. (1999). Quality control by DNA repair. Science *286*, 1897-1905.

Lisby,M. and Rothstein,R. (2004a). DNA damage checkpoint and repair centers. Curr. Opin. Cell Biol. *16*, 328-334.

Lisby,M. and Rothstein,R. (2004b). DNA repair: keeping it together. Curr. Biol. *14*, R994-R996.

Liu,D., Aguirre,G.J., Estrada,Y., and Ossowski,L. (2002). EGFR is a transducer of the urokinase receptor initiated signal that is required for in vivo growth of a human carcinoma. Cancer Cell *1*, 445-457.

Liu,Y., Martindale,J.L., Gorospe,M., and Holbrook,N.J. (1996). Regulation of p21WAF1/CIP1 expression through mitogen-activated protein kinase signaling pathway. Cancer Res. *56*, 31-35.

Lo,H.W., Hsu,S.C., li-Seyed,M., Gunduz,M., Xia,W., Wei,Y., Bartholomeusz,G., Shih,J.Y., and Hung,M.C. (2005). Nuclear interaction of EGFR and STAT3 in the activation of the iNOS/NO pathway. Cancer Cell *7*, 575-589.

Lo,H.W., Hsu,S.C., and Hung,M.C. (2006). EGFR signaling pathway in breast cancers: from traditional signal transduction to direct nuclear translocalization. Breast Cancer Res. Treat. *95*, 211-218.

Lonardo,F., Di,M.E., King,C.R., Pierce,J.H., Segatto,O., Aaronson,S.A., and Di Fiore,P.P. (1990). The normal erbB-2 product is an atypical receptor-like tyrosine kinase with constitutive activity in the absence of ligand. New Biol. *2*, 992-1003.

Long,B.H., Musial,S.T., and Brattain,M.G. (1985). Single- and double-strand DNA breakage and repair in human lung adenocarcinoma cells exposed to etoposide and teniposide. Cancer Res. *45*, 3106-3112.

Longva,K.E., Pedersen,N.M., Haslekas,C., Stang,E., and Madshus,I.H. (2005). Herceptin-induced inhibition of ErbB2 signaling involves reduced phosphorylation of Akt but not endocytic down-regulation of ErbB2. Int. J. Cancer *116*, 359-367.

Lopez-Girona,A., Furnari,B., Mondesert,O., and Russell,P. (1999). Nuclear localization of Cdc25 is regulated by DNA damage and a 14-3-3 protein. Nature *397*, 172-175.

Lorick,K.L., Jensen,J.P., Fang,S., Ong,A.M., Hatakeyama,S., and Weissman,A.M. (1999). RING fingers mediate ubiquitin-conjugating enzyme (E2)-dependent ubiquitination. Proc. Natl. Acad. Sci. U. S. A *96*, 11364-11369.

Lou,Z., Minter-Dykhouse,K., and Chen,J. (2005). BRCA1 participates in DNA decatenation. Nat. Struct. Mol. Biol. *12*, 589-593.

Lowe,S.W. and Lin,A.W. (2000). Apoptosis in cancer. Carcinogenesis *21*, 485-495.

Lowry,O.H., Rosebrough,N.J., Farr,A.L., and Randall,R.J. (1951). Protein measurement with the Folin phenol reagent. J. Biol. Chem. *193*, 265-275.

Lu,Y., Zi,X., Zhao,Y., Mascarenhas,D., and Pollak,M. (2001). Insulin-like growth factor-I receptor signaling and resistance to trastuzumab (Herceptin). J. Natl. Cancer Inst. *93*, 1852-1857.

Lynch,T.J., Bell,D.W., Sordella,R., Gurubhagavatula,S., Okimoto,R.A., Brannigan,B.W., Harris,P.L., Haserlat,S.M., Supko,J.G., Haluska,F.G., Louis,D.N., Christiani,D.C., Settleman,J., and Haber,D.A. (2004). Activating mutations in the epidermal growth factor receptor underlying responsiveness of non-small-cell lung cancer to gefitinib. N. Engl. J. Med. *350*, 2129-2139.

MacKay,A., Jones,C., Dexter,T., Silva,R.L., Bulmer,K., Jones,A., Simpson,P., Harris,R.A., Jat,P.S., Neville,A.M., Reis,L.F., Lakhani,S.R., and O'Hare,M.J. (2003). cDNA microarray analysis of genes associated with ERBB2 (HER2/neu) overexpression in human mammary luminal epithelial cells. Oncogene *22*, 2680-2688.

MacLachlan,T.K. and El-Deiry,W.S. (2002). Apoptotic threshold is lowered by p53 transactivation of caspase-6. Proc. Natl. Acad. Sci. U. S. A *99*, 9492-9497.

MacLachlan,T.K., Takimoto,R., and El-Deiry,W.S. (2002). BRCA1 directs a selective p53-dependent transcriptional response towards growth arrest and DNA repair targets. Mol. Cell Biol. *22*, 4280-4292.

Maier,L.A., Xu,F.J., Hester,S., Boyer,C.M., McKenzie,S., Bruskin,A.M., Argon,Y., and Bast,R.C., Jr. (1991). Requirements for the internalization of a murine monoclonal antibody directed against the HER-2/neu gene product c-erbB-2. Cancer Res. *51*, 5361-5369.

Malinge,J.M., Perez,C., and Leng,M. (1994). Base sequence-independent distorsions induced by interstrand cross-links in cis-diamminedichloroplatinum (II)-modified DNA. Nucleic Acids Res. *22*, 3834-3839.

Marches,R. and Uhr,J.W. (2004). Enhancement of the p27Kip1-mediated antiproliferative effect of trastuzumab (Herceptin) on HER2-overexpressing tumor cells. Int. J. Cancer *112*, 492-501.

Marmor,M.D., Skaria,K.B., and Yarden,Y. (2004). Signal transduction and oncogenesis by ErbB/HER receptors. Int. J. Radiat. Oncol. Biol. Phys. *58*, 903-913.

Marti,U. and Wells,A. (2000). The nuclear accumulation of a variant epidermal growth factor receptor (EGFR) lacking the transmembrane domain requires coexpression of a full-length EGFR. Mol. Cell Biol. Res. Commun. *3* , 8-14.

Mass,R.D., Press,M.F., Anderson,S., Cobleigh,M.A., Vogel,C.L., Dybdal,N., Leiberman,G., and Slamon,D.J. (2005). Evaluation of clinical outcomes according to HER2 detection by fluorescence in situ hybridization in women with metastatic breast cancer treated with trastuzumab. Clin. Breast Cancer *6* , 240-246.

Massie,C. and Mills,I.G. (2006). The developing role of receptors and adaptors. Nat. Rev. Cancer *6*, 403-409.

Mastropaolo,D., Camerman,A., Luo,Y., Brayer,G.D., and Camerman,N. (1995). Crystal and molecular structure of paclitaxel (taxol). Proc. Natl. Acad. Sci. U. S. A *92*, 6920-6924.

Masumoto,N., Nakano,S., Fujishima,H., Kohno,K., and Niho,Y. (1999). v-src induces cisplatin resistance by increasing the repair of cisplatin-DNA interstrand cross-links in human gallbladder adenocarcinoma cells. Int. J. Cancer *80*, 731-737.

Mateo,C., Moreno,E., Amour,K., Lombardero,J., Harris,W., and Perez,R. (1997). Humanization of a mouse monoclonal antibody that blocks the epidermal growth factor receptor: recovery of antagonistic activity. Immunotechnology. *3*, 71-81.

Matsuoka,S., Huang,M., and Elledge,S.J. (1998). Linkage of ATM to cell cycle regulation by the Chk2 protein kinase. Science *282*, 1893-1897.

Mayfield,S., Vaughn,J.P., and Kute,T.E. (2001). DNA strand breaks and cell cycle perturbation in herceptin treated breast cancer cell lines. Breast Cancer Res. Treat. *70*, 123-129.

McDonald,E.R., III, Wu,G.S., Waldman,T., and El-Deiry,W.S. (1996). Repair Defect in p21 WAF1/CIP1 -/- human cancer cells. Cancer Res. *56* , 2250-2255.

McHugh,P.J., Spanswick,V.J., and Hartley,J.A. (2001). Repair of DNA interstrand crosslinks: molecular mechanisms and clinical relevance. Lancet Oncol. *2*, 483-490.

Medema,R.H., Kops,G.J., Bos,J.L., and Burgering,B.M. (2000). AFX-like Forkhead transcription factors mediate cell-cycle regulation by Ras and PKB through p27kip1. Nature *404*, 782-787.

Meier,R. and Hemmings,B.A. (1999). Regulation of protein kinase B. J. Recept. Signal. Transduct. Res. *19*, 121-128.

Mellinghoff,I.K., Wang,M.Y., Vivanco,I., Haas-Kogan,D.A., Zhu,S., Dia,E.Q., Lu,K.V., Yoshimoto,K., Huang,J.H., Chute,D.J., Riggs,B.L., Horvath,S., Liau,L.M., Cavenee,W.K., Rao,P.N., Beroukhim,R., Peck,T.C., Lee,J.C., Sellers,W.R., Stokoe,D., Prados,M., Cloughesy,T.F., Sawyers,C.L., and Mischel,P.S. (2005). Molecular determinants of the response of glioblastomas to EGFR kinase inhibitors. N. Engl. J. Med. *353*, 2012-2024.

Mendelsohn,J. (2000). Blockade of receptors for growth factors: an anticancer therapy--the fourth annual Joseph H Burchenal American Association of Cancer Research Clinical Research Award Lecture. Clin. Cancer Res. *6* , 747-753.

Mendelsohn,J. and Baselga,J. (2003). Status of epidermal growth factor receptor antagonists in the biology and treatment of cancer. J. Clin. Oncol. *21*, 2787-2799.

Michel,B., Flores,M.J., Viguera,E., Grompone,G., Seigneur,M., and Bidnenko,V. (2001). Rescue of arrested replication forks by homologous recombination. Proc. Natl. Acad. Sci. U. S. A *98*, 8181-8188.

Miki,Y., Swensen,J., Shattuck-Eidens,D., Futreal,P.A., Harshman,K., Tavtigian,S., Liu,Q., Cochran,C., Bennett,L.M., Ding,W., and . (1994). A strong candidate for the breast and ovarian cancer susceptibility gene BRCA1. Science *266*, 66-71.

Miyashita,T., Krajewski,S., Krajewska,M., Wang,H.G., Lin,H.K., Liebermann,D.A., Hoffman,B., and Reed,J.C. (1994). Tumor suppressor p53 is a regulator of bcl-2 and bax gene expression in vitro and in vivo. Oncogene *9*, 1799-1805.

Moasser,M.M., Basso,A., Averbuch,S.D., and Rosen,N. (2001). The tyrosine kinase inhibitor ZD1839 ("Iressa") inhibits HER2-driven signaling and suppresses the growth of HER2-overexpressing tumor cells. Cancer Res. *61*, 7184-7188.

Mohsin,S.K., Weiss,H.L., Gutierrez,M.C., Chamness,G.C., Schiff,R., Digiovanna,M.P., Wang,C.X., Hilsenbeck,S.G., Osborne,C.K., Allred,D.C., Elledge,R., and Chang,J.C. (2005). Neoadjuvant trastuzumab induces apoptosis in primary breast cancers. J. Clin. Oncol. *23*, 2460-2468.

Molina,M.A., Codony-Servat,J., Albanell,J., Rojo,F., Arribas,J., and Baselga,J. (2001). Trastuzumab (herceptin), a humanized anti-Her2 receptor monoclonal antibody, inhibits basal and activated Her2 ectodomain cleavage in breast cancer cells. Cancer Res. *61*, 4744-4749.

Molina,M.A., Saez,R., Ramsey,E.E., Garcia-Barchino,M.J., Rojo,F., Evans,A.J., Albanell,J., Keenan,E.J., Lluch,A., Garcia-Conde,J., Baselga,J., and Clinton,G.M. (2002). NH(2)-terminal truncated HER-2 protein but not full-length receptor is associated with nodal metastasis in human breast cancer. Clin. Cancer Res. *8*, 347-353.

Monteiro,A.N. (2000). BRCA1: exploring the links to transcription. Trends Biochem. Sci. *25*, 469-474.

Moro,L., Dolce,L., Cabodi,S., Bergatto,E., Boeri,E.E., Smeriglio,M., Turco,E., Retta,S.F., Giuffrida,M.G., Venturino,M., Godovac-Zimmermann,J., Conti,A., Schaefer,E., Beguinot,L., Tacchetti,C., Gaggini,P., Silengo,L., Tarone,G., and Defilippi,P. (2002). Integrin-induced epidermal growth factor (EGF) receptor activation requires c-Src and p130Cas and leads to phosphorylation of specific EGF receptor tyrosines. J. Biol. Chem. *277*, 9405-9414.

Moroni,M.C., Hickman,E.S., Lazzerini,D.E., Caprara,G., Colli,E., Cecconi,F., Muller,H., and Helin,K. (2001). Apaf-1 is a transcriptional target for E2F and p53. Nat. Cell Biol. *3*, 552-558.

Motoyama,A.B., Hynes,N.E., and Lane,H.A. (2002). The efficacy of ErbB receptor-targeted anticancer therapeutics is influenced by the availability of epidermal growth factor-related peptides. Cancer Res. *62*, 3151-3158.

Motti,M.L., Califano,D., Troncone,G., De,M.C., Migliaccio,I., Palmieri,E., Pezzullo,L., Palombini,L., Fusco,A., and Viglietto,G. (2005). Complex regulation of the cyclin-dependent kinase inhibitor p27kip1 in thyroid cancer cells by the PI3K/AKT pathway: regulation of p27kip1 expression and localization. Am. J. Pathol. *166*, 737-749.

Moulder,S.L. and Arteaga,C.L. (2003). A Phase I/II Trial of trastuzumab and gefitinib in patients with Metastatic Breast Cancer that overexpresses HER2/neu (ErbB-2). Clin. Breast Cancer *4*, 142-145.

Moynahan,M.E., Chiu,J.W., Koller,B.H., and Jasin,M. (1999). Brca1 controls homology-directed DNA repair. Mol. Cell *4*, 511-518.

Moynahan,M.E., Pierce,A.J., and Jasin,M. (2001). BRCA2 is required for homology-directed repair of chromosomal breaks. Mol. Cell *7*, 263-272.

Mu,D., Bessho,T., Nechev,L.V., Chen,D.J., Harris,T.M., Hearst,J.E., and Sancar,A. (2000). DNA interstrand cross-links induce futile repair synthesis in mammalian cell extracts. Mol. Cell Biol. *20*, 2446-2454.

Muss,H.B., Thor,A.D., Berry,D.A., Kute,T., Liu,E.T., Koerner,F., Cirrincione,C.T., Budman,D.R., Wood,W.C., Barcos,M., and . (1994). c-erbB-2 expression and response to adjuvant therapy in women with node-positive early breast cancer. N. Engl. J. Med. *330*, 1260-1266.

Myers,J.M., Martins,G.G., Ostrowski,J., and Stachowiak,M.K. (2003). Nuclear trafficking of FGFR1: a role for the transmembrane domain. J. Cell Biochem. *88*, 1273-1291.

Nagata,Y., Lan,K.H., Zhou,X., Tan,M., Esteva,F.J., Sahin,A.A., Klos,K.S., Li,P., Monia,B.P., Nguyen,N.T., Hortobagyi,G.N., Hung,M.C., and Yu,D. (2004). PTEN activation contributes to tumor inhibition by trastuzumab, and loss of PTEN predicts trastuzumab resistance in patients. Cancer Cell *6*, 117-127.

Nahta,R., Hung,M.C., and Esteva,F.J. (2004). The HER-2-targeting antibodies trastuzumab and pertuzumab synergistically inhibit the survival of breast cancer cells. Cancer Res. *64*, 2343-2346.

Nahta,R. and Esteva,F.J. (2006). Herceptin: mechanisms of action and resistance. Cancer Lett. *232*, 123-138.

Nakanishi,K., Yang,Y.G., Pierce,A.J., Taniguchi,T., Digweed,M., D'Andrea,A.D., Wang,Z.Q., and Jasin,M. (2005). Human Fanconi anemia monoubiquitination pathway promotes homologous DNA repair. Proc. Natl. Acad. Sci. U. S. A *102*, 1110-1115.

Narod,S.A. and Foulkes,W.D. (2004). BRCA1 and BRCA2: 1994 and beyond. Nat. Rev. Cancer *4*, 665-676.

Naruse,I., Fukumoto,H., Saijo,N., and Nishio,K. (2002). Enhanced anti-tumor effect of trastuzumab in combination with cisplatin. Jpn. J. Cancer Res. *93*, 574-581.

Neve,R.M., Sutterluty,H., Pullen,N., Lane,H.A., Daly,J.M., Krek,W., and Hynes,N.E. (2000). Effects of oncogenic ErbB2 on G1 cell cycle regulators in breast tumour cells. Oncogene *19*, 1647-1656.

Newmeyer,D.D. and Forbes,D.J. (1988). Nuclear import can be separated into distinct steps in vitro: nuclear pore binding and translocation. Cell *52*, 641-653.

Ni,C.Y., Murphy,M.P., Golde,T.E., and Carpenter,G. (2001). gamma -Secretase cleavage and nuclear localization of ErbB-4 receptor tyrosine kinase. Science *294*, 2179-2181.

Ni,Z., Lou,W., Leman,E.S., and Gao,A.C. (2000). Inhibition of constitutively activated Stat3 signaling pathway suppresses growth of prostate cancer cells. Cancer Res. *60*, 1225-1228.

Nicholson,R.I., Gee,J.M., Knowlden,J., McClelland,R., Madden,T.A., Barrow,D., and Hutcheson,I. (2003). The biology of antihormone failure in breast cancer. Breast Cancer Res. Treat. *80 Suppl 1*, S29-S34.

Nieuwenhuis,B., Van Assen-Bolt,A.J., Van Waarde-Verhagen,M.A., Sijmons,R.H., Van der Hout,A.H., Bauch,T., Streffer,C., and Kampinga,H.H. (2002). BRCA1 and BRCA2 heterozygosity and repair of X-ray-induced DNA damage. Int. J. Radiat. Biol. *78*, 285-295.

Nishii,K., Kabarowski,J.H., Gibbons,D.L., Griffiths,S.D., Titley,I., Wiedemann,L.M., and Greaves,M.F. (1996). ts BCR-ABL kinase activation confers increased resistance to genotoxic damage via cell cycle block. Oncogene *13*, 2225-2234.

Nitiss,J.L. (1998). Investigating the biological functions of DNA topoisomerases in eukaryotic cells. Biochim. Biophys. Acta *1400*, 63-81.

Nkondjock,A. and Ghadirian,P. (2004). Epidemiology of breast cancer among BRCA mutation carriers: an overview. Cancer Lett. *205*, 1-8.

Normanno,N., Campiglio,M., De,L.A., Somenzi,G., Maiello,M., Ciardiello,F., Gianni,L., Salomon,D.S., and Menard,S. (2002). Cooperative inhibitory effect of ZD1839 (Iressa) in combination with trastuzumab (Herceptin) on human breast cancer cell growth. Ann. Oncol. *13*, 65-72.

Offterdinger,M., Schofer,C., Weipoltshammer,K., and Grunt,T.W. (2002). c-erbB-3: a nuclear protein in mammary epithelial cells. J. Cell Biol. *157*, 929-939.

Offterdinger,M., Schneider,S.M., and Grunt,T.W. (2003). Heregulin and retinoids synergistically induce branching morphogenesis of breast cancer cells cultivated in 3D collagen gels. J. Cell Physiol *195*, 260-275.

Ohgaki,H., Dessen,P., Jourde,B., Horstmann,S., Nishikawa,T., Di Patre,P.L., Burkhard,C., Schuler,D., Probst-Hensch,N.M., Maiorka,P.C., Baeza,N., Pisani,P., Yonekawa,Y., Yasargil,M.G., Lutolf,U.M., and Kleihues,P. (2004). Genetic pathways to glioblastoma: a population-based study. Cancer Res. *64*, 6892-6899.

Okobia,M.N. and Bunker,C.H. (2003). Molecular epidemiology of breast cancer: a review. Afr. J. Reprod. Health *7*, 17-28.

Olayioye,M.A., Neve,R.M., Lane,H.A., and Hynes,N.E. (2000). The ErbB signaling network: receptor heterodimerization in development and cancer. EMBO J. *19*, 3159-3167.

Olive,P.L. (2002). The comet assay. An overview of techniques. Methods Mol. Biol. *203*, 179-194.

Orr,M.S., O'Connor,P.M., and Kohn,K.W. (2000). Effects of c-erbB2 overexpression on the drug sensitivities of normal human mammary epithelial cells. J. Natl. Cancer Inst. *92*, 987-994.

Osborne,C.K., Bardou,V., Hopp,T.A., Chamness,G.C., Hilsenbeck,S.G., Fuqua,S.A., Wong,J., Allred,D.C., Clark,G.M., and Schiff,R. (2003). Role of the estrogen receptor coactivator AIB1 (SRC-3) and HER-2/neu in tamoxifen resistance in breast cancer. J. Natl. Cancer Inst. *95*, 353-361.

Ostling,O. and Johanson,K.J. (1984). Microelectrophoretic study of radiation-induced DNA damage in individual mammalian cells. Biochem. Biophys. Res. Commun. *123*, 291-298.

Ouchi,T., Monteiro,A.N., August,A., Aaronson,S.A., and Hanafusa,H. (1998). BRCA1 regulates p53-dependent gene expression. Proc. Natl. Acad. Sci. U. S. A *95*, 2302-2306.

Ouchi,T., Lee,S.W., Ouchi,M., Aaronson,S.A., and Horvath,C.M. (2000). Collaboration of signal transducer and activator of transcription 1 (STAT1) and BRCA1 in differential regulation of IFN-gamma target genes. Proc. Natl. Acad. Sci. U. S. A *97*, 5208-5213.

Owen-Schaub,L.B., Angelo,L.S., Radinsky,R., Ware,C.F., Gesner,T.G., and Bartos,D.P. (1995). Soluble Fas/APO-1 in tumor cells: a potential regulator of apoptosis? Cancer Lett. *94*, 1-8.

Paez,J.G., Janne,P.A., Lee,J.C., Tracy,S., Greulich,H., Gabriel,S., Herman,P., Kaye,F.J., Lindeman,N., Boggon,T.J., Naoki,K., Sasaki,H., Fujii,Y., Eck,M.J., Sellers,W.R., Johnson,B.E., and Meyerson,M. (2004). EGFR mutations in lung cancer: correlation with clinical response to gefitinib therapy. Science *304*, 1497-1500.

Pao,W., Miller,V., Zakowski,M., Doherty,J., Politi,K., Sarkaria,I., Singh,B., Heelan,R., Rusch,V., Fulton,L., Mardis,E., Kupfer,D., Wilson,R., Kris,M., and Varmus,H. (2004). EGF receptor gene mutations are common in lung cancers from "never smokers" and are associated with sensitivity of tumors to gefitinib and erlotinib. Proc. Natl. Acad. Sci. U. S. A *101*, 13306-13311.

Pao,W. and Miller,V.A. (2005). Epidermal growth factor receptor mutations, small-molecule kinase inhibitors, and non-small-cell lung cancer: current knowledge and future directions. J. Clin. Oncol. *23*, 2556-2568.

Pao,W., Wang,T.Y., Riely,G.J., Miller,V.A., Pan,Q., Ladanyi,M., Zakowski,M.F., Heelan,R.T., Kris,M.G., and Varmus,H.E. (2005). KRAS mutations and primary resistance of lung adenocarcinomas to gefitinib or erlotinib. PLoS. Med. *2*, e17.

Park,J.W., Stagg,R., Lewis,G.D., Carter,P., Maneval,D., Slamon,D.J., Jaffe,H., and Shepard,H.M. (1992). Anti-p185HER2 monoclonal antibodies: biological properties and potential for immunotherapy. Cancer Treat. Res. *61*, 193-211.

Pastink,A., Eeken,J.C., and Lohman,P.H. (2001). Genomic integrity and the repair of double-strand DNA breaks. Mutat. Res. *480-481*, 37-50.

Pastwa,E. and Blasiak,J. (2003). Non-homologous DNA end joining. Acta Biochim. Pol. *50*, 891-908.

Pegram,M., Hsu,S., Lewis,G., Pietras,R., Beryt,M., Sliwkowski,M., Coombs,D., Baly,D., Kabbinavar,F., and Slamon,D. (1999). Inhibitory effects of combinations of HER-2/neu antibody and chemotherapeutic agents used for treatment of human breast cancers. Oncogene *18*, 2241-2251.

Pegram,M.D., Finn,R.S., Arzoo,K., Beryt,M., Pietras,R.J., and Slamon,D.J. (1997). The effect of HER-2/neu overexpression on chemotherapeutic drug sensitivity in human breast and ovarian cancer cells. Oncogene *15*, 537-547.

Pegram,M.D., Lipton,A., Hayes,D.F., Weber,B.L., Baselga,J.M., Tripathy,D., Baly,D., Baughman,S.A., Twaddell,T., Glaspy,J.A., and Slamon,D.J. (1998). Phase II study of receptor-enhanced chemosensitivity using recombinant humanized anti-p185HER2/neu monoclonal antibody plus cisplatin in patients with HER2/neu-overexpressing metastatic breast cancer refractory to chemotherapy treatment. J. Clin. Oncol. *16*, 2659-2671.

Pegram,M.D. and Slamon,D.J. (1999). Combination therapy with trastuzumab (Herceptin) and cisplatin for chemoresistant metastatic breast cancer: evidence for receptor-enhanced chemosensitivity. Semin. Oncol. *26*, 89-95.

Pegram,M.D., Konecny,G.E., O'Callaghan,C., Beryt,M., Pietras,R., and Slamon,D.J. (2004a). Rational combinations of trastuzumab with chemotherapeutic drugs used in the treatment of breast cancer. J. Natl. Cancer Inst. *96*, 739-749.

Pegram,M.D., Pienkowski,T., Northfelt,D.W., Eiermann,W., Patel,R., Fumoleau,P., Quan,E., Crown,J., Toppmeyer,D., Smylie,M., Riva,A., Blitz,S., Press,M.F., Reese,D., Lindsay,M.A., and Slamon,D.J. (2004b). Results of two open-label, multicenter phase II studies of docetaxel, platinum salts, and trastuzumab in HER2-positive advanced breast cancer. J. Natl. Cancer Inst. *96*, 759-769.

Peles,E., Ben-Levy,R., Tzahar,E., Liu,N., Wen,D., and Yarden,Y. (1993). Cell-type specific interaction of Neu differentiation factor (NDF/heregulin) with Neu/HER-2 suggests complex ligand-receptor relationships. EMBO J. *12*, 961-971.

Pemberton,L.F. and Paschal,B.M. (2005). Mechanisms of receptor-mediated nuclear import and nuclear export. Traffic. *6*, 187-198.

Perez,E.A. (2004). Carboplatin in combination therapy for metastatic breast cancer. Oncologist. *9*, 518-527.

Petak,I., Tillman,D.M., and Houghton,J.A. (2000). p53 dependence of Fas induction and acute apoptosis in response to 5-fluorouracil-leucovorin in human colon carcinoma cell lines. Clin. Cancer Res. *6*, 4432-4441.

Petit,A.M., Rak,J., Hung,M.C., Rockwell,P., Goldstein,N., Fendly,B., and Kerbel,R.S. (1997). Neutralizing antibodies against epidermal growth factor and ErbB-2/neu receptor tyrosine kinases down-regulate vascular endothelial growth factor production by tumor cells in vitro and in vivo: angiogenic implications for signal transduction therapy of solid tumors. Am. J. Pathol. *151*, 1523-1530.

Pfaffl,M.W. (2001). A new mathematical model for relative quantification in real-time RT-PCR. Nucleic Acids Res. *29*, e45.

Pichierri,P. and Rosselli,F. (2004). Fanconi anemia proteins and the s phase checkpoint. Cell Cycle *3*, 698-700.

Pichierri,P., Franchitto,A., and Rosselli,F. (2004). BLM and the FANC proteins collaborate in a common pathway in response to stalled replication forks. EMBO J. *23*, 3154-3163.

Pietenpol,J.A. and Stewart,Z.A. (2002). Cell cycle checkpoint signaling: cell cycle arrest versus apoptosis. Toxicology *181-182*, 475-481.

Pietras,R.J., Fendly,B.M., Chazin,V.R., Pegram,M.D., Howell,S.B., and Slamon,D.J. (1994). Antibody to HER-2/neu receptor blocks DNA repair after cisplatin in human breast and ovarian cancer cells. Oncogene *9*, 1829-1838.

Pietras,R.J., Pegram,M.D., Finn,R.S., Maneval,D.A., and Slamon,D.J. (1998). Remission of human breast cancer xenografts on therapy with humanized monoclonal antibody to HER-2 receptor and DNA-reactive drugs. Oncogene *17*, 2235-2249.

Pietras,R.J., Poen,J.C., Gallardo,D., Wongvipat,P.N., Lee,H.J., and Slamon,D.J. (1999). Monoclonal antibody to HER-2/neureceptor modulates repair of radiation-induced DNA damage and enhances radiosensitivity of human breast cancer cells overexpressing this oncogene. Cancer Res. *59*, 1347-1355.

Porter,A.C. and Vaillancourt,R.R. (1998). Tyrosine kinase receptor-activated signal transduction pathways which lead to oncogenesis. Oncogene *17*, 1343-1352.

Powell,S.N. and Kachnic,L.A. (2003). Roles of BRCA1 and BRCA2 in homologous recombination, DNA replication fidelity and the cellular response to ionizing radiation. Oncogene *22*, 5784-5791.

Prewett,M.C., Hooper,A.T., Bassi,R., Ellis,L.M., Waksal,H.W., and Hicklin,D.J. (2002). Enhanced antitumor activity of anti-epidermal growth factor receptor monoclonal antibody IMC-C225 in combination with irinotecan (CPT-11) against human colorectal tumor xenografts. Clin. Cancer Res. *8*, 994-1003.

Pu,Q.Q. and Bezwoda,W.R. (1999). Induction of alkylator (melphalan) resistance in HL60 cells is accompanied by increased levels of topoisomerase II expression and function. Mol. Pharmacol. *56*, 147-153.

Pupa,S.M., Menard,S., Morelli,D., Pozzi,B., De,P.G., and Colnaghi,M.I. (1993). The extracellular domain of the c-erbB-2 oncoprotein is released from tumor cells by proteolytic cleavage. Oncogene *8*, 2917-2923.

Quinn,J.E., Kennedy,R.D., Mullan,P.B., Gilmore,P.M., Carty,M., Johnston,P.G., and Harkin,D.P. (2003). BRCA1 functions as a differential modulator of chemotherapy-induced apoptosis. Cancer Res. *63*, 6221-6228.

Raderschall,E., Stout,K., Freier,S., Suckow,V., Schweiger,S., and Haaf,T. (2002). Elevated levels of Rad51 recombination protein in tumor cells. Cancer Res. *62*, 219-225.

Raymond,E., Faivre,S., and Armand,J.P. (2000). Epidermal growth factor receptor tyrosine kinase as a target for anticancer therapy. Drugs *60 Suppl 1*, 15-23.

Riese,D.J. and Stern,D.F. (1998). Specificity within the EGF family/ErbB receptor family signaling network. Bioessays *20*, 41-48.

Rivard,N., Boucher,M.J., Asselin,C., and L'Allemain,G. (1999). MAP kinase cascade is required for p27 downregulation and S phase entry in fibroblasts and epithelial cells. Am. J. Physiol *277*, C652-C664.

Robert,N., Leyland-Jones,B., Asmar,L., Belt,R., Ilegbodu,D., Loesch,D., Raju,R., Valentine,E., Sayre,R., Cobleigh,M., Albain,K., McCullough,C., Fuchs,L., and Slamon,D. (2006). Randomized phase III study of trastuzumab, paclitaxel, and carboplatin compared with trastuzumab and paclitaxel in women with HER-2-overexpressing metastatic breast cancer. J. Clin. Oncol. *24*, 2786-2792.

Ruffner,H., Joazeiro,C.A., Hemmati,D., Hunter,T., and Verma,I.M. (2001). Cancer-predisposing mutations within the RING domain of BRCA1: loss of ubiquitin protein ligase activity and protection from radiation hypersensitivity. Proc. Natl. Acad. Sci. U. S. A *98*, 5134-5139.

Rusnak,D.W., Affleck,K., Cockerill,S.G., Stubberfield,C., Harris,R., Page,M., Smith,K.J., Guntrip,S.B., Carter,M.C., Shaw,R.J., Jowett,A., Stables,J., Topley,P., Wood,E.R., Brignola,P.S., Kadwell,S.H., Reep,B.R., Mullin,R.J., Alligood,K.J., Keith,B.R., Crosby,R.M., Murray,D.M., Knight,W.B., Gilmer,T.M., and Lackey,K. (2001). The characterization of novel, dual ErbB-2/EGFR, tyrosine kinase inhibitors: potential therapy for cancer. Cancer Res. *61*, 7196-7203.

Salloukh,H.F., Vowles,I., Heisterkamp,N., Groffen,J., and Laneuville,P. (2000). Early events in leukemogenesis in P190Bcr-abl transgenic mice. Oncogene *19*, 4362-4374.

Salomoni,P., Condorelli,F., Sweeney,S.M., and Calabretta,B. (2000). Versatility of BCR/ABL-expressing leukemic cells in circumventing proapoptotic BAD effects. Blood *96*, 676-684.

Saltz,L.B., Lenz,H.J., Kindler,H.L., Hochster,H.S., Wadler,S., Hoff,P.M., Kemeny,N.E., Hollywood,E.M., Gonen,M., Quinones,M., Morse,M., and Chen,H.X. (2007). Randomized Phase II Trial of Cetuximab, Bevacizumab, and Irinotecan Compared With Cetuximab and Bevacizumab Alone in Irinotecan-Refractory Colorectal Cancer: The BOND-2 Study. J. Clin. Oncol.

Sanchez,Y., Wong,C., Thoma,R.S., Richman,R., Wu,Z., Piwnica-Worms,H., and Elledge,S.J. (1997). Conservation of the Chk1 checkpoint pathway in mammals: linkage of DNA damage to Cdk regulation through Cdc25. Science *277*, 1497-1501.

Sarbassov,D.D., Guertin,D.A., Ali,S.M., and Sabatini,D.M. (2005). Phosphorylation and regulation of Akt/PKB by the rictor-mTOR complex. Science *307*, 1098-1101.

Sawyers,C.L. (1997). Signal transduction pathways involved in BCR-ABL transformation. Baillieres Clin. Haematol. *10*, 223-231.

Schaefer,G., Shao,L., Totpal,K., and Akita,R.W. (2007). Erlotinib directly inhibits HER2 kinase activation and downstream signaling events in intact cells lacking epidermal growth factor receptor expression. Cancer Res. *67*, 1228-1238.

Schlessinger,J. (2000). Cell signaling by receptor tyrosine kinases. Cell *103*, 211-225.

Schlessinger,J. (2002). Ligand-induced, receptor-mediated dimerization and activation of EGF receptor. Cell *110*, 669-672.

Scully,R., Anderson,S.F., Chao,D.M., Wei,W., Ye,L., Young,R.A., Livingston,D.M., and Parvin,J.D. (1997a). BRCA1 is a component of the RNA polymerase II holoenzyme. Proc. Natl. Acad. Sci. U. S. A *94*, 5605-5610.

Scully,R., Chen,J., Ochs,R.L., Keegan,K., Hoekstra,M., Feunteun,J., and Livingston,D.M. (1997b). Dynamic changes of BRCA1 subnuclear location and phosphorylation state are initiated by DNA damage. Cell *90*, 425-435.

Scully,R., Chen,J., Plug,A., Xiao,Y., Weaver,D., Feunteun,J., Ashley,T., and Livingston,D.M. (1997c). Association of BRCA1 with Rad51 in mitotic and meiotic cells. Cell *88*, 265-275.

Scully,R., Ganesan,S., Vlasakova,K., Chen,J., Socolovsky,M., and Livingston,D.M. (1999). Genetic analysis of BRCA1 function in a defined tumor cell line. Mol. Cell *4*, 1093-1099.

Seidman,A., Hudis,C., Pierri,M.K., Shak,S., Paton,V., Ashby,M., Murphy,M., Stewart,S.J., and Keefe,D. (2002). Cardiac dysfunction in the trastuzumab clinical trials experience. J. Clin. Oncol. *20*, 1215-1221.

Seidman,A.D., Fornier,M.N., Esteva,F.J., Tan,L., Kaptain,S., Bach,A., Panageas,K.S., Arroyo,C., Valero,V., Currie,V., Gilewski,T., Theodoulou,M., Moynahan,M.E., Moasser,M., Sklarin,N., Dickler,M., D'Andrea,G., Cristofanilli,M., Rivera,E., Hortobagyi,G.N., Norton,L., and Hudis,C.A. (2001). Weekly trastuzumab and paclitaxel therapy for metastatic breast cancer with analysis of efficacy by HER2 immunophenotype and gene amplification. J. Clin. Oncol. *19*, 2587-2595.

Sekiguchi,I., Suzuki,M., Tamada,T., Shinomiya,N., Tsuru,S., and Murata,M. (1996). Effects of cisplatin on cell cycle kinetics, morphological change, and cleavage pattern of DNA in two human ovarian carcinoma cell lines. Oncology *53*, 19-26.

Shah,N.P., Tran,C., Lee,F.Y., Chen,P., Norris,D., and Sawyers,C.L. (2004). Overriding imatinib resistance with a novel ABL kinase inhibitor. Science *305*, 399-401.

Shapiro,G.I. and Harper,J.W. (1999). Anticancer drug targets: cell cycle and checkpoint control. J. Clin. Invest *104*, 1645-1653.

Shapiro,P.S., Whalen,A.M., Tolwinski,N.S., Wilsbacher,J., Froelich-Ammon,S.J., Garcia,M., Osheroff,N., and Ahn,N.G. (1999). Extracellular signal-regulated kinase activates topoisomerase IIalpha through a mechanism independent of phosphorylation. Mol. Cell Biol. *19*, 3551-3560.

Sheaff,R.J., Groudine,M., Gordon,M., Roberts,J.M., and Clurman,B.E. (1997). Cyclin E-CDK2 is a regulator of p27Kip1. Genes Dev. *11*, 1464-1478.

Sherr,C.J. and Roberts,J.M. (1999). CDK inhibitors: positive and negative regulators of G1-phase progression. Genes Dev. *13*, 1501-1512.

Shigematsu,H., Takahashi,T., Nomura,M., Majmudar,K., Suzuki,M., Lee,H., Wistuba,I.I., Fong,K.M., Toyooka,S., Shimizu,N., Fujisawa,T., Minna,J.D., and Gazdar,A.F. (2005). Somatic mutations of the HER2 kinase domain in lung adenocarcinomas. Cancer Res. *65*, 1642-1646.

Sirotnak,F.M., Zakowski,M.F., Miller,V.A., Scher,H.I., and Kris,M.G. (2000). Efficacy of cytotoxic agents against human tumor xenografts is markedly enhanced by coadministration of ZD1839 (Iressa), an inhibitor of EGFR tyrosine kinase. Clin. Cancer Res. *6*, 4885-4892.

Skehan,P., Storeng,R., Scudiero,D., Monks,A., McMahon,J., Vistica,D., Warren,J.T., Bokesch,H., Kenney,S., and Boyd,M.R. (1990). New colorimetric cytotoxicity assay for anticancer-drug screening. J. Natl. Cancer Inst. *82*, 1107-1112.

Slamon,D.J., Clark,G.M., Wong,S.G., Levin,W.J., Ullrich,A., and McGuire,W.L. (1987). Human breast cancer: correlation of relapse and survival with amplification of the HER-2/neu oncogene. Science *235*, 177-182.

Slamon,D.J., Leyland-Jones,B., Shak,S., Fuchs,H., Paton,V., Bajamonde,A., Fleming,T., Eiermann,W., Wolter,J., Pegram,M., Baselga,J., and Norton,L. (2001). Use of chemotherapy plus a monoclonal antibody against HER2 for metastatic breast cancer that overexpresses HER2. N. Engl. J. Med. *344*, 783-792.

Sliwkowski,M.X., Lofgren,J.A., Lewis,G.D., Hotaling,T.E., Fendly,B.M., and Fox,J.A. (1999). Nonclinical studies addressing the mechanism of action of trastuzumab (Herceptin). Semin. Oncol. *26*, 60-70.

Slupianek,A., Schmutte,C., Tombline,G., Nieborowska-Skorska,M., Hoser,G., Nowicki,M.O., Pierce,A.J., Fishel,R., and Skorski,T. (2001). BCR/ABL regulates mammalian RecA homologs, resulting in drug resistance. Mol. Cell *8*, 795-806.

Slupianek,A., Hoser,G., Majsterek,I., Bronisz,A., Malecki,M., Blasiak,J., Fishel,R., and Skorski,T. (2002). Fusion tyrosine kinases induce drug resistance by stimulation of homology-dependent recombination repair, prolongation of G(2)/M phase, and protection from apoptosis. Mol. Cell Biol. *22*, 4189-4201.

Smith,K., Houlbrook,S., Greenall,M., Carmichael,J., and Harris,A.L. (1993). Topoisomerase II alpha co-amplification with erbB2 in human primary breast cancer and breast cancer cell lines: relationship to m-AMSA and mitoxantrone sensitivity. Oncogene *8*, 933-938.

Snouwaert,J.N., Gowen,L.C., Latour,A.M., Mohn,A.R., Xiao,A., DiBiase,L., and Koller,B.H. (1999). BRCA1 deficient embryonic stem cells display a decreased homologous recombination frequency and an increased frequency of non-homologous recombination that is corrected by expression of a brca1 transgene. Oncogene *18*, 7900-7907.

Soldani,C. and Scovassi,A.I. (2002). Poly(ADP-ribose) polymerase-1 cleavage during apoptosis: an update. Apoptosis. *7*, 321-328.

Somasundaram,K., Zhang,H., Zeng,Y.X., Houvras,Y., Peng,Y., Zhang,H., Wu,G.S., Licht,J.D., Weber,B.L., and El-Deiry,W.S. (1997). Arrest of the cell cycle by the tumour-suppressor BRCA1 requires the CDK-inhibitor p21WAF1/CiP1. Nature *389*, 187-190.

Sorkin,A., Di Fiore,P.P., and Carpenter,G. (1993). The carboxyl terminus of epidermal growth factor receptor/erbB-2 chimerae is internalization impaired. Oncogene *8*, 3021-3028.

Spanswick,V.J., Craddock,C., Sekhar,M., Mahendra,P., Shankaranarayana,P., Hughes,R.G., Hochhauser,D., and Hartley,J.A. (2002). Repair of DNA interstrand crosslinks as a mechanism of clinical resistance to melphalan in multiple myeloma. Blood *100*, 224-229.

Stachowiak,M.K., Maher,P.A., Joy,A., Mordechai,E., and Stachowiak,E.K. (1996). Nuclear localization of functional FGF receptor 1 in human astrocytes suggests a novel mechanism for growth factor action. Brain Res. Mol. Brain Res. *38*, 161-165.

Stephens,P., Hunter,C., Bignell,G., Edkins,S., Davies,H., Teague,J., Stevens,C., O'Meara,S., Smith,R., Parker,A., Barthorpe,A., Blow,M., Brackenbury,L., Butler,A., Clarke,O., Cole,J., Dicks,E., Dike,A., Drozd,A., Edwards,K., Forbes,S., Foster,R., Gray,K., Greenman,C., Halliday,K., Hills,K., Kosmidou,V., Lugg,R., Menzies,A., Perry,J., Petty,R., Raine,K., Ratford,L., Shepherd,R., Small,A., Stephens,Y., Tofts,C., Varian,J., West,S., Widaa,S., Yates,A., Brasseur,F., Cooper,C.S., Flanagan,A.M., Knowles,M., Leung,S.Y., Louis,D.N., Looijenga,L.H., Malkowicz,B., Pierotti,M.A., Teh,B., Chenevix-Trench,G., Weber,B.L., Yuen,S.T., Harris,G., Goldstraw,P.,

Nicholson,A.G., Futreal,P.A., Wooster,R., and Stratton,M.R. (2004). Lung cancer: intragenic ERBB2 kinase mutations in tumours. Nature *431*, 525-526.

Tallarida,R.J. (2001). Drug synergism: its detection and applications. J. Pharmacol. Exp. Ther. *298*, 865-872.

Talpaz,M., Rakhit,A., Rittweger,K., O'Brien,S., Cortes,J., Fettner,S., Hooftman,L., and Kantarjian,H. (2005). Phase I evaluation of a 40-kDa branched-chain long-acting pegylated IFN-alpha-2a with and without cytarabine in patients with chronic myelogenous leukemia. Clin. Cancer Res. *11*, 6247-6255.

Taniguchi,T., Tischkowitz,M., Ameziane,N., Hodgson,S.V., Mathew,C.G., Joenje,H., Mok,S.C., and D'Andrea,A.D. (2003). Disruption of the Fanconi anemia-BRCA pathway in cisplatin-sensitive ovarian tumors. Nat. Med. *9*, 568-574.

Tassone,P., Tagliaferri,P., Perricelli,A., Blotta,S., Quaresima,B., Martelli,M.L., Goel,A., Barbieri,V., Costanzo,F., Boland,C.R., and Venuta,S. (2003). BRCA1 expression modulates chemosensitivity of BRCA1-defective HCC1937 human breast cancer cells. Br. J. Cancer *88*, 1285-1291.

Testa,J.R. and Bellacosa,A. (2001). AKT plays a central role in tumorigenesis. Proc. Natl. Acad. Sci. U. S. A *98*, 10983-10985.

Thatcher,N., Chang,A., Parikh,P., Rodrigues,P.J., Ciuleanu,T., Von,P.J., Thongprasert,S., Tan,E.H., Pemberton,K., Archer,V., and Carroll,K. (2005). Gefitinib plus best supportive care in previously treated patients with refractory advanced non-small-cell lung cancer: results from a randomised, placebo-controlled, multicentre study (Iressa Survival Evaluation in Lung Cancer). Lancet *366*, 1527-1537.

Thompson,L.H. and Schild,D. (2001). Homologous recombinational repair of DNA ensures mammalian chromosome stability. Mutat. Res. *477*, 131-153.

Tibbetts,R.S., Cortez,D., Brumbaugh,K.M., Scully,R., Livingston,D., Elledge,S.J., and Abraham,R.T. (2000). Functional interactions between BRCA1 and the checkpoint kinase ATR during genotoxic stress. Genes Dev. *14*, 2989-3002.

Tice,R.R., Agurell,E., Anderson,D., Burlinson,B., Hartmann,A., Kobayashi,H., Miyamae,Y., Rojas,E., Ryu,J.C., and Sasaki,Y.F. (2000). Single cell gel/comet assay: guidelines for in vitro and in vivo genetic toxicology testing. Environ. Mol. Mutagen. *35*, 206-221.

Tilby,M.J., Styles,J.M., and Dean,C.J. (1987). Immunological detection of DNA damage caused by melphalan using monoclonal antibodies. Cancer Res. *47*, 1542-1546.

Tilby,M.J., Johnson,C., Knox,R.J., Cordell,J., Roberts,J.J., and Dean,C.J. (1991). Sensitive detection of DNA modifications induced by cisplatin and carboplatin in vitro and in vivo using a monoclonal antibody. Cancer Res. *51*, 123-129.

Toker,A. and Newton,A.C. (2000). Akt/protein kinase B is regulated by autophosphorylation at the hypothetical PDK-2 site. J. Biol. Chem. *275*, 8271-8274.

Tokuda,Y., Watanabe,T., Omuro,Y., Ando,M., Katsumata,N., Okumura,A., Ohta,M., Fujii,H., Sasaki,Y., Niwa,T., and Tajima,T. (1999). Dose escalation and pharmacokinetic study of a humanized anti-HER2 monoclonal antibody in patients with HER2/neu-overexpressing metastatic breast cancer. Br. J. Cancer *81*, 1419-1425.

Trenz,K., Schutz,P., and Speit,G. (2005). Radiosensitivity of lymphoblastoid cell lines with a heterozygous BRCA1 mutation is not detected by the comet assay and pulsed field gel electrophoresis. Mutagenesis *20*, 131-137.

Tsai,C.M., Chang,K.T., Perng,R.P., Mitsudomi,T., Chen,M.H., Kadoyama,C., and Gazdar,A.F. (1993). Correlation of intrinsic chemoresistance of non-small-cell lung cancer cell lines with HER-2/neu gene expression but not with ras gene mutations. J. Natl. Cancer Inst. *85*, 897-901.

Tsujimoto,Y. (2003). Cell death regulation by the Bcl-2 protein family in the mitochondria. J. Cell Physiol *195*, 158-167.

Turini,M.E. and DuBois,R.N. (2002). Cyclooxygenase-2: a therapeutic target. Annu. Rev. Med. *53*, 35-57.

Turner,N., Tutt,A., and Ashworth,A. (2005). Targeting the DNA repair defect of BRCA tumours. Curr. Opin. Pharmacol. *5*, 388-393.

Tutt,A., Bertwistle,D., Valentine,J., Gabriel,A., Swift,S., Ross,G., Griffin,C., Thacker,J., and Ashworth,A. (2001). Mutation in Brca2 stimulates error-prone homology-directed repair of DNA double-strand breaks occurring between repeated sequences. EMBO J. *20*, 4704-4716.

Tzahar,E., Waterman,H., Chen,X., Levkowitz,G., Karunagaran,D., Lavi,S., Ratzkin,B.J., and Yarden,Y. (1996). A hierarchical network of interreceptor interactions determines signal transduction by Neu differentiation factor/neuregulin and epidermal growth factor. Mol. Cell Biol. *16*, 5276-5287.

Vahteristo,P., Bartkova,J., Eerola,H., Syrjakoski,K., Ojala,S., Kilpivaara,O., Tamminen,A., Kononen,J., Aittomaki,K., Heikkila,P., Holli,K., Blomqvist,C., Bartek,J., Kallioniemi,O.P., and Nevanlinna,H. (2002). A CHEK2 genetic variant contributing to a substantial fraction of familial breast cancer. Am. J. Hum. Genet. *71*, 432-438.

Vakkala,M., Kahlos,K., Lakari,E., Paakko,P., Kinnula,V., and Soini,Y. (2000). Inducible nitric oxide synthase expression, apoptosis, and angiogenesis in in situ and invasive breast carcinomas. Clin. Cancer Res. *6*, 2408-2416.

Valone,F.H., Kaufman,P.A., Guyre,P.M., Lewis,L.D., Memoli,V., Deo,Y., Graziano,R., Fisher,J.L., Meyer,L., Mrozek-Orlowski,M., and . (1995). Phase Ia/Ib trial of bispecific antibody MDX-210 in patients with advanced breast or ovarian cancer that overexpresses the proto-oncogene HER-2/neu. J. Clin. Oncol. *13*, 2281-2292.

Van Hemert,M.J., Steensma,H.Y., and van Heusden,G.P. (2001). 14-3-3 proteins: key regulators of cell division, signalling and apoptosis. Bioessays *23*, 936-946.

Van,C.E. (2006). Challenges in the use of epidermal growth factor receptor inhibitors in colorectal cancer. Oncologist. *11*, 1010-1017.

Vanhoefer,U., Tewes,M., Rojo,F., Dirsch,O., Schleucher,N., Rosen,O., Tillner,J., Kovar,A., Braun,A.H., Trarbach,T., Seeber,S., Harstrick,A., and Baselga,J. (2004). Phase I study of the humanized antiepidermal growth factor receptor monoclonal antibody EMD72000 in patients with advanced solid tumors that express the epidermal growth factor receptor. J. Clin. Oncol. *22*, 175-184.

Velu,T.J. (1990). Structure, function and transforming potential of the epidermal growth factor receptor. Mol. Cell Endocrinol. *70*, 205-216.

Venkitaraman,A.R. (2002). Cancer susceptibility and the functions of BRCA1 and BRCA2. Cell *108*, 171-182.

Viloria-Petit,A., Crombet,T., Jothy,S., Hicklin,D., Bohlen,P., Schlaeppi,J.M., Rak,J., and Kerbel,R.S. (2001). Acquired resistance to the antitumor effect of epidermal growth factor receptor-blocking antibodies in vivo: a role for altered tumor angiogenesis. Cancer Res. *61*, 5090-5101.

Vivanco,I. and Sawyers,C.L. (2002). The phosphatidylinositol 3-Kinase AKT pathway in human cancer. Nat. Rev. Cancer *2*, 489-501.

Vlahovic,G. and Crawford,J. (2003). Activation of tyrosine kinases in cancer. Oncologist. *8*, 531-538.

Vogel,C.L., Cobleigh,M.A., Tripathy,D., Gutheil,J.C., Harris,L.N., Fehrenbacher,L., Slamon,D.J., Murphy,M., Novotny,W.F., Burchmore,M., Shak,S., Stewart,S.J., and Press,M. (2002). Efficacy and safety of trastuzumab as a single agent in first-line treatment of HER2-overexpressing metastatic breast cancer. J. Clin. Oncol. *20*, 719-726.

Voigt,W. (2005). Sulforhodamine B assay and chemosensitivity. Methods Mol. Med. *110*, 39-48.

Vousden,K.H. (2002). Activation of the p53 tumor suppressor protein. Biochim. Biophys. Acta *1602*, 47-59.

Wada,T., Qian,X.L., and Greene,M.I. (1990). Intermolecular association of the p185neu protein and EGF receptor modulates EGF receptor function. Cell *61*, 1339-1347.

Waga,S., Hannon,G.J., Beach,D., and Stillman,B. (1994). The p21 inhibitor of cyclin-dependent kinases controls DNA replication by interaction with PCNA. Nature *369*, 574-578.

Walworth,N.C. (2000). Cell-cycle checkpoint kinases: checking in on the cell cycle. Curr. Opin. Cell Biol. *12*, 697-704.

Wang,H., Zeng,Z.C., Bui,T.A., DiBiase,S.J., Qin,W., Xia,F., Powell,S.N., and Iliakis,G. (2001). Nonhomologous end-joining of ionizing radiation-induced DNA double-stranded breaks in human tumor cells deficient in BRCA1 or BRCA2. Cancer Res. *61*, 270-277.

Wang,Q., Zambetti,G.P., and Suttle,D.P. (1997). Inhibition of DNA topoisomerase II alpha gene expression by the p53 tumor suppressor. Mol. Cell Biol. *17*, 389-397.

Wang,S.C., Lien,H.C., Xia,W., Chen,I.F., Lo,H.W., Wang,Z., li-Seyed,M., Lee,D.F., Bartholomeusz,G., Ou-Yang,F., Giri,D.K., and Hung,M.C. (2004). Binding at and transactivation of the COX-2 promoter by nuclear tyrosine kinase receptor ErbB-2. Cancer Cell *6*, 251-261.

Wang,S.E., Narasanna,A., Perez-Torres,M., Xiang,B., Wu,F.Y., Yang,S., Carpenter,G., Gazdar,A.F., Muthuswamy,S.K., and Arteaga,C.L. (2006). HER2 kinase domain mutation results in constitutive phosphorylation and activation of HER2 and EGFR and resistance to EGFR tyrosine kinase inhibitors. Cancer Cell *10*, 25-38.

Wang,X., Martindale,J.L., and Holbrook,N.J. (2000a). Requirement for ERK activation in cisplatin-induced apoptosis. J. Biol. Chem. *275*, 39435-39443.

Wang,X.W., Zhan,Q., Coursen,J.D., Khan,M.A., Kontny,H.U., Yu,L., Hollander,M.C., O'Connor,P.M., Fornace,A.J., Jr., and Harris,C.C. (1999a). GADD45 induction of a G2/M cell cycle checkpoint. Proc. Natl. Acad. Sci. U. S. A *96*, 3706-3711.

Wang,Y., Cortez,D., Yazdi,P., Neff,N., Elledge,S.J., and Qin,J. (2000b). BASC, a super complex of BRCA1-associated proteins involved in the recognition and repair of aberrant DNA structures. Genes Dev. *14*, 927-939.

Wang,Y., Pennock,S., Chen,X., and Wang,Z. (2002). Internalization of inactive EGF receptor into endosomes and the subsequent activation of endosome-associated EGF receptors. Epidermal growth factor. Sci. STKE. *2002*, L17.

Wang,Z., Morris,G.F., Reed,J.C., Kelly,G.D., and Morris,C.B. (1999b). Activation of Bcl-2 promoter-directed gene expression by the human immunodeficiency virus type-1 Tat protein. Virology *257*, 502-510.

Waterman,H., Alroy,I., Strano,S., Seger,R., and Yarden,Y. (1999). The C-terminus of the kinase-defective neuregulin receptor ErbB-3 confers mitogenic superiority and dictates endocytic routing. EMBO J. *18*, 3348-3358.

Wedge,S.R., Ogilvie,D.J., Dukes,M., Kendrew,J., Chester,R., Jackson,J.A., Boffey,S.J., Valentine,P.J., Curwen,J.O., Musgrove,H.L., Graham,G.A., Hughes,G.D., Thomas,A.P., Stokes,E.S., Curry,B., Richmond,G.H., Wadsworth,P.F., Bigley,A.L., and Hennequin,L.F. (2002). ZD6474 inhibits vascular endothelial growth factor signaling, angiogenesis, and tumor growth following oral administration. Cancer Res. *62*, 4645-4655.

Weiner,D.B., Kokai,Y., Wada,T., Cohen,J.A., Williams,W.V., and Greene,M.I. (1989). Linkage of tyrosine kinase activity with transforming ability of the p185neu oncoprotein. Oncogene *4*, 1175-1183.

Weinert,T. (1997). A DNA damage checkpoint meets the cell cycle engine. Science *277*, 1450-1451.

Weiss,J.R., Moysich,K.B., and Swede,H. (2005). Epidemiology of male breast cancer. Cancer Epidemiol. Biomarkers Prev. *14*, 20-26.

Welcsh,P.L., Owens,K.N., and King,M.C. (2000). Insights into the functions of BRCA1 and BRCA2. Trends Genet. *16*, 69-74.

Whitehouse,C.J., Taylor,R.M., Thistlethwaite,A., Zhang,H., Karimi-Busheri,F., Lasko,D.D., Weinfeld,M., and Caldecott,K.W. (2001). XRCC1 stimulates human polynucleotide kinase activity at damaged DNA termini and accelerates DNA single-strand break repair. Cell *104*, 107-117.

Wiener,J.R., Windham,T.C., Estrella,V.C., Parikh,N.U., Thall,P.F., Deavers,M.T., Bast,R.C., Mills,G.B., and Gallick,G.E. (2003). Activated SRC protein tyrosine kinase is overexpressed in late-stage human ovarian cancers. Gynecol. Oncol. *88*, 73-79.

Williams,C.C., Allison,J.G., Vidal,G.A., Burow,M.E., Beckman,B.S., Marrero,L., and Jones,F.E. (2004). The ERBB4/HER4 receptor tyrosine kinase regulates gene expression by functioning as a STAT5A nuclear chaperone. J. Cell Biol. *167*, 469-478.

Williamson,E.A., Dadmanesh,F., and Koeffler,H.P. (2002). BRCA1 transactivates the cyclin-dependent kinase inhibitor p27(Kip1). Oncogene *21*, 3199-3206.

Woessner,R.D., Mattern,M.R., Mirabelli,C.K., Johnson,R.K., and Drake,F.H. (1991). Proliferation- and cell cycle-dependent differences in expression of the 170 kilodalton and 180 kilodalton forms of topoisomerase II in NIH-3T3 cells. Cell Growth Differ. *2*, 209-214.

Wolff,B., Willingham,M.C., and Hanover,J.A. (1988). Nuclear protein import: specificity for transport across the nuclear pore. Exp. Cell Res. *178*, 318-334.

Wong,T.W., Lee,F.Y., Yu,C., Luo,F.R., Oppenheimer,S., Zhang,H., Smykla,R.A., Mastalerz,H., Fink,B.E., Hunt,J.T., Gavai,A.V., and Vite,G.D. (2006). Preclinical antitumor activity of BMS-599626, a pan-HER kinase inhibitor that inhibits HER1/HER2 homodimer and heterodimer signaling. Clin. Cancer Res. *12*, 6186-6193.

Woodburn,J.R. (1999). The epidermal growth factor receptor and its inhibition in cancer therapy. Pharmacol. Ther. *82*, 241-250.

Wooster,R., Bignell,G., Lancaster,J., Swift,S., Seal,S., Mangion,J., Collins,N., Gregory,S., Gumbs,C., and Micklem,G. (1995). Identification of the breast cancer susceptibility gene BRCA2. Nature *378*, 789-792.

Wright,C., Nicholson,S., Angus,B., Sainsbury,J.R., Farndon,J., Cairns,J., Harris,A.L., and Horne,C.H. (1992). Relationship between c-erbB-2 protein product expression and response to endocrine therapy in advanced breast cancer. Br. J. Cancer *65*, 118-121.

Wynford-Thomas,D. (1999). Cellular senescence and cancer. J. Pathol. *187*, 100-111.

Xia,W., Mullin,R.J., Keith,B.R., Liu,L.H., Ma,H., Rusnak,D.W., Owens,G., Alligood,K.J., and Spector,N.L. (2002). Anti-tumor activity of GW572016: a dual tyrosine kinase inhibitor blocks EGF activation of EGFR/erbB2 and downstream Erk1/2 and AKT pathways. Oncogene *21*, 6255-6263.

Xia,W., Gerard,C.M., Liu,L., Baudson,N.M., Ory,T.L., and Spector,N.L. (2005). Combining lapatinib (GW572016), a small molecule inhibitor of ErbB1 and ErbB2 tyrosine kinases, with therapeutic anti-ErbB2 antibodies enhances apoptosis of ErbB2-overexpressing breast cancer cells. Oncogene *24*, 6213-6221.

Xian,M.Y., Fan,S., Xiong,J., Yuan,R.Q., Meng,Q., Gao,M., Goldberg,I.D., Fuqua,S.A., Pestell,R.G., and Rosen,E.M. (2003). Role of BRCA1 in heat shock response. Oncogene *22*, 10-27.

Xiong,Y., Hannon,G.J., Zhang,H., Casso,D., Kobayashi,R., and Beach,D. (1993). p21 is a universal inhibitor of cyclin kinases. Nature *366* , 701-704.

Xu,B., Kim,S., and Kastan,M.B. (2001). Involvement of Brca1 in S-phase and G(2)-phase checkpoints after ionizing irradiation. Mol. Cell Biol. *21*, 3445-3450.

Xu,B., Kim,S.T., Lim,D.S., and Kastan,M.B. (2002). Two molecularly distinct G(2)/M checkpoints are induced by ionizing irradiation. Mol. Cell Biol. *22*, 1049-1059.

Xu,J.M., Azzariti,A., Severino,M., Lu,B., Colucci,G., and Paradiso,A. (2003). Characterization of sequence-dependent synergy between ZD1839 ("Iressa") and oxaliplatin. Biochem. Pharmacol. *66*, 551-563.

Xu,X., Weaver,Z., Linke,S.P., Li,C., Gotay,J., Wang,X.W., Harris,C.C., Ried,T., and Deng,C.X. (1999). Centrosome amplification and a defective G2-M cell cycle checkpoint induce genetic instability in BRCA1 exon 11 isoform-deficient cells. Mol. Cell *3*, 389-395.

Yakes,F.M., Chinratanalab,W., Ritter,C.A., King,W., Seelig,S., and Arteaga,C.L. (2002). Herceptin-induced inhibition of phosphatidylinositol-3 kinase and Akt Is required for antibody-mediated effects on p27, cyclin D1, and antitumor action. Cancer Res. *62*, 4132-4141.

Yamamoto,K., Hirano,S., Ishiai,M., Morishima,K., Kitao,H., Namikoshi,K., Kimura,M., Matsushita,N., Arakawa,H., Buerstedde,J.M., Komatsu,K., Thompson,L.H., and Takata,M. (2005). Fanconi anemia protein FANCD2 promotes immunoglobulin gene conversion and DNA repair through a mechanism related to homologous recombination. Mol. Cell Biol. *25*, 34-43.

Yamane,K., Katayama,E., and Tsuruo,T. (2000). The BRCT regions of tumor suppressor BRCA1 and of XRCC1 show DNA end binding activity with a multimerizing feature. Biochem. Biophys. Res. Commun. *279*, 678-684.

Yamauchi,H., O'Neill,A., Gelman,R., Carney,W., Tenney,D.Y., Hosch,S., and Hayes,D.F. (1997). Prediction of response to antiestrogen therapy in advanced breast cancer patients by pretreatment circulating levels of extracellular domain of the HER-2/c-neu protein. J. Clin. Oncol. *15*, 2518-2525.

Yan,Y., Haas,J.P., Kim,M., Sgagias,M.K., and Cowan,K.H. (2002). BRCA1-induced apoptosis involves inactivation of ERK1/2 activities. J. Biol. Chem. *277*, 33422-33430.

Yarden,R.I., Pardo-Reoyo,S., Sgagias,M., Cowan,K.H., and Brody,L.C. (2002). BRCA1 regulates the G2/M checkpoint by activating Chk1 kinase upon DNA damage. Nat. Genet. *30*, 285-289.

Yarden,Y. (1990). Receptor-like oncogenes: functional analysis through novel experimental approaches. Mol. Immunol. *27*, 1319-1324.

Yarden,Y. (2001a). Biology of HER2 and its importance in breast cancer. Oncology *61 Suppl 2*, 1-13.

Yarden,Y. (2001b). The EGFR family and its ligands in human cancer. signalling mechanisms and therapeutic opportunities. Eur. J. Cancer *37 Suppl 4*, S3-S8.

Yarden,Y. and Sliwkowski,M.X. (2001). Untangling the ErbB signalling network. Nat. Rev. Mol. Cell Biol. *2*, 127-137.

Ye,Q., Hu,Y.F., Zhong,H., Nye,A.C., Belmont,A.S., and Li,R. (2001). BRCA1-induced large-scale chromatin unfolding and allele-specific effects of cancer-predisposing mutations. J. Cell Biol. *155*, 911-921.

Yoneda,Y., Imamoto-Sonobe,N., Yamaizumi,M., and Uchida,T. (1987). Reversible inhibition of protein import into the nucleus by wheat germ agglutinin injected into cultured cells. Exp. Cell Res. *173*, 586-595.

Yoshida,K. and Miki,Y. (2004). Role of BRCA1 and BRCA2 as regulators of DNA repair, transcription, and cell cycle in response to DNA damage. Cancer Sci. *95*, 866-871.

Yoshimura,N., Kudoh,S., Kimura,T., Mitsuoka,S., Matsuura,K., Hirata,K., Matsui,K., Negoro,S., Nakagawa,K., and Fukuoka,M. (2006). EKB-569, a new irreversible epidermal growth factor receptor tyrosine kinase inhibitor, with clinical activity in patients with non-small cell lung cancer with acquired resistance to gefitinib. Lung Cancer *51*, 363-368.

Yu,D., Liu,B., Tan,M., Li,J., Wang,S.S., and Hung,M.C. (1996). Overexpression of c-erbB-2/neu in breast cancer cells confers increased resistance to Taxol via mdr-1-independent mechanisms. Oncogene *13*, 1359-1365.

Yu,D., Jing,T., Liu,B., Yao,J., Tan,M., McDonnell,T.J., and Hung,M.C. (1998a). Overexpression of ErbB2 blocks Taxol-induced apoptosis by upregulation of p21Cip1, which inhibits p34Cdc2 kinase. Mol. Cell *2*, 581-591.

Yu,D., Liu,B., Jing,T., Sun,D., Price,J.E., Singletary,S.E., Ibrahim,N., Hortobagyi,G.N., and Hung,M.C. (1998b). Overexpression of both p185c-erbB2 and p170mdr-1 renders breast cancer cells highly resistant to taxol. Oncogene *16*, 2087-2094.

Zamble,D.B., Mu,D., Reardon,J.T., Sancar,A., and Lippard,S.J. (1996). Repair of cisplatin--DNA adducts by the mammalian excision nuclease. Biochemistry *35*, 10004-10013.

Zheng,L., Pan,H., Li,S., Flesken-Nikitin,A., Chen,P.L., Boyer,T.G., and Lee,W.H. (2000). Sequence-specific transcriptional corepressor function for BRCA1 through a novel zinc finger protein, ZBRK1. Mol. Cell *6*, 757-768.

Zhong,Q., Chen,C.F., Li,S., Chen,Y., Wang,C.C., Xiao,J., Chen,P.L., Sharp,Z.D., and Lee,W.H. (1999). Association of BRCA1 with the hRad50-hMre11-p95 complex and the DNA damage response. Science *285*, 747-750.

Zhong,Q., Boyer,T.G., Chen,P.L., and Lee,W.H. (2002). Deficient nonhomologous end-joining activity in cell-free extracts from Brca1-null fibroblasts. Cancer Res. *62*, 3966-3970.

Zhou,B.B. and Elledge,S.J. (2000). The DNA damage response: putting checkpoints in perspective. Nature *408*, 433-439.

Zhou,B.B. and Bartek,J. (2004). Targeting the checkpoint kinases: chemosensitization versus chemoprotection. Nat. Rev. Cancer *4*, 216-225.

Zhou,B.P., Liao,Y., Xia,W., Zou,Y., Spohn,B., and Hung,M.C. (2001a). HER-2/neu induces p53 ubiquitination via Akt-mediated MDM2 phosphorylation. Nat. Cell Biol. *3*, 973-982.

Zhou,B.P., Liao,Y., Xia,W., Spohn,B., Lee,M.H., and Hung,M.C. (2001b). Cytoplasmic localization of p21Cip1/WAF1 by Akt-induced phosphorylation in HER-2/neu-overexpressing cells. Nat. Cell Biol. *3*, 245-252.

Zhou,C., Smith,J.L., and Liu,J. (2003). Role of BRCA1 in cellular resistance to paclitaxel and ionizing radiation in an ovarian cancer cell line carrying a defective BRCA1. Oncogene *22*, 2396-2404.

Zwelling,L.A., Anderson,T., and Kohn,K.W. (1979). DNA-protein and DNA interstrand cross-linking by cis- and trans-platinum(II) diamminedichloride in L1210 mouse leukemia cells and relation to cytotoxicity. Cancer Res. *39*, 365-369.

Zwelling,L.A., Michaels,S., Schwartz,H., Dobson,P.P., and Kohn,K.W. (1981). DNA cross-linking as an indicator of sensitivity and resistance of mouse L1210 leukemia to cis-diamminedichloroplatinum(II) and L-phenylalanine mustard. Cancer Res. *41*, 640-649.

Web site visited:

www.3dchem.com

www.appliedbiosystems.com (ABI, User Bulletin #2 and #5)

www.bmb.uga.edu

www.cambio.co.uk

www.cancerresearchuk.org

www.cellsignal.com

www.clontech.com

www.invitrogen.com

www.ncbi.nlm.nih.gov

www.ovc.uoguelph.ca

www.promega.com

www.roche.com

Appendices

Appendix 1: Student *t*-test

The Student *t*-test was established by William Sealy Gosset. Data (in our case IC_{50}), of two independent treatments to be compared, were listed and the number of replicates (n_1 and n_2) treatment was recorded (in our case 3). The mean (x) and the variance (σ^2) were calculated for each treatment. The variance of the difference between the two means (σd^2) was calculated as follow:

$$\sigma d^2 = \frac{\sigma_1^2}{n_1} + \frac{\sigma_2^2}{n_2}$$

Using the standard error ($SE^2 = \sigma^2/n$), we obtain:

$$\sigma d^2 = SE_1^2 + SE_2^2$$

Hence the *t* value was finally obtained using:

$$t = (x_1 - x_2)/ \square d$$

With $x_1 \geq x_2$

Having determined the degree of freedom (n_1+n_2-2) and the level of significance (p = 0.01 or 0.05), the tabulated *t* value is read from the table below (Table I). Hence, if the calculated *t* value is superior to the tabulated value, the IC_{50} are significantly different at 95% or 99% probability. So we can be reasonably confident that the IC_{50} differ from one another, but there is still a 5% chance of being wrong in reaching this conclusion.

		Level of significance p						
		0.1	**0.05**	**0.01**	**0.005**	**0.0025**	**0.001**	**0.0005**
Degree of freedom	**1**	3.078	6.314	31.82	63.66	127.3	318.3	636.6
	2	1.886	2.92	6.965	9.925	14.09	22.33	31.6
	3	1.638	2.353	4.541	5.841	7.453	10.21	12.92
	4	1.533	**2.132**	**3.747**	4.604	5.598	7.173	8.61
	5	1.476	2.015	3.365	4.032	4.773	5.893	6.869
	6	1.44	1.943	3.143	3.707	4.317	5.208	5.959
	7	1.415	1.895	2.998	3.499	4.029	4.785	5.408
	8	1.397	1.86	2.896	3.355	3.833	4.501	5.041
	9	1.383	1.833	2.821	3.25	3.69	4.297	4.781
	10	1.372	1.812	2.764	3.169	3.581	4.144	4.587

Table I – Tabulated *t* values. The values are read using a calculated degree of freedom and a determined level of significance (www.socr.ucla.edu). Tabulated *t* values highlighted in bold correspond to the values obtained when each independent experiment is done in triplicate, so the degree of freedom is 4, and the level of significance *p* is 0.01 or 0.05.

Appendix 2: Design of TaqMan probes and primers using Primer Express software

For our studies, probes were all labelled FAM (fluorescent dye) / TAMRA (quencher dye). The criteria for primer design are the following (Perkin-Elmer Applied Biosystems, UK – www.appliedbiosystems.com):

Design of probes:

- Probes should chosen before the primers
- The Tm (melting point) should be 10°C higher than the primer Tm and kept between 68 – 70°C
- GC content should be between 20 – 80%
- Probes should be 9 – 40bp long
- Runs of identical nucleotides should be avoided, especially G's (no more than 4 contiguous)
- No G's at the 5' end
- It should not have more G's than C's

Design of the primers:

- Primers should be as close as possible to the probe without overlapping the probe
- GC content should be between 30 – 80%
- Primers should be 9 – 40bp long
- The Tm should be between 58 – 60°C
- Runs of identical nucleotides should be avoided, especially G's (no more than 4 contiguous)
- The five nucleotides at the 3' end, of each primer should have no more than two G and/or C bases.
- The difference of Tm between the two primers should be no more than 2%
- Amplicons should be 50 – 150bp long